University of Strathclyde Glasgow

Depression-like behaviour in a mouse model of Alzheimer's disease: a reverse translational study.

Nicole Edwards

A thesis submitted in partial fulfilment of the requirements for the degree of Doctor of Philosophy

Strathclyde Institute of Pharmacy & Biomedical Sciences

Supervisor: Dr Trevor Bushell

2025

Declaration

Strathclyde Institute of Pharmacy and Biomedical Sciences, University of Strathclyde, Glasgow G4 0RE

This thesis is the result of the author's original research. It has been composed by the author and has not been previously submitted for examination which has led to the award of degree.

Signed: *NEdwards*

Date: 17/11/25

Acknowledgements

I am very thankful to my supervisor, Trevor Bushell, for his continued support, advice, and guidance during this journey. I have truly enjoyed working and learning from him, and his supervision has greatly contributed to my development as a scientist.

I am also grateful to my second supervisor, Shuzo Sakata, for allowing me to work in his lab under his licence and for providing the codes and resources essential to my project. I would also like to thank Gail McConnell for the use of the Mesolens, which has been instrumental for the analyses in this project.

I would like to acknowledge the funding from Alzheimer's Society that supported this project, along with the monitors who oversaw my progress. I am also thankful to ARUK Scotland for additional contributions to this project.

I am very grateful to the entire team in the BPU, for all their help, support, and laughter during my project. In particular, I would like to thank Lee, who would drop everything to assist me with my work and who has also been a great friend and listener during my time at Strathclyde.

I am also extremely lucky to have met some wonderful friends along the way who have made this experience such a fun and enjoyable time in my life. A special thanks to my former desk mate, flatmate, and all-around mate, Cristina, who has been a constant source of joy, encouragement, and chaos in the very best way.

To my family, I am incredibly thankful to my mum, dad, and sisters, Emma and Lauren, for their continuous love, support, and patience over the past three years. I know my mind has often been preoccupied with work, and I probably haven't said it enough, but I love you all very much and I am truly grateful for everything you do for me.

Finally, I would like to acknowledge all the mice used in this study and throughout the history of scientific research. They have paid the ultimate sacrifice in order to advance scientific knowledge, and ultimately save lives, for which we should be eternally grateful.

Conferences and Achievements

Strathclyde institute of Pharmacy and Biomedical Science Research Day, Glasgow - Feb 2023 (poster presentation: “Does pharmacologically induced depression-like behaviour exacerbate Alzheimer’s disease pathology?”, best poster prize).

ECR Life Sciences Symposium, University of Glasgow – Feb 2023 (poster presentation: “Does pharmacologically-induced depression-like behaviour exacerbate Alzheimer’s disease pathology?”).

Alzheimer’s Research UK annual conference, Aberdeen - March 2023 (poster presentation: “Does pharmacologically induced depression-like behaviour exacerbate Alzheimer’s disease pathology?”).

Scottish Dementia Research Consortium annual meeting, Glasgow – April 2023 (poster presentation: “Does pharmacologically-induced depression-like behaviour exacerbate Alzheimer’s disease pathology?”, best poster prize).

Alzheimer’s Society annual retreat meeting, Newcastle – June 2023.

Alzheimer’s Research UK Scottish network meeting, Dundee - Aug 2023 (short oral and poster presentation: “Does pharmacologically induced depression-like behaviour exacerbate Alzheimer’s disease pathology?”).

Alzheimer’s Research UK Scottish network small grant award - awarded December 2023 (£3000).

Alzheimer’s Research UK annual conference, Liverpool – March 2024 (poster presentation: “Pharmacologically-induced depression-like behaviour is genotype and sex independent in a mouse model of amyloid pathology”)

Measuring behaviour international conference, Aberdeen – May 2024 (Invited speaker: “The splash test as a model of rodent apathy”).

Strathclyde institute of Pharmacy and Biomedical Science PGR research day, Glasgow – June 2024 (poster presentation: “Astrocytic immunomodulation as a potential novel treatment for Alzheimer’s disease”).

Scottish Dementia Research Consortium celebrating Scottish research Dundee – June 2024 (poster presentation: “Astrocytic immunomodulation as a potential novel treatment for Alzheimer’s disease”).

Alzheimer’s Society annual retreat meeting, Solihull – June 2024.

Strathclyde Optical Microscopy Course, Glasgow – July 2024 (poster presentation: “Astrocytic immunomodulation as a potential novel treatment for Alzheimer’s disease”, best microscope image prize).

Alzheimer’s Research UK Scottish network meeting, Dundee – Aug 2024 (Invited speaker: “Is there a link between depression-like behaviour and amyloid pathology in 5xFAD mice?”).

Alzheimer’s Research UK annual conference, Birmingham - February 2025 (poster presentation: “Pharmacologically-impaired astrocytic reactivity reduces amyloid plaque pathology in female 5xFAD mice”, best poster prize).

Alzheimer’s Research UK Scottish network ECR training grant award - awarded March 2025 (£250).

University of Strathclyde PGR travel fund award - awarded April 2025 (£480).

Brain travel fund award – awarded June 2025 (£800).

XVII European Meeting on Glial Cells in Health and Disease, Marseille – July 2025 (poster presentation: “Reducing astrocytic reactivity as a potential novel pathway for impairing amyloid pathology”).

Abstract

Alzheimer's disease (AD) represents a major global health burden, with prevalence continuing to rise and current treatments offering limited efficacy. Growing evidence highlights neuroinflammation as a key driver of AD progression, with activated microglia and reactive astrocytes contributing to and accelerating AD pathology. Similarly, major depressive disorder (MDD) is characterised by enhanced neuroinflammation, including elevated levels of pro-inflammatory cytokines, and is recognised as a risk factor for AD. Furthermore, patients experiencing both MDD and AD show accelerated disease progression and a worse prognosis, suggesting that MDD could act as an early biomarker or intervention target for AD therapeutics. Recent findings demonstrate that protease-activated receptor 2 (PAR2) activation induced behavioural changes associated with depression-like behaviour and cytokine release *in vivo*. Based on this, we hypothesised that PAR2 activation via activator AC264613, as well as LPS-induced inflammation, would elicit depression-like behaviour and exacerbate neuroinflammation and amyloid-beta (Aβ) deposition in the 5xFAD mouse model.

10-12-week-old mice ($5xFAD^{-/-}$ and $5xFAD^{+/-}$ littermates and C57BL6/J wild-types) were injected with either vehicle (i.p.), AC264613 (AC: 100 mg kg^{-1} i.p.) or lipopolysaccharide (LPS: 0.5 mg kg^{-1} i.p.) and locomotor activity, anhedonia and apathy were investigated 2h and 24h post-injection. Both AC and LPS induced behavioural changes associated with depression-like behaviour, demonstrated by reduced locomotor activity, sucrose preference, and

grooming behaviour, which were exacerbated under environmental stress. Immunohistochemistry revealed that AC and LPS induced transient immunomodulatory effects, reducing astrocyte reactivity and Aβ plaque deposition at 3 weeks post-injection in female 5xFAD$^{+/-}$ mice but had no effect on activated or phagocytic microglia. Both AC and LPS altered pro- and anti-inflammatory cytokine release in 5xFAD$^{-/-}$ mice, while AC had minimal effects in 5xFAD$^{+/-}$ mice. In addition, PAR2 activation increased blood brain barrier (BBB) permeability, whereas PAR2 inhibition maintained BBB integrity and prevented AC induced disruption.

Overall, this study expands our knowledge on the neuroprotective and immunomodulatory properties of PAR2, highlighting its potential as a therapeutic target for modulating neuroinflammation, Aβ plaque deposition and BBB integrity, offering promising new avenues for AD treatments.

Table of Contents

Declaration ii
Acknowledgements iii
Conferences and Achievements iv
Abstract vi
List of figures xiv
List of tables xviii
Abbreviations xix
Chapter 1: General Introduction 1
1.1. Alzheimer's disease 2
1.1.1. History and prevalence of Alzheimer's disease 2
1.1.2. Alzheimer's disease pathology 4
1.1.2.1. Amyloid cascade hypothesis 4
1.1.2.2. Neurofibrillary Tau tangles 6
1.1.2.3. Pathological and structural brain changes 8
1.1.2.4. Amyloid plaques and neurofibrillary tau interactions 9
1.1.3. Genetics of Alzheimer's disease 11
1.1.3.1. Familial Alzheimer's disease 11
1.1.3.2. Sporadic Alzheimer's disease 12
1.1.4. Risk factors of Alzheimer's disease 13
1.1.5. Biomarkers of Alzheimer's disease 15
1.1.6. Treatments for Alzheimer's disease 18
1.1.6.1. Symptomatic treatments 18
1.1.6.2. Disease-modifying treatments 20
1.1.7. Animal models of Alzheimer's disease 21
1.1.7.1. Cognitive and behavioural tests of Alzheimer's disease 22
1.1.7.2. 5xFAD mouse model 25
1.2. Neuroinflammation 26
1.2.1. The inflammatory response 26
1.2.2. Microglia 27
1.2.2.1. The role of microglia in AD 28
1.2.3. Astrocytes 30
1.2.3.1. The role of astrocytes in AD 32
1.2.4. Microglia and astrocyte interactions 35
1.2.5. Cytokines and chemokines 37
1.2.5.1 Cytokines and chemokines in AD 38
1.2.6. LPS model of inflammation 39

1.2.6.1. LPS in AD models 39
1.3. Major depression disorder 41
1.3.1. Epidemiology and symptoms of MDD 41
1.3.2. Biomarkers and risk factors of MDD 42
1.3.3. Pathophysiology of MDD 43
1.3.3.1. The monoamine theory 43
1.3.3.2. Stress, the HPA axis and glucocorticoid cascade hypothesis 45
1.3.3.3. Glutamatergic neurotransmitter receptor dysfunction 46
1.3.3.4. Pathological changes and neurogenesis 47
1.3.4. Neuroinflammation in MDD 48
1.3.5. MDD and AD 50
1.3.6. Rodent models of MDD 54
1.3.6.1. Chronic stress-induced models 55
1.3.6.2. Genetic models 55
1.3.6.3. Pharmacological models 56
1.3.6.4. Behavioural tests of depression 57
1.3.6.5. Targeting MDD and neurodegeneration 59
1.4. Protease-activated receptors 61
1.4.1. PAR activation and expression 61
1.4.2. PAR functions 62
1.4.3. PAR2 63
1.4.3.1. PAR2 in the CNS 65
1.4.3.2. PAR2, neuroinflammation and depression-like behaviour 66
1.5. Hypothesis 67
Chapter 2: Materials and methods 68
2.1. *In vivo* experiments 69
2.1.1. Mice 69
2.1.1.1. Breeding and genotyping 69
2.1.2. Study groups 70
2.1.3. Treatments 71
2.1.4. Behavioural tests 74
2.1.4.1. Open field test 75
2.1.4.2. Sucrose preference test 77
2.1.4.3. Splash test 78
2.1.4.4. Exclusion criteria 79
2.1.5. Perfusion fixation 79
2.2. Immunohistochemistry 80
2.2.1. Microtomy 80

2.2.2. IHC....81
2.3. Imaging....83
2.3.1. Mesolens imaging....83
2.3.2. Cadaverine and lectin imaging....84
2.3.2.1. Mesolens imaging....84
2.3.2.2. Confocal imaging....84
2.4. Cytokine arrays....84
2.4.1. Blood sampling....84
2.4.2. Sample preparation....85
2.4.3. Membrane exposure....86
2.5. Data and statistics....87
2.5.1. Power calculations....88
Chapter 3: The effects of AC- and LPS-injection on behaviour in C57BL6/J and 5xFAD$^{-/-}$ mice....89
3.1. Introduction and aims....90
3.1.1. C57BL6/J and 5xFAD$^{-/-}$ mice....91
3.2. AC- and LPS-injection reduced locomotor activity independent of sex and genotype....91
3.2. AC- and LPS-injection reduced time spent in centre square independent of sex and genotype....97
3.3. AC-injection reduced sucrose preference independent of sex and genotype....101
3.4. LPS- but not AC-injection reduced time spent grooming....105
3.4.1. AI machine learning analysis suggested AC-injection increased grooming behaviour 2h post-injection....105
3.4.2. Manual scoring analysis reveals LPS- but not AC-injection reduced grooming behaviour....108
3.4.3. Sex and genotype had no effect on time spent grooming 2h post-injection independent of treatment....111
3.5. AC- and LPS-injection induced temporary weight loss....114
3.6. Discussion....116
3.6.1. AC264613 and LPS induce behavioural changes associated with depression-like behaviour in C57BL6/J and 5xFAD$^{-/-}$ mice....116
3.6.2. AC264613 and LPS reduced locomotor activity and increased anxiety-like behaviour in C57BL6/J and 5xFAD$^{-/-}$ mice....116
3.6.3. AC264613 and LPS reduced sucrose preference in C57BL6/J and 5xFAD$^{-/-}$ mice....118
3.6.4. LPS but not AC264613 induced apathy-like behaviour in C57BL6/J and 5xFAD$^{-/-}$ mice....120
3.6.5. AC264613 did not affect general animal health....123

3.6.6. Sex and genotype do not influence AC264613 or LPS-induced depression-like behaviour. 124
3.6.7. Conclusion 126
Chapter 4: The effects of AC- and LPS-injection on behaviour and neuropathology in 5xFAD$^{-/-}$ and 5xFAD$^{+/-}$ mice. 127
4.1. Introduction and aims. 128
4.1.1 5xFAD mice 129
4.2. 5xFAD$^{+/-}$ mice have higher locomotor activity upon first exposure to the open field arena. 130
4.3. AC- and LPS-injection reduced locomotor activity is independent of sex and genotype. 133
4.4. LPS- but not AC-injection reduced time spent at the centre square of the OFT arena independent of sex and genotype. 138
4.5. Injection per se reduced sucrose preference independent of sex and genotype. 142
4.6. AC- and LPS-injection reduced grooming behaviour in 5xFAD$^{+/-}$ mice. 147
4.7. LPS-injection induced a temporary weight reduction independent of sex or genotype. 153
4.8. Immunohistochemistry results 156
4.8.1. Two injections of AC and LPS reduced GFAP and C3 expression in female but not male 5xFAD$^{+/-}$ mice at 3 weeks post-injection. 157
4.8.2. Two injections of AC reduced Iba1 expression in some brain regions of female but not male 5xFAD$^{+/-}$ mice at 3 weeks post-injection. 164
4.8.3. Two injections of AC and LPS reduced Aβ plaque load in female but not male 5xFAD$^{+/-}$ mice at 3 weeks post-injection. 167
4.8.4. Two injections of AC and LPS had no influence on CD68 expression or CD68 to Iba1 ratio at 3 weeks post-injection. 172
4.9. AC-injection has no influence on peripheral cytokines in 5xFAD$^{+/-}$ mice. 178
4.10. Discussion 182
4.10.1. AC264613 and LPS induced behavioural changes associated with depression-like behaviour. 182
4.10.2. AC264613 and LPS reduced locomotor activity in both 5xFAD$^{-/-}$ and 5xFAD$^{+/-}$ mice, while LPS alone increased anxiety-like behaviour. 183
4.10.3. Vehicle, AC- and LPS-injection all induced anhedonia-like behaviour in 5xFAD$^{-/-}$ and 5xFAD$^{+/-}$ mice. 185
4.10.4. 5xFAD$^{+/-}$ but not 5xFAD$^{-/-}$ mice are susceptible to pharmacologically-induced apathy-like behaviour. 187
4.10.5. AC264613 and LPS reduced astrocyte reactivity in female but not male 5xFAD$^{+/-}$ mice at 3 weeks post-injection. 188
4.10.6. AC264613 and LPS have no effect on activated microglia at 3 weeks post-injection. 191
4.10.7. AC264613 and LPS reduce Aβ plaque load in female but not male 5xFAD$^{+/-}$ mice at 3 weeks post-injection. 192

4.10.8. AC264613 and LPS have no effect on phagocytic microglia at 3 weeks post-injection. 193
4.10.9. Methodological limitations of immunohistochemical analysis....195
4.10.10. Sex differences in pathology results....196
4.10.11. Cytokine changes in 5xFAD$^{-/-}$ and 5xFAD$^{+/-}$ mice. 199
4.10.12. Conclusion....201
Chapter 5: The longevity and effect of additional dosing of AC and LPS on behaviour and neuropathology in 5xFAD$^{+/-}$ mice. 202
5.1. Introduction and aims. 203
5.1.1. 5xFAD mice 204
5.2. AC- and LPS-injection reduced locomotor activity with no prolonged behavioural or health changes at 10 weeks post-injection. 204
5.3. Immunohistochemistry results at 10 weeks post-injection. 207
5.3.1. Two injections of AC and LPS had no effect on GFAP or C3 expression at 10 weeks post-injection. 207
5.3.2. Two injections of AC and LPS had no influence on Iba1 or CD68 expression at 10 weeks post-injection. 212
5.3.3. Two injections of AC and LPS did not affect Aβ plaque load at 10 weeks post-injection. 218
5.4. Multiple-injections of AC or LPS had no lasting influence on locomotor activity or animal health at 3 weeks post-injection in 5xFAD$^{+/-}$ mice. 221
5.5. Immunohistochemistry results of four weekly-injections of AC or LPS. 224
5.5.1. Four injections of AC and LPS had no effect on GFAP or C3 expression at 3 weeks post-injection. 224
5.5.2. Four injections of AC and LPS had no effect on Iba1 or CD68 expression at 3 weeks post-injection. 230
5.5.3. Four injections of AC and LPS did not influence Aβ plaque load at 3 weeks post-injection. 238
5.6. Discussion 241
5.6.1. AC264613 and LPS had no effect long-term effect on locomotor activity or animal health at 10 weeks post-injection. 241
5.6.2. LPS but not AC264613 reduced sucrose preference at 2h post-injection. 241
5.6.3. AC264613 and LPS did not induce apathy-like behaviour in female 5xFAD$^{+/-}$ mice. 243
5.6.4. AC264613 and LPS had no effect astrocytic reactivity at 10 weeks post-injection. 244
5.6.5. AC264613 and LPS had no effect on activated microglia or their phagocytic activity at 10 weeks post-injection. 246
5.6.5. AC264613 and LPS had no effect Aβ plaque load at 10 weeks post-injection. 249
5.6.6. Multiple doses of AC264613 and LPS had no long-lasting effect on locomotor activity or animal health at 3 weeks post-injection. 250

5.6.7. LPS reduced sucrose preference in both sexes, while AC264613 reduced sucrose preference in only female 5xFAD$^{+/-}$ mice at 2h post-injection. 251
5.6.8. AC264613 and LPS induce apathy-like behaviour in male 5xFAD$^{+/-}$ mice. 252
5.6.9. Four injections of AC264613 and LPS had no effect astrocytic reactivity in either male or female 5xFAD$^{+/-}$ mice at 3 weeks post-injection. 253
5.6.10. Four injections of AC264613 and LPS had no effect activated microglia or phagocytic activity in either male or female 5xFAD$^{+/-}$ mice at 3 weeks post-injection. 255
5.6.11. Four injections of AC264613 and LPS had no effect Aβ plaque burden in either male or female 5xFAD$^{+/-}$ mice at 3 weeks post-injection. 256
5.6.12. Conclusion 257
Chapter 6: The effects of PAR2 inhibition on behaviour and blood brain barrier integrity. 258
6.1. Introduction and aims. 259
6.1.1. 5xFAD mice. 260
6.2. AZ pre-treatment enhanced AC-induced reductions in locomotor activity 2h post-injection, while AZ alone had no effect. 261
6.3. AC- but not AZ-injection increases cadaverine and lectin levels across the brain. 264
6.3.1. AC-injection increases cadaverine expression in across the brain. 264
6.3.1 AC-injection increases lectin expression in some brain regions. 265
6.4. Confocal imaging reveals no increase in parenchymal cadaverine or vascular lectin in the CA1 following AC-injection. 269
6.4.1. AC-injection has no significant effect on cadaverine expression in the parenchyma. 269
6.4.2. AC-injection has no significant effect on lectin expression in the blood vessels. 269
6.5. Discussion. 273
6.5.1. AZ8838 pre-treatment exacerbates AC264613-induced reductions in locomotor activity. 273
6.5.2. PAR2 activation increases BBB permeability, whereas PAR2 inhibition preserves barrier integrity. 274
6.5.3. Conclusion 278
Chapter 7: General discussion 279
7.1. Summary of aims and results. 280
7.2. Clinical relevance 282
7.3. Limitations 283
7.4. Future directions 286
References 288

List of figures

Figure 1.1: Schematic representation of amyloidogenic and non-amyloidogenic APP processing pathways. 5
Figure 1.2: Pathology of healthy brain vs Alzheimer's disease brain. 9
Figure 1.3: Genetic variant mutations contributing to AD risk. 13
Figure 1.4: 14 modifiable risk factors contributing to AD prevalence. 14
Figure 1.5: Biomarkers and progression of AD. 17
Figure 1.6: Microglia activation. 29
Figure 1.7: Astrocyte activation. 33
Figure 1.8: Major theories of MDD pathophysiology. 44
Figure 1.9: The role of MDD in AD risk. 51
Figure 1.10: Schematic representation of PAR2 activation. 64
Figure 2.1: Protocol for breeding heterozygous 5xFAD mice. 70
Figure 2.2: Schematic representation of the 7 experimental mouse groups. 73
Figure 2.3: Schematic representation of the behavioural testing schedule for group 2 mice: double-injection 3-week protocol. 75
Figure 2.4: OFT set up. 76
Figure 2.5: DLC tracking of individual mouse body parts and respective tracing images generated for each. 77
Figure 2.6: Sucrose preference set up. 78
Figure 2.7: The Allen mouse brain atlas diagram of a sagittal cerebrum section. 81
Figure 2.8: Representative Mesolens image of a 5xFAD$^{+/-}$ mouse brain. 83
Figure 2.9: Cytokine array method. 86
Figure 3.1: AC- and LPS-injection significantly reduced locomotor activity 2h post-injection. 94
Figure 3.2: AC- and LPS-injection significantly reduced locomotor activity 2h post-injection in both C57BL6/J and 5xFAD$^{-/-}$ mice independent of sex. 95
Figure 3.3: AC-injection significantly reduced locomotor activity in C57BL6/J compared to 5xFAD$^{-/-}$ mice at 2h post-injection. 96
Figure 3.4: AC-injection significantly reduced time spent in the centre square 2h post-injection. 97
Figure 3.5: AC-injection reduced time spent in centre square 2h post-injection and is independent of sex. 99
Figure 3.6: AC- and LPS-injection reduced time spent in the centre square 2h post-injection is genotype independent. 100
Figure 3.7: AC-injection significantly reduced sucrose preference 2h post-injection. 101
Figure 3.8: AC-injection reduced sucrose preference 2h post-injection in both C57BL6/J and 5xFAD$^{-/-}$ mice and is independent of sex. 103
Figure 3.9: AC- and LPS-injection reduced sucrose preference across the timepoints with no difference between genotypes. 104
Figure 3.10: AI machine learning analysis suggests that AC-injection significantly increased time spent grooming 2h post-injection. 107

Figure 3.11: Manual scored grooming revealed that AC-injection had no effect on time spent grooming. 110
Figure 3.12: AC- and LPS-injection had no influence on time spent grooming in either sex within the genotypes 2h post-injection. 112
Figure 3.13: Genotype has no effect on total time spent grooming at 2h post- or 24h post-injection independent of treatment group. 113
Figure 3.14: AC- and LPS-injection cause a temporary reduction in weight independent of genotype. 115
Figure 4.1: 5xFAD$^{+/-}$ mice have significantly increased locomotor activity compared to 5xFAD$^{-/-}$ at naïve habituation day 1. 132
Figure 4.2: AC- and LPS-injection significantly reduced locomotor activity 2h post-injection. 135
Figure 4.3: AC- and LPS-injection reduced locomotor activity 2h post-injection in both 5xFAD$^{-/-}$ and 5xFAD$^{+/-}$ mice independent of sex. 136
Figure 4.4: AC- and LPS-injection significantly reduced locomotor activity independent of genotype. 137
Figure 4.5: LPS-injection reduced time spent at the centre square 2h post-injection. 139
Figure 4.6: Sex did not influence time spent at the centre square of the OFT arena. 140
Figure 4.7: LPS-injection significantly time spent at centre independent of genotype. 141
Figure 4.8: Injection per se significantly reduced sucrose preference 2h post-injection independent of treatment. 144
Figure 4.9: Injection per se reduced sucrose preference 2h post-injection in both 5xFAD$^{-/-}$ and 5xFAD$^{+/-}$ mice independent of sex. 145
Figure 4.10: Injection per se reduced sucrose preference 2h post-injection independent of genotype. 146
Figure 4.11: AC- and LPS-injection reduced grooming behaviour 2h post-injection. 150
Figure 4.12: AC-injection reduced grooming time 2h post-injection with differences found between sex in 5xFAD$^{+/-}$ mice. 151
Figure 4.13: 5xFAD$^{+/-}$ mice are more susceptible to reduced grooming behaviour following AC- and LPS-injection. 152
Figure 4.14: Male 5xFAD$^{+/-}$ mice have significantly reduced overall body weight compared to male 5xFAD$^{-/-}$ mice. 154
Figure 4.15: LPS-injection induced a temporary reduction in weight in female mice of both genotypes. 155
Figure 4.16: LPS-injection caused a temporary reduction in weight in male mice of both genotypes. 156
Figure 4.17: Representative Mesolens images of GFAP IHC in female and male 5xFAD$^{-/-}$ and 5xFAD$^{+/-}$ mice. 160
Figure 4.18: AC and LPS-injection reduced GFAP expression in female but not male 5xFAD$^{+/-}$ mice. 161
Figure 4.19: Representative Mesolens images of C3 IHC in female and male 5xFAD$^{-/-}$ and 5xFAD$^{+/-}$ mice. 162

Figure 4.20: AC and LPS-injection reduced C3 expression across the brain of female but not male 5xFAD$^{+/-}$ mice. 163
Figure 4.21: Representative Mesolens images of Iba1 IHC in female and male 5xFAD$^{-/-}$ and 5xFAD$^{+/-}$ mice. 165
Figure 4.22: AC-injection reduced Iba1 expression in some brain regions of female 5xFAD$^{+/-}$ mice. 166
Figure 4.23: Representative Mesolens images of Aβ plaques in female and male 5xFAD$^{+/-}$ mice following vehicle, AC- and LPS-injection. 169
Figure 4.24: AC- and LPS-injection reduced Aβ plaque load across several brain regions of female but not male 5xFAD$^{+/-}$ mice. 170
Figure 4.25: AC- and LPS-injection reduced Aβ plaque size in some regions of female but not male 5xFAD$^{+/-}$ mice. 171
Figure 4.26: Representative Mesolens images of CD68 IHC in female and male 5xFAD$^{+/-}$ mice following vehicle, AC- and LPS-injection. 175
Figure 4.27: AC- and LPS-injection had no influence on CD68 expression in female or male 5xFAD$^{+/-}$ mice. 176
Figure 4.28: AC- and LPS-injection had no significant effect on CD68 to Iba1 ratio in male or female 5xFAD$^{+/-}$ mice. 177
Figure 4.29: Cytokine analysis of 5xFAD$^{-/-}$ mice following vehicle, AC- and LPS-injection. 180
Figure 4.30: Cytokine analysis of 5xFAD$^{+/-}$ mice following vehicle, AC- and LPS-injection. 181
Figure 5.1: Figure 5.1: AC- and LPS-injection reduced locomotor activity and sucrose preference 2h post-injection with no prolonged effects on locomotor activity at 10 weeks post-injection. 206
Figure 5.2: Representative Mesolens images of GFAP and C3 IHC in female 5xFAD$^{+/-}$ mice at 10 weeks post-injection. 209
Figure 5.3: AC- and LPS-injection had no effect GFAP expression at 10 weeks post-injection in female 5xFAD$^{+/-}$ mice. 210
Figure 5.4: AC- and LPS-injection had no effect C3 expression at 10 weeks post-injection in female 5xFAD$^{+/-}$ mice. 211
Figure 5.5: Representative Mesolens images of Iba1 and CD68 IHC in female 5xFAD$^{+/-}$ mice at 10 weeks post-injection. 214
Figure 5.6: AC- and LPS-injection had no effect Iba1 expression at 10 weeks post-injection in female 5xFAD$^{+/-}$ mice. 215
Figure 5.7: AC- and LPS-injection had no influence on CD68 expression at 10 weeks post-injection. 216
Figure 5.8: AC- and LPS-injection had no effect on the ratio of CD68 to IBA1 at 10 weeks post-injection. 217
Figure 5.9: Representative Mesolens images of Thioflavin S staining Aβ plaques in female 5xFAD$^{+/-}$ mice at 10 weeks post-injection. 219
Figure 5.10: AC- and LPS-injection did not alter Aβ plaque load at 10 weeks post-injection in female 5xFAD$^{+/-}$ mice. 220
Figure 5.11: AC- and LPS-injection reduced locomotor activity 2h post-injection with additional doses having no lasting influence on activity at 3 weeks post-injection. 223

Figure 5.12: Representative Mesolens images of GFAP IHC in female and male 5xFAD$^{+/-}$ mice following multiple-injections. 226
Figure 5.13: GFAP expression was unchanged in both female and male 5xFAD$^{+/-}$ mice following multiple injections of AC and LPS. 227
Figure 5.14: Representative Mesolens images of C3 IHC in female and male 5xFAD$^{+/-}$ mice following multiple-injections. 228
Figure 5.15: C3 expression was unaffected in both female and male 5xFAD$^{+/-}$ mice following multiple injections of AC and LPS. 229
Figure 5.16: Representative Mesolens images of Iba1 IHC in female and male 5xFAD$^{+/-}$ mice following multiple-injections. 233
Figure 5.17: Iba1 expression was unaltered in both female and male 5xFAD$^{+/-}$ mice following multiple injections of AC and LPS. 234
Figure 5.18: Representative Mesolens images of CD68 IHC in female and male 5xFAD$^{+/-}$ mice following multiple-injections. 235
Figure 5.19: CD68 expression was unchanged in both female and male 5xFAD$^{+/-}$ mice following multiple injections of AC and LPS. 236
Figure 5.20: CD68 to IBA1 ratio was unaffected by multiple injections of AC and LPS in both female and male 5xFAD$^{+/-}$ mice at 3 weeks post-injection 237
Figure 5.21: Representative Mesolens images of thioflavin S staining in female and male 5xFAD$^{+/-}$ mice following multiple-injections. 239
Figure 5.22: Multiple injections of AC and LPS had no influence on Aβ plaque load in either female or male 5xFAD$^{+/-}$ mice. 240
Figure 6.1: AZ-injection followed by AC-injection reduced locomotor activity 2h post-injection while AZ-injection alone had no effects. 263
Figure 6.2: Representative Mesolens images of cadaverine and lectin expression in the hippocampus, VC and SSC. 267
Figure 6.3: AC-injection increases cadaverine and lectin expression across brain regions. 268
Figure 6.4: Representative confocal images of cadaverine and lectin expression in the hippocampal CA1 region. 271
Figure 6.5: AC-injection did not significantly influence the expression of cadaverine in the parenchyma or lectin in the blood vessels in the CA1. 272

List of tables

Table 1.1: Examples of commonly used mouse models of Alzheimer's disease. 24
Table 1.2: Common behavioural tests used to assess depression-like behaviour in rodents. 60
Table 2.1: List of primary and secondary antibodies and dyes used in IHC. 82
Table 2.2: All cytokines, chemokines and acute phase proteins detected by the mouse array proteome profiler. 85
Table 1.1: Number of mice included and excluded in each treatment group. 91
Table 4.1: Number of mice included and excluded in each treatment group. 130

Abbreviations

5-HT	Serotonin
ACh	Acetylcholine
AD	Alzheimer's Disease
APOE	Apolipoprotein E
APP	β-amyloid precursor protein
Aβ	Amyloid beta
BACE1	β-secretase
BBB	Blood brain barrier
BDNF	Brain derived neurotrophic factor
C3	Complement component 3
CA (1)	Cornu ammonis 1
CAA	Cerebral amyloid angiopathy
CD33	Cluster of differentiation 33
ChAT	Choline acetyltransferase
ChEI	Cholinesterase inhibitor
CNS	Central nervous system
CSF	Cerebral spinal fluid
DAA	Disease-associated astrocyte
DAM	Disease-associated microglia
DAMPs/PAMPs	Damage/Pathogen-associated molecular patterns
DG	Dentate gyrus
DMT	Disease-modifying therapy
EOAD	Early-onset Alzheimer's disease
FAD	Familial Alzheimer's disease
FST	Forced swim test
GFAP	Glial fibrillary acidic protein
GWAS	Genome-wide association studies
HPA	Hypothalamic-pituitary-adrenal
Iba1	Ionized calcium-binding adaptor molecule 1
IL	Interleukin
KO	Knockout
LOAD	Late-onset Alzheimer's disease
LPS	Lipopolysaccharide
LTP	Long-term potentiation
mAb	Monoclonal antibody
MAPT	Microtubule associated protein tau
MCI	Mild cognitive impairment
MDD	Major depressive disorder
NFT	Neurofibrillary tangle
NMDA	N-methyl-D-aspartate
NPS	Neuropsychiatric symptom
NSAID	Non-steroidal anti-inflammatory drug
OFT	Open field test
PAR	Protease-activated receptor

PET	Positron emission tomography
PHF	Paired helical fibrils
PSEN	Presenilin
p-tau	Phosphorylated tau
ROS	Reactive oxygen species
SPT	Sucrose preference test
SSC	Somatosensory cortex
SSRIs	Selective serotonin reuptake inhibitors
TNF-α	Tumor necrosis factor alpha
TRD	Treatment resistant depression
TREM2	Triggering receptor expressed on myeloid cells 2
TST	Tail suspension test
t-tau	Total tau
VC	Visual cortex
WT	Wild-type

Chapter 1: General Introduction

1.1. Alzheimer's disease

1.1.1. History and prevalence of Alzheimer's disease

Alzheimer's disease (AD) is the most common form of dementia, accounting for 60-70% of all cases, and is recognised as the leading cause of disability and dependency worldwide. Globally, over 55 million people are currently living with dementia, with approximately 10 million new cases each year, and prevalence is projected to rise to 140 million cases by 2050 (Long *et al.*, 2023; World Health Organisation [WHO], 2023). In the UK, dementia and AD has been the leading cause of death since 2022, responsible for 12% of all deaths in England and Wales (Office for National Statistics (ONS), 2024). It is estimated that 70% of care homes residents have dementia, and the economic health and social care burden exceeds £25bn in the UK alone (Alzheimer's Society, 2024; Landeiro *et al.*, 2024). As life expectancy increases, and with no cure and only limited treatments to slow progression, the WHO has declared AD 'a global public health priority' (The World Health Organisation, 2012; Zhang, Zhang, *et al.*, 2024).

First described in 1906 by German psychiatrist Alois Alzheimer, AD is a progressive neurodegenerative disorder clinically characterised by memory loss and cognitive decline, eventually leading to behavioural changes and impairments in speech and motor function (Alzheimer, 1906; De-Paula *et al.*, 2012). Pathologically, the disease is defined by the accumulation and aggregation of extracellular amyloid beta (Aβ) peptide in the form of neuritic plaques and hyperphosphorylated tau protein (p-tau) in the form of intracellular neurofibrillary tangles (NFTs) (Alzheimer *et al.*, 1995; Ferencz *et al.*, 2015).

Inflammatory responses, neuronal apoptosis, and synaptic loss results in atrophy in the cortical regions, hippocampus, and entorhinal cortex, correlating with the cognitive and memory symptoms of AD (Jellinger, 1998).

Neuropsychiatric symptoms (NPS) comprise a core feature of AD, with nearly all patients suffering early or late stage NPS. Depression and apathy are the most frequent early onset NPS that continue as the disease progresses, with agitation, aggression, and psychotic symptoms becoming more common in the later stages of disease (Lyketsos *et al.*, 2011). Early cognitive symptoms are often subtle and mistaken for normal age-related decline, complicating early diagnosis (Knopman *et al.*, 2021). Mild cognitive impairment (MCI) represents the earliest symptomatic stage of cognitive decline, characterised by slight but noticeable changes in memory and thinking abilities. Although not all cases of MCI go onto develop AD, MCI is often the transitional stage between normal ageing and AD progression, therefore MCI can act as an indication of dementia risk (Petersen, 2004). Deposition of amyloid pathology can begin 15-20 years before symptoms, followed by tau pathology and cognitive changes (Bateman *et al.*, 2012).

Ongoing research has focused on understanding the molecular mechanisms driving AD, identifying genetic and environmental risk factors, and developing disease-modifying treatments. Growing evidence highlights the importance of neuroinflammation in the development and progression of AD pathogenesis (Heneka *et al.*, 2024). Although, whether the immune response is a driver or consequence of disease, and whether it represents a viable therapeutic target remains under debate.

1.1.2. Alzheimer's disease pathology

1.1.2.1. Amyloid cascade hypothesis

Aβ peptide, identified as the primary component of Aβ plaques, has been proposed as the initiating factor in AD pathogenesis, forming the basis of the amyloid cascade hypothesis (Glenner *et al.*, 1984; Hardy *et al.*, 1992). This hypothesis posits that abnormal Aβ production acts as the driving force, causing subsequent pathological changes including tau pathology and neurodegeneration (Hardy *et al.*, 1992).

Aβ is derived by sequential cleavage of the β-amyloid precursor protein (APP) (Kang *et al.*, 1987). APP is an integral membrane protein highly expressed in the brain, particularly at neuronal synapses, and is involved in synaptic function and repair, intracellular transport, signalling, and neuronal homeostasis (Chen *et al.*, 2017). APP can be processed via two cleavage pathways: the non-amyloidogenic pathway via α-secretase or the amyloidogenic pathway via β-secretase (BACE1). Most APP is cleaved via α-secretase, producing a soluble secreted APP-fragment (sAPP)α and membrane-bound C-terminal fragment 83 (C83), which γ-secretase further cleaves to produce P3 peptide, a truncated form of Aβ ($Aβ_{17-40/42}$). Alternatively, cleavage by β-secretase generates soluble sAPPβ and C-terminal fragment 99 (C99). Further cleavage of C99 by γ-secretase creates monomers, $Aβ_{40}$ and $Aβ_{42}$, which are released into the extracellular space, forming the basis of Aβ plaques (Fig. 1.1) (Haass *et al.*, 1993; Wang *et al.*, 2012; Zhang *et al.*, 2013). Normally, extracellular Aβ is degraded but the abnormal APP processing by BACE1 and an imbalance in the production and

clearance leads to the accumulation of $A\beta_{40}$ and $A\beta_{42}$. Due to the slightly longer amino acid sequence, $A\beta_{42}$ is more hydrophobic and readily aggregates into oligomers, which in turn form misfolded insoluble fibrils, ultimately resulting in the formation of amyloid neuritic plaques (Rambaran *et al.*, 2008; Chen *et al.*, 2017). BACE1 inhibition has been explored to reduce $A\beta_{40/42}$ production, but clinical trials were halted due to off-target toxicity and selectivity issues (Zhang *et al.*, 2023).

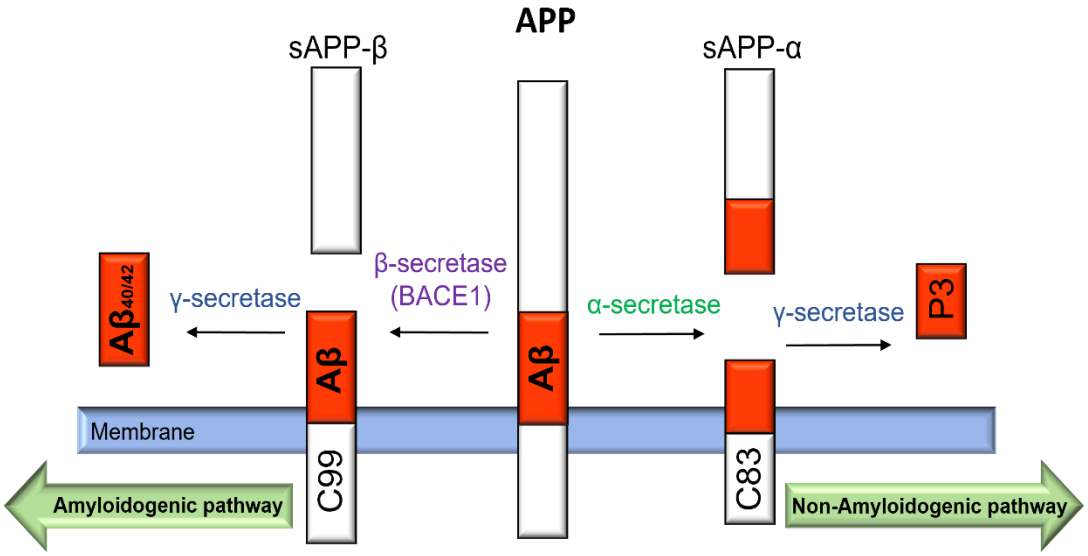

Figure 1.1: Schematic representation of amyloidogenic and non-amyloidogenic APP processing pathways. Transmembrane protein APP is usually cleaved via α-secretase within the Aβ region (indicated in orange), generating the soluble secreted APP-fragment (sAPP)α and C83, which is further cleaved by γ-secretase to produce P3 peptide. Alternatively, β-secretase cleaves APP, producing sAPPβ and C99. C99 is further cleaved by γ-secretase producing monomers $A\beta_{40}$ and $A\beta_{42}$. (Figure adapted: Wang *et al.*, 2012).

Aβ deposits initially accumulate in the neocortex, spreading to the entorhinal cortex and hippocampus, then to the subcortical nuclei, and finally to the brainstem and cerebellum inducing neurotoxicity, tau deposition, synaptic loss, and neuronal apoptosis (Jellinger, 1998; van der Kant *et al.*, 2020). The mechanisms of plaque propagation are not fully understood but the 'seeding'

hypothesis suggests that small Aβ aggregations can act as 'seeds' that are released from synapses to propagate Aβ plaques in adjacent brain regions, spreading throughout the brain in a prion-like manner (Walker *et al.*, 2016). Studies have shown Aβ injected into AD mouse brains demonstrate a seeding-like spread from the site of injection (Li *et al.*, 2022).

Aβ plaques are typically classified as diffuse and neuritic plaques. Diffuse plaques are an amorphous, poorly defined collection of aggregated Aβ peptide not yet fibrillar in form and are not usually associated with a glial reaction, frequently occurring in normal ageing. Neuritic, dense-core or senile plaques consist of fibrillar Aβ with a compact central core, surrounded by dystrophic neurites, reactive microglia and astrocytes, and are associated with neurotoxicity and synaptic degeneration (Wippold *et al.*, 2008; Serrano-Pozo *et al.*, 2011). Aβ deposits can also accumulate in cerebral blood vessel walls, known as cerebral amyloid angiopathy (CAA), leading to weakened vasculature and increased vulnerability to intracerebral haemorrhages. CAA is frequently observed in AD brains and may contribute to cognitive decline (Serrano-Pozo *et al.*, 2011; Jäkel *et al.*, 2022).

1.1.2.2. Neurofibrillary Tau tangles

Tau is a soluble microtubule-associated protein highly expressed in axons and plays an essential role in axonal transport, microtubule assembly, and stability (Grundke-Iqbal *et al.*, 1986; Medeiros *et al.*, 2011). Encoded by the microtubule associated protein tau (*MAPT*) on chromosome 17, tau is spliced into six isoforms, differing in the number of N-terminal and C- terminal inserts. Depending on the repeat domain, tau proteins become either 3R or 4R, three

or four repeats, respectively (Goedert *et al.*, 1989; Hutton *et al.*, 1998). In the adult human brain, 3R and 4R isoforms are expressed at approximately equal levels but this ratio is altered in tau-related neurodegenerative diseases, collectively known as tauopathies (Hernández *et al.*, 2007; Medeiros *et al.*, 2011).

Under normal homeostasis, tau undergoes various post-translational modifications including phosphorylation, glycosylation, ubiquitination, methylation, and oxidation. Typically, only two or three residues are phosphorylated but under certain conditions, tau is prone to misfolding resulting in increased phosphorylation known as hyperphosphorylation. Hyperphosphorylated tau (p-tau) molecules misfold and aggregate within the neuronal soma, dendrites, and synapses forming insoluble paired helical fibrils (PHF), the main component of NFTs (Grundke-Iqbal *et al.*, 1986; Köpke *et al.*, 1993; Medeiros *et al.*, 2011). This process impairs axonal transport and microtubule support resulting in microtubule instability and cytoskeletal disintegration (Köpke *et al.*, 1993; Alonso *et al.*, 2018).

Alongside Aβ plaques, NFTs are a fundamental hallmark of AD. However, NFTs are observed in several other tauopathies, including frontotemporal dementia, chronic traumatic encephalopathy, progressive supranuclear palsy, and corticobasal degeneration (Hernández *et al.*, 2007; Alonso *et al.*, 2018). Tauopathies can often be classified by predominant isoform of tau accumulating in NFTs, with 3R tau characteristic of Pick's disease and 4R of supranuclear palsy. Both 3R and 4R tau occur in the NFTs in AD (Hernández *et al.*, 2007; Medeiros *et al.*, 2011).

The progression and regional distribution of NFTs are described by Braak staging (Braak *et al.*, 1991). NFTs initially develop in the entorhinal cortex, spreading to the limbic system and hippocampus, and eventually the neocortical areas through synaptic seeding and propagation mechanisms. This progressive accumulation of tau pathology correlates strongly with cognitive decline in AD patients (Braak *et al.*, 1995; Nelson *et al.*, 2012; Ferrari *et al.*, 2021).

1.1.2.3. Pathological and structural brain changes

Atrophy of the hippocampus and amygdala represents one of the earliest structural changes in AD, contributing to the memory and mood disturbances of early disease. As atrophy progresses, it spreads through the temporal lobe and entorhinal cortex to the thalamus and striatum, and subsequently to widespread cortical areas, including the prefrontal cortex responsible for executive functions (Jellinger, 1998). Synapse loss and degeneration, driven by Aβ- and tau-induced synaptic toxicity, strongly correlates with cognitive decline as the disease progresses (DeKosky *et al.*, 1990; Tzioras *et al.*, 2023). Ventricle enlargement and thinning of the corpus callosum are also observed resulting from neuronal and synaptic atrophy (Fig. 1.2). Several of the brain regions vulnerable to AD pathology are also susceptible to other neurodegenerative disease pathologies, including α-synucleinopathy and TDP-43 proteinopathy. Mixed dementia pathology is therefore common, and overlapping or heterogeneous clinical symptoms can often complicate accurate diagnosis (Srivastava *et al.*, 2021).

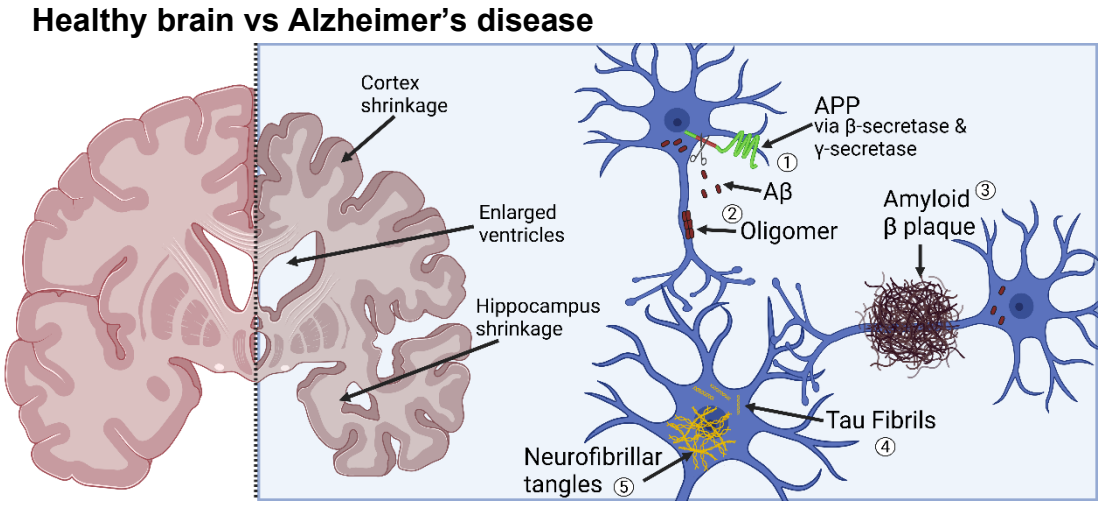

Figure 1.2: Pathology of healthy brain vs Alzheimer's disease brain. (1-2) APP is cleaved via the amyloidogenic pathway by β-secretase and γ-secretase, producing $A\beta_{40}/A\beta_{42}$ that aggregate into Aβ oligomers. (3) Aβ oligomers aggregate into extracellular Aβ plaques, accumulating around neurons. (4) Intracellular tau proteins become hyperphosphorylated, forming insoluble paired helical fibrils. (5) Tau fibrils form into neurofibrillary hyperphosphorylated tau tangles aggregated in the neuronal soma. Additional pathological changes include generalised brain atrophy, cerebral cortex atrophy, ventricle enlargement, thinning of the corpus callosum, and shrinkage of the hippocampus and amygdala. (Figure made in biorender.com).

1.1.2.4. Amyloid plaques and neurofibrillary tau interactions

A neuropathological diagnosis of AD requires the presence of both Aβ plaques and NFTs (Jellinger, 1998). However, there remains debate regarding which pathological change initiates and drives AD progression. The amyloid cascade hypothesis, introduced in 1991, has been the central framework for understanding AD pathogenesis following the discovery that three familial mutations promote Aβ plaque aggregation and early onset AD (Hardy *et al.*, 1992). This hypothesis has continued to guide drug development, with recent monoclonal antibodies designed to reduce Aβ deposition and/or enhance Aβ clearance (Sims *et al.*, 2023; van Dyck *et al.*, 2023).

Biomarker studies, including cerebral spinal fluid (CSF) analysis, neuroimaging, and post-mortem samples, indicate that Aβ accumulation precedes the appearance of p-tau pathology (Fagan *et al.*, 2006; Tolboom *et al.*, 2009). Over time, the amyloid hypothesis has evolved to encompass additional mechanisms including neuroinflammation, oxidative stress, and dysregulation of protein homeostasis, highlighting the multifactorial nature of AD and the need for multi-targeted therapeutic approaches (Selkoe *et al.*, 2016; van der Kant *et al.*, 2020). However, many disagree with the amyloid hypothesis due to the lack of correlation in cognitive decline between Aβ in MCI and AD, and presence of amyloid pathology in cognitively normal individuals (Aizenstein *et al.*, 2008).

An alternate theory posits tau as the primary instigator of AD, having been identified in the medial temporal lobe in the absence of amyloid plaques in cognitively normal individuals. Tau pathology is proposed to begin very early in the brain, as pretangles in the brain stem nuclei, progressing to NFTs subsequently triggering Aβ plaque deposition (Braak *et al.*, 2011). Others argue this represents age-related tau pathology rather than a true precursor to AD (Crary *et al.*, 2014; Schöll *et al.*, 2016). A contrasting hypothesis proposes that NFTs only spread beyond the medial temporal lobe in the presence of Aβ plaques, reinforcing that Aβ is the initiating factor (Schöll *et al.*, 2016; Vogel *et al.*, 2021). Interestingly, substantial Aβ and tau pathology comparable to that in AD, has also been reported in cognitively normal individuals suggesting a potential resilience to the effects of these neuropathological changes (Neuner *et al.*, 2022; Zhang, Ganz, *et al.*, 2022; Ahangari *et al.*, 2023).

Synaptic degeneration driven by Aβ and p-tau toxicity correlates strongly with cognitive decline in both humans and animals models (Sri *et al.*, 2019; Colom-Cadena *et al.*, 2020; Tzioras *et al.*, 2023). Animal studies have demonstrated Aβ clearance via antibody immunotherapy can improve or even reverse synaptic loss (Rozkalne *et al.*, 2009; Spires-Jones *et al.*, 2009). Similarly, tau reduction or tau knockout (KO) has been shown to restore memory and behavioural deficits while protecting against Aβ-induced synaptic degeneration (Roberson *et al.*, 2007; Cisternas *et al.*, 2022). Deletion of the Aβ cleaving enzyme BACE1 in the 5xFAD mouse model also completely reversed amyloid deposition, improving long-term potentiation (LTP) and synaptic function (Hu *et al.*, 2018).

Although clear links exist between Aβ plaque formation and NFT propagation, the underlying cause of these pathological processes remain uncertain. AD is now recognised as a multifactorial disease, associated with several risk factors including ageing, genetics, and environmental factors.

1.1.3. Genetics of Alzheimer's disease

1.1.3.1. Familial Alzheimer’s disease

Although most AD cases are sporadic, approximately 1-2% are familial (FAD, familial Alzheimer’s disease), presenting with early-onset symptoms (EOAD) (Guerreiro *et al.*, 2012). Mutations in three major genes have been identified; *APP*, presenilin 1 (*PSEN1*) and presenilin 2 (*PSEN2*) (Chartier-Harlin *et al.*, 1991; Levy-Lahad *et al.*, 1995; Sherrington *et al.*, 1995). These mutations alter APP processing, favouring $A\beta_{42}$ production and promoting amyloid accumulation. Over 200 pathogenic variants have been identified across these

genes, contributing to AD risk and progression (Ferencz *et al.*, 2015; Xiao *et al.*, 2021).

1.1.3.2. Sporadic Alzheimer's disease

Late-onset AD (LOAD) accounts for 98-99% of cases, with many associated variants affecting Aβ metabolism (Ferencz *et al.*, 2015). The strongest genetic risk factor for LOAD is a polymorphism in the apolipoprotein E (*APOE*) gene, which encodes a glycoprotein involved in lipid transport and neuronal repair (Liu *et al.*, 2013; Shen *et al.*, 2016). Humans possess three isoforms of the *APOE* gene: ε2, ε3, and ε4 alleles, with ε4 allele increasing AD risk by approximately 3-4-fold in heterozygotes and approximately 9-15-fold in homozygous allele inheritance (Corder *et al.*, 1993; Frick *et al.*, 2024). ε4 promotes Aβ aggregation and impairs clearance, accelerating AD pathogenesis (Tachibana *et al.*, 2019; Husain *et al.*, 2021). Conversely, ε2 is considered protective with a decreased risk of developing AD (Liu *et al.*, 2013; Li *et al.*, 2020).

Recent genome-wide association studies (GWAS) have identified over 40 loci, associated with LOAD risk, including *APOE*, many of which relate to inflammation and microglial function (Novikova *et al.*, 2021; Wightman *et al.*, 2021). Variants in triggering receptor expressed on myeloid cells 2 (*TREM2*) and cluster of differentiation 33 (*CD33*), both expressed by microglia and involved in phagocytosis, are linked to impaired immune responses and increased AD susceptibility (Fig. 1.3). Notably, TREM2-activating antibodies have shown promise in restoring microglial function (Misra *et al.*, 2018; van Lengerich *et al.*, 2023). Several of the identified loci are linked to the immune

response, highlighting the importance of inflammation in AD risk (Fig.1.3) (Karch *et al.*, 2015).

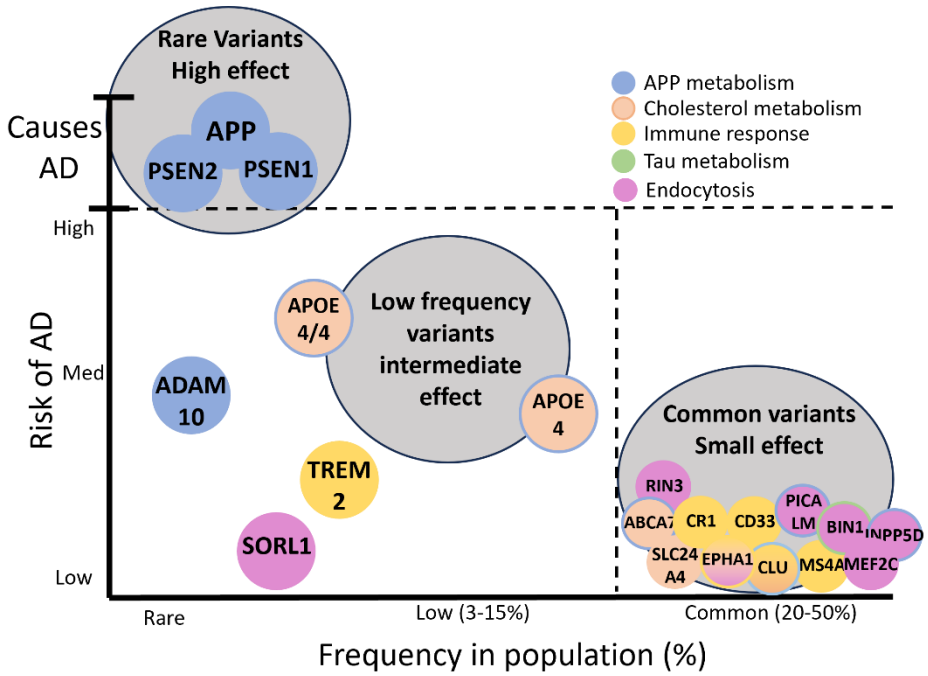

Figure 1.3: Genetic variant mutations contributing to AD risk. Genetic variants are shown according to their associated AD risk level, either low, medium, or high risk, and frequency in the general population. (Figure adapted: Karch and Goate, 2015).

1.1.4. Risk factors of Alzheimer's disease

Age is the highest risk factor for AD with the typical onset 65 years old, and risk increases exponentially with age (Livingston *et al.*, 2024). Ageing is also associated with co-morbidities, including cardiovascular diseases, diabetes, bowel disease, and depression. These disorders can precede or occur concomitantly with AD, and their presence may influence AD progression. Chronic inflammation represents a common feature linking these conditions, though whether it is a cause or consequence of AD remains debated (Santiago *et al.*, 2021).

Biological sex is another important determinant, with women exhibiting a higher prevalence of AD independent of lifespan. This disparity may reflect both biological influences, such as hormonal changes, and sociocultural factors including education and lifestyle differences (Lopez-Lee *et al.*, 2024).

A recent review published in The Lancet identified a series of modifiable risk factors associated with a 45% increased risk in developing AD (Fig. 1.4).

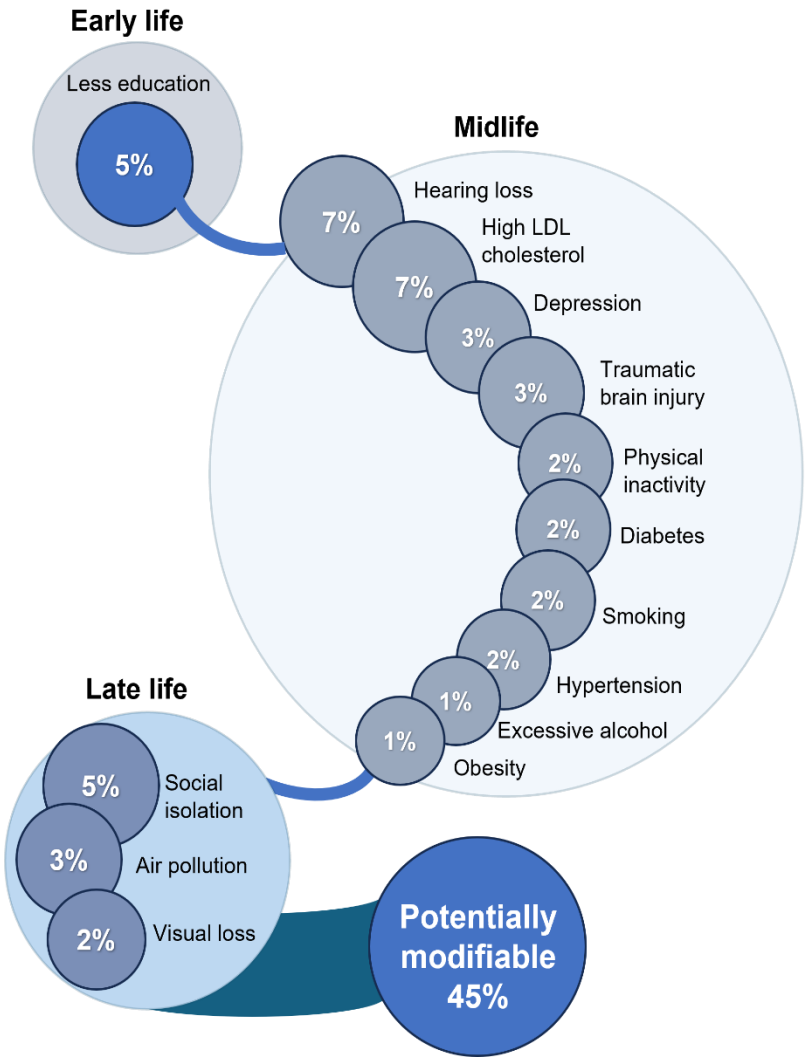

Figure 1.4: 14 modifiable risk factors contributing to AD prevalence. These factors collectively account for 45% of the increased risk of developing AD and are distributed across different life stages, with each factor indicating the potential reduction in dementia risk if eliminated. (Figure adapted: Livingston *et al.*, 2024).

These risk factors were identified across the life-course highlighting areas to practice preventative measures to reduce AD risk (Livingston *et al.*, 2024).

Depression is recognised as a midlife risk, with long-term depression associated with cognitive decline. Further, meta-analyses have identified a 2-3-fold risk in developing AD in individuals who have suffered depression through life (Sáiz-Vázquez *et al.*, 2021). Notably, depression is more prevalent in women, highlighting sex-specific vulnerability across both affective and neurodegenerative disorders (Kim *et al.*, 2021).

1.1.5. Biomarkers of Alzheimer's disease

The lack of effective AD treatments in clinical practice may be attributed to the advanced disease state during clinical trials and pharmacological intervention. As Aβ deposition can begin up to 20 years before symptom onset, developing specific early-stage diagnostic tools is crucial for both early detection and therapeutic intervention (Zetterberg *et al.*, 2021; Klyucherev *et al.*, 2022). Currently, the main biomarkers include neuroimaging and CSF testing, with emerging blood-based biomarkers offering promising advances in accessibility and costs.

Positron emission tomography (PET) remains the leading neuroimaging technique, enabling detection of amyloid, tau, and glucose metabolism in the brain. Radioligands, such as [^{18}F]florbetapir, [^{18}F] flortaucipir, and ^{18}F-2-fluoro-2-deoxy-D-glucose ([^{18}F]FDG), cross the blood brain barrier (BBB) to bind Aβ plaques, p-tau, or glucose, respectively, allowing accurate quantification of pathology (Maschio *et al.*, 2022). Development of new radiotracers targeting

neuroinflammatory markers, including glia, could offer new insights into the disease progression of AD (Zhou *et al.*, 2021; Liu *et al.*, 2022).

CSF analysis provides biochemical evidence of amyloid and tau pathology, as well as neurodegeneration by measuring $A\beta_{42}$, $A\beta_{42}/A\beta_{40}$ ratio, p-tau and total tau (t-tau), and neurofilament light polypeptide (NfL), respectively (Dhiman *et al.*, 2020; Zetterberg *et al.*, 2021). In AD, reduced $A\beta_{42}$ and increased $A\beta_{40/42}$ ratio reflect plaque deposition, while increases in p-tau and t-tau correlate with tau pathology (Zetterberg *et al.*, 2021; Klyucherev *et al.*, 2022). Elevated NfL indicates axonal degeneration, hippocampal atrophy, and grey matter loss, making them useful predicters of cognitive impairment (Dhiman *et al.*, 2020) (Fig. 1.5). Despite their diagnostic accuracy, CSF tests are limited by cost and invasiveness.

Recent progress in plasma and serum biomarker assays offers a less invasive alternative with high diagnostic potential. Plasma levels of p-tau217 and p-tau181 show strong correlations with early Aβ load, while levels of t-tau indicate neurodegeneration (Balogun *et al.*, 2023). Additionally, markers such as NfL can reflect neurodegeneration and astrocytic activation, supporting the use of blood-based biomarkers as a practical, scalable diagnostic tool for AD (Chatterjee *et al.*, 2023; Grande *et al.*, 2025).

Although current biomarkers are highly specific, testing usually occurs only after clinical symptoms emerge. Identifying earlier indicators of disease risk is a major research focus. Monitoring modifiable factors, such as chronic depression, may provide early insight into neuroinflammatory processes

preceding amyloid or tau pathology, acting as a biomarker and potentially enabling intervention before irreversible neurodegeneration (Howlett *et al.*, 2021; Roccati *et al.*, 2024).

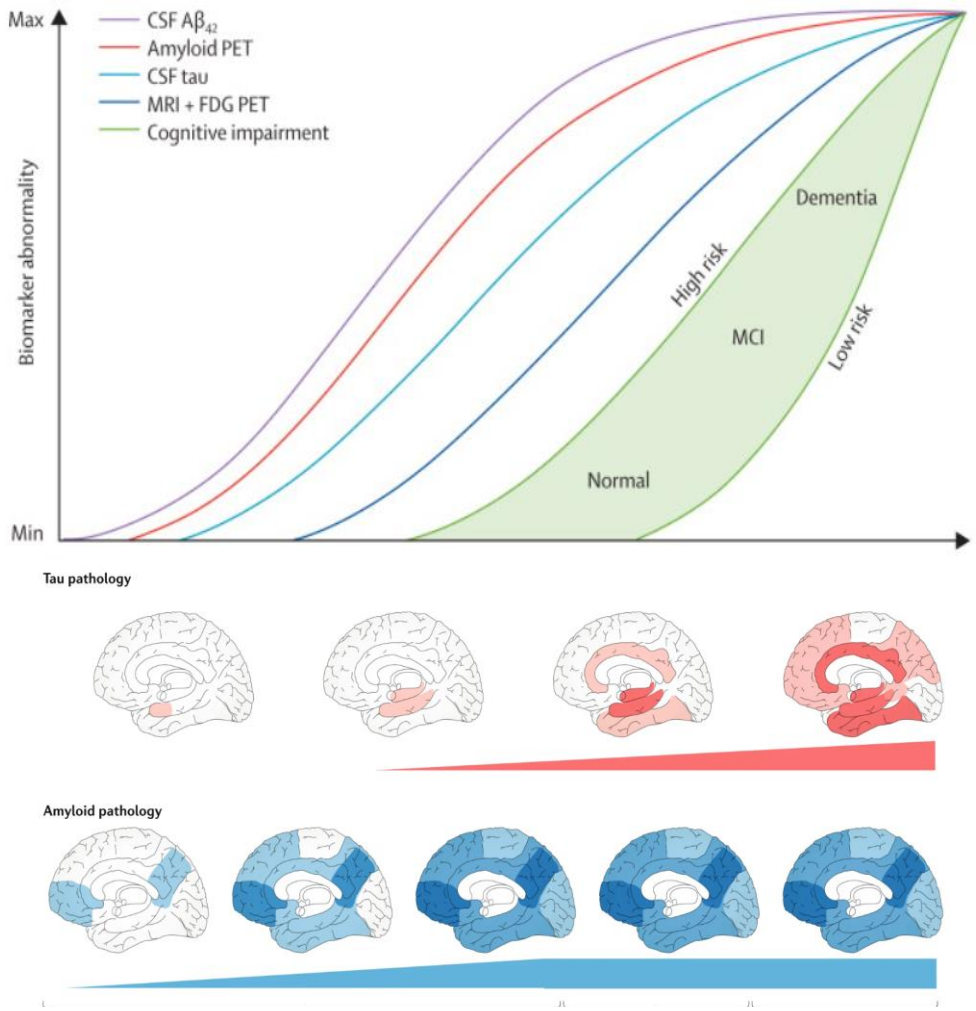

Figure 1.5: Biomarkers and progression of AD. $A\beta_{42}$ detection identified by CSF and PET is followed by p-tau detection, with neurodegeneration measured by FDG-PET and MRI scans. Cognitive decline (green zone) progresses from MCI to dementia as $A\beta_{42}$ and p-tau levels increase. (Red brain) Tau pathology spreads from the entorhinal cortex, hippocampus, and temporal regions to the cortical regions. (Blue brain) Aβ deposition begins in the neocortex, spreading to the hippocampus, entorhinal cortex, and amygdala, then to the subcortical nuclei. Widespread Aβ accumulation occurs in preclinical AD, while tau pathology develops later, suggesting amyloid may drive tau aggregation. (Figure sources: Jack *et al.*, 2013; van der Kant, Goldstein and Ossenkoppele, 2020).

1.1.6. Treatments for Alzheimer's disease

Current treatments for AD can be divided into symptomatic agents, which aim to improve cognitive and behavioural features, and disease-modifying therapies (DMT), which aim to alter the underlying processes to prevent or reduce disease progression. Developing effective and specific DMTs remains a priority and as of 2025, 138 agents were in various phases of clinical trials, with DMT representing 75% of these treatments (Cummings *et al.*, 2025). There has been increasing development and success with the use of monoclonal antibodies (mAbs) as DMTs to specifically target and remove Aβ (Cummings *et al.*, 2024).

1.1.6.1. Symptomatic treatments

Four drugs are currently approved by both the Medicines and Healthcare products Regulatory Agency (MHRA, UK) and Food and Drug Administration (FDA, US) for the management of cognitive and behavioural symptoms in AD; acetyl cholinesterase inhibitors (AChEIs), donepezil, rivastigmine, and galantamine, and N-methyl-D-aspartate (NMDA) receptor antagonist, memantine (National Institute for Health and Care Excellence, 2018; Cummings, 2021). In addition, two further drugs for AD symptoms have been approved by the FDA in the USA, brexpiprazole for agitation and suvorexant for insomnia, though neither is currently approved for use in the UK.

The cholinergic hypothesis, derived in the 1970s, arose from findings that cholinergic antagonists induced memory impairment and neocortical deficits in the enzyme choline acetyltransferase (ChAT), which is responsible for the synthesis of acetylcholine (ACh) (Deutsch, 1971). ACh is essential for learning

and memory, and cholinergic degeneration is associated with cognitive decline and Aβ-related neurotoxicity. AChEIs inhibit acetylcholinesterase (AChE) from breaking down ACh, thereby increasing ACh in the synaptic cleft (Pákáski *et al.*, 2008; Huang *et al.*, 2022).

Excitatory glutamatergic neurotransmission via NMDA receptors is essential for synaptic plasticity but overactivation leads to calcium (Ca^{2+})-mediated excitotoxicity and neuronal death. Memantine blocks NMDA receptor overactivation, restoring physiological glutamatergic signalling (Zhou *et al.*, 2014; Liu *et al.*, 2019). Memantine is recommended by National Institute for Health and Care Excellence (NICE, UK) in combination with donepezil for moderate to severe AD (National Institute for Health and Care Excellence, 2018; McShane *et al.*, 2019). Both drug classes provide modest cognitive and neuropsychiatric symptom (NPS) improvement, particularly in mild-to-moderate disease, but do not halt neurodegeneration (Rodda *et al.*, 2009; Dou *et al.*, 2018; Guo *et al.*, 2020).

Brexpiprazole is an atypical antipsychotic that modulates neurotransmitter activity in the brain, acting as a partial agonist at serotonin (5-HT1A) and dopamine D2 receptors, as well as an antagonist at serotonin 5-HT2A receptors, thereby influencing both serotonin and dopamine signalling. Commonly used in schizophrenia, brexpiprazole is the first FDA-approved drug for the treatment of agitation associated with AD (Edinoff *et al.*, 2021; Lee, Clark, *et al.*, 2024). Suvorexant is an orexin receptor antagonist that promotes sleep by inhibiting wakefulness-promoting orexin neurons through binding OX1R and OX2R receptors, and was FDA-approved for treating insomnia in

mild to moderate AD (Herring *et al.*, 2020; Ragsdale *et al.*, 2025). Depression and anxiety are the most prevalent NPSs of AD, and patients are frequently prescribed selective serotonin reuptake inhibitors (SSRIs) to manage mood disturbances; however, evidence suggests that these treatments have limited efficacy and do not alter the underlying progression of the disease (Costello *et al.*, 2023; Lenouvel *et al.*, 2024).

1.1.6.2. Disease-modifying treatments

The first DMT, aducanumab, an immunoglobulin G1 (IgG1) mAb was approved by the FDA in 2021 for AD treatment. Aducanumab targets and removes Aβ oligomers, fibrils, and plaques, most successfully in mild cases of AD or MCI (Sevigny *et al.*, 2016). Its approval was controversial due to limited evidence of cognitive benefit, early fast-track approval, and significant adverse effects, including amyloid-related imaging abnormalities (ARIA) such as cerebral oedema (35%) and haemorrhage (19%), alongside high treatment cost (Walsh *et al.*, 2021; Beshir *et al.*, 2022).

Subsequent Aβ targeting mAbs, Lecanemab and Donanemab, were FDA approved in 2023 and 2024, after demonstrating reduced amyloid burden and modest slowing of cognitive decline over 12–18 months (McDade *et al.*, 2022; H. *et al.*, 2023; Sims *et al.*, 2023). However, both were rejected by NICE due to limited clinical benefit, ARIA risk, and cost (Mahase, 2024).

Despite these challenges, the approval of Aβ-targeting antibodies is a major milestone in AD therapeutics. Numerous agents targeting tau pathology,

neuroinflammation, and neurotransmitters are currently in clinical trials, aiming to deliver more effective and safer DMTs (Cummings *et al.*, 2025).

1.1.7. Animal models of Alzheimer's disease

Experimental models are essential for understanding the complex mechanisms underlying AD pathology, and for testing novel therapeutics. Models are established based on three basic constructs: face validity (phenotype similar to human disease), construct validity (shared underlying mechanisms), and predictive validity (response to treatments) (Willner, 1984). Additional refinements, such as mechanistic (similar cognitive or biological mechanisms) and pathogenic validity (etiological and biomarker validity), further improve translational relevance (Belzung *et al.*, 2011; Wang *et al.*, 2017).

Genetically modified animal models, particularly rodent models, are widely used due to their comparable brain structure and function, short lifespan allowing longitudinal observations, and the ability to introduce human relevant genetic variants that reproduce key AD hallmarks such as Aβ plaques and NFTs (Drummond *et al.*, 2017; Yokoyama *et al.*, 2022). The discovery of genetic mutations in *APP/PSEN*, linked to FAD, and *MAPT*, associated with tauopathies, has led to the creation of diverse transgenic, knock-in, and knock-out models that develop Aβ and tau pathology, as well as associated inflammatory responses (Zhong *et al.*, 2024) (table 1.1).

Models can be designed to capture different stages of disease progression, with rapidly developing pathology in transgenic lines such as 5xFAD (Oakley

et al., 2006), while knock-in models develop pathology more gradually, providing a closer approximation to human disease progression (Saito *et al.*, 2014; Zhong *et al.*, 2024). Although no single model fully recapitulates the combined Aβ, p-tau, and neurodegeneration pathology seen in AD, these models effectively represent various disease stages, providing valuable platforms to study disease progression, cognitive deficits, and behavioural changes (Kosel *et al.*, 2020).

1.1.7.1. Cognitive and behavioural tests of Alzheimer's disease

Rodent cognitive and behavioural tests are designed to assess functions that decline in AD, including memory, executive function, and attention. Common paradigms include maze-based tasks and object recognition test, to evaluate reference, working, and recognition memory (Olton *et al.*, 1976; Barnes, 1979; Morris *et al.*, 1982; Ennaceur *et al.*, 1988). Executive function can be tested with discrimination tasks (Birrell *et al.*, 2000), while attention can be modelled with multiple-choice time selective tasks (Carli *et al.*, 1983).

These tests provide insight into neurological functions affected by disease progression, with performance deficits indicating AD-like cognitive decline. Rodent models can also be used to assess the efficacy of potential therapeutic interventions. However, rodent models replicate only specific aspects of AD pathology, limiting their translational accuracy from preclinical to clinical settings (Webster *et al.*, 2014; Drummond *et al.*, 2017).

Behavioural symptoms associated with neuropsychiatric features of AD, such as depression-like and anxiety-like behaviour can also be examined in rodent

models using various tests including forced swim test (Porsolt *et al.*, 1977), sucrose preference (Willner *et al.*, 1987), grooming behaviour, (Isingrini *et al.*, 2010) and nesting building tests (Deacon, 2006). These are discussed in more depth in ‘rodent models of MDD’ (section 1.3.6).

Table 1.1: Examples of commonly used mouse models of Alzheimer's disease.

Mouse model	Mutations	Aβ plaques	p-Tau	Inflammation	Cognitive & Behaviour
Tg2576 (Hsiao *et al.*, 1996)	*APP* Swedish mutation: (KM670/671NL)	+ (6-8 months of age - amyloid, 11-13 months of age - plaque formation)	-	↑ Reactive astrocytes ↑ Activated microglia ↓ Synaptic density ↑ IL1β, IL6, IL10	↓ Cognition (6-8 months of age) ↓ Spatial & working memory ↑ Hyperexcitability & Anxiety↑ Social withdrawal ↑ Aggression
APP/PS1 (Jankowsky *et al.*, 2004)	*APP* Swedish mutation: (KM670/671NL) *PSEN1* mutation: (PS1dE9)	+ (high levels of plaques at 6 months of age)	-	↑ Reactive astrocytes ↑ Activated microglia ↓ Synapse function	↓ Cognition (6-9 months of age) ↓ Spatial & working memory ↓ Fear conditioning ↑ Anxiety & social withdrawal ↑ Hyperexcitability
5xFAD (Oakley *et al.*, 2006)	*APP* Swedish mutations: (K670N/M671L), Florida (1716V), London (V717I), *PSEN1* mutations: (M146L and L286V)	+ (2 months of age - plaque formation with high plaque level by 6 months of age)	-	↑ Reactive astrocytes ↑ Activated microglia ↓ Synaptic density ↑ Neurodegeneration ↑ IL1β, TNF-α	↓ Cognition (6-12 months of age) ↓ Spatial & working memory ↑ Hyperexcitability & Aggression ↓ Anxiety ↑ Depression-like behaviour
3xTg (Oddo *et al.*, 2003)	*APP* Swedish mutation: (KM670/671NL), *PSEN1* mutation (M146V), *MAPT*-tau mutation (P301L)	+ (6-12 months of age - amyloid plaques)	+ (NFTs from 12 months of age)	↑ Inflammation ↑ Neurodegeneration ↑ Synapse dysfunction ↑ LTP deficits	↓Cognition (3-5 months of age) ↓ Spatial & working memory ↑ Depression-like behaviour (18 months of age) ↑ Aggression
APP^{NLF} Knock-in (Saito *et al.*, 2014)	*APP Swedish mutation: (K670N/M671L), APP* Beyreuther/Iberian mutation: (I716F)	+ (6 months of age - amyloid deposition, 24 months of age cortical amyloidosis	-	↑ Reactive astrocytes ↑ Activated microglia ↓ Synapses	↓ Cognition (18 months of age) ↓ Working memory

1.1.7.2. 5xFAD mouse model

The 5xFAD transgenic mouse model was developed as an aggressive model of AD, characterised by rapid development of Aβ plaques, as early as 2 months of age, and the onset of cognitive and behavioural deficits at approximately 6 months of age. The 5xFAD model carries five FAD mutations: three *APP* mutations, the Swedish (K670N/M671L); the Florida (1716V) and London (V717I) mutations, driven by a Thy1 promotor, and two *PSEN1* mutations (M146L and L286V), on a C57BL/6 background. These mutations alter APP processing, favouring $A\beta_{42}$ production (Oakley *et al.*, 2006).

5xFAD mice develop extensive amyloid pathology beginning in the deep cortical layers and the subiculum, progressing with age through the hippocampal CA1–CA3 regions, dentate gyrus, neocortex, thalamus, and brainstem (Oakley *et al.*, 2006; Forner *et al.*, 2021). Female mice exhibit greater Aβ deposition than male mice due to the oestrogen-mediated Thy1 promoter (Oakley *et al.*, 2006; Sadleir *et al.*, 2015; Zhong *et al.*, 2024). The model also displays heightened neuroinflammatory responses, including activated microglia and reactive astrocytes, as demonstrated by F4/80 and GFAP markers, and increased pro-inflammatory cytokine levels, including Interleukin (IL)-1β and tumor necrosis factor alpha (TNF-α) (Oakley *et al.*, 2006; Oblak *et al.*, 2021), which may act as both drivers and consequences of Aβ deposition.

Cognitive and behavioural deficits emerge from 6-12 months of age, with impairments in spatial and working memory observed in the Morris water maze, radial arm maze, and novel object recognition tests (Oakley *et al.*, 2006;

Pádua *et al.*, 2024). Mice also display reduced anxiety-like behaviour in open arm and elevated plus mazes, and some studies have reported depression-like behaviour in forced swim tests (Jawhar *et al.*, 2012; Locci *et al.*, 2021). Male 5xFAD mice have been known to show increased aggression (Kosel *et al.*, 2020, 2021) while both sexes often show reduced weight and hyperactivity compared to wild type (WT) littermates (Kosel *et al.*, 2020, 2021; Forner *et al.*, 2021).

Overall, the 5xFAD mouse model provides a robust platform to study early and rapid amyloid pathology, neuroinflammatory mechanisms, and potential neuropsychiatric behaviours in AD pathogenesis. Importantly, the presence of amyloidosis before the onset of cognitive decline allows for study of potential drivers of disease and biomarker discovery (Oblak *et al.*, 2021; Zhong *et al.*, 2024).

1.2. Neuroinflammation

1.2.1. The inflammatory response

Neuroinflammation is a key feature of neurodegenerative diseases and is recognised as the third core hallmark of AD pathogenesis (Heneka *et al.*, 2024). Neuroinflammation refers to an inflammatory response within the CNS in response to injuries, illness, or infections, leading to the release of pro-inflammatory cytokines, chemokines, and reactive oxygen species (ROS) from the innate immune cells, including microglia and astrocytes (Morales *et al.*, 2014; Kwon *et al.*, 2020).

Primarily, neuroinflammation is an acute protective mechanism to promote recovery. However, prolonged chronic activation can lead to synapse dysfunction, neuronal death and impaired neurogenesis, driving AD progression (Kempuraj *et al.*, 2016; Leng *et al.*, 2021). Thus, the balance between neuroprotective and neurotoxic effects remains a major focus of research.

Epidemiological studies have reported long-term use of non-steroidal anti-inflammatory drugs (NSAIDs) is associated with reduced AD risk, with meta-analyses indicating a 19% lower risk compared to controls (Zhang *et al.*, 2018; Vom Hofe *et al.*, 2025). However, despite these associations, clinical trials have shown that NSAIDs do not slow or alter the progression of established AD and are therefore not recommended by NICE guidelines, highlighting the challenge of translating anti-inflammatory strategies into effective treatments (National Institute for Health and Care Excellence, 2018). Despite this, compounds targeting neuroinflammation currently comprise 17% of the DMTs in clinical trials (Cummings *et al.*, 2025). Furthermore, immune receptors, such as TREM2 and CD33, and gene variants involved in inflammatory pathways, have been identified as AD risk factors. Modulation of microglial and astrocytic activation to alleviate neuroinflammation has been proposed as a potential therapeutic strategy (Singh, 2022; Chen *et al.*, 2025).

1.2.2. Microglia

Microglia are the resident immune cells of the brain, derived from embryonic yolk sac precursors, they act as the primary line of surveillance and defence in the CNS. Microglia comprise approximately 10% of all brain cells, and are

highly motile, constantly surveying for pathogens, clearing debris, and maintaining homeostasis (Colonna *et al.*, 2017; Leng *et al.*, 2021). In response to such stimuli, damage- or pathogen-associated molecular patterns (DAMPs and PAMPs) trigger microglial activation to the site of injury to initiate the immune response. Microglia can clear debris via phagocytosis and release proinflammatory cytokines, such as TNF-α, IL-1β, IL-6, and chemokines, as well as anti-inflammatory cytokines, such as IL-4 and IL-10, to recruit additional immune cells to support pathological agent removal (Hansen *et al.*, 2018; Kwon *et al.*, 2020).

Microglia alter their morphology from a ramified, branched 'resting' state to a rounded, ameboid 'activated' state in response to stimuli (Gao, Jiang, *et al.*, 2023). Traditionally, they were classified as either M1 (pro-inflammatory) or M2 (anti-inflammatory), with M1 microglia releasing cytokines and chemokines to limit further damage, and M2 microglia promoting tissue repair and neuroprotection (Fig.1.6) (Heneka *et al.*, 2015; Wang *et al.*, 2022). However, the M1/M2 classifications are now regarded as an oversimplification, and transcriptomics has revealed microglia exist on a spectrum of activation states influenced by different stimuli, microenvironments, and CNS regions. Fine regulation of microglia activation is essential for normal function, and dysregulation or overreaction contributes to neurodegenerative disease pathology (Colonna *et al.*, 2017; Guo, Wang, *et al.*, 2022).

1.2.2.1. The role of microglia in AD

In AD, microglia adopt a reactive phenotype and are recruited to sites of Aβ deposition (Gao, Jiang, *et al.*, 2023). Recent transcriptomics identified a

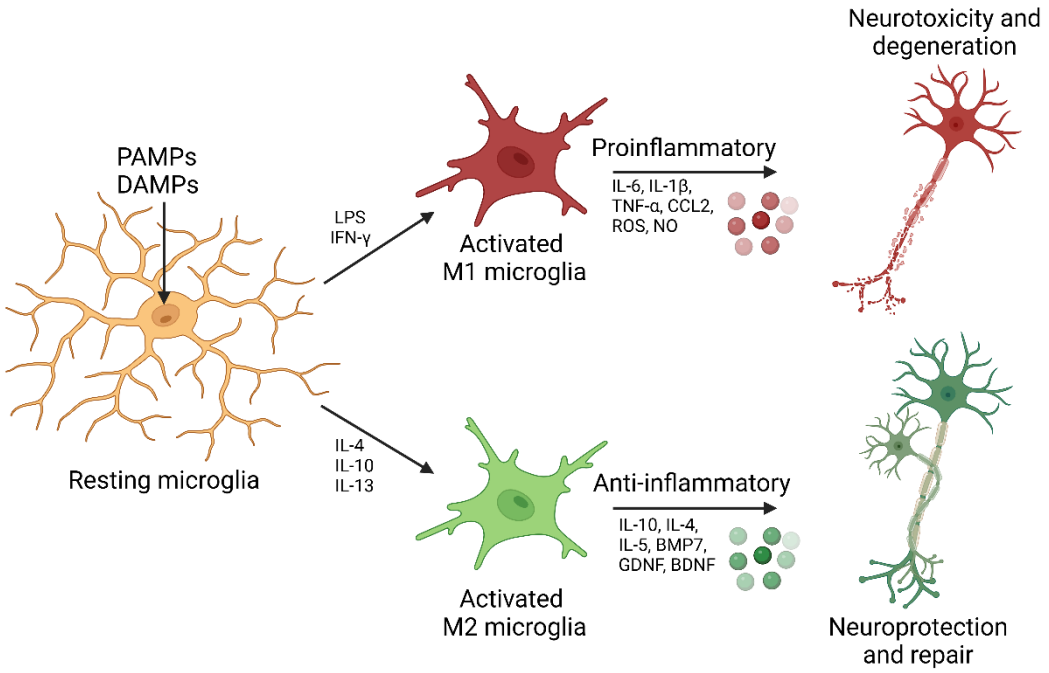

Figure 1.6: Microglia activation. Resting ramified microglia are stimulated by PAMPS or DAMPs and alter to a pro- or anti-inflammatory ameboid conformation resulting in cytokine and chemokine release. Chronic activation of pro-inflammatory pathways can induce neurotoxicity and degeneration, while anti-inflammatory responses promote repair and neurogenesis. (Figure created in Biorender.com; adapted: Wang *et al.*, 2022).

distinct subpopulation, termed disease-associated microglia (DAM), which are associated with neurodegenerative diseases, including AD. DAMs act to downregulate homeostatic pathways, while upregulating phagocytosis and lipid metabolism, suggesting a transition toward an activated, neuroprotective state in early disease (Keren-Shaul *et al.*, 2017; Takatori *et al.*, 2025). However, ongoing formation, impaired clearance, and positive feedback loops result in chronic non-resolving inflammation that promotes further Aβ accumulation (Heneka *et al.*, 2015). TREM2 signalling is essential for the transition to the DAM phenotype, and TREM2 mutations can impair this process, limiting Aβ clearance (Keren-Shaul *et al.*, 2017). Prolonged exposure to Aβ, cytokines, and other inflammatory mediators leads to microglial

dysfunction at the plaque sites, contributing to synaptic dysfunction and neuronal death (Krabbe *et al.*, 2013; Heneka *et al.*, 2024).

Microglia also regulate synaptic maintenance and plasticity through secretion of brain-derived neurotrophic factor (BDNF), with age-related reductions in BDNF potentially impairing synaptic plasticity and memory formation in AD (Norden *et al.*, 2013; Cornell *et al.*, 2022). Ageing microglia display heightened sensitivity to inflammatory stimuli and a reduced activation threshold resulting in increased pro-inflammatory cytokine release. This ageing, termed microglia 'priming', is associated with functional decline and microglial senescence (Hoeijmakers *et al.*, 2016; Greenwood *et al.*, 2021). Elevated levels of both pro-, IL-1β, IL-6, IL-18, TNFα, and anti-inflammatory cytokines, interleukin-1 receptor antagonist (IL-1RA) and IL-10, have been detected in the CSF of patients with AD (Dionisio-Santos *et al.*, 2019). Interestingly, some AD mouse models have shown IL-1β overexpression can reduce Aβ plaque load, potentially by enhancing microglial clearance. Conversely, cytokines such as IL-1β, IL-6, and TNF-α, have been linked to exacerbated tau hyperphosphorylation (Shaftel *et al.*, 2007; Ghosh *et al.*, 2013; Domingues *et al.*, 2017). Furthermore, mutations within the microglial immune receptors TREM2 and CD33 impair Aβ phagocytic clearance, heightening inflammatory response and accelerating AD progression (Griciuc *et al.*, 2021).

1.2.3. Astrocytes

Astrocytes are specialised glial cells that play essential roles in maintaining CNS homeostasis. Derived from a common progenitor shared with neurons

and oligodendrocytes, astrocytes are the most abundant cell type in the CNS (Liddelow *et al.*, 2020). Originally thought to merely provide structural ‘glue’ for neurons, they are now recognised as morphologically and functionally diverse, with two major subtypes: protoplasmic astrocytes, predominantly found in grey matter, and fibrous, found in white matter. Both subtypes have extensive major ‘branches’ as well as secondary and tertiary “branchlets’ that form interactions with other neurons and synapses throughout the brain (Zhang *et al.*, 2021; Baldwin *et al.*, 2024). In addition, single-cell and spatial transcriptomic studies have revealed region-specific astrocyte subtypes, reflecting the diversity of different brain areas (Batiuk *et al.*, 2020; Sofroniew, 2020).

Astrocytes form part of the tripartite synapse, interacting with both pre- and post-synaptic neurons to enable bidirectional communication between glia and neurons, allowing modulation of synaptic transmission and plasticity. (Monterey *et al.*, 2021). Key functions include ion regulation, synapse formation and support, metabolic support to neurons, maintenance of the blood–brain barrier (BBB), and clearance of neurotoxic waste (Leng *et al.*, 2021; Monterey *et al.*, 2021). Astrocytic endfeet enwrap capillaries and secrete factors required for BBB formation and tight-junction maintenance. The BBB regulates the exchange of ions and molecules in and out of the brain and protects the brain from pathogens and toxic substances. BBB disruption and increased permeability are common in several neurological disorders, including AD (Cabezas *et al.*, 2014; Nehra *et al.*, 2022).

Astrocytes regulate synaptic transmission through the uptake of neurotransmitters such as glutamate, GABA, and adenosine. Proper

regulation of glutamatergic transmission and clearance is essential to prevent excitotoxic build-up, a key feature of cognitive decline in neuropsychiatric and neurodegenerative diseases (Ziar *et al.*, 2025).

In response to stimuli such as toxins, oxidative stress, or infections, resting astrocytes become reactive, undergoing morphological and functional changes. Traditionally, these were classified as proinflammatory, A1-like, or anti-inflammatory, A2-like, astrocytes (Fig.1.7) (Li *et al.*, 2019; Sarkar *et al.*, 2022). However, as with microglia, this binary classification oversimplifies their response as astrocytic activation occurs across a continuum of states influenced by environmental and pathological factors (Fan *et al.*, 2021). These reactive astrocytes trigger relevant signalling pathways to release pro- or anti-inflammatory cytokines and chemokines. Activated microglia can also induce astrocyte reactivity through the release of cytokines, amplifying both pro- and anti-inflammatory signalling cascades (Escartin *et al.*, 2021; Sarkar *et al.*, 2022).

1.2.3.1. The role of astrocytes in AD

Neuropathological and neuroimaging studies demonstrate significant atrophy and dysfunction of astrocytes in AD, which disrupts synaptic connectivity, neurotransmitter homeostasis, and neuronal survival through increased excitotoxicity (Zhang *et al.*, 2021). Historically, much of the research into understanding neuroinflammation in AD focused on microglia. However, post-mortem samples of AD brains have revealed abundant reactive astrocytes surrounding amyloid plaques and blood vessels with Aβ deposits (Monterey *et al.*, 2021; Viejo *et al.*, 2022).

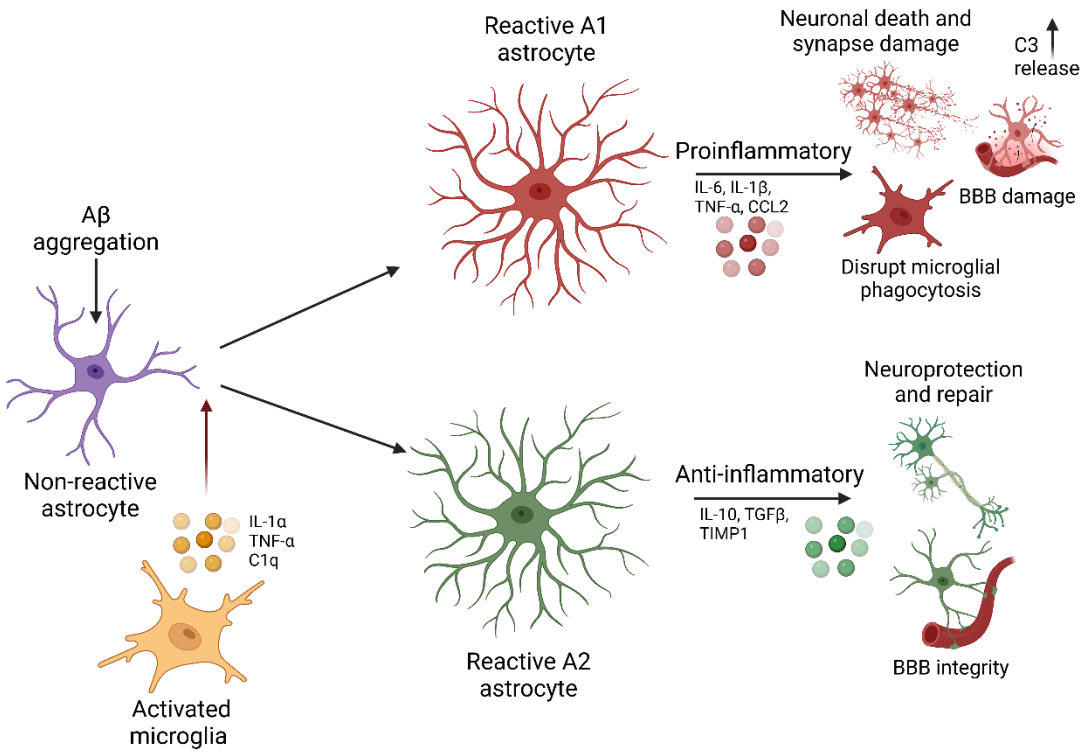

Figure 1.7: Astrocyte activation. Resting non-reactive astrocytes are activated directly by Aβ, or in response to microglial activation, to a pro- or anti-inflammatory reactive state resulting in cytokine and chemokine release. Chronic pro-inflammatory pathway activation can induce neurotoxicity, synapse damage, and neuronal death, while anti-inflammatory responses promote synaptic repair and neurogenesis. (Figure created in Biorender.com; adapted: Sarkar et al., 2022).

Astrocytes are central mediators of the neuroinflammatory response through reactive gliosis, characterised by an upregulation of glial fibrillary acidic protein (GFAP). Although GFAP is widely used as a marker for astrocytic reactivation, it does not fully capture the molecular and functional diversity of astrocytic reactivity (Zhang *et al.*, 2021; Heneka *et al.*, 2024). In AD, astrocytes are stimulated by Aβ deposition, triggering morphological and functional transformation into reactive states. They adopt both pro- or anti-inflammatory responses and release cytokines, chemokines, and growth factors that influence disease progression. The early astrocytic response is thought to be neuroprotective, enhancing neuronal viability and mitochondrial biogenesis to

counter amyloid induced inflammation (Li *et al.*, 2019; Leng *et al.*, 2021). However, chronic activation sustains a pro-inflammatory response, increasing cytokines and chemokine release and promoting neurotoxicity, synapse dysfunction, and neuronal death (Kwon *et al.*, 2020; Sarkar *et al.*, 2022).

The complement system plays a crucial role in innate immune defence and clearance of pathogens; however, excessive activation can result in neuronal damage. Upregulation of complement component 3 (C3) is hallmark of neurotoxic reactive astrocytes, which are induced by microglial cytokines such as IL-1α, TNF-α, and C1q (Liddelow *et al.*, 2017; Lawrence *et al.*, 2023). Elevated C3 levels have been detected in both AD brain tissue and CSF, where they contribute to synaptic dysfunction and neuronal loss, and correlate with increased neuroinflammation and tau-associated cognitive decline (Litvinchuk *et al.*, 2018; Wu *et al.*, 2019).

Recent single nucleus RNA-sequencing studies have identified a spatially and transcriptionally distinct subpopulation of astrocytes, termed disease-associated astrocytes (DAAs), which share similarities with DAMs, and are located in proximity to Aβ plaques (Batiuk *et al.*, 2020; Habib *et al.*, 2020). DAAs upregulate genes involved in lipid and cholesterol metabolism, responses to toxic compounds, and inflammatory signalling pathways, suggesting they contribute to both protective clearance mechanisms but also neurotoxic inflammation in AD (Habib *et al.*, 2020; Lee, Rone, *et al.*, 2024).

Activated microglia can further induce reactive astrocytes through cytokine release, including IL-1α, IL-1β, IL-6, and TNF-α, which stimulates β-secretase

and γ-secretase to cleave APP, leading to further Aβ production by astrocytes and amplification of plaque formation. (Zhao *et al.*, 2011; Zhou *et al.*, 2023). In addition, dysfunction in astrocytic glutamatergic transmission disrupts excitatory neurotransmitter clearance, elevating Aβ and tau burden contributing to memory impairment in AD (González-Reyes *et al.*, 2017).

In AD, chronic astrocytic reactivity contributes to BBB disruption and increased vascular permeability. Structural and functional impairment of astrocytic endfeet reduces tight-junction integrity and alters the secretion of trophic and signalling factors required for BBB maintenance. This results in leakage of plasma proteins, infiltration of peripheral immune cells, and reduced clearance of Aβ and other neurotoxic molecules from the brain, further exacerbating neuroinflammation and neuronal dysfunction (Cabezas *et al.*, 2014; Nehra *et al.*, 2022).

1.2.4. Microglia and astrocyte interactions

Microglia and astrocytes have traditionally been studied as separate contributors to neuroinflammation. However, recent evidence highlights extensive crosstalk between these glial cells in both healthy and diseased brains. In the healthy brain, microglia and astrocytes coordinate to maintain homeostasis, modulate synaptic activity, and support neuronal metabolism. However, under pathological conditions, such as amyloid deposition in AD, this microglia-astrocytic crosstalk becomes dysregulated (Matejuk *et al.*, 2020; Wu *et al.*, 2023).

Activated microglia are typically the first responders to Aβ accumulation, releasing cytokines including IL-1α, complement C1q and TNF-α. These mediators drive the transformation of resting astrocytes to A1-like reactive astrocytes, which in turn activate NF- κB pathways to release C3, along with other pro-inflammatory mediators (Liddelow *et al.*, 2017; Jha *et al.*, 2019; Gomes *et al.*, 2024). The astrocytic release of C3 and cytokines further activates microglia via complement receptor 3 (CR3) and other signalling pathways, amplifying the neuroinflammatory response (Litvinchuk *et al.*, 2018; Wu *et al.*, 2019) .

Conversely, astrocytes can detect Aβ and other DAMPs, and through NF-κB activation, secrete cytokines such as IL-6, IL-1β, and CCL2, as well as C3, to further stimulate microglial activation (Wu *et al.*, 2019). This creates a positive feedback loop, sustaining chronic inflammation and oxidative stress, and resulting in a dysregulated, self-amplifying inflammatory response (Jha *et al.*, 2019; Leng *et al.*, 2021). Activation of the toll-like receptor (TLR) and NLRP3 inflammasome pathways in microglia, enhances IL-1β and IL-18 secretion, which further extenuates reactive astrocytes and exacerbates neuronal damage (Van Zeller *et al.*, 2021; Soraci *et al.*, 2023).

Spatial and single-cell transcriptomic analyses have shown DAMs and DAAs frequently co-localise near Aβ plaques, often sharing upregulation genes involved in lipid metabolism, complement signalling, and cytokine responses (Mallach *et al.*, 2024; Chen *et al.*, 2025). While the initial responses of microglia and astrocytes are intended to facilitate Aβ clearance and promote neuroprotection, chronic activation shifts this response towards a dysregulated

self-perpetuating inflammatory state that exacerbates synaptic dysfunction, BBB disruption, and neuronal death (Matejuk *et al.*, 2020; Heneka *et al.*, 2024).

Given the central role of microglia–astrocyte crosstalk in sustaining chronic neuroinflammation in AD, therapeutic approaches have a focus on disrupting this interaction to restore homeostasis and limit disease progression. Inhibition of key pro-inflammatory cytokines, including IL-1α, C1q and TNF-α, as well as targeting the complement cascade to suppress astrocyte-derived C3–signalling, has been shown to attenuate neuroinflammation and synapse loss (Lian *et al.*, 2016; Lawrence *et al.*, 2023). Studies in C3 knockout mice or C3-inhibited mice demonstrated rescued synapse integrity and improved cognitive function, while deletion of the C3 receptor reduced tau pathology and neurodegeneration in AD models (Lian *et al.*, 2016; Shi *et al.*, 2017; Litvinchuk *et al.*, 2018). Astrocytic priming following transient immune stimulation has been shown to enhance microglial Aβ clearance but this effect is impaired in APOE4 astrocyte carriers (Lee, Yu, *et al.*, 2025). Enhancing TREM2 signalling has also shown potential to restore microglial phagocytosis, thereby limiting Aβ accumulation and inflammatory responses, providing neuroprotection (Li *et al.*, 2023).

1.2.5. Cytokines and chemokines

Cytokines and chemokines are small, secreted proteins that mediate immune signalling, facilitate communication between glia and neurons, and are essential components of the neuroinflammatory response. In the CNS, they are released primarily by microglia and astrocytes, and play key roles in cell proliferation, gliogenesis, neurogenesis, cell migration, apoptosis, and

synaptic release of neurotransmitters as well as responding to pathological stimuli. Although they are usually classified as pro- or anti-inflammatory, many cytokines exhibit context dependent dual functions, therefore balance is essential for homeostasis (Zheng *et al.*, 2016; Domingues *et al.*, 2017; Chen *et al.*, 2024).

1.2.5.1 Cytokines and chemokines in AD

In AD, Aβ deposition and tau aggregation trigger microglia and astrocytes to release pro-inflammatory cytokines, including interleukins IL-1β, IL-6, IL-2, and IL-12, TNF-α and interferon-γ (IFN-γ), which activate downstream signalling pathways, such as NF-κB and MAPK, promoting reactive gliosis and amplifying inflammatory responses. Chemokines, including CCL2 (MCP-1), CCL5 (RANTES) and CXCL10, are involved in cell recruitment and glial activation, which amplifies inflammatory responses and contributes to the chronic neuroinflammation seen in AD (Zheng *et al.*, 2016; Domingues *et al.*, 2017; Kwon *et al.*, 2020). Sustained elevation of these cytokines and chemokines contributes to neuronal dysfunction, synaptic loss, and neurodegeneration.

Anti-inflammatory cytokines, including IL-1ra, IL-4, IL-10, and IL-13, are also released in AD to prevent excessive pro-inflammatory responses and support tissue repair, thereby providing neuroprotection (Bhol *et al.*, 2024; Chen *et al.*, 2024). A balance between pro- and anti-inflammatory cytokine release is therefore crucial to limit neuroinflammation and prevent AD-associated neurodegeneration.

1.2.6. LPS model of inflammation

To investigate the role of inflammation on neurological processes, lipopolysaccharide (LPS) is widely used as a pharmacological agent to induce an immune response (Nazem *et al.*, 2015). LPS is an endotoxin derived from a gram-negative bacterium that acts on pattern recognition receptor, toll-like receptor 4 (TLR4), to initiate inflammation. Upon LPS stimulation, microglia become activated and release pro-inflammatory cytokines, such as IL-1β, IL-6, and TNFα, as well as chemokines, complement proteins, and anti-inflammatory cytokines, such as IL-10 and TGF-β (Nazem *et al.*, 2015; Zhao *et al.*, 2019). LPS has also been shown to disrupt the BBB, increasing permeability and promoting further neuroinflammation (Zhao *et al.*, 2019; Peng *et al.*, 2021).

In rodent models, LPS induces a rapid 'sickness-like behaviour' similar to sepsis, resulting in fever, loss of appetite and decreased activity (Dantzer, 2006; Xie *et al.*, 2022). Furthermore, LPS can induce cognitive impairments, such as spatial memory deficits, and behavioural changes similar to depressive- and anxiety-like behaviour (Zhao *et al.*, 2019; Yin *et al.*, 2023). As such, LPS is often used to study neuroinflammatory-related diseases, including Parkinson's disease (Deng *et al.*, 2020), but numerous studies have also used LPS-induced neuroinflammation to examine the effects on AD pathology (Jendresen *et al.*, 2019; Xie *et al.*, 2021; Yang *et al.*, 2023).

1.2.6.1. LPS in AD models

As neuroinflammation is recognised as a key driver of AD progression, studies have investigated LPS-induced inflammation on AD pathology. Several studies

using AD models, including Tg2576 and APP/PS1 mice, reported increased Aβ deposition following with LPS administration (Sly *et al.*, 2001; Lee *et al.*, 2008; Michaud *et al.*, 2013; Tejera *et al.*, 2019). However, other studies using the same models, reported reductions in Aβ burden but increased neuroinflammation (Herber *et al.*, 2004; Go *et al.*, 2016; Thygesen *et al.*, 2018). In the 5xFAD model, a single dose of LPS administered prior to Aβ plaque deposition was shown to induce microglial priming, and reduce plaque burden at 6 months of age (Yang *et al.*, 2023).

Variation in results could be due to different dosages, duration of administration, age of animals, and time of sacrifice. Notably, short-term, low-dosages of LPS often reduced Aβ deposition, whereas long-term administration, weekly dosing for 12-13 weeks, were more likely to display increased plaque burden (Xie *et al.*, 2022). These studies support that neuroinflammation has an initial neuroprotective role, which after sustained chronic activation, becomes neurotoxic and exacerbates AD progression (Nazem *et al.*, 2015; Xie *et al.*, 2022).

A study in wild-type Sprague Dawley rats found a single dose of LPS increased soluble Aβ and plaques, as well as increased p-tau levels, potentially as a downstream consequence of Aβ plaque aggregation (Wang, Wu, *et al.*, 2018). Furthermore, LPS administered to CD1 mice mothers in late gestation, resulted in long-term neuropathological and behavioural changes in the offspring, with increased levels of $A\beta_{42}$, p-tau, and GFAP, and impairment in cognitive tasks starting at 12 months of age (Wang *et al.*, 2020).

Continuous LPS infusion into the fourth ventricle of rats led to upregulation of microglial activation, as well as shrinkage of the temporal lobe, enlargement of the ventricles, and neuronal loss in the hippocampus and entorhinal cortex, pathologies similar to AD (Hauss-Wegrzyniak *et al.*, 2000; Nazem *et al.*, 2015). Additionally, sustained inflammation impaired microglial Aβ clearance resulting in increased plaque deposition in APP/PS1 mice (Tejera *et al.*, 2019). Cognitive impairment is also reported following repeated LPS administration, demonstrated as deficits in the MWM, memory avoidance tasks, and fear conditioning in models of AD (Kahn *et al.*, 2012; Zhao *et al.*, 2019).

Overall, LPS is a valuable tool for examining neuroinflammatory responses, glial activation, and behavioural and cognitive changes. Furthermore, findings that a single or low doses of LPS can have neuroprotective effects highlight that immune modulation may represent a potential therapeutic strategy for targeting AD pathology.

1.3. Major depression disorder

1.3.1. Epidemiology and symptoms of MDD

Major depressive disorder (MDD), also known as clinical depression, is a neuropsychiatric disorder characterised by persistent low mood, loss of interest or motivation (apathy), loss of pleasure in pleasurable activities (anhedonia), feelings of worthlessness, fatigue, appetite and weight changes, and in extreme cases, thoughts and acts of self-harm and suicide (Cui *et al.*, 2024). As one of the leading causes of disability worldwide, MDD affects 5% of the population, with the lifetime prevalence as high as 15-20% (Kamran *et*

al., 2022). Further, the prevalence is higher in women than men, with an incidence of approximately 10-25% and 5-12%, respectively (Sabic *et al.*, 2021; Bains *et al.*, 2023).

The duration and severity of MDD vary widely, ranging from a moderate singular event to a recurrent lifelong condition. In extreme cases, patients may experience severe chronic psychosis distinguished by delusions and hallucinations. Other types of depression include melancholic depression, peri- and post-partum depression, and seasonal affective disorder, each characterised by distinct symptoms and triggers (Fekadu *et al.*, 2017). Diagnosis of MDD is made through psychiatric evaluation using the Diagnostic and Statistical Manual of Mental Disorders (DSM-5), developed by the American Psychiatric Association, or the diagnostic criteria set out by the International Classification of Disease (ICD-11) (First *et al.*, 2021). MDD is diagnosed when the three prominent features; low mood, anhedonia, and apathy, are present for a minimum period of two weeks (Kamran *et al.*, 2022; Cui *et al.*, 2024).

1.3.2. Biomarkers and risk factors of MDD

Due to the variability in clinical symptoms, there are currently no validated biomarkers for MDD diagnosis. However, research on growth factors, inflammatory and oxidative stress markers, genetic features, and neuroimaging may provide invaluable information in understanding the aetiology and pathophysiology, therefore may be strong candidates for diagnostic biomarkers (Hacimusalar *et al.*, 2018; Dadkhah *et al.*, 2023).

The aetiology of MDD is multifactorial, involving genetic, environmental, and psychological factors. GWAS have identified over 100 independent variants and more than 200 genes associated with MDD, many of which are associated with synaptic function and neurotransmission (Howard *et al.*, 2019; Amare *et al.*, 2020; Levey *et al.*, 2021). Environmental factors such as adverse life experiences, prolonged stress, trauma as well as other health conditions can contribute to the risk of MDD.

MDD is a common co-morbidity in chronic diseases, such as cancer, cardiovascular disease, inflammatory disorders, and neurodegenerative diseases, adding significant psychological burden (Berk *et al.*, 2013; Gold *et al.*, 2020). Long-term MDD has been linked to cognitive decline, particularly in elderly individuals, with impairments in executive function and memory. MDD concomitantly with a neurodegenerative disease, such as AD, is thought to exacerbate disease progression and worsen prognosis (Martín-Sánchez *et al.*, 2021; Sevil-Pérez *et al.*, 2024).

1.3.3. Pathophysiology of MDD

The biological mechanisms of MDD are not fully understood, likely due to the complexity of genetic and environmental influences, but several hypotheses have been proposed (Fig.1.8) (Cui *et al.*, 2024).

1.3.3.1. The monoamine theory

Neurotransmitter monoamines, noradrenaline, dopamine, and serotonin (5-HT) modulate various physiological processes including memory, behaviour, reward, and cognition (Perez-Caballero *et al.*, 2019). Low levels of these

neurotransmitters have been reported MDD and suicide cases (Kamran *et al.*, 2022). The first generation of antidepressants, monoamine oxidase inhibitors (MAOIs) and tricyclic anti-depressants, impaired the breakdown or blocked the reuptake of monoamines, thus increasing noradrenaline, dopamine, and serotonin levels in the synaptic cleft (Perez-Caballero *et al.*, 2019).

Antidepressant development has progressed, with selective serotonin reuptake inhibitors (SSRIs) and serotonin and noradrenaline reuptake inhibitors (SNRIs) being the first-line treatment for MDD due to their improved safety profile (Perez-Caballero *et al.*, 2019). Despite this, individual responses to antidepressants vary, with approximately 30% of patients achieving remission after a single treatment, rising to 60% after multiple courses (Rush *et al.*, 2006; Troubat *et al.*, 2021). Cognitive behavioural therapy (CBT) is the most well documented psychological intervention for MDD, with meta-analyses reporting improved MDD symptoms with CBT alone, and even greater benefits

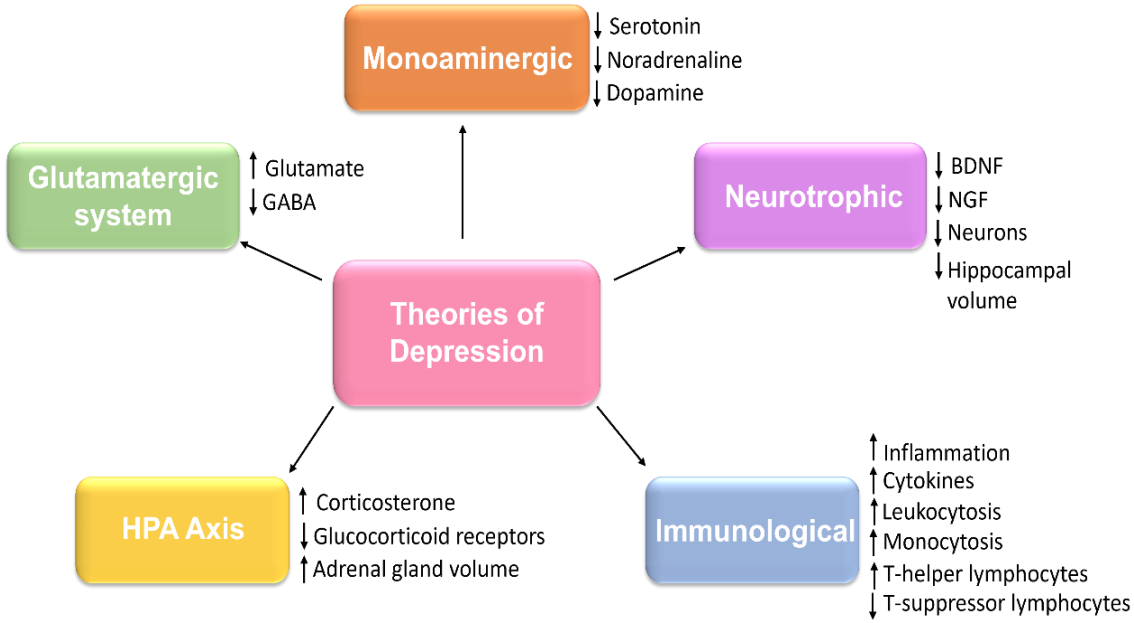

Figure 1.8: Major theories of MDD pathophysiology. Highlighting the numerous contributors to MDD and their effects on signalling pathways. (Figure adapted: Mlyniec, 2015).

in combination with pharmacological treatments. Relapse rates are also lower in patients treated with CBT compared to pharmacological treatments alone (Gautam *et al.*, 2020; Cuijpers *et al.*, 2023). However, 30-40% of patients experience treatment resistant depression (TRD), expressing the need for novel intervention methods (Perez-Caballero *et al.*, 2019).

1.3.3.2. Stress, the HPA axis and glucocorticoid cascade hypothesis

The hypothalamic-pituitary-adrenal (HPA) axis regulates stress responses through the release of corticosteroids. During stress, corticotropin-releasing hormone (CRH) is released from the hypothalamus to stimulate the pituitary to secrete adrenocorticotropic hormone (ACTH), which promotes cortisol release from the adrenal gland. Cortisol then inhibits further secretion of CRH in a negative feedback loop.

Cortisol acts through glucocorticoid (GR) and mineralocorticoid (MR) receptors, which are highly expressed in the hippocampus, amygdala, and prefrontal cortex. These regions regulate emotion and memory, as well as influence HPA axis activity, and are strongly implicated in MDD (Keller *et al.*, 2017; Mikulska *et al.*, 2021). Chronic stress and early-life stress can disrupt this feedback system, causing HPA axis dysregulation and downregulated GRs and MRs, thus increasing the levels of cortisol in the brain (Keller *et al.*, 2017; Troubat *et al.*, 2021). Rodents subjected early life stress, such as maternal separation, experienced HPA axis dysregulation, and while short term separation was associated with resilience, long-term separation increased vulnerability to HPA axis dysregulation and depression-like behaviour (Levine, 2005; Wang *et al.*, 2017). Furthermore, patients with MDD

also displayed up to 40-60% hyperactivity of the HPA axis and elevated cortisol in the brain (Keller *et al.*, 2017; Troubat *et al.*, 2021).

This increase in cortisol forms the basis of the 'glucocorticoid cascade hypothesis,' in that chronic glucocorticoid activation and reduced GRs can induce hippocampal neurotoxicity, resulting in neuronal loss and reduced hippocampal volume, furthering HPA dysfunction. Administration of glucocorticoids increased levels of APP and BACE1, promoting Aβ plaque deposition and p-tau accumulation in models of AD (Green *et al.*, 2006; Canet *et al.*, 2019). These studies support that prolonged stress, causes HPA dysfunction, contributing to both MDD pathophysiology and increased vulnerability to neurodegenerative diseases.

1.3.3.3. Glutamatergic neurotransmitter receptor dysfunction

Dysfunction in the glutamatergic, GABAergic, dopaminergic, and serotonergic neurotransmitter systems has been implicated in MDD. Altered receptor expression causes an imbalance in neurotransmission, resulting in behavioural and cognitive changes (Wang *et al.*, 2021; Cui *et al.*, 2024). Stress-induced reductions in AMPA receptor expression, along with deficits in the inhibitory neurotransmitter GABA and its receptor, $GABA_A$, have been shown to impair hippocampal and prefrontal cortex function and synaptic plasticity, contributing to the cognitive changes observed in MDD (Ren *et al.*, 2016; He *et al.*, 2023).

Abnormal expression of NMDA receptors, GluN2A and GluN2B, due to hypermethylation of genes *GRIN2A* and *GRIN2B* in the hippocampus and

PFC, has been linked to increased susceptibility to MDD. *Grin2a* and *Grin2b* knockout mice exhibit heightened depressive-like behaviours (Boyce-Rustay *et al.*, 2006; Miller *et al.*, 2014), while treatment with NMDA receptor antagonists, such as ketamine, restored impaired synaptic transmission and promotes neurogenesis (Amidfar *et al.*, 2019; Wang *et al.*, 2021).

Serotonin (5-HT) is a key inhibitory neurotransmitter with 14 receptor subtypes widely distributed in the cortex and synapses. Dysfunction of the 5-HT_{1A} receptor reduces serotonergic signalling, contributing to MDD. Mouse models with reduced 5-HT_{1A} receptor expression have shown greater resilience to stress and improved responses to SSRIs, compared to those with receptor overexpression (Richardson-Jones *et al.*, 2011; Yohn *et al.*, 2017).

Dopamine, a precursor of noradrenaline, regulates emotion and reward pathways, and dysfunction in dopamine receptor 2 (D2) is implicated in MDD and anxiety. Polymorphisms in the D_2 receptor gene, *DRD2*, have been associated with early-life and maternal-deprivation stress, with DRD2 knockout mice displaying increased depression-like behaviour (Wang *et al.*, 2021; Guo, Li, *et al.*, 2022).

1.3.3.4. Pathological changes and neurogenesis

Abnormalities in brain regions that regulate emotional response and memory, such as the amygdala and hippocampus, have been reported in MDD, potentially due to corticosteroid imbalance. Imaging and post-mortem studies revealed reduced grey matter volume in the prefrontal cortex and

hippocampus, which may impair function and disrupt HPA axis regulation (Colla *et al.*, 2007; Fekadu *et al.*, 2017).

Chronic stress reduces BDNF expression, which is essential for synaptic plasticity and hippocampal neurogenesis, and is implicated in neurodegenerative diseases. Reduced BDNF levels contribute to neuronal atrophy and cognitive deficits observed in MDD, and antidepressants have been shown to increase BDNF expression and promote neurogenesis (Cui *et al.*, 2024; Han *et al.*, 2025).

Chronic stress can also cause epigenetic modifications through DNA methylation, inducing lifelong changes to the genome resulting in increased susceptibility to MDD. Maternal separation studies in rodent induced epigenetic modifications, leading to increased depression- and anxiety-like behavioural changes in adulthood (Levine, 2005; Becker *et al.*, 2021).

Together, these neurobiological and pathological changes contribute to MDD pathophysiology, but neuroinflammation is increasingly recognised as a key driver of the disorder.

1.3.4. Neuroinflammation in MDD

Neuroinflammation is recognised as a key driver of MDD and may provide a mechanistic link to neurodegenerative diseases, including AD. Patients with MDD display elevated pro-inflammatory cytokines, including IL-1β, TNF-α, IL-6, and C-reactive protein (CRP), in blood and CSF, along with reduced anti-inflammatory cytokines, such as IL-10 (Min *et al.*, 2023; Kouba *et al.*, 2024). Chronic, low-grade inflammation is associated with decreased dopamine

synthesis and reduced monoamine neurotransmission, contributing to MDD (Miller *et al.*, 2016).

Evidence has shown microglial activation, measured by translocator protein (TSPO) total distribution volume, occurs in the prefrontal and anterior cingulate cortex, correlating with the severity of a depressive episode (Setiawan *et al.*, 2018; Wang *et al.*, 2022). Prolonged microglial activation becomes chronic in untreated MDD, and may 'prime' microglia, increasing their reactivity to subsequent injuries and insults, providing a link between MDD and neurodegenerative disease (Dafsari *et al.*, 2020; Richardson *et al.*, 2022). Increased microglial density has also been observed in the anterior cingulate cortex of suicide patients (Steiner *et al.*, 2011; Wang *et al.*, 2022). Supporting evidence in animal models of depression, either induced by chronic stress or LPS, have demonstrated similar microglial immune response with increased levels of pro-inflammatory cytokines (Nazem *et al.*, 2015; Zhao *et al.*, 2019).

Astrocytes also show pathological alterations in MDD, with reduced density and GFAP expression, particularly in the prefrontal and anterior cingulate cortex, and decreased coverage of blood vessels in the grey matter (Si *et al.*, 2004; Kruyer *et al.*, 2023; González-Arias *et al.*, 2025). Disrupted astrocytic glutamate synthesis and transmission contributes to excitotoxicity and depressive-like behaviour in rodent models (Kruyer *et al.*, 2023). Astrocytes are also key producers of BDNF, and their dysfunction, along with chronic stress, reduces BDNF expression and impairs hippocampal neurogenesis and synaptic plasticity, increasing susceptibility to MDD. BDNF deficits may further amplify neuroinflammatory responses, creating a feed-forward loop, that

promotes chronic inflammation and contribute to neurodegeneration (Puentes-Orozco *et al.*, 2024; González-Arias *et al.*, 2025).

Clinical studies have shown that anti-inflammatory treatments, including NSAIDs and cytokine inhibitors, can improve depressive symptoms to a certain degree, as both a monotherapy and in combination with antidepressants (Kohler *et al.*, 2016; Bay-Richter *et al.*, 2022). Antidepressants also possess anti-inflammatory properties, with SSRIs, such as fluoxetine, shown to reduce microglial and astrocytic activation, downregulate pro-inflammatory cytokine production, reverse stress-induced hippocampal changes, and promote BDNF release to improve synaptic plasticity and promote neurogenesis (Zhang *et al.*, 2012; Dafsari *et al.*, 2020; Fang *et al.*, 2022). However, despite evidence suggesting modest symptomatic benefit, NSAIDs are not included in current NICE guidelines for the treatment of MDD due to inconsistent efficacy and concerns regarding long-term safety (National Institute for Health and Care Excellence, 2022).

Collectively, the chronic inflammation, impaired neurogenesis, and glial dysfunction observed in MDD overlap with pathological features of AD, highlighting mechanisms through which depression may contribute to cognitive decline and increase the risk of AD.

1.3.5. MDD and AD

Epidemiological and clinical studies increasingly indicate that MDD is associated with cognitive decline and dementia (Fig.1.9) (Cassano *et al.*, 2019). MDD is the most common NPS in patients with AD, and a history of

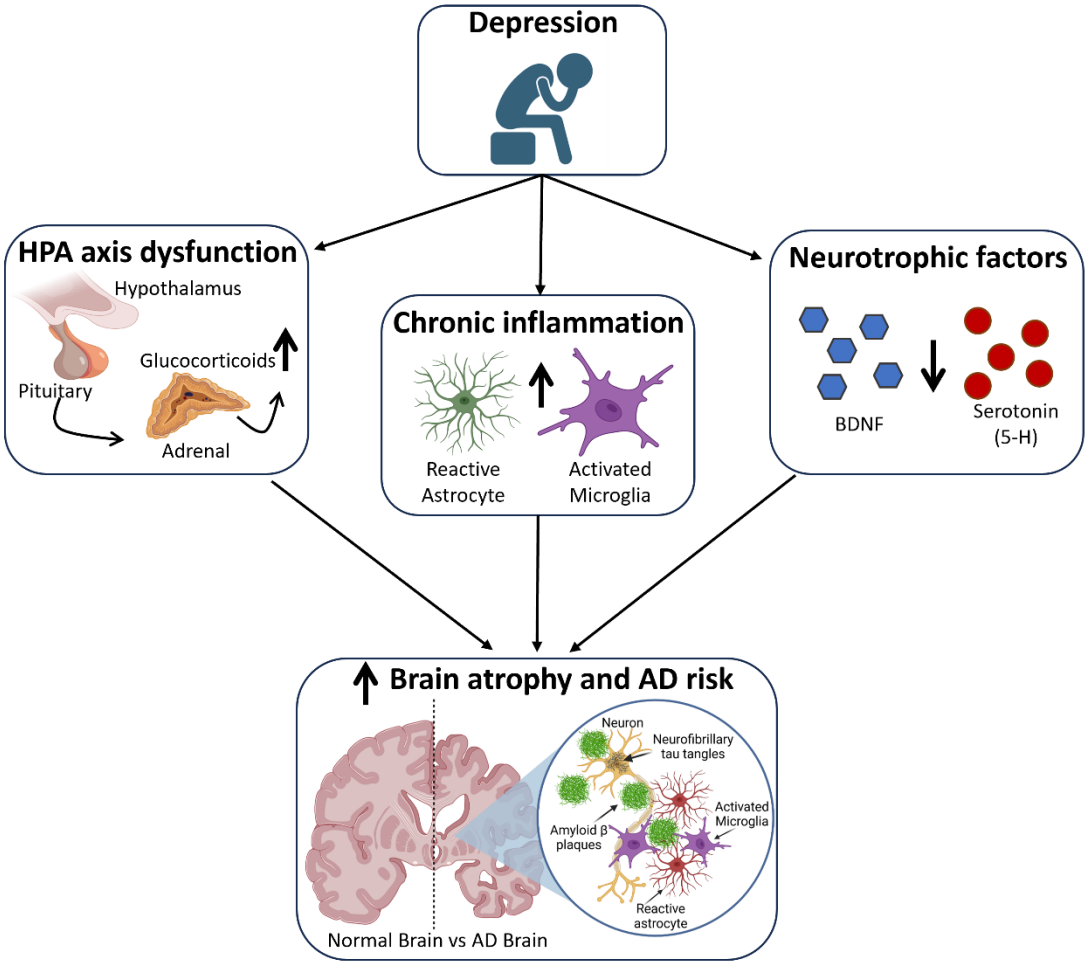

Figure 1.9: The role of MDD in AD risk. Dysfunction of the HPA axis, chronic inflammation, and reduced neurotransmission in MDD contribute to an increased vulnerability of Aβ deposition and hippocampal atrophy accelerating the progression of AD. (Figure created using biorender.com; adapted: Cassano *et al.*, 2019).

MDD is associated with a 2-3 fold increased risk of developing AD (Ownby *et al.*, 2006; Sáiz-Vázquez *et al.*, 2021). Longitudinal studies suggest the number of depressive episodes correlates with AD risk, with each recurrent episode increasing risk by 14% (Dafsari *et al.*, 2020; Sáiz-Vázquez *et al.*, 2021). Furthermore, meta-analyses have shown that MDD increased AD risk even when the depressive episodes occurred up to 25 years prior to cognitive changes, highlighting the long-term effect of psychiatric disorders on neurodegeneration (Green *et al.*, 2003).

MDD may accelerate progression from normal cognition to MCI, and from MCI to dementia. Studies show older adults with both MCI and recently active depression are particularly vulnerable to this progression (Brendel *et al.*, 2015; Gallagher *et al.*, 2018). Dysfunction of the HPA axis in MDD has been linked to hippocampal atrophy and cognitive deficits, which may further contribute to AD development (Canet *et al.*, 2019). Chronic inflammation associated with MDD increases glial activation and pro-inflammatory cytokines, which may exacerbate Aβ deposition and p-tau accumulation in AD. Supporting evidence from rodent models of AD has shown increased Aβ accumulation following stress-inducing glucocorticoid administration (Dafsari *et al.*, 2020), and stress-induced MDD increased Aβ production in cognitively normal older adults, suggesting that MDD could act as a prodromal indicator or biomarker of MCI and AD progression (Gatchel *et al.*, 2019).

Glucocorticoids can accelerate NFT formation, with PET imaging studies showing increased tau phosphorylation in the entorhinal cortex and inferior temporal lobe of depressed but cognitively normal older adults (Gatchel *et al.*, 2017). Rodent stress models have demonstrated that CRH overexpression increases tau phosphorylation and aggregation, brain atrophy, and cognitive deficits (Campbell *et al.*, 2015). However, treatment with CRH receptor 1 antagonists reduced Aβ deposition, synaptic loss, and stressed-induced behavioural and cognitive changes in AD models, potentially by restoring HPA axis function (Dong *et al.*, 2014, 2018; Zhang *et al.*, 2016; Canet *et al.*, 2019).

Both MDD and AD have multi-factorial aetiologies, including environmental risk factors and genetic mutations affecting fundamental neurophysiological

processes. Both diseases share closely linked inflammatory aetiologies, with increased activated microglia and reactive astrocytes, and enhanced pro-inflammatory cytokine release, including IL-1β, IL-6, and TNF-α, as well as reduced anti-inflammatory cytokines, including IL-10 (Dafsari *et al.*, 2020; Kwon *et al.*, 2020; Min *et al.*, 2023).

While antidepressants, particularly SSRIs, are often prescribed to manage depressive symptoms in patients with established AD, evidence suggests they have limited efficacy in treating MDD once neurodegeneration is present and do not improve disease progression (Costello *et al.*, 2023; Lenouvel *et al.*, 2024). In contrast, retrospective studies have shown that long-term treatment, using SSRIs, may be associated with a reduced risk of developing AD, alongside improved cognitive and memory function, and decreased Aβ accumulation in patients with MCI or early AD (Kessing *et al.*, 2009; Bartels *et al.*, 2018; Dafsari *et al.*, 2020). Furthermore, antidepressant citalopram decreased CSF Aβ by 40% compared to controls, suggesting a neuroprotective role (Sheline *et al.*, 2014). The effects of antidepressants have also been demonstrated in rodent models of AD, with fluoxetine reducing Aβ deposition, as well as improving spatial memory, learning, and behavioural deficits in the APP/PS1 model (Wang *et al.*, 2014). Mechanistically, antidepressants may exert neuroprotective effects by reducing glial activation, lowering pro-inflammatory cytokines, promoting BDNF expression, enhancing synaptic plasticity, and supporting hippocampal neurogenesis, which together may reduce AD risk (Zhang *et al.*, 2012; Dafsari *et al.*, 2020; Fang *et al.*, 2022).

However, contradicting studies have reported little to no effect of antidepressants on AD (AlDawsari *et al.*, 2022; Ramos-Cejudo *et al.*, 2024; Belessiotis-Richards *et al.*, 2025), while others have shown an increased risk of AD development with prolonged SSRI and MAOI treatment (Wang, Tai, *et al.*, 2018; Mo *et al.*, 2025), highlighting variability in treatment efficacy. Furthermore, long-term antidepressant use has been associated with negative effects such as impaired emotion regulation, withdrawal symptoms and side effects, and increased risk of cardiovascular disease (Cartwright *et al.*, 2016; Jang *et al.*, 2020). These findings highlight the need for novel more effective interventions to prevent or slow AD progression in patients with MDD.

1.3.6. Rodent models of MDD

Animal models have been vital for advancing understanding of MDD pathophysiology and testing antidepressant efficacy. However, many of the complex symptoms of MDD, such as hallucinations, feelings of worthlessness, ruminations, and self-harm and suicide ideation, are considered uniquely human and cannot be replicated in rodent models. Therefore, behavioural tests rely on behavioural paradigms that reproduce measurable aspects of MDD, such as reduced activity, anhedonia, apathy, and social withdrawal (Table 1.2) (Nestler *et al.*, 2010; Petković *et al.*, 2022).

As previously discussed, the translational relevance of animal models is commonly assessed using established validity criteria, including face, construct, predictive, mechanistic, and pathogenic validity, to determine how effectively models recapitulate key features of human disease (Willner, 1984; Belzung *et al.*, 2011; Wang *et al.*, 2017). Given the complex aetiology of MDD,

rodent models are typically generated through chronic stress exposure, genetic manipulation, or pharmacological intervention to replicate behavioural and molecular hallmarks of the disorder (Nestler *et al.*, 2010; Wang *et al.*, 2017).

1.3.6.1. Chronic stress-induced models

Chronic stress paradigms, such as chronic mild stress (CMS) or chronic unpredictable mild stress (CUMS) models are widely used to induce depression-like behaviour by exposing rodent to repeated mild stressors, including fear conditioning, food/water deprivation, restraint, loud noises, cage shaking, and unsuitable home cage environments, over a period of several weeks (Willner, 1997, 2017). These models have strong face validity, as prolonged stress is a major risk factor for MDD. Depression-like behaviour is commonly evaluated by forced swim (FST) and tail suspension tests (TST), where increased immobility indicates behavioural despair (Porsolt *et al.*, 1977; Steru *et al.*, 1985). Learned helplessness similarly measures failure to escape from escapable foot shocks (Maier *et al.*, 2016). While these stresses reproduce core depression-like behaviours, they can also induce anxiety-like behaviour, reflecting the overlapping symptoms of anxiety and MDD.

1.3.6.2. Genetic models

Genetically modified rodents provide valuable insights into molecular mechanisms underlying genes associated with MDD vulnerability. Various KO and overexpression transgenic models targeting the serotoninergic and noradrenergic neurotransmission systems, as well as HPA axis regulation have been developed (Planchez *et al.*, 2019; Becker *et al.*, 2021). Mutations

in 5-HT_{1A} and 5-HT_{1B} receptors increased sensitivity to stress, reversible by SSRIs, while 5-HT_{1A} KO mice show antidepressant-resistant depression- and anxiety-like behaviour (Richardson-Jones *et al.*, 2011; Willner *et al.*, 2015). Mice with reduced glucocorticoid receptors, $GR^{+/-}$ mice, exhibit HPA axis dysfunction and stress-induced depression- and anxiety-like behaviour, whereas GR overexpression induced resilience in learned helplessness tests (Ridder *et al.*, 2005). In addition, serotonin transporter $SERT^{-/-}$ mice also demonstrated heightened sensitivity to stress with reduced GR expression and impaired HPA axis function (Jiang *et al.*, 2009). Although such models lack full face validity due to the multifactorial nature of MDD, they remain valuable for mechanistic studies.

1.3.6.3. Pharmacological models

Pharmacological models provide reproducible and reversible methods for inducing MDD, making them highly useful for understanding mechanisms and drug responses. Chronic glucocorticoids or corticosterone administration mimics long-term stress exposure, decreases hippocampal BDNF, and induces HPA axis dysfunction, resulting in depression-like behaviour (Ding *et al.*, 2018; Wang *et al.*, 2024). BDNF infusion restores hippocampal function and reversed depression-like behaviour (Gourley *et al.*, 2008; Ding *et al.*, 2018). Other studies report additional behavioural changes, including social avoidance, decreased grooming, impaired memory, and increased anxiety-like behaviour following prolonged corticosterone administration, which are reserved with antidepressant fluoxetine or ketamine treatment (Planchez *et al.*, 2019; Becker *et al.*, 2021). Reserpine, a vesicle reuptake inhibitor which

prevents the reuptake of neurotransmitters, depletes noradrenaline, dopamine, and serotonin in the synaptic cleft, inducing depression- and anxiety-like behaviour, reflecting the monoamine depletion theories of MDD (Qian *et al.*, 2023).

LPS-induced depression has gained increasing relevance as a model of inflammation-driven MDD (Yin *et al.*, 2023). Systemic administration of LPS, activates the immune system leading to elevated circulating pro-inflammatory cytokines, such as IL-1β, IL-6, and TNFα, and suppressed anti-inflammatory IL-10 (Xie *et al.*, 2022). These cytokines cross the BBB, promoting glial activation and further cytokine release, as well as disrupting monoaminergic signalling and neurogenesis (Nazem *et al.*, 2015; Zhao *et al.*, 2019). This induced inflammatory response produces a sickness-like behaviour followed by depression-like behavioural changes, including reduced locomotor activity, anhedonia, weight loss, and cognitive impairment (Dantzer, 2006; Yin *et al.*, 2023). Antidepressant treatment with SSRIs, such as fluoxetine, has been shown to attenuate LPS-induced behavioural and inflammatory responses (Liu *et al.*, 2011; Zhang, Zhang, *et al.*, 2022).

1.3.6.4. Behavioural tests of depression

Once a model has been established, a variety of behavioural tests are used to evaluate specific depression-like symptoms (Table 1.2). These tests capture measurable behaviours that correlate with core MDD features, including behavioural despair, anhedonia, apathy, and motivational deficits (Becker *et al.*, 2021; Petković *et al.*, 2022).

Behavioural despair is typically assessed using the forced swim test (FST) or tail suspension test (TST), where increased immobility reflects loss of coping or hopelessness (Porsolt *et al.*, 1977; Steru *et al.*, 1985). Learned helplessness models also assess coping ability through escape latency following mild foot shocks, providing strong construct validity for stress-induced depressive behaviour (Maier *et al.*, 2016).

Anhedonia is assessed using the sucrose preference test (SPT), where reduced sucrose consumption in a two-bottle paradigm indicates depression-like behaviour (Oddo *et al.*, 2003). Apathy and reduced motivation, reflecting reduced goal-directed behaviour, is assessed by unkempt fur due to lack of self-care, impaired nest formation, reduced social interest, and reduced maternal care. The splash test, using sucrose solution sprayed onto the dorsal coat, measures grooming duration and latency to groom with reductions associated with depression-like behaviour (Isingrini *et al.*, 2010; Cathomas *et al.*, 2015). Nest building is a natural behaviour in rodents for comfort and the housing of pups. In testing, animals are scored on nest completion and timing, and slow or incomplete nesting is associated with a depression-like phenotype (Deacon, 2006; Kraeuter *et al.*, 2019).

The open field test (OFT) measures locomotor activity and exploration, with reduced activity and more time at the edge of the arena, thigmotaxis, associated with both anxiety- and depression-like phenotypes (Seibenhener *et al.*, 2015). Furthermore, the novelty-suppressed feeding test assesses rodents' exploratory behaviour and fear of open and bright environments against its motivation to eat after being food-deprived (Stedenfeld *et al.*, 2011).

1.3.6.5. Targeting MDD and neurodegeneration

Collectively, clinical and experimental studies highlight neuroinflammation and glial dysfunction as key mechanisms linking MDD to neurodegeneration, potentially driving AD progression. Consequently, there is a need to identify new therapeutic strategies that target these shared inflammatory pathways. Recent evidence has shown activation of protease-activated receptor 2 (PAR2) induces both inflammatory responses and depression-like behaviour (Moudio *et al.*, 2022), indicating it may be a useful tool for examining the mechanistic links between MDD and neurodegeneration.

Table 1.2: Common behavioural tests used to assess depression-like behaviour in rodents.

Test	Behaviour assessed	Measure	Depression-like effect
Forced swim test (FST) (Porsolt *et al.*, 1977)	Behavioural despair	Immobility time in water	↑ Immobility = despair-like behaviour
Tail suspension test (TST) (Steru *et al.*, 1985)	Behavioural despair	Immobility time when suspended by tail	↑ Immobility = despair-like behaviour
Open field test (OFT) (Seibenhener *et al.*, 2015)	General locomotion and anxiety-like behaviour	Distance travelled; time in centre vs edge	↓ Locomotor activity = low mood ↓ Time at centre = anxiety-like behaviour
Sucrose preference test (SPT) (Oddo *et al.*, 2003)	Anhedonia	Preference for sucrose over water	↓ Sucrose preference = Anhedonia
Splash test (Isingrini *et al.*, 2010)	Apathy: Self-care/motivation	Grooming duration; latency to groom	↓ Grooming = apathy-like behaviour ↑ Latency to groom
Nest building (Deacon, 2006)	Apathy: Goal directed behaviour	Nest quality and completion	↓ Nest quality = apathy/reduced motivation ↑ Time to build nest
Learned helplessness (Maier *et al.*, 2016)	Coping behaviour/ behavioural despair	Latency to escape from foot shocks	↑ Latency = helplessness
Novelty-suppressed feeding (Stedenfeld *et al.*, 2011)	Anxiety/motivational conflict	Latency to approach food in novel environment	↑ Latency = anxiety/depression-like behaviour

1.4. Protease-activated receptors

1.4.1. PAR activation and expression

Protease-activated receptors (PARs) are a family of transmembrane G protein-couple receptors (GPCRs) consisting of four members: PAR1, PAR2, PAR3 and PAR4 (Heuberger *et al.*, 2019). They possess a unique activation mechanism in which endogenous or exogenous proteases irreversibly cleave N-terminal peptides, exposing a new N-terminal peptide chain. These new peptides act as tethered activation ligands, binding to a conserved region on the second extracellular loop, initiating conformational changes and activating intracellular signalling cascades (McIntosh *et al.*, 2020; Lyu *et al.*, 2025).

PAR1 was first described in 1991, when it was discovered as a key receptor for thrombin-mediated coagulation on human platelets (Vu *et al.*, 1991). Subsequently, PAR1 KO models led to the discovery of the other PAR members, PAR2, PAR3 and PAR4 (Nystedt *et al.*, 1994; Ishihara *et al.*, 1997; Xu *et al.*, 1998), which are highly expressed on endothelial cells, myocyte muscle cells, immune cells, and neurons (Heuberger *et al.*, 2019).

PAR1, 3 and 4 are primarily activated by the serine protease thrombin at differing potencies, whereas PAR2 is preferentially activated by trypsin, tryptase and some coagulation factors (McIntosh *et al.*, 2020). PARs can be activated by numerous endogenous proteases from coagulation, inflammatory, and digestive pathways, as well as exogenous proteases from plants, bacteria, and insects (Heuberger *et al.*, 2019). In addition, PARs can be activated by short synthetic peptides, such as SLIGRL in rodents or SLIGKV

in humans, which correspond to the tethered ligand sequence in humans, and activate PARs without proteolytic cleavage, enabling controlled experimental activation (Price *et al.*, 2021).

1.4.2. PAR functions

Due to their wide tissue distribution, PARs contribute to a range of physiological processes, including platelet regulation through haemostasis and thrombosis, regulation of vascular smooth muscle, cell proliferation and migration, and inflammatory signalling (Alberelli *et al.*, 2014; Heuberger *et al.*, 2019).

Beyond their peripheral functions, PARs are also expressed throughout the CNS, including regions relevant to MDD and AD, such as the hippocampus, prefrontal cortex, amygdala, and hypothalamus. Their localisation to neurons, astrocytes, and microglia underlies their diverse roles in modulating synaptic transmission, plasticity, nociception, and neuroinflammatory processes (Noorbakhsh *et al.*, 2003; Price *et al.*, 2021).

PAR1 and PAR2 are particularly abundant in neurons and glial cells, suggesting roles in both neuroprotection and neurotoxicity (Greenwood *et al.*, 2010; Han *et al.*, 2011; Moudio *et al.*, 2025). Dysregulated PAR signalling has been implicated in numerous diseases, including cardiovascular disease, cancer, inflammatory conditions including asthma, bowel disease and arthritis, and neurodegenerative diseases including Parkinson's disease and AD (Russell *et al.*, 2009; Hara *et al.*, 2023; Peach *et al.*, 2023; Khoon *et al.*, 2025). Among these, PAR2 has emerged as a key modulator of neuroinflammation

and glial activation, making it a potential therapeutic target for MDD and AD (Noorbakhsh *et al.*, 2006; Zhuo *et al.*, 2022).

1.4.3. PAR2

PAR2 was first described in 1994 when a GPCR-DNA sequence homologous to PAR1 was isolated from a mouse genome library and found to be activated by trypsin and the synthetic peptide SLIGRL (Nystedt *et al.*, 1994). Since its discovery, PAR2 has been found to be widely distributed throughout the body, including the gastrointestinal tract, vasculature, immune systems, and CNS (Price *et al.*, 2021; Peach *et al.*, 2023; Reches *et al.*, 2024; Habibi *et al.*, 2025). Its activation by trypsin, mast cell tryptase, and coagulation factors VIIa and Xa, as well as synthetic agonists such as SLIGRL or SLIGKV, triggers multiple intracellular signalling cascades (McIntosh *et al.*, 2020; Han, Aiyer, *et al.*, 2021).

Upon activation, with trypsin or a synthetic peptide, PAR2 couples primarily to $G_{\alpha q}$, $G_{\alpha 12/13}$, G_i proteins, leading to increased intracellular Ca^{2+}, phospholipase C (PLCβ) activation, MAPK pathways, including ERK1/2, JNK, and p38, as well as downstream inflammatory signalling pathways (Fig. 1.10) (Han, Aiyer, *et al.*, 2021; Zhuo *et al.*, 2022). PAR2 signalling can also engage NF-κB and β-arrestin-mediated pathways (Nichols *et al.*, 2012; Bang *et al.*, 2021).

Although PAR2 is often associated with pro-inflammatory signalling, research has indicated that its effects are context dependant, acting as either pro- or anti- inflammatory, varying by tissue type and disease state (Bushell, 2007; McCulloch *et al.*, 2018). Studies have shown in rodent models of arthritis,

PAR2 agonists induce joint swelling and cytokine release, whereas antagonists or PAR2 KO models show reduced inflammation and tissue damage (Ferrell *et al.*, 2010; Crilly *et al.*, 2012). This duality suggests that regulated PAR2 activation may support tissue repair or neuroprotection under acute stress, while chronic or excessive activation promotes pathological inflammation and neurodegeneration (Noorbakhsh *et al.*, 2003; Zhuo *et al.*, 2022).

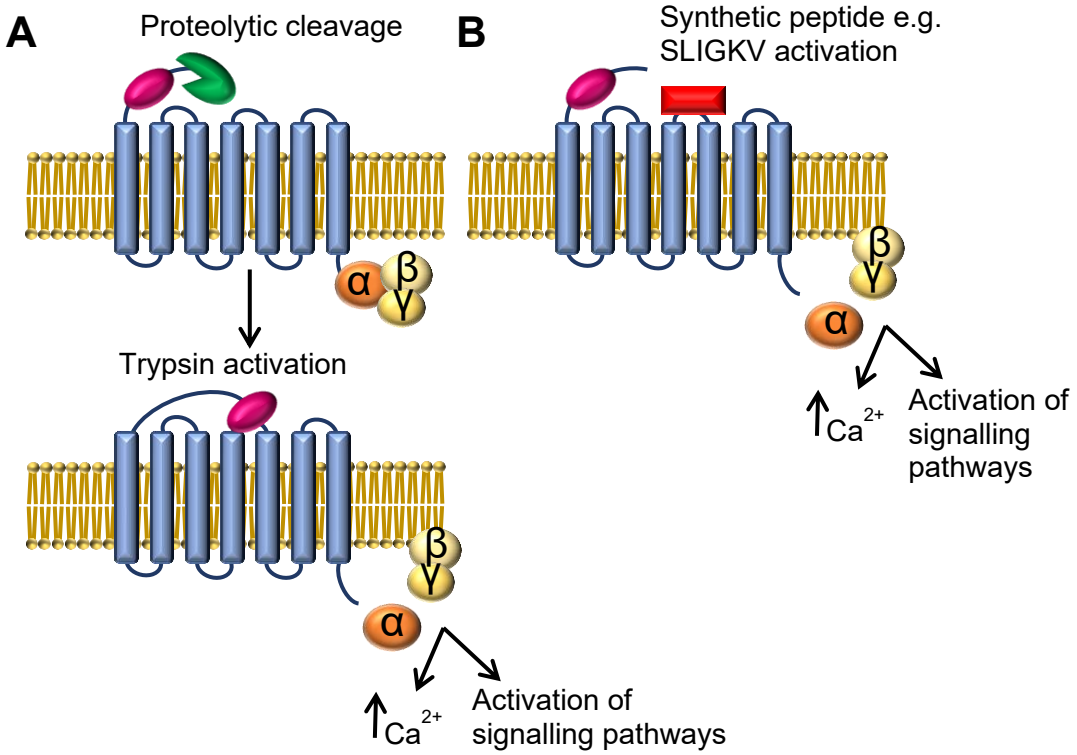

Figure 1.10: Schematic representation of PAR2 activation. (A) Endogenous activation via cleavage of the N-terminus by trypsin, reveals a tethered ligand which binds to the second extracellular loop inducing GPCR activation, resulting in Ca^{2+} release and intracellular signalling cascade activation. (B) Alternative activation via a synthetic peptide, e.g. SLIGKV, binds the second extracellular loop, activating downstream signalling cascades, in the absence of proteolytic cleavage. (Figure adapted: Reches and Piran, 2024).

1.4.3.1. PAR2 in the CNS

Within the CNS, PAR2 is expressed in neurons, astrocytes, and microglia across multiple brain regions, including the hippocampus, CA1-CA3 regions and the dentate gyrus, cortex, amygdala, thalamus, and striatum (Striggow *et al.*, 2001; Bushell, 2007; Price *et al.*, 2021). Activation of PAR2 increases intracellular Ca^{2+} levels in neurons and astrocytes (Bushell *et al.*, 2006) and modulates synaptic activity, including induction of NMDA-receptor dependant long-term depression in hippocampal CA1-CA3 regions (Gan *et al.*, 2011; Shavit-Stein *et al.*, 2017).

PAR2 has shown neuroprotective properties, with PAR2 activation protecting against kainate-induced excitotoxicity in organotypic hippocampal cultures (Greenwood *et al.*, 2010; Moudio *et al.*, 2025) and ceramide-induced neuronal death (Wang *et al.*, 2007). However, other studies have shown PAR2 activation is neurotoxic in a concentration dependant manner (Smith-Swintosky *et al.*, 1997), suggesting PAR2 plays an important role in the balance between neuroprotection and neurotoxicity.

Upregulated PAR2 expression is reported in several neuroinflammatory diseases including multiple sclerosis, HIV dementia, and AD (Afkhami-Goli *et al.*, 2007; Sachan *et al.*, 2019; Eftekhari *et al.*, 2024), while deficiency of the PAR2 gene increases acute ischemic brain damage (Jin *et al.*, 2005). In addition, PAR2 is associated with neurogenic inflammation and pain pathways, with studies targeting PAR2 for migraine treatments (Mason *et al.*, 2023). PAR2 activation is also associated with increased pro-inflammatory cytokines, including TNF-α, IL-6, and IL-12 expression (Bang *et al.*, 2021; Khoon *et al.*,

2025), similar to those observed in MDD (Min *et al.*, 2023; Kouba *et al.*, 2024), suggesting potential shared inflammatory pathways.

1.4.3.2. PAR2, neuroinflammation and depression-like behaviour

Recent studies have highlighted PAR2 as a modulator of neuroinflammatory and behavioural changes associated with MDD. PAR2 KO mice show delayed onset and faster recovery from LPS-induced depression-like behaviour (Abulkassim *et al.*, 2016). Further, a reportedly potent selective, BBB-permeable PAR2 activator, AC264613 (Gardell *et al.*, 2008), has recently been shown to induce behavioural changes associated with depression-like behaviour *in vivo*, including reduced locomotor activity and anhedonia, core symptoms of MDD. AC264613 also elevated peripheral levels of pro-inflammatory cytokine IL-6, again an inflammatory change observed in MDD (Moudio *et al.*, 2022). Additionally, PAR2 inhibition with antagonist, AZ8838 produced anti-inflammatory effects in a model of paw inflammatory oedema *in vivo* (Kennedy *et al.*, 2020). Together, these findings demonstrate that PAR2 activation can induce both inflammatory and behavioural changes similar to those observed in MDD and LPS-induced inflammatory models of depression (Yin *et al.*, 2023).

Given that MDD is an established risk factor for AD, with neuroinflammation underlying both pathologies, and PAR2s established role in activating inflammatory signalling pathways and inducing depression-like behaviour, PAR2 may provide a valuable pharmacological tool for modelling depression-like behaviour and inflammation in transgenic AD models, enabling investigation into how MDD and inflammation accelerates AD pathology.

1.5. Hypothesis

Based on evidence that MDD increases the risk of developing AD, and that neuroinflammation contributes to the pathophysiology of both diseases, we hypothesise that pharmacologically-inducing depression-like behaviour, utilising PAR2 activation and LPS-induced inflammation, will amplify the neuroinflammatory response and exacerbate amyloid pathology in a mouse model of AD, thus accelerating disease progression.

Using the 5xFAD mouse model of amyloid pathology, a combination of behavioural testing, immunohistochemistry, and cytokine profiling will be performed to test the hypothesis through the following research questions:

1. Does PAR2 activation and LPS induce depression-like behaviour in 5xFAD$^{-/-}$ and C57BL6/J wild-type controls?
2. Do 5xFAD$^{+/-}$ mice exhibit depression-like behaviour, and/or are 5xFAD$^{+/-}$ mice more susceptible to pharmacologically-induced depression-like behaviour compared to 5xFAD$^{-/-}$ littermate controls?
3. Does double-dose intervention or multi-dose intervention of pharmacologically induced depression-like behaviour exacerbate behavioural, inflammatory, and molecular pathology in 5xFAD$^{+/-}$ mice?
4. Does PAR2 inhibition affect blood brain barrier integrity and influence behaviour and pathological changes following pharmacologically-induced depression-like behaviour in 5xFAD$^{+/-}$ mice.

Chapter 2: Materials and methods

2.1. *In vivo* experiments

2.1.1. Mice

All *in vivo* experimental procedures were in accordance with UK legislation (Animals (Scientific Procedures) Act 1986), ARRIVE guidelines v2.0 and with approval by the University of Strathclyde Ethics Committee, under the project licence PLL:PP0688944. Experiments were performed using transgenic 5xFAD heterozygous mice ((5xFAD$^{+/-}$ and 5xFAD$^{-/-}$ male and female littermates, (strain: B6SJL-Tg (*APP*SwFILon, *PSEN1**M146L*L286 V) 6799Vas/Mmjax: genetic background: CJ57BL/6J) and CJ57BL6/J wild-type (WT) mice at 11-12 weeks-old, which were group-housed under standard conditions: 21 ± 2°C, 45–65% humidity, 12h dark/light cycle (7am - 7pm) or 14h dark/light cycle (7am - 9pm) in MB1 cages (45 × 28 × 13 cm) lined with grade 6 wood bedding, containing a plastic house, tunnel, and nesting material. During week one, mice were singly housed for the sucrose preference test and regrouped after the last measurement. Mice had free access to food and water, and all behavioural procedures were carried out between 8am - 5pm. As per animal welfare guidelines, any lone mice were given cage buddies.

2.1.1.1. Breeding and genotyping

All 5xFAD heterozygous mice were bred using a C57BL6/J female (purchased from stock colony at biological procedures unit, University of Strathclyde or Envigo, UK) and 5xFAD$^{+/-}$ male (purchased from Jackson Laboratories or from colony breeders) on a B6SJL-Tg, genetic background: CJ57BL6/J. This breeding strategy generated pups that inherited either the human *APP* and

PSEN1 transgenes (5xFAD$^{+/-}$) or did not carry the transgenes (5xFAD$^{-/-}$), producing transgene-positive and -negative littermates (Fig.2.1). In this study, the notation "$^{+/-}$" and "$^{-/-}$" therefore denotes the presence or absence of the 5xFAD transgene. Pups were weaned at approximately 3 weeks old. Ear notching was used for individual identification, and ear punch samples were collected from pups at 3-9 weeks old and genotyped by automated genotyping service, Transnetyx, USA, using probes designed to identify *APP*sw Tg and hu*PSEN1* Tg mutations. Genotype results were received approximately 1 week after sampling.

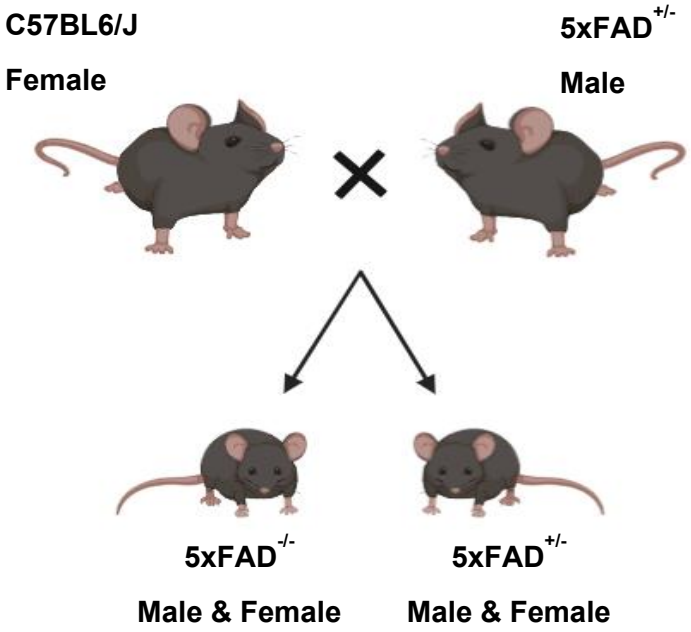

Figure 2.1: Protocol for breeding heterozygous 5xFAD mice. Male 5xFAD$^{+/-}$ mice are bred with female C57BL6/J mice to produce transgenic-positive, 5xFAD$^{+/-}$, and transgenic-negative, 5xFAD$^{-/-}$, pups. (Image created with biorender.com).

2.1.2. Study groups

The initial experiments were conducted in C57BL6/J WT and 5xFAD$^{-/-}$ mice (group 1) to establish that PAR2 activation, using activator AC264613 (Gardell *et al.*, 2008), induced depression-like behaviour. Once depression-like behaviour was confirmed, groups 2, 3, and 4 tested the effects of PAR2

activation and LPS on behaviour and pathology in 5xFAD$^{+/-}$, with varying time courses and dosing regimens. Group 5 were used to assess the peripheral inflammatory response to PAR2 activation and LPS. Groups 6 and 7 were used to study the effect of PAR2 inhibition, using the inhibitor AZ8838 (Cheng *et al.*, 2017), on behaviour and the BBB integrity, respectively (Fig.2.2).

2.1.3. Treatments

Mice were randomly assigned to their treatment groups. Group 1-5 mice received either vehicle, AC264613 (AC) or LPS via intraperitoneal (i.p.) injection. The dose of AC (100 mg kg $^{-1}$) was selected based on previous pharmacokinetic and *in vivo* studies demonstrating that AC peaks in the brain 1h post-injection, produces measurable behavioural changes at 2h post-injection, and is undetectable with behaviours returning to baseline at 24h post-injection (Moudio *et al.*, 2022). The dose of LPS (0.5 mg kg $^{-1}$) was selected based on previous studies showing that this dose rapidly induces cytokine release and sickness-like, inflammation-driven behavioural changes, primes microglia, and reduces Aβ load in the 5xFAD model (Xie *et al.*, 2022; Yang *et al.*, 2023; Yin *et al.*, 2023).

Group 6 mice received the PAR2 inhibitor AZ8838 (AZ) either alone or in combination with vehicle or AC, while group 7 mice received either vehicle, AC, AZ, or AZ followed by AC. The dose of AZ (100 mg kg $^{-1}$) was selected based on unpublished pharmacokinetics data generated within the research group, indicating that AZ crosses the BBB and reaches peak brain concentrations 1h post-injection. Accordingly, AZ was administered 1h prior to AC injection to ensure maximal PAR2 inhibition.

Vehicle control was made up of 0.9% sodium chloride (NaCl) saline solution (Fisher scientific, UK) with 1% tween 80 (Sigma-Aldrich, UK). AC was given as 100 mg kg $^{-1}$ (Tocris/Bio-Techne, UK) sonicated and suspended in vehicle. LPS was given as 0.5 mg kg $^{-1}$ (Sigma-Aldrich, UK) suspended in vehicle. AZ was given as 100 mg kg $^{-1}$ (Neo-Biotech CliniSciences, UK) sonicated and suspended in vehicle, given either alone or 1h prior to AC or vehicle where applicable. Mice were perfused 2h post i.p. injection. In cases were mice received both AZ and AC, mice were perfused 2h post AC-injection. All treatments were heated to approximately 37°C and administrated intraperitoneally to the right-side abdomen of the mouse. In cases where mice received two i.p. injections, the left-side abdomen was used for the second injection (i.p., maximum volume 0.7 mL).

To examine BBB permeability following PAR2 activation and inhibition, polar tracer and protein marker cadaverine-A555 and vascular marker fluorescein conjugated Tomato lectin (*Lycopersicon esculentum*) were used to examine the brain parenchyma and blood vessels. The doses and administration timings of cadaverine and lectin were based on a prior study examining BBB dysfunction (Bravo-Ferrer *et al.*, 2025). Alexa Fluor™ 555 Cadaverine (A30677, ThermoFisher Scientific, UK) was dissolved with 1% phosphate buffered saline (PBS) (Millipore Merck, UK) to 1 mg kg $^{-1}$. Cadaverine was given at 7 mg kg $^{-1}$ intravenously (i.v.) 30 min post i.p. injection (1.5h prior to perfusion fixation). Fluorescein conjugated tomato Lectin (FL-1171-1 Vector Laboratories by 2BScientific, UK) was given at 5 mg kg $^{-1}$ i.v. 5 min prior to perfusion fixation.

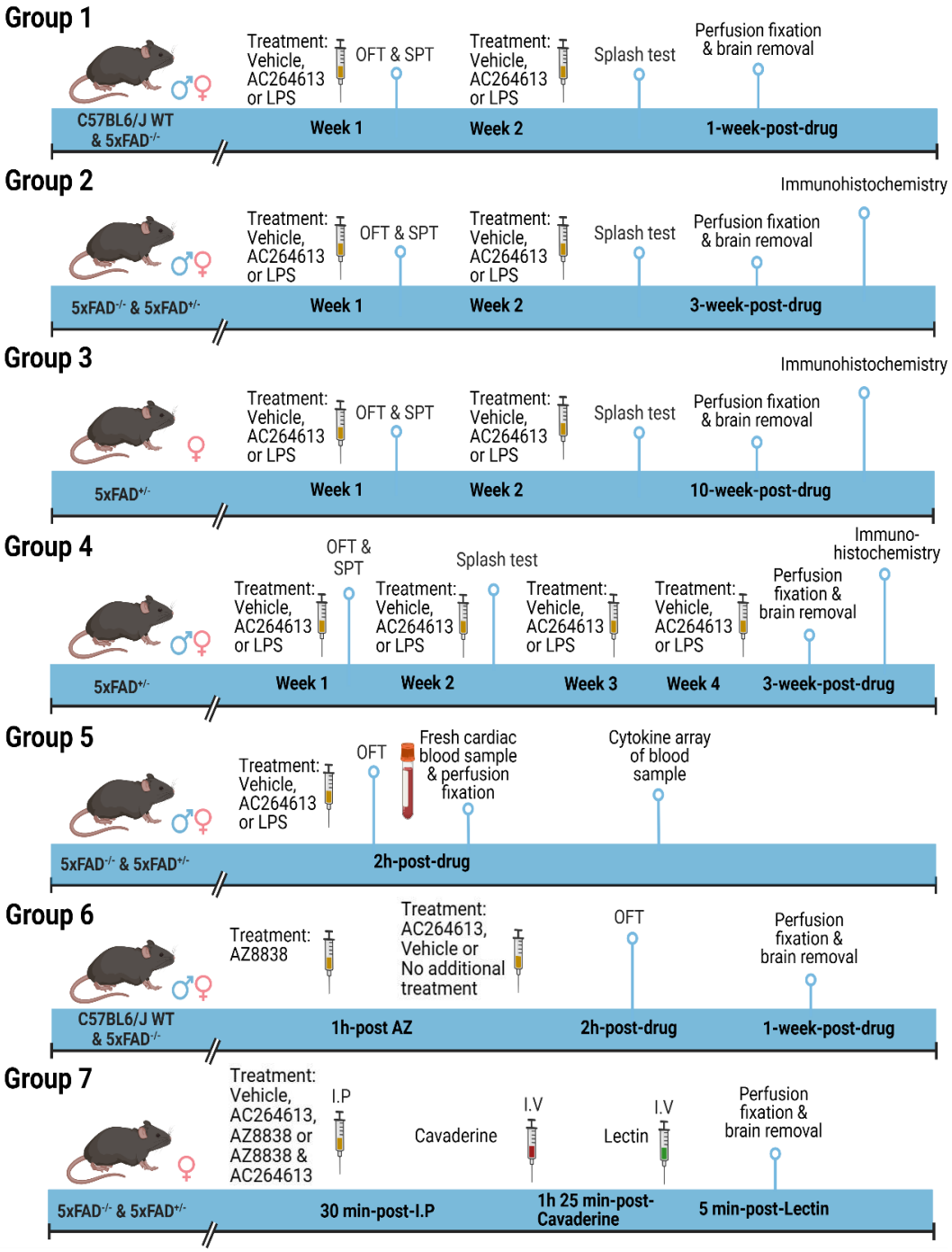

Figure 2.2: Schematic representation of the 7 experimental mouse groups. Figure highlights the treatments, testing protocols, behavioural tests, sex, and genotypes included in each group. (Image created with biorender.com).

2.1.4. Behavioural tests

Prior to experiments, all mice were handled for a minimum of two sessions in a habituation week prior to testing at 10 weeks old. For all behavioural tests, mice were habituated to the relevant apparatus prior to treatments. All apparatus was cleaned thoroughly with safe4 disinfectant cleaner (DMB, UK) before and after use. Mice underwent two naïve habituation and two pre-drug OFT sessions prior to treatment to establish baseline locomotor activity. All videos were recorded using open broadcaster software (OBS) studio. Mice were 11 weeks old upon receiving their first i.p. treatment.

Based on prior studies demonstrating that AC peaks in the brain at 1h post-injection and produces behavioural changes at 2h post-injection, and that LPS induces rapid inflammatory responses and behavioural changes within hours of administration, behavioural testing was conducted at 2h post-injection to capture acute effects. Behavioural testing was also performed at 24h post-injection, when AC is undetectable in the brain and behaviour has been reported to return to baseline. Behavioural testing took place over two weeks, with one injection given per week (Fig. 2.3: example of group 2 testing protocol).

The open field test and sucrose preference test took place in week one and the splash test was conducted in week two, allowing animals one week to fully recover from the treatment. Mice in group 4 received two additional injections without further behavioural testing. Mice were weighed daily as a marker of health, starting from naïve hab 1 until one week post final injection. Mice were aged for 3- or 10-weeks post final injection, before a final OFT and weighing.

Mice in group 1 and 6 were perfused 1-week-post treatment. Mice were then perfusion fixed, and brain removed for immunohistochemistry.

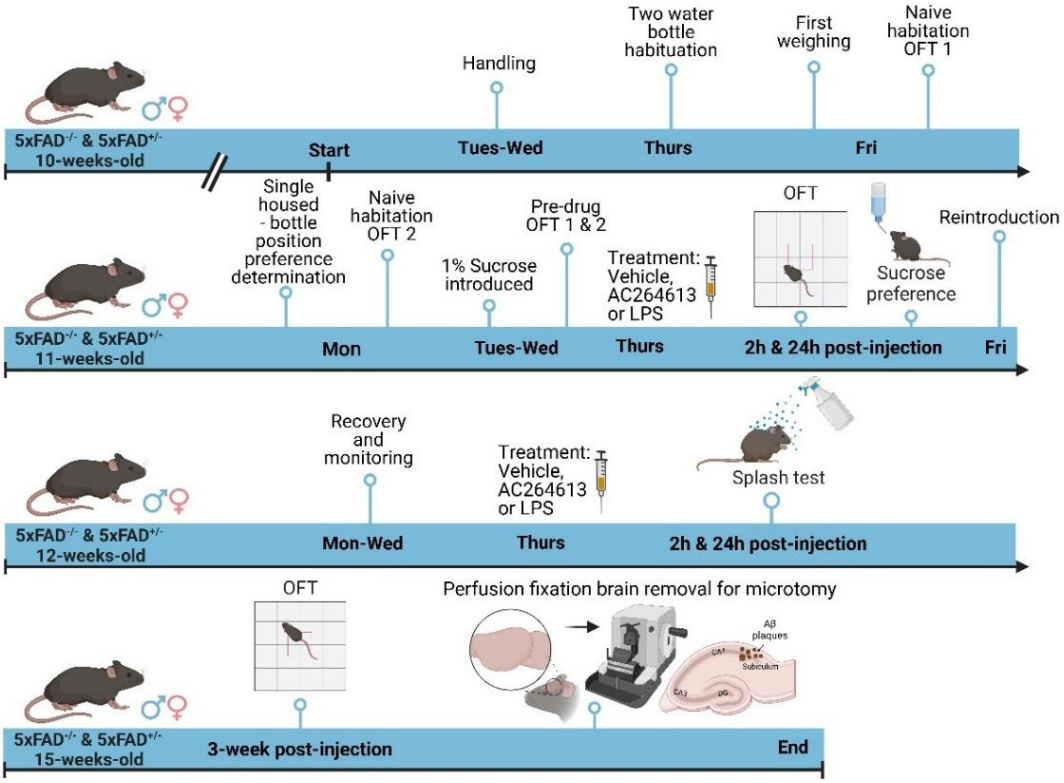

Figure 2.3: Schematic representation of the behavioural testing schedule for group 2 mice: double-injection 3-week protocol. Mice were handled and habituated to the apparatus and testing arena then were separated and singly-house for the sucrose preference test. Mice underwent two pre-drug OFT recordings. Following i.p. injection, behavioural tests were carried out 2h and 24h post injection, over a period of two weeks with OFT and sucrose preference conducted in week 1 and the splash test conducted in week 2. Mice were aged for 3 weeks then underwent a final OFT before perfusion fixation and brain removal for immunohistochemical analysis. (Image created with biorender.com).

2.1.4.1. Open field test

Mice were individually placed in a 40x40x40cm white Perspex box (IKEA, UK), with a webcam (Nulaxy HD 1080p, Amazon, UK) situated overhead (Fig. 2.4) and habituated for two, 20 min naïve OFT habituation recordings (naïve hab 1 and 2) (Seibenhener *et al.*, 2015). Following habituation, mice were recorded for 20 min for two pre-injection (pre-drug 1 and 2) OFT sessions on consecutive days to determine baseline locomotor activity. Following i.p.

injection, mice were recorded in the OFT arena for 20 min at 2h and 24h post-injection with 5xFAD mice receiving a final OFT, 3- or 10-week post final injection.

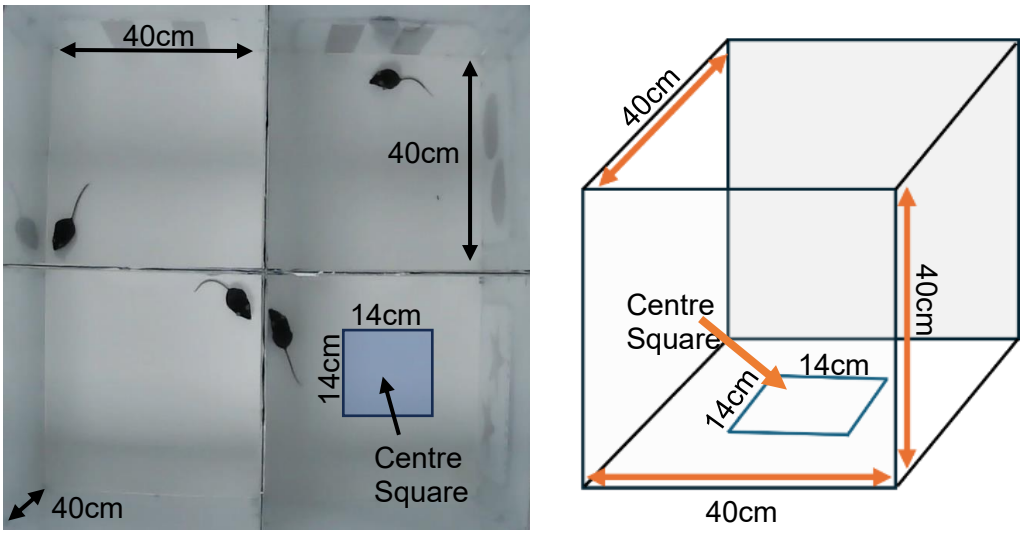

Figure 2.4: OFT set up. Four 40 x 40 x 40 cm white Perspex boxes with a single webcam directly overhead to record locomotor activity. The centre square was defined as 14 x 14 cm but not physically marked on the box.

Locomotor activity was measured as distance travelled, determined using an artificial intelligence (AI) software python package, DeepLabCut (DLC) (Mathis *et al.*, 2018) to track animal movement. Each video had 11-body parts tracked that generate coordinates reflecting the movement of each body part for the 20 min OFT (Fig.2.5). These co-ordinates generated in DLC were imported into MatLab script (written by Professor Shuzo Sakata, University of Strathclyde) to plot body position trajectories and calculate animal speed and distance travelled. The centre of the box was defined in the MatLab script as a 14 x 14 cm centre square but not physically marked on the box base. Time spent at the centre vs the edge was calculated as a marker of anxiety. Naïve habituation OFT and 1 week post OFT sessions were not recorded for

behaviour tests in the group 1 or group 6 mice. Mice in group 5 received a 2h post-injection OFT before immediate perfusion for blood sampling.

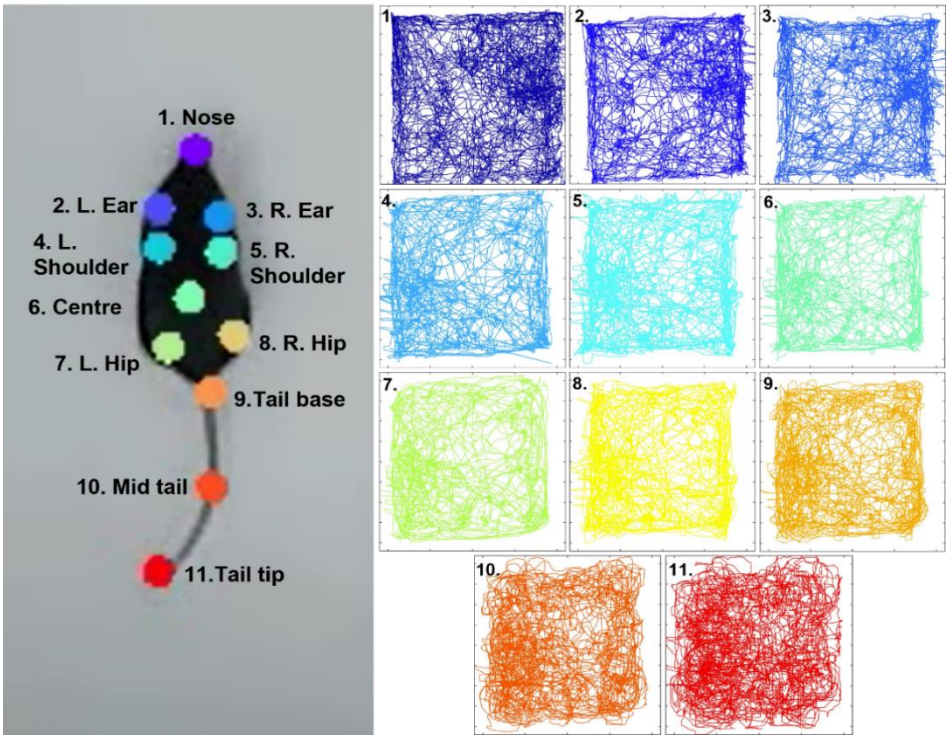

Figure 2.5: DLC tracking of individual mouse body parts and respective tracing images generated for each. Body parts tracked: nose, left and right ear, left and right shoulder, centre, left and right hip, tail base, mid tail, tail tip.

2.1.4.2. Sucrose preference test

Prior to experiments, mice were singly housed with two identical bottles of water, with the amount of water consumed for each measured over 24h to determine bottle position preference (Oddo *et al.*, 2003). For the next 2 days, mice were habituated to sucrose by replacing the water bottle in the non-preferred position with an identical bottle containing 1% sucrose solution, made up with sucrose (Fisher Scientific, UK) and fresh tap water (Fig. 2.6). The weights of both bottles were recorded daily, and the sucrose and water bottle positions were switched after 24h to allow mice to habituate to the sucrose bottle in both positions. Following habituation, sucrose and water

consumption was measured pre-injection, 2h and 24h post-injection with sucrose consumption (%) and total volume drunk calculated at each time point. Sucrose was deemed preferred over water at 50% sucrose consumption at the pre-injection measurement. Mice below this threshold were excluded from results and further testing or reassigned to another study group. Mice were regrouped in MB1 cages after the 24h sucrose weighing and monitored.

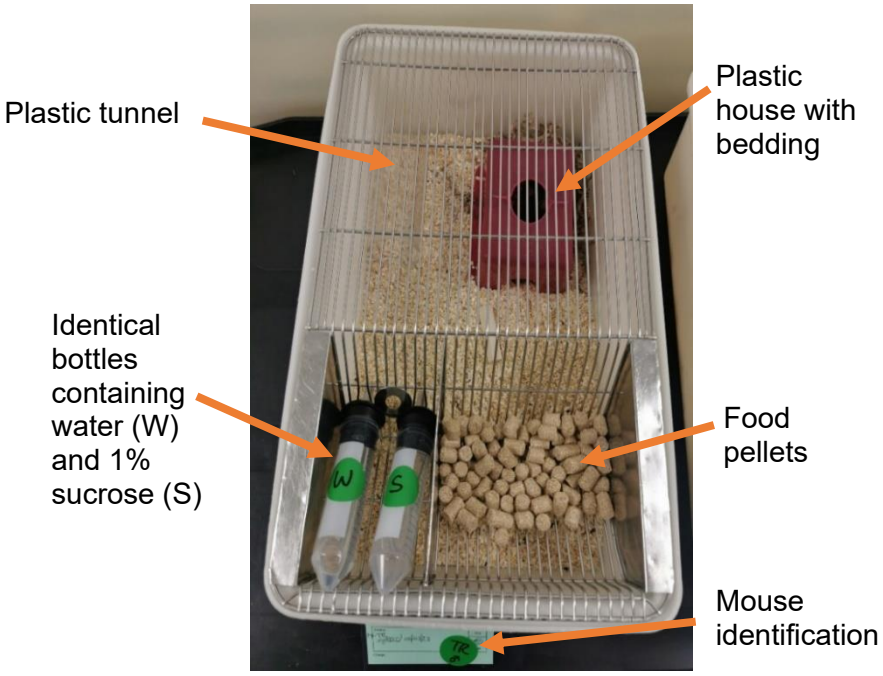

Figure 2.6: Sucrose preference set up. MB1 cage with two identical bottles one containing tap water (W) and one containing 1% sucrose water (S). Mice had free access to food pellets, a plastic tunnel and house with bedding material.

2.1.4.3. Splash test

In preparation for the splash test (Isingrini *et al.*, 2010), mice were habituated to the OFT box, with an individual webcam fixed atop each box, for 10 min in an unrecorded session. Mice received their appropriate second i.p. injection and at 2h and 24h post injection, mice were sprayed on their dorsal coat twice with a freshly made 10% sucrose solution, made up of sucrose (Fisher scientific, UK) and fresh tap water, then immediately placed in the OFT box

and recorded for 10 min. Grooming behaviour was measured as total duration of grooming, time to first groom, and number of grooming episodes using DLC to track animal movement and a MatLab script, SaLSa, (written by Professor Shuzo Sakata, University of Strathclyde) to analyse animal pose co-ordinates in a semi-automatic learning classification model (Sakata, 2023). All grooming videos were also scored manually using a stopwatch. Total time spent grooming, time to first face wipe, and time to first sit and groom >5 sec were recorded. Any mice excluded from the sucrose preference did not undertake the splash test.

2.1.4.4. Exclusion criteria

All mice were checked to be healthy for the study prior to inclusion. Mice were excluded if they displayed one of the following: excessive locomotor activity >120 m in 20 min, sucrose preference <50% at pre-drug measurement or health defects such as teeth malocclusion. Excluded mice were reassigned where appropriate to alternate groups where behavioural testing was not necessary, i.e. cytokine or BBB. Any mice under 19 grams on the day of dosing were assigned to vehicle injections, as a previous study found mice with low weight had a prolonged recovery from AC- and LPS-injection. This ensured that excessive animals were not excluded unnecessarily.

2.1.5. Perfusion fixation

Mice were lethally injected with pentobarbital, 200 mg/mL (Dolethal, Vetoquinol, UK). The chest cavity was opened, and the right atrium of the heart was snipped to allow desanguination. Mice were perfused transcardially with 10 ml of 1% PBS followed by 10 ml of 4% paraformaldehyde (PFA,

ThermoFisher Scientific, UK). The brain was removed and further fixed in 4% PFA for 24h, then stored in 30% sucrose solution for cryoprotection at 4°C until cutting. Mice in the cytokine group were injected with their assigned drug and perfused 2h post-injection. Upon snipping the right atrium, blood was collected for cytokine analysis. The mice were then perfused and brains collected as described above. The blood samples were stored at -20°C until analysis.

2.2. Immunohistochemistry

Immunohistochemistry (IHC) was performed on the collected brains to visualise Aβ plaque pathology and neuroinflammatory markers. Thioflavin S stain was utilised to visualise Aβ structures including Aβ sheets and dense plaques. Monoclonal anti-GFAP (Glial fibrillary acidic protein) and anti-C3 (complement component 3) were used as markers for reactive astrocytes. Monoclonal anti-Iba1 (Ionized calcium-binding adaptor molecule 1) was used as a marker of microglia, with anti-CD68 (Cluster of Differentiation 68) used as a marker of phagocytic microglia.

2.2.1. Microtomy

Brain samples were dissected into left and right hemispheres with the cerebellum and brain stem removed. For microtomy, each hemisphere was embedded onto a sliding microtome (Leica SM2010R) using freezing optimal cutting temperature (OCT) compound (CellPath, UK). Each sample was trimmed until the full hippocampal formation (HPF), and medial geniculate (MG) complex were visible below the dentate gyrus (DG) (Fig. 2.7). Sagittal

serial sections were cut at 40 µm and collected into a 24-well plate containing 1% PBS, with three replicates per well. Samples were stored at 4°C until IHC.

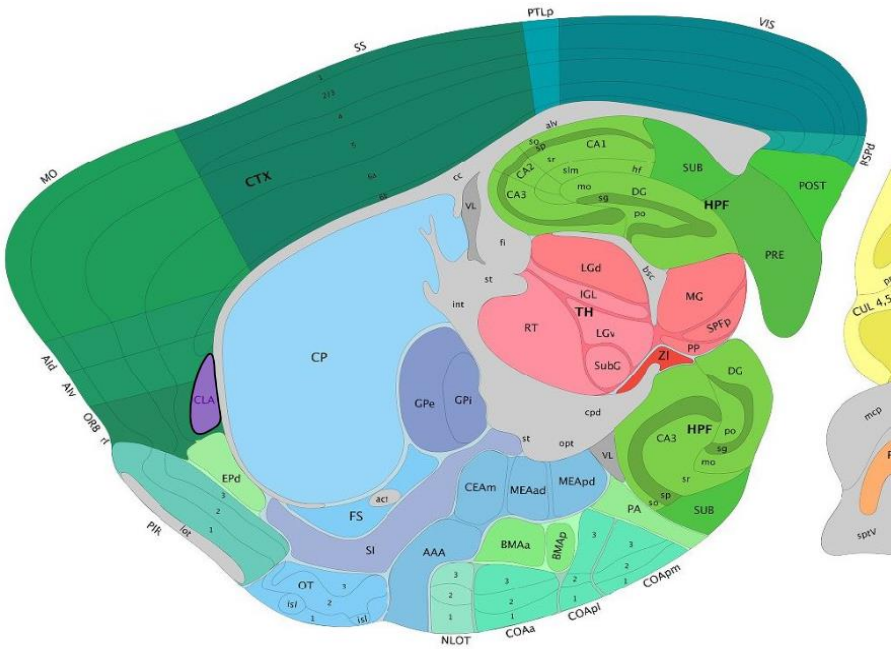

Figure 2.7: The Allen mouse brain atlas diagram of a sagittal cerebrum section. Sections were collected for IHC when the full HPF was visible, and the MG was visible below the DG. (Figure source: Allen Institution of Brain Sciences, 2004).

2.2.2. IHC

The free-floating brain sections were washed in PBS then permeabilised using 1% Triton X-100 (Sigma-Aldrich, UK) in PBS for 1h on a mini orbital shaker at 80 rpm (Stuart SSM1). Sections were then blocked for 1h in PBS with 0.5% Triton X-100, 1% (w/v) bovine serum albumin (BSA, Sigma-Aldrich, UK) and 5% (v/v) foetal calf serum (FCS). Sections were incubated overnight at 4°C with relevant primary antibodies diluted in 0.5% Triton X-100, 1% BSA and 5% FCS. Sections were then washed with PBS and incubated for 3h with secondary antibody diluted in 0.5% Triton X-100, 1% BSA and 5% FCS, on the orbital shaker at 80 rpm. Sections were washed with PBS then relevant sections were counterstained for Aβ plaques using 10% Thioflavin-S (1:1000,

T1892, Sigma-Aldrich, UK) in PBS for 15 min on the orbital shaker at 80 rpm. Sections were washed with PBS and mounted on slides with VectaMount Express Mounting medium (H-5700, Vector Laboratories by 2BScientific UK). Primary and secondary antibodies, and dyes are listed below (Table 2.1).

Table 2.1: List of primary and secondary antibodies, and dyes used in IHC.

Antibodies/Dyes	Species	Dilution	ID	Target
Thioflavin S	NA	1:1000	T1892, Sigma Aldrich	Aβ structures including Aβ sheets and dense plaques
GFAP	Mouse	1:1000	MAB360, Sigma Aldrich	Reactive astrocytes
C3	Mouse	1:100	HM1045, Hycult Biotech, Cambridge bioscience	Reactive astrocytes
Iba1	Rabbit	1:2000/1:1000 if co-labelling with CD68	AB178846, Abcam	Activated microglia
CD68	Rat	1:1000	MCA1957GA, Bio-Rad	Phagocytic microglia
Alexa Fluor 555 Cadaverine	NA	NA	A30677, ThermoFisher Scientific, UK	Leakage of BBB proteins to parenchyma
Fluorescein conjugated tomato Lectin	NA	NA	FL-1171-1, Vector Laboratories 2BScientific, UK	Vascular endothelium
Alexa Fluor 555	Donkey anti-mouse	1:500	A31570, Life technologies	GFAP & C3
Alexa Fluor 555	goat anti-rabbit	1:500	A21428, Life technologies	Iba1
Alexa Fluor 555	goat anti-rat	1:500	A21434, Life technologies	CD68
Alexa Fluor 488	goat anti-rabbit	1.500	A11008, Life technologies	Iba1

2.3. Imaging

2.3.1. Mesolens imaging

Images were acquired using a custom built wide-field epi-fluorescence microscope (Mesolens, designed and built by Professor Gail McConnell, University of Strathclyde (McConnell *et al.*, 2016)). Excitation wavelengths of 435 nm (Thioflavin S) and 585 nm (GFAP, C3 and Iba1), or 490 nm (Iba1) and 585 nm (CD68) were used, respectively. Each image included the full hippocampus and subiculum, as well as partial regions of visual cortex (VC) and somatosensory cortex (SSC) (Fig.2.8). Images were processed and quantified using the open-source software Fiji ImageJ to analyse fluorescence intensity. Aβ plaque load, size, and number were analysed using Fiji plugin

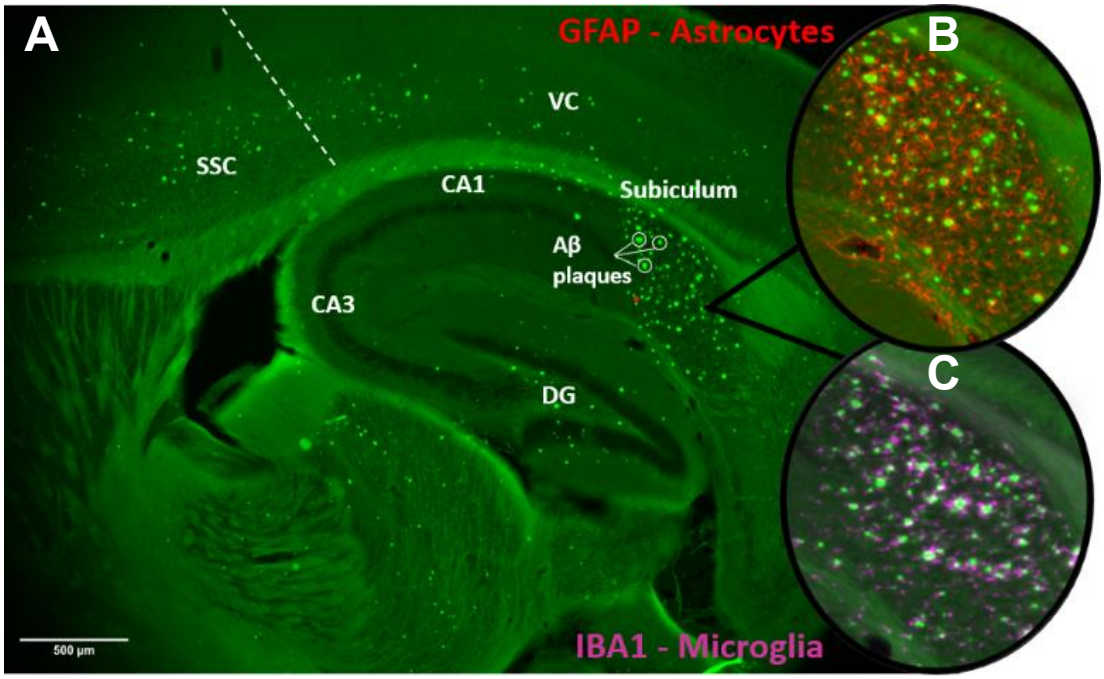

Figure 2.8: Representative Mesolens image of a 5xFAD$^{+/-}$ mouse brain. (A) Brain section stained with thioflavin S to visualise Aβ plaques in the hippocampus, subiculum, VC and SSC. (B) Magnified image of the subiculum with thioflavin S and GFAP co-stain to highlight the colocalisation of astrocytes to Aβ plaques. (C) Magnified image of the subiculum with thioflavin S and Iba1 co-stain to highlight the colocalization of microglia to Aβ plaques.

Trainable Weka Segmentation. Brain regions analysed were the subiculum, cornu Ammonis (CA) 1 and CA3, DG, VC and SSC.

2.3.2. Cadaverine and lectin imaging

2.3.2.1. Mesolens imaging

Brains from mice injected with fluorescently labelled cadaverine and lectin were dissected and 9 serial sections at 40 µm were collected into PBS, as described in section 2.2.1. Sections were mounted directly onto slides without further preparation. Images were acquired using the Mesolens at excitation wavelengths of 490 nm (lectin) and 585 nm (cadaverine) to visualise the hippocampus, VC, SSC, and motor cortex. Images were processed and quantified using Fiji ImageJ to analyse fluorescence intensity.

2.3.2.2. Confocal imaging

Sections from mice injected with fluorescently labelled cadaverine and lectin were also examined using a TCS SP8 Leica Microsystems confocal microscope (Leica, UK). Images of blood vessels were acquired as a z-stack at x63 magnification, using excitation wavelengths of 488 nm (lectin) and 552 nm (cadaverine) in the CA1 region of the hippocampus. Images were processed and quantified using Fiji ImageJ to analyse fluorescence intensity in the parenchyma and vasculature.

2.4. Cytokine arrays

2.4.1. Blood sampling

Cytokine assays were utilised to examine cytokine and chemokine release in the periphery following PAR2 activation and LPS in 5xFAD$^{+/-}$ and 5xFAD$^{-/-}$

mice. Mice received either vehicle, AC264613 (100 mg kg $^{-1}$) or LPS (0.5 mg kg $^{-1}$) and at 2h post-injection, cardiac blood was collected for profiling prior to perfusion fixation. The Proteome Profiler Mouse Cytokine Array Kit (ARY006, R&D Systems, UK) was used to detect 40 different cytokines, chemokines, and acute phase proteins simultaneously (Table 2.2).

Table 2.2: Cytokines, chemokines, and acute phase proteins detected by the mouse array proteome profiler.

Cytokines, chemokines, and acute phase proteins detected				
CXCL13/BLC/ BCA-1	IL-1 alpha/ IL-1F1	IL-7	CXCL10/IP-10	CCL4/MIP-1 beta
C5a	IL-1 beta/IL-1F2	IL-10	CXCL11/I-TAC	CXCL2/MIP-2
G-CSF	IL-1ra/IL-1F3	IL-12 p70	CXCL1/KC	CCL5/RANTES
GM-CSF	IL-2	IL-13	M-CSF	CXCL12/SDF-1
CCL1/I-309	IL-3	IL-16	CCL2/JE/MCP-1	CCL17/TARC
CCL11/Eotaxin	IL-4	IL-17	CCL12/MCP-5	TIMP-1
ICAM-1	IL-5	IL-23	CXCL9/MIG	TNF-alpha
IFN-gamma	IL-6	IL-27	CCL3/MIP-1 alpha	TREM-1

2.4.2. Sample preparation

Cardiac blood samples were collected and stored at -20°C until analysis. Samples were thawed and centrifuged at 1600 rpm, 4°C (Labofuge 400R, Heraeus) for 20 min to separate blood serum and plasma. The blood serum was collected and 28 µl was used per sample, with 4 samples (2 per sex) analysed for each treatment per genotype in accordance with the kit protocol. Membranes were blocked with array buffer for 1h on a rocking platform shaker (HS250, IKA). Plasma samples were prepared with array buffers 4 and 6 then incubated with 15 µl of reconstituted mouse cytokine array panel A detection

antibody cocktail for 1h. The plasma sample/antibody mixes were added to the membranes and incubated on the rocking platform shaker at 2-8°C overnight. Following incubation, the membranes were washed with wash buffer then incubated with Streptavidin-HRP for 30 min on rocking platform shaker. The membranes were washed thoroughly before 1 ml of chemi reagent mix was added to the membranes and gently shaken for even spread for 1 min. Excess reagent mix was blotted off the membranes in preparation for exposure.

2.4.3. Membrane exposure

Membranes were placed in an autoradiography film cassette and covered with plastic wrap, removing any air bubbles. Blue sensitive autoradiography X-ray film (UltraCruz, Fisher Scientific, UK) was applied, and samples were exposed for 5 min. The film was then developed in an automatic X-ray film processor (JP-33, JPI). All 5xFAD$^{+/-}$ membranes were developed on one film and all 5xFAD$^{-/-}$ on another, to compare treatments within the genotypes (Fig.2.9). Membranes were scanned and processed using Fiji ImageJ to analyse the

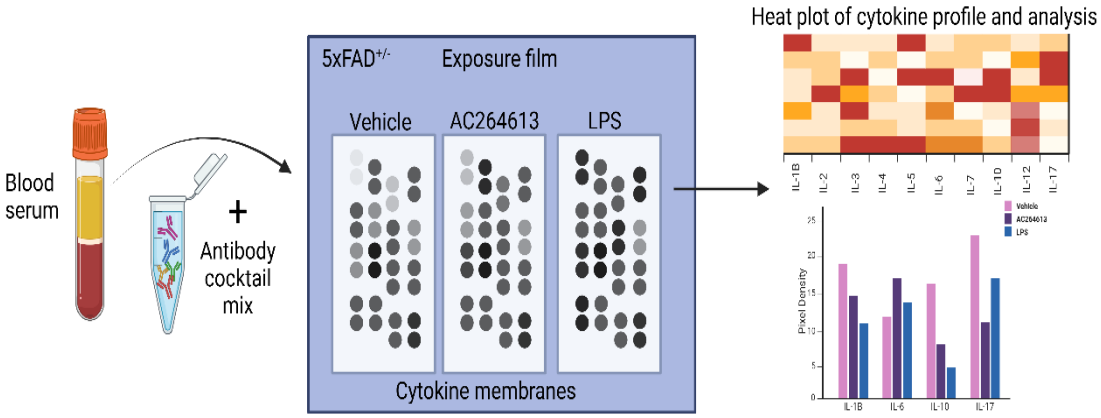

Figure 2.9: Cytokine array method. Cardiac blood samples from vehicle, AC and LPS-injected mice were centrifuged, and serum was collected and incubated with the cytokine array panel A detection antibody cocktail. The membranes were exposed and developed then the pixel density of each array spot was analysed to determine a relative change between samples. (Image created using biorender.com).

pixel density of each array spot to determine a relative change between samples. Each array spot was analysed in duplicate, and the mean density after background subtraction, was calculated.

2.5. Data and statistics

All data are reported as mean ± S.E.M. with individual data points, where *n* = the number of animals used. Sex and genotypic differences were compared to identify any differences in drug effects, with data presented separately by sex and genotype, as well as combined to show overall treatment effects. Statistical analyses were performed using GraphPad Prism (v8.4.3). Statistical tests are indicated in the relevant figure legends and included one-way repeated-measures ANOVA with Tukey's post hoc test, two-way repeated-measures ANOVA with Sidak's or Tukey's post hoc tests, and unpaired two-tailed t-tests. Significance is reported when $p<0.05$. Asterisks shown with brackets indicate significant pairwise differences between groups, while asterisks shown without brackets represent significant overall effects identified by ANOVA. Data were examined for normality using the Shapiro-Wilk test, alongside inspection of Q-Q plots and assessment of Gaussian distribution.

To maintain clarity given the sample sizes, analyses compared drug effects by sex or genotype across timepoints, or by assessing overall drug effects using two-way repeated-measures ANOVA. This approach assumes normality, homogeneity of variance, and sphericity for repeated-measures data, which may be less robust in complex designs with multiple variables and could potentially over- or under-represent statistical significance.

2.5.1. Power calculations

Based on the data from previous projects, the normalised mean ± standard deviation (SD) under the null hypothesis was predicted to be 1 ± 0.2, whereas the alternative hypothesis was predicted to be 0.6. Group 1 mice were used to confirm that AC264613 induced depression-like behaviour, and to assess genotypic differences between wild-type C57BL6/J and 5xFAD$^{-/-}$ mice. As no difference in genotype or sex were predicted for behavioural outcomes, an n = 3 per sex and genotype was used. To assess AC264613 on behaviour and brain pathology in 5xFAD$^{+/-}$ mice, using an anticipated change of 40% with a 90% power and a 5% significance level (alpha = 0.05), the sample size was calculated at a minimum of 5 animals per group. Hence, a minimum of 5 mice per sex and genotype were used for each treatment group in mice groups 2-4.

To examine cytokines in the blood, previous data were consulted, with the normalised mean ± SD predicted to be 1 ± 0.2 and an expected change of approximately ± 0.4. With a 90% power and a 5% significance level, the minimum sample size was calculated as 2 animals per treatment group. A small project grant was awarded to examine peripheral cytokines, and an n = 2 per sex and genotype were used for each treatment group.

To examine BBB integrity following PAR2 activation and antagonism, a small pilot grant was awarded. As the effects of PAR2 on the BBB were unexplored, an n = 3 female mice of each genotype and treatment were used to establish preliminary data. To examine the effects on PAR2 antagonism on behaviour, surplus C57BL6/J or 5xFAD$^{-/-}$ colony mice, were used with an n = 3 per sex per treatment to establish preliminary data.

Chapter 3: The effects of AC- and LPS-injection on behaviour in C57BL6/J and 5xFAD$^{-/-}$ mice.

3.1. Introduction and aims.

Previous research demonstrated that PAR2 activation induced depression-like behaviour in vivo (Moudio et al., 2022). As we planned to use PAR2 activation to induce depression-like behaviour in a mouse model of AD, we first wanted to confirm these previous findings. To control for potential effects of genetic background, behavioural responses were examined in both C57BL6/J WT and 5xFAD$^{-/-}$ mice, which do not express the APP or PSEN1 transgenes. This comparison ensured that observed behavioural effects were not driven by transgenic background and confirmed the replicability of pharmacological effects in non-diseased mice. Hence, PAR2 activator AC264613, was examined alongside vehicle and LPS, to measure three core features of MDD, low mood/fatigue, anhedonia, and apathy in both genotype. It was hypothesised that AC and LPS would induce depression-like behaviour, displayed as reduced locomotor activity, sucrose preference, and grooming behaviour in both C57BL6/J and 5xFAD$^{-/-}$ mice.

The work in this chapter aims to answer the following research questions:

- Do AC and LPS induce depression-like behaviour in both C57BL6/J and 5xFAD$^{-/-}$ mice?
- Does sex influence the effects of AC- and LPS-induced behavioural changes?
- Are there any behavioural genotypic differences between C57BL6/J and 5xFAD$^{-/-}$ mice prior to, or following pharmacologically induced-depression-like behaviour?

3.1.1. C57BL6/J and 5xFAD$^{-/-}$ mice

In total 15 mice received vehicle, 16 mice received AC, and 16 mice received LPS. After exclusions, each treatment group had 12, 14 and 13 mice, respectively (Table 3.1).

Table 3.1: Number of mice included and excluded in each treatment group.

Total Number		Total after exclusion	C57BL6/J vs 5xFAD$^{-/-}$	
Vehicle	15	12		
AC461613	16	14		
LPS	16	13		
	Total after Exclusions			
	C57BL6/J		5xFAD$^{-/-}$	
	F	M	F	M
Vehicle	3	3	3	3
AC461613	4	3	4	3
LPS	3	3	3	4
	Excluded			
	C57BL6/J		5xFAD$^{-/-}$	
	F	M	F	M
Vehicle	1	1	0	1
AC461613	0	0	0	2
LPS	1	1	1	0

3.2. AC- and LPS-injection reduced locomotor activity independent of sex and genotype.

Comparing locomotor activity from pre-drug to 2h post-drug, AC- and LPS-injection significantly reduced locomotor activity at 2h post-injection ($F_{(3\text{-}108)}$ = 41.8, $p<0.001$ vs pre-drug) with AC- ($p<0.001$ vs vehicle, n=14, Fig. 3.1B) and LPS-injection ($p<0.001$ vs vehicle, n=14, Fig. 3.1B) reducing locomotor activity 2h post-injection when compared to vehicle injection. At 24h post-injection, locomotor activity in the AC- and LPS-injected mice was fully recovered. In

contrast, vehicle injection had no effect on locomotor activity at either 2h or 24h post-injection (p=0.99 vs pre-drug, n=12, Fig.3.1B).

Having shown that AC and LPS reduced locomotor activity, we investigated whether this was dependent on the sex of the mice. Within genotypes, AC- and LPS-injection reduced locomotor activity 2h post-injection in both C57BL6/J (AC: $F_{(2-11)}$ = 5.2, p=0.02 vs pre-drug, n=7, Fig. 3.2C; LPS: $F_{(2-9)}$ = 12.17, p=0.002 vs pre-drug, n=6, Fig. 3.2E) and 5xFAD$^{-/-}$ mice (AC: $F_{(2-9)}$ = 21.06, p=0.0005 vs pre-drug, n=6, Fig. 3.2D; LPS: $F_{(2-12)}$ = 34.64, p<0.0001 vs pre-drug, n=7, Fig.3.2F). When comparing sex within the genotypes, no differences in locomotor activity were observed between male and female mice prior to, or following injection of vehicle, AC or LPS (vehicle: $F_{(1-4)}$ = 0.1, p=0.77 C57BL6/J male vs female, n=3, Fig.3.2A; $F_{(1-4)}$ = 1.55, p=0.28 5xFAD$^{-/-}$ male vs female, n=3, Fig.3.2B; AC: $F_{(1-5)}$ = 0.18, p=0.69 C57BL6/J male, n=3, vs female, n=4, Fig.3.2C; $F_{(1-5)}$ = 0.02, p=0.89 5xFAD$^{-/-}$ male, n=3, vs female, n=4, Fig.3.2D; LPS: $F_{(1-4)}$ = 4.38, p=0.1 C57BL6/J male vs female, n=3, Fig.3.2E; $F_{(1-5)}$ = 1.94, p=0.22 5xFAD$^{-/-}$ male vs female, n=3, Fig.3.2F).

We also examined whether drug-induced changes were genotype dependent. No differences in locomotor activity were found between C57BL6/J and 5xFAD$^{-/-}$ mice within the treatment groups prior to injection (vehicle: p>0.99 C57BL6/J vs 5xFAD$^{-/-}$, n=6, Fig.3.3A; AC: p=0.67 C57BL6/J vs 5xFAD$^{-/-}$, Fig.3.3B, n=7; LPS: p=0.29 C57BL6/J, n=6, vs 5xFAD$^{-/-}$, n=7, Fig.3.3C, at pre-drug 2 for all treatments). However, AC injection reduced locomotor activity in C57BL6/J mice compared to 5xFAD$^{-/-}$ mice at 2h post-injection (p=0.04 C57BL6/J vs 5xFAD$^{-/-}$, n=7, Fig.3.2B). This genotypic difference was not

observed at 24h post-injection (p=0.46 C57BL6/J vs 5xFAD$^{-/-}$, n=7). No genotypic differences were observed in vehicle- or LPS-injected mice 2h post injection (vehicle: p=0.35 C57BL6/J vs 5xFAD$^{-/-}$, n=7; LPS: p=0.65 C57BL6/J, n=6, vs 5xFAD$^{-/-}$, n=7).

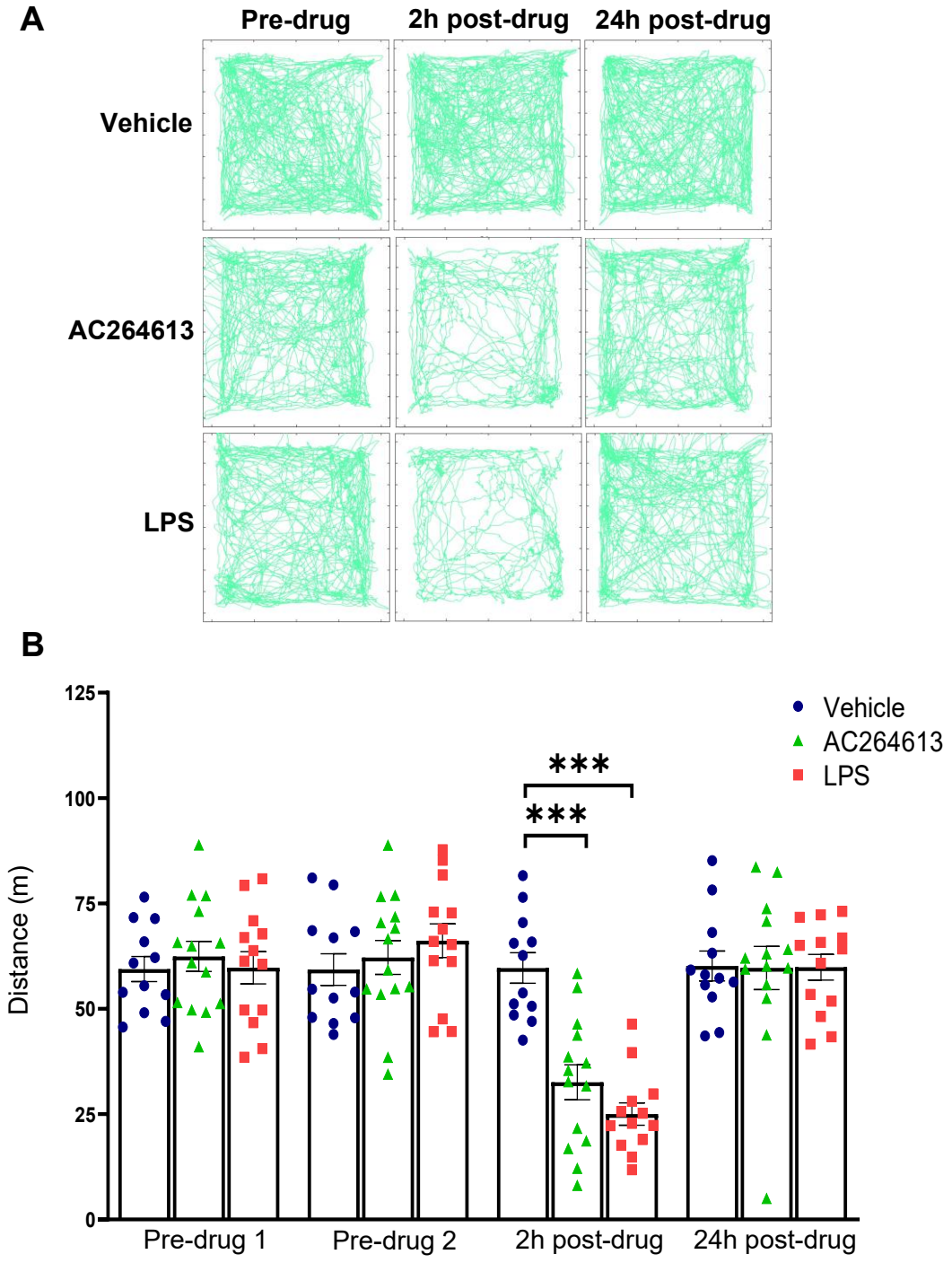

Figure 3.1: AC- and LPS-injection significantly reduced locomotor activity 2h post-injection. (A) Representative OFT tracking traces of an individual mouse's movement during the pre-drug, 2h post- and 24h post-injection for vehicle, AC and LPS. (B) AC (100 mg kg^{-1} i.p.) and LPS (0.5 mg kg^{-1} i.p.) injection significantly reduced locomotor activity in C57BL6/J and $5xFAD^{-/-}$ mice 2h post-injection (AC: ***p<0.001; LPS: ***p<0.001 vs vehicle). Two-way repeated-measures ANOVA with Tukey's post hoc test (n=12 vehicle, n=14 AC, n=13 LPS).

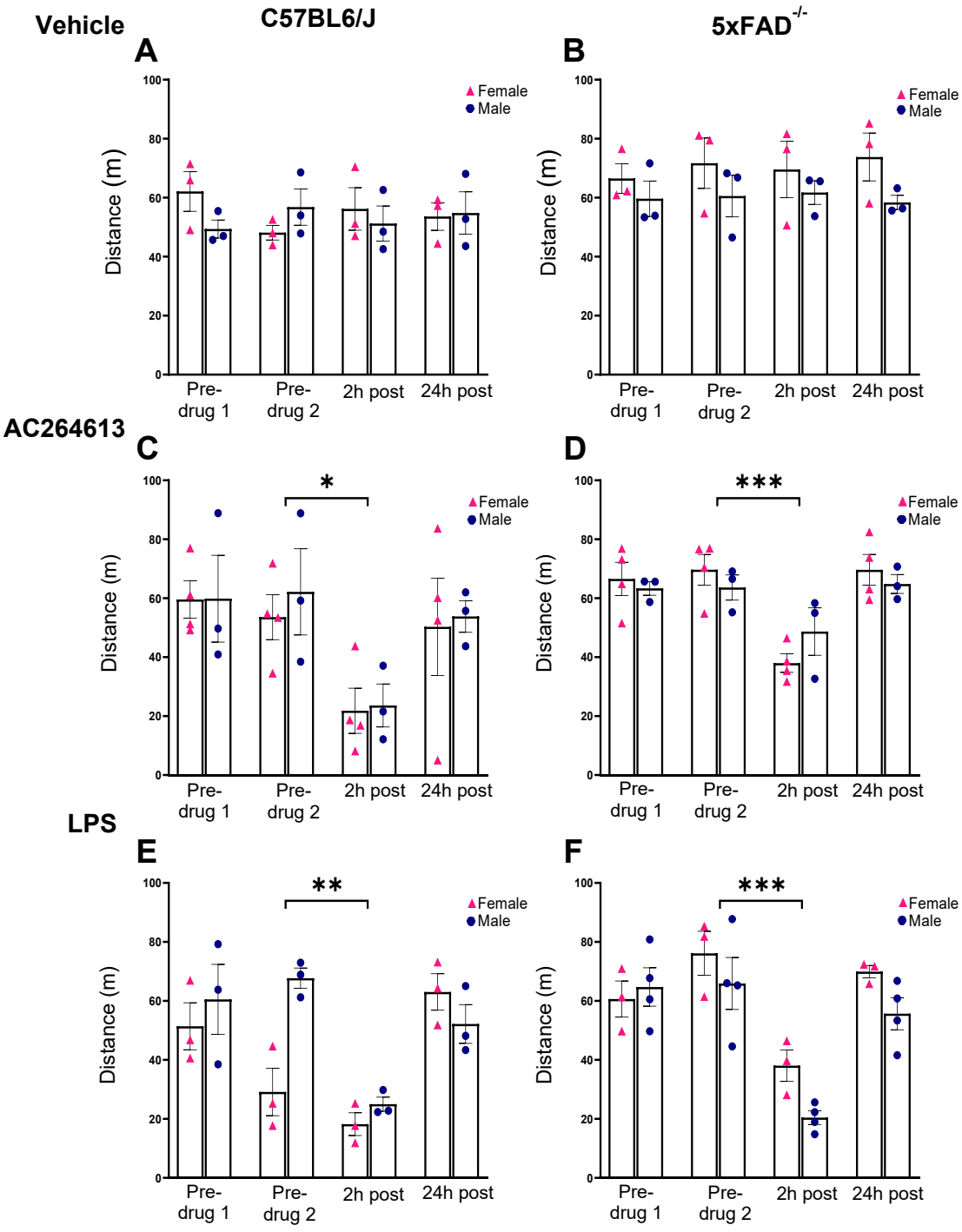

Figure 3.2: AC- and LPS-injection significantly reduced locomotor activity 2h post-injection in both C57BL6/J and 5xFAD$^{-/-}$ mice independent of sex. No sex differences within the genotypes were observed at any time point or following injection of vehicle, AC or LPS. (C-D) AC- and (E-F) LPS-injection significantly reduced locomotor activity overall at 2h-post injection in both C57BL6/J (AC: *p<0.05 vs pre-drug; LPS **p<0.01 vs pre-drug) and 5xFAD$^{-/-}$ mice (AC: ***p<0.001 vs pre-drug; LPS ***p<0.001 vs pre-drug). Two-way repeated-measures ANOVA with Sidak's post hoc test (vehicle: n=3 male vs female; AC: n=4 female vs n=3 male; LPS: n=3 male vs female C57BL6/J, n=3 female vs n=4 male 5xFAD$^{-/-}$).

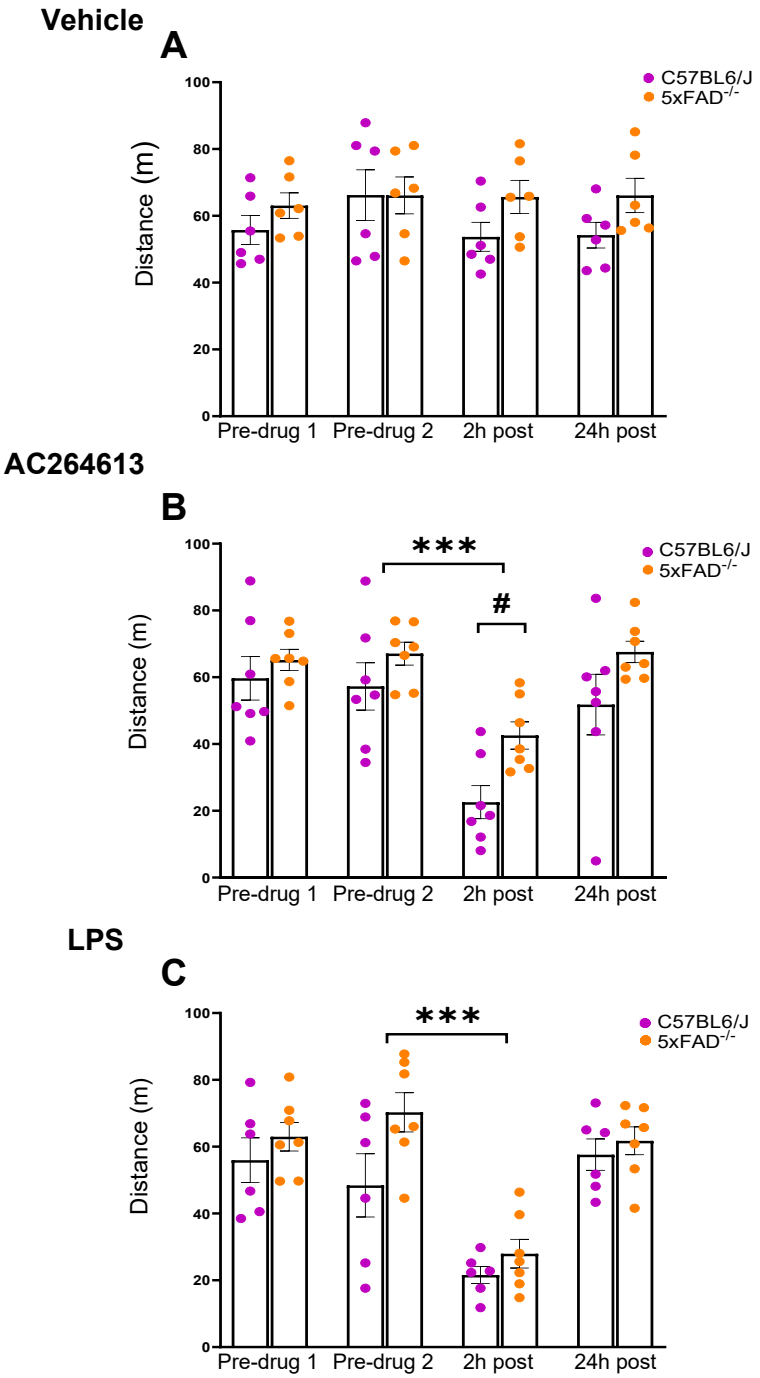

Figure 3.3: AC-injection significantly reduced locomotor activity in C57BL6/J compared to 5xFAD$^{-/-}$ mice at 2h post-injection. No genotypic differences in locomotor activity were observed prior to injection of vehicle, AC or LPS, or post-injection with vehicle or LPS between C57BL6/J and 5xFAD$^{-/-}$ mice. However, at 2h post AC-injection (B), C57BL6/J mice had reduced locomotor activity compared to 5xFAD$^{-/-}$ mice ($^{\#}p<0.05$ C57BL6/J vs 5xFAD$^{-/-}$). This genotypic difference was not observed at 24h post-injection. Overall, AC- and LPS-injection significantly reduced locomotor activity at 2h post injection (AC: ***p<0.001; LPS: ***p<0.001 vs pre-drug). Two-way repeated-measures ANOVA with Sidak's post hoc test (vehicle: n=6 C57BL6/J vs 5xFAD$^{-/-}$; AC: n=7 C57BL6/J vs 5xFAD$^{-/-}$; LPS: n=6 C57BL6/J vs n=7 5xFAD$^{-/-}$).

3.2. AC- and LPS-injection reduced time spent in centre square independent of sex and genotype.

A common test of anxiety-like behaviour in rodent studies measures the amount of time spent in the centre vs edge of the OFT arena, with a greater time spent at the edge relating to higher anxiety-like behaviour. We examined time spent in the centre square, prior to and following injection in the C57BL6/J and 5xFAD$^{-/-}$ mice.

AC- and LPS-injection significantly reduced time spent in centre 2h post-injection (AC: p=0.04 vs pre-drug, n=14; LPS: p=0.01 vs pre-drug, n=13, Fig. 3.4) compared to pre-drug, but no changes were observed 24h post-injection.

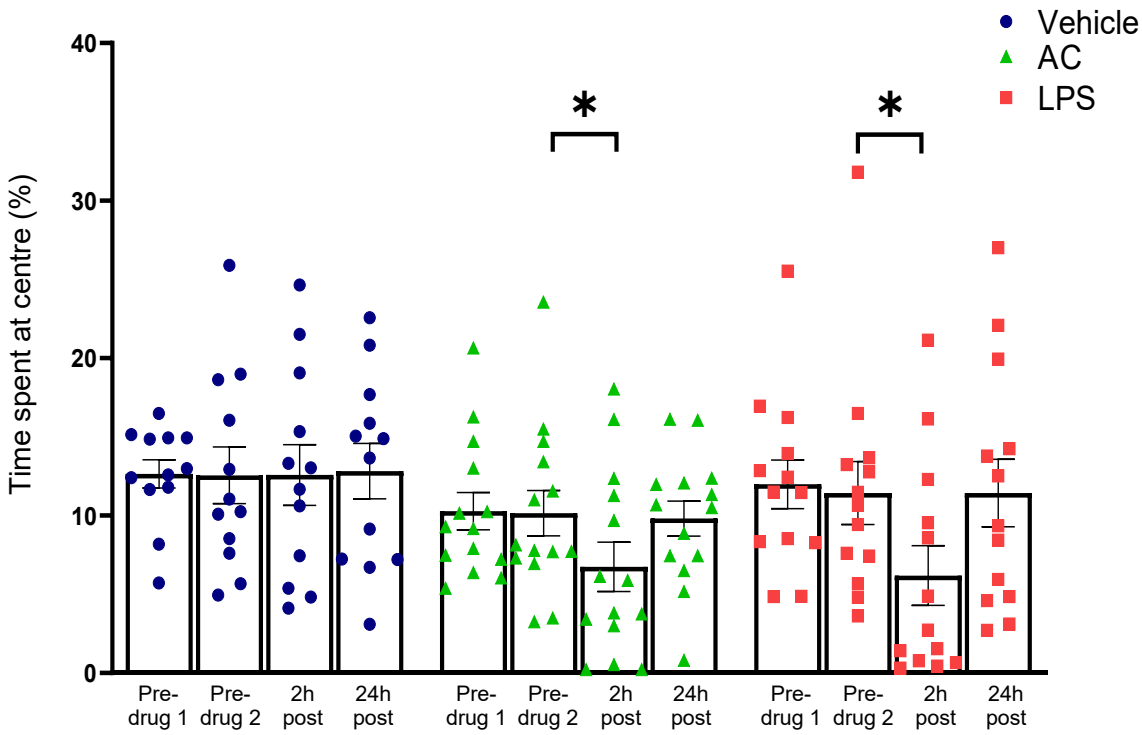

Figure 3.4: AC-injection significantly reduced time spent in the centre square 2h post-injection. AC- and LPS-injection significantly reduced time spent in the centre of the OFT box in C57BL6/J and 5xFAD$^{-/-}$ mice 2h post-injection (AC: *p<0.05; LPS: *p<0.05, vs pre-drug). Two-way repeated-measures ANOVA with Tukey's post hoc test (n=12 vehicle, n=14 AC, n=13 LPS).

In contrast, vehicle injection had no effect on time spent in centre at 2h or 24h post-injection ($p>0.99$ vs pre-drug, n=12, Fig. 3.4).

Examining sex within the genotypes found no differences between males and females in time spent in centre prior to, or following injection of vehicle, AC or LPS (vehicle: $F_{(1-4)} = 0.03$, $p=0.88$ C57BL6/J male vs female, n=3, Fig.3.5A; $F_{(1-4)} = 4.25$, $p=0.11$ 5xFAD$^{-/-}$ male vs female, n=3, Fig.3.5B; AC: $F_{(1-5)} = 1.43$, $p=0.29$ C57BL6/J male, n=3, vs female, n=4, Fig.3.5C; $F_{(1-5)} = 0.09$, $p=0.78$ 5xFAD$^{-/-}$ male, n=3, vs female, n=4, Fig.3.5; LPS: $F_{(1-4)} = 5.74$, $p=0.07$ C57BL6/J male vs female, n=3, Fig.3.5E, $F_{(1-5)} = 1.54$, $p=0.27$ 5xFAD$^{-/-}$ male, n=4, vs female, n=3, Fig.3.5F). However, LPS-injected C57BL6/J female mice showed a trend towards increased time spent at centre compared to males across the time points ($p=0.07$, male vs female, n=3, Fig 3.5E). Overall, AC-injection reduced time spend at centre at 2h post-injection in C57BL6/J ($p=0.02$ vs pre-drug, n=7, Fig.3.5C) but not 5xFAD$^{-/-}$ mice.

Genotypic differences were also examined and no differences were found in time spent in the centre square between C57BL6/J and 5xFAD$^{-/-}$ mice prior to or following injection (vehicle: $F_{(1-10)} = 0.06$, $p=0.82$, C57BL6/J vs 5xFAD$^{-/-}$, n=6, Fig.3.6A; AC: $F_{(1-12)} = 0.27$, $p=0.62$, C57BL6/J vs 5xFAD$^{-/-}$, n=7, Fig.3.6B; LPS: $F_{(1-11)} = 0.08$, $p=0.78$, C57BL6/J, n=6, vs 5xFAD$^{-/-}$, n=7, Fig.3.6C). Overall, at 2h post-injection, AC and LPS significantly reduced time spent in the centre (AC: $p=0.05$ vs pre-drug, n=14, Fig.3.6B; LPS: $p=0.02$ vs pre-drug, n=13, Fig.3.6C).

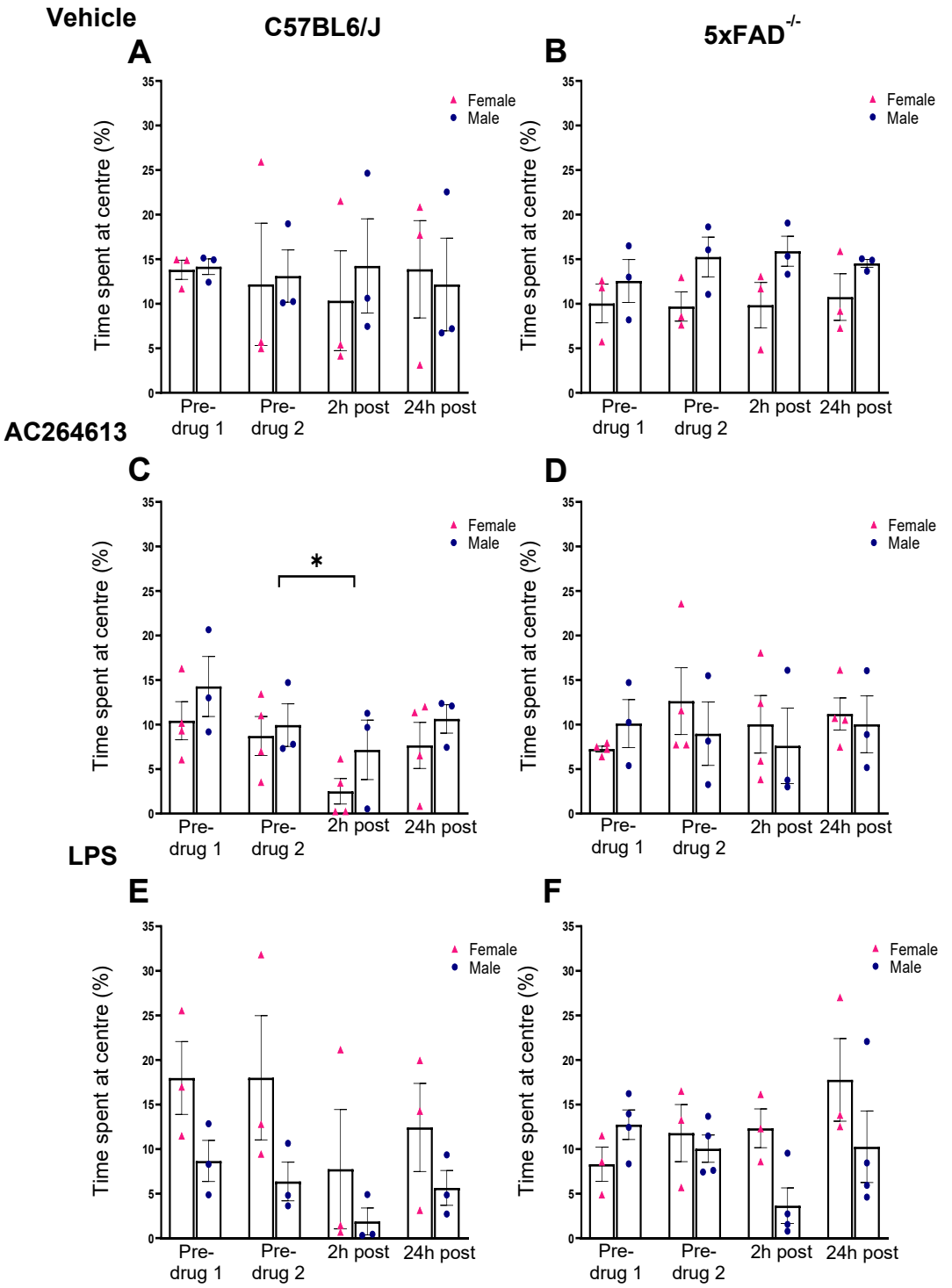

Figure 3.5: AC-injection reduced time spent in centre square 2h post-injection and is independent of sex. No sex differences within the genotypes were observed at any time point or following injection of vehicle, AC or LPS in time spent at centre in the OFT arena. AC-injection significantly reduced time spent at centre overall at 2h-post injection in C57BL6/J (*$p<0.05$ vs pre-drug) but not 5xFAD$^{-/-}$ mice. Two-way repeated-measures ANOVA with Sidak's post hoc test (vehicle: n=3 male vs female; AC: n=4 female vs n=3 male; LPS: n=3 male vs female C57BL6/J, n=3 female vs n=4 male 5xFAD$^{-/-}$).

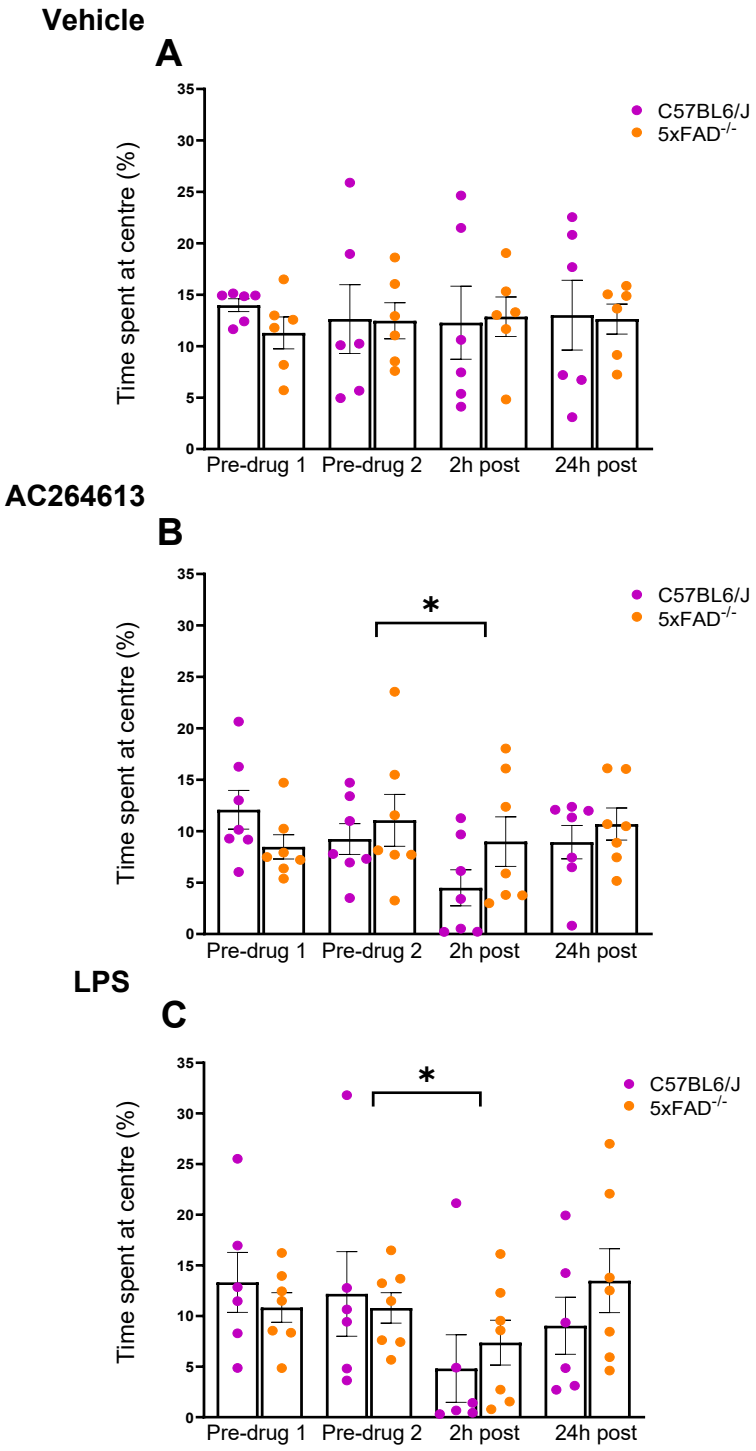

Figure 3.6: AC- and LPS-injection reduced time spent in the centre square 2h post-injection is genotype independent. No genotypic differences in time spent at centre of the OFT arena were observed at any time point prior to, or post injection with vehicle, AC or LPS between C57BL6/J and 5xFAD$^{-/-}$ mice. AC- and LPS-injection significantly reduced time spent at centre overall at 2h post injection (AC: *p<0.05 vs pre-drug; LPS: *p<0.05 vs pre-drug). Two-way repeated-measures ANOVA with Sidak's post hoc test (vehicle: n=6 C57BL6/J vs 5xFAD$^{-/-}$; AC: n=7 C57BL6/J vs 5xFAD$^{-/-}$; LPS: n=6 C57BL6/J vs n=7 5xFAD$^{-/-}$).

3.3. AC-injection reduced sucrose preference independent of sex and genotype.

The sucrose preference test was used to examine anhedonia in the mice. AC-injection significantly reduced sucrose preference 2h post-injection (p=0.02 vs pre-drug, n=14, Fig.3.7) when compared to pre-drug. This reduction was recovered by 24h post-injection. LPS-injection non-significantly reduced sucrose preference at 2h post-injection (p=0.06 vs pre-drug, n=13, Fig.3.7). No significant change in sucrose preference was observed following vehicle injection (p=0.5 vs pre-drug, n=12, Fig.3.7).

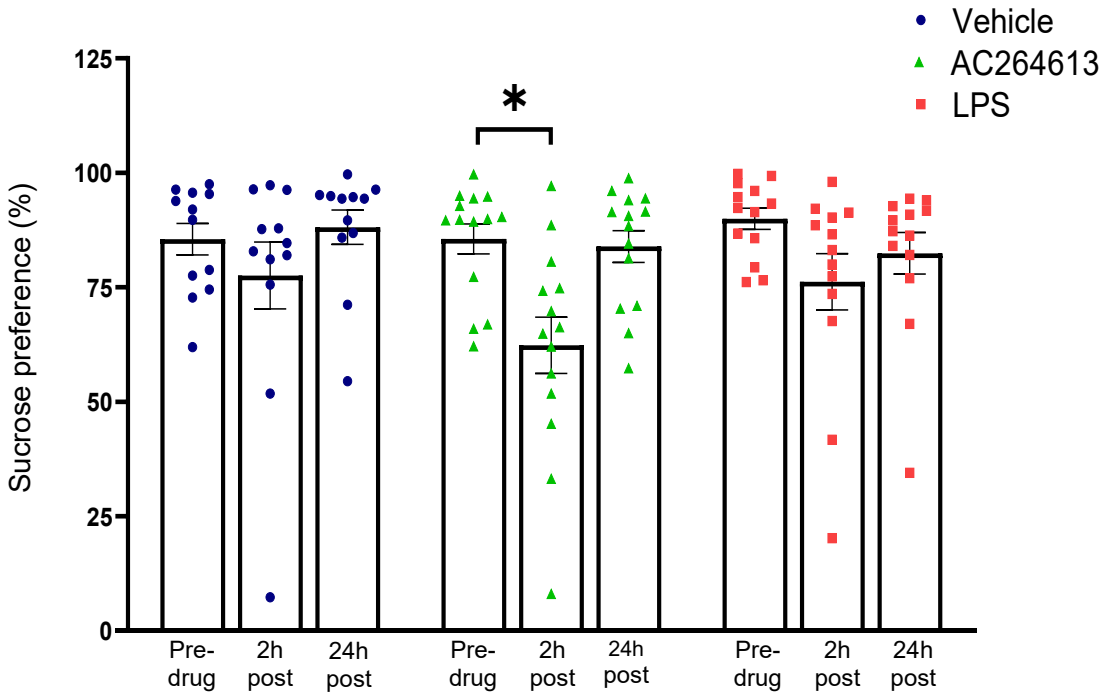

Figure 3.7: AC-injection significantly reduced sucrose preference 2h post-injection. AC-injection significantly reduced sucrose preference in C57BL6/J and 5xFAD$^{-/-}$ mice 2h post-injection (*p<0.05 vs pre-drug) which was recovered by 24h post-injection. LPS-injection non-significantly reduced sucrose preference 2h post-injection (p=0.06 vs pre-drug). No significant change in sucrose preference was observed following vehicle-injection. Two-way repeated-measures ANOVA with Tukey's post hoc test (n=12 vehicle, n=14 AC, n=13 LPS).

The observed reduction in sucrose preference was independent of sex when examined within genotypes following vehicle, AC- and LPS-injection (vehicle: $F_{(1-4)}$ = 0.95, p=0.38 C57BL6/J male vs female, n=3, Fig 3.8A; $F_{(1-4)}$ = 0.38, p=0.57 5xFAD$^{-/-}$ male vs female, n=3, Fig.3.8B; AC: $F_{(1-5)}$ = 1.22, p=0.32 C57BL6/J male, n=3, vs female, n=4, Fig.3.8C; $F_{(1-5)}$ = 0.17, p=0.7 5xFAD$^{-/-}$ male, n=3, vs female, n=4, Fig.3.8D; LPS: $F_{(1-4)}$ = 7.42, p=0.053 C57BL6/J male vs female, n=3, Fig.3.8E, $F_{(1-5)}$ = 0.58, p=0.48 5xFAD$^{-/-}$ male, n=4, vs female, n=3, Fig.3.8F). Overall, AC-injection non-significantly reduced sucrose preference in both C57BL6/J ($F_{(1-7)}$ = 4.9, p=0.058 vs pre-drug, n=7, Fig.3.8C) and 5xFAD$^{-/-}$ mice 2h post-injection ($F_{(1-5)}$ = 5.42, p=0.066 vs pre-drug, n=7, Fig.3.8D).

When sucrose preference was examined between the genotypes, no differences were found between C57BL6/J and 5xFAD$^{-/-}$ prior to or following injection (vehicle: $F_{(1-10)}$ = 0.37, p=0.56 C57BL6/J vs 5xFAD$^{-/-}$, n=6, Fig.3.9A; AC: $F_{(1-12)}$ = 0.43, p=0.52 C57BL6/J vs 5xFAD$^{-/-}$, n=7, Fig.3.9B; LPS: $F_{(1-11)}$ = 1.43, p=0.26 C57BL6/J, n=6, vs 5xFAD$^{-/-}$, n=7, Fig.3.9C). Overall, AC- and LPS-injection reduced sucrose preference across the time points (AC: $F_{(1-14)}$ = 10.01, p=0.005, n=14, Fig.3.9B; LPS: $F_{(2-18)}$ = 5.78, p=0.015, n=13, Fig.3.9C).

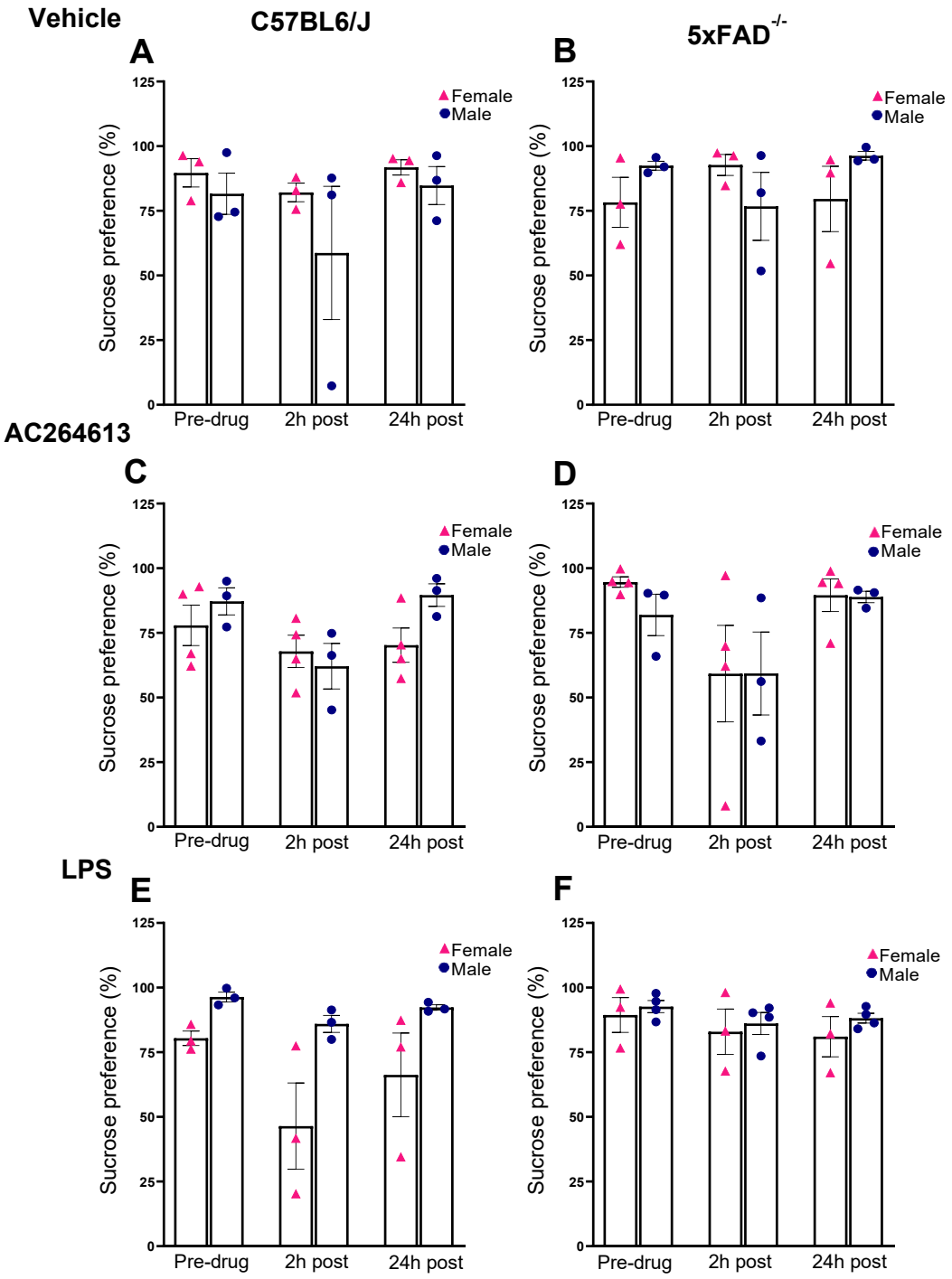

Figure 3.8: AC-injection reduced sucrose preference 2h post-injection in both C57BL6/J and 5xFAD$^{-/-}$ mice and is independent of sex. No sex differences within the genotypes were observed following injection of vehicle, AC or LPS. AC-injection non-significantly reduced sucrose preference 2h-post injection in both C57BL6/J ($p=0.058$ vs pre-drug) and 5xFAD$^{-/-}$ mice ($p=0.066$ vs pre-drug). Two-way repeated-measures ANOVA with Sidak's post hoc test (vehicle: n=3 male vs female; AC: n=4 female vs n=3 male; LPS: n=3 male vs female C57BL6/J, n=3 female vs n=4 male 5xFAD$^{-/-}$).

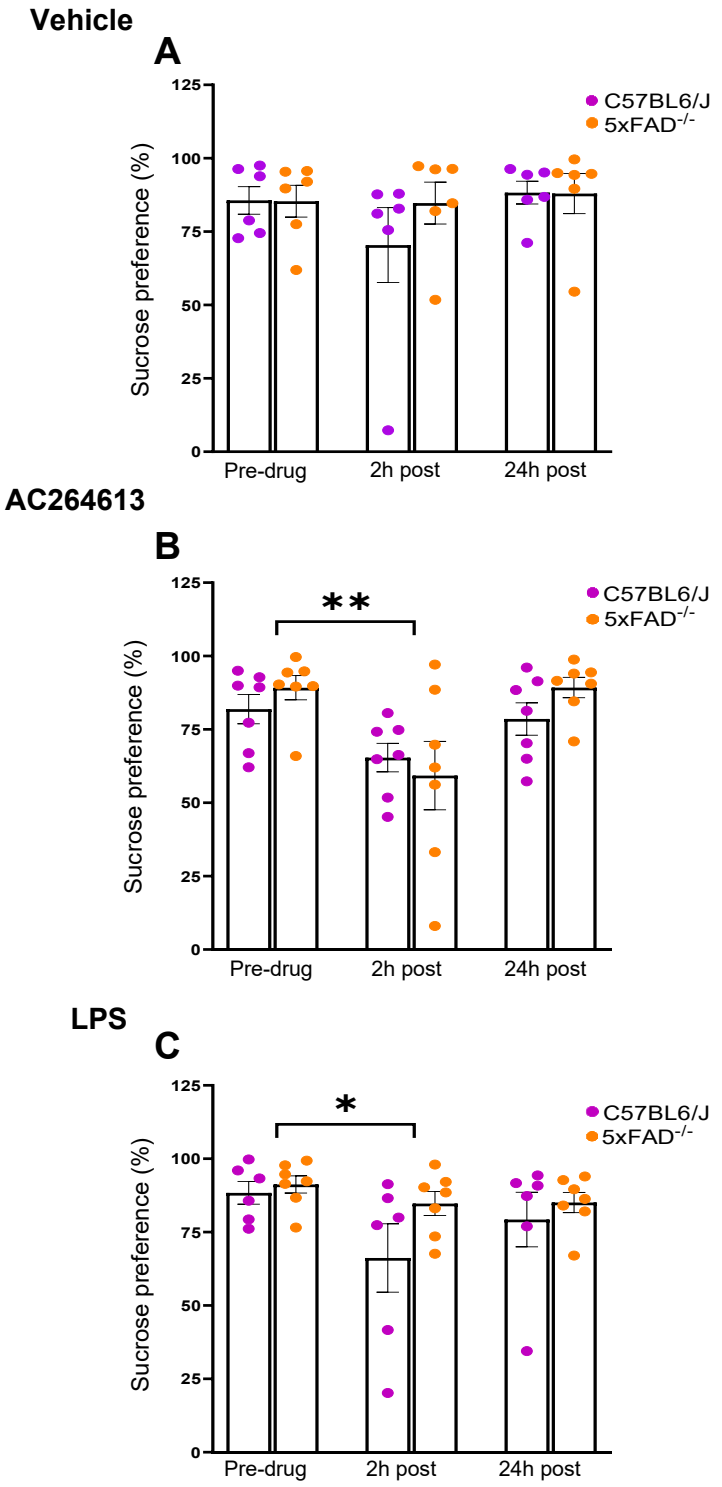

Figure 3.9: AC- and LPS-injection reduced sucrose preference across the timepoints with no difference between genotypes. No genotypic differences in sucrose preference were observed prior to, or following injection of vehicle, AC or LPS. Overall, AC- and LPS-injection induced a significant reduction in sucrose preference across the timepoints (AC: **p<0.01; LPS: *p<0.01, vs pre-drug). Two-way repeated-measures ANOVA with Sidak's post hoc test (vehicle: n=6 C57BL6/J vs 5xFAD$^{-/-}$; AC: n=7 C57BL6/J vs 5xFAD$^{-/-}$; LPS: n=6 C57BL6/J vs n=7 5xFAD$^{-/-}$).

3.4. LPS- but not AC-injection reduced time spent grooming.

Having established that both AC and LPS induced behavioural changes associated with depression-like behaviour, we next examined grooming behaviour using the splash test to assess apathy-like behaviour following AC- and LPS-injection. To analyse the grooming behaviour recordings, we implemented AI machine learning using DLC software (Mathis *et al.*, 2018) followed by the SaLSa MatLab script (Sakata, 2023) to measure total time spent grooming, time to first groom, and number of grooming episodes. We also scored the recordings manually with a stopwatch and measured total time spent grooming, time to first face wipe, and time to sit and groom for >5 seconds. The two methods of analysis yielded differing results suggesting sensitivity issues with AI machine learning analysis.

3.4.1. AI machine learning analysis suggested AC-injection increased grooming behaviour 2h post-injection.

AI machine learning analysis of the splash test found a significant increase in the total time spent grooming 2h post-injection in AC-injected mice (p=0.002 vs vehicle, n=14, Fig.3.10A) when compared to vehicle-injected mice. LPS-injection had no effect on total time spent grooming compared to vehicle at 2h post-injection (p=0.17 vs vehicle, n=13, Fig.3.10A). There was an overall increase in time spent grooming at 2h post-injection compared to 24h post-injection across the treatment groups ($F_{(1\text{-}36)}$ = 48.55, p<0.001 2h post-vs 24h post-drug, n=39, Fig.3.10A).

No difference in time to first groom was observed between the treatment groups at 2h post-injection (AC: p=0.96 vs vehicle, n=14, Fig.3.10B; LPS:

p=0.95 vs vehicle, n=13, Fig.3.10B) or 24h post-injection (AC: p=0.13 vs vehicle, n=14, Fig.3.10B; LPS: p=0.74 vs vehicle, n=13, Fig.3.10B), and no difference was observed in time to first groom across the timepoints ($F_{(1-36)}$ = 0.94, p=0.34 2h post-vs 24h post-drug, n=39, Fig.3.10B).

There was a significant increase in the number of grooming episodes at 2h post-injection compared to 24h post-injection ($F_{(1-36)}$ = 18.63, p<0.001 2h post-vs 24h post-drug, n=39, Fig.3.10C) but no significant differences in were found between the treatment groups at 2h post-injection (AC: p=0.09 vs vehicle, n=14, Fig.3.10C; LPS: p=0.47 vs vehicle, n=13, Fig.3.10).

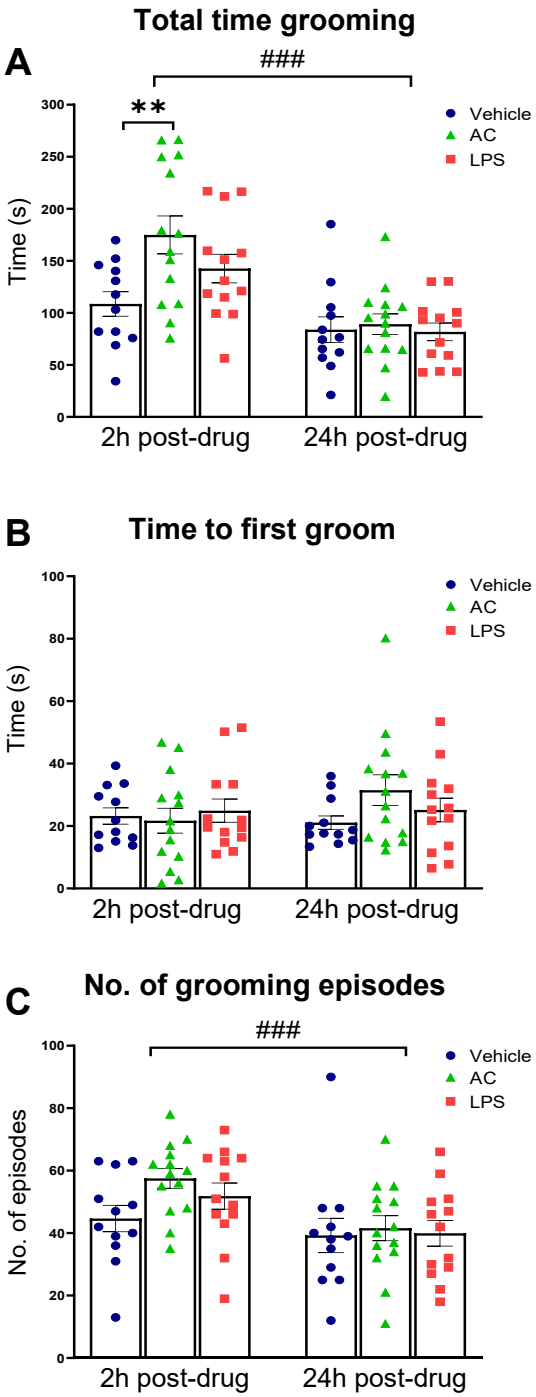

Figure 3.10: AI machine learning analysis suggests that AC-injection significantly increased time spent grooming 2h post-injection. When analysed with AI machine learning, AC-injection increased total time spent grooming (**p<0.01 vs vehicle) 2h post-injection. Overall, grooming time was increased 2h post-injection across the treatments ($^{###}$p<0.001 2h post- vs 24h post-drug). No differences in time to first groom were observed between the treatments or timepoints. There was an overall increase in number of grooming episodes at 2h post-injection across the treatment groups ($^{###}$p<0.001 2h post- vs 24h post-drug) but no differences in grooming episodes were observed between the treatments. Two-way repeated-measures ANOVA with Tukey's post hoc test (n=12 vehicle, n=14 AC, n=13 LPS).

3.4.2. Manual scoring analysis reveals LPS- but not AC-injection reduced grooming behaviour.

As manual scoring was the standard method described in the literature to assess grooming behaviour (Isingrini *et al.*, 2010), we also used manual scoring to verify our splash test results. Manual scoring revealed that AC-injection had no effect on time spent grooming at either 2h post-injection (p=0.99 vs vehicle, n=14, Fig.3.11A) or 24h post-injection (p=0.93 vs vehicle, n=14, Fig.3.11A). However, LPS-injection significantly reduced time spent grooming 2h post-injection (p=0.004 vs vehicle, n=13, Fig.3.11A) compared to vehicle. At 24h post-injection, LPS-injected mice had recovered and significantly increased their time spent grooming compared to 2h post-injection (p=0.03 2h post vs 24h post-drug, n=13, Fig.3.11A).

As the mice frequently exhibited brief hyperactive behaviour following sucrose water spraying and placement in the test box, the time to first wipe their face and the latency to settle and initiate grooming for at least 5 seconds was also measured. No differences in time to first face wipe were observed between the treatment groups at 2h post-injection (AC: p=0.62 vs vehicle, n=14, Fig.3.11B; LPS: p=0.99 vs vehicle, n=13, Fig.3.11B) or 24h post-injection (AC: p=0.41 vs vehicle, n=14, Fig.3.11B; LPS: p=0.15 vs vehicle, n=13, Fig.3.11B), and no differences were observed in time to first face wipe across the timepoints ($F_{(1-36)}$ = 0.09, p=0.77 2h post-vs 24h post-drug, n=39, Fig.3.11B). Further, no differences in time to sit and groom > 5 s were observed between the treatment groups at 2h post-injection (AC: p=0.99 vs vehicle, n=14, Fig.3.11C; LPS: p=0.32 vs vehicle, n=13, Fig.3.11C) or 24h post-injection (AC: p=0.22 vs

vehicle, n=14, Fig.3.11C; LPS: p=0.11 vs vehicle, n=13, Fig.3.11C), and no differences were observed in time to sit and groom > 5 s across the timepoints ($F_{(1-36)}$ = 0.44, p=0.51 2h post-vs 24h post-drug, n=39, Fig.3.11C).

When the videos were analysed with hand scoring, it was observed that the behaviour displayed in the recording often misaligned with the machine learning classifications, highlighting sensitivity issues with the AI software. Due to this, behaviour that was not grooming, such as being immobile, was being classified as grooming, thus giving inaccurate results. Therefore, it was deemed that manual hand scoring was more accurate for analysing grooming behaviour, hence manual scoring was the adopted method for analysing the splash test data.

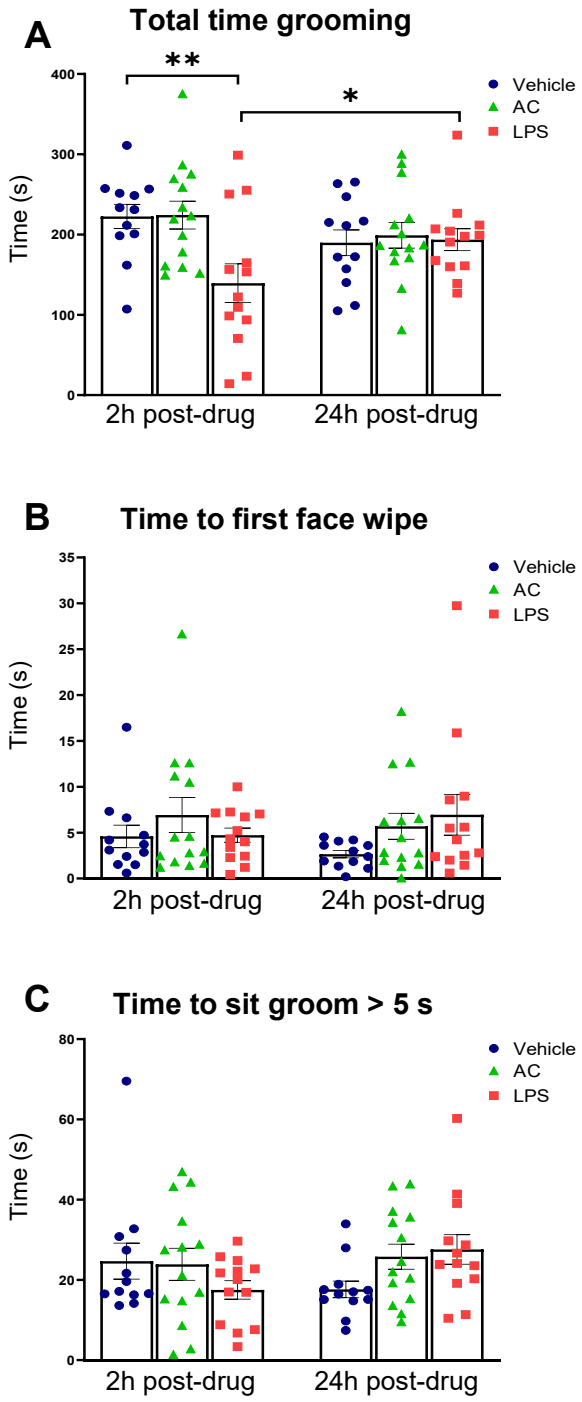

Figure 3.11: Manual scored grooming revealed that AC-injection had no effect on time spent grooming. When analysed using manual scoring, AC-injection had no effect on grooming time 2h post-injection. LPS-injection significantly reduced total time grooming 2h post-injection (**p<0.01 vs vehicle). Overall, there was no difference in time spent grooming between 2h post- or 24h post-injection across the treatments, however there was a significant decrease in total time grooming in LPS-injected mice at 2h post-injection compared to 24h post-injection (*p<0.05 2h post- vs 24h post-drug). No differences in time to first face wipe or time to sit and groom for > 5 s were observed between the treatments or timepoints. Two-way repeated-measures ANOVA with Tukey's and Sidak's post hoc test (n=12 vehicle, n=14 AC, n=13 LPS).

3.4.3. Sex and genotype had no effect on time spent grooming 2h post-injection independent of treatment.

When sex was examined within the genotypes, no differences were found in grooming time between male and female mice 2h post-injection following vehicle, AC- or LPS-injection (vehicle: $F_{(1-4)}$ = 0.8, p=0.42 C57BL6/J male vs female, n=3, Fig.3.12A; $F_{(1-4)}$ = 0.03, p=0.87 5xFAD$^{-/-}$ male vs female, n=3, Fig.3.12B; AC: $F_{(1-5)}$ = 3.4, p=0.12 C57BL6/J male, n=3, vs female, n=4, Fig.3.12C; $F_{(1-5)}$ = 0.79, p=0.42 5xFAD$^{-/-}$ male, n=3, vs female, n=4, Fig.3.12D; LPS: $F_{(1-4)}$ = 4.7, p=0.1 C57BL6/J male vs female, n=3, Fig.3.12E; $F_{(1-5)}$ = 0.38 p=0.56 5xFAD$^{-/-}$ male, n=4, vs female, n=3, Fig.3.12F). No sex differences were found at 24h post-injection in the vehicle or LPS-injected mice but AC-injected female C57BL6/J mice groomed more than males (p=0.03 male, n=3, vs female, n=4, Fig.3.12C). No sex differences were found in AC-injected 5xFAD$^{-/-}$ mice. Overall, vehicle-injected female C57BL6/J mice groomed more at 2h post-injection than 24h post-injection (p=0.048 2h post-vs 24h post-drug).

No differences were observed in time spent grooming between C57BL6/J and 5xFAD$^{-/-}$ mice within the treatment groups at 2h or 24h post-injection (vehicle: $F_{(1-10)}$ = 1.96, p=0.19 C57BL6/J vs 5xFAD$^{-/-}$, n=6, Fig.3.13A; AC: $F_{(1-12)}$ = 0.29, p=0.6 C57BL6/J vs 5xFAD$^{-/-}$, n=7, Fig.3.13B; LPS: $F_{(1-11)}$ = 0.65, p=0.44, C57BL6/J, n=6, vs 5xFAD$^{-/-}$, n=7, Fig.3.13C). Overall, vehicle-injected C57BL6/J mice groomed more at 2h post-injection compared to 24h post-injection (p=0.04 2h post-vs 24h post-drug, n=6, Fig.3.13A) and AC-injected 5xFAD$^{-/-}$ mice groomed more at 2h post-injection than at 24h post-injection (p=0.04 2h post-vs 24h post-drug, n=7, Fig.3.13B).

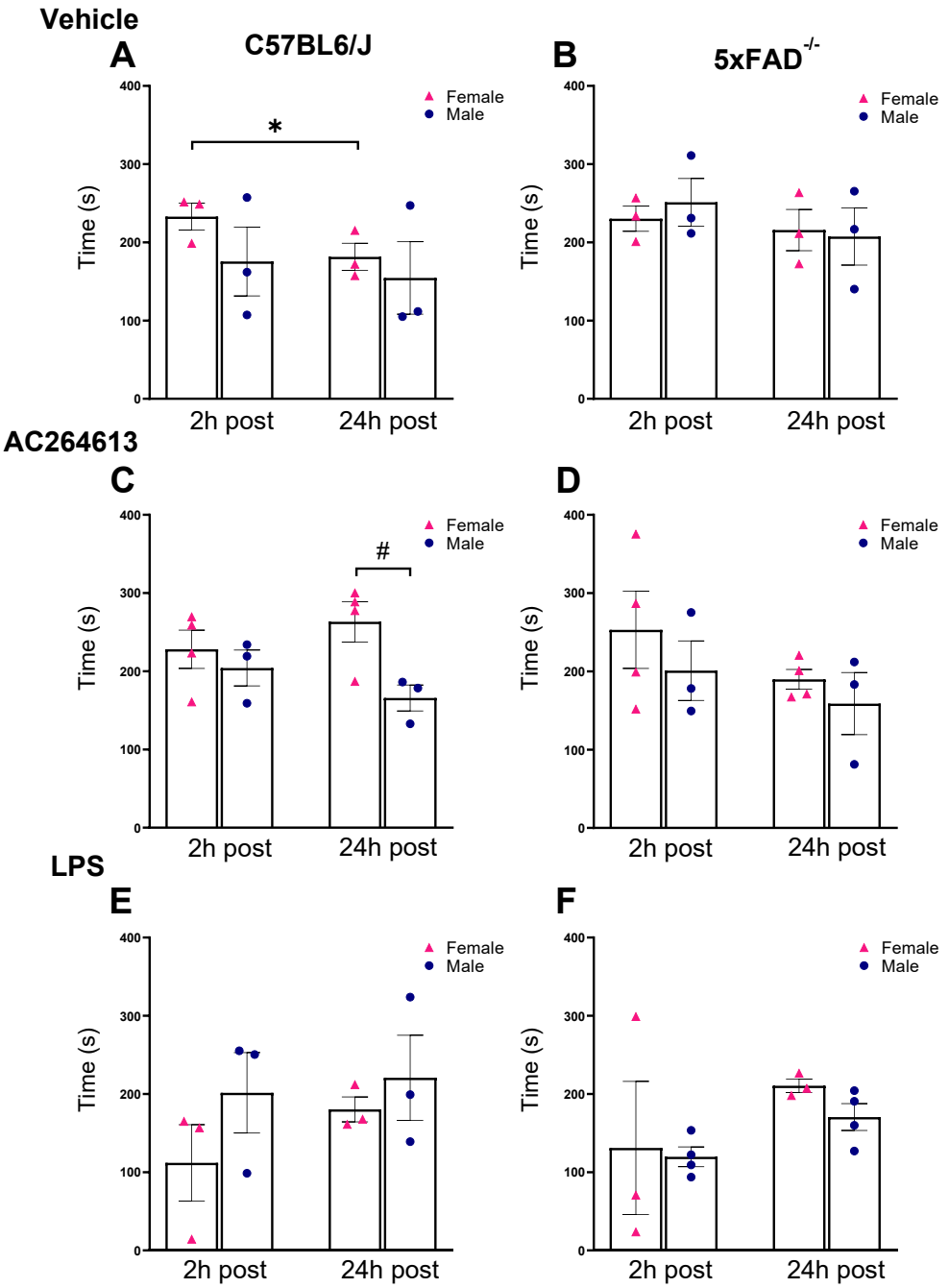

Figure 3.12: AC- and LPS-injection had no influence on time spent grooming in either sex within the genotypes 2h post-injection. No differences in total time grooming between males and females of either genotype were found 2h post-injection with vehicle, AC or LPS. However, at 24h post AC-injection, female C57BL6/J mice groomed significantly longer than male C57BL6/J ($^{\#}p<0.05$ male vs female). This behaviour was not observed in AC-injected 5xFAD$^{-/-}$ mice. Overall, vehicle-injected female C57BL6/J mice groomed significantly more at 2h post-injection compared to 24h post-injection (*p<0.05 2h post vs 24h post-drug). Two-way repeated-measures ANOVA with Sidak's post hoc test (vehicle: n=3 male vs female; AC: n=4 female vs n=3 male; LPS: n=3 male vs female C57BL6/J, n=3 female vs n=4 male 5xFAD$^{-/-}$).

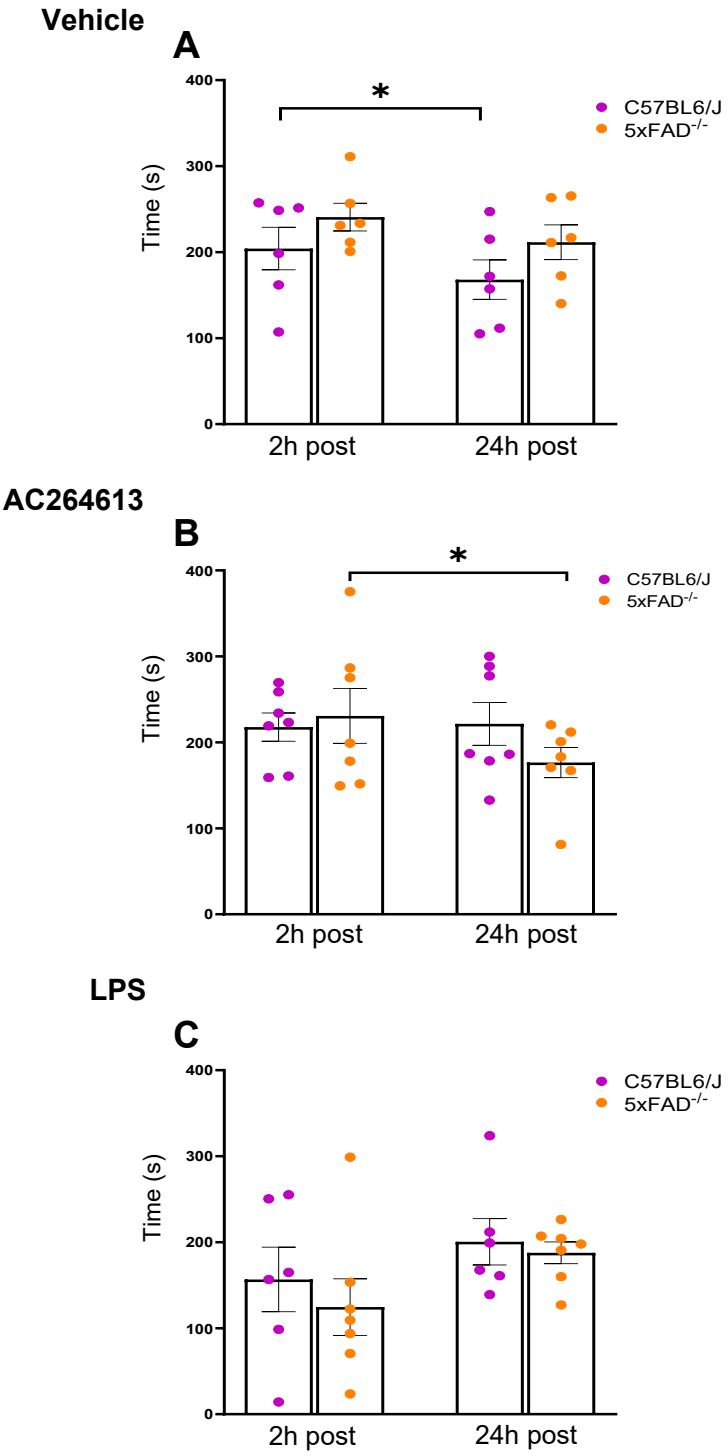

Figure 3.13: Genotype has no effect on total time spent grooming at 2h post- or 24h post-injection independent of treatment group. No genotypic differences in time spent grooming were observed prior to, or following injection of vehicle, AC or LPS. Overall, C57BL6/J mice that received vehicle-injection groomed longer at 2h post-injection compared to 24h post-injection (*p<0.01 2h post- vs 24h post-drug) and AC-injected 5xFAD$^{-/-}$ mice groomed significantly more at 2h post-injection compared to 24h post-injection (*p<0.01 2h post- vs 24h post-drug). Two-way repeated-measures ANOVA with Sidak's post hoc test (vehicle: n=6 C57BL6/J vs 5xFAD$^{-/-}$; AC: n=7 C57BL6/J vs 5xFAD$^{-/-}$; LPS: n=6 C57BL6/J vs n=7 5xFAD$^{-/-}$).

3.5. AC- and LPS-injection induced temporary weight loss.

Mice were weighed daily starting from the pre-drug OFT recordings, until 1 week post final injection. During the first week of testing, at 24h post-injection, AC-injection significantly reduced female mice weight compared to pre-drug weight ($p=0.048$ vs pre-drug, n=8, Fig.3.14A). LPS-injection significantly reduced weight 24h post-injection in both female ($p=0.009$ vs pre-drug, n=6 Fig.3.14A) and male ($p<0.001$ vs pre-drug, n=7, Fig.3.14B) mice. During the second week of testing, AC-injection had no significant effect on weight at 24h post- injection in female ($p=0.38$ vs pre-drug, n=8, Fig.3.14A) or male mice ($p>0.99$ vs pre-drug, n=6, Fig.3.14B). LPS-injection had no significant effect on female mice ($p=0.21$ vs pre-drug, n=6, Fig.3.14A) but male mice had significantly reduced weight at 24h post-injection ($p<0.001$ vs pre-drug, n=7, Fig.3.14B). Any weight lost was temporary and never > 20% of the mouse's pre-drug weight, and all mice had fully recovered by the next weighing timepoint (day 7 and 12).

No genotypic differences in weight were found at any timepoint across any of the treatment groups for female mice (vehicle: $F_{(1-4)} = 0.11$, $p=0.76$ C57BL6/J vs 5xFAD$^{-/-}$, n=3; AC: $F_{(1-6)} = 0.11$, $p=0.74$ C57BL6/J vs 5xFAD$^{-/-}$, n=4; LPS: $F_{(1-4)} = 0.33$, $p=0.6$ C57BL6/J vs 5xFAD$^{-/-}$, n=3) or male mice (vehicle: $F_{(1-7)} = 1.2$, $p=0.31$ C57BL6/J vs 5xFAD$^{-/-}$, n=3; AC: $F_{(1-4)} = 0.32$, $p=0.6$ C57BL6/J vs 5xFAD$^{-/-}$, n=3; LPS: $F_{(1-5)} = 0.004$, $p=0.95$ C57BL6/J vs 5xFAD$^{-/-}$, n=3). Therefore, weight graphs were combined to display mean ± S.E.M. weight across time for female and male mice.

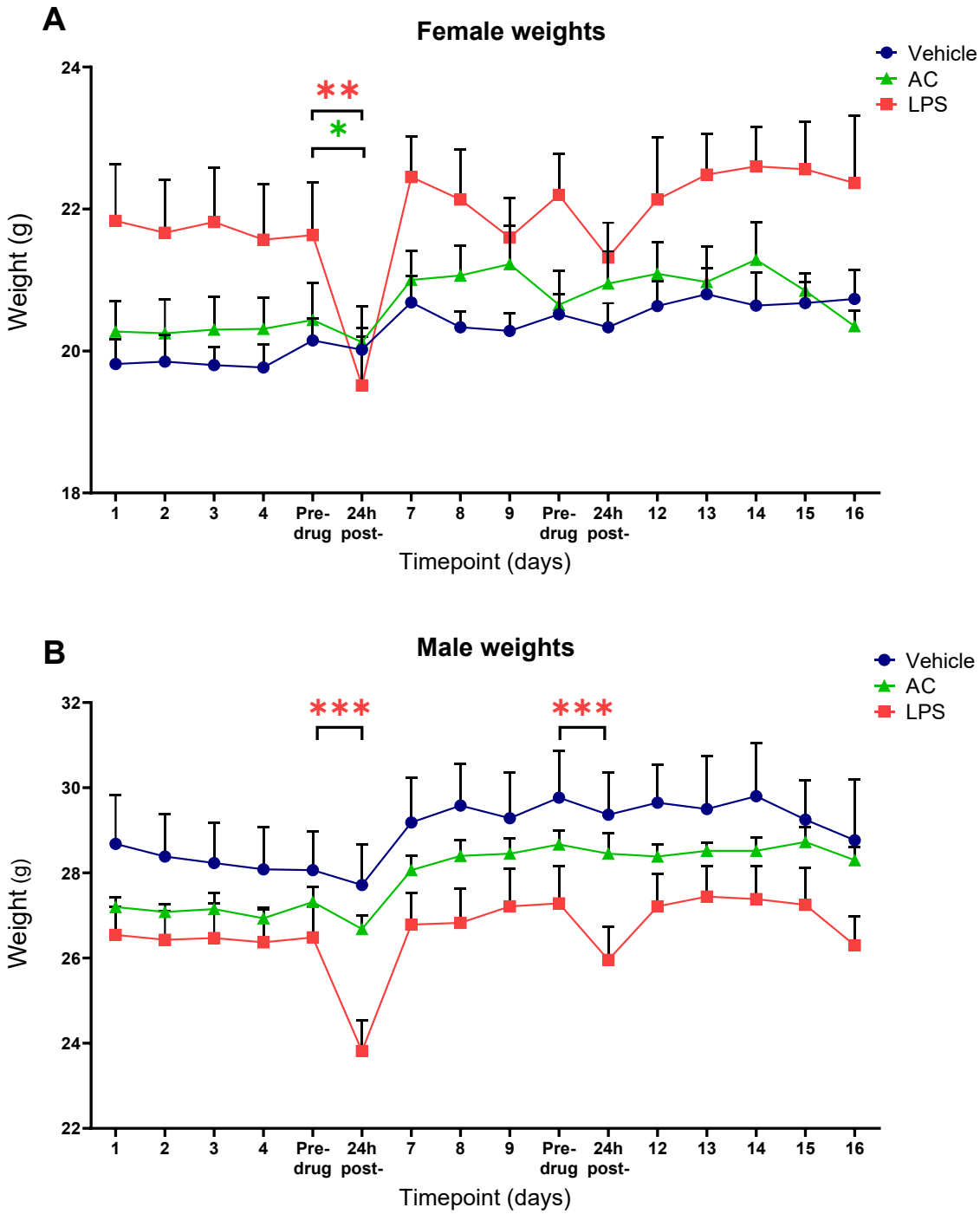

Figure 3.14: AC- and LPS-injection cause a temporary reduction in weight independent of genotype. AC- and LPS-injection induced a significant reduction in weight at 24h-post injection in the first week of testing in female (AC: *p<0.05; LPS: **p<0.01 pre-drug vs 24h post-drug) mice, whilst LPS but not AC-injection induced a significant reduction in male weight post-injection (***p<0.001 pre-drug vs 24h post-drug). AC-injection had no effect on weight in the second week of testing, but LPS induced a trend of weight loss in female mice and a significant reduction in weight in male mice (***p<0.001 pre-drug vs 24h post-drug). Weight displayed as mean ± SEM. Mixed model's analysis with Tukey's post hoc test (vehicle: n=6 female, 6 male; AC: n=8 female, 6 male; LPS: n=6 female, 7 male).

3.6. Discussion

3.6.1. AC264613 and LPS induce behavioural changes associated with depression-like behaviour in C57BL6/J and 5xFAD$^{-/-}$ mice.

Our data from both C57BL6/J and 5xFAD$^{-/-}$ mice confirmed that AC (100 mg kg^{-1}) and LPS (0.5 mg kg^{-1}) induced behavioural changes associated with depression-like behaviour as demonstrated by reduced locomotor activity and reduced sucrose preference, suggesting the mice are experiencing low mood, fatigue, and anhedonia, which are major symptoms in patients with MDD. These findings further support previous studies within the research group that AC induces depression-like behaviour similar to LPS induced sickness-like behaviour (Abulkassim *et al.*, 2016; Moudio *et al.*, 2022).

3.6.2. AC264613 and LPS reduced locomotor activity and increased anxiety-like behaviour in C57BL6/J and 5xFAD$^{-/-}$ mice.

Locomotor and exploratory activity are natural behaviours in rodents and reductions in these behaviours are associated with anxiety- and depression-like behaviour (Seibenhener *et al.*, 2015; Wang *et al.*, 2017; Becker *et al.*, 2021). Studies of social defeat and stress-induced depression-like behaviour models report decreased locomotor activity and exploratory behaviour that can be reversed with anxiolytic or antidepressant treatments (Rygula *et al.*, 2008; Krishnan *et al.*, 2011). As fatigue, low mood and reduced activity are symptoms of MDD, this reduced locomotor and exploratory behaviour observed in the AC and LPS-treated groups suggests the mice may be experiencing depression-like behaviour (Seibenhener *et al.*, 2015; Gencturk *et al.*, 2024). This reduction

in locomotor activity was not present 24h post-injection, indicating that AC and LPS do not induce prolonged behavioural changes.

Previous work from our lab group established the pharmacokinetic profile for AC (100 mg kg^{-1}), showing that AC crosses the BBB, peaks at 1h post-injection, and is almost undetectable at 24h post-injection, highlighting it short-lived effects (Moudio *et al.*, 2022). Multiple studies also support the transient nature of LPS administration, with rapid inflammatory cytokines peaking within hours of systemic injection, while behavioural changes are usually fully recovered by 24h (Biesmans *et al.*, 2013; Lasselin *et al.*, 2020).

AC and LPS also reduced the time spent at the centre of the OFT arena, suggesting possible anxiety-like behavioural changes. The centre vs edge ratio in the OFT is a common behavioural assay, where reduced time spent exploring the centre and increased time spent exploring the edges of the arena (thigmotaxis) are associated with higher levels of anxiety (Seibenhener *et al.*, 2015; La-Vu *et al.*, 2020). This behaviour mimics natural behaviour, whereby mice would avoid open areas to avoid potential predation, with the centre vs edge behavioural measure often used to assess the effects of anxiolytics. Administration of anxiolytics such as benzodiazepines have shown increased time spent at the centre of the OFT arena, which is interpreted as decreased anxiety-like behaviour in rodents (Prut *et al.*, 2003; La-Vu *et al.*, 2020).

It is important to differentiate “sickness-like behaviour” from depression- or anxiety-like behaviour when interrupting *in vivo* studies as they share overlapping symptoms. Sickness-like behaviours are acute responses to an

immune challenge, including reduced locomotor and exploratory behaviour, social withdrawal, decreased food and water intake, and changes in body temperature (Dantzer, 2006). In contrast, depression-like behaviour encompasses specific phenotypes such as anhedonia, apathy, and low mood, while anxiety-like behaviour is reflected in avoidance behaviours (Nestler *et al.*, 2010).

In our study, reduced time spent at centre following AC and LPS may be interpreted as anxiety-like behaviour. Previous behavioural testing using the elevated plus maze, as well as OFT and forced swim test demonstrated that PAR2 activation did not induce anxiety-like behaviour in C57BL6/J mice (Moudio *et al.*, 2022). Instead, mice were often immobile at the edges of the arena, as opposed to exploring only around the periphery. In addition, AC- and LPS-injected mice were often found immobile in their home cage immediately prior to OFT testing suggesting fatigue. This immobility could be associated with transient sickness-like behaviour induced by AC264613 or LPS, rather than fatigue alone. However, the concurrent reductions in sucrose preference and grooming indicate the mice were experiencing anhedonia and apathy, consistent with depression-like behavioural changes, supporting the conclusion that the observed behavioural changes are not solely attributable to sickness.

3.6.3. AC264613 and LPS reduced sucrose preference in C57BL6/J and 5xFAD$^{-/-}$ mice.

AC reduced sucrose preference 2h post-injection, further supporting previous findings suggesting that PAR2 activation induces anhedonia in mice, a key

symptom in MDD (Abulkassim *et al.*, 2016; Moudio *et al.*, 2022). The sucrose preference test is a common behavioural assay used in induced stress and depression-like behaviour models, where reduced preference to sucrose consumption is considered indicative of anhedonia (Markov, 2022). Mice injected with LPS also showed a trend towards reduced sucrose preference, partially supporting previous findings that LPS induces anhedonia (Salazar *et al.*, 2012; Biesmans *et al.*, 2016). These varying effects may reflect differences in LPS dosage used in other studies, as higher doses have been more consistently associated with significant reductions in sucrose preference (Salazar *et al.*, 2012; Biesmans *et al.*, 2016). However, reduced sucrose preference has also been observed using the same dosage employed in the present study (Li *et al.*, 2015).

Overall, there was a degree of variability in sucrose preference across mice in all treatment groups prior to injection, ranging from 61% to 99% preference. Sucrose was considered the preferred drinking solution when consumption exceeded 50% compared to water; however, several studies suggest a threshold of 65%, with lower values indicative of anhedonia (Scheggi *et al.*, 2018; Berrio *et al.*, 2023). This would therefore suggest some mice were experiencing anhedonia prior to treatment.

Furthermore, several mice excluded from the results showed no preference for sucrose prior to treatment, instead preferring tap water even in the absence of induced stress or pharmacological intervention. Although these cases were few and occurred in both sexes, they highlight individual variability despite all mice being of the same strain, raised in the same environment and housing

conditions, within the same age range and subjected to prior handling and habituation. It has been suggested that, although the sucrose preference test is a widely used assay for assessing anhedonia, the numerous variations in experimental protocols, such as environmental and housing conditions, light-dark cycle, food and water deprivation, duration of testing and habituation procedures, can increase variability and limit reproducible results (Primo *et al.*, 2023).

3.6.4. LPS but not AC264613 induced apathy-like behaviour in C57BL6/J and 5xFAD$^{-/-}$ mice.

Apathy, defined as a reduction in goal-directed behaviour, is one of the core features of MDD (Cathomas *et al.*, 2015). The splash test is commonly used to model apathy-like behaviour by assessing self-care and motivational behaviour in rodents. Most protocols employ a 10% sucrose solution and measure total time spent grooming and latency to first groom (Isingrini *et al.*, 2010; Planchez *et al.*, 2019). Reduced grooming behaviour is associated with depression-like behaviour, as animals may no longer experience pleasure from the sweetness of sucrose and show a lack of motivation to groom (Isingrini *et al.*, 2010; Planchez *et al.*, 2019; Becker *et al.*, 2021).

To reduce potential experimenter bias in assessing grooming behaviour, machine learning AI was implemented using a MatLab script designed to classify behaviour based on movement and body part co-ordination (Sakata, 2023). The AI machine learning classifier was trained using several videos of mice grooming. However, results from the C57BL6/J and 5xFAD$^{-/-}$ cohorts

suggested that AC increased time spent grooming, contrary to our hypothesis that AC would reduce grooming.

When the videos were subsequently analysed by manual scoring, it was found that the AI results were inaccurate. Upon reviewing the videos, it was discovered that mice form a range of postures and movements while grooming, and machine learning was not sensitive enough to detect all grooming behaviours. Furthermore, the machine learning could not reliably distinguish between a mouse sitting immobile and a mouse sitting and grooming. As a result, periods of immobility were often misclassified as grooming. Consequently, it appeared that AC increased total grooming time, although the mice were often immobile.

Several other machine learning options were explored, including B-SOiD, SimBA, and JAABA (Kabra *et al.*, 2013; Hsu *et al.*, 2021; Goodwin *et al.*, 2024). However, the majority of previous studies using the splash test to assess apathy-like behaviour employed manual scoring (Kalueff *et al.*, 2004b; Isingrini *et al.*, 2010; Bouguiyoud *et al.*, 2022).Therefore, given the limitations of the MatLab script, manual scoring was deemed to more accurately capture grooming behaviour and was used as the standard method for all subsequent studies.

AC had no effect on grooming behaviour when examined 2h post-injection. It was hypothesised that AC would decrease grooming time, consistent with findings from chronic stress- and blindness-indued depression-like behavioural models (Isingrini *et al.*, 2010; Hu *et al.*, 2017; Bouguiyoud *et al.*,

2022). However, AC-injected mice groomed for a similar duration as vehicle-injected mice, suggesting that AC may not induce apathy-like behaviour. In contrast, LPS reduced grooming behaviour, consistent with previous reports (Sabedra Sousa *et al.*, 2019; Watanabe *et al.*, 2025), but grooming recovered to levels comparable to vehicle by 24h post-injection, again supporting a short-lived effect.

Grooming is a complex, innate behaviour in rodents, with mice spending 30-50% of their waking time grooming (Kalueff *et al.*, 2007; Shiota *et al.*, 2016). Grooming is considered a 'self-soothing' behaviour in stressful situations, and both the duration and frequency of self-grooming can vary depending on stress and anxiety levels (Estanislau *et al.*, 2013; Kalueff *et al.*, 2016). Rats have shown longer time spent grooming in response to restraint-induced stress (Zhang *et al.*, 2011; Kalueff *et al.*, 2016). Grooming behaviour also varies across strains and species, with research demonstrating that C57BL/6J mice groom more than 129S1/SvImJ mice (Kalueff *et al.*, 2004a).

Although AC reduced locomotor activity and sucrose preference and was therefore expected to induce apathy-like behaviour, it is possible that AC-injected mice experienced mild stress, expressed as grooming for comfort. Similar to MDD, in which some individuals engage in excessive eating or "comfort" behaviours, mice may exhibit a similar "comfort eating" or "self-soothing" response (Kalueff *et al.*, 2016; Burton *et al.*, 2019; Liu *et al.*, 2021). AC-injected mice may have found comfort or pleasure in the 10% sucrose water spray; however, as AC also induced anhedonia-like behaviour, it

remains unclear whether the grooming was driven by comfort-seeking or to taste the sucrose water.

LPS-injected mice displayed reduced locomotor activity, likely reflecting fatigue, which may have also contributed to decreased grooming behaviour (Sabedra Sousa *et al.*, 2019; Carregosa *et al.*, 2024). At 24h post-injection, grooming times were comparable across all three treatments, further supporting that both AC and LPS-induced behavioural changes are transient.

3.6.5. AC264613 did not affect general animal health.

Mice received two injections of each treatment one week apart, and neither AC nor LPS had any adverse effects on general health and wellbeing beyond two days post-injection. Body weight was recorded daily, and while both AC and LPS caused temporary weight loss within 24h following injection, this reduction never exceeded 20% of their pre-drug weight and had fully recovered by 48h post-injection.

This transient weight loss may reflect temporary fatigue or reduced appetite in response to the AC and LPS, both features of MDD (Shin *et al.*, 2024). Further, LPS is known to reduce body weight primarily due to the body's breakdown of proteins, lipids and carbohydrates to support the immune inflammatory response, with sustained LPS administration capable of inducing fat loss and anorexia (Dantzer *et al.*, 2008; Yang *et al.*, 2022). Daily weighing allowed for mice to be monitored as a marker of health throughout the study.

Notably, the second dose of AC did not significantly reduce body weight, suggesting a level of tolerability to PAR2 activation. Mice were also checked

daily, and no health or welfare concerns were found following either AC or LPS-injection, supporting that PAR2 induced depression-like behaviour is transient and not associated with long-term behavioural or welfare concerns. Locomotor activity was examined 3- and 10-weeks post-injection in 5xFAD$^{-/-}$ and 5xFAD$^{+/-}$ to further evaluate potential long-term behavioural effects of PAR2 activation (see chapters 4.3 and 5.2, respectively).

3.6.6. Sex and genotype do not influence AC264613 or LPS-induced depression-like behaviour.

Across all behavioural tests, few sex or genotype differences were observed following AC or LPS administration, suggesting that induced behavioural changes occur independently of sex and genotype. Sex differences remain an underexplored area in biomedical. Historically, females were often excluded from studies due to assumptions that the oestrous cycle would introduce variability in results (Dayton *et al.*, 2016; Lovick *et al.*, 2021), despite MDD and other neuropsychiatric disorders being more prevalent in women (Eid *et al.*, 2019; Green *et al.*, 2019). However, comparative studies of male and female rodents in depression-like behaviour has yielded inconsistent results, with some demonstrating greater depression-like behaviour in females, others in males, and many show no differences (Pitzer *et al.*, 2022; Bowman *et al.*, 2025). These discrepancies may be attributed to numerous factors including variations in strain, age, experimental design, and the specific model of depression used.

Sex differences in PAR2 activation are not well studied, with mostly male animals being used (Abulkassim *et al.*, 2016; Hassler *et al.*, 2020; Moudio *et*

al., 2022). A recent PAR2 migraine model reported no sex differences in pain-related behaviour (Mason *et al.*, 2023), which supports the absence of sex effects in our study. Together, these findings suggest that PAR2 activation, and the resulting depression-like behaviour, are not strongly influenced by sex.

Similarly, no major genotypic differences were found between C57BL6/J and 5xFAD$^{-/-}$ mice. As 5xFAD$^{-/-}$ mice do not express the *APP* or *PSEN1* transgenes, they served as a transgene-negative control, but it was unknown if 5xFAD$^{-/-}$ would display the same behaviour as a standard C57BL6/J wild-type mouse. The largely overlapping behavioural profiles observed indicate that pharmacologically induced behavioural changes were not driven by transgenic background. While, AC-injected C57BL6/J mice exhibited a small reduction in locomotor behaviour, as no genotypic differences were observed in LPS-injected mice or at other time points or behavioural tests, this effect likely reflects individual variability rather than true genetic difference.

In literature, 5xFAD$^{-/-}$ mice are commonly referred to as wild-type littermates of heterozygous 5xFAD mice but due to the inclusion of C57BL6/J in this study, it was necessary to differentiate the breeding parentage (Forner *et al.*, 2021). There is little evidence of comparisons between C57BL6/J and 5xFAD$^{-/-}$ mice as most behavioural comparisons are between 5xFAD$^{+/-}$ and wild-type mice. Here, the use of both C57BL6/J and 5xFAD$^{-/-}$ mice provided important validation that AC- and LPS-induced behavioural effects were reproducible in non-diseased mice and not confounded by transgenic lineage. Further, these initial experiments were conducted to generate baseline behavioural responses and to establish working protocols for conducting the three

behavioural tests post-injection. Also, due to a genotyping error at the outset of the study, 5xFAD$^{+/-}$ breeders were unavailable, and therefore only C57BL6/J and 5xFAD$^{-/-}$ mice were available for the first 8 months of the project.

3.6.7. Conclusion

We confirm that PAR2 activation and LPS induce behavioural changes associated with depression-like behaviour. AC elicited short-term behavioural changes indicative of low mood, fatigue and anhedonia as demonstrated by reduced locomotor and exploratory activity and decreased sucrose preference, while LPS reduced activity and produced signs of apathy-like behaviour. Furthermore, sex and genotype did not appear to influence AC- or LPS-induced depression-like behavioural changes in C57BL6/J and 5xFAD$^{-/-}$ mice.

Chapter 4: The effects of AC- and LPS-injection on behaviour and neuropathology in 5xFAD$^{-/-}$ and 5xFAD$^{+/-}$ mice.

4.1. Introduction and aims.

MDD is a known risk factor for developing AD, and evidence suggests that individuals with AD and MDD concomitantly suffer a worse prognosis and accelerated disease progression (Brendel *et al.*, 2015; Cassano *et al.*, 2019). After confirming that AC- and LPS-injection induced depression-like behaviour in C57BL6/J and 5xFAD$^{-/-}$ mice, we then examined whether pharmacologically-induced depression-like behaviour was altered in the 5xFAD$^{+/-}$ mouse model of amyloid pathology compared to littermate controls and whether two doses in successive weeks of AC or LPS exacerbated molecular pathology. Based on clinical and preclinical evidence, we hypothesised that 5xFAD$^{+/-}$ mice would be more likely to display and be more susceptible to depression-like behaviour than 5xFAD$^{-/-}$ mice. Furthermore, we hypothesised that induced-depression-like behaviour would accelerate Aβ plaque pathology and increase neuroinflammation compared to vehicle injection in the 5xFAD$^{+/-}$ mice.

Previous work on PAR2 activation revealed elevated levels of pro-inflammatory cytokine IL-6 in the blood sera of WT mice following AC-injection, while other pro-inflammatory markers, TNF-α, IL-1β and INF-γ, were unaffected (Moudio *et al.*, 2022). Peripheral inflammation is increasingly recognised as a contributor to the pathogenesis of MDD, with IL-6 upregulation associated with MDD (Beurel *et al.*, 2020; Roohi *et al.*, 2021). Given the links between peripheral inflammation, MDD, and AD progression, we aimed to examine whether pharmacologically-induced depression-like behaviour influenced peripheral cytokines in 5xFAD$^{+/-}$ mice. We hypothesised that AC- and LPS-injection would increase pro-inflammatory cytokine levels and reduce

anti-inflammatory cytokines in the 5xFAD$^{-/-}$ and 5xFAD$^{+/-}$ mice, similar to that observed in patients with MDD.

The work in this chapter aims to answer the following research questions:

- Do 5xFAD$^{+/-}$ mice display depression-like behaviour and/or are more susceptible to AC- and LPS-induced depression-like behaviour compared to 5xFAD$^{-/-}$ mice?
- Does two doses of AC- and LPS-induced depression-like behaviour influence neuroinflammation and Aβ plaque pathology in 5xFAD$^{-/-}$ and 5xFAD$^{+/-}$ mice at 3 weeks post-injection?
- Do AC- and LPS-induced depression-like behaviour influence inflammatory peripheral cytokines in 5xFAD$^{-/-}$ and 5xFAD$^{+/-}$ mice in a similar manner to cytokine changes observed in MDD?

4.1.1 5xFAD mice

In total 30 mice received vehicle, 30 mice received AC, and 31 mice received LPS. After exclusions, each treatment group had 23, 23 and 24 mice, respectively (Table.4.1).

Table 4.1: Number of mice included and excluded in each treatment group.

Total Number		Total after exclusion	5xFAD$^{-/-}$ VS 5xFAD$^{+/-}$	
Vehicle	30	23		
AC461613	30	23		
LPS	31	34		
	Total after Exclusions			
	5xFAD$^{-/-}$		5xFAD$^{+/-}$	
	F	M	F	M
Vehicle	8	5	5	5
AC461613	8	5	5	5
LPS	8	6	5	5
	Excluded			
	5xFAD$^{-/-}$		5xFAD$^{+/-}$	
	F	M	F	M
Vehicle	2	1	3	1
AC461613	0	1	2	4
LPS	2	0	3	2

4.2. 5xFAD$^{+/-}$ mice have higher locomotor activity upon first exposure to the open field arena.

5xFAD$^{+/-}$ mice are reported to have increased hyperactivity and anxiety-like behaviour compared to WT mice (Oblak *et al.*, 2021; Zhong *et al.*, 2024). Therefore, locomotor activity at the first naïve habituation session in the OFT was examined. At the first habituation session (naïve hab 1), 5xFAD$^{+/-}$ mice exhibited significantly increased locomotor activity ($F_{(1\text{-}68)}$ = 5.053, p=0.02, 5xFAD$^{+/-}$ n=30, vs 5xFAD$^{-/-}$ n=40, Fig. 4.1A) compared to 5xFAD$^{-/-}$ mice. In contrast, on the second habitation day (naïve hab 2), no difference in locomotor activity was observed between the genotypes (p=0.22, 5xFAD$^{+/-}$, n=30 vs 5xFAD$^{-/-}$, n=40, Fig. 4.1A). From naïve hab 1 to naïve hab 2, there was an overall reduction in locomotor activity in both genotypes ($F_{(1\text{-}68)}$ = 199.6, p<0.001, naïve hab 1 vs naïve hab 2, N=70, Fig. 4.1A) confirming the mice were becoming habituated to the OFT arena. Furthermore, no differences in

locomotor activity between male and female 5xFAD$^{+/-}$ mice were found at either time points ($F_{(1-28)}$ = 0.01, p=0.91, male vs female, n=15).

To examine anxiety-like behaviour in the 5xFAD$^{+/-}$ mice at first habituation session, the time spend at the centre square was calculated. No difference in time spent at the centre square was found between the genotypes at either timepoint ($F_{(1-68)}$ = 0.27, p=0.61, 5xFAD$^{+/-}$, n=30 vs 5xFAD$^{-/-}$, n=40, Fig. 4.1B) and no change in time spent at centre square was observed from naïve hab 1 to naïve hab 2 ($F_{(1-68)}$ = 0.09, p=0.76, , 5xFAD$^{+/-}$, n=30 vs 5xFAD$^{-/-}$, n=40, Fig. 4.1B). Further, no sex differences in 5xFAD$^{+/-}$ mice were found at either timepoint ($F_{(1-28)}$ = 0.12, p=0.73, male vs female, n=15).

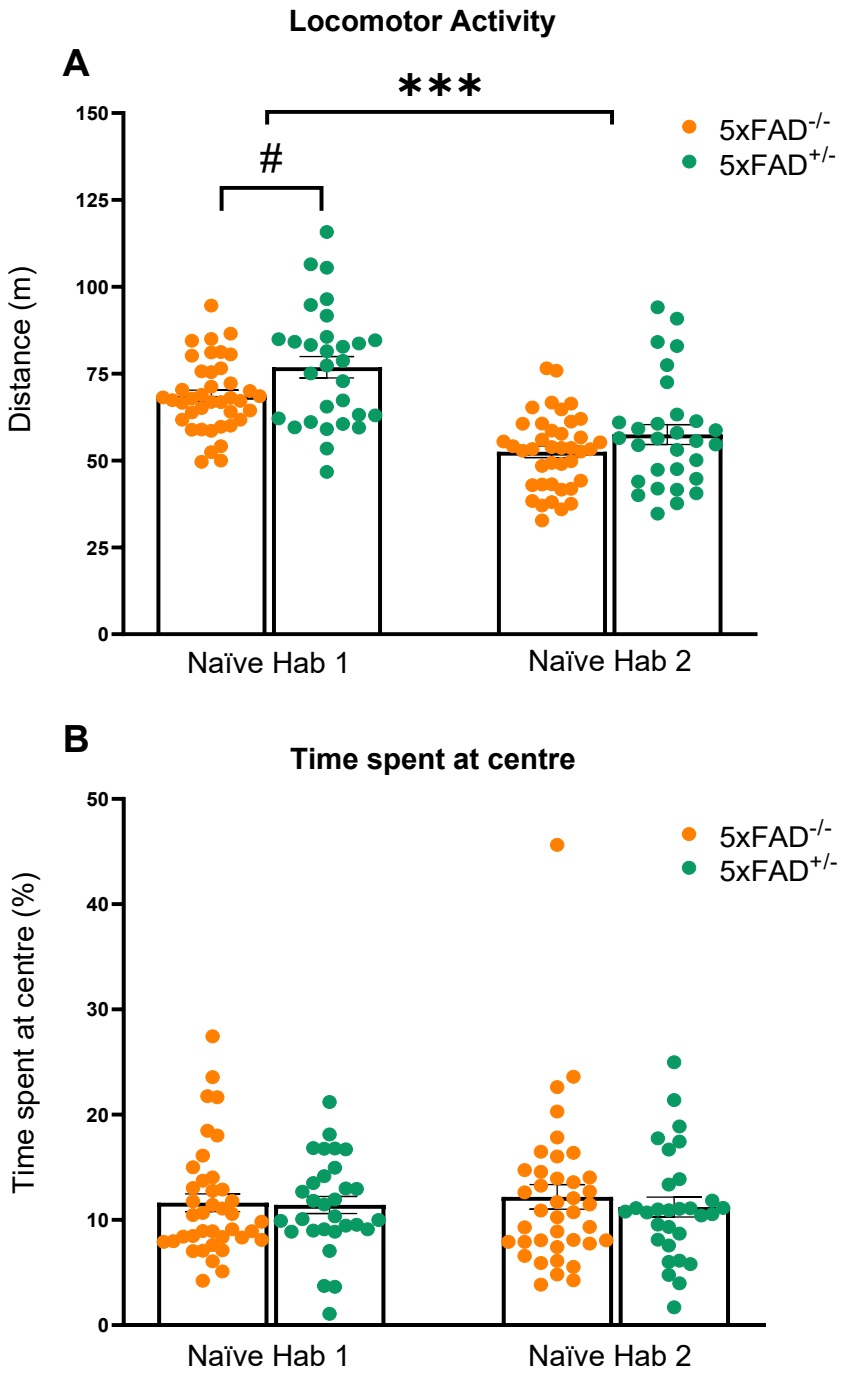

Figure 4.1: 5xFAD$^{+/-}$ mice have significantly increased locomotor activity compared to 5xFAD$^{-/-}$ at naïve habituation day 1. (A) 5xFAD$^{+/-}$ mice had higher locomotor activity compared to 5xFAD$^{-/-}$ mice at naïve hab 1 ($^{\#}p<0.05$ 5xFAD$^{+/-}$ vs 5xFAD$^{-/-}$). No difference in locomotor activity between the genotypes was found at naïve hab 2 but there was an overall decrease in locomotor activity at naïve hab 2 compared to naïve hab 1 (***p<0.001 naïve hab 1 vs naïve hab 2). (B) No difference in time spent at the centre square was observed between 5xFAD$^{-/-}$ and 5xFAD$^{+/-}$ mice, or between naïve hab 1 and naïve hab 2. Two-way repeated-measures ANOVA with Sidak's post hoc test (n=40 5xFAD$^{-/-}$, n=30 5xFAD$^{+/-}$).

4.3. AC- and LPS-injection reduced locomotor activity is independent of sex and genotype.

Following habituation and pre-drug measurements, locomotor activity was then examined 2h post-injection. AC- (100 mg kg^{-1}) and LPS-injection (0.5 mg kg^{-1}) significantly reduced locomotor activity at 2h post-injection compared to pre-drug ($F_{(3-192)}$ = 39.26, p<0.001 vs pre-drug, Fig 4.2B), with AC- (p=0.004 vs vehicle, n=23, Fig. 4.2B) and LPS-injection (p<0.001 vs vehicle, n=24, Fig. 4.2B) significantly reducing locomotor activity compared to vehicle injection. At 24h post-injection, locomotor activity in the AC- (p>0.99 vs vehicle, n=23, Fig.4.2B) and LPS-injected (p>0.99 vs vehicle, n=24, Fig.4.2B) mice was fully recovered. Vehicle injection had no effect on locomotor activity at either 2h or 24h post-injection (p>0.99 vs pre-drug, n=23, Fig.4.2B). A final OFT was done at 3-weeks post-injection to confirm there were no long-term adverse effects on locomotor activity following AC- and LPS-injection. AC- (p=0.64 vs vehicle, n=23, Fig.4.2B) and LPS-injection (p=0.79 vs vehicle, n=24, Fig.4.2B) had no effect on locomotor activity at 3-weeks post injection compared to vehicle injection.

Having shown that AC- and LPS-injection reduced locomotor activity, sex differences were then investigated within the genotypes. Both AC- and LPS-injection reduced locomotor activity 2h post-injection independent of sex in $5xFAD^{-/-}$ (AC: p=0.008 vs pre-drug, n=13, Fig. 4.3C; LPS: p<0.001 vs pre-drug, n=14, Fig. 4.3E) and $5xFAD^{+/-}$ mice (AC: p=0.053 vs pre-drug, n=10, Fig. 4.3D; LPS: p<0.001 vs pre-drug, n=10, Fig. 4.3F). No differences in locomotor activity were observed between males and females, prior to or following AC-

and LPS-injection in either genotype (AC: $F_{(1-11)}$ = 1.22, p=0.29, 5xFAD$^{-/-}$ male, n=5, vs female, n=8, Fig.4.3C; $F_{(1-8)}$ = 0.02 p=0.89 5xFAD$^{+/-}$ male vs female, n=5, Fig.4.3D; LPS: $F_{(1-12)}$ = 0.93, p=0.36 5xFAD$^{-/-}$ male, n=6 vs female, n=8, Fig.4.3E; $F_{(1-8)}$ = 1.91, p=0.2 5xFAD$^{+/-}$ male vs female, n=5, Fig.4.3F). Vehicle injection had no effect on locomotor activity 2h post-injection in either sex of 5xFAD$^{-/-}$ (p=0.96 vs pre-drug, n=13, Fig. 4.3A) or 5xFAD$^{+/-}$ mice (p=0.99 vs pre-drug, n=10, Fig. 4.3B).

Drug-induced changes were also examined for genotype dependence. No genotypic differences were observed at any time point in the vehicle-injected mice ($F_{(1-21)}$ = 1.7, p=0.2 5xFAD$^{-/-}$, n=13 vs 5xFAD$^{+/-}$, n=10, Fig 4.4A). Both AC- (p<0.001 vs pre-drug, n=23, Fig. 4.4B) and LPS-injection (p<0.001 vs pre-drug, n=24, Fig. 4.4C) reduced locomotor activity 2h post-injection with no differences observed between the 5xFAD$^{-/-}$ and 5xFAD$^{+/-}$ mice, prior to or following injection (AC: $F_{(1-21)}$ = 1.17, p=0.29 5xFAD$^{-/-}$, n=13 vs 5xFAD$^{+/-}$, n=10, Fig 4.4B; LPS: $F_{(1-22)}$ = 0.01, p=0.91 5xFAD$^{-/-}$, n=14 vs 5xFAD$^{+/-}$, n=10, Fig 4.4C).

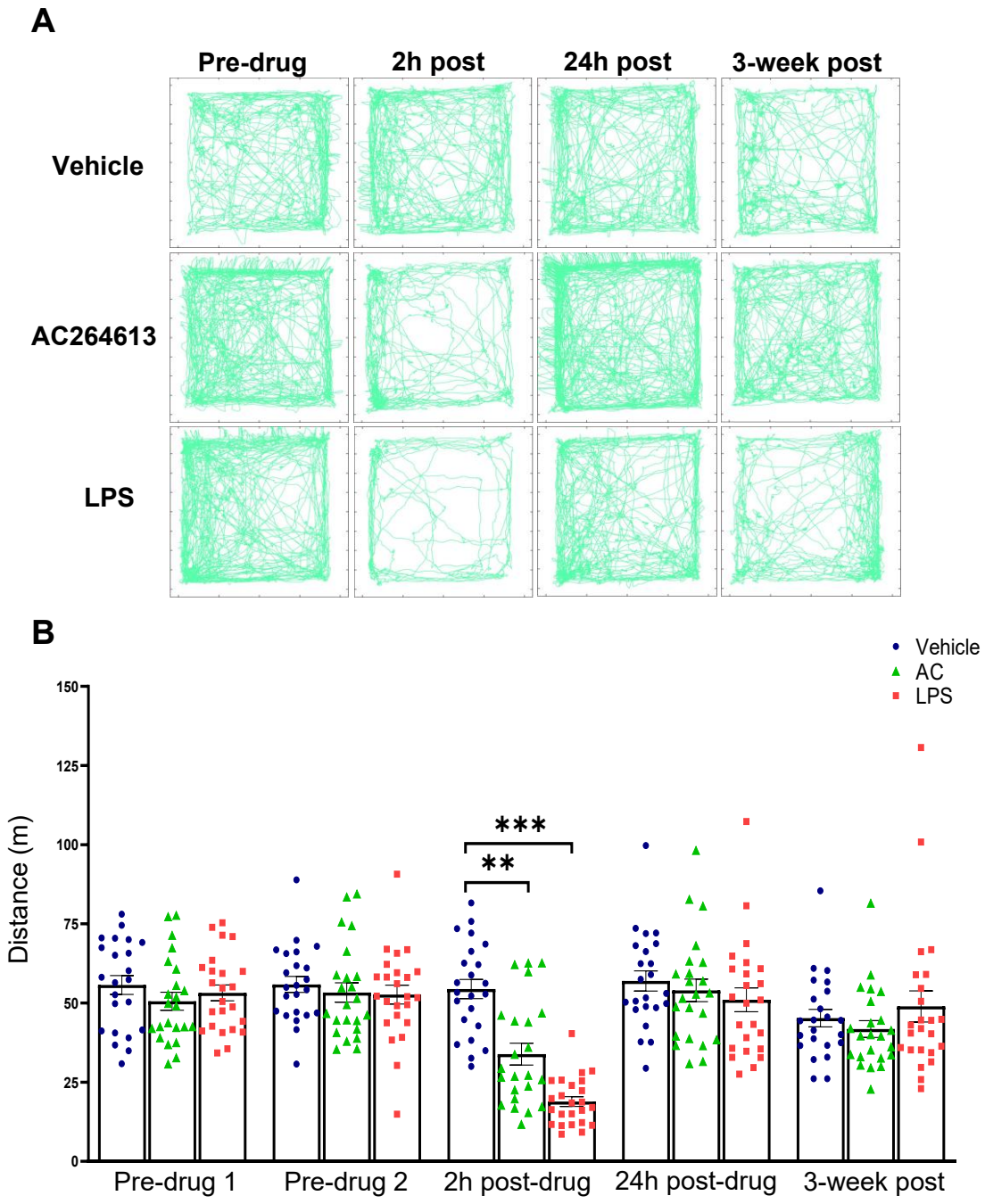

Figure 4.2: AC- and LPS-injection significantly reduced locomotor activity 2h post-injection. (A) Representative OFT tracking traces of an individual mouse's movement during the pre-drug, 2h post-drug, 24h post-drug and 3-week post-drug for vehicle, AC and LPS. (B) AC- (100 mg kg^{-1} i.p.) and LPS- (0.5 mg kg^{-1} i.p.) injection significantly reduced locomotor activity in the mice 2h post-injection (AC: **p<0.01; LPS: ***p<0.001, vs vehicle). Two-way repeated-measures ANOVA with Tukey's post hoc test (n=23 vehicle, n=23 AC, n=24 LPS).

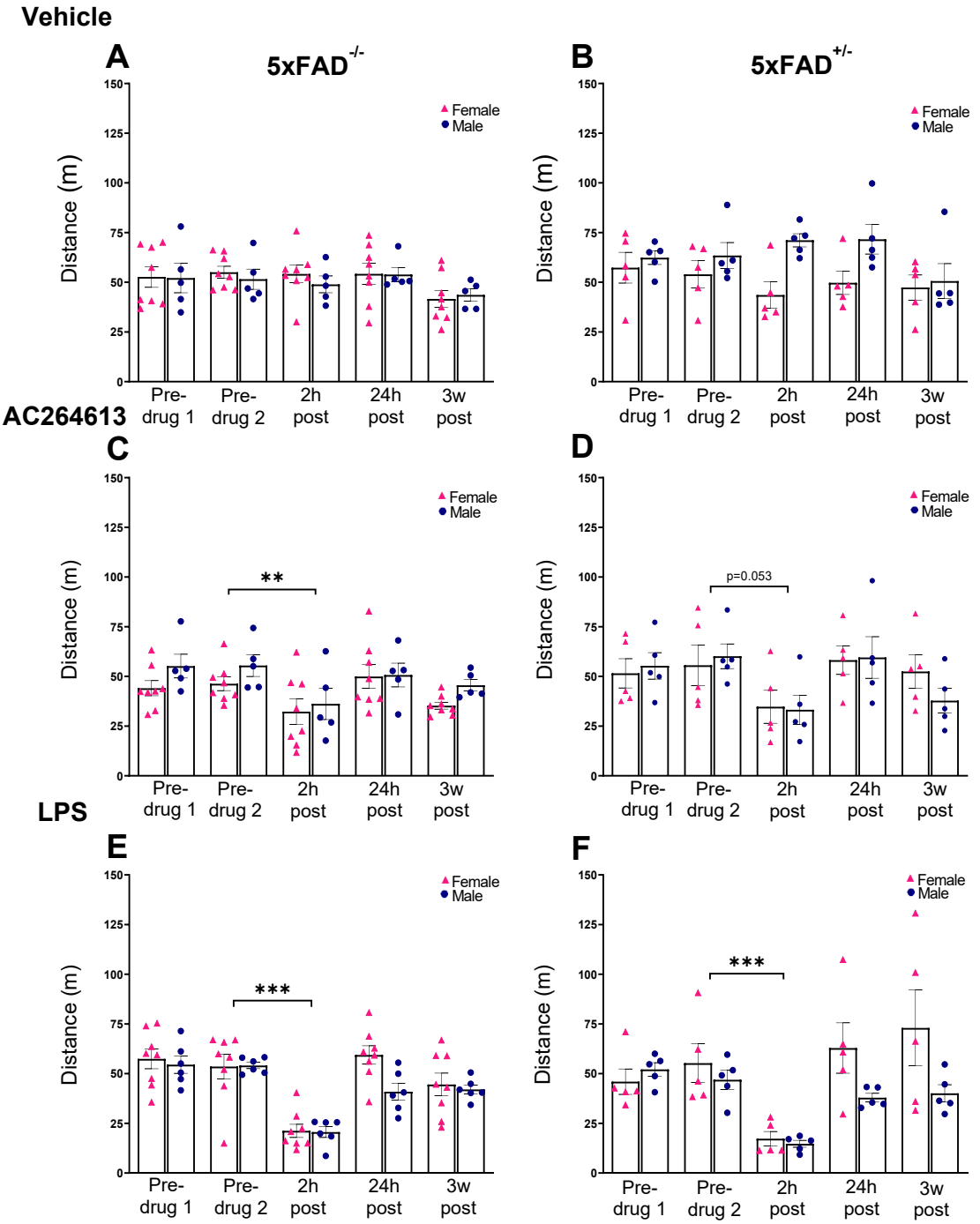

Figure 4.3: AC- and LPS-injection reduced locomotor activity 2h post-injection in both 5xFAD$^{-/-}$ and 5xFAD$^{+/-}$ mice independent of sex. (A-B) Vehicle injection had no effect on locomotor activity between the genotypes or sexes. (C-D) AC-injection reduced locomotor activity 2h post-drug in both 5xFAD$^{-/-}$ (**p<0.01 vs pre-drug) and 5xFAD$^{+/-}$ mice (p=0.053 vs pre-drug) independent of sex. (E-F) LPS-injection reduced locomotor activity in both 5xFAD$^{-/-}$ (***p<0.001 vs pre-drug) and 5xFAD$^{+/-}$ mice (***p<0.001 vs pre-drug) 2h post-injection independent of sex. Two-way repeated-measures ANOVA with Tukey's and Sidak's post hoc test (vehicle: n=5 male vs 8 female 5xFAD$^{-/-}$, n=5 male vs female 5xFAD$^{+/-}$; AC: n=5 male vs 8 female 5xFAD$^{-/-}$, n=5 male vs female 5xFAD$^{+/-}$; LPS: n=6 male vs 8 female 5xFAD$^{-/-}$, n=5 male vs female 5xFAD$^{+/-}$).

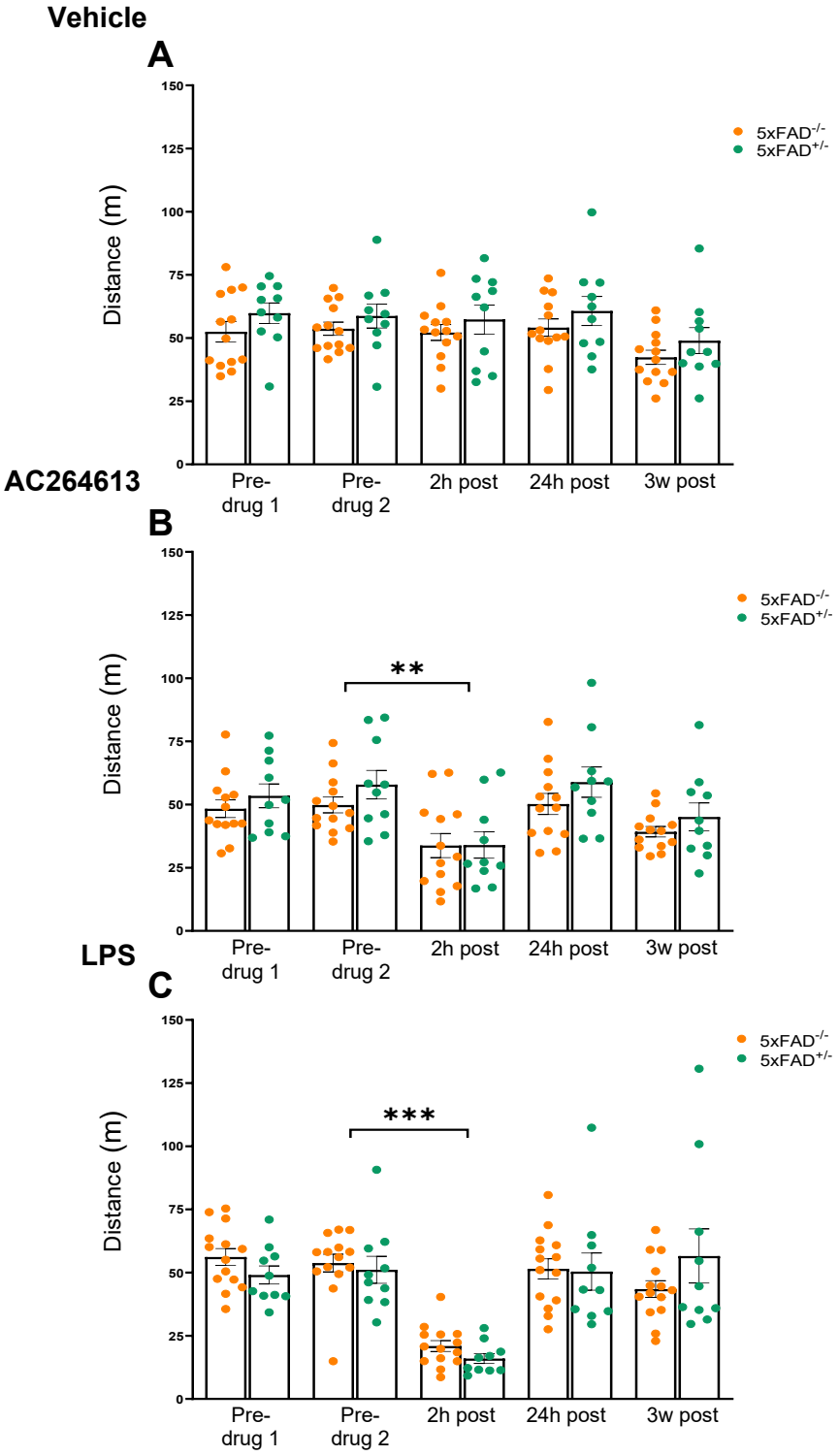

Figure 4.4: AC- and LPS-injection significantly reduced locomotor activity independent of genotype. (A) Vehicle injection had no effect on locomotor activity in either 5xFAD$^{-/-}$ or 5xFAD$^{+/-}$ mice. (B-C) Both AC- and LPS-injection significantly reduced locomotor activity 2h post-injection in both 5xFAD$^{-/-}$ and 5xFAD$^{+/-}$ mice (AC: **p<0.01; LPS: ***p<0.001, vs pre-drug) with no genotypic differences. Two-way repeated-measures ANOVA with Tukey's and Sidak's post hoc test (vehicle: n=13 5xFAD$^{-/-}$ vs 10 5xFAD$^{+/-}$; AC: n=13 5xFAD$^{-/-}$ vs 10 5xFAD$^{+/-}$; LPS: n=14 5xFAD$^{-/-}$ vs 10 5xFAD$^{+/-}$).

4.4. LPS- but not AC-injection reduced time spent at the centre square of the OFT arena independent of sex and genotype.

To examine anxiety-like behaviour, time spent at the centre square of the OFT arena was analysed across the treatment groups. LPS-injection reduced time spent at the centre square 2h post-injection ($p=0.057$ vs pre-drug, n=24, Fig. 4.5) compared to pre-drug whilst vehicle and AC-injection had no effect (vehicle: $p=0.54$; AC: $p=0.86$, vs pre-drug for both treatments, n=23, Fig. 4.5). No change in time spent at centre was observed at 24h- or 3-week post-injection in any of the treatment groups.

Sex was compared within the genotypes with LPS-injection having no effect on time spent at the centre square in male or female 5xFAD$^{-/-}$ mice ($p=0.29$ vs pre-drug, n=14, Fig. 4.6E) at 2h post-injection but LPS did induce a non-significant reduction in time at the centre square in male and female 5xFAD$^{+/-}$ mice ($p=0.07$ vs pre-drug, n=10, Fig. 4.6F) independent of sex. No sex differences were found in either vehicle injected 5xFAD$^{-/-}$ ($F_{(1-11)} = 0.93$, $p=0.36$, n=13, Fig 4.6A) or 5xFAD$^{+/-}$ mice ($F_{(1-8)} = 1.77$, $p=0.22$, n=10, Fig 4.6B), or in AC-injected 5xFAD$^{-/-}$ mice ($F_{(1-11)} = 0.05$, $p=0.82$, n=13, Fig 4.6C) or 5xFAD$^{+/-}$ mice ($F_{(1-8)} = 0.009$, $p=0.93$, n=10, Fig 4.6D).

Genotypes were also compared and no difference in time spent at the centre square between 5xFAD$^{-/-}$ and 5xFAD$^{+/-}$ mice were observed in any of the treatment groups (vehicle: $F_{(1-21)} = 1.6$, $p=0.2$ 5xFAD$^{-/-}$, n=13 vs 5xFAD$^{+/-}$, n=10, Fig 4.7A; AC: $F_{(1-21)} = 0.56$, $p=0.46$ 5xFAD$^{-/-}$, n=13 vs 5xFAD$^{+/-}$, n=10, Fig 4.7B; LPS: $F_{(1-22)} = 0.47$, $p=0.5$ 5xFAD$^{-/-}$, n=14 vs 5xFAD$^{+/-}$, n=10, Fig

4.7C). Overall, LPS but not vehicle or AC-injection, significantly reduced time spend at the centre square 2h post injection (p=0.018 vs pre-drug, n=24, Fig 4.7C) compared to pre-drug.

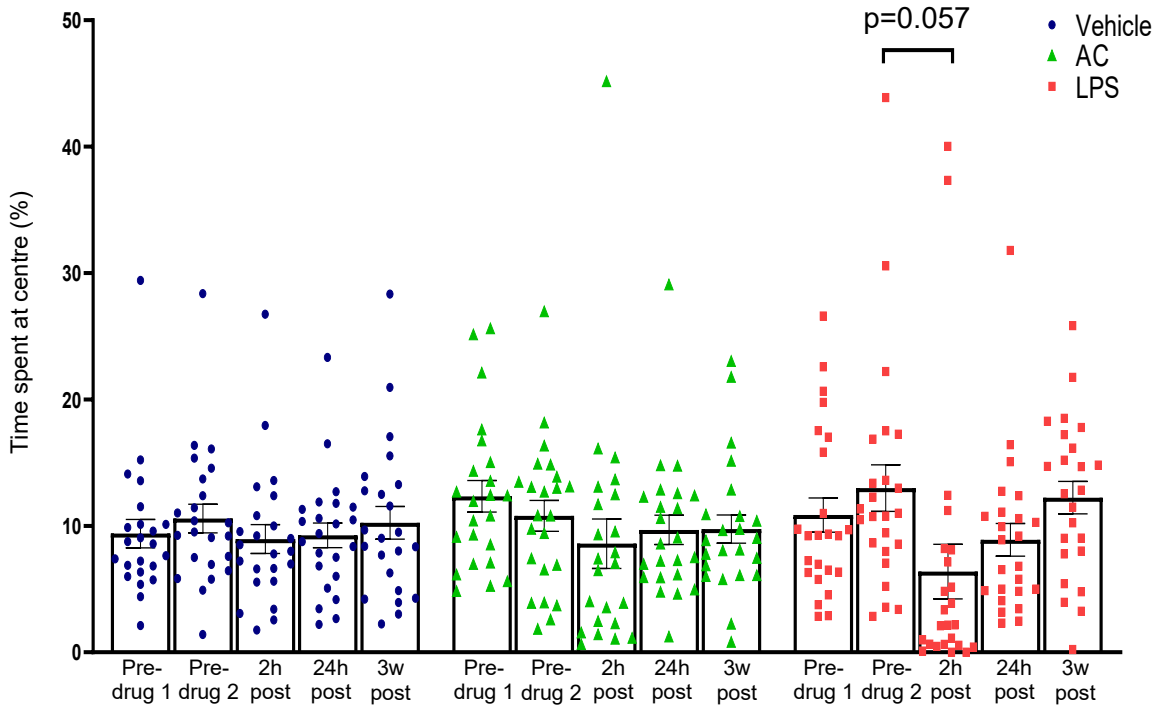

Figure 4.5: LPS-injection reduced time spent at the centre square 2h post-injection. LPS-injection but not vehicle or AC-injection reduced time spent at the centre square of the OFT arena 2h post-injection (p=0.057 vs pre-drug. Two-way repeated-measures ANOVA with Tukey's post hoc test (n=23 vehicle, n=23 AC, n=24 LPS).

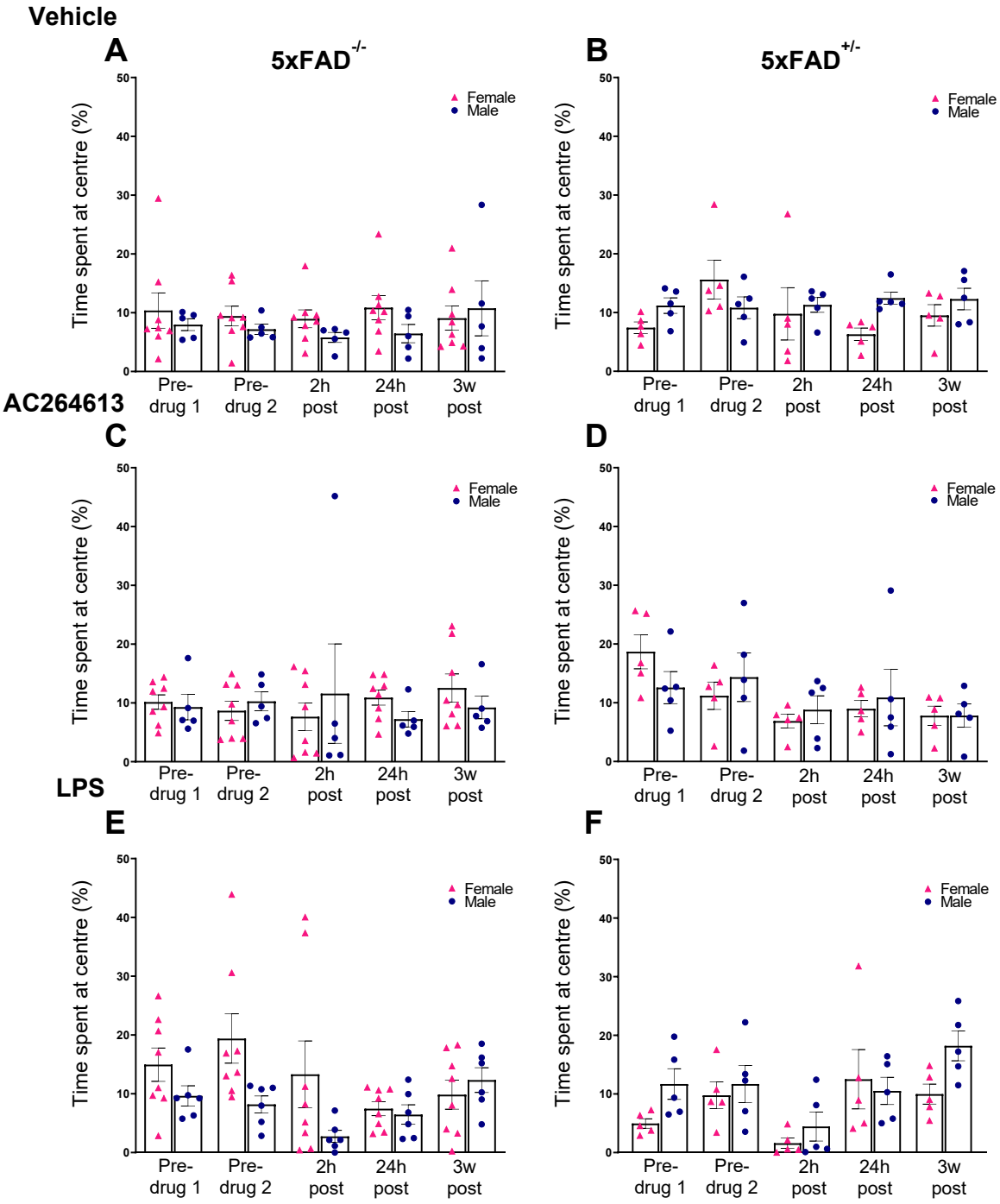

Figure 4.6: Sex did not influence time spent at the centre square of the OFT arena. (A-B) Vehicle injection had no effect on time spent at the centre of the OFT box in either sex of 5xFAD$^{-/-}$ or 5xFAD$^{+/-}$ mice. (C-D) AC-injection had no effect on time spent at centre in male or female 5xFAD$^{-/-}$ mice 2h post-injection. (E-F) LPS-injection had no effect on time spent at the centre square in 5xFAD$^{-/-}$ mice but non-significantly reduced time spent at the centre in 5xFAD$^{+/-}$ mice (p=0.07 vs pre-drug) independent of sex. Two-way repeated-measures ANOVA with Tukey's post hoc test (vehicle: n=5 male vs 8 female 5xFAD$^{-/-}$, n=5 male vs female 5xFAD$^{+/-}$; AC: n=5 male vs 8 female 5xFAD$^{-/-}$, n=5 male vs female 5xFAD$^{+/-}$; LPS: n=6 male vs 8 female 5xFAD$^{-/-}$, n=5 male vs female 5xFAD$^{+/-}$).

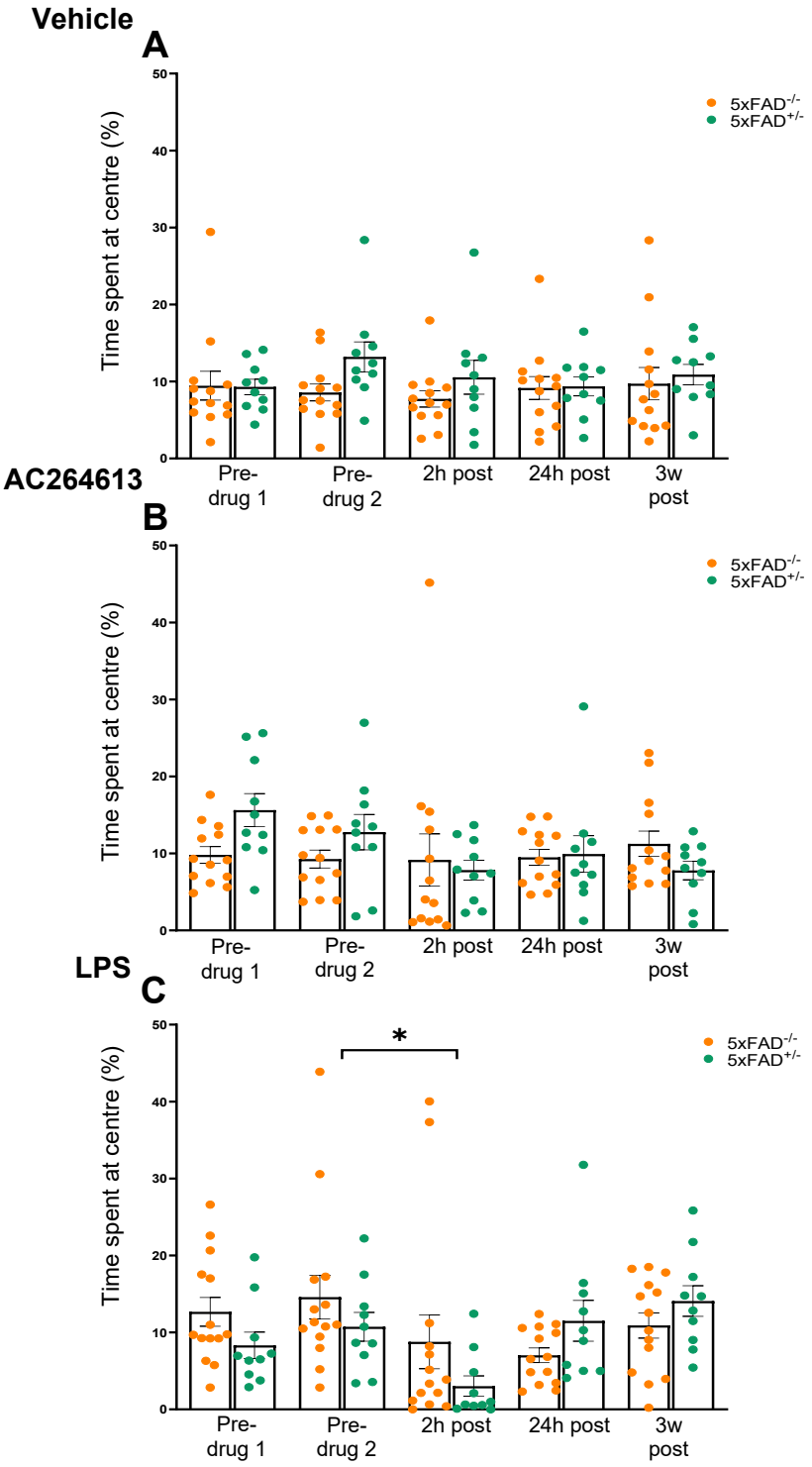

Figure 4.7: LPS-injection significantly reduced time spent at the centre square independent of genotype. No genotypic differences in time spent at the centre of the OFT arena were observed at any time point prior to, or following injection of vehicle, AC or LPS between 5xFAD$^{-/-}$ and 5xFAD$^{+/-}$ mice. (A-B) Overall, vehicle and AC-injection did not affect time spent at centre. (C) LPS-injection significantly reduced time spent at centre 2h post-injection (*p<0.05 vs pre-drug). Two-way repeated-measures ANOVA with Tukey's and Sidak's post hoc test (vehicle: n=13 5xFAD$^{-/-}$ vs 10 5xFAD$^{+/-}$; AC: n=13 5xFAD$^{-/-}$ vs 10 5xFAD$^{+/-}$; LPS: n=14 5xFAD$^{-/-}$ vs 10 5xFAD$^{+/-}$).

4.5. Injection per se reduced sucrose preference independent of sex and genotype.

When sucrose preference was examined, we revealed that vehicle, AC and LPS all reduced sucrose preference 2h post-injection in 5xFAD$^{-/-}$ vs 5xFAD$^{+/-}$ mice (vehicle: $p<0.001$ vs pre-drug, n=23; AC: $p<0.001$ vs pre-drug, n=23; LPS: $p<0.001$ vs pre-drug, n=24, Fig 4.8). This reduction in sucrose preference was recovered at 24h post-injection in the vehicle and AC-injected mice. However, sucrose preference in the LPS-injected mice remained reduced at the 24h post injection measurement (LPS: $p<0.001$ vs pre-drug n=24, Fig 4.8).

When sex was examined within the genotypes, sucrose preference was reduced 2h post-injection in both vehicle and AC-injected male and female 5xFAD$^{-/-}$ and 5xFAD$^{+/-}$ mice compared to pre-drug, with no difference found between the sexes (vehicle 5xFAD$^{-/-}$: $p=0.006$ vs pre-drug, n=13, sex differences: $F_{(1-11)} = 0.62$, $p=0.45$, male, n=5, vs female, n=8, Fig.4.9A; Vehicle 5xFAD$^{+/-}$: $p=0.012$ vs pre-drug, n=10, sex differences: $F_{(1-8)} = 2.55$, $p=0.15$, male, n=5, vs female, n=5, Fig.4.9B; AC 5xFAD$^{-/-}$: $p<0.001$ vs pre-drug, n=13, sex differences: $F_{(1-11)} = 0.08$, $p=0.77$, male, n=5, vs female, n=8, Fig.4.9C; AC 5xFAD$^{+/-}$: $p=0.003$ vs pre-drug, n=10, sex differences: $F_{(1-8)} = 1.14$, $p=0.32$, male, n=5, vs female, n=5, Fig.4.9D). In LPS-injected mice, there was an overall reduction in sucrose preference in both 5xFAD$^{-/-}$ and 5xFAD$^{+/-}$ mice across the timepoints, independent of sex (LPS 5xFAD$^{-/-}$: $F_{(1-16)} = 4.4$, $p=0.04$, n=14, sex differences: $F_{(1-12)} = 0.006$, $p=0.94$, male, n=6, vs female, n=8, Fig.4.9E; LPS 5xFAD$^{+/-}$: $F_{(2-15)} = 4.03$, $p=0.04$, n=10, sex differences: $F_{(1-8)} = 6.1$, *$p=0.04$, male, n=5, vs female, n=5, Fig.4.9F). LPS-injected male 5xFAD$^{+/-}$

mice had a non-significant reduction in sucrose preference at 24h post-injection compared to females (p=0.08 males vs female, n=5, Fig 4.8F) but no significant differences were found between the sexes.

When genotypes were compared, no significant genotypic differences in sucrose preference were found prior to or following injection of vehicle ($F_{(1-21)}$ = 7.6, p=0.99 5xFAD$^{-/-}$, n=13 vs 5xFAD$^{+/-}$, n=10, Fig 4.10A), AC ($F_{(1-21)}$ = 2.87, p=0.1 5xFAD$^{-/-}$, n=13 vs 5xFAD$^{+/-}$, n=10, Fig 4.10B) or LPS ($F_{(1-22)}$ = 0.77, p=0.39 5xFAD$^{-/-}$, n=14 vs 5xFAD$^{+/-}$, n=10, Fig 4.10C). 5xFAD$^{+/-}$ mice in the AC-injection group had a non-significant preference for sucrose prior to injection compared to 5xFAD$^{-/-}$ mice (p=0.06 5xFAD$^{-/-}$, n=13 vs 5xFAD$^{+/-}$, n=10, Fig 4.10B). However, this different was not observed in other treatment groups or timepoints. Overall, vehicle, AC- and LPS-injection reduced sucrose preference at 2h post injection (Vehicle: p<0.001 vs pre-drug, n=23, Fig 4.10A; AC: p<0.001 vs pre-drug, n=23, Fig 4.10B; LPS: p=0.002 vs pre-drug, n=24, Fig 4.10C) and sucrose preference remained reduced at 24h post-injection in the LPS-injected mice (p=0.007 vs pre-drug, n=24, Fig 4.10C).

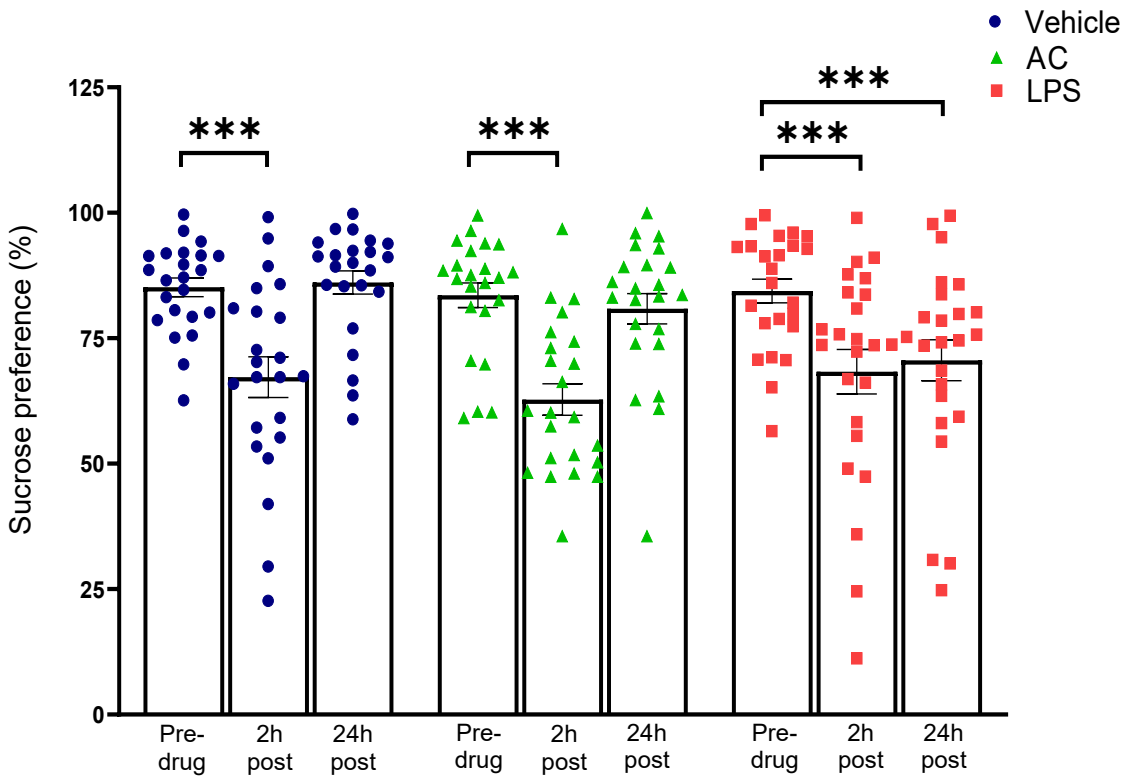

Figure 4.8: Injection per se significantly reduced sucrose preference 2h post-injection independent of treatment. Sucrose preference was significantly reduced across vehicle, AC- and LPS-injected 5xFAD$^{-/-}$ and 5xFAD$^{+/-}$ mice at 2h post injection (vehicle: ***p<0.001, AC: ***p<0.001; LPS: ***p<0.001, vs pre-drug). At 24h post-injection, sucrose preference was recovered in vehicle and AC-injected mice but not LPS-injected mice (***p<0.001 pre-drug vs 24h post-drug). Two-way repeated-measures ANOVA with Tukey's post hoc test (n=23 vehicle, n=23 AC, n=24 LPS).

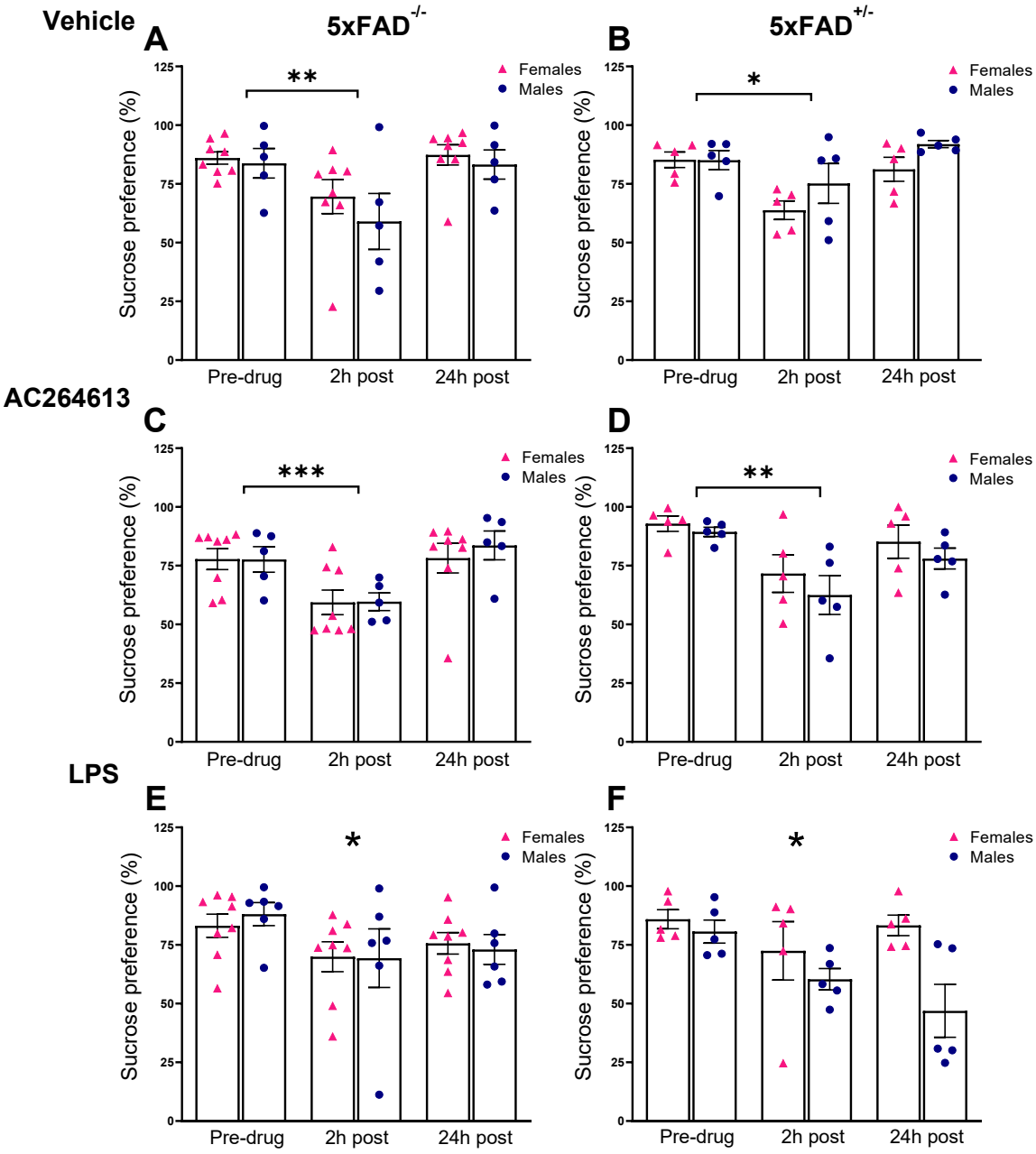

Figure 4.9: Injection per se reduced sucrose preference 2h post-injection in both 5xFAD$^{-/-}$ and 5xFAD$^{+/-}$ mice independent of sex. No sex differences within the genotypes were observed prior to or following injection of vehicle, AC or LPS. (A-B) Vehicle injection reduced sucrose preference 2h post-injection in both 5xFAD$^{-/-}$ (**p<0.01 vs pre-drug) and 5xFAD$^{+/-}$ (*p<0.05 vs pre-drug) mice. (C-D) AC-injection reduced sucrose preference 2h post-injection in both 5xFAD$^{-/-}$ (***p<0.001 vs pre-drug) and 5xFAD$^{+/-}$ (**p<0.01 vs pre-drug) mice. (E-F) Overall, LPS-injection reduced sucrose preference across the timepoints in both 5xFAD$^{-/-}$ and 5xFAD$^{+/-}$ (*p<0.05) mice. At 24h post-injection, male 5xFAD$^{+/-}$ mice had non-significantly reduced sucrose preference compared to female 5xFAD$^{+/-}$ mice (p=0.08 male vs female). Two-way repeated-measures ANOVA with Tukey's and Sidak's post hoc test (vehicle: n=5 male vs 8 female 5xFAD$^{-/-}$, n=5 male vs female 5xFAD$^{+/-}$; AC: n=5 male vs 8 female 5xFAD$^{-/-}$, n=5 male vs female 5xFAD$^{+/-}$; LPS: n=6 male vs 8 female 5xFAD$^{-/-}$, n=5 male vs female 5xFAD$^{+/-}$).

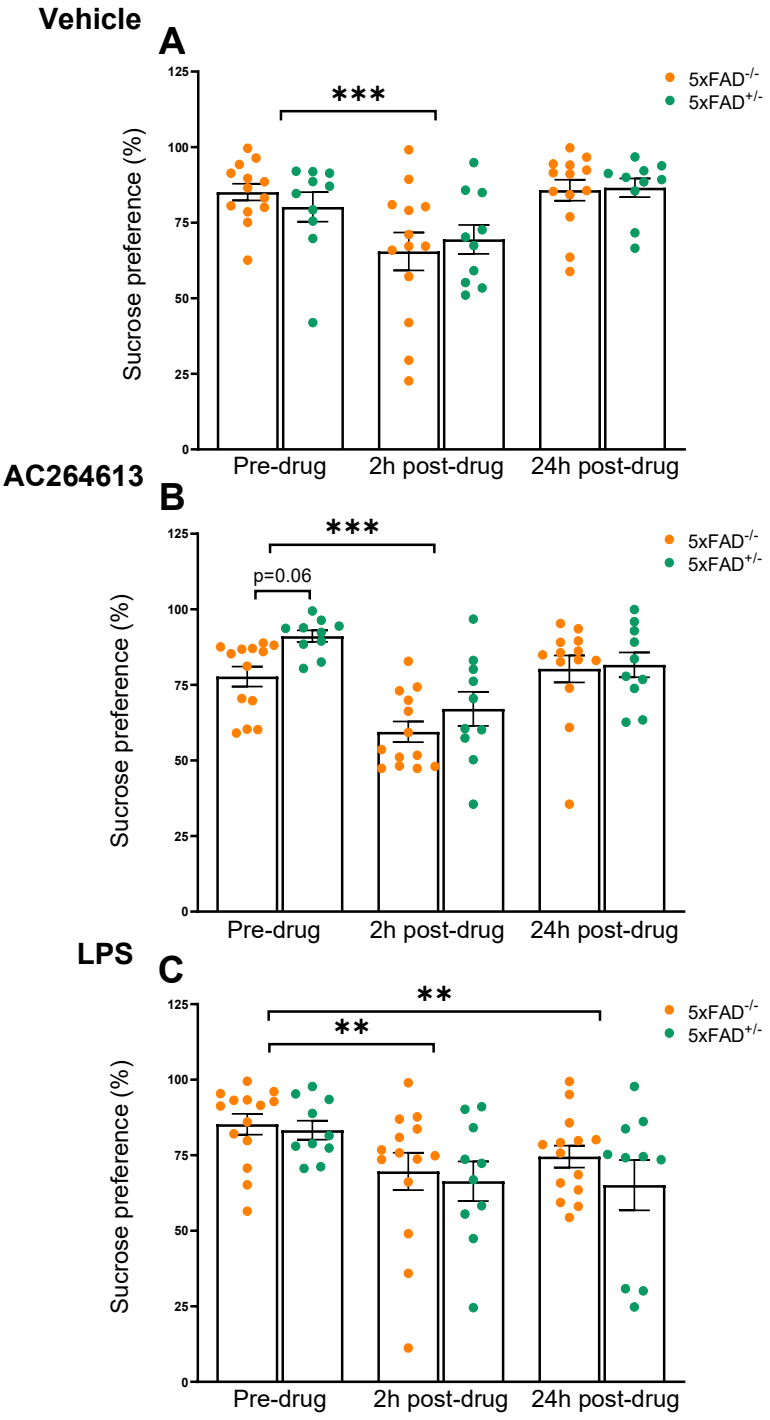

Figure 4.10: Injection per se reduced sucrose preference 2h post-injection independent of genotype. No genotypic differences in sucrose preference were observed following injection of vehicle, AC or LPS between 5xFAD$^{-/-}$ and 5xFAD$^{+/-}$ mice. However, 5xFAD$^{+/-}$ mice had a higher preference to sucrose prior to AC-injection (p=0.06 5xFAD$^{+/-}$ vs 5xFAD$^{-/-}$). Injection per se reduced sucrose preference 2h post-injection in all treatment groups (vehicle: ***p<0.001, AC: ***p<0.001; LPS: **p<0.01, vs pre-drug). Sucrose preference remained reduced 24h post-injection in LPS-injected mice (**p<0.01 24h post vs pre-drug). Two-way repeated-measures ANOVA with Tukey's and Sidak's post hoc test (vehicle: n=13 5xFAD$^{-/-}$ vs 10 5xFAD$^{+/-}$; AC: n=13 5xFAD$^{-/-}$ vs 10 5xFAD$^{+/-}$; LPS: n=14 5xFAD$^{-/-}$ vs 10 5xFAD$^{+/-}$).

4.6. AC- and LPS-injection reduced grooming behaviour in 5xFAD$^{+/-}$ mice.

Based on the grooming behavioural results from the C57BL6/J vs 5xFAD$^{-/-}$ mice cohort, it was determined that manual scoring was more accurate to analyse grooming behavioural recordings than AI machine learning. This was also the most commonly used method in the literature, therefore was the adopted method to analyse the 5xFAD$^{-/-}$ vs 5xFAD$^{+/-}$ mice data.

Both, AC- and LPS-injection reduced total time spent grooming 2h post-injection compared to vehicle (AC: $p<0.001$ vs vehicle, n=23; LPS: $p=0.02$ vs vehicle, n=24, Fig 4.11A) but grooming levels had recovered 24h post-injection (AC: $p=0.99$ vs vehicle, n=23; LPS: $p=0.83$ vs vehicle, n=24, Fig 4.11A). At 2h post-injection, AC- but not LPS-injection delayed the time for mice to first wipe their face compared to vehicle ($p=0.039$ vs vehicle, n=23, Fig 4.11B). No difference in time to first face wipe was observed between the treatments at 24h post injection (AC: $p=0.87$ vs vehicle, n=23; LPS: $p=0.6$ vs vehicle, n=24, Fig 4.11B). As the mice frequently exhibited hyperactive behaviour following sucrose water spraying and placement in the test box, the latency to settle and initiate grooming for at least 5 seconds was also measured. No difference was found between the treatments in time to sit and groom > 5 seconds at 2h post- (AC: $p=0.39$ vs vehicle, n=23; LPS: $p=0.5$ vs vehicle, n=24, Fig 4.11C) or 24h post-injection (AC: $p=0.27$ vs vehicle, n=23; LPS: $p=0.8$ vs vehicle, n=24, Fig 4.11C).

The influence of sex and genotype on total grooming time was then examined. When sex was compared within the genotypes, vehicle injection had no influence on time spent grooming in either 5xFAD$^{-/-}$ ($F_{(1-11)}$ = 0.31 p=0.59 2h post- vs 24h post-drug, n=13, Fig 4.12A) or 5xFAD$^{+/-}$ mice ($F_{(1-8)}$ = 0.85 p=0.38 2h post- vs 24h post-drug, n=10, Fig 4.12B) but female 5xFAD$^{-/-}$ mice groomed significantly more than males at 24h post-injection (p=0.45 female, n=8, vs male, n=5, Fig.4.12A). AC-injection significantly reduced grooming time overall in 5xFAD$^{-/-}$ mice ($F_{(1-11)}$ = 0.68 p=0.02 2h post- vs 24h post-drug, n=13, Fig 4.12C). In 5xFAD$^{+/-}$ mice, AC-injection reduced grooming time 2h post-injection in female (p=0.06 2h post- vs 24h post-drug, n=5, Fig. 4.12D) and male mice (p=0.01 2h post- vs 24h post-drug, n=5, Fig. 4.12D). Also, at 2h post-injection, AC-injected male 5xFAD$^{+/-}$ mice groomed significantly less than females (p=0.03 male vs female, n=5, Fig.4.12D) but no difference was observed 24h post-injection. LPS-injection had no effect on grooming time in 5xFAD$^{-/-}$ mice ($F_{(1-12)}$ = 0.003 p=0.96 2h post- vs 24h post-drug, n=14, Fig 4.12E) but decreased grooming time overall 2h post injection in 5xFAD$^{+/-}$ mice ($F_{(1-8)}$ = 12.2 p=0.008 2h post- vs 24h post-drug, n=10, Fig 4.12F). No sex differences were found in the LPS-injected mice of either genotype.

When genotypes were compared it was revealed that 5xFAD$^{+/-}$ mice were more susceptible to reduced grooming at 2h post-injection with AC and LPS compared to 5xFAD$^{-/-}$ mice (AC: p=0.037 5xFAD$^{+/-}$, n=10, vs 5xFAD$^{+/-}$, n=13, Fig.4.13B; LPS: p=0.06 5xFAD$^{+/-}$, n=10, vs 5xFAD$^{+/-}$, n=14, Fig.4.13C). These genotypic differences were not observed at 24h post-injection. Overall, AC- and LPS-injection reduced grooming behaviour 2h post-injection (AC: $F_{(1-21)}$ =

26.9 p<0.001 2h post- vs 24h post-drug, n=23, Fig 4.13B; LPS: $F_{(1-22)}$ = 8.5 p=0.08 2h post- vs 24h post-drug, n=24, Fig 4.13C).

No sex or genotypic differences were found within the treatment groups for time to first face wipe or for time to sit and groom > 5 seconds, apart from AC-injected 5xFAD$^{+/-}$ male mice had a delayed time to sit and groom at 2h post-injection compared to females (p=0.03 males vs females, n=10). This delay to groom in males was not observed at 24h post-injection.

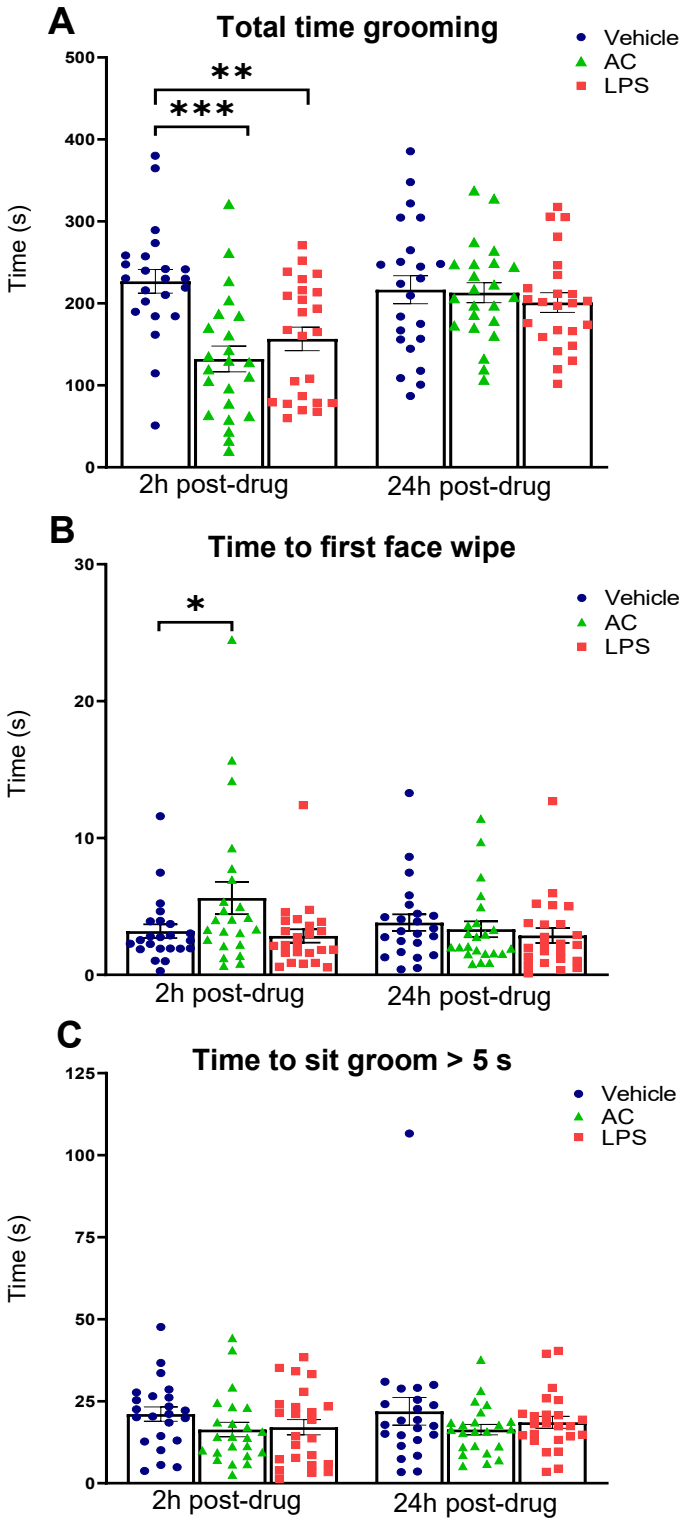

Figure 4.11: AC- and LPS-injection reduced grooming behaviour 2h post-injection. (A) AC- and LPS-injection significantly reduced grooming time 2h post injection compared to vehicle (AC: ***p<0.001; LPS: **p<0.01, vs vehicle) but no change was observed 24h post-injection. (B) AC-injected mice had a delayed time to first face wipe at 2h post-injection compared to vehicle (*p<0.05 vs vehicle). Which was not observed 24h post-injection. (C) No difference in time to sit and groom > 5 secs were found between the treatments or timepoints. Two-way repeated-measures ANOVA with Tukey's and Sidak's post hoc test (n=23 vehicle, n=23 AC, n=24 LPS).

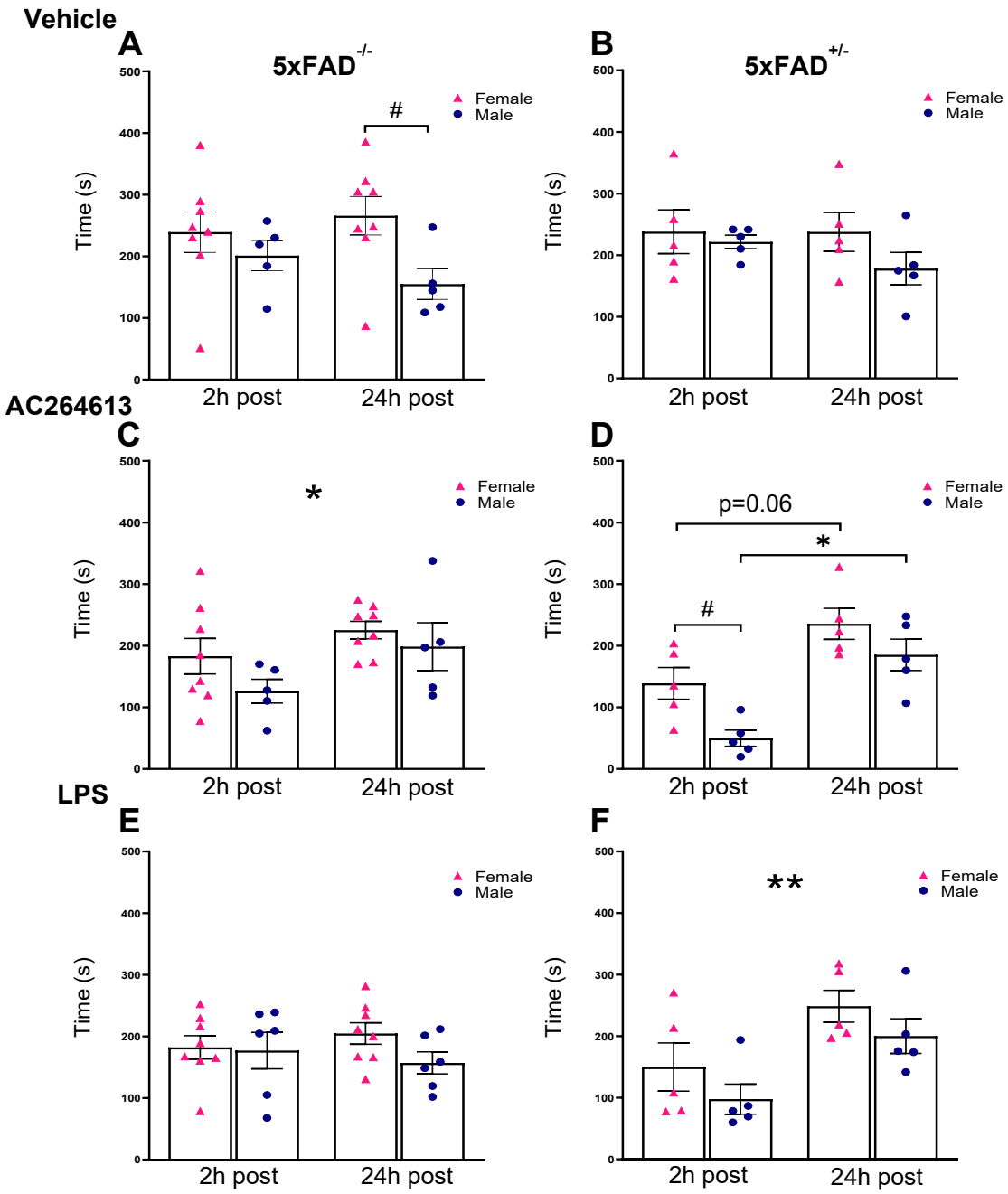

Figure 4.12: AC-injection reduced grooming 2h post-injection with differences found between sex in 5xFAD$^{+/-}$ mice. (A-B) Vehicle injection had no effect on grooming time within the genotypes at either timepoint. However, at 24h post-injection, female 5xFAD$^{-/-}$ mice groomed more than males ($^{\#}p<0.05$ male vs female). (C-D) AC-injection reduced overall grooming 2h post-injection in 5xFAD$^{-/-}$ mice ($^{*}p<0.05$ 2h vs 24h post-drug). In 5xFAD$^{+/-}$ mice, AC-injection reduced grooming 2h post-injection in females (p=0.06 2h vs 24h post-drug) and males ($^{*}p=0.01$ 2h vs 24h post-drug), with male mice grooming less than females ($^{\#}p<0.05$ male vs female). (E-F) Overall, LPS reduced grooming 2h post-injection in 5xFAD$^{+/-}$ ($^{**}p<0.01$) but not 5xFAD$^{-/-}$ mice, with no sex differences observed. Asterisks without brackets denote significant main effects. Two-way repeated-measures ANOVA with Sidak's post hoc test (vehicle: n=5 male vs 8 female 5xFAD$^{-/-}$, n=5 male vs female 5xFAD$^{+/-}$; AC: n=5 male vs 8 female 5xFAD$^{-/-}$, n=5 male vs female 5xFAD$^{+/-}$; LPS: n=6 male vs 8 female 5xFAD$^{-/-}$, n=5 male vs female 5xFAD$^{+/-}$).

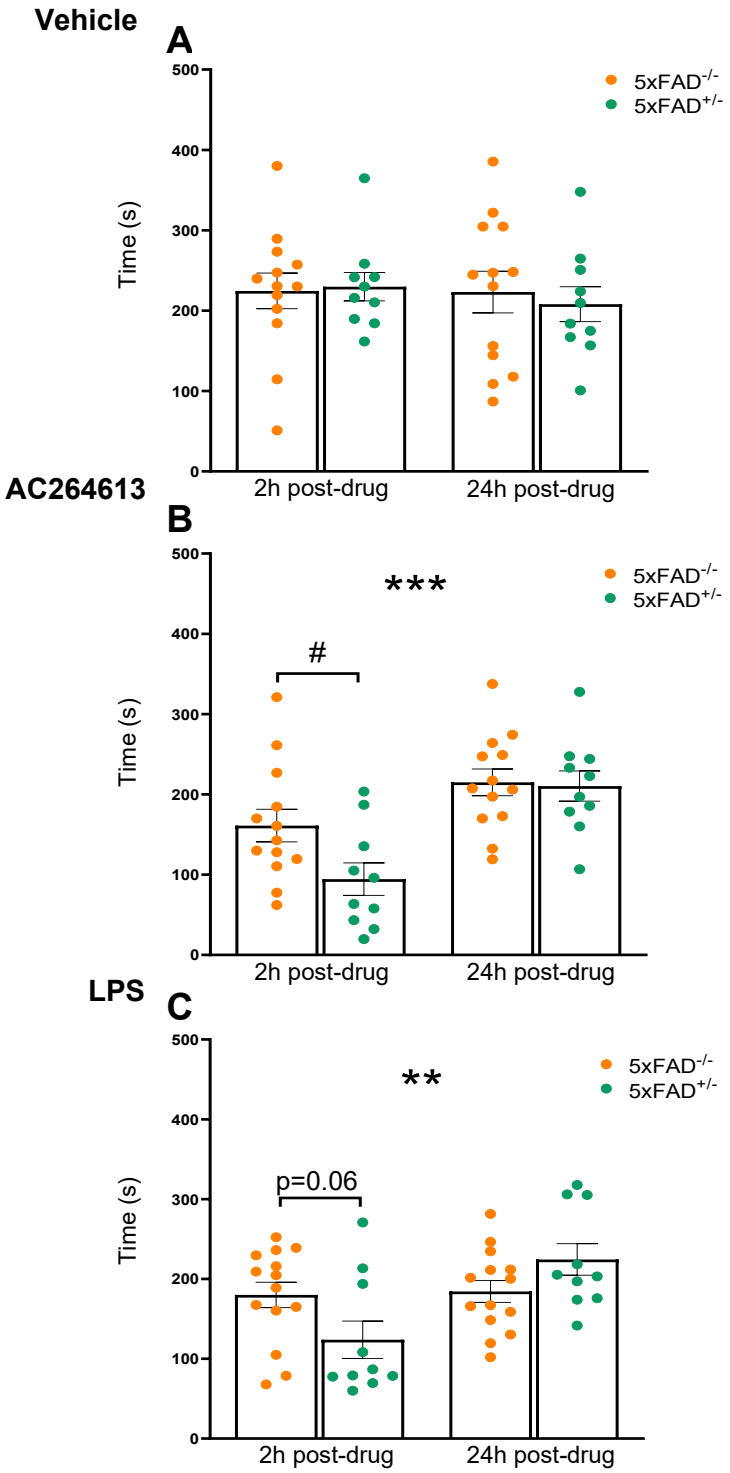

Figure 4.13: 5xFAD$^{+/-}$ mice are more susceptible to reduced grooming behaviour following AC- and LPS-injection. (A) Vehicle injection had no effect on grooming behaviour independent of genotype. (B-C) Overall, AC- and LPS-injection reduced grooming behaviour 2h post-injection (AC: ***p<0.001; LPS: **p<0.01, 2h post- vs 24h post-drug). At 2h post-injection, 5xFAD$^{+/-}$ mice were more susceptible to reduced grooming time following AC- and LPS-injection compared to 5xFAD$^{-/-}$ mice (AC: $^{\#}$p<0.05; LPS: p=0.06, 5xFAD$^{+/-}$ vs 5xFAD$^{-/-}$). Asterisks without brackets denote significant main effects. Two-way repeated-measures ANOVA with Sidak's post hoc test (vehicle: n=13 5xFAD$^{-/-}$ vs 10 5xFAD$^{+/-}$; AC: n=13 5xFAD$^{-/-}$ vs 10 5xFAD$^{+/-}$; LPS: n=14 5xFAD$^{-/-}$ vs 10 5xFAD$^{+/-}$).

4.7. LPS-injection induced a temporary weight reduction independent of sex or genotype.

Mice were weighed daily starting from the first naïve habituation day, until 1-week post-injection, and at a final 3-week post injection weighing prior to perfusion-fixation. It was observed that 5xFAD$^{+/-}$ mice were often smaller than their 5xFAD$^{-/-}$ littermates and at first weighing, male but not female 5xAD$^{+/-}$ mice had significantly reduced body weight compared to 5xFAD$^{-/-}$ mice (female: p=0.41 5xFAD$^{+/-}$, n=15, vs 5xFAD$^{-/-}$, n=24, Fig.4.14A; male: p=0.004 5xFAD$^{+/-}$, n=15, vs 5xFAD$^{-/-}$, n=16, Fig.4.14B).

Weights were compared within the genotypes for each sex. During the first week of testing, LPS- but not AC- or vehicle-injection, induced a temporary weight reduction at 24h post-injection compared to pre-drug in both 5xFAD$^{-/-}$ (p<0.001 vs pre-drug, n=8, Fig.4.15A) and 5xFAD$^{+/-}$ female mice (p<0.002 vs pre-drug, n=5, Fig.4.15B). During the second week of testing, LPS-injection significantly reduced body weight in the female 5xFAD$^{-/-}$ mice (p=0.04 vs pre-drug, n=8, Fig.4.15A) but not female 5xFAD$^{+/-}$ mice (p=0.19 vs pre-drug, n=5, Fig.4.15B). LPS-injection induced a temporary weight loss in male 5xFAD$^{-/-}$ (p<0.001 vs pre-drug, n=6, Fig.4.16A) and 5xFAD$^{+/-}$ mice (p<0.001 vs pre-drug, n=5, Fig.4.16B) during the first week of testing, and again in male 5xFAD$^{+/-}$ (p=0.03 vs pre-drug, n=5, Fig.4.16A) but not 5xFAD$^{-/-}$ mice in the second week of testing. No weight loss was observed in vehicle or AC-injected males of either genotype. Any weight lost was temporary and never exceeded 20% of the mouse's pre-drug weight, and all mice had fully recovered by the next weighing time point (day 7 and 12).

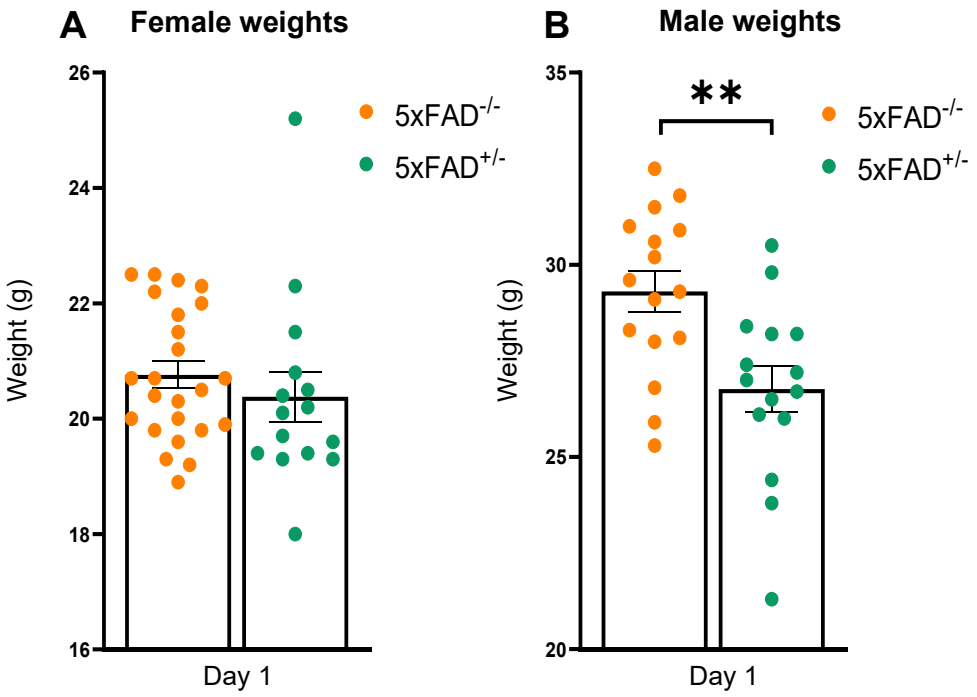

Figure 4.14: Male 5xFAD$^{+/-}$ mice have significantly reduced overall body weight compared to male 5xFAD$^{-/-}$ mice. When genotypes were compared at day 1 timepoint, male but not female 5xFAD$^{+/-}$ mice have a reduced body weight compared to age-matched male 5xFAD$^{-/-}$ mice (**p>0.01 5xFAD$^{+/-}$ vs 5xFAD$^{-/-}$). Weight displayed as mean ± SEM. Unpaired two-tailed t-test (Females: n=24 5xFAD$^{-/-}$, 15 5xFAD$^{+/-}$; Male; n=16 5xFAD$^{-/-}$, 15 5xFAD$^{+/-}$).

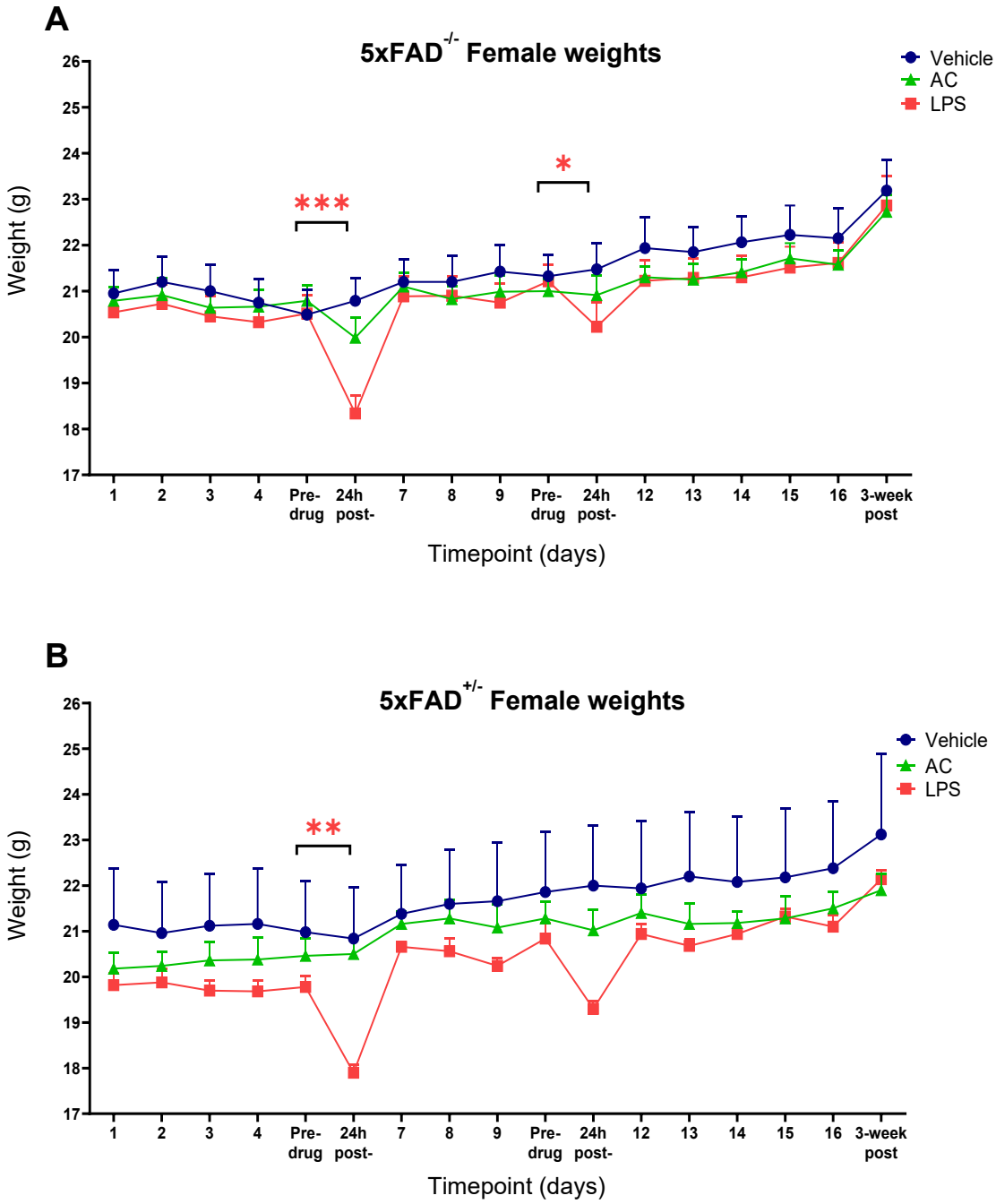

Figure 4.15: LPS-injection induced a temporary reduction in weight in female mice of both genotypes. LPS-injection induced a significant reduction in weight at 24h-post injection in the first week of testing in both 5xFAD$^{-/-}$ (***p<0.001 vs pre-drug) and 5xFAD$^{+/-}$ (**p<0.01 vs pre-drug) female mice. In the second week of testing, LPS-injection induced a significant reduction in weight in 5xFAD$^{-/-}$ mice (*p<0.05 vs pre-drug) and a trend of weight loss in 5xFAD$^{+/-}$ female mice. Weight displayed as mean ± S.E.M. Two-way repeated-measures ANOVA with Tukey's post hoc test (5xFAD$^{-/-}$: vehicle n=8, AC n=8, LPS n=8; 5xFAD$^{+/-}$: vehicle n=5, AC n=5, LPS n=6).

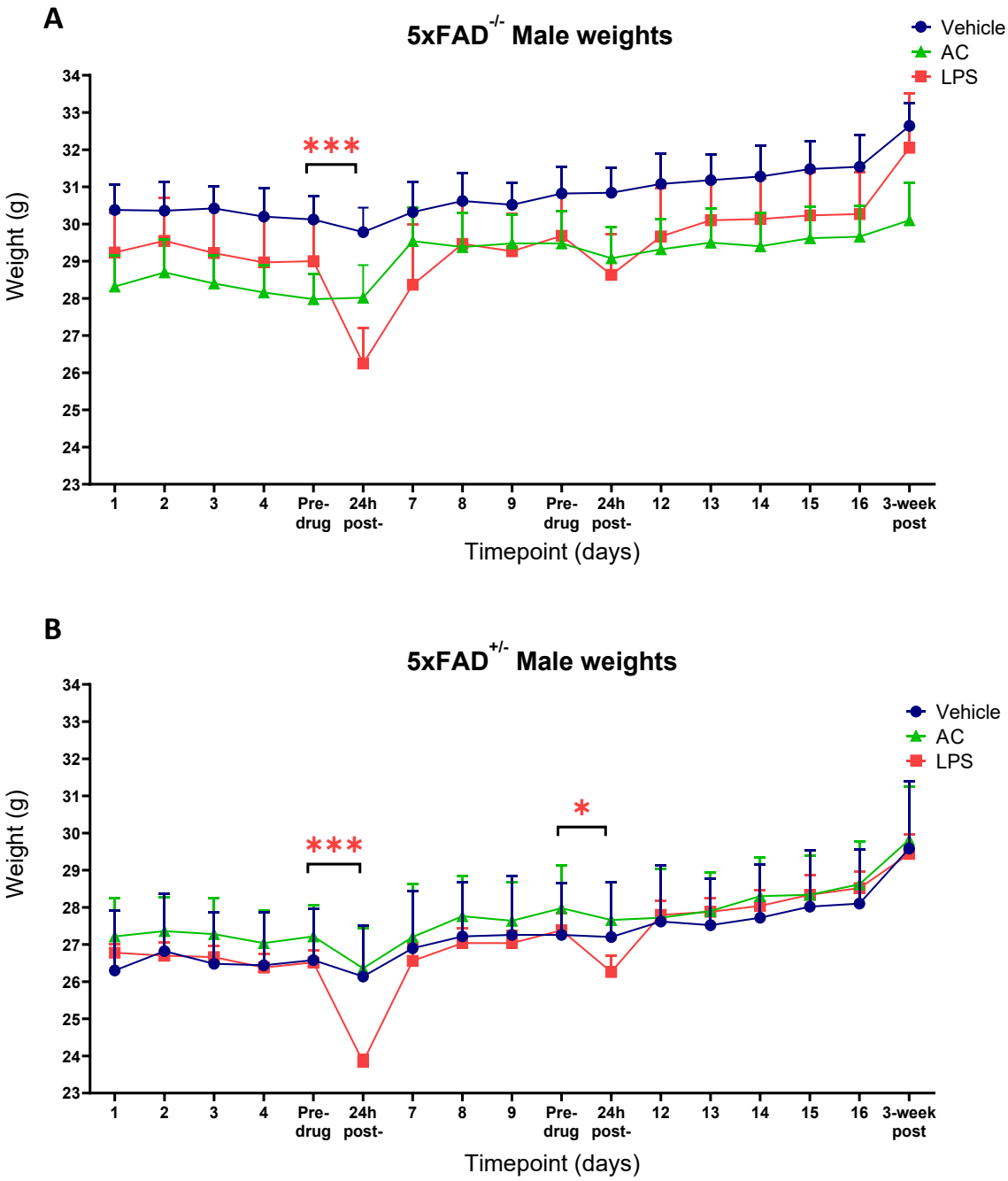

Figure 4.16: LPS-injection caused a temporary reduction in weight in male mice of both genotypes. LPS-injection induced a significant reduction in weight at 24h-post injection in the first week of testing in both 5xFAD$^{-/-}$ (***p<0.001 vs pre-drug) and 5xFAD$^{+/-}$ (***p<0.001 vs pre-drug) male mice. In the second week of testing, LPS-injection induced a trend of reduced weight in male 5xFAD$^{-/-}$ mice, and a significant weight reduction in male 5xFAD$^{+/-}$ mice (*p<0.05 vs pre-drug). Weight displayed as mean ± S.E.M. Two-way repeated-measures ANOVA with Tukey's post hoc test (5xFAD$^{-/-}$: vehicle n=8, AC n=8, LPS n=8; 5xFAD$^{+/-}$: vehicle n=5, AC n=5, LPS n=6).

4.8. Immunohistochemistry results

Following behavioural testing and treatments, mice were aged for 3 weeks to allow neuropathology to develop, then brains were fixed and IHC performed to examine astrocytes, microglia, and Aβ plaques in the following regions: subiculum, cornu Ammonis (CA) 1 and CA3, dentate gyrus (DG), visual cortex (VC) and somatosensory cortex (SSC).

4.8.1. Two injections of AC and LPS reduced GFAP and C3 expression in female but not male 5xFAD$^{+/-}$ mice at 3 weeks post-injection.

Astrocytic reactivity was determined using GFAP and C3 antibodies, with images of sagittal sections taken using the Mesolens. When astrocytes were examined using GFAP fluorescence (Fig.4.17), there was an overall increase in GFAP expression in the subiculum of both male and female 5xFAD$^{+/-}$ mice ($F_{(3\text{-}58)}$ = 89.75, $p<0.001$ 5xFAD$^{-/-}$, n=40, vs 5xFAD$^{+/-}$, n=30, Fig 4.18A) compared to 5xFAD$^{-/-}$ mice. Across the other brain regions examined, female vehicle-injected 5xFAD$^{+/-}$ mice had increased GFAP expression compared to female vehicle-injected 5xFAD$^{-/-}$ mice (CA1: $p<0.001$, Fig.4.18B; CA3: $p=0.007$, Fig.4.18C; DG: $p<0.001$, Fig.4.18D; VC: $p<0.001$, Fig.4.18E; SSC: $p<0.001$, Fig.4.18F, 5xFAD$^{-/-}$, n=8, vs 5xFAD$^{+/-}$, n=5, for all regions). Male 5xFAD$^{+/-}$ mice were found to have reduced overall GFAP expression compared to 5xFAD$^{+/-}$ females in the subiculum, DG, VC and SSC ($p<0.001$ males vs females, n=5) but no differences were found between male 5xFAD$^{-/-}$ and 5xFAD$^{+/-}$ mice or between treatments and sexes in 5xFAD$^{-/-}$ mice.

In 5xFAD$^{+/-}$ mice, it was revealed that AC-injection reduced GFAP expression across all examined brain regions in female 5xFAD$^{+/-}$ mice compared to vehicle

injection (subiculum: p=0.002, Fig.4.18A; CA1: p=0.005, Fig.4.18B; CA3: p=0.005, Fig.4.18C; DG: p<0.001, Fig.4.18D; VC: p=0.007, Fig.4.18E; SSC: p=0.002, Fig.4.18F, n=5 vs vehicle for all regions). AC-injection had no effect on GFAP fluorescence in male 5xFAD$^{+/-}$ mice in any region (subiculum: p=0.65, Fig.4.18A; CA1: p=0.91, Fig.4.18B; CA3: p=0.92, Fig.4.18C; DG: p=0.73, Fig.4.18D; VC: p=0.97, Fig.4.18E; SSC: p=0.91, Fig.4.18F, n=5 vs vehicle for all regions).

In 5xFAD$^{+/-}$ mice, LPS-injection also reduced GFAP expression in female 5xFAD$^{+/-}$ mice compared to vehicle injection in all regions (subiculum: p=0.004, Fig.4.18A; CA1: p=0.003, Fig.4.18B; CA3: p=0.013, Fig.4.18C; DG: p=0.002, Fig.4.18D; VC: p=0.03, Fig.4.18E; SSC: p=0.002, Fig.4.18F, n=5 vs vehicle for all regions). GFAP expression was unaffected by LPS-injection in male 5xFAD$^{+/-}$ mice (subiculum: p=0.34, Fig.4.18A; CA1: p=0.99, Fig.4.18B; CA3: p=0.79, Fig.4.18C; DG: p=0.99, Fig.4.18D; VC: p=0.94, Fig.4.18E; SSC: p=0.88, Fig.4.18F, n=5 vs vehicle for all regions).

When C3 fluorescence was examined (Fig.4.19), vehicle-injected female 5xFAD$^{+/-}$ mice had increased C3 expression across the brain compared to vehicle-injected female 5xFAD$^{-/-}$ mice (subiculum: p<0.001, Fig.4.20A; CA1: p=0.003, Fig.4.20B; CA3: p=0.03, Fig.4.20C; DG: p=0.02, Fig.4.20D; VC: p=0.02, Fig.4.20E; SSC: p=0.008, Fig.4.20F, 5xFAD$^{-/-}$, n=8, vs 5xFAD$^{+/-}$, n=5 vs vehicle for all regions). Male 5xFAD$^{+/-}$ mice had reduced overall C3 expression compared to 5xFAD$^{+/-}$ female mice in several brain regions (subiculum: p=0.01; CA1: p=0.02; DG: p=0.05; VC: p=0.008; SSC: p=0.009, males vs females, n=5). No difference in C3 expression was observed

between male 5xFAD$^{-/-}$ and 5xFAD$^{+/-}$ mice, or between the treatments in 5xFAD$^{-/-}$ mice of either sex.

Similar to GFAP, AC-injection reduced C3 expression in female 5xFAD$^{+/-}$ mice (subiculum: p=0.006, Fig.4.20A; CA1: p=0.04, Fig.4.20B; CA3: p=0.052, Fig.4.20C; DG: p=0.04, Fig.4.20D; VC: p=0.015, Fig.4.20E; SSC: p=0.035, Fig.4.20F, n=5 vs vehicle for all regions). However, no change was observed in male 5xFAD$^{+/-}$ mice following AC-injection (subiculum: p=0.88, Fig.4.20A; CA1: p=0.99, Fig.4.20B; CA3: p=0.98, Fig.4.20C; DG: p=0.82, Fig.4.20D; VC: p=0.78, Fig.4.20E; SSC: p=0.44, Fig.4.20F, n=5 vs vehicle for all regions).

LPS-injection also reduced C3 expression in female 5xFAD$^{+/-}$ mice (subiculum: p=0.003, Fig.4.20A; CA1: p=0.011, Fig.4.20B; CA3: p=0.03, Fig.4.20C; DG: p=0.04, Fig.4.20D; SSC: p=0.005, Fig.4.20F, n=5 vs vehicle for all regions) but LPS-injection had no effect in male 5xFAD$^{+/-}$ mice (subiculum: p=0.93, Fig.4.20A; CA1: p=0.75, Fig.4.20B; CA3: p=0.99, Fig.4.20C; DG: p=0.99, Fig.4.20D; VC: p=0.99, Fig.4.20E; SSC: p=0.78, Fig.4.20F, n=5 vs vehicle for all regions).

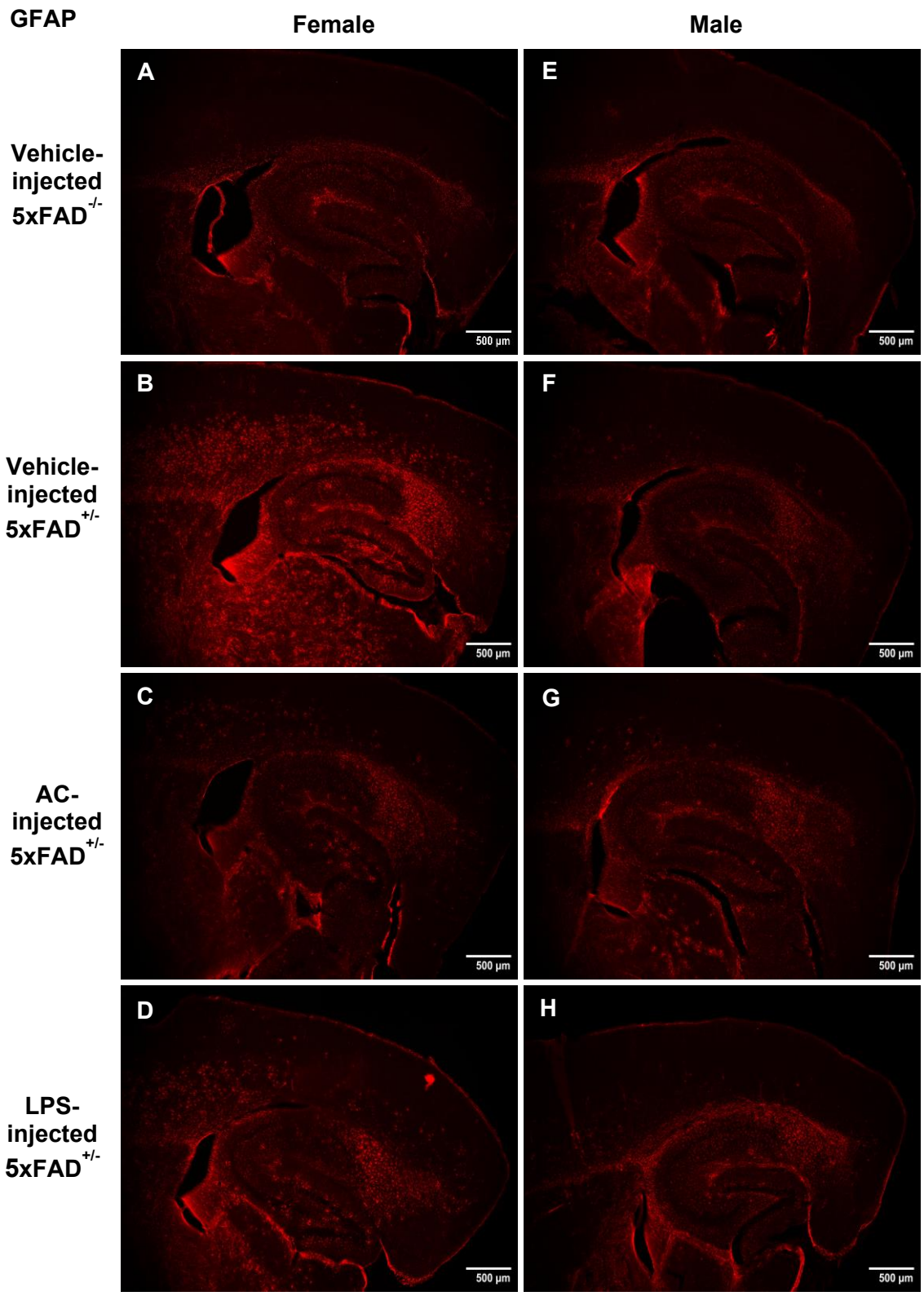

Figure 4.17: Representative Mesolens images of GFAP IHC in female and male 5xFAD$^{-/-}$ and 5xFAD$^{+/-}$ mice. (A-B) GFAP expression was increased in female 5xFAD$^{+/-}$ mice compared to 5xFAD$^{-/-}$ mice. (C-D) AC- and LPS-injection reduced GFAP expression across the brain regions in female but not male 5xFAD$^{+/-}$ mice at 3 weeks post-injection. Scale bar: 500µm.

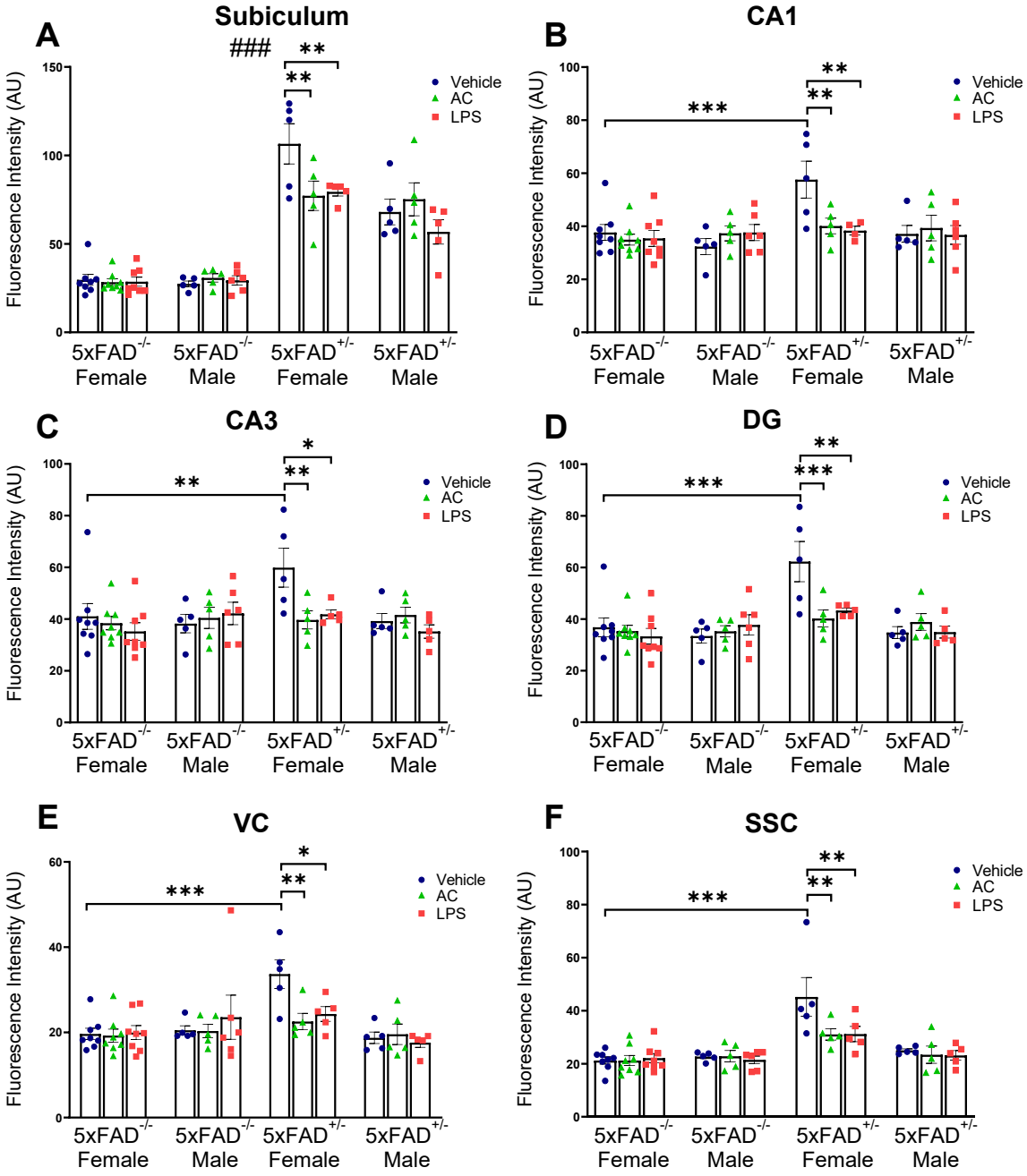

Figure 4.18: AC- and LPS-injection reduced GFAP expression in female but not male 5xFAD$^{+/-}$ mice. (A) Overall, GFAP expression was increased in the subiculum of 5xFAD$^{+/-}$ mice compared to 5xFAD$^{-/-}$ mice ($^{###}$p<0.001 5xFAD$^{-/-}$ vs 5xFAD$^{+/-}$). (B-F) GFAP expression was increased in vehicle-injected female 5xFAD$^{+/-}$ mice compared to 5xFAD$^{-/-}$ mice (CA1, DG, VC, SSC: ***p<0.001; CA3: **p<0.01, 5xFAD$^{-/-}$ vs 5xFAD$^{+/-}$, for all regions). (A-F) AC- and LPS-injection reduced GFAP expression in female but not male 5xFAD$^{+/-}$ mice compared to vehicle ((A) subiculum: AC: **p<0.01; LPS: **p<0.01 (B) CA1: AC: **p<0.01; LPS: **p<0.01 (C) CA3: AC: **p<0.01; LPS: *p<0.05 (D) DG: AC: ***p<0.001; LPS: **p<0.01 (E) VC: AC: **p<0.01; LPS: *p<0.05 (F) SSC: AC: **p<0.01; LPS: **p<0.01, vs vehicle for all regions). Fluorescence intensity measured as arbitrary units (AU). Two-way repeated-measures ANOVA with Tukey's post hoc test (Female: 5xFAD$^{-/-}$ n=8 all treatments, 5xFAD$^{+/-}$ n=5 all treatments; Male: 5xFAD$^{-/-}$ n=5 vehicle, n=5 AC, n=6 LPS, 5xFAD$^{+/-}$ n=5 all treatments).

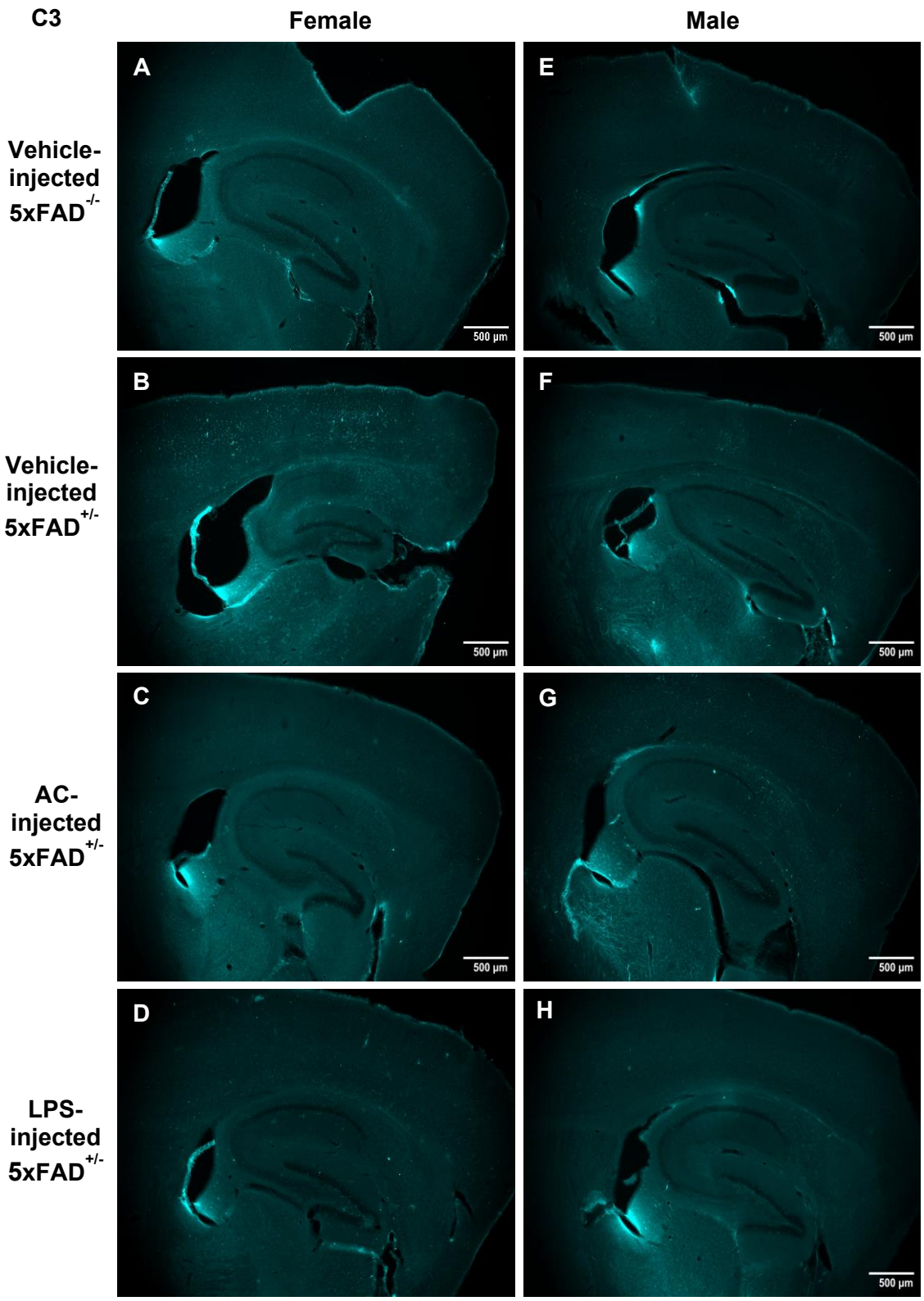

Figure 4.19: Representative Mesolens images of C3 IHC in female and male 5xFAD$^{-/-}$ and 5xFAD$^{+/-}$ mice. (A-B) C3 expression was increased in female 5xFAD$^{+/-}$ mice compared to 5xFAD$^{-/-}$ mice. (C-D) AC- and LPS-injection reduced C3 expression across the brain regions in female but not male 5xFAD$^{+/-}$ mice at 3 weeks post-injection. Scale bar: 500µm.

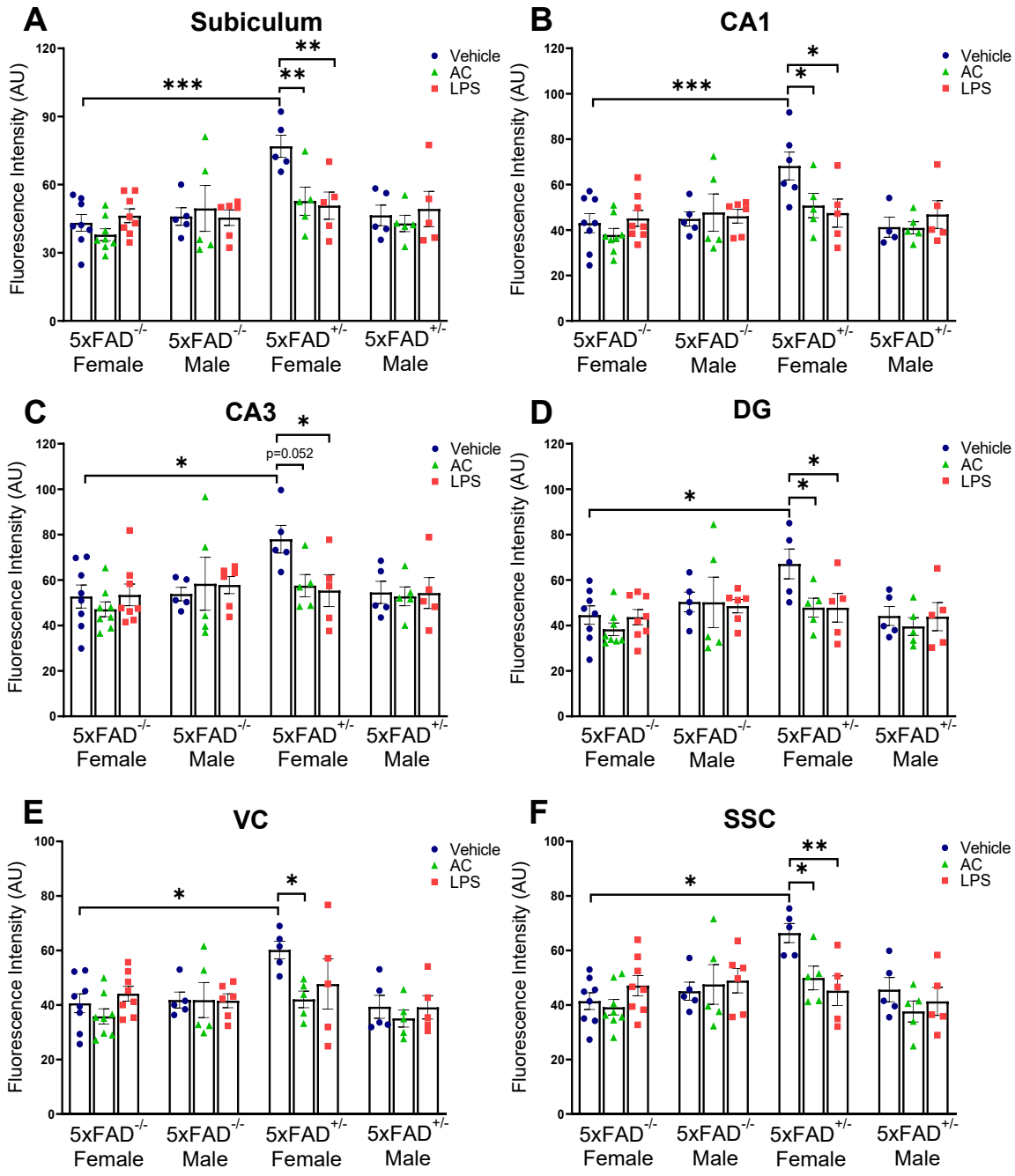

Figure 4.20: AC- and LPS-injection reduced C3 expression across the brain of female but not male 5xFAD$^{+/-}$ mice. (A-F) Vehicle injected female 5xFAD$^{+/-}$ mice had increased C3 expression across the brain compared to 5xFAD$^{-/-}$ mice (subiculum and CA1: ***p<0.001; CA3, DG, VC and SSC: *p<0.05, 5xFAD$^{-/-}$ vs 5xFAD$^{+/-}$, for all regions). AC- and LPS-injection reduced C3 expression in female but not male 5xFAD$^{+/-}$ mice compared to vehicle-injection (A) Subiculum: AC: **p<0.01; LPS: **p<0.01 (B) CA1: AC: *p<0.05; LPS: *p<0.05 (C) CA3: AC: p=0.052; LPS: *p<0.05 (D) DG: AC: *p<0.05; LPS: *p<0.05 (E) VC: AC: *p<0.05 (F) SSC: AC: *p<0.05; LPS: **p<0.01, vs vehicle for all regions. Fluorescence intensity measured as arbitrary units (AU). Two-way repeated-measures ANOVA with Tukey's post hoc test (Female: 5xFAD$^{-/-}$ n=8 all treatments, 5xFAD$^{+/-}$ n=5 all treatments; Male: 5xFAD$^{-/-}$ n=5 vehicle, n=5 AC, n=6 LPS, 5xFAD$^{+/-}$ n=5 all treatments).

4.8.2. Two injections of AC reduced Iba1 expression in some brain regions of female but not male 5xFAD$^{+/-}$ mice at 3 weeks post-injection.

Activated microglia were examined using Iba1 expression (Fig.4.21). There was an overall increase in Iba1 expression in 5xFAD$^{+/-}$ mice compared to 5xFAD$^{-/-}$ mice across several brain regions (subiculum: $F_{(3\text{-}58)} = 57.5$ $p<0.001$; CA1: $F_{(3\text{-}58)} = 4.4$ $p<0.01$; CA3: $F_{(3\text{-}58)} = 3.1$ $p<0.05$; DG: $F_{(3\text{-}58)} = 2.78$ $p<0.05$; SSC: $F_{(3\text{-}58)} = 6.8$ $p<0.001$, 5xFAD$^{-/-}$, n=40, vs 5xFAD$^{-/-}$, n=30 for all regions, Fig 4.21A-D, F). In the subiculum, male 5xFAD$^{+/-}$ mice had reduced Iba1 expression compared to female mice ($p<0.05$ males vs females, n=5). No differences were found between treatments or sex in 5xFAD$^{-/-}$ mice.

In 5xFAD$^{+/-}$ mice, AC-injection reduced Iba1 expression in only the CA3 ($p=0.048$ vs vehicle, n=5, Fig 4.22C) and SSC ($p=0.047$ vs vehicle, n=5, Fig 4.22F) of female 5xFAD$^{+/-}$ mice compared to vehicle-injection. AC-injection had no effect on Iba1 expression in male 5xFAD$^{+/-}$ mice in any region (subiculum: $p=0.29$, Fig.4.22A; CA1: $p=0.16$, Fig.4.22B; CA3: $p=0.22$, Fig.4.22C; DG: $p=0.51$, Fig.4.22D; VC: $p=0.27$, Fig.4.22E; SSC: $p=0.09$, Fig.4.22F, n=5 vs vehicle for all regions).

LPS-injection had no significant effect on Iba1 expression in either female (subiculum: $p=0.99$, Fig.4.22A; CA1: $p=0.68$, Fig.4.22B; CA3: $p=0.63$, Fig.4.22C; DG: $p=0.99$, Fig.4.22D; VC: $p=0.42$, Fig.4.22E; SSC: $p=0.51$, Fig.4.22F, n=5 vs vehicle for all regions) or male 5xFAD$^{+/-}$ (subiculum: $p=0.26$, Fig.4.22A; CA1: $p=0.29$, Fig.4.22B; CA3: $p=0.37$, Fig.4.22C; DG: $p=0.36$, Fig.4.22D; VC: $p=0.32$, Fig.4.22E; SSC: $p=0.75$, Fig.4.22F, n=5 vs vehicle for all regions) mice compared to vehicle injection.

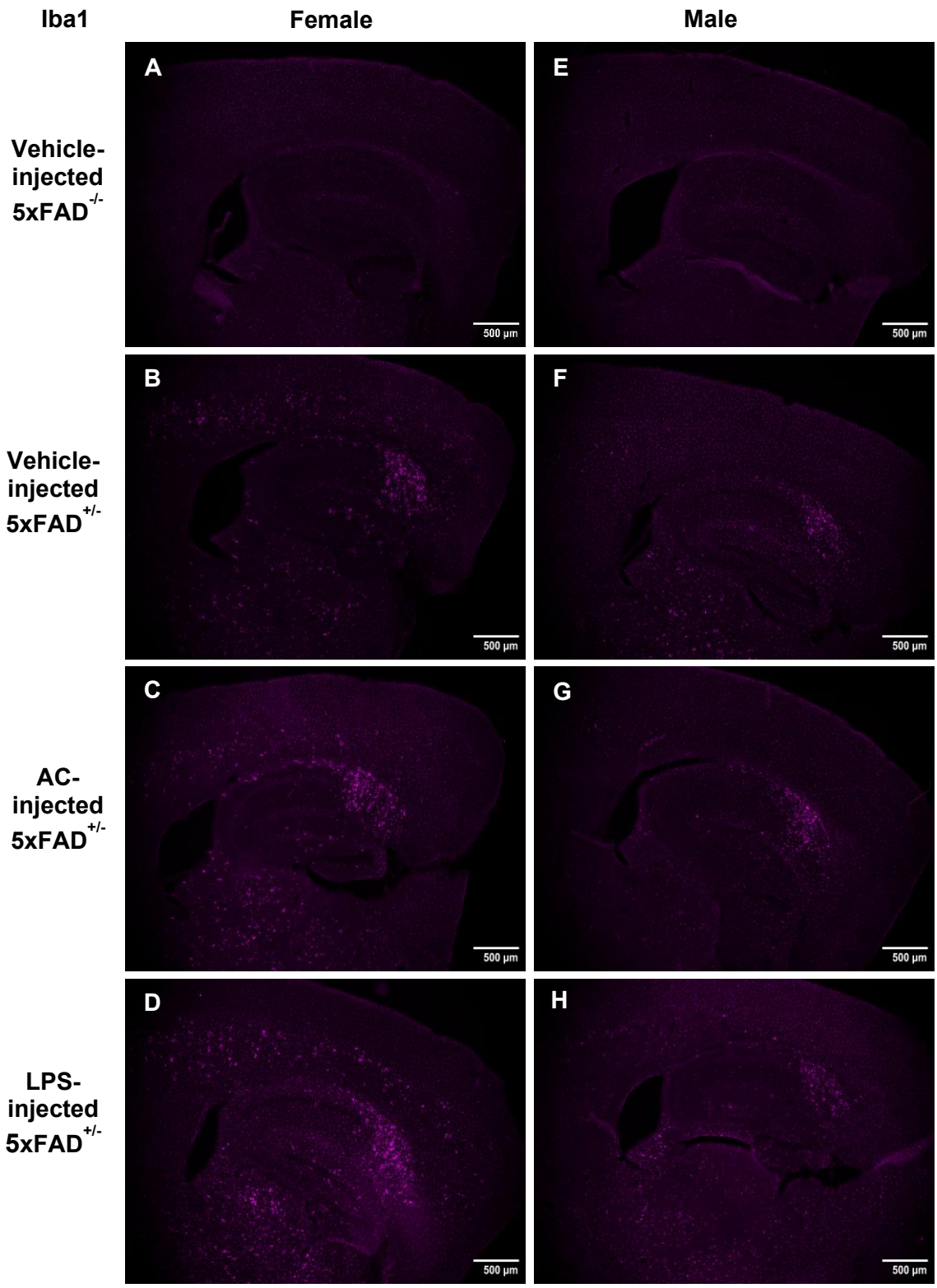

Figure 4.21: Representative Mesolens images of Iba1 IHC in female and male 5xFAD$^{-/-}$ and 5xFAD$^{+/-}$ mice. (A-B, E-F) There was an overall increase in Iba1 expression in 5xFAD$^{+/-}$ mice compared to 5xFAD$^{-/-}$ mice. (C-D) AC-injection reduced Iba1 expression in some brain regions in female 5xFAD$^{+/-}$ mice but LPS-injection had no effect. (G-H) Neither AC- nor LPS-injection influenced Iba1 expression in male 5xFAD$^{+/-}$ mice at 3 weeks post-injection. Scale bar: 500µm.

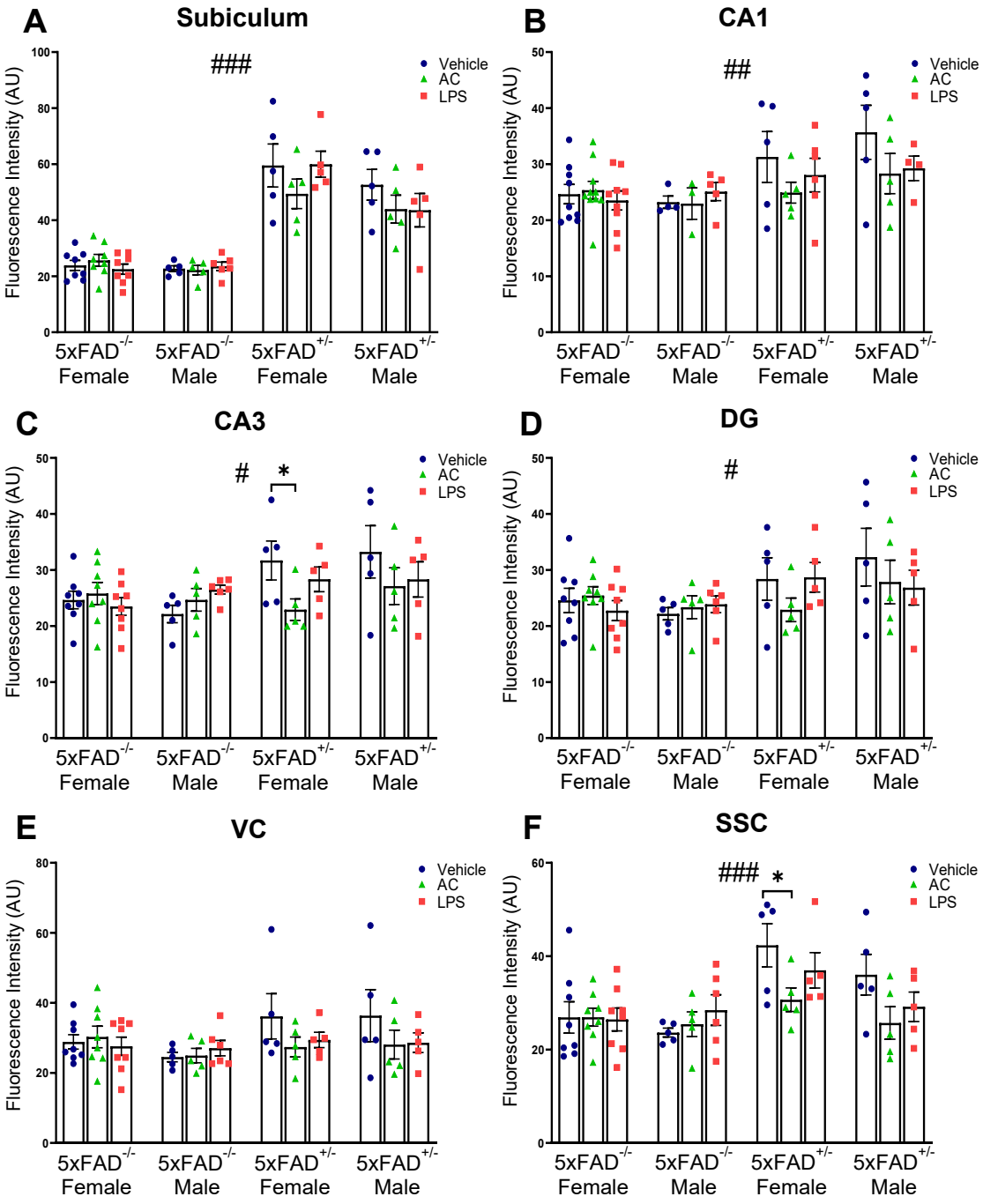

Figure 4.22: AC-injection reduced Iba1 expression in some brain regions of female 5xFAD$^{+/-}$ mice. (A-D, F) Iba1 expression was increased in 5xFAD$^{+/-}$ mice compared to 5xFAD$^{-/-}$ mice across the brain (subiculum: $^{###}p<0.001$; CA1: $^{\#}p<0.05$; CA3: $^{\#}p<0.05$; DG: $^{\#}p<0.05$; SSC $^{###}p<0.001$, 5xFAD$^{-/-}$ vs 5xFAD$^{+/-}$ for all regions). (C, F) AC-injection reduced Iba1 expression in some brain regions of female 5xFAD$^{+/-}$ mice (CA3: $^{*}p<0.05$; SSC: $^{*}p<0.05$, vs vehicle) but LPS-injection had no effect on Iba1 expression in any region of female 5xFAD$^{+/-}$ mice. Neither AC- nor LPS-injection significantly influenced Iba1 expression in male 5xFAD$^{+/-}$ mice. Fluorescence intensity measured as arbitrary units (AU). Two-way repeated-measures ANOVA with Tukey's post hoc test (Female: 5xFAD$^{-/-}$ n=8 all treatments, 5xFAD$^{+/-}$ n=5 all treatments; Male: 5xFAD$^{-/-}$ n=5 vehicle, n=5 AC, n=6 LPS, 5xFAD$^{+/-}$ n=5 all treatments).

4.8.3. Two injections of AC and LPS reduced Aβ plaque load in female but not male 5xFAD$^{+/-}$ mice at 3 weeks post-injection.

Thioflavin S was used to visualise Aβ plaques in 5xFAD$^{+/-}$ mice (Fig.4.23). Overall, female 5xFAD$^{+/-}$ mice had a higher plaque load than males across all brain regions (subiculum: $F_{(1-24)}$ = 18.21 p<0.001; CA1: $F_{(1-24)}$ = 13.58 p=0.0012; CA3: $F_{(1-24)}$ = 38.5 p<0.001; DG: $F_{(1-24)}$ = 56.4 p<0.001; VC: $F_{(1-24)}$ = 65.04 p<0.001; SSC: $F_{(1-24)}$ = 56.37 p<0.001, male vs female, n=5, for all regions, Fig 4.24A-F).

AC-injection reduced Aβ plaque load compared to vehicle in several brain regions of female 5xFAD$^{+/-}$ mice (subiculum: p=0.03, Fig.4.24A; CA3: p<0.001, Fig.4.24C; DG: p<0.001, Fig.4.24D; VC: p=0.001, Fig.4.24E; SSC: p=0.008, Fig.4.24F, n=5 vs vehicle for all regions). However, AC-injection had no effect on Aβ plaque load in male 5xFAD$^{+/-}$ mice (subiculum: p=0.76, Fig.4.24A; CA1: p=0.92, Fig.4.24B; CA3: p=0.86, Fig.4.24C; DG: p=0.99, Fig.4.24D; VC: p=0.65, Fig.4.24E; SSC: p=0.96, Fig.4.24F, n=5 vs vehicle for all regions).

It was also revealed that LPS-injection reduced Aβ plaque load in some brain regions of female 5xFAD$^{+/-}$ mice compared to vehicle (CA3: p<0.001, Fig.4.24C; DG: p<0.001, Fig.4.24D; VC: p=0.04, Fig.4.24E, n=5 vs vehicle for all regions). However, similar to AC, LPS-injection did not influence Aβ plaque load in male 5xFAD$^{+/-}$ mice (subiculum: p=0.9, Fig.4.24A; CA1: p=0.89, Fig.4.24B; CA3: p=0.92, Fig.4.24C; DG: p=0.96, Fig.4.24D; VC: p=0.84, Fig.4.24E; SSC: p=0.9, Fig.4.24F, n=5 vs vehicle for all regions).

Furthermore, the size of Aβ plaques in 5xFAD$^{+/-}$ mice were analysed. Overall, female 5xFAD$^{+/-}$ mice had significantly larger Aβ plaques than males in all brain regions (subiculum: $F_{(1-24)} = 13.75$ $p=0.002$; CA1: $F_{(1-24)} = 14.65$ $p<0.001$; CA3: $F_{(1-24)} = 6.74$ $p<0.015$; DG: $F_{(1-24)} = 22.18$ $p<0.001$; VC: $F_{(1-24)} = 25.52$ $p<0.001$; SSC: $F_{(1-24)} = 35.69$ $p<0.001$, male vs female, n=5, for all regions, Fig 4.25A-F).

In female 5xFAD$^{+/-}$ mice, AC-injection reduced Aβ plaque size across some brain regions compared to vehicle injection (subiculum: p=0.052, Fig.4.25A; DG: p=0.009, Fig.4.25D; VC: p=0.04, Fig.4.25E, n=5 vs vehicle for all regions). AC-injection did not alter Aβ plaque size in male 5xFAD$^{+/-}$ mice (subiculum: p=0.99, Fig.4.25A; CA1: p=0.99, Fig.4.25B; CA3: p=0.56, Fig.4.25C; DG: p=0.99, Fig.4.25D; VC: p=0.41, Fig.4.25E; SSC: p=0.74, Fig.4.25F, n=5 vs vehicle for all regions).

When Aβ plaque size was examined in LPS-injected mice, plaque size was only reduced in the DG of female 5xFAD$^{+/-}$ mice (p=0.051, Fig.4.25D, n=5 vs vehicle). In male 5xFAD$^{+/-}$ mice, LPS-injection had no effect on Aβ plaque size (subiculum: p=0.94, Fig.4.25A; CA1: p=0.97, Fig.4.25B; CA3: p=0.85, Fig.4.25C; DG: p>0.99, Fig.4.25D; VC: p=0.76, Fig.4.25E; SSC: p=0.46, Fig.4.25F, n=5 vs vehicle for all regions).

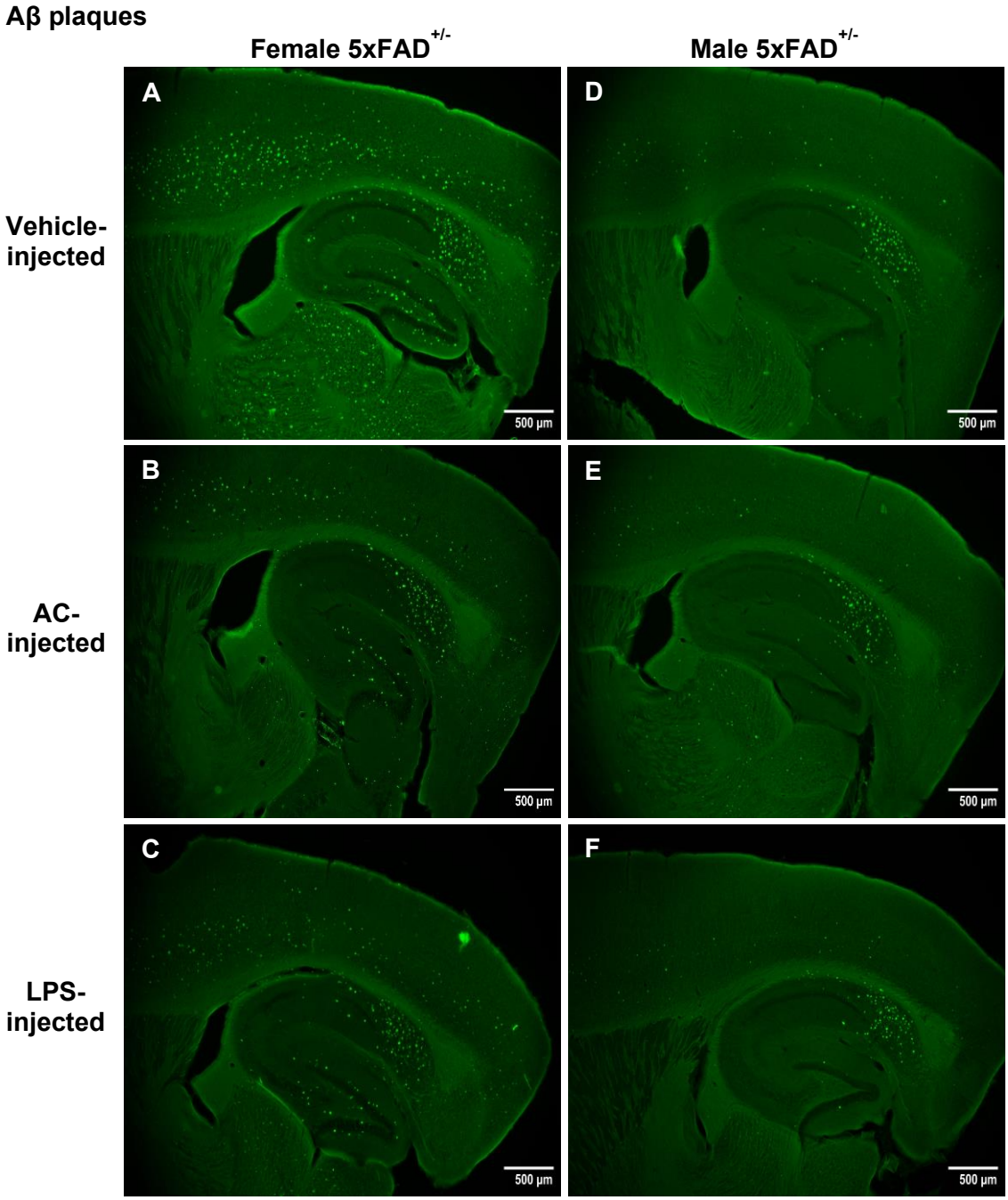

Figure 4.23: Representative Mesolens images of Aβ plaques in female and male 5xFAD$^{+/-}$ mice following vehicle, AC- and LPS-injection. (A&D) Female 5xFAD$^{+/-}$ mice had significantly increased Aβ plaque load than male 5xFAD$^{+/-}$ mice. (B-C) AC- and LPS-injection reduced Aβ plaque load in several brain regions in female but not male 5xFAD$^{+/-}$ mice at 3 weeks post-injection. Scale bar: 500µm.

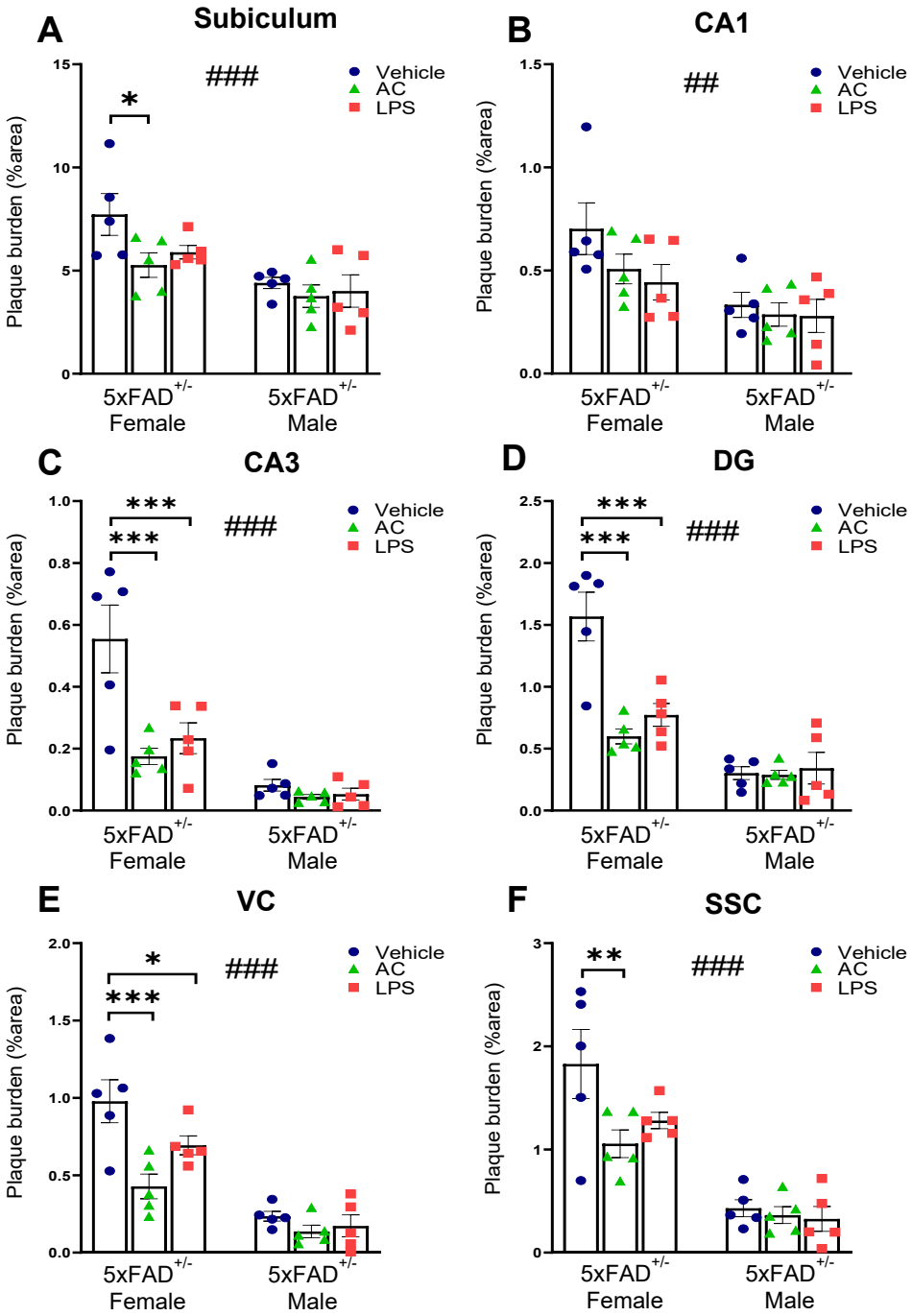

Figure 4.24: AC- and LPS-injection reduced Aβ plaque load across several brain regions of female but not male 5xFAD$^{+/-}$ mice. (A-F) Thioflavin S staining revealed an overall increase in Aβ plaque load in female 5xFAD$^{+/-}$ mice compared to males across all regions (subiculum: $^{###}$p<0.001; CA1: $^{##}$p<0.01; CA3: $^{###}$p<0.001; DG: $^{###}$p<0.001; VC $^{###}$p<0.001; SSC $^{###}$p<0.001, male vs female for all regions). Across many brain regions, AC- and LPS-injected female but not male 5xFAD$^{+/-}$ mice had significantly reduced Aβ plaque load compared to vehicle-injection ((A) subiculum: AC: *p<0.05 (C) CA3: AC: ***p<0.001; LPS: ***p<0.001 (D) DG: AC: ***p<0.001; LPS: ***p<0.001 (E) VC: AC: ***p<0.001; LPS: *p<0.05 (F) SSC: AC: **p<0.01, vs vehicle for all regions). Two-way repeated-measures ANOVA with Tukey's post hoc test (n=5 all treatments and sex).

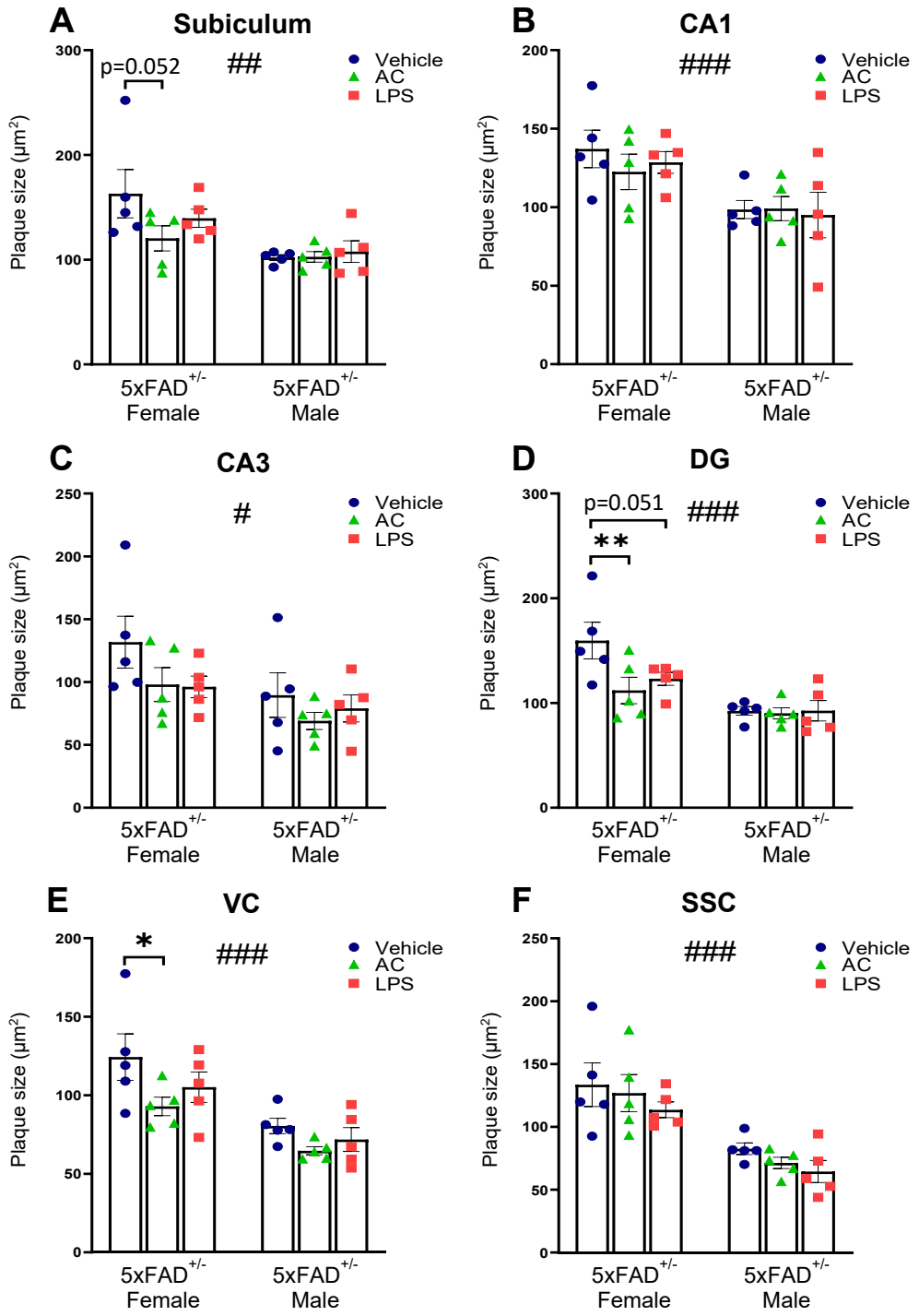

Figure 4.25: AC- and LPS-injection reduced Aβ plaque size in some regions of female but not male 5xFAD$^{+/-}$ mice. (A-F) Thioflavin S staining revealed an overall increase in Aβ plaque size in female 5xFAD$^{+/-}$ mice compared to males across all regions (subiculum: $^{\#\#}$p<0.01; CA1: $^{\#\#\#}$p<0.001; CA3: $^{\#}$p<0.05; DG: $^{\#\#\#}$p<0.001; VC $^{\#\#\#}$p<0.001; SSC $^{\#\#\#}$p<0.001, male vs female for all regions). In some regions, AC- and LPS-injected female but not male 5xFAD$^{+/-}$ mice had reduced Aβ plaque size compared to vehicle-injection ((A) Subiculum: AC: p=0.052 (D) DG: AC: **p<0.01; LPS: p=0.051 (E) VC: AC: *p<0.05, vs vehicle for all regions). Two-way repeated-measures ANOVA with Tukey's post hoc test (n=5 all treatments and sex).

4.8.4. Two injections of AC and LPS had no influence on CD68 expression or CD68 to Iba1 ratio at 3 weeks post-injection.

Following the observation that AC- and LPS-injection reduced astrocytic reactivity and Aβ plaque load in the female 5xFAD$^{+/-}$ mice, it was hypothesised that AC and LPS may modulate microglia-astrocyte cross-talk (Rostami *et al.*, 2021; Lee, Yu, *et al.*, 2025), thereby promoting a more phagocytic microglial phenotype and thereby reducing Aβ plaque burden. To investigate this, CD68 antibody was utilised to examine phagocytic microglia, both as CD68 expression (Fig.4.26), and as the ratio of CD68 to Iba1 expression in 5xFAD$^{+/-}$ mice.

In female 5xFAD$^{+/-}$ mice, CD68 expression was significantly increased across the brain compared to male 5xFAD$^{+/-}$ mice (subiculum: $F_{(1-23)}$ = 23.05 p<0.001; CA1: $F_{(1-23)}$ = 14.57 p<0.001; CA3: $F_{(1-23)}$ = 5.48 p=0.03; DG: $F_{(1-23)}$ = 10.69 p=0.003; VC: $F_{(1-23)}$ = 8.57 p<0.008; SSC: $F_{(1-23)}$ = 21.4 p<0.001, male vs female, n=5 females all treatments; n=4 vehicle, n=5 AC, n=5 LPS males, for all regions, Fig 4.27A-F).

AC-injection had no effect on CD68 expression in either female (subiculum: p=0.5, Fig.4.27A; CA1: p=0.49, Fig.4.27B; CA3: p=0.35, Fig.4.27C; DG: p=0.5, Fig.4.27D; VC: p=0.2, Fig.4.27E; SSC: p=0.09, Fig.4.27F, n=5 vs vehicle for all regions) or male 5xFAD$^{-/-}$ mice (subiculum: p=0.9, Fig.4.27A; CA1: p=0.84, Fig.4.27B; CA3: p=0.82, Fig.4.27C; DG: p=0.66, Fig.4.27D; VC: p=0.95, Fig.4.27E; SSC: p=0.99, Fig.4.27F, n=5 vs vehicle for all regions).

LPS-injection significantly reduced CD68 expression in only the SSC of female 5xFAD$^{+/-}$ mice (p=0.03 vs vehicle, n=5) but had no further significant effects across the brain in either female (subiculum: p=0.2, Fig.4.27A; CA1: p=0.42, Fig.4.27B; CA3: p=0.19, Fig.4.27C; DG: p=0.13, Fig.4.27D; VC: p=0.37, Fig.4.27E, n=5 vs vehicle for all regions) or male 5xFAD$^{+/-}$ mice (subiculum: p=0.99, Fig.4.27A; CA1: p=0.76, Fig.4.27B; CA3: p=0.88, Fig.4.27C; DG: p=0.83, Fig.4.27D; VC: p=0.89, Fig.4.27E; SSC: p=0.8, Fig.4.27F, n=5 vs vehicle for all regions).

When CD68 was examined as a ratio with Iba1, there was overall increase in CD68 labelled phagocytic microglia compared to Iba1 labelled activated microglia in the CA3 and VC of female 5xFAD$^{+/-}$ mice compared to males (CA3: $F_{(1-23)}$ = 10.04 p=0.004, Fig.4.28C; VC: $F_{(1-23)}$ = 12.54 p=0.002, Fig.4.28E, male vs female, n=5 females all treatments; n=4 vehicle, n=5 AC, n=5 LPS males, for both regions).

AC-injection had no effect on CD68 to Iba1 ratio in either female (subiculum: p=0.73, Fig.4.28A; CA1: p=0.97, Fig.4.28B; CA3: p=0.8, Fig.4.28C; DG: p=0.99, Fig.4.28D; VC: p=0.09, Fig.4.28E; SSC: p=0.94, Fig.4.28F, n=5 vs vehicle for all regions) or male 5xFAD$^{+/-}$ mice (subiculum: p>0.99, Fig.4.28A; CA1: p=0.99, Fig.4.28B; CA3: p=0.28, Fig.4.28C; DG: p=0.99, Fig.4.28D; VC: p=0.83, Fig.4.28E; SSC: p=0.99, Fig.4.28F, n=5 vs vehicle for all regions).

In LPS-injected mice, there was an increase in CD68 to Iba1 ratio in the VC of female 5xFAD$^{+/-}$ (p=0.055 vs vehicle, Fig. 4.27E, n=5). However, LPS-injection did not alter CD68 to Iba1 ratio in any other region of female (subiculum: p=0.8,

Fig.4.28A; CA1: p=0.94, Fig.4.28B; CA3: p=0.54, Fig.4.28C; DG: p=0.94, Fig.4.28D; SSC: p=0.13, Fig.4.28F, n=5 vs vehicle for all regions) or male 5xFAD$^{+/-}$ (subiculum: p=0.1, Fig.4.28A; CA1: p=0.15, Fig.4.28B; CA3: p=0.27, Fig.4.28C; DG: p=0.25, Fig.4.28D; VC: p=0.91, Fig.4.28E, SSC: p>0.99, Fig.4.28F, n=5 vs vehicle for all regions).

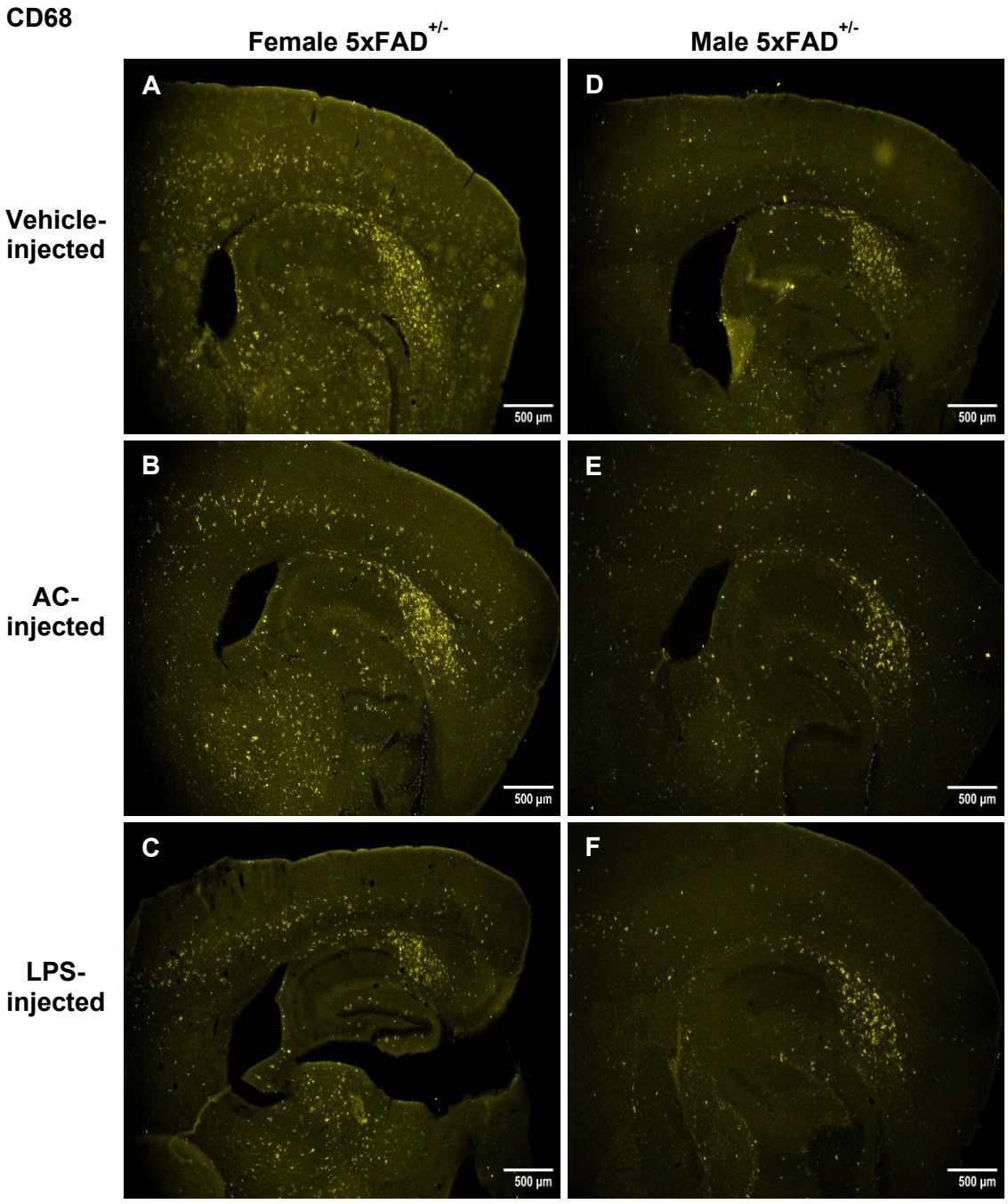

Figure 4.26: Representative Mesolens images of CD68 IHC in female and male 5xFAD$^{+/-}$ mice following vehicle, AC- and LPS-injection. (A&D) Female 5xFAD$^{+/-}$ mice had significantly increased CD68 expression than male 5xFAD$^{+/-}$ mice. (B-C & E-F) AC- and LPS-injection had no significant effect on CD68 in either female or male 5xFAD$^{+/-}$ mice at 3 weeks post-injection. Scale bar: 500µm.

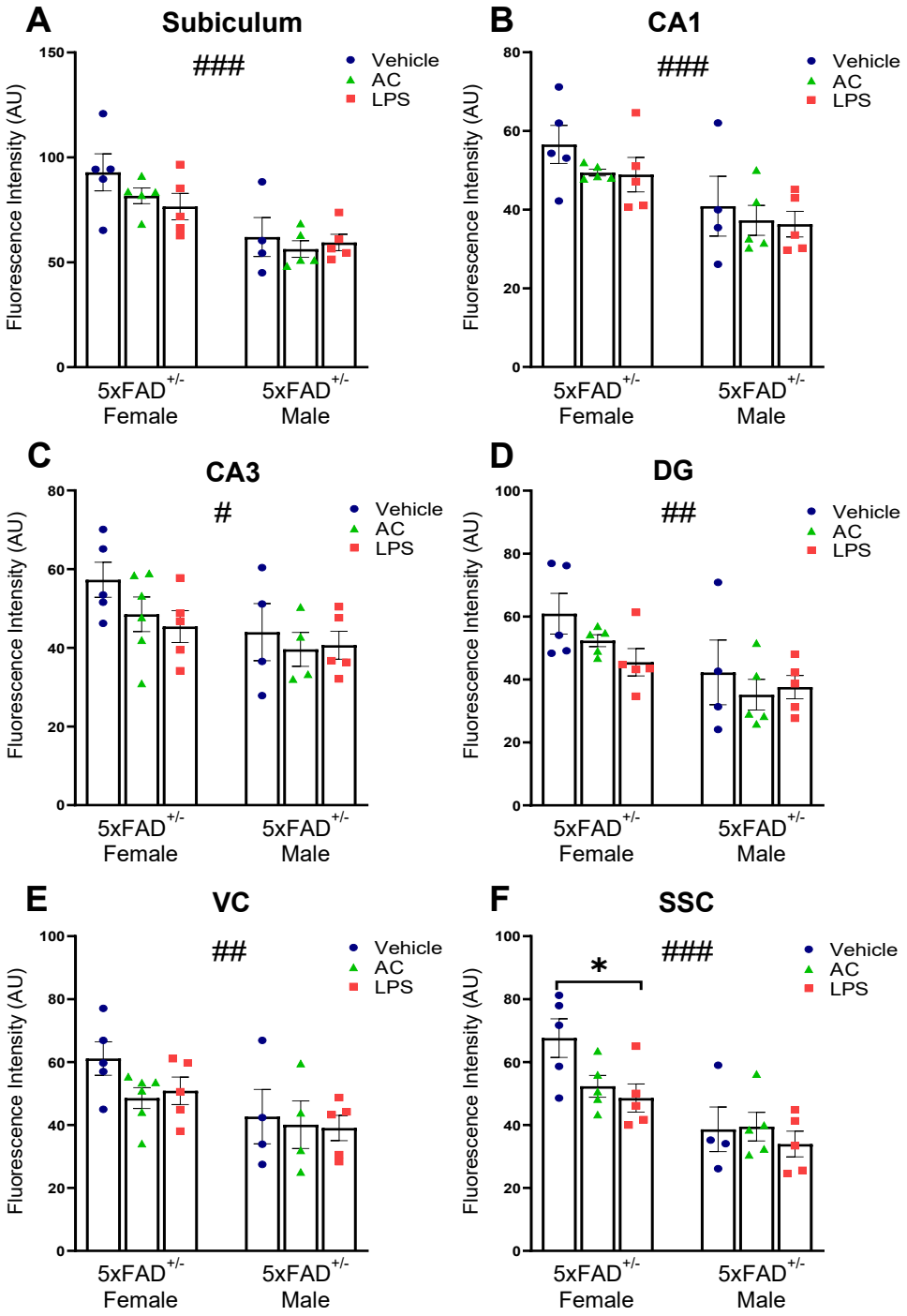

Figure 4.27: AC- and LPS-injection had no influence on CD68 expression in female or male 5xFAD$^{+/-}$ mice. (A-F) CD68 expression was significantly increased in female 5xFAD$^{+/-}$ mice compared to males across the brain (subiculum: $^{###}p<0.001$; CA1: $^{###}p<0.001$; CA3: $^{\#}p<0.05$; DG: $^{\#\#}p<0.01$; VC: $^{\#\#}p<0.01$; SSC $^{###}p<0.001$, male vs female all regions). Across the brain, AC- and LPS-injection had no effect on CD68 expression in either female or male 5xFAD$^{+/-}$ mice. (F) However, in the SSC, LPS-injection reduced CD68 expression compared to vehicle (*p<0.05 vs vehicle. Fluorescence intensity measured as arbitrary units (AU). Two-way repeated-measures ANOVA with Tukey's post hoc test (Female: n=5 all treatments; Male: n=4 vehicle, n=5 AC, n=5 LPS).

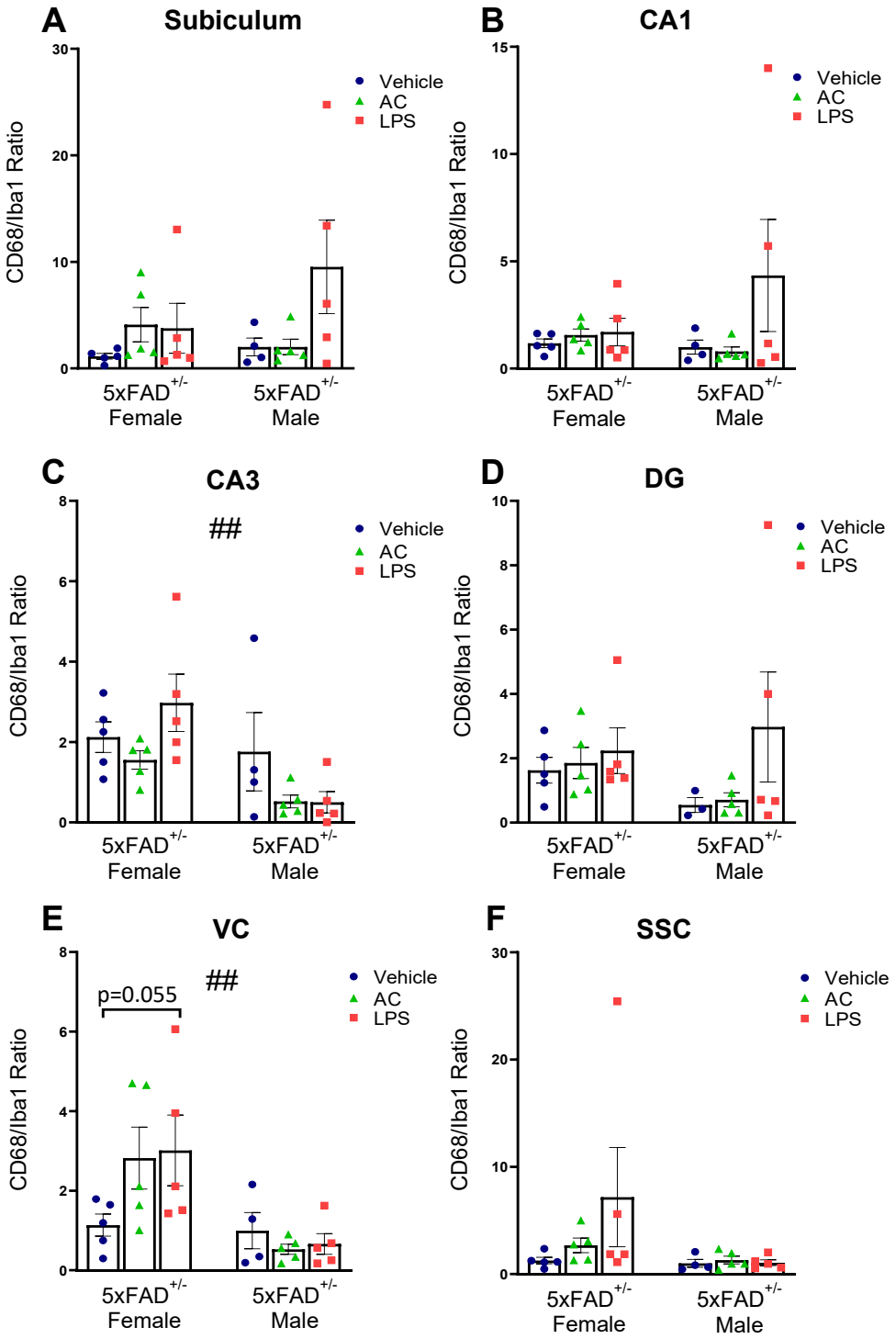

Figure 4.28: AC- and LPS-injection had no significant effect on CD68 to Iba1 ratio in male or female 5xFAD$^{+/-}$ mice. (C, E) In the CA3 and VC, CD68 to Iba1 ratio was increased in female 5xFAD$^{+/-}$ mice compared to males (CA3: $^{\#\#}p<0.01$; VC: $^{\#\#}p<0.01$, male vs female for both regions). (E) In the VC, LPS-injection increased CD68 to IBA1 ratio compared to vehicle (p=0.055 vs vehicle). However, AC- and LPS-injection did not alter CD68 to Iba1 ratio in any other brain region in either female or male 5xFAD$^{+/-}$ mice. Two-way repeated-measures ANOVA with Tukey's post hoc test (Female: n=5 all treatments; Male: n=4 vehicle, n=5 AC, n=5 LPS).

4.9. AC-injection has no influence on peripheral cytokines in 5xFAD$^{+/-}$ mice.

Given the established link between peripheral inflammation and MDD (Beurel *et al.*, 2020; Roohi *et al.*, 2021), peripheral cytokine levels were examined following AC- and LPS-induced depression-like behaviour to assess systemic inflammatory responses and determine whether cytokine changes correspond to those observed in MDD.

Cytokines were examined within the genotypes. In 5xFAD$^{-/-}$ mice, AC- and LPS-injection influenced several cytokines (Fig.4.29). LPS-injection increased pro-inflammatory IL-6 levels ($p<0.001$ vs vehicle, n=4, Fig.4.29) compared to vehicle injection but AC-injection had no effect on IL-6 ($p=0.17$ vs vehicle, n=4, Fig.4.29). LPS-injection had no effect on pro-inflammatory cytokines IL-1β ($p=0.29$ vs vehicle, n=4, Fig.4.29) and TNF-α ($p=0.16$ vs vehicle, n=4, Fig.4.29). However, AC-injection significantly reduced several proinflammatory cytokines in 5xFAD$^{-/-}$ mice (IL-1β: $p=0.01$; TNF-α: $p=0.008$; IL-12: $p=0.01$, n=4 vs vehicle for all cytokines, Fig.4.29). In 5xFAD$^{-/-}$ mice, some anti-inflammatory cytokines were reduced by both AC- (IL-4: $p<0.001$; IFN-γ: $p<0.001$, n=4 vs vehicle for both cytokines, Fig.4.29) and LPS-injection (IL-4: $p<0.001$; IFN-γ: $p=0.009$, n=4 vs vehicle for both cytokines, Fig.4.29) but no change was observed in anti-inflammatory IL-10 following either AC- or LPS-injection (AC: $p=0.4$; LPS: $p=0.12$, n=4 vs vehicle for both cytokines). Furthermore, AC- and LPS-injection increased pro-inflammatory levels of several CC chemokine ligands (CCL) and chemokine (C-X-C motif) ligands (CXCL), including CXCL1 (AC: $p=0.046$; LPS: $p<0.001$, n=4 vs vehicle

for both chemokines, Fig.4.29) and CCL2 (LPS: $p<0.001$ vs vehicle, n=4, Fig.4.29).

When cytokines were examined in the 5xFAD$^{+/-}$ mice (Fig.4.30), AC-injection only increased pro-inflammatory CXCL1 (AC: $p=0.036$ vs vehicle, n=4, Fig.4.30). LPS-injection again increased several pro-inflammatory cytokines and chemokines (IL-6: $p<0.001$; CXCL1: $p<0.001$; CCL2: $p<0.001$, n=4 vs vehicle for all cytokines, Fig.4.30) but neither AC- nor LPS-injection altered IL-1β , IL-12 or TNF-α (IL-1β: AC: $p=0.96$; LPS: $p=0.98$; IL-12: AC: $p=0.77$; LPS: $p=0.15$; TNF-α: AC: $p=0.86$; LPS: 0.85, Fig.4.30, n=4 vs vehicle for all cytokines). LPS-injection also reduced anti-inflammatory cytokines IL-4 ($p=0.002$ vs vehicle, n=4, Fig.4.30) and IFN-γ ($p<0.001$ vs vehicle, n=4, Fig.4.30) but no change was observed in these anti-inflammatory cytokines following AC-injection.

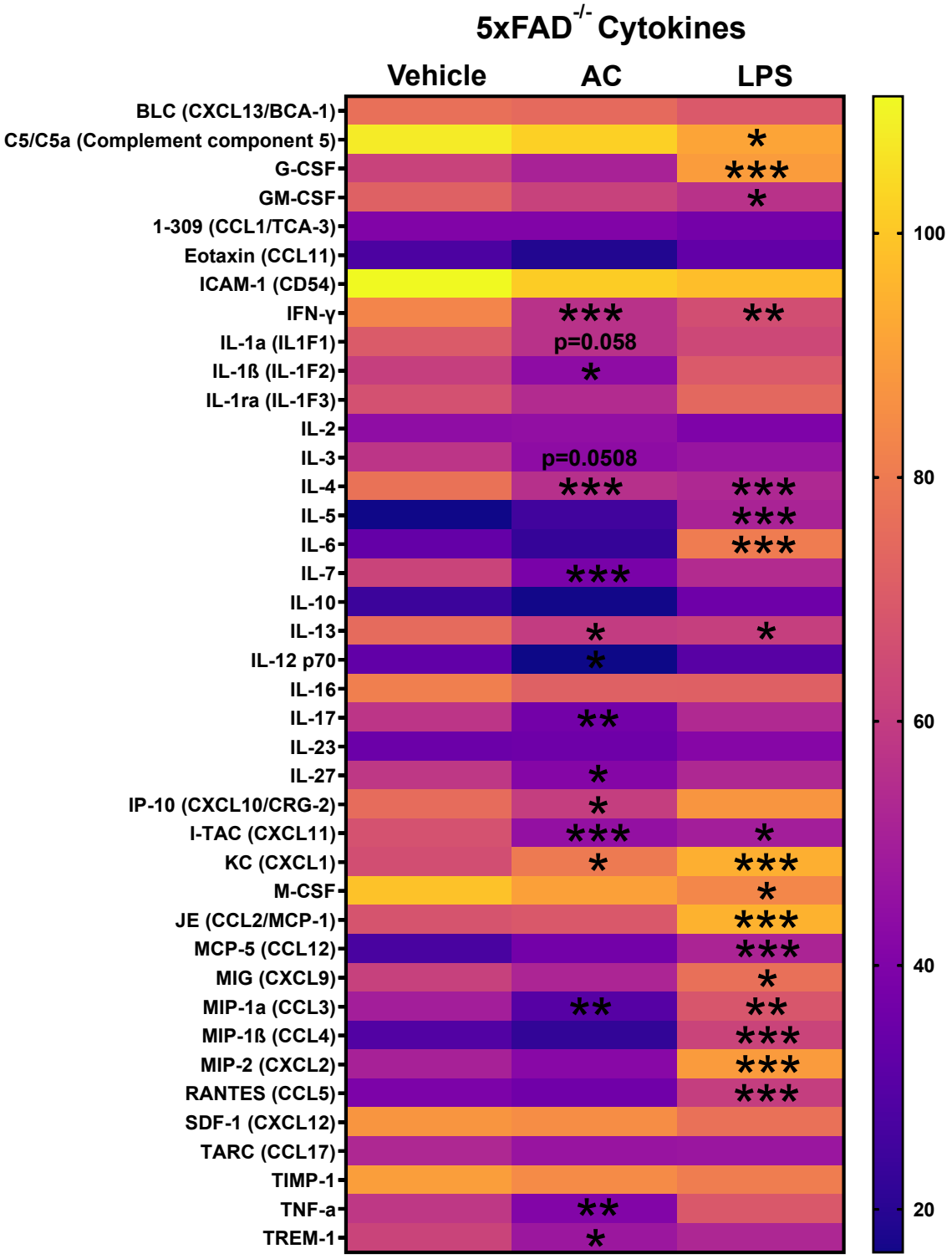

Figure 4.29: Cytokine analysis of 5xFAD$^{-/-}$ mice following vehicle, AC- and LPS-injection. Several cytokines were increased or decreased in response to AC- or LPS-injection compared to vehicle. Notably, IL-6 was increased in response to LPS-injection (***p<0.001) but not AC-injection. Cytokine heat plot displayed as mean, sex combined data (*p<0.05, **p<0.01, ***p<0.001 vs vehicle). Two-way repeated-measures ANOVA with Tukey's post hoc test (n=4; 2 male, 2 female per treatment).

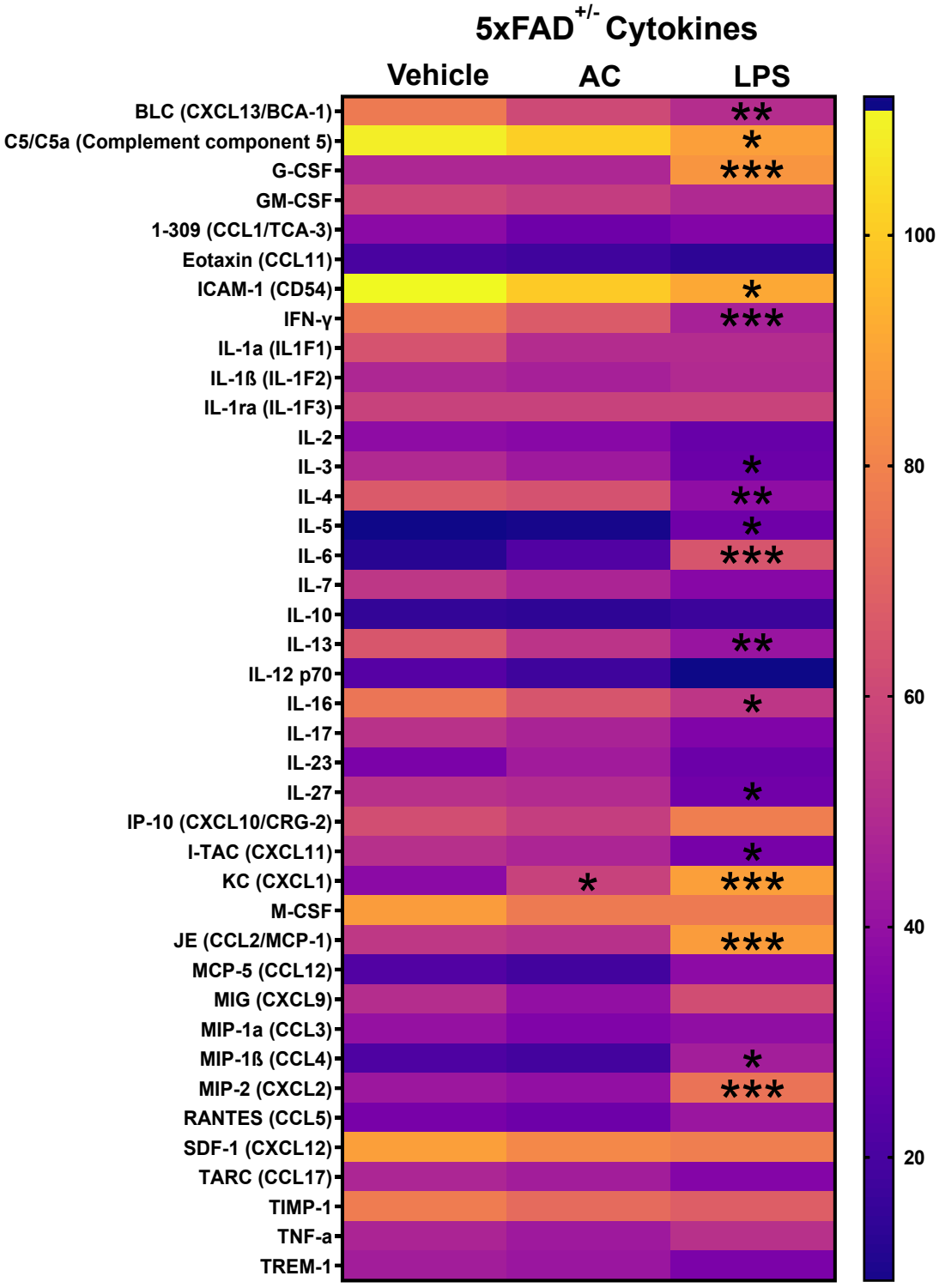

Figure 4.30: Cytokine analysis of 5xFAD$^{+/-}$ mice following vehicle, AC- and LPS-injection. Several cytokines were increased or decreased in response to LPS-injection. However, in 5xFAD$^{+/-}$ mice only pro-inflammatory CXCL1 was increased following AC-injection (*p<0.05). Notably, IL-6 was increased in response to LPS-injection (***p<0.001) but not AC-injection. Cytokine heat plot displayed as mean, sex combined data (*p<0.05, **p<0.01, ***p<0.001). Two-way repeated-measures ANOVA with Tukey's post hoc test (n=4; 2 male, 2 female per treatment).

4.10. Discussion

4.10.1. AC264613 and LPS induced behavioural changes associated with depression-like behaviour.

The results from the 5xFAD$^{-/-}$ vs 5xFAD$^{+/-}$ mice cohort further confirmed that AC264613 (100 mg kg^{-1}) and LPS (0.5 mg kg^{-1}) induce behavioural changes associated with depression-like behaviour 2h post-injection. Reductions in locomotor activity, reduced sucrose preference, and grooming behaviour suggest the mice are experiencing low mood, anhedonia, and apathy, core features of MDD. While AC-induced behavioural changes were recovered by 24h post-injection, LPS-induced anhedonia persisted at 24h post-injection, although changes in grooming and locomotor activity were recovered. These findings further support our data from the C57BL6/J and 5xFAD$^{-/-}$ mice cohort, as well as previous studies within the research group (Abulkassim *et al.*, 2016; Moudio *et al.*, 2022).

Neuropsychiatric symptoms are a core feature of AD, with a higher incidence of depression reported in patients living with dementia (16-32%) compared to the general population (5%) (Kamran *et al.*, 2022; Huang *et al.*, 2024). Therefore, we hypothesised that 5xFAD$^{+/-}$ mice would be more likely to display and would be more susceptible to depression-like behaviour compared to their 5xFAD$^{-/-}$ littermates. However, few genotypic differences were observed, with the most notable being a greater reduction in grooming behaviour in 5xFAD$^{+/-}$ mice following AC and LPS. This suggests that while both genotypes display depression-like responses to AC and LPS, 5xFAD$^{+/-}$ mice may be more vulnerable to pharmacologically induced apathy-like behaviour.

4.10.2. AC264613 and LPS reduced locomotor activity in both 5xFAD$^{-/-}$ and 5xFAD$^{+/-}$ mice, while LPS alone increased anxiety-like behaviour.

In our 5xFAD$^{-/-}$ vs 5xFAD$^{+/-}$ cohort, we observed an initial increase in locomotor activity in 5xFAD$^{+/-}$ mice upon first exposure to the OFT arena, which may indicate hyperactivity. However, in subsequent sessions, no differences in locomotor behaviour were found between 5xFAD$^{+/-}$ and 5xFAD$^{-/-}$ mice. Furthermore, we did not observe any change in anxiety-like behaviour in 5xFAD$^{+/-}$ mice during any OFT sessions.

Hyperactivity and increased anxiety-like behaviour has been reported in 5xFAD$^{+/-}$ mice compared to WT controls (Oblak *et al.*, 2021; Zhong *et al.*, 2024). However, these behavioural changes are typically observed in older animals, between 6–12 months of age (Oblak *et al.*, 2021), suggesting that the mice used in our study, 3 months of age at the time of testing, may have been too young to display such changes. The age of the mice selected for this research was chosen due to the early formation of Aβ plaque pathology, therefore behavioural changes associated with low mood and anhedonia may be seen between the genotypes in aged animals.

Reports in the literature vary considerably, with some suggesting 5xFAD$^{+/-}$ mice display altered behaviour, including locomotor and exploratory behaviour from 6–9 months, while others report earlier onset at 4–5 months (Oblak *et al.*, 2021; Medina-Vera *et al.*, 2023; Pádua *et al.*, 2024). Interestingly, reduced anxiety-like behaviour has also been observed in 5xFAD$^{+/-}$ mice at 12 months of age (Forner *et al.*, 2021; Zhong *et al.*, 2024), and previous reviews have highlighted significant inconsistencies related to the exploratory behaviour of

5xFAD$^{+/-}$ mice, both in the nature and age of onset of behavioural changes (Pádua *et al.*, 2024).

Both 5xFAD$^{-/-}$ and 5xFAD$^{+/-}$ mice exhibited reduced locomotor activity following AC and LPS treatment, indicating that both genotypes were equally susceptible to AC- and LPS-induced sickness or depression-like behavioural changes affecting locomotion and exploratory behaviour. This reduction supports previous findings, and may reflect low mood and fatigue in the mice, key features of MDD (Seibenhener *et al.*, 2015; Gencturk *et al.*, 2024). As observed in the previous cohort, locomotor activity recovered by 24h post-injection in both genotypes, indicating that AC and LPS did not induce prolonged behavioural changes. Furthermore, no long-term alterations in locomotor activity were observed at 3-weeks post injection, supporting the transient effect of AC and LPS-induced behavioural changes (Biesmans *et al.*, 2013; Lasselin *et al.*, 2020; Moudio *et al.*, 2022).

LPS, but not AC, induced a decrease in time spent in the centre of the OFT arena, which may indicate increased anxiety-like behaviour, particularly in the 5xFAD$^{+/-}$ mice. Although previous studies have reported anxiety-like behaviour following LPS treatment (Sulakhiya *et al.*, 2016; Yu *et al.*, 2022), this increased time spent at the edges may also be attributable to general fatigue, with the mice simply resting, rather than exhibiting anxiety-like behaviour per se, similar to the effects observed with C57BL6/J and 5xFAD$^{-/-}$ cohort.

4.10.3. Vehicle, AC- and LPS-injection all induced anhedonia-like behaviour in 5xFAD$^{-/-}$ and 5xFAD$^{+/-}$ mice.

Both AC- and LPS-injected mice exhibited reduced sucrose preference, indicating anhedonia-like behaviour consistent with findings in the WT cohort and previous reports (Salazar *et al.*, 2012; Biesmans *et al.*, 2016; Moudio *et al.*, 2022). There were no significant differences between 5xFAD$^{-/-}$ and 5xFAD$^{+/-}$ mice in the degree of reduction, suggesting that both genotypes were equally susceptible to the effects of AC and LPS treatment.

A notable discrepancy between the C57BL6/J vs 5xFAD$^{-/-}$ cohort and the 5xFAD$^{-/-}$ vs 5xFAD$^{+/-}$ mice experiments was the incidence of reduced sucrose preference in the vehicle-injected mice, suggesting they were experiencing anhedonia-like behaviour despite no change in locomotor activity or grooming behaviour. The sucrose preference test is widely used to assess anhedonia; however, its reliability and reproducibility have been questioned, particularly in chronic stress studies (Markov, 2022; Berrio *et al.*, 2024).

Although the experimental protocols remained identical between cohorts, is it possible that external factors influenced the vehicle-injected group. At the time of these experiments, major construction work was being carried out in the animal facility and despite best efforts to minimise any disruption, it is difficult to determine whether environmental stress may have contributed to reduced sucrose consumption post-injection (Liu *et al.*, 2018). No genotypic differences were observed within the vehicle-injected group, suggesting that 5xFAD$^{+/-}$ mice were not inherently more susceptible, but potentially that the injection alone or the environmental conditions may have induced anhedonia-like behaviour.

As observed in the WT studies, there was variability in baseline sucrose preference across the mice of all treatment groups prior to injection ranging from 56% to 99% preference. The inclusion threshold remained > 50% preference to maintain consistency with the initial WT studies and to minimise exclusions in line with the 3Rs principles. Although studies have suggested a higher threshold of 65% preference (Scheggi *et al.*, 2018; Berrio *et al.*, 2023).

More 5xFAD$^{+/-}$ mice (15 mice) were excluded than 5xFAD$^{-/-}$ mice (6 mice). Of these, 13 were excluded due to sucrose preference of < 50%, 10 of which were 5xFAD$^{+/-}$ mice, and 3 were 5xFAD$^{-/-}$ mice. This finding suggests that 5xFAD$^{+/-}$ mice may experience elevated anhedonia-like behaviour even in the absence of pharmacological intervention. Clinically, patients with AD often experience anhedonia, either independently or alongside MDD (Turner *et al.*, 2022). Anhedonia has also been proposed as a potential preclinical symptom of cognitive decline, or a neuropsychiatric risk factor for AD (Lee *et al.*, 2019; Vaquero-Puyuelo *et al.*, 2021).

Although anhedonia is less reported in the 5xFAD model than other behavioural impairments, reduced sucrose preference has been observed at 5 months of age in heterozygous (5xFAD$^{+/-}$) and homozygous (5xFAD$^{+/+}$) mice when compared to non-transgenic controls (Medina-Vera *et al.*, 2023), suggesting anhedonia may be an under-reported feature of this model.

4.10.4. 5xFAD$^{+/-}$ but not 5xFAD$^{-/-}$ mice are susceptible to pharmacologically-induced apathy-like behaviour.

When grooming behaviour was analysed, AC- and LPS-injected 5xFAD$^{+/-}$ mice showed reduced grooming durations compared to 5xFAD$^{-/-}$ mice at 2h but not 24h post-injection, suggesting that 5xFAD$^{+/-}$ mice may be more susceptible to pharmacologically-induced apathy-like behaviour. AC-injection also delayed the time to first groom at the 2h splash test but not 24h post-injection splash test, further indicating transient apathy-like behaviour.

Apathy-like behaviour has been reported in the 5xFAD model starting from approximately 6-months of age, deteriorating with age when examined using nest building and marble burrowing (Keszycki *et al.*, 2023; Pádua *et al.*, 2024). This further supports that the mice used in this study, 3 months of age, may have been too young to display baseline naïve apathy-like behaviour but, 5xFAD$^{+/-}$ mice were still more susceptible to pharmacologically-induced apathy-like behaviour.

Grooming behaviour is known to vary between species, strains, age and sex (Kalueff *et al.*, 2004a, 2016; Tran *et al.*, 2021). Naïve grooming behaviour was not examined between the genotypes to avoid habituation and maintain novelty of the splash test sucrose spray. Reduced grooming in the 5xFAD model has been observed between 3–6 months of age; however, differences in testing protocols within the study produced variable outcomes (O'Leary *et al.*, 2024). The 5xFAD$^{+/-}$ mice were indistinguishable from 5xFAD$^{-/-}$ mice in their home cage highlighting both genotypes were well groomed throughout the duration of this study. Future studies could explore baseline grooming in

absence of pharmacological intervention to determine whether 5xFAD$^{+/-}$ mice groom less than 5xFAD$^{-/-}$ mice and exhibit inherent apathy-like behaviour.

Male 5xFAD$^{+/-}$ AC-injected mice exhibited reduced grooming duration and increased latency to sit and groom compared to females at 2h but not 24h post-injection. This may indicate transient sex differences in susceptibility to apathy-like behaviour. Pathological sex differences are well established in the 5xFAD model, with female mice exhibiting greater Aβ plaque load and heightened neuroinflammation due to the oestrogen-mediated Thy1 promoter (Sil *et al.*, 2022; Zhong *et al.*, 2024). However, despite this increased pathology, female 5xFAD$^{+/-}$ mice displayed less apathy-like behaviour than male 5xFAD$^{+/-}$ mice following AC-injection.

Sex differences in MDD are well documented, but studies investigating sex differences in rodent apathy are limited. Some report increased grooming in C57BL6/J mice compared to their female counterparts (Pitzer *et al.*, 2022; Sil *et al.*, 2022), though other findings remain inconsistent due to lack of research studying both sexes (Isingrini *et al.*, 2010; Bangasser *et al.*, 2021).

4.10.5. AC264613 and LPS reduced astrocyte reactivity in female but not male 5xFAD$^{+/-}$ mice at 3 weeks post-injection.

The incidence of MDD is linked to an acceleration in AD pathology and a worse prognosis for people diagnosed with AD (Sáiz-Vázquez *et al.*, 2021). Therefore, we hypothesised that pharmacologically-induced depression-like behaviour would exacerbate neuroinflammation and Aβ plaque pathology. Unexpectedly, it was discovered that two doses in successive weeks of AC

and LPS reduced astrocytic reactivity in all examined brain regions in female but not male 5xFAD$^{+/-}$ mice at 3 weeks post-injection.

Astrocyte reactivity is increasingly recognised as a core component of neuroinflammatory and neurodegenerative diseases (Kwon *et al.*, 2020; Verkhratsky *et al.*, 2023), and emerging research has shown astrocytes play important roles in disease states, with cross-talk between microglia and astrocytes modulating disease pathology (Rostami *et al.*, 2021; Singh, 2022). Communication between microglia and astrocytes modulated by astrocyte sourced IL-3 has been shown to direct microglia to reduce plaque burden and improve cognition in the 5xFAD model (McAlpine *et al.*, 2021; Rodríguez-Giraldo *et al.*, 2022). Interestingly, in our cytokine array analysis, LPS but not AC reduced IL-3 levels in the 5xFAD$^{+/-}$ mice, contradicting previous reports that describe a protective role for IL-3 in AD (Chen *et al.*, 2024).

Complement component 3 (C3) is an astrocyte-released factor found to be correlated with cognitive decline and tau Braak staging in AD (Litvinchuk *et al.*, 2018; Rodríguez-Giraldo *et al.*, 2022). When C3 receptor C3aR1 was knocked out in a tau mouse model, neuroinflammation and tau pathology was attenuated (Litvinchuk *et al.*, 2018). Further, a C3aR antagonist reduced neuroinflammation and Aβ plaques, improving cognitive deficits in a Tg mouse model (Yao *et al.*, 2023). C3 is involved in the astrocyte-microglia crosstalk, with C3 effecting downstream NF-κB signalling resulting in greater Aβ plaque deposition. This increase in plaques is suggested to lead to astrocytic release of further C3, initiating a feed-forward loop (Lian *et al.*, 2016). Prolonged C3 activation also reduces microglial phagocytosis (Fu *et al.*, 2012). As we found

that AC and LPS reduced C3 expression in the female 5xFAD$^{+/-}$ mice, this may have alleviated some of the excessive neuroinflammatory responses, allowing for more efficient phagocytic clearance of Aβ plaques.

Previous studies have shown that modulation of the astrocytic pathways can directly influence Aβ plaque pathology. Inhibition of the JAK2-STAT3 pathway, reduces astrocytic reactivity and Aβ plaques, restoring synaptic function and cognitive performance in AD models (Ceyzériat *et al.*, 2018; Reichenbach *et al.*, 2019). However, astrocytic inhibition of NF-κB accelerated Aβ plaque deposition and tau accumulation in models (Jong Huat *et al.*, 2024), highlighting that reactive astrocytes possess beneficial neuroprotective effects, or detrimental neurotoxic effects, depending on their activation state (Ding *et al.*, 2021; Lawrence *et al.*, 2023). Previous research within the lab group demonstrated neuroprotective properties of PAR2 activation against kainite-induced neurotoxicity via astrocytic activation (Greenwood *et al.*, 2010). PAR2 signalling has also been linked to modulation of glial reactivity and cytokine release via ERK1/2 and NF-κB pathways (Noorbakhsh *et al.*, 2006; Peach *et al.*, 2023), suggesting that AC-induced PAR2 activation may have contributed to the observed reduction in astrocytic activation and Aβ plaque pathology.

Together, our findings suggest that AC and LPS may modulate astrocyte reactivity and astrocyte-derived factors such as C3, potentially influencing Aβ plaque clearance, thus reducing plaque burden in female 5xFAD$^{+/-}$ mice.

4.10.6. AC264613 and LPS have no effect on activated microglia at 3 weeks post-injection.

When activated microglia were examined across the 5xFAD$^{+/-}$ mice brains, there were region-specific reductions, CA3 and SSC, in Iba1 expression in the AC-injected female mice but no further changes throughout the brain. However, there was no change in Iba1 expression in any region of LPS-treated females compared with vehicle controls. Similarly, AC and LPS treatment had no effect on activated microglia expression in male 5xFAD$^{+/-}$ mice.

PAR2 is expressed on microglia, and PAR2 activation can influence microglial activation to initiate inflammatory signalling cascades, including the MAPK and NF-κB pathways, leading to cytokine release (Noorbakhsh *et al.*, 2006; Quarta *et al.*, 2024). Studies have shown both neuroprotective (Moudio *et al.*, 2025) and neurotoxic (Afkhami-Goli *et al.*, 2007; Park *et al.*, 2010) properties for PAR2 activation. However, in our study we demonstrated limited effects of PAR2 activation on microglia expression when examined at 3 weeks post-injection, suggesting that AC may have short-live effects on microglial activity.

LPS is an endotoxin that activates microglia via TLR4, and the administration of LPS in varying dosages and methods has been associated with a reduction in Aβ deposition in several studies (Go *et al.*, 2016; Thygesen *et al.*, 2018; Wendeln *et al.*, 2018; Xie *et al.*, 2022). Furthermore, recent research has suggested that a single administration of LPS (1mg kg^{-1}), before the development of plaques in 6-week-old 5xFAD mice, 'primes' the innate immune memory of the microglia, altering microglial activation. This alteration can increase phagocytosis, thus reducing Aβ plaque deposition, as well as

improving cognitive performance, suggesting low-dose LPS treatment in the pre-clinical stages of AD may therapeutically beneficial (Yang *et al.*, 2023).

For our study, we selected a dose of 0.5 mg kg^{-1}, which was well tolerated and previously shown to lower Aβ plaque burden (Thygesen *et al.*, 2018). Our results confirm previous findings in that a low dose of LPS reduces Aβ plaque burden but there was no change in microglial activity in response to LPS. The 5xFAD mouse model displays pronounced and early microglial activation, with clustering of reactive microglia around Aβ plaques as early as 2 months of age (Oakley *et al.*, 2006; Forner *et al.*, 2021). This heightened basal activation may reduce the effects of AC and LPS on microglial expression hence the limited effects we observed at 3 weeks post-injection. However, due to the microglial-astrocytic cross-talk (Singh, 2022), we proposed that modulation of astrocytic reactivity by AC and LPS could reduce excessive neuroinflammation. Such a reduction may restore glial cells to a more efficient functional state, thereby enhancing microglial phagocytosis and ultimately reducing Aβ plaque burden.

4.10.7. AC264613 and LPS reduce Aβ plaque load in female but not male 5xFAD$^{+/-}$ mice at 3 weeks post-injection.

When Aβ plaques were examined, we revealed that, in contrary to our hypothesis, two injections in successive weeks of AC and LPS reduced Aβ plaque load and size in female but not male 5xFAD$^{+/-}$ mice suggesting that short-term priming of the immune responses with AC and LPS may be beneficial to Aβ pathology.

Evidence of PAR2 activation directly influencing AD pathology is limited, but upregulated PAR2 expression has been found in glia clustered around Aβ plaques in human post-mortem tissue (Afkhami-Goli *et al.*, 2007). On the other hand, LPS has been widely used to modulate Aβ plaque pathology, with several studies reporting reduced plaque deposition, following single or multi-treatments with LPS (Go *et al.*, 2016; Thygesen *et al.*, 2018; Wendeln *et al.*, 2018; Xie *et al.*, 2022). These reductions have been linked to 'priming' of the immune cells, and 'primed' microglia and astrocytes have demonstrated increased Aβ plaque clearance (Yang *et al.*, 2023; Lee, Yu, *et al.*, 2025). Based on these findings, we decided to investigate microglial phagocytosis, to determine whether AC and LPS increased phagocytic microglia activity, thus reducing plaque burden.

4.10.8. AC264613 and LPS have no effect on phagocytic microglia at 3 weeks post-injection.

When phagocytic microglia were explored, it was found that two injections in successive weeks of AC and LPS had no significant effects on phagocytic microglia expression in male or female 5xFAD$^{+/-}$ mice. Interestingly, there was a trend of reduced phagocytic microglial expression in female AC and LPS-treated mice. However, when phagocytic microglia were compared to overall microglial expression, there was in increase in phagocytic microglia in CA3 and VC of LPS-injected females. Several studies have shown that LPS treatment reduces Aβ plaque burden (Go *et al.*, 2016; Thygesen *et al.*, 2018; Wendeln *et al.*, 2018; Xie *et al.*, 2022), with a single dose found to 'prime' microglia and enhance this effect (Yang *et al.*, 2023). However, CD68-marked

phagocytosis was only altered in the dentate gyrus of 5xFAD mice, suggesting region-specific modulation (Yang *et al.*, 2023). In another study a single dose of LPS shifted Aβ plaques from an insoluble to a soluble state, favouring plaque clearance, thus reducing plaque burden (Jendresen *et al.*, 2019).

In our study, consistent with patterns observed for astrocyte and microglial expression, female 5xFAD$^{+/-}$ mice showed greater phagocytic microglial activity than males, which may be attributable to the more advanced progression of disease. Overall, there was a higher degree of variability in the CD68 IHC results compared to the rest of IHC performed. Brain slices were sectioned in advance and stored in PBS with sodium azide at 4 °C for several months while antibody optimisation was performed. When the samples were finally stained, the tissue quality was compromised, resulting in fewer usable replicates and the exclusion of some brains from analysis. This may have contributed to the variability observed in CD68 staining.

As our findings suggest phagocytosis via microglia was largely unaffected by AC and LPS, it is worth considering alternative mechanisms of Aβ clearance. Given that astrocyte reactivity was modulated by AC and LPS, future studies should investigate astrocytic phagocytosis to better understand the reduction in Aβ plaques observed. Although microglia are considered the primary phagocytic cells in the brain, growing body of evidence highlights an important role for astrocytes in phagocytosis (Lee *et al.*, 2021; Konishi *et al.*, 2022).

Studies have shown that astrocytic phagocytic receptors such as Multiple-EGF like domains 10 (MEGF10) and MER-proto-oncogene tyrosine kinase

(MERTK) contribute to Aβ plaque clearance, and knockdown models of MEGF10 or MERTK inhibits the uptake and clearance mechanisms (Singh *et al.*, 2010; Fujita *et al.*, 2020; Hulshof *et al.*, 2022). Astrocytes can also internalise Aβ plaques via endocytosis which are then degraded by lysosomal enzymes. Further, astrocytic lysosomal-associated membrane protein 1 (LAMP1) is often elevated and co-localised with Aβ plaques, indicating enhanced lysosomal activity and a potential role in plaque degradation (Li *et al.*, 2024). In addition, astrocytes can produce various Aβ degrading proteases, including neprilysin, insulin-degrading enzyme, and matrix metalloproteinases, which are suggested to aid in the clearance of plaques (Ries *et al.*, 2016; Park *et al.*, 2024). As mentioned above, the compromised tissue quality prevented further analysis of astrocyte activity.

4.10.9. Methodological limitations of immunohistochemical analysis

A methodological limitation of the IHC analysis throughout this project was the reliance on fluorescence intensity as a quantitative measure of astrocyte reactivity and microglial activation and phagocytosis. While fluorescence intensity is widely for protein expression, molecular localisation, and cellular studies, it can be influenced by technical factors including tissue storage, antibody penetration, tissue thickness, staining efficiency, and imaging parameters. As such, changes in signal intensity may not directly reflect absolute differences in astrocyte or microglia activity (Waters, 2009; Shakya *et al.*, 2020). In addition, IHC was performed without the inclusion of negative controls, such as no-primary antibody controls, limiting the ability to fully exclude non-specific binding or background fluorescence. Although antibody

concentrations, staining protocols, and imaging parameters were kept consistent across experimental groups to minimise technical variability, the absence of negative controls represents a limitation when analysing across different IHC batches. Future studies should incorporate appropriate negative controls and potentially other methods of analysis, such as astrocyte and microglia density or burden, to strengthen IHC results.

4.10.10. Sex differences in pathology results

Behaviourally, only minor sex differences were observed in grooming, but pathology revealed a pronounced effect of sex. Analysis of our data revealed that alterations in astrocyte reactivity, microglial activation, and Aβ plaque burden in response to AC and LPS were observed exclusively in female 5xFAD$^{+/-}$ mice. Female 5xFAD$^{+/-}$ mice are known to exhibit higher levels of Aβ plaques compared to males, thus exhibit higher levels of neuroinflammation (Sil *et al.*, 2022; Poon *et al.*, 2023). As discussed in section 1.1.7.2, the five familial AD mutations in the 5xFAD model are expressed under the control of the neuron-specific Thy1 promoter. Thy1 drives overexpression of mutant *APP* and *PSEN1* in forebrain excitatory neurons, resulting in rapid Aβ42 overproduction and early plaque deposition (Oakley *et al.*, 2006). Oestrogen influences the Thy1 promoter, enhancing the expression of APP and PSEN1 thus contributing to the increased Aβ plaque burden in female mice (Forner *et al.*, 2021; Zhong *et al.*, 2024).

A recent study reported that parental origin of the transgenes also influences Aβ plaque burden in 5xFAD$^{+/-}$ mice, with paternal inheritance producing a two-fold increase in Aβ plaque load compared to maternal inheritance, while

grandparental origin had no effect. This study highlighted a potential neuroprotective role of maternal inheritance of the transgenes (Sasmita *et al.*, 2025). In our study, mice inherited the transgene paternally and thus exhibited higher plaque burden. However, due to breeding challenges there was a lack of male 5xFAD$^{+/-}$ mice, therefore, additional males were sourced from another colony. These mice were later found to carry maternally inherited transgenes and displayed significantly fewer plaques. To maintain consistency, they were excluded and subsequently replaced with paternal-inherited mice.

Evidence has shown sex-specific differences in astrocytes and microglia, including functional, developmental and morphological variations influenced by hormones and early life experiences in both humans and rodents (Han, Fan, *et al.*, 2021; Gozlan *et al.*, 2024). While male astrocytes have been reported to reach full maturation faster than females, sex differences are region specific, and males show a greater number of astrocytes, and more extensive branching in the hypothalamus, whereas females exhibit increased astrocyte density with shorter branches in the hippocampal regions, including CA1 and DG (Gozlan *et al.*, 2024; Bortolanza *et al.*, 2025). Females also tend to express higher levels of GFAP, potentially reflecting greater astrocyte reactivity or numbers. The introduction of testosterone or oestrogen into females or males, reduces or increases GFAP levels, respectively. Astrocyte sex-specific responses to injury and disease are also recognised, with male astrocytes reported to secrete higher levels of proinflammatory cytokines (Crespo-Castrillo *et al.*, 2020), while chronic stress and inflammation induce increased astrocyte activation in females (Zhang, Elias, *et al.*, 2024).

Similarly, microglia also display well-characterised sex-specific differences throughout development and in disease states. Microglial maturation is regulated by sex hormones such as oestradiol and testosterone, leading to distinct regional activation profiles (Villa *et al.*, 2018; Han, Fan, *et al.*, 2021). In rodents, male brains exhibit higher densities of amoeboid microglia during early postnatal development, particularly within the hippocampus and amygdala, whereas females have more ramified and activated microglia within the hippocampus and cortex (Han, Fan, *et al.*, 2021; Lynch, 2022). In adulthood, males display increased Iba1 dense microglia at baseline, while female microglia demonstrate a more rapid response to pathological stimuli such as Aβ plaques and increased phagocytic capacity (Villa *et al.*, 2018; Crespo-Castrillo *et al.*, 2020).

These inherent sex differences in glial function may partly explain why AC and LPS reduced astrocyte reactivity and Aβ plaque pathology in female, but not male 5xFAD$^{+/-}$ mice. Female glia have been reported to exhibit more dynamic morphological and activation changes in response to inflammatory stimuli, which could contribute to sex-specific differences in Aβ plaque reduction. (Villa *et al.*, 2018; Crespo-Castrillo *et al.*, 2020; Han, Fan, *et al.*, 2021). This enhanced glial responsiveness is likely further influenced by oestrogen, which is known to exert neuroprotective effects. Reduced oestrogen levels are associated with increased Aβ plaque deposition. Whereas oestrogen can suppress pro-inflammatory cytokine expression in response to LPS. Furthermore, oestrogen receptor agonists have been shown to enhance anti-inflammatory responses, reduce Aβ plaques and improve cognitive function

(Chakrabarti *et al.*, 2014; Price *et al.*, 2025). Although the oestrous cycle was not examined in this study, it may contribute to the observed reduction in astrocyte reactivity and Aβ plaques in female mice. Investigating how AC influences oestrogen levels in the brain could provide further insight into its effect on astrocyte and plaque modulation.

4.10.11. Cytokine changes in 5xFAD$^{-/-}$ and 5xFAD$^{+/-}$ mice.

Given the established link between cytokines, particularly IL-6, and MDD (Beurel *et al.*, 2020), cytokine analysis was performed to explore whether peripheral cytokine release following AC- and LPS-injection contributed to the induced depression-like behaviour in 5xFAD mice. Previous work in WT mice showed that AC increased pro-inflammatory IL-6 levels while other markers, TNF-α, IL-1β and INF-γ were unaffected (Moudio *et al.*, 2022). In the current study, we assessed whether similar effects occur in 5xFAD mice following AC- and LPS-injection. Cytokine profiles were examined within the genotypes.

AC altered several cytokines associated with MDD in the 5xFAD$^{-/-}$ mice, notably decreasing pro-inflammatory cytokines IL1β, IL-12, while increasing CXCL1, and decreasing anti-inflammatory IL-4 and INF-γ. However, in 5xFAD$^{+/-}$ mice, AC only significantly increased CXCL1. Research has shown that 5xFAD mice exhibit elevated baseline levels of pro-inflammatory cytokines both peripherally and centrally due to Aβ plaque burden compared to wild-types (Oblak *et al.*, 2021). These findings suggest that the heightened baseline inflammatory state in 5xFAD$^{+/-}$ mice dampens their responsiveness to AC, while the comparatively homeostatic immune environment of the 5xFAD$^{-/-}$ mice enables AC to elicit wider cytokine changes.

In contrast, LPS produced robust cytokine changes in both genotypes, increasing pro-inflammatory cytokines IL-6, CXCL1 and CCL2, while decreasing the anti-inflammatory cytokines IL-4 and IFN-γ. Unlike AC, which signals through the selective PAR2 pathway, LPS activates via TLR4, to produce more potent and broad cytokine changes across both 5xFAD$^{-/-}$ and 5xFAD$^{+/-}$ mice regardless of disease or baseline inflammatory state (Wendeln *et al.*, 2018; Yang *et al.*, 2023).

The cytokine changes observed by AC and LPS only partially reflect the peripheral cytokine profile reported in MDD. IL-6 is consistently upregulated patients with MDD (Roohi *et al.*, 2021; Kouba *et al.*, 2024), and while LPS increased IL-6 in our study, AC had no effect. TNF-α is also often elevated in MDD, while IL-1β reports are variable (Dowlati *et al.*, 2010; Das *et al.*, 2021). Anti-inflammatory cytokines such as IL-4 and IFN-γ show inconsistent patterns in MDD, with some reports of increase or no change at all (Dowlati *et al.*, 2010; Daria *et al.*, 2020; Sarmin *et al.*, 2024). Chemokines CXCL1 and CCL2 have been reported in stress-induced models and some elderly MDD studies (Eyre *et al.*, 2016; Chai *et al.*, 2019; Fanelli *et al.*, 2019). Overall, our LPS data aligns more closely to the changes observed in MDD, whereas AC-induced changes in the 5xFAD$^{-/-}$ mice do not reflect the typical MDD profile, suggesting that the depression-like behavioural changes we observed are not driven by the peripheral cytokine response.

Our study utilised cytokine multiplex immunoassays which provide broad profiling but are less sensitive than ELISAs for detecting subtle changes, such as the IL-6 increase previously reported with AC in wild-type mice (Moudio *et*

al., 2022). Finally, no sex differences were detected; however, the sample size per sex was small (n=2 per treatment per genotype), limiting statistical power to detect sex-specific effects.

4.10.12. Conclusion

From the work in this chapter, we conclude that 5xFAD$^{+/-}$ mice do not inherently exhibit depression-like behaviour. Under the influence of AC and LPS-injections, 5xFAD$^{+/-}$ mice are not more susceptible to depression-like behavioural changes such as low mood and anhedonia but they may be more prone to induced apathy-like behaviour. Two injections in successive weeks of AC and LPS, reduced astrocytic reactivity and Aβ plaque burden exclusively in female 5xFAD$^{+/-}$ mice but had limited influence on activated and phagocytic microglia in either sex. Furthermore, LPS, but not AC, induced peripheral cytokine alterations that correlate with MDD. Overall, these results suggest that AC and LPS may be potentially useful therapeutic tools to modulate neuroinflammatory and Aβ plaque pathology in AD. To further explore this potential, the long-term effects, and the impact of additional dosing of AC or LPS on neuroinflammation and Aβ plaque pathology were investigated.

Chapter 5: The longevity and effect of additional dosing of AC and LPS on behaviour and neuropathology in 5xFAD$^{+/-}$ mice.

5.1. Introduction and aims.

Evidence has shown that a single dose of LPS could prime the immune system to enhance Aβ plaque phagocytosis, leading to reduced plaque load at 140 days post-injection in 5xFAD mice (Yang *et al.*, 2023). Having established that two doses in successive weeks of AC (100 mg kg^{-1}) and LPS (0.5 mg kg^{-1}) reduced astrocytic reactivity and Aβ plaque pathology at 3 weeks post-injection, we then examined the longevity of this effect, and whether additional injections could further modulate these changes. We hypothesised that the impaired reactivity and plaque load observed following two injections of AC or LPS would remain for an extended period. However, as this effect was only observed in female 5xFAD$^{+/-}$ mice, we investigated the long-term impact of two doses in successive weeks of AC or LPS at 10 weeks post-injection only in female 5xFAD$^{+/-}$ mice. We further hypothesised that additional injections of AC and LPS would elicit more pronounced effects, reducing astrocytic reactivity and Aβ plaque load further in female mice, and also induce pathological changes in male 5xFAD$^{+/-}$ mice. Therefore, we examined the effects of four injections in successive weeks of AC or LPS in both male and female 5xFAD mice.

The work in this chapter aims to answer the following research questions:

- Do two AC and LPS injections produce prolonged reductions in astrocytic reactivity and Aβ plaque load at 10 weeks post-injection?
- Do four AC and LPS injections further enhance astrocyte modulation and further reduce Aβ plaque load in 5xFAD mice?

5.1.1. 5xFAD mice

To ensure that behavioural testing did not influence pathological outcomes and to maintain consistency with previous experiments, locomotor activity, sucrose preference, and grooming behaviour were assessed using the same protocols, with all mice receiving a final OFT prior to perfusion. To examine the longevity of AC and LPS treatment, female 5xFAD$^{+/-}$ mice received two doses of either vehicle, AC or LPS during the behavioural testing phase, then were aged for 10 weeks. Each treatment group consisted of five mice.

To investigate the effects of additional doses of AC and LPS, both male and female 5xFAD$^{+/-}$ mice underwent the standard two weeks of behavioural testing and injections, followed by two additional weeks of injections with no further behavioural testing, then were aged for 3 weeks. Each treatment group consisted of five mice per sex.

5.2. AC- and LPS-injection reduced locomotor activity with no prolonged behavioural or health changes at 10 weeks post-injection.

When locomotor activity was examined in the female 5xFAD$^{+/-}$ mice, AC (100 mg kg^{-1}) and LPS-injection (0.5 mg kg^{-1}) once again reduced activity 2h post-injection compared to pre-drug ($F_{(2\text{-}24)}$ = 15.21, $p<0.001$ vs pre-drug, Fig 5.1A) with AC- ($p<0.001$ vs vehicle, n=5, Fig.5.1A) and LPS-injection ($p<0.001$ vs vehicle, n=5, Fig.5.1A) reducing locomotor activity compared to vehicle injection. Locomotor activity was recovered at 24h post-injection (AC: p=0.99 vs vehicle, n=5, Fig.5.1A; LPS: p=0.92 vs vehicle, n=5, Fig.5.1A). When

locomotor activity was examined at 10 weeks post-injection, no long-term behavioural changes were observed in either AC- p=0.65 vs vehicle, n=5, Fig.5.1A) or LPS-injected (p=0.28 vs vehicle, n=5, Fig.5.1A) female 5xFAD$^{+/-}$ mice.

When sucrose preference was examined 2h post-injection, LPS-injection reduced sucrose preference (p=0.03 vs pre-drug, n=5, Fig.5.1B) but no significant changes were observed in AC- or vehicle-injected mice (vehicle: p=0.09 vs pre-drug, n=5, Fig.5.1B; AC: p=0.79 vs pre-drug, n=5, Fig.5.1B). At 24h post-injection, the LPS-induced reduction in sucrose preference was not significant when compared to pre-drug (p=0.17 vs pre-drug, n=5, Fig.5.1B).

In contrast to previous findings, AC- and LPS-injection had no effect on grooming behaviour compared to vehicle at 2h post-injection in this cohort of female 5xFAD$^{+/-}$ mice (AC: p=0.99 vs vehicle, n=5, Fig.5.1C; LPS: p=0.84 vs vehicle, n=5, Fig.5.1C). Furthermore, when grooming was compared from 2h post-injection to 24h post-injection within the treatment groups, no significant difference in time spent grooming were observed between the timepoints ($F_{(1-12)}$ = 3.56, p=0.08 2h post- vs 24h post-drug, n=15, Fig 5.1C).

As with previous experiments, mice were weighed daily during the behavioural testing and treatments phase. At 10-weeks post-injection, mice underwent a final weighing and no difference in weight was found between the female 5xFAD$^{+/-}$ mice given AC (p=0.45 vs vehicle, n=5) or LPS (p=0.5 vs vehicle, n=5) treatment compared to vehicle injection.

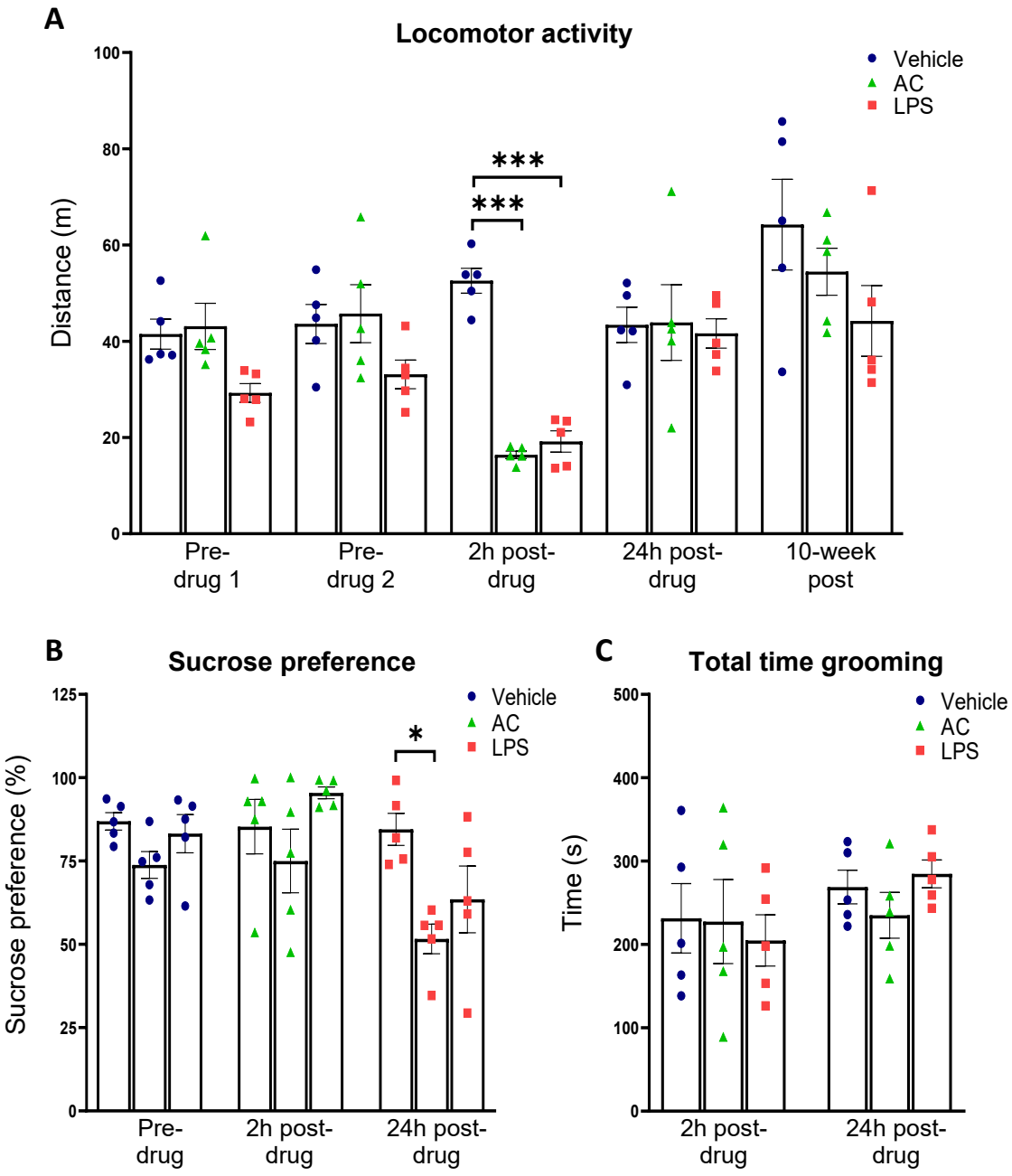

Figure 5.1: AC- and LPS-injection reduced locomotor activity and sucrose preference 2h post-injection with no prolonged effects on locomotor activity at 10 weeks post-injection. (A) AC- (100 mg kg^{-1} i.p.) and LPS-injection (0.5 mg kg^{-1} i.p.) significantly reduced locomotor activity in female $5xFAD^{+/-}$ mice 2h post-injection (***p<0.001 vs vehicle). No long-term effects of AC- and LPS-injection on locomotor activity persisted at 10 weeks post-injection. (B) LPS- but not AC-injection significantly reduced sucrose preference in female $5xFAD^{+/-}$ mice 2h post-injection (*p<0.05 2h post- vs 24h post-injection). (C) AC- and LPS-injection had no effect on time spent grooming at either 2h or 24h post-injection. Two-way repeated-measures ANOVA with Tukey's post hoc test (n=5 all treatments).

5.3. Immunohistochemistry results at 10 weeks post-injection.

Following behavioural testing and treatments, female 5xFAD$^{+/-}$ mice were aged for 10 weeks to determine if the neuroprotective effects observed at 3 weeks post-injection were still present. IHC was conducted using the established protocols, and brains were labelled for astrocytes, microglia, and Aβ plaques.

5.3.1. Two injections of AC and LPS had no effect on GFAP or C3 expression at 10 weeks post-injection.

When reactive astrocytes were examined using GFAP fluorescence (Fig.5.2A-C), it was revealed that AC-injection had no effect on GFAP expression at 10 weeks post-injection in any brain region in female 5xFAD$^{+/-}$ mice (subiculum: p=0.96, Fig.5.3A; CA1: p=0.98, Fig.5.3B; CA3: p=0.92, Fig.5.3C; DG: p=0.83, Fig.5.3D; VC: p=0.9, Fig.5.3E; SSC: p=0.99, Fig.5.3F, n=5 vs vehicle for all regions).

LPS-injection also had no influence on GFAP expression at 10 weeks post-injection in female 5xFAD$^{+/-}$ mice (subiculum: p=0.98, Fig.5.3A; CA1: p=0.99, Fig.5.3B; CA3: p=0.94, Fig.5.3C; DG: p=0.99, Fig.5.3D; VC: p=0.96, Fig.5.3E; SSC: p=0.99, Fig.5.3F, n=5 vs vehicle for all regions).

As with GFAP, IHC with reactive astrocyte marker C3 (Fig.5.2D-F) revealed that AC-injection did not affect C3 expression compared to vehicle in female 5xFAD$^{+/-}$ mice at 10 weeks post-injection (subiculum: p=0.95, Fig.5.4A; CA1: p=0.93, Fig.5.4B; CA3: p=0.87, Fig.5.4C; DG: p=0.84, Fig.5.4D; p=0.97, Fig.5.4E; SSC: p=0.92, Fig.5.4F, n=5 vs vehicle for all regions).

Similarly, LPS-injection did not alter C3 expression at 10 weeks post-injection in any brain region of female 5xFAD$^{+/-}$ mice (subiculum: p=0.99, Fig.5.4A; CA1: p=0.99, Fig.5.4B; CA3: p=0.98, Fig.5.4C; DG: p=0.99, Fig.5.4D; VC: p=0.97, Fig.5.4E; SSC: p=0.98, Fig.5.4F, n=5 vs vehicle for all regions).

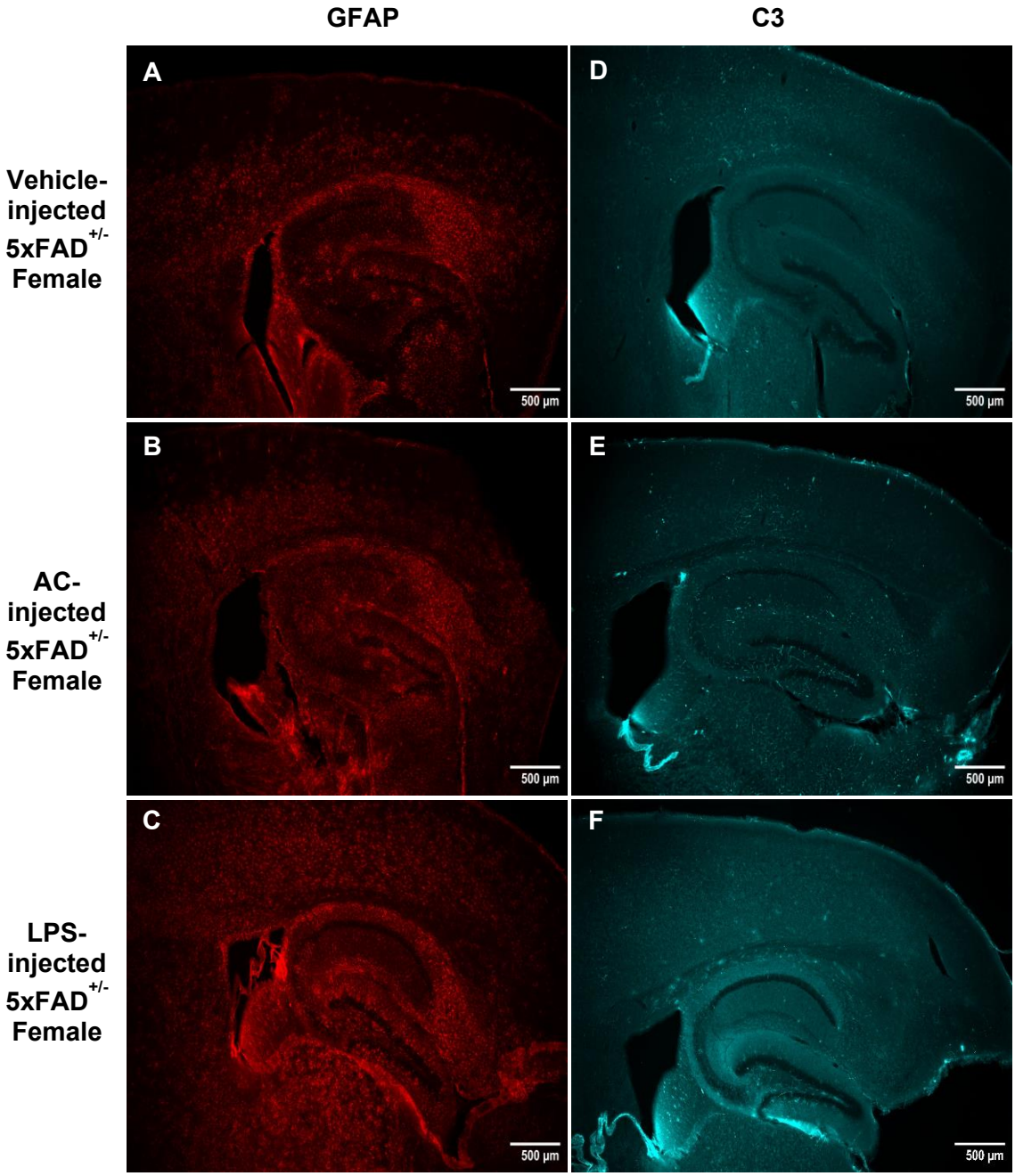

Figure 5.2: Representative Mesolens images of GFAP and C3 IHC in female 5xFAD$^{+/-}$ mice at 10 weeks post-injection. AC- and LPS-injection had no effect on GFAP (A-C) or C3 (D-F) expression compared to vehicle across the brain regions at 10 weeks post-injection in female 5xFAD$^{+/-}$ mice. Scale bar: 500µm.

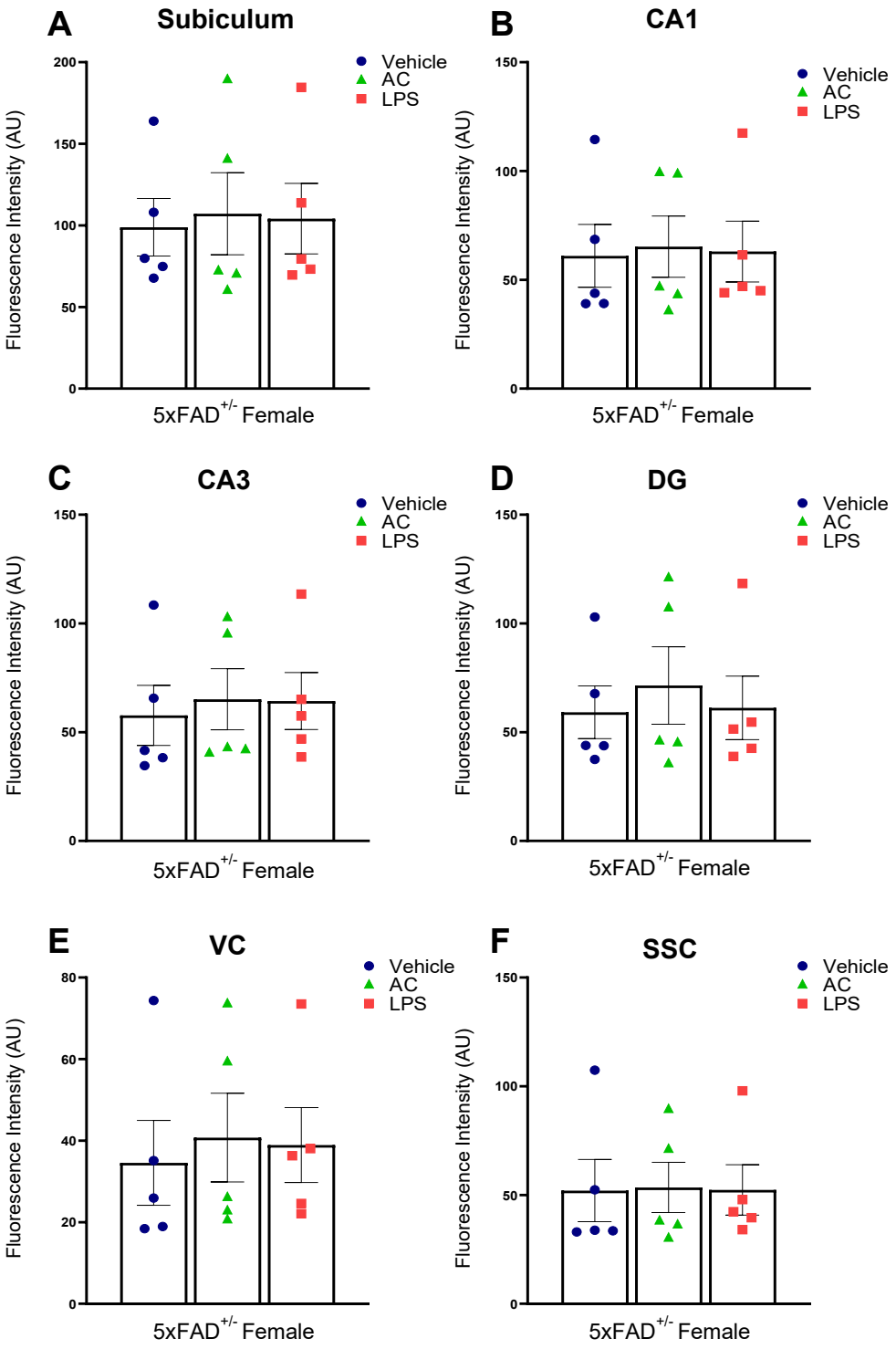

Figure 5.3: AC- and LPS-injection had no effect GFAP expression at 10 weeks post-injection in female 5xFAD$^{+/-}$ mice. (A-F) Across all brain regions, GFAP expression was unchanged by AC or LPS-injection compared to vehicle when examined at 10-week post-injection in 5xFAD$^{+/-}$ mice. Fluorescence intensity measured as arbitrary units (AU). One-way repeated-measures ANOVA with Tukey's post hoc test (n=5 all treatments).

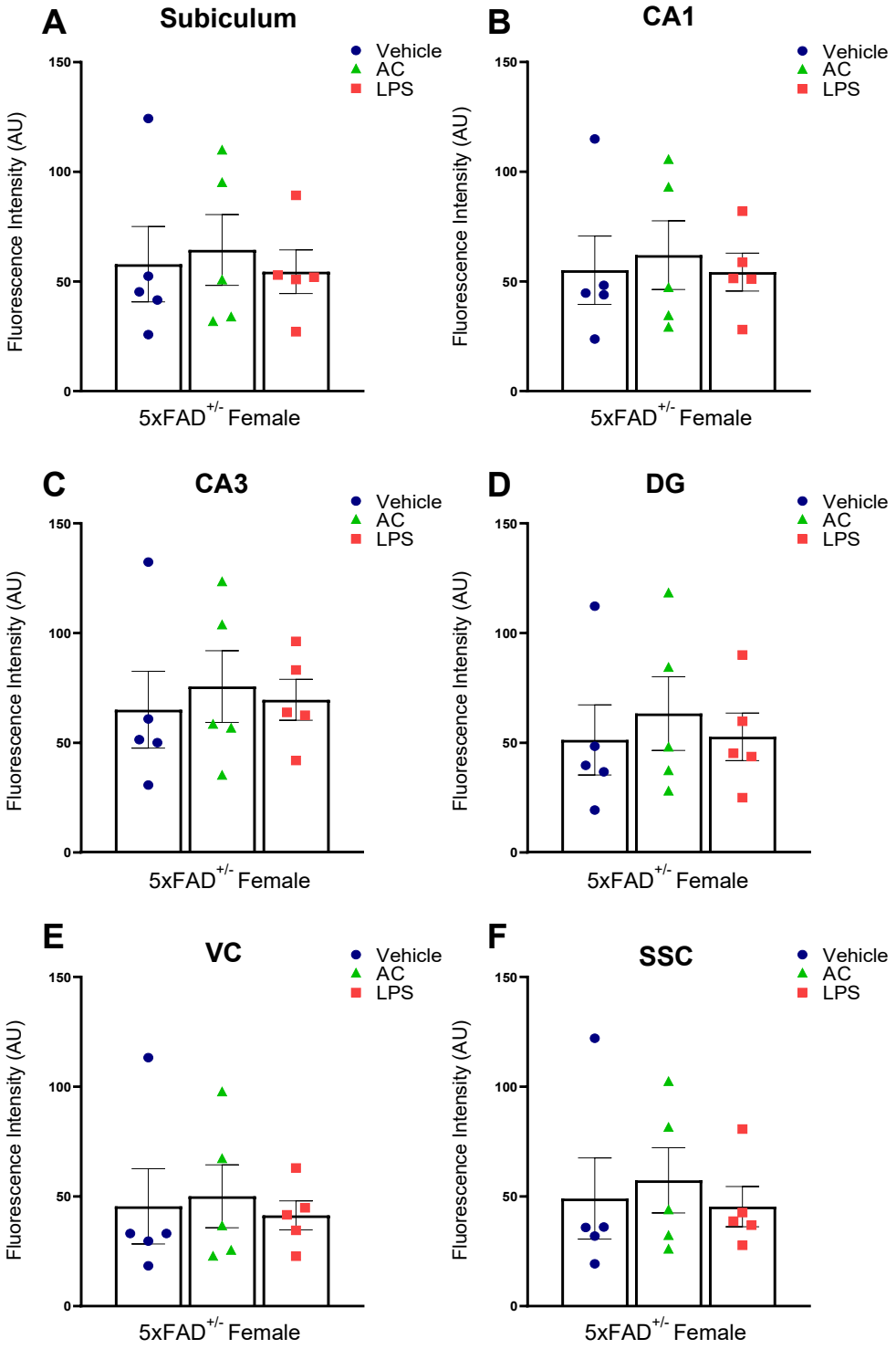

Figure 5.4: AC- and LPS-injection had no effect C3 expression at 10 weeks post-injection in female 5xFAD$^{+/-}$ mice. (A-F) Across all brain regions, AC and LPS-injection had no effect on C3 expression compared to vehicle at 10-week post-injection in 5xFAD$^{+/-}$ mice. Fluorescence intensity measured as arbitrary units (AU). One-way repeated-measures ANOVA with Tukey's post hoc test (n=5 all treatments).

5.3.2. Two injections of AC and LPS had no influence on Iba1 or CD68 expression at 10 weeks post-injection.

When activated microglia were examined with Iba1 (Fig.5.5A-C), it was found that AC-injection had no effect on Iba1 expression at 10 weeks post in female 5xFAD$^{+/-}$ mice (subiculum: p=0.98, Fig.5.6A; CA1:p=0.97, Fig.5.6B; CA3: p=0.99, Fig.5.6C; DG: p=0.98, Fig.5.6D; VC: p=0.97, Fig.5.6E; SSC: p=0.95, Fig.5.6F, n=5 vs vehicle for all regions).

In LPS-injected female 5xFAD$^{+/-}$ mice, Iba1 expression was unchanged compared to vehicle-injection at 10 weeks post-injection (subiculum: p=0.99, Fig.5.6A; CA1: p=0.99, Fig.5.6B; CA3: p=0.99, Fig.5.6C; DG: p=0.99, Fig.5.6D; VC: p=0.99, Fig.5.6E; SSC: p=0.99, Fig.5.6F, n=5 vs vehicle for all regions).

We also examined whether treatments affected phagocytic microglia using CD68 (Fig.5.5D-F) but AC-injection had no influence on CD68 expression at 10 weeks post-injection in female 5xFAD$^{+/-}$ mice (subiculum: p=0.99, Fig.5.7A; CA1:p=0.98, Fig.5.7B; CA3:p=0.9, Fig.5.7C; DG: p=0.99, Fig.5.7D; VC: p=0.98, Fig.5.7E; SSC: p=0.99, Fig.5.7F, n=5 vs vehicle for all regions).

Similarly, LPS-injection also did not alter CD68 expression at 10 weeks post-injection in female 5xFAD$^{+/-}$ mice (subiculum: p=0.63, Fig.5.7A; CA1: p=0.92, Fig.5.7B; CA3: p=0.85, Fig.5.7C; DG: p=0.89, Fig.5.7D; VC: p=0.71, Fig.5.7E; SSC: p=0.95, Fig.5.7F, n=5 vs vehicle for all regions).

Furthermore, when phagocytic microglia vs activated microglia were investigated using CD68 to Iba1 ratio, AC-injected mice displayed no change

in CD68 to Iba1 ratio compared to vehicle-injected female 5xFAD$^{+/-}$ mice at 10 weeks post-injection (subiculum: p=0.99, Fig.5.8A; CA1: p=0.98, Fig.5.8B; CA3: p=0.99, Fig.5.8C; DG: p=0.99, Fig.5.8D; VC: p=0.83, Fig.5.8E; SSC: p=0.99, Fig.5.8F, n=5 vs vehicle for all regions).

LPS-injection also had no effect on CD68 to Iba1 ratio examined at 10 weeks post-injection in female 5xFAD$^{+/-}$ mice (subiculum: p=0.84, Fig.5.8A; CA1: p=0.96, Fig.5.8B; CA3: p=0.91, Fig.5.8C; DG: p=0.93, Fig.5.8D; VC: p=0.73, Fig.5.8E; SSC: p=0.98, Fig.5.8F, n=5 vs vehicle for all regions).

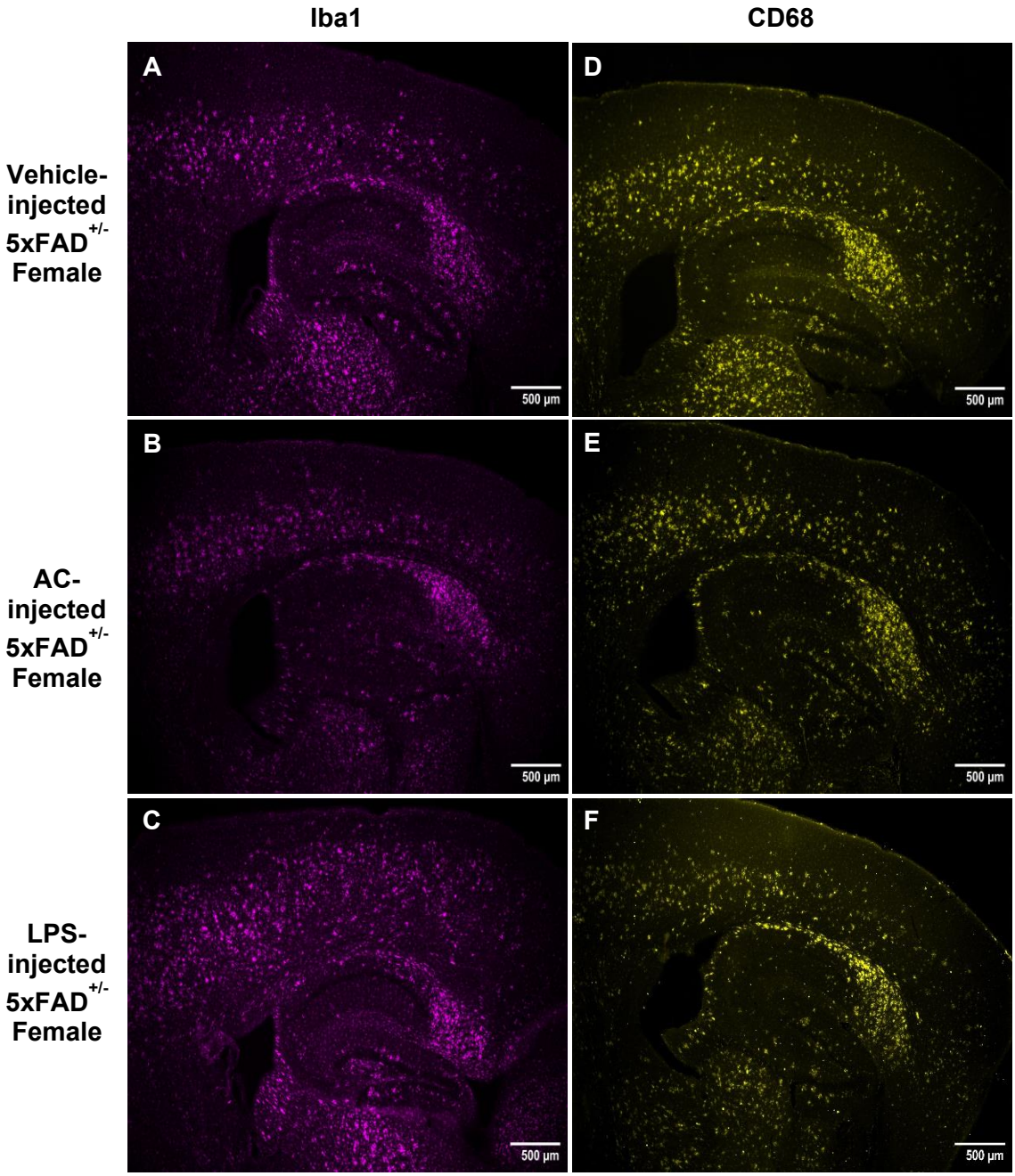

Figure 5.5: Representative Mesolens images of Iba1 and CD68 IHC in female 5xFAD$^{+/-}$ mice at 10 weeks post-injection. AC- and LPS-injection had no effect on Iba1 (A-C) or CD68 (D-F) expression compared to vehicle across the brain regions at 10 weeks post-injection in female 5xFAD$^{+/-}$ mice. Scale bar: 500µm.

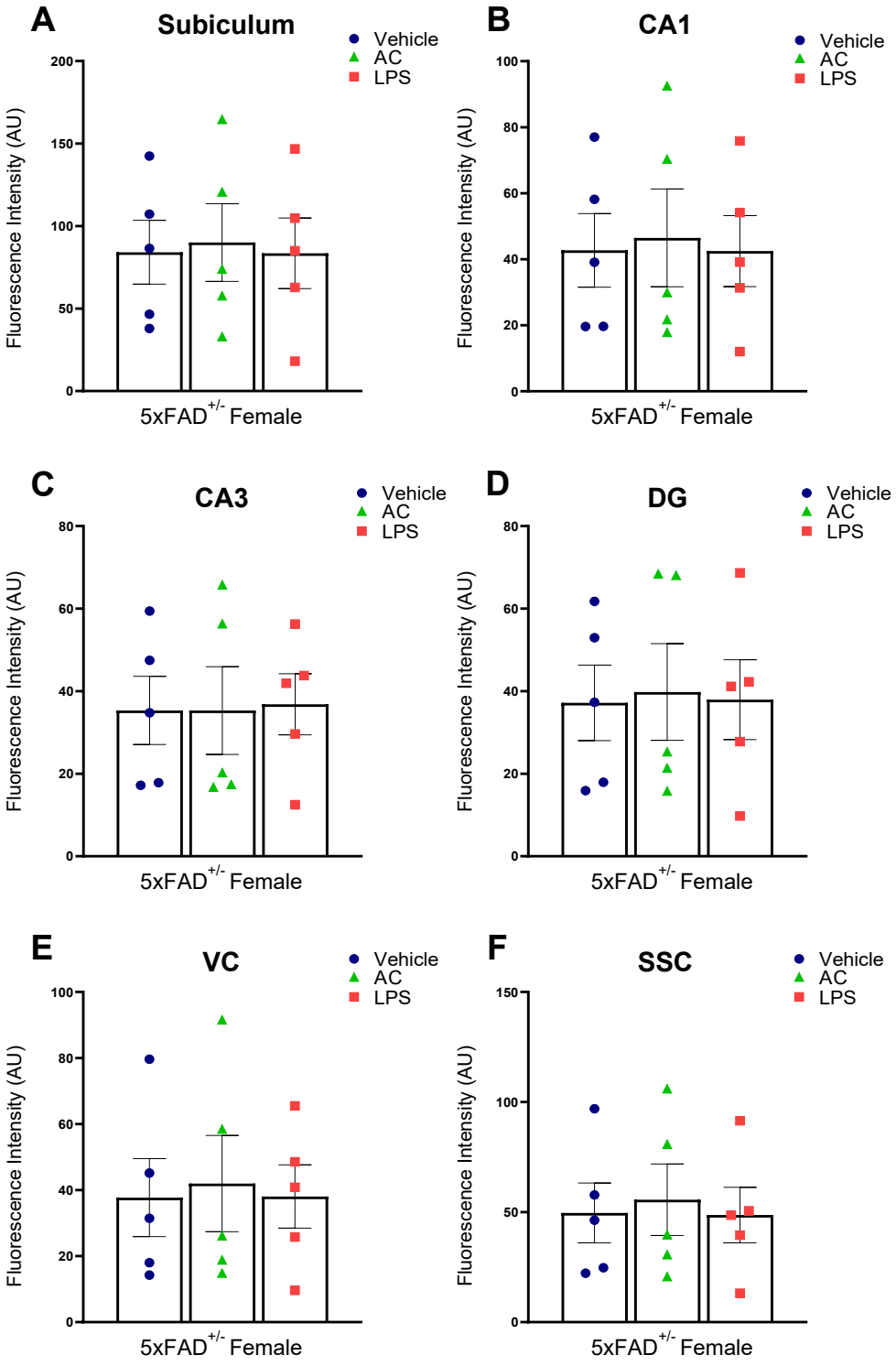

Figure 5.6: AC- and LPS-injection had no effect Iba1 expression at 10 weeks post-injection in female 5xFAD$^{+/-}$ mice. (A-F) Across all brain regions, AC and LPS-injection had no influence on Iba1 expression compared to vehicle injection in female 5xFAD$^{+/-}$ mice at 10 weeks post-injection. Fluorescence intensity measured as arbitrary units (AU). One-way repeated-measures ANOVA with Tukey's post hoc test (n=5 all treatments).

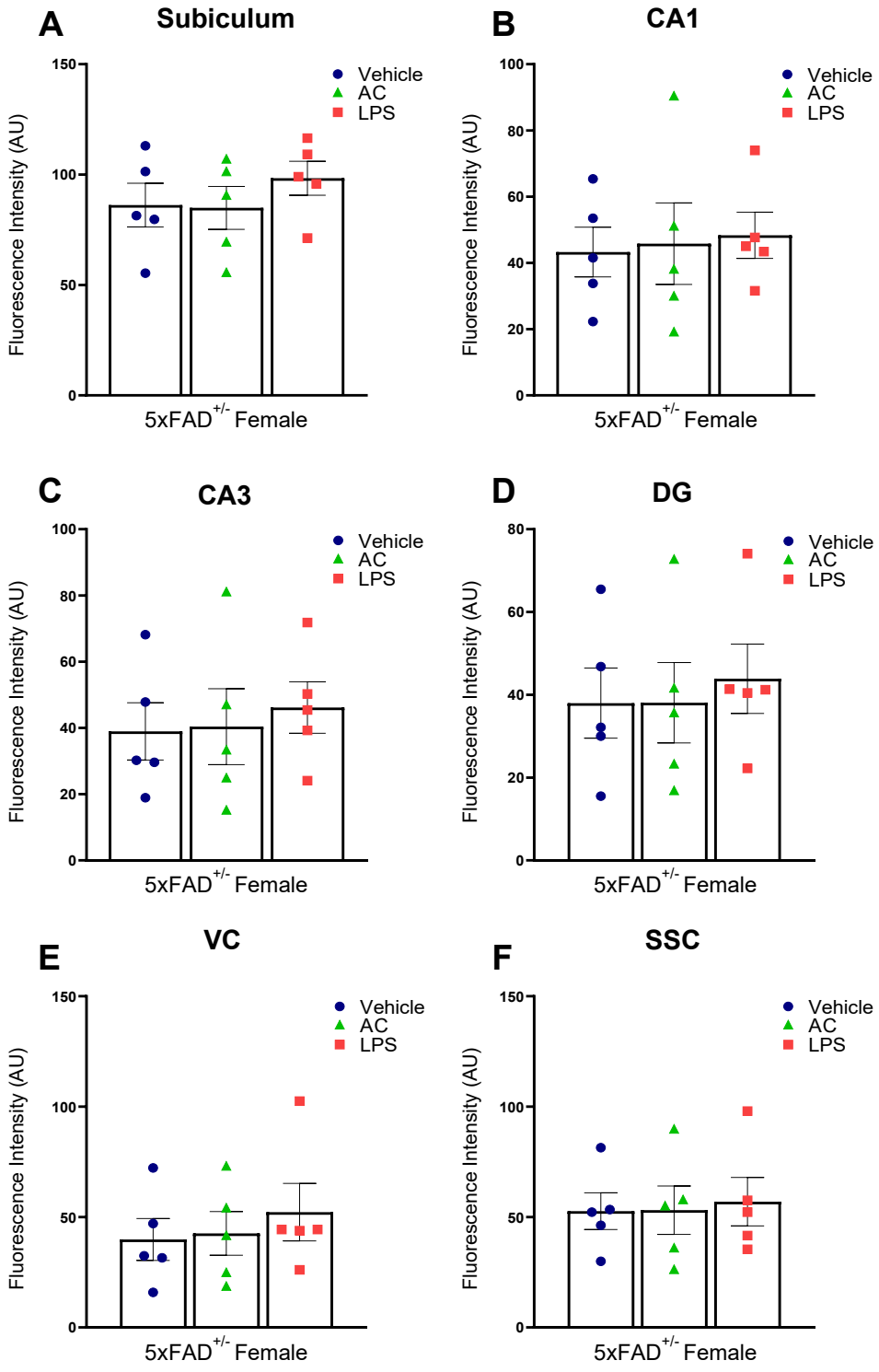

Figure 5.7: AC- and LPS-injection had no influence on CD68 expression at 10 weeks post-injection. (A-F) CD68 expression was unchanged across the brain in AC- and LPS-injected female 5xFAD$^{+/-}$ mice at 10 weeks post-injection compared to vehicle injection. Fluorescence intensity measured as arbitrary units (AU). One-way repeated-measures ANOVA with Tukey's post hoc test (Female: n=5 all treatments).

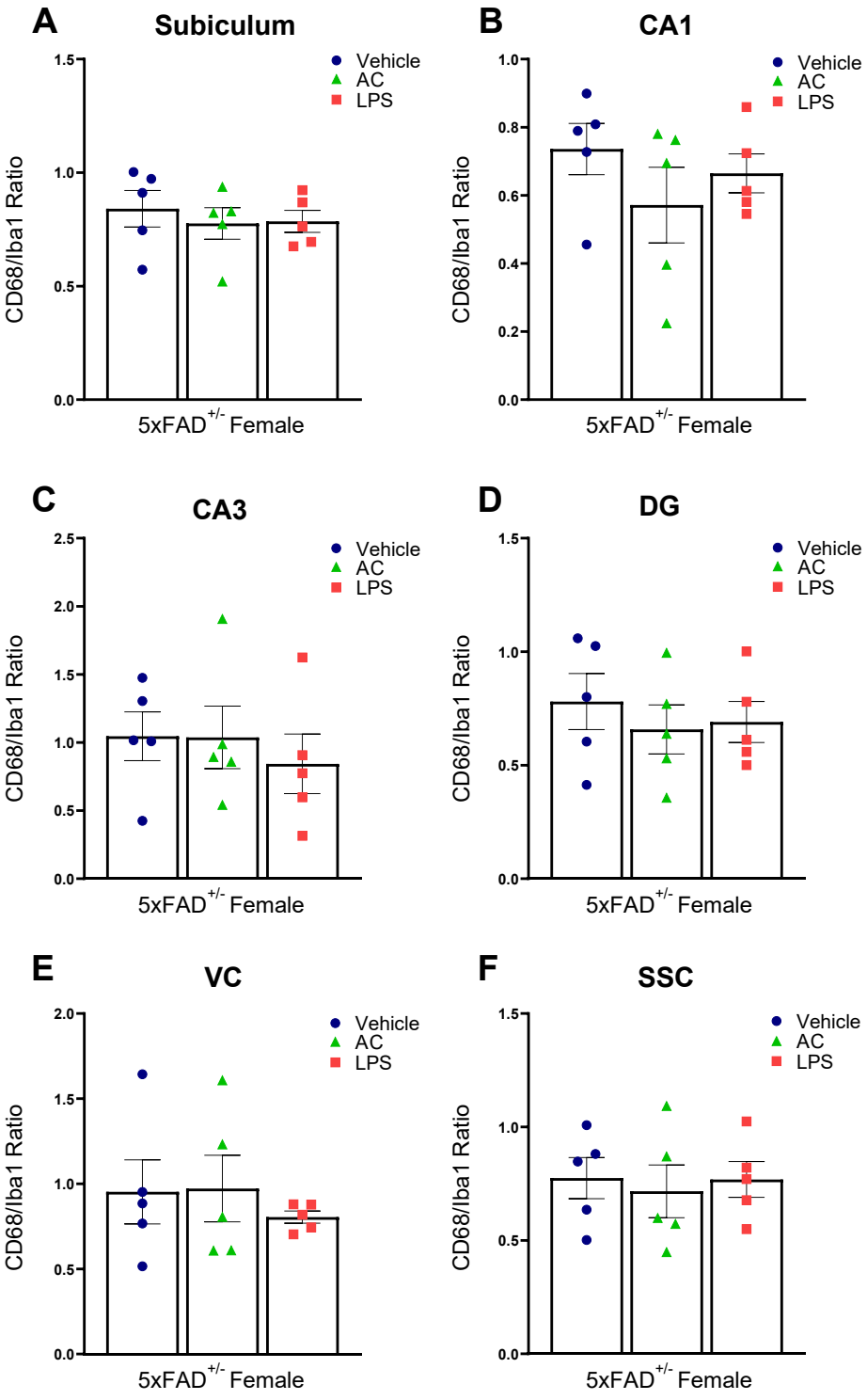

Figure 5.8: AC- and LPS-injection had no effect on the ratio of CD68 to IBA1 at 10 weeks post-injection. (A-F) Across the brain, AC- and LPS-injection had no effect on CD68 to Iba1 ratio at 10 weeks post-injection in female 5xFAD$^{+/-}$ mice compared to vehicle injection. One-way repeated-measures ANOVA with Tukey's post hoc test (Female: n=5 all treatments).

5.3.3. Two injections of AC and LPS did not affect Aβ plaque load at 10 weeks post-injection.

When Aβ plaques were examined in the female 5xFAD$^{+/-}$ mice at 10 weeks post injection (Fig.5.9), AC-injection did not influence Aβ plaque load in any of the examined brain regions (subiculum: p=0.99, Fig.5.10A; CA1: p=0.9, Fig.5.10B; CA3: p=0.9, Fig.5.10C; DG: p=0.83, Fig.5.10D; VC: p=0.85, Fig.5.10E; SSC: p=0.99, Fig.5.10F, n=5 vs vehicle for all regions).

Similarly, LPS-injection also had no effect on Aβ plaque load across the brain at 10 weeks post-injection when compared to vehicle injection (subiculum: p=0.81, Fig.5.10A; CA1: p=0.84, Fig.5.10B; CA3: p=0.84, Fig.5.10C; DG: p=0.97, Fig.5.10D; VC: p=0.61, Fig.5.10E; SSC: p=0.55, Fig.5.10F, n=5 vs vehicle for all regions).

The size of Aβ plaques were also examined but no changes were found following AC- and LPS-injection at 10 weeks post-injection.

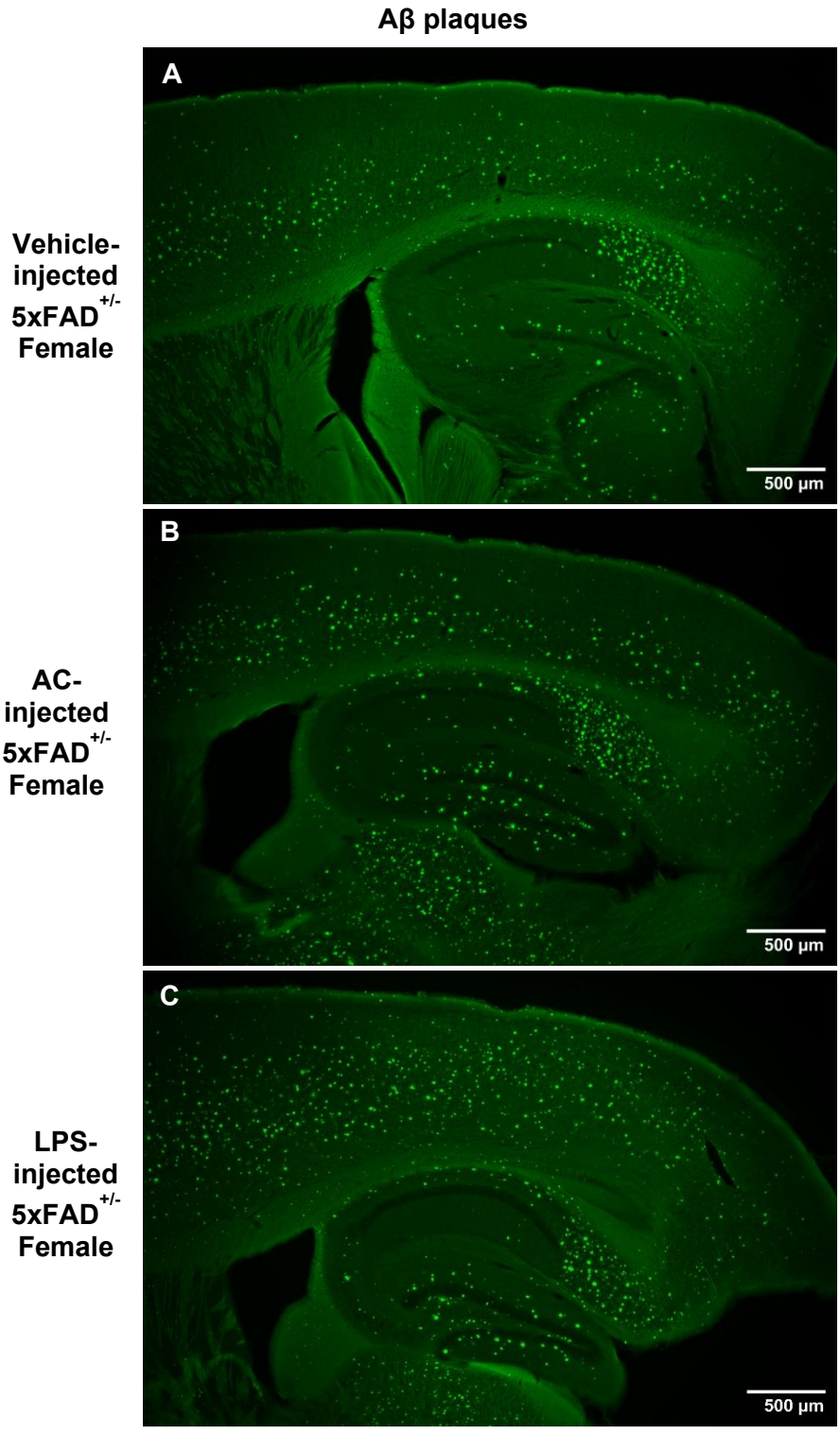

Figure 5.9: Representative Mesolens images of thioflavin S staining Aβ plaques in female 5xFAD$^{+/-}$ mice at 10 weeks post-injection. Compared to vehicle injection, neither AC- nor LPS-injection had any effect on Aβ plaque load or size across all the examined brain regions at 10 weeks post-injection in female 5xFAD$^{+/-}$ mice. Scale bar: 500µm.

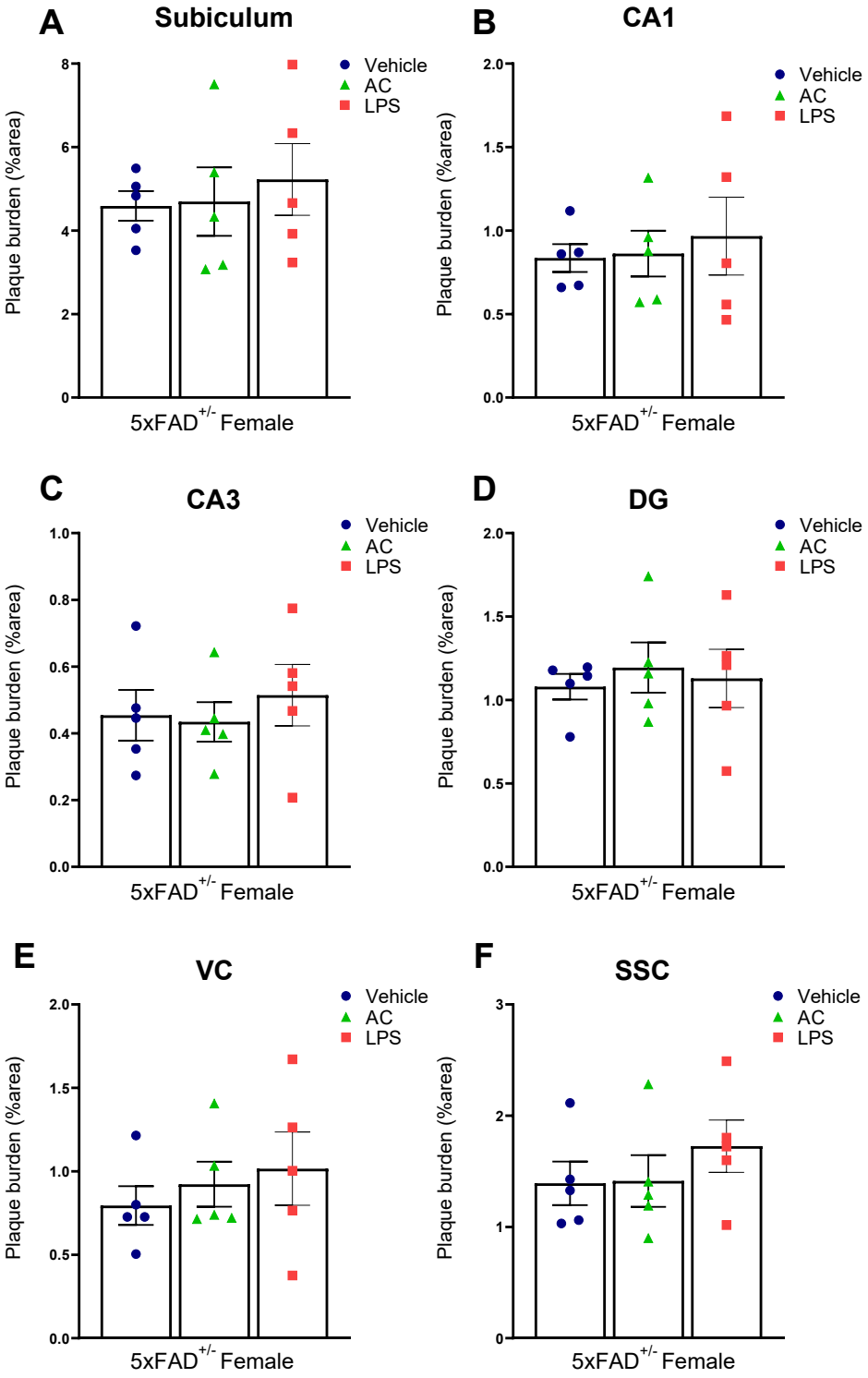

Figure 5.10: AC- and LPS-injection did not alter Aβ plaque load at 10 weeks post-injection in female 5xFAD$^{+/-}$ mice. (A-F) Thioflavin S staining revealed that AC- and LPS-injection had no effect Aβ plaque load in any brain region compared to vehicle injection at 10-week post-injection in 5xFAD$^{+/-}$ female mice. One-way repeated-measures ANOVA with Tukey's post hoc test (n=5 all treatments).

5.4. Multiple-injections of AC or LPS had no lasting influence on locomotor activity or animal health at 3 weeks post-injection in 5xFAD$^{+/-}$ mice.

Male and female 5xFAD$^{+/-}$ mice in the multiple-injection cohort, received four weekly-doses of either vehicle, AC or LPS, with the OFT and sucrose preference in week 1 and splash test in week 2.

Consistent with previous findings, AC and LPS injections again reduced locomotor activity 2h post-injection compared to pre-drug ($F_{(1\text{-}38)}$ = 6.67, p=0.007 vs pre-drug, Fig 5.11A) with AC- (p=0.03 vs vehicle, n=10, Fig.5.11A) and LPS-injection (p=0.002 vs vehicle, n=10, Fig.5.11A) reducing locomotor activity compared to vehicle injection. No sex differences were observed at any time point. However, hyperactivity was observed in two animals at 24h post-injection, one vehicle-injected and one LPS-injected. This increased activity partially recovered in the vehicle-injected mouse but persisted in the LPS-injected mouse. When locomotor activity was examined 3-weeks post-injection, additional doses of AC and LPS had no lasting behavioural changes on the 5xFAD$^{+/-}$ mice (AC: p=0.83 vs vehicle, n=10, Fig.5.11A; LPS: p=0.89 vs vehicle, n=10, Fig.5.11A).

To maintain consistency, sucrose preference was examined to find that LPS-injection again reduced sucrose preference 2h post-injection (, p=0.03 vs pre-drug, n=10, Fig.5.11B) but no significant changes were observed in AC- or vehicle-injected mice (Vehicle: p=0.26 vs pre-drug, n=10, Fig.5.11B; AC: p=0.09 vs pre-drug, n=10, Fig.5.11B). At 24h post-injection, the LPS-induced

reduction in sucrose preference was not significant when compared to pre-drug (p=0.25 vs pre-drug, n=10, Fig.5.11B). When sex was examined, AC- and LPS-injection significantly reduced sucrose preference 2h post-injection in female (AC: p=0.05; LPS: p=0.04, n=5 vs pre-drug for both treatments) but not male mice when compared to pre-drug.

When grooming behaviour was examined in this cohort of mice, there was an overall reduction in time spent grooming in the AC-injected mice 2h post injection (p=0.046 vs vehicle, n=10, Fig.5.11C), whereas LPS-injection had no effect (p=0.36 vs vehicle, n=10, Fig.5.11C). When sex differences were examined, it was noticed that male 5xFAD$^{+/-}$ mice were more susceptible to reduced grooming 2h post-injection following both AC (p=0.02 male vs female, n=5) and LPS (p=0.02 male vs female, n=5). Overall, no difference in time spent grooming was found between 2h post-injection and 24h post-injection ($F_{(1\text{-}27)}$ = 1.56, p=0.22 2h post- vs 24h post-drug, n=30, Fig 5.11C).

Consistent with the previous studies, mice were weighed daily during the behavioural testing and treatments phase. Additional doses of AC and LPS had no effect on final body weight in either male or female 5xFAD$^{+/-}$ mice at 3-weeks post-injection compared to vehicle injection (AC: p=0.44 vs vehicle, n=10 males; p=0.62 vs vehicle, n=10 females; LPS: p=0.33 vs vehicle, n=10 males; p=0.13 vs vehicle, n=10 females).

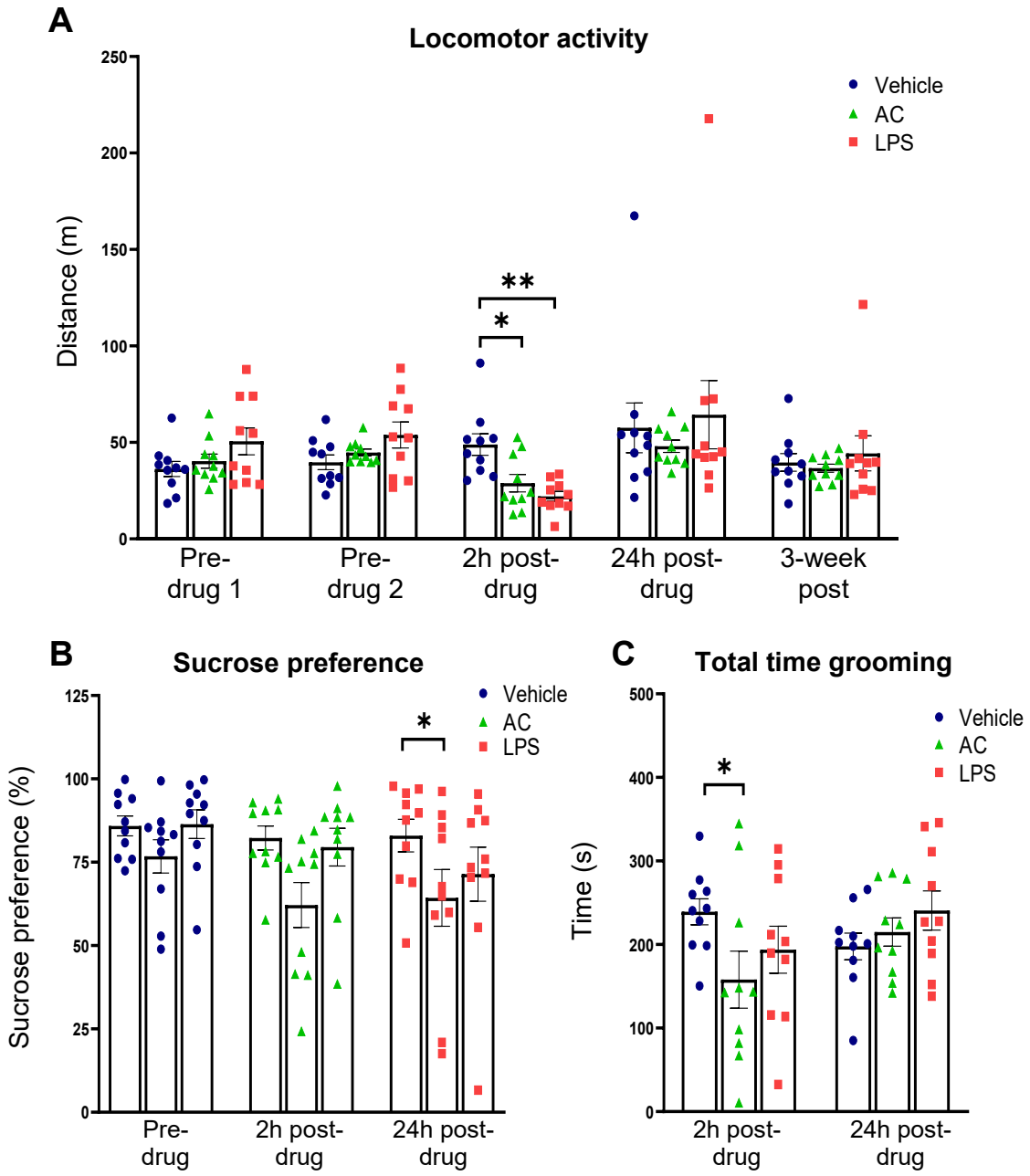

Figure 5.11: AC- and LPS-injection reduced locomotor activity 2h post-injection with additional doses having no lasting influence on activity at 3 weeks post-injection. (A) AC- and LPS-injection significantly reduced locomotor activity 2h post-injection (AC: *p<0.05 vs vehicle; LPS: **p<0.01 vs vehicle). Additional doses of AC and LPS had no lasting effects on locomotor activity at 3-weeks post-injection. (B) LPS- but not AC-injection significantly reduced sucrose preference 2h post-injection (*p<0.05 2h post- vs 24h post-injection). (C) AC- but not LPS-injection reduced grooming time 2h post-injection (*p<0.05 vs vehicle). Two-way repeated-measures ANOVA with Tukey's post hoc test (n=10 all treatments).

5.5. Immunohistochemistry results of four weekly-injections of AC or LPS.

Following the established behavioural testing protocol, with two injections in successive weeks alongside behaviour testing, both male and female 5xFAD$^{+/-}$ mice received two additional injections in successive weeks (four injections in total) and were aged for 3 weeks to determine if the neuroprotective effects were enhanced with further dosing in female 5xFAD$^{+/-}$ mice, and whether any pathological changes were observed in male 5xFAD$^{+/-}$ mice.

5.5.1. Four injections of AC and LPS had no effect on GFAP or C3 expression at 3 weeks post-injection.

GFAP fluorescence was used to examine astrocyte reactivity (Fig.5.12) to reveal that additional AC-injections did not influence GFAP expression across the brain in female (subiculum: p=0.81, Fig.5.13A; CA1: p=0.55, Fig.5.13B; CA3: p=0.8, Fig.5.13C; DG: p=0.49, Fig.5.13D; VC: p=0.51, Fig.5.13E; SSC: p=0.54, Fig.5.13F, n=5 vs vehicle for all regions) or male 5xFAD$^{+/-}$ mice (subiculum: p=0.85, Fig.5.13A; CA1: p=0.87, Fig.5.13B; CA3: p=0.98, Fig.5.13C; DG: p=0.94, Fig.5.13D; VC: p=0.99, Fig.5.13E; SSC: p=0.9, Fig.5.13F, n=5 vs vehicle for all regions). Furthermore, no differences in GFAP expression were found between the sexes in any brain region.

When LPS-injected mice were examined, we also found that additional injections of LPS had no effect on GFAP expression when compared to vehicle injection in either female (subiculum: p=0.93, Fig.5.13A; CA1: p=0.9, Fig.5.13B; CA3: p=0.98, Fig.5.13C; DG: p=0.99 Fig.5.13D; VC: p=0.98,

Fig.5.13E; SSC: p=0.99, Fig.5.13F, n=5 vs vehicle for all regions) or male 5xFAD$^{+/-}$ mice (subiculum: p=0.99, Fig.5.13A; CA1: p=0.99, Fig.5.13B; CA3: p=0.71, Fig.5.13C; DG: p=0.92, Fig.5.13D; VC: p>0.99, Fig.5.13E; SSC p=0.94, Fig.5.13F, n=5 vs vehicle for all regions). Also, no differences in GFAP expression were found between male and female 5xFAD$^{+/-}$ mice following multiple LPS-injections across the brain.

When C3 expression was examined (Fig.5.14), multiple injections of AC revealed no change C3 expression in female 5xFAD$^{+/-}$ mice compared to vehicle-injected mice (subiculum: p=0.92, Fig.5.15A; CA1: p=0.91, Fig.5.15B; CA3: p=0.97, Fig.5.15C; DG: p=0.84, Fig.5.15D; VC: p=0.91, Fig.5.15E; SSC: p=0.95, Fig.5.15F, n=5 vs vehicle for all regions). There was also no effect of additional AC-injections on C3 expression in male 5xFAD$^{+/-}$ mice (subiculum: p=0.58, Fig.5.1A; CA1: p=0.6, Fig.5.15B; CA3: p=0.81, Fig.5.15C; DG: p=0.5, Fig.5.15D; VC: p=0.55, Fig.5.1E; SSC: p=0.69, Fig.5.15F, n=5 vs vehicle for all regions). When sex was compared, no differences between C3 expression were found between AC-injected male and female 5xFAD$^{+/-}$ mice.

Further, additional injections of LPS also had no effects on C3 expression in either female (subiculum: p=0.76, Fig.5.15A; CA1: p=0.79, Fig.5.15B; CA3: p=0.58, Fig.5.15C; DG: p=0.58, Fig.5.15D; VC: p=0.83, Fig.5.15E; SSC: p=0.8, Fig.5.15F, n=5 vs vehicle for all regions) or male 5xFAD$^{+/-}$ mice (subiculum: p=0.99, Fig.5.1A; CA1: p=0.99, Fig.5.15B; CA3: p=0.94, Fig.5.15C; DG: p=0.99, Fig.5.15D; VC: p=0.87, Fig.5.1E; SSC: p=0.94, Fig.5.15F, n=5 vs vehicle for all regions). In addition, no sex differences in C3 expression were found between LPS-injection male and female 5xFAD$^{+/-}$ mice.

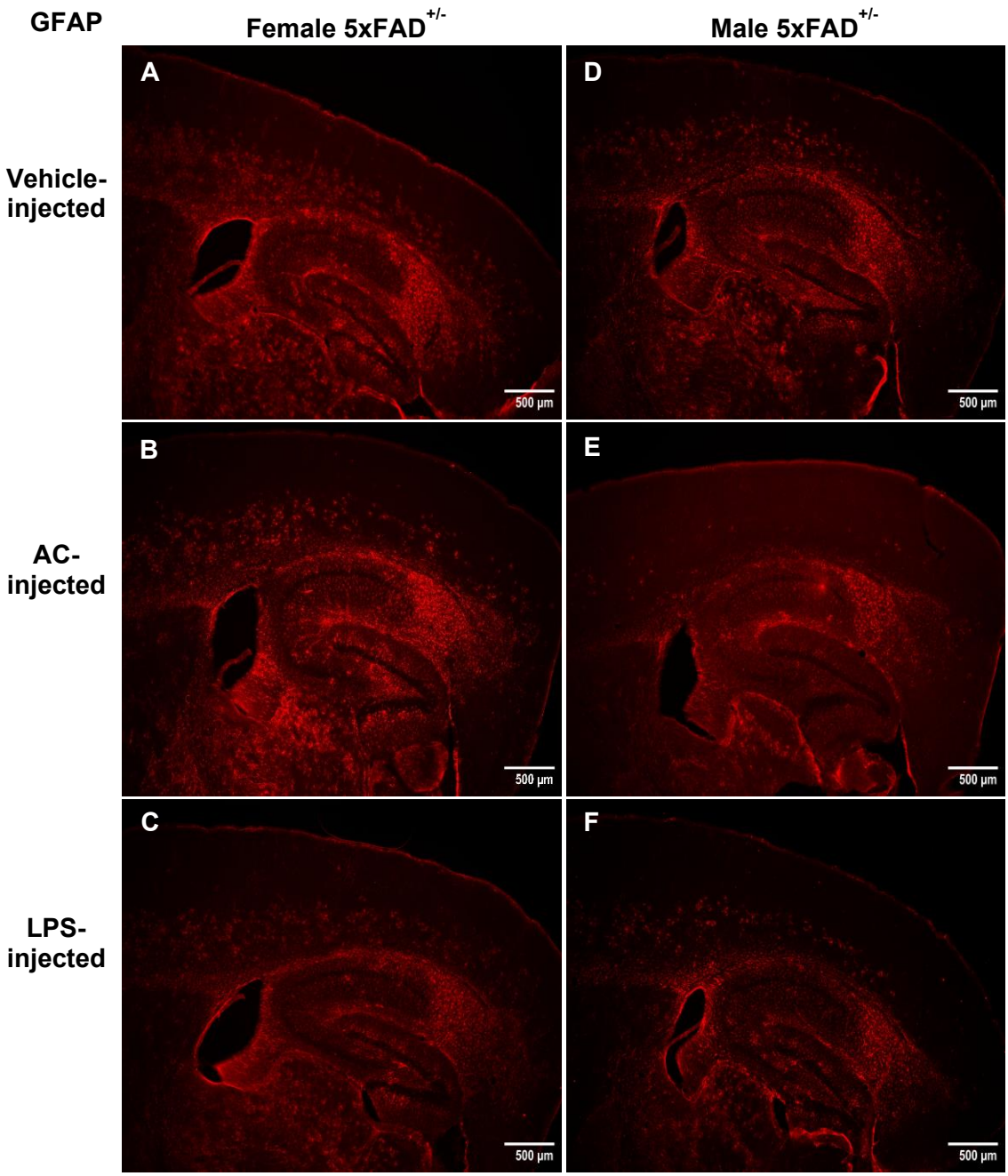

Figure 5.12: Representative Mesolens images of GFAP IHC in female and male 5xFAD$^{+/-}$ mice following multiple-injections. Additional doses of AC- and LPS-injection had no effect on GFAP expression compared to vehicle in either female (A-C) or male (D-F) 5xFAD$^{+/-}$ mice across the brain regions at 3 weeks post-injection. Scale bar: 500µm.

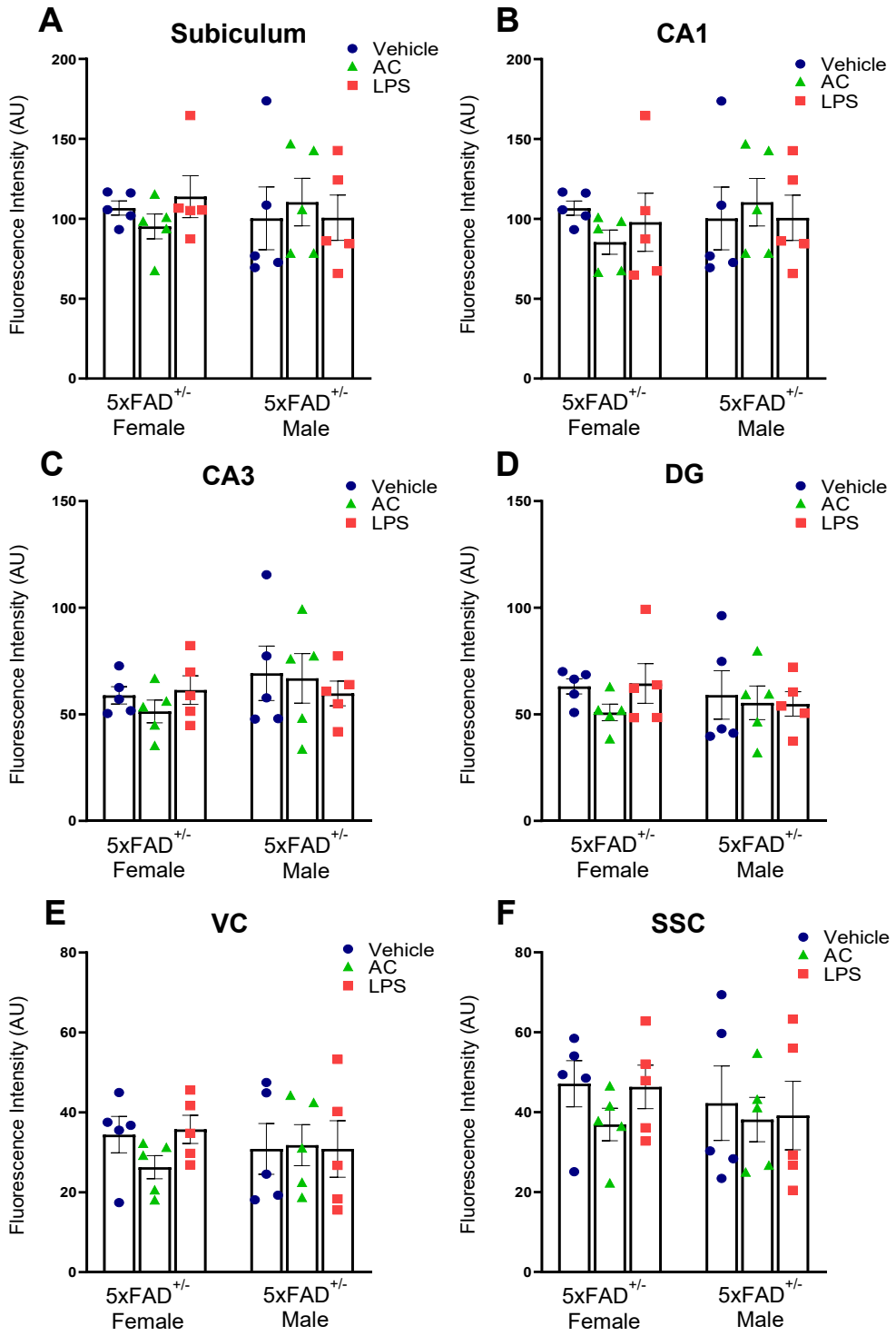

Figure 5.13: GFAP expression was unchanged in both female and male 5xFAD$^{+/-}$ mice following multiple injections of AC or LPS. (A-F) Across the brain, multiple injections of AC and LPS-injections had no effect on GFAP expression at 3 weeks post injection in either male or female 5xFAD$^{+/-}$ mice compared to vehicle. Further, no significant differences in astrocytic reactivity were found between male and female 5xFAD$^{+/-}$ mice. Fluorescence intensity measured as arbitrary units (AU). Two-way repeated-measures ANOVA with Tukey's post hoc test (n=5 all treatments and sex).

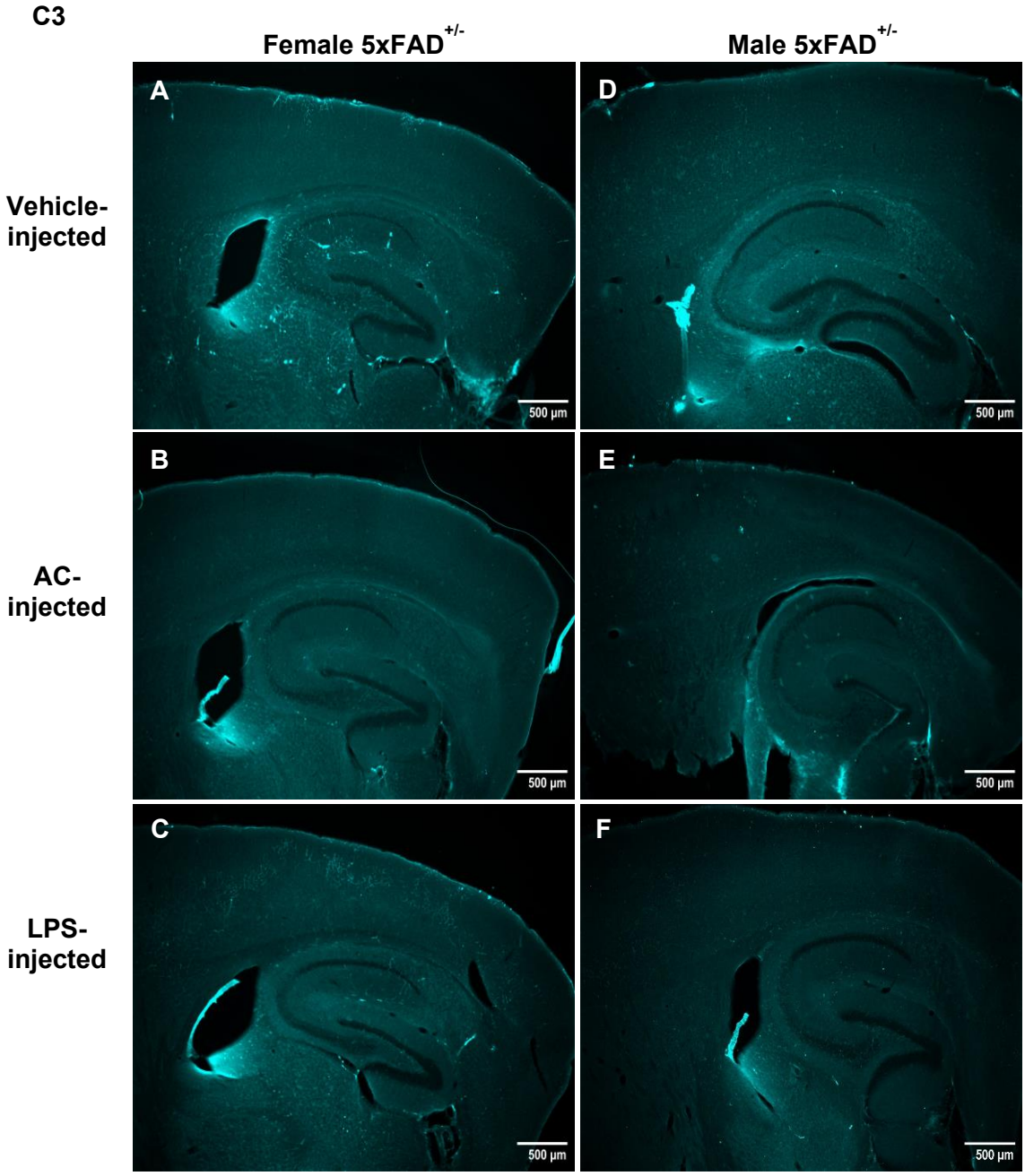

Figure 5.14: Representative Mesolens images of C3 IHC in female and male 5xFAD$^{+/-}$ mice following multiple-injections. Additional doses of AC- and LPS-injection had no effect on C3 expression compared to vehicle in either female (A-C) or male (D-F) 5xFAD$^{+/-}$ mice across the brain regions at 3 weeks post-injection. Scale bar: 500µm.

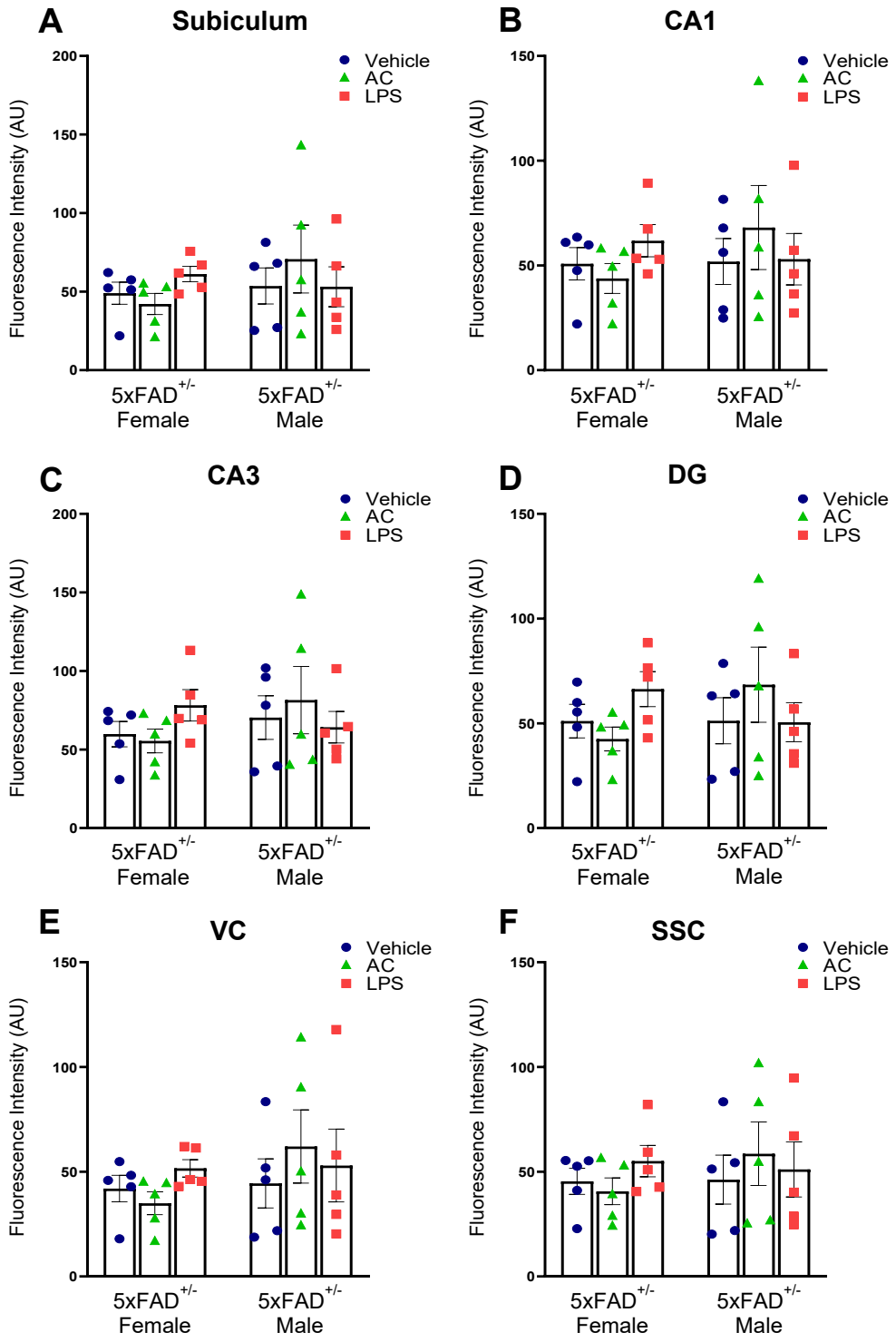

Figure 5.15: C3 expression was unaffected in both female and male 5xFAD$^{+/-}$ mice following multiple injections of AC or LPS. (A-F) Multiple injections of AC and LPS had no effect on C3 expression when examined across the brain in either male or female 5xFAD$^{+/-}$ mice at 3 weeks post-injection. There were also no differences in C3 expression found between sex of any treatment. Fluorescence intensity measured as arbitrary units (AU). Two-way repeated-measures ANOVA with Tukey's post hoc test (n=5 all treatments and sex).

5.5.2. Four injections of AC and LPS had no effect on Iba1 or CD68 expression at 3 weeks post-injection.

When activated microglia were examined using Iba1 expression (Fig.5.16), we found that additional doses of AC had no effect on Iba1 expression when compared to vehicle in both female (subiculum: p=0.92, Fig.5.17A; CA1: p=0.99, Fig.5.17B; CA3: p=0.99, Fig.5.17C; DG: p=0.99, Fig.5.17D; VC: p=0.78, Fig.5.17E; SSC: p=0.79, Fig.5.17F, n=5 vs vehicle for all regions) and male 5xFAD$^{+/-}$ mice (subiculum: p=0.67, Fig.5.17A; CA1: p=0.79, Fig.5.17B; CA3: p=0.75, Fig.5.17C; DG: p=0.88, Fig.5.17D; VC: p=0.88, Fig.5.17E; SSC: p=0.99, Fig.5.17F, n=5 vs vehicle for all regions). Furthermore, there was no difference in Iba1 expression between AC-injected male and female 5xFAD$^{+/-}$ mice in any brain region.

We also revealed that additional doses of LPS did not influence Iba1 expression compared to vehicle in either female (subiculum: p=0.99, Fig.5.17A; CA1: p=0.9, Fig.5.17B; CA3: p=0.95, Fig.5.17C; DG: p=0.96, Fig.5.17D; VC: p=0.85, Fig.5.17E; SSC: p=0.99, Fig.5.17F, n=5 vs vehicle for all regions) or male 5xFAD$^{+/-}$ mice (subiculum: p=0.99, Fig.5.17A; CA1: p=0.79, Fig.5.17B; CA3: p=0.75, Fig.5.17C; DG: p=0.91, Fig.5.17D; VC: p>0.99, Fig.5.17E; SSC: p=0.99, Fig.5.17F, n=5 vs vehicle for all regions). Furthermore, no sex differences were found in Iba1 expression following additional injections of LPS.

Phagocytic microglia, assessed using CD68 expression (Fig.5.18), were unaffected by additional doses of AC in female 5xFAD$^{+/-}$ mice (subiculum: p=0.96, Fig.5.19A; CA1: p=0.99, Fig.5.19B; CA3: p=0.99, Fig.5.19C; DG:

p=0.95, Fig.5.19D; VC: p>0.99, Fig.5.19E; SSC: p=0.99, Fig.5.19F, n=5 vs vehicle for all regions). Further, CD68 expression in male 5xFAD$^{+/-}$ mice was unchanged compared to vehicle following additional doses of AC (subiculum: p=0.73, Fig.5.19A; CA1: p=0.63, Fig.5.19B; CA3: p=0.67, Fig.5.19C; DG: p=0.58, Fig.5.19D; VC: p=0.84, Fig.5.19E; SSC: p=0.77, Fig.5.19F, n=5 vs vehicle for all regions).

Additional doses of LPS also had no effect on CD68 expression in both female (subiculum: p=0.99, Fig.5.19A; CA1: p=0.99, Fig.5.19B; CA3: p=0.97, Fig.5.19C; DG: p=0.98, Fig.5.19D; VC: p=0.95, Fig.5.19E; SSC: p=0.95, Fig.5.19F, n=5 vs vehicle for all regions) and male 5xFAD$^{+/-}$ mice (subiculum: p=0.92, Fig.5.19A; CA1: p=0.81, Fig.5.19B; CA3: p=0.78, Fig.5.19C; DG: p=0.88, Fig.5.19D; VC: p=0.85, Fig.5.19E; SSC: p=0.73, Fig.5.19F, n=5 vs vehicle for all regions).

There was a general trend towards increased CD68 expression across the treatment groups in male 5xFAD$^{+/-}$ mice in the CA3 ($F_{(1-23)}$ = 4.06, p=0.056 male vs female, n=15, Fig 5.19C), DG ($F_{(1-23)}$ = 3.31, p=0.08 male vs female, n=15, Fig 5.19D) and SSC ($F_{(1-23)}$ = 3.2, p=0.087 male vs female, n=15, Fig 5.19F).

Finally, when the CD68 to Iba1 ratio was examined, we found no change following additional doses of AC compared to vehicle in either female (subiculum: p>0.99, Fig.5.20A; CA1: p=0.62, Fig.5.20B; CA3: p>0.99, Fig.5.20C; DG: p=0.93, Fig.5.20D; VC: p=0.58, Fig.5.20E; SSC: p=0.79, Fig.5.20F, n=5 vs vehicle for all regions) or male 5xFAD$^{+/-}$ mice (subiculum:

p>0.99, Fig.5.19A; CA1: p=0.97, Fig.5.20B; CA3: p=0.99, Fig.5.20C; DG: p=0.99, Fig.5.20D; VC: p=0.81, Fig.5.20E; SSC: p=0.97; LPS: Fig.5.20F, n=5 vs vehicle for all regions).

There was also no change in CD68 to Iba1 ratio following additional doses of LPS compared to vehicle in either female (subiculum: p=0.82, Fig.5.20A; CA1: p=0.78, Fig.5.20B; CA3: p=0.93, Fig.5.20C; DG: p=0.89, Fig.5.20D; VC: p=0.88, Fig.5.20E; SSC: p=0.96, Fig.5.20F, n=5 vs vehicle for all regions) or male 5xFAD$^{+/-}$ mice (subiculum: p=0.5, Fig.5.19A; CA1: p=0.98, Fig.5.20B; CA3: p=0.43, Fig.5.20C; DG: p=0.61, Fig.5.20D; VC: p=0.97, Fig.5.20E; SSC: p=0.94, Fig.5.20F, n=5 vs vehicle for all regions). No sex differences in CD68 to Iba1 ratio were observed following additional doses of vehicle, AC or LPS.

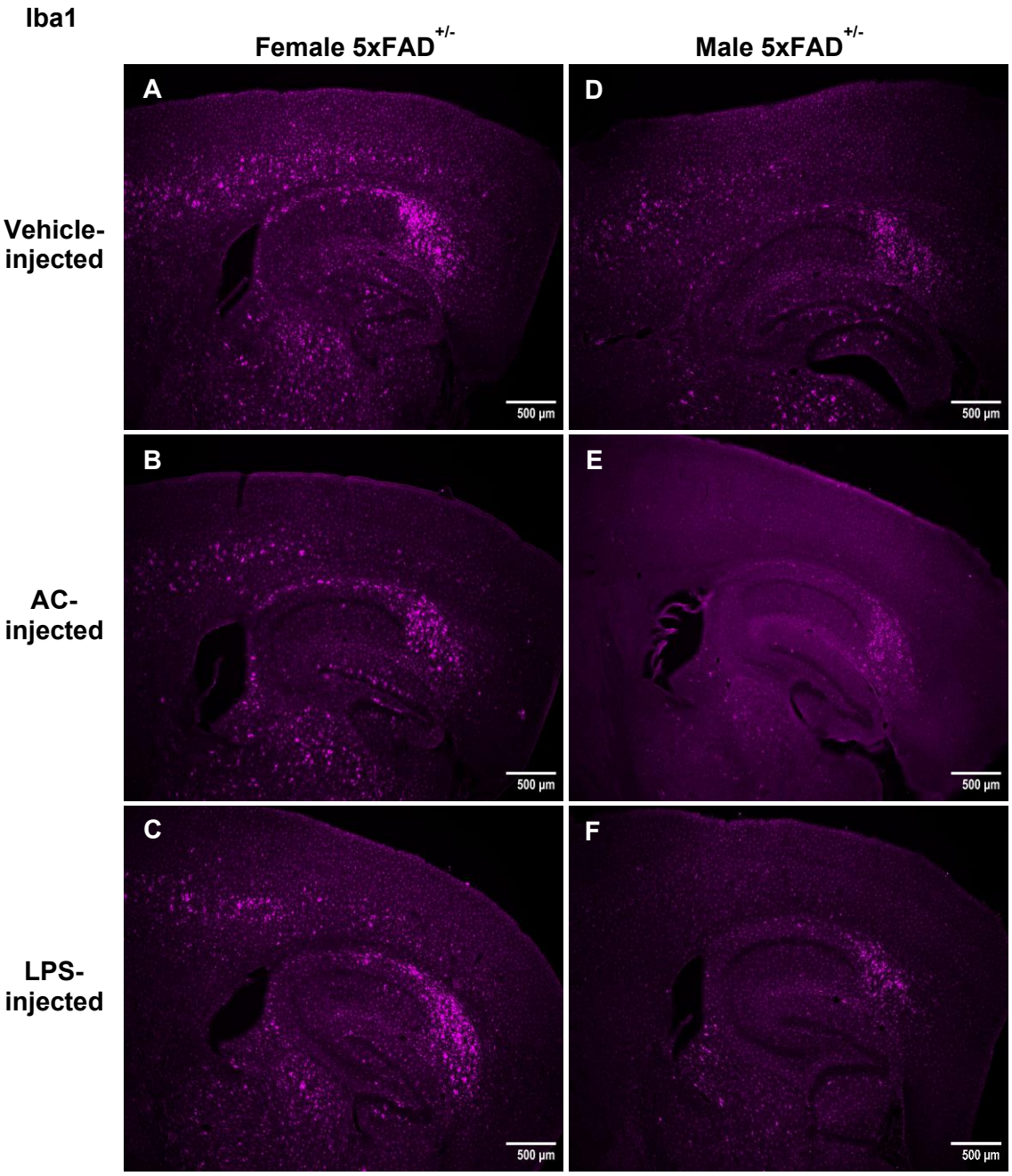

Figure 5.16: Representative Mesolens images of Iba1 IHC in female and male 5xFAD$^{+/-}$ mice following multiple-injections. Additional doses of AC- and LPS-injection had no effect on Iba1 expression compared to vehicle in either female (A-C) or male (D-F) 5xFAD$^{+/-}$ mice across the brain regions at 3 weeks post-injection. Scale bar: 500µm.

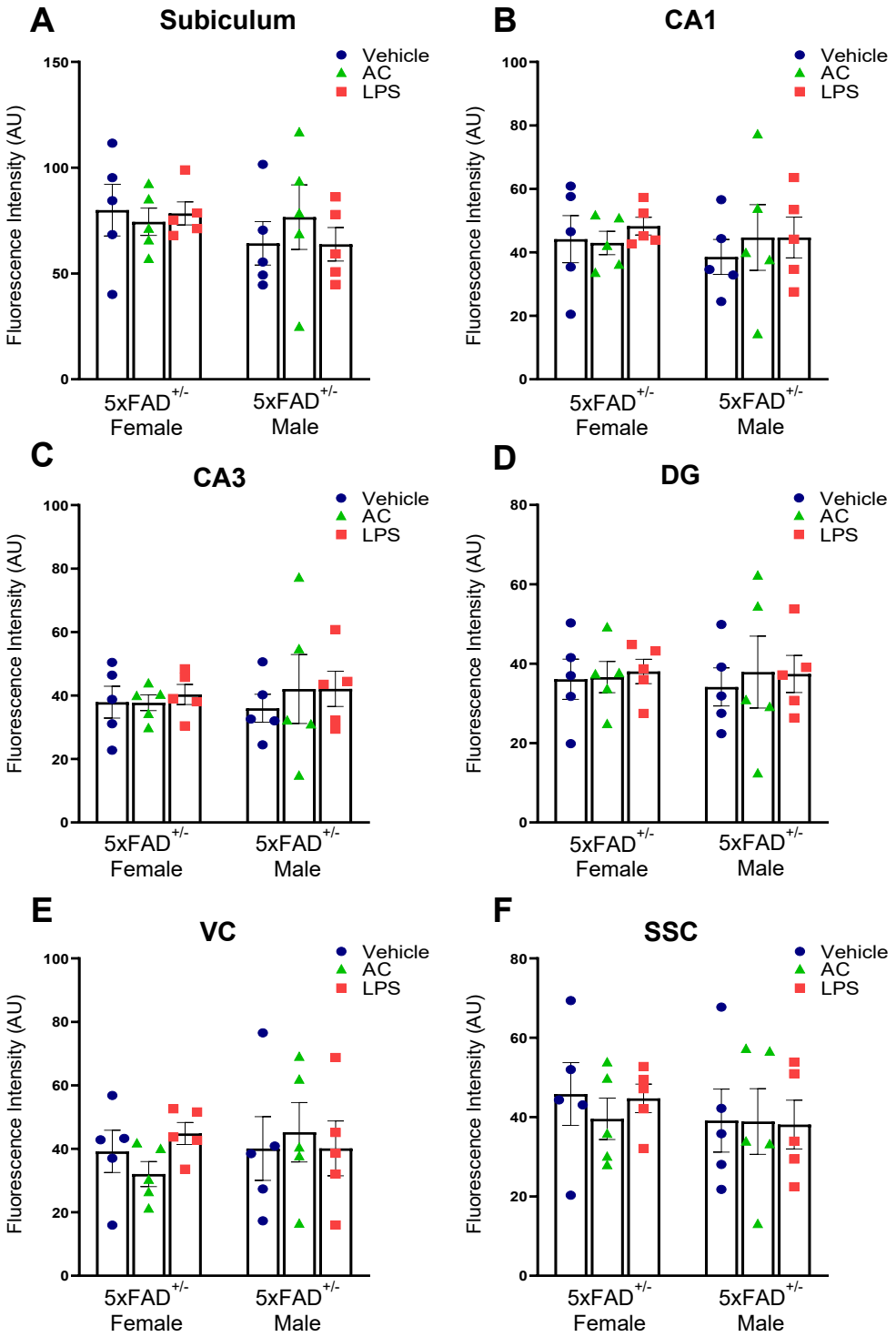

Figure 5.17: Iba1 expression was unaltered in both female and male 5xFAD$^{+/-}$ mice following multiple injections of AC or LPS. (A-F) In both male and female 5xFAD$^{+/-}$ mice, multiple injections of AC and LPS had no effect on Iba1 expression compared to vehicle when examined across the brain at 3 weeks post-injection. Also, no differences in Iba1 expression were found between sex of any treatment. Fluorescence intensity measured as arbitrary units (AU). Two-way repeated-measures ANOVA with Tukey's post hoc test (n=5 all treatments and sex).

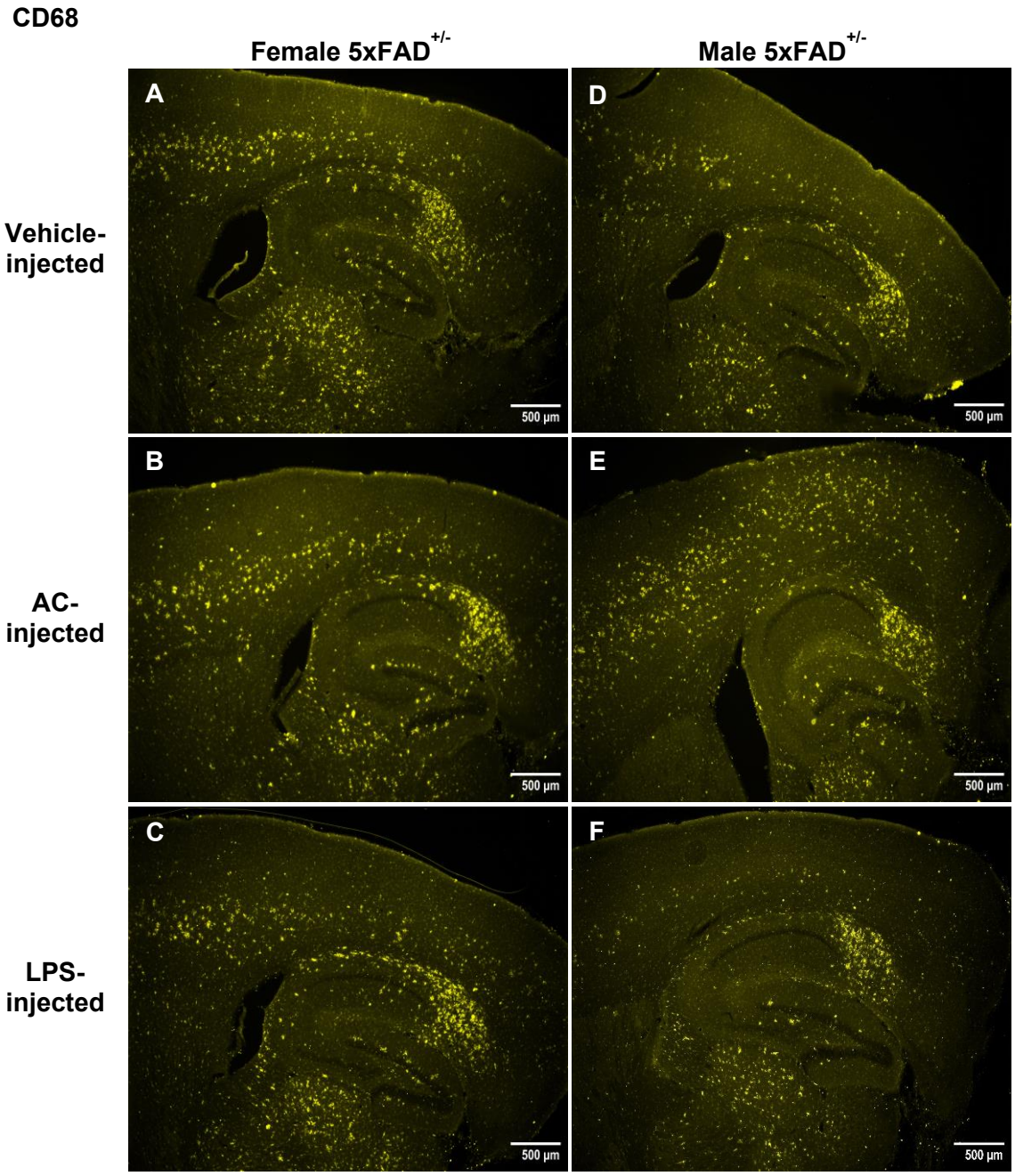

Figure 5.18: Representative Mesolens images of CD68 IHC in female and male 5xFAD$^{+/-}$ mice following multiple-injections. Additional doses of AC- and LPS-injection had no effect on CD68 expression compared to vehicle in either female (A-C) or male (D-F) 5xFAD$^{+/-}$ mice across the brain regions at 3 weeks post-injection. Scale bar: 500µm.

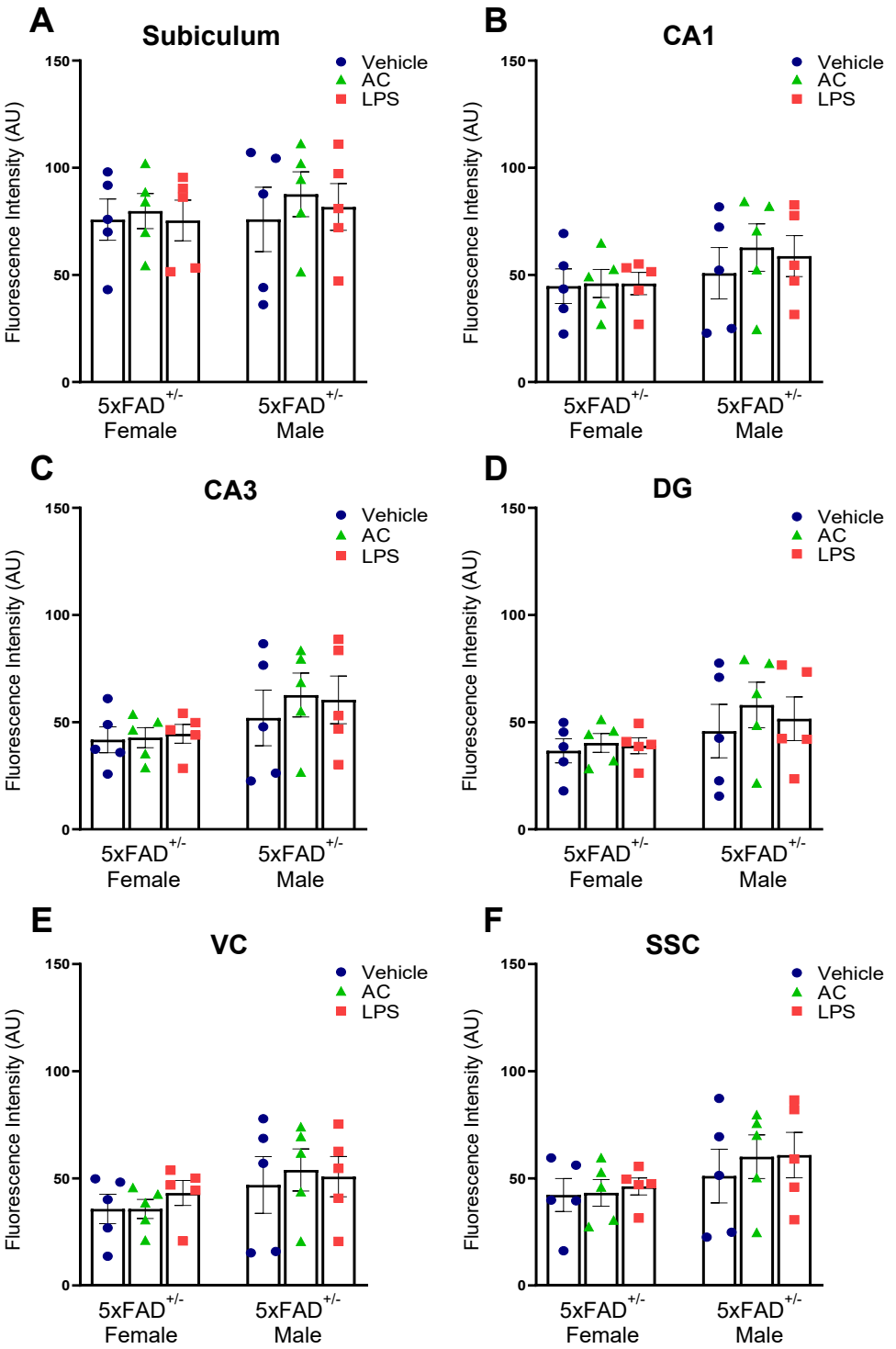

Figure 5.19: CD68 expression was unchanged in both female and male 5xFAD$^{+/-}$ mice following multiple injections of AC or LPS. (A-F) When CD68 expression was examined, multiple injections of AC and LPS had no effect in either male or female 5xFAD$^{+/-}$ mice compared to vehicle when examined across the brain regions at 3 weeks post-injection. There was also no significant difference in CD68 expression between male and female mice of any treatment. Fluorescence intensity measured as arbitrary units (AU). Two-way repeated-measures ANOVA with Tukey's post hoc test (n=5 all treatments and sex).

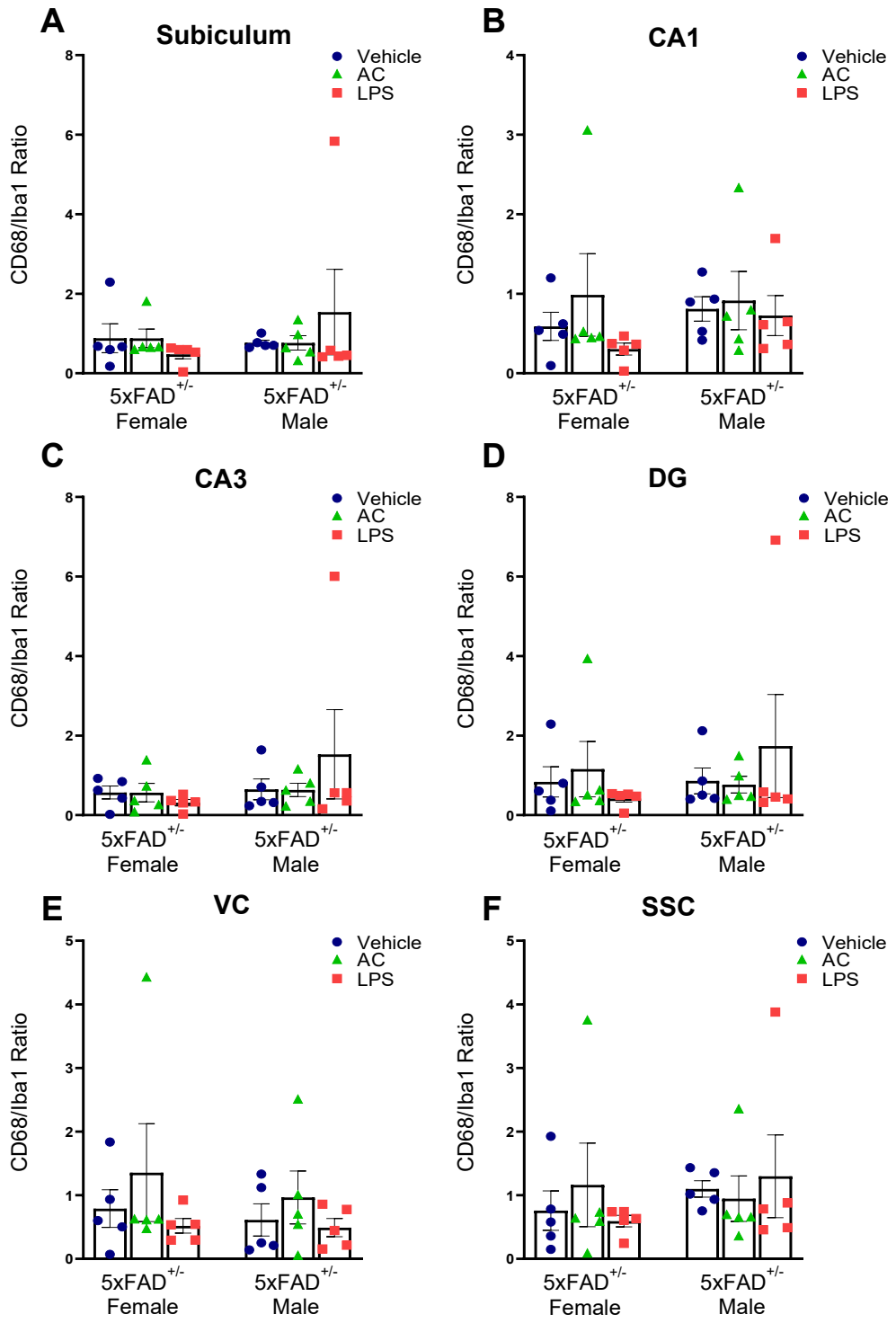

Figure 5.20: CD68 to Iba1 ratio was unaffected by multiple injections of AC or LPS in both female and male 5xFAD$^{+/-}$ mice at 3 weeks post-injection. (A-F) When the CD68 to Iba1 ratio was compared across the brain regions, it revealed that multiple doses of AC and LPS had no effect on the ratio of phagocytic microglia to activated microglia compared to vehicle in either female or male 5xFAD$^{+/-}$ mice. Two-way repeated-measures ANOVA with Tukey's post hoc test (n=5 all treatments and sex).

5.5.3. Four injections of AC and LPS did not influence Aβ plaque load at 3 weeks post-injection.

When Aβ plaques were examined using thioflavin S staining (Fig.5.21), we found that multiple injections of AC had no influence on Aβ plaque load in any of the examined brain regions in either female (subiculum: p=0.38, Fig.5.22A; CA1: p=0.85, Fig.5.22B; CA3: p=0.97, Fig.5.22C; DG: p=0.95, Fig.5.22D; VC: p=0.64, Fig.5.22E; SSC: p=0.53, Fig.5.22F, n=5 vs vehicle for all regions) or male 5xFAD$^{+/-}$ mice (subiculum: p=0.97, Fig.5.22A; CA1: p=0.99, Fig.5.22B; CA3: p=0.83, Fig.5.22C; DG: p=0.78, Fig.5.22D; VC: p=0.99, Fig.5.22E; SSC: p=0.55, Fig.5.22F, n=5 vs vehicle for all regions).

Furthermore, additional doses of LPS also had no effect on Aβ plaque load in either female (subiculum: p=0.33, Fig.5.22A; CA1: p=0.53, Fig.5.22B; CA3: p=0.96, Fig.5.22C; DG: p=0.93, Fig.5.22D; VC: p=0.9, Fig.5.22E; SSC: p=0.12, Fig.5.22F, n=5 vs vehicle for all regions) or male 5xFAD$^{+/-}$ mice (subiculum: p=0.99, Fig.5.22A; CA1: p=0.5, Fig.5.22B; CA3: p=0.42, Fig.5.22C; DG: p=0.92, Fig.5.22D; VC: p=0.39 Fig.5.22E; SSC: p=0.99, Fig.5.22F, n=5 vs vehicle for all regions).

In several brain regions, there was an overall increase in Aβ plaque load in female mice compared to males (CA1: $F_{(1-24)} = 4.81$, p=0.4, Fig 5.22B; DG: $F_{(1-24)} = 6.1$, p=0.02, Fig 5.22D; SSC: $F_{(1-24)} = 10.7$, p=0.003, Fig 5.22F, n=15 male vs female for all regions). In addition, the size of Aβ plaques were examined but we found no changes following additional doses of AC and LPS in either sex.

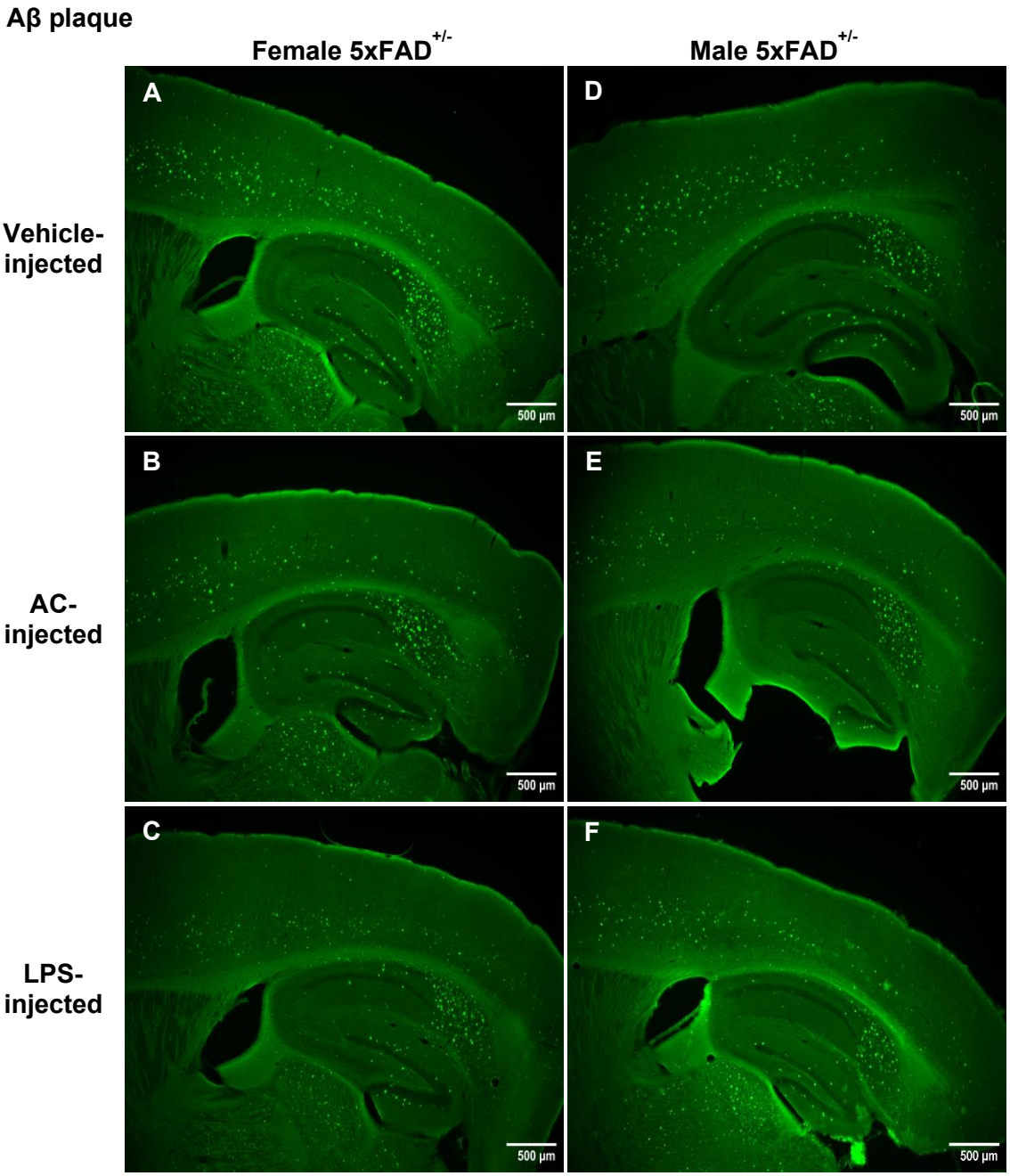

Figure 5.21: Representative Mesolens images of thioflavin S staining in female and male 5xFAD$^{+/-}$ mice following multiple-injections. Additional doses of AC- and LPS-injection had no significant effect on Aβ plaque load compared to vehicle in either female (A-C) or male (D-F) 5xFAD$^{+/-}$ mice across the brain regions at 3 weeks post-injection. Female mice were observed to have increased Aβ plaque load in several regions compared to male mice. Scale bar: 500µm.

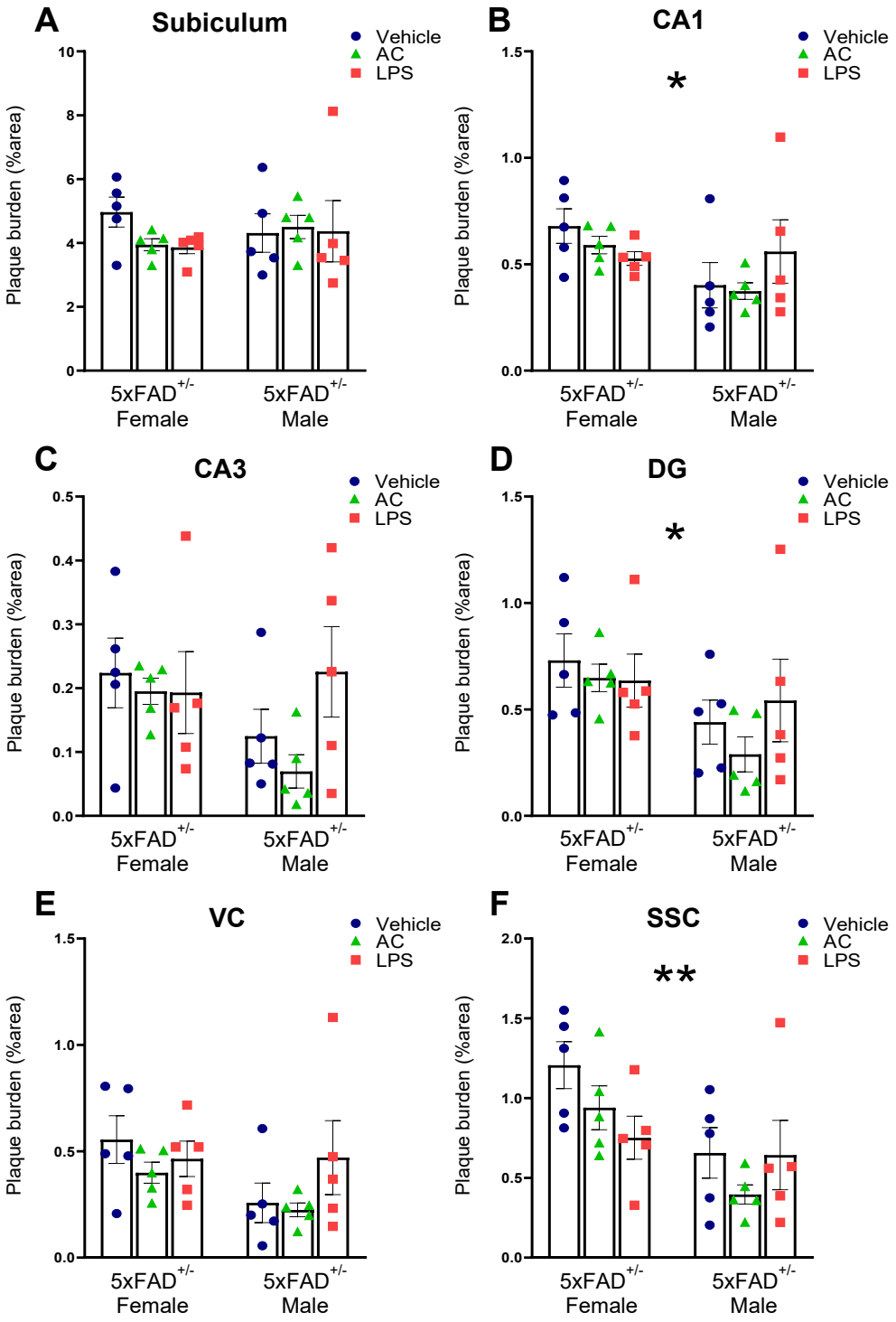

Figure 5.22: Multiple injections of AC or LPS had no influence on Aβ plaque load in either female or male 5xFAD$^{+/-}$ mice. (A-F) Thioflavin S staining revealed that additional doses of AC and LPS had no effect Aβ plaque load compared to vehicle injection in any brain region in either male or female 5xFAD$^{+/-}$ mice at 3 weeks post-injection. (B, D, F) Female mice had significantly increased Aβ plaque load in the CA1 (*p<0.05), DG (*p<0.05) and SSC (**p<0.01) compared to male 5xFAD $^{+/-}$ mice. Two-way repeated-measures ANOVA with Tukey's post hoc test (n=5 all treatments and sex).

5.6. Discussion

5.6.1. AC264613 and LPS had no effect long-term effect on locomotor activity or animal health at 10 weeks post-injection.

Consistent with previous experiments, we observed that AC and LPS reduced locomotor activity 2h post-injection, suggesting the mice were experiencing low mood-like behaviour (Petković *et al.*, 2022). This reduction was recovered at 24h post-injection, again highlighting the short-lived effects of AC (100 mg kg^{-1}) and LPS (0.5 mg kg^{-1}) on activity (Dang *et al.*, 2019; Moudio *et al.*, 2022). As we previously found no long-term effects of AC and LPS on locomotor activity at 3 weeks post-injection, we also confirmed activity remained unchanged at 10 weeks post-injection.

Furthermore, we found no long-term changes in body weight in the animals that received AC and LPS at 10 weeks post-injection. Although locomotor activity was only examined in female $5xFAD^{+/-}$ mice at 10 weeks post-injection, prior cohorts comparing WT and $5xFAD^{-/-}$ vs $5xFAD^{+/-}$ mice revealed no sex differences in locomotor activity, suggesting that male $5xFAD^{+/-}$ mice would likely also exhibit no lasting effects of AC or LPS at this time point. Taken together, these results indicate that, at the doses and frequency used, AC and LPS do not induce persistent behavioural or general health changes in mice.

5.6.2. LPS but not AC264613 reduced sucrose preference at 2h post-injection.

In this cohort of female $5xFAD^{+/-}$ mice, LPS reduced sucrose preference at 2h post-injection, whereas AC had no significant effect. These results contrast to our previous $5xFAD^{-/-}$ vs $5xFAD^{+/-}$ mice cohort, where both AC- and vehicle-

injection also induced reductions in sucrose preference. This variability in our results highlights the reported reliability and reproducibility issues often associated with the sucrose preference test (Markov, 2022; Berrio *et al.*, 2024).

In particular, the previous 5xFAD$^{-/-}$ vs 5xFAD$^{+/-}$ mice cohort experiments were conducted during major construction to the animal facility, exposing animals to environmental stressors such as noise and room changes. Several studies show that acoustic and environmental stressors increase susceptibility to depression-like and anhedonia-like behaviours in rodents. Chronic aversive noise has been shown to reduce sucrose preference and induce other depressive-like behaviours in mice (Dong *et al.*, 2016), while intense auditory stress impaired cognitive function, as well as inducing depression-like behaviour, including reduced sucrose preference and hyperactivity (Gao, Zhang, *et al.*, 2023). Therefore, the mice from our earlier 5xFAD$^{-/-}$ vs 5xFAD$^{+/-}$ cohort may have been more susceptible to stress-induced anhedonia-like behaviour following AC and vehicle-injection.

In contrast, the later cohorts of mice, including the female 5xFAD$^{+/-}$ mice maintained for 10 weeks post-injection, and the male and female 5xFAD$^{+/-}$ that received four weekly injections, were born and tested after construction had finished. These mice were maintained in a quieter and more stable environment, likely reducing their susceptibility to stress-related behavioural alterations. Although these cohorts were maintained in a quieter environment, they still experienced LPS-induced reduced sucrose preference suggesting that LPS-induces anhedonia regardless of environment. LPS is widely used to induce anhedonia (Dantzer, 2006; Biesmans *et al.*, 2016), and studies have

shown LPS-induced anhedonia is exacerbated in the presence of environmental stressors (Couch *et al.*, 2016). Evidence of environmental stress effects can also be observed in the locomotor activity between these cohorts of mice, as the 5xFAD$^{-/-}$ vs 5xFAD$^{+/-}$ mice exhibited higher baseline locomotor activity compared to later cohorts, suggesting stress may have induced some degree of hyperactivity in the mice (Boulle *et al.*, 2014; Deal *et al.*, 2021). Overall, these results highlight that environmental stress can influence baseline and vehicle or AC-induced sucrose preference, but LPS consistently produces a transient anhedonia-like behaviour.

5.6.3. AC264613 and LPS did not induce apathy-like behaviour in female 5xFAD$^{+/-}$ mice.

In contrast to the 5xFAD$^{-/-}$ vs 5xFAD$^{+/-}$ mice cohort where we found 5xFAD$^{+/-}$ mice were more susceptible to pharmacologically-induced apathy-like behaviour, AC and LPS had no effect on grooming in the 5xFAD$^{+/-}$ female mice cohort 2h post-injection. There was also no overall change in grooming time between 2h and 24h post-injection.

This difference may also be attributable to environmental stress. The earlier 5xFAD$^{-/-}$ vs 5xFAD$^{+/-}$ mice cohort was exposed to major construction in the animal facility, which may have led to increased susceptibility to stress-induced reductions in grooming and apathy-like behaviour (Atrooz *et al.*, 2021; Nollet, 2021). By contrast, the 5xFAD$^{+/-}$ female mice cohort was maintained in a quieter, more stable environment, therefore were less likely to display stress-induced apathetic behaviour. Studies have shown environmental stressors exacerbate pharmacologically-induced depression- and apathy-like behaviour

(Couch *et al.*, 2016; Kwatra *et al.*, 2021). This further supports that stress influences responses to apathy-like behaviour, and suggests that in our study, AC, may only induce apathetic-like behavioural changes in stress-sensitised animals. Interestingly, in the WT cohort, which was conducted before the animal facility construction commenced, we also found that AC did not alter grooming behaviour whereas LPS reduced grooming, suggesting LPS-induced behavioural changes can occur regardless of environmental stress, but the consistency may vary across cohorts.

Overall, these findings highlight that environmental conditions can influence susceptibility to depression- and apathy-like behaviour, and that pharmacologically-induced effects, such as AC or LPS, may be variable across cohorts depending on both stress history and other cohort-specific factors.

5.6.4. AC264613 and LPS had no effect astrocytic reactivity at 10 weeks post-injection.

The 5xFAD$^{+/-}$ female mice cohort were maintained for an additional 7 weeks, reaching 10 weeks post-injection (22-23 weeks old) when the brains were examined. Our previous results demonstrated that two injections of AC and LPS reduced astrocyte reactivity and Aβ plaque burden at 3 weeks-post injection. However, we found at 10 weeks post-injection these pathological changes did not persist, and astrocyte reactivity between vehicle, AC and LPS was indistinguishable.

Astrocyte reactivity is increasingly recognised as a hallmark of neuroinflammatory and neurodegenerative diseases, with astrocytes

undergoing progressive changes that contribute to disease pathogenesis (Verkhratsky *et al.*, 2023; Huang *et al.*, 2025). Depending on their activation state, reactive astrocytes can have beneficial neuroprotective effects, or detrimental neurotoxic effects that can influence disease progression (Lawrence *et al.*, 2023; Zhao *et al.*, 2024). Previous research within the lab group has shown PAR2 activation induces neuroprotection against kainate-induced neurotoxicity via astrocytic activation, highlighting the potential of PAR2 astrocytic modulation (Greenwood *et al.*, 2010). In the 5xFAD mouse model, astrocyte reactivity is associated with Aβ plaque burden (Oakley *et al.*, 2006) and multiple studies have demonstrated modulation of astrocyte reactivity can influence Aβ plaque burden. Indeed inhibition or knock-out models of regulators involved with astrogliosis, such as STAT3 and YKL-40, have shown to reduce astrocyte reactivity and Aβ plaque burden in mouse models of AD (Reichenbach *et al.*, 2019; Zeng *et al.*, 2023). Furthermore, pharmacological interventions of STAT3 signalling, reduced astrocyte expression, as well as reduced Aβ plaque deposition and improved cognitive function in the APP/PSN1 mouse model (Gao *et al.*, 2022). Conversely, several studies have also shown that ablation or reduction of astrocyte activity can impair Aβ plaque clearance and worsen Aβ plaque burden, often resulting in further cognitive decline (Kraft *et al.*, 2013; Katsouri *et al.*, 2020).

From our results at 3 weeks-post injection, we proposed that AC and LPS were modulating astrocytes to reduce reactivity, thus facilitating Aβ plaque clearance. However, as we see no change in GFAP or C3 expression following two injections of AC and LPS at 10 weeks post-injection, this effect appears to

be short-lived. This may be due to the progressive and aggressive pathology of the 5xFAD model, where astrocyte reactivity and Aβ plaque advance rapidly potentially overtaking any early pharmacological effect (Oblak *et al.*, 2021). Further, it could suggest that the dose and frequency of AC and LPS given in our study were only sufficient for short-term modulation. A study using low-dose LPS demonstrated astrocyte and microglia activation, resulting in Aβ plaque reduction up to 14 days post-injection. However, after 14 days post-injection astrocyte reactivity returned to baseline, while Aβ plaque burden was restored by 28 days post-injection (Herber *et al.*, 2004). Taken together, our results suggest a transient neuroprotective role of astrocytic modulation in 5xFAD mice but potentially dosage and frequency may influence the duration of efficacy.

5.6.5. AC264613 and LPS had no effect on activated microglia or their phagocytic activity at 10 weeks post-injection.

We found that at 10 weeks post-injection, AC and LPS had no effect on activated microglia levels, measured using Iba1 expression, or phagocytic activity, measured using CD68 expression. From our 3 week-post injection data, we observed region specific reductions in microglial activity following two injections of AC, but we found no changes in microglial phagocytic activity. We also did not observe any changes in microglial or phagocytic activity following LPS treatment. Our 10-week post-injection findings further substantiate that AC and LPS produce little to no effect on microglial and phagocytic activity in the 5xFAD mouse model at the dosage and frequency used.

Upregulated microglial activation is a hallmark of neuroinflammatory and neurodegenerative diseases, including AD (Leng *et al.*, 2021; Valiukas *et al.*, 2025). Microglia play a crucial role in Aβ plaque clearance but as disease progresses, chronic microglial activation contributes to a dysfunctional inflammatory response, leading to impaired Aβ plaque clearance, and even increased Aβ plaque deposition (Valiukas *et al.*, 2025). In the 5xFAD model, activated microglia cluster around Aβ plaques, and studies have shown increased activated microglia levels starting at 2 months of age (Oakley *et al.*, 2006; Forner *et al.*, 2021). This heightened and sustained inflammatory environment may limit the ability of pharmacological agents, such as AC or LPS, to further modulate microglial activity at more developed disease stages.

PAR2 activation has been shown to modulate microglial responses, though its effects are context-dependent. Studies have shown PAR2 activation can induce pro-inflammatory responses via microglia, releasing cytokines that result in neuronal death (Park *et al.*, 2010). Conversely, others have shown PAR2 stimulation can release protective neurotrophic factors and delay inflammatory cytokine release (Chen *et al.*, 2012). However, previous studies within the lab group demonstrated that AC did not induce cytokine release from primary microglia (Moudio *et al.*, 2022). The results from both our 3-week and 10-week post-injection cohorts suggests that PAR2 activation via AC-injection has limited effects on activated microglia and does not influence microglial phagocytosis. This again may be due to the disease state of the 5xFAD model, or the dose of AC used in our study is not sufficient to produce effects on microglia.

LPS is widely used in to induce microglial inflammatory responses. However, several studies have shown that LPS-induced microglial activation often produces short-lived effects, peaking within a few hours or days post-injection but returning to baseline levels shortly after (Reinert *et al.*, 2014; Jung *et al.*, 2023). Whereas other research demonstrated that repeated LPS injections induced long-lasting immune training and tolerance effects in microglia that persisted for 6 months (Wendeln *et al.*, 2018). Whilst these studies may vary by dosage and frequency of administration, these findings suggest that the microglial response to a single LPS exposure can be limited in duration and may not produce long-lasting effects on microglial activity or Aβ clearance. Notably, only a fraction of systemically administered LPS enters the brain, as the BBB prevents most from penetrating. Instead, LPS primarily mediates its effects indirectly via peripheral immune activation, leading to cytokine release that can cross the BBB to initiate a neuroinflammatory response. Additionally, disruption of the BBB may allow further LPS into the CNS (Nordgreen *et al.*, 2018; Batista *et al.*, 2019). In contrast, AC, as a small molecule, can readily cross the BBB and directly affect the CNS directly (Moudio *et al.*, 2022). These differences in CNS accessibility may influence the extent of behavioural effects and immunomodulation, although in our study, behavioural and pathological outcomes were broadly similar between AC and LPS.

Together, the results from both our 3 week and 10-week post-injection cohorts, suggest that, at the dose and frequency used, AC and LPS are insufficient at influencing microglial activity in the 5xFAD model.

5.6.5. AC264613 and LPS had no effect Aβ plaque load at 10 weeks post-injection.

Although we observed significant reductions in Aβ plaque load at 3 weeks post-injection following two injections of AC and LPS treatment, by 10 weeks post-injection neither AC nor LPS altered Aβ plaque load in female 5xFAD$^{+/-}$ mice. These findings, alongside unchanged astrocytic and microglial activity, further support that AC and LPS exert only transient effects on AD related pathology in the 5xFAD model.

Whilst extensive research supports the role of PAR2 in glial expression (Bushell, 2007; Price *et al.*, 2021), evidence linking PAR2 activation directly to Aβ plaque pathology is limited. Upregulated PAR2 expression has been found in glial cells clustered around Aβ plaques in human post-mortem tissue (Afkhami-Goli *et al.*, 2007). Furthermore, a PAR2 inhibitor was found to decrease amyloid aggregates and neuroinflammation in human fibroblasts from Parkison's patients (Quarta *et al.*, 2024). These studies support an association between PAR2 and amyloid related neuroinflammation.

Conversely, LPS has been used to influence Aβ plaque pathology in various models to differing effects. A single administration of LPS prior to plaque formation induced long-term microglial priming and reduced Aβ plaques for up to 6 months in the 5xFAD model, indicating that the timing of immune stimulation influences sustained neuroprotection (Yang *et al.*, 2023). Additional studies have also reported decreases in Aβ plaque burden following repeated or low-dose LPS administration in mouse models of differing ages (Go *et al.*, 2016; Thygesen *et al.*, 2018; Jendresen *et al.*, 2019). In contrast, others report

systemic or chronic LPS exposure can exacerbate amyloid pathology and neuroinflammation (Michaud *et al.*, 2013; Xie *et al.*, 2021, 2022). Such discrepancies likely arise from differences in LPS dosage, frequency, route of administration, and the disease stage at which interventions occur.

In our 3-week post-injection cohort, we revealed that both AC and LPS reduced Aβ plaque burden in female 5xFAD$^{+/-}$ mice, but not in males. Hence, we focused on females for the 10-week cohort. However, the absence of an effect at 10 weeks post-injection suggests that these interventions produce only short-lived modulation of Aβ pathology. This may be due the aggressive and progressive inflammatory state of the 5xFAD model. Taken together with our astrocytic and microglial findings, these data indicate that AC- and LPS-induced modulation may induce transient neuroprotective effects in female 5xFAD$^{+/-}$ mice, which diminish as disease pathology advances.

5.6.6. Multiple doses of AC264613 and LPS had no long-lasting effect on locomotor activity or animal health at 3 weeks post-injection.

After observing reductions in astrocytic reactivity and Aβ plaques in female 5xFAD$^{+/-}$ mice following two injections in successive weeks of either AC or LPS, we sought to determine whether additional doses could further potentiate these effects or elicit responses in male 5xFAD$^{+/-}$ mice. To maintain consistency with the initial experimental design, both male and female 5xFAD$^{+/-}$ mice received two injections in successive weeks alongside behavioural testing in accordance with previous protocols for the first two weeks. This was followed by two additional injections in successive weeks, for

a total of four injections. Mice were then maintained for 3 weeks post-final injection.

As seen in previous experiments, AC (100 mg kg^{-1}) and LPS (0.5 mg kg^{-1}) reduced locomotor activity 2h post-injection, consistent with short-term low mood-like behavioural effects, which were recovered by 24h post-injection. We also revealed that additional doses of AC and LPS had no lasting effects on activity, further confirming the short-lived nature of the treatments on behaviour (Moudio *et al.*, 2022). In addition, repeated injections of AC and LPS did not affect long-term changes in body weight in the animals when examined at 3 weeks post-injection. These findings further confirm that, at the doses and frequency used, AC and LPS do not induce persistent behavioural or general health alterations in 5xFAD mice.

5.6.7. LPS reduced sucrose preference in both sexes, while AC264613 reduced sucrose preference in only female 5xFAD$^{+/-}$ mice at 2h post-injection.

As with the 10-week post-injection cohort, the mice in the multi-injection cohort were maintained and tested in a quieter and more stable environment. Overall, LPS, but not AC, reduced sucrose preference in both sexes; however, AC reduced sucrose preference in female 5xFAD$^{+/-}$ mice, suggesting sex-dependant susceptibility of AC-induced anhedonia.

Interestingly, previous research from our lab group found that AC (10 mg kg^{-1}) reduced sucrose preference 2h post-injection in WT male mice (Moudio *et al.*, 2022). However, despite a higher dose of AC in the present study, only female mice exhibited anhedonia-like behaviour again highlighting variability in the

sucrose preference test, as well as the influence of environmental conditions, strain, age, and sex on behavioural outcomes (Verharen *et al.*, 2023).

Taken together with the 10-week cohort, these findings highlight that AC-induced anhedonia-like behaviour is context dependant but under conditions of environmental stress, behavioural responses can be potentiated. Whereas LPS still produces anhedonia-like behaviour regardless of environment.

5.6.8. AC264613 and LPS induce apathy-like behaviour in male 5xFAD$^{+/-}$ mice.

When grooming behaviour was assessed in the multi-injection mice cohort, which were maintained in a quieter, more stable environment, both AC and LPS induced apathy-like behaviour in male 5xFAD$^{+/-}$ mice. These findings are consistent with those observed in previous cohorts, firstly in that 5xFAD$^{+/-}$ mice were more susceptible to pharmacologically-induced apathy, and secondly aligning with the absence of grooming changes observed in the 10-week female 5xFAD$^{+/-}$ mice.

Sex differences in apathy-like behaviour are well reported in rodents, particularly in grooming tests. As previously discussed, grooming behaviour can vary between sex, strain, age, and environmental contexts (Kalueff *et al.*, 2004a). Studies have reported that males of various strains can have increased or decreased baseline grooming compared to females (Pitzer *et al.*, 2022; Murta *et al.*, 2023). Females have also been reported to be more susceptible to reduced grooming following LPS intervention (Sens *et al.*, 2017) or in stress-inducing conditions (Bekhbat *et al.*, 2018).

In our 5xFAD$^{-/-}$ vs 5xFAD$^{+/-}$ mice cohort, we found a trend towards reduced grooming in males. In the present cohort, we suggest that male 5xFAD$^{+/-}$ mice exhibit lower baseline grooming but also are more susceptible to AC- and LPS-induced apathy, even in the absence of environmental stress. We have also shown that male 5xFAD$^{+/-}$ mice exhibit lower levels of neuroinflammation and Aβ plaques than females. Therefore, the inflammatory effects induced by AC and LPS may exacerbate behavioural deficits in males, while female 5xFAD$^{+/-}$ mice may be less affected due to their heightened inflammatory state.

5.6.9. Four injections of AC264613 and LPS had no effect astrocytic reactivity in either male or female 5xFAD$^{+/-}$ mice at 3 weeks post-injection.

The multi-injection 5xFAD$^{+/-}$ mice cohort received four weekly injections and were maintained for 3 weeks post-injection (17-18 weeks old) when brains were examined. Our previous results demonstrated two injections reduced astrocyte reactivity and Aβ plaque burden in female 5xFAD$^{+/-}$ mice, therefore we expected to find further reductions or potential changes in male mice. However, our results revealed that additional doses of AC and LPS had no effect on astrocyte reactivity in either sex.

The absence of effects on astrocytic reactivity following repeated AC and LPS treatment may be due to several mechanisms. One possibility is a saturation or ceiling effect in astrocytic modulation, limiting further pathological changes, despite continued stimulation, as observed in other models of pharmacological intervention (Chistyakov *et al.*, 2019; Kim *et al.*, 2024). Repeated activation of PAR2 could also cause receptor desensitisation, resulting in diminished responsiveness pathologically to AC-injection (Ricks *et al.*, 2009). However,

PAR2 is known to resensitise within hours, therefore prolonged desensitisation across several days is unlikely (Bühm *et al.*, 1996). Despite AC repeatedly producing daily behavioural responses (Moudio *et al.*, 2022), astrocytes may have reached a modulation threshold after two injections, thus additional doses are ineffective. Similarly, repeated LPS exposure has been shown to induce immune tolerance, resulting in reduced cytokine release and glial activation (Wendeln *et al.*, 2018).

Environmental stress and prior immune history can alter astrocytic responsiveness to pharmacological interventions. Studies have shown prior stress can blunt LPS-induced astrocytic reactivity (Biesmans *et al.*, 2015), while others have shown stress can potentiate neuroinflammatory responses to LPS (Munhoz *et al.*, 2006). The 5xFAD$^{-/-}$ vs 5xFAD$^{+/-}$ cohort were exposed to construction-related environmental stress, which may have altered astrocytic baselines or changed reactivity profiles, and as such AC and LPS produced measurable reductions in astrocyte reactivity. Whereas mice tested in the later quieter environment, including the 10-week and multi-injection cohorts, did not show the same astrocytic modulation to AC and LPS (Miguel-Hidalgo, 2022).

Another contributing factor could be the advancing disease state of the 5xFAD model at 17-18 weeks of age, where extensive neuroinflammation and Aβ plaque deposition, may further limit the capacity for pharmacological modulation (Forner *et al.*, 2021). Finally, we observed considerable variability in GFAP intensity. Whist all IHC and imaging protocols remained consistent

throughout the project, such variability was noted across multiple stains and may have contributed to variation within the analyses.

5.6.10. Four injections of AC264613 and LPS had no effect activated microglia or phagocytic activity in either male or female 5xFAD$^{+/-}$ mice at 3 weeks post-injection.

Consistent with previous cohorts, additional injections of AC and LPS did not alter activated microglial or phagocytic activity in either sex. Taken together, the results from our 3-week, 10-week and multi-injection cohorts, suggest that, at the dose and frequency used, AC and LPS are insufficient to modulate microglial activity in the 5xFAD model.

Previous studies using prolonged repeated exposure to LPS (12-13 weeks), found increased microglial activation and clustering around Aβ plaques, and while some reported decreases in Aβ plaque burden (Thygesen *et al.*, 2018), others report increases in plaque burden (Sheng *et al.*, 2003). These discrepancies in findings could be due to different transgenic models, ages, and varying treatment regimens, all of which can significantly influence immunomodulatory outcomes.

As the experimental cohorts in our study expand over the period of, and conclusion of major construction in the animal unit, the absence of microglial activity following AC and LPS suggests that environmental stress did not influence our findings. Potentially, the lack of response of AC and LPS on microglial activity is due to the advancing disease state of the 5xFAD model. At 17–18 weeks of age, microglia in 5xFAD mice are already chronically

activated and may have reached a plateau of reactivity, limiting further pharmacological modulation.

5.6.11. Four injections of AC264613 and LPS had no effect Aβ plaque burden in either male or female 5xFAD$^{+/-}$ mice at 3 weeks post-injection.

Despite our initial results demonstrating reductions in Aβ plaque load in female 5xFAD$^{+/-}$ mice at 3 weeks post-injection following AC and LPS treatment, additional injections did not influence Aβ plaque burden in either sex. Our results suggest a potential ceiling effect or receptor desensitisation to additional doses of AC and LPS, thus Aβ plaque clearance is limited. While we observed an initial transient neuroprotective effect of AC and LPS in female 5xFAD$^{+/-}$ mice, these effects plateau potentially due to the advancing state of disease in the 5xFAD model.

It was observed that overall, the 10-week and the multi-injection cohort, had similar or slightly reduced Aβ plaques load, regardless of treatment than the mice in the 5xFAD$^{-/-}$ vs 5xFAD$^{+/-}$ cohort despite being older. This may be due to the construction-inducing environmental stress in the mice, resulting in exacerbated neuroinflammation and Aβ plaque load in the 5xFAD$^{-/-}$ vs 5xFAD$^{+/-}$ cohort. Chronic stress has been widely shown to potentiate neuroinflammation and accelerate Aβ plaque deposition, and increase the risk of cognitive decline in both humans and mouse models of AD (Dong *et al.*, 2009; Wallensten *et al.*, 2023; Shlomi-Loubaton *et al.*, 2025). Together, these findings suggest that stress in our study may have modulated baseline pathology and influenced the efficacy of AC and LPS intervention.

In several regions of the brain, we still observed female 5xFAD$^{+/-}$ mice had a higher plaque burden, consistent with known pathology in the 5xFAD model (Oakley *et al.*, 2006). These sex-specific differences may contribute to the lack of detectable effects in males, as 5xFAD$^{+/-}$ males display lower baseline Aβ levels and glial reactivity, potentially limiting the observable impact of AC or LPS. Together, our results indicated that, at the frequency and dosages, additional injections of AC and LPS were insufficient to reduce Aβ plaques in the progressing 5xFAD model, and environmental conditions and disease progression are factors to consider in pharmacological immunomodulation.

5.6.12. Conclusion

From the work in this chapter, we conclude that AC and LPS do not produce any long-term behavioural changes in 5xFAD$^{+/-}$ mice. Both AC and LPS intervention produce only limited, transient neuroprotective effects on astrocyte reactivity and Aβ plaque pathology, which do not persist to 10 weeks post-injection. Furthermore, additional treatments with AC and LPS were insufficient to modulate neuroinflammation and plaque pathology. Our findings suggest that environmental stress can highly influence AC- and LPS-induced changes in both behaviour and pathology, while the progressive and aggressive nature of disease in the 5xFAD model limits pharmacological immunomodulation.

Chapter 6: The effects of PAR2 inhibition on behaviour and blood brain barrier integrity.

6.1. Introduction and aims.

PAR2 has been implicated in a range of inflammatory processes, and accumulating evidence indicates that pharmacological inhibition of PAR2 can suppress its pro-inflammatory signalling pathways, offering potential therapeutic avenues for inflammatory disease (Villano *et al.*, 2024). The selective PAR2 inhibitor, AZ8838 (AZ), has been reported to act as a competitive inhibitor at the receptor, preventing PAR2 activation-induced inflammation and exerting anti-inflammatory effects *in vivo* (Kennedy *et al.*, 2020). From our results, we revealed that PAR2 activator AC (100 mg kg^{-1}) consistently reduced locomotor activity. Therefore, we investigated the effects of AZ (100 mg kg^{-1}) on activity and hypothesised that AZ inhibition would diminish AC-induced reductions in locomotor activity.

It is well-established that astrocytes play a crucial role in maintaining blood brain barrier (BBB) integrity, with astrocyte endfeet enwrapping blood vessels to support tight junctions and regulate BBB permeability (Yue *et al.*, 2023). BBB dysfunction is a common feature of neurodegenerative diseases, including AD, and is often associated with increased astrocytic reactivity (Chen *et al.*, 2023). BBB leakage has also been shown in the 5xFAD mouse model of amyloid pathology (Liu *et al.*, 2020). Evidence also suggests that PAR2 contributes in BBB maintenance, potentially through astrocytic regulation, where balanced PAR2 activity supports BBB integrity (Xu *et al.*, 2022). However, it remains unclear whether PAR2-induced astrocytic modulation directly influences BBB permeability.

In our previous results, we demonstrated that astrocytic GFAP and C3 expression is reduced by AC-injection in female 5xFAD$^{+/-}$ mice at 3-weeks post-injection, which suggests that this reduction of astrocytic reactivity may also influence the BBB integrity. Therefore, we investigated the effects of PAR2 activation and inhibition, using AC- and AZ-injection, on BBB permeability. We hypothesised that astrocytic reactivity contributes to increased BBB permeability, thus PAR2 activation will reduce BBB permeability, whereas PAR2 inhibition would increase BBB permeability.

The work in this chapter aims to answer the following research questions:

- Does AZ influence activity and/or inhibit AC-induced changes in locomotor behaviour in mice?
- Do AC and/or AZ alter BBB permeability in 5xFAD$^{-/-}$ or 5xFAD$^{+/-}$ mice?

6.1.1. 5xFAD mice.

In previous experiments, we found no sex differences in locomotor activity following vehicle or AC-injection. To ensure PAR2 inhibition did not influence sex in behavioural testing, both male and female WT and 5xFAD$^{-/-}$ mice were examined. Each treatment group consisted of a minimum of three mice per sex.

As reduced astrocytic reactivity was only observed in female 5xFAD$^{+/-}$ mice following AC-injection, we subsequently examined PAR2 activation and inhibition on BBB integrity in female 5xFAD$^{-/-}$ and 5xFAD$^{+/-}$ mice. Brain regions examined were the hippocampus (HC), motor cortex (MC), visual cortex (VC),

somatosensory cortex (SSC), and Cornu ammonis 1 (CA1). Each treatment group consisted of a minimum of three mice per genotype.

6.2. AZ pre-treatment enhanced AC-induced reductions in locomotor activity 2h post-injection, while AZ alone had no effect.

AC-injection (100 mg kg^{-1}) reduced locomotor activity 2h post-injection compared to pre-drug as previously shown ($F_{(2-29)}$ = 15.69, p<0.001 vs pre-drug, n=14, Fig.6.1B) with AC-injection significantly reducing activity compared to vehicle (p<0.001 vs vehicle, n=14, Fig.6.1B). No sex differences were found in the AC-treated group ($F_{(1-12)}$ = 0.05, p=0.82 male, n=6 vs female, n=8).

At 2h post-injection, AZ-injection (100 mg kg^{-1}) alone did not alter locomotor activity compared to pre-drug ($F_{(2-11)}$ = 1.08, p=0.38 vs pre-drug, n=6, Fig.6.1B) or when examined with vehicle injection (p=0.87 vs vehicle, n=6, Fig.6.1B). Similarly, no differences in activity were found between males and females ($F_{(1-4)}$ = 2.35, p=0.2 male vs female, n=3).

Having shown that AZ alone did not affect behaviour, we then examined a combination of AZ-injection (100 mg kg^{-1}) followed 1h later by vehicle-injection. No difference in locomotor activity was observed at 2h post-injection in the AZ- and vehicle-injected mice compared to pre-drug ($F_{(3-14)}$ = 0.04, p=0.99 vs pre-drug, n=6, Fig.6.1B) or when compared to vehicle-injection alone (p=0.14 vs vehicle, n=6, Fig.6.1B). There was a trend towards reduced locomotor activity in females across all timepoints ($F_{(1-4)}$ = 6.39, p=0.06 male vs female, n=3) but sex had no influence on treatment at 2h post-injection (p=0.51 male vs female, n=3).

To determine whether AZ pre-treatment affected AC-induced behavioural changes, AZ (100 mg kg^{-1}) was injected followed 1h later by AC-injection (100 mg kg^{-1}), with locomotor activity measured 2h post AC-injection. In AZ- and AC-injected mice, locomotor activity was significantly reduced compared to pre-drug ($F_{(1-6)}$ = 24.97, $p<0.001$ vs pre-drug, n=6, Fig.6.1B) and when examined with vehicle ($p<0.001$ vs vehicle, n=6, Fig.6.1B). Interestingly, AZ pre-treatment further enhanced the AC-induced reduction in activity compared to AC-injection alone ($p=0.008$ vs AC, n=6, Fig.6.1B). No sex differences were found within the AZ and AC-injection ($F_{(1-4)}$ = 1.6, $p=0.27$ male vs female, n=3).

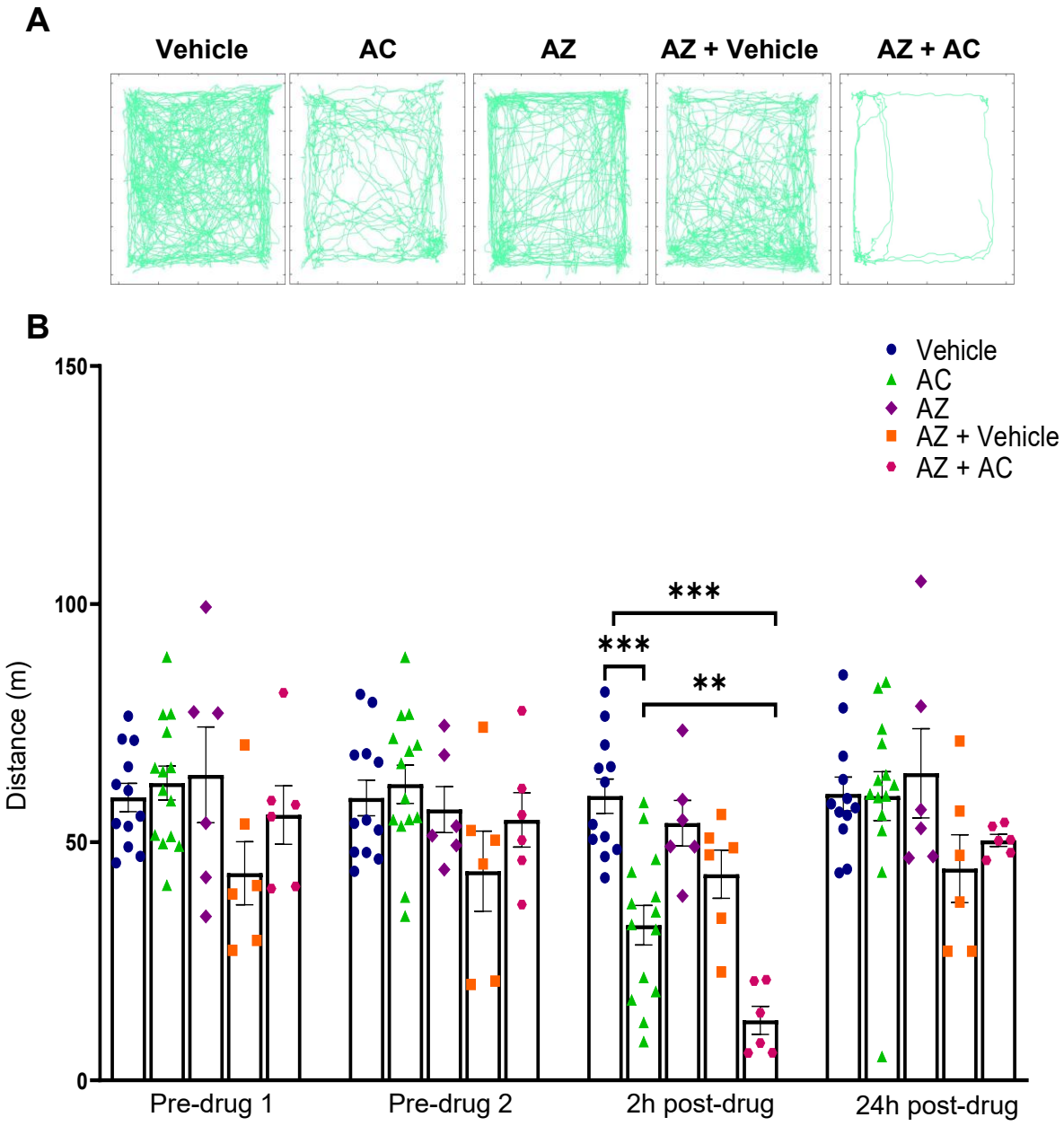

Figure 6.1: AZ-injection followed by AC-injection reduced locomotor activity 2h post-injection while AZ-injection alone had no effects. (A) Representative OFT tracking traces at 2h post-injection following vehicle, AC, AZ, AZ + Vehicle and AZ + AC. (B) AZ + AC-injection (100 mg kg^{-1} i.p.) significantly reduced locomotor activity 2h post-injection compared to vehicle (***p<0.001 vs vehicle) and AC alone (**p<0.01 vs AC). AZ-injection (100 mg kg^{-1} i.p.) alone and AZ (100 mg kg^{-1} i.p.) + Vehicle-injection had no effect on locomotor activity at 2h post-injection. AC-injection (100 mg kg^{-1} i.p.) significantly reduced locomotor activity 2h post-injection (***p<0.001 vs vehicle). Two-way repeated-measures ANOVA with Tukey's post hoc test (n= 12 vehicle, 14 AC, 6 AZ, 6 AZ + Vehicle, 6 AZ + AC).

6.3. AC- but not AZ-injection increases cadaverine and lectin levels across the brain.

6.3.1. AC-injection increases cadaverine expression in across the brain.

To investigate BBB permeability, cadaverine (7 mg kg $^{-1}$) (Bravo-Ferrer *et al.*, 2025), a small polar tracer and protein marker which does not normally cross the BBB, was administered intravenously to examine BBB leakage into the brain parenchyma. Cadaverine is often used to detect paracellular or transcytotic leakage, as it rapidly diffuses into areas of BBB disruption but is largely excluded from healthy brain tissue (Munoz-Ballester *et al.*, 2024). Mice received either vehicle, AC (100 mg kg $^{-1}$), AZ (100 mg kg $^{-1}$), or AZ pre-treatment (100 mg kg $^{-1}$) followed 1h later by AC (100 mg kg $^{-1}$), intraperitoneally, with brain fixation and removal occurring 2h post-injection. Cadaverine was given 30 min after i.p. treatment.

Mesolens imaging of cadaverine fluorescence (Fig.6.2A-D) revealed no difference in cadaverine fluorescence between 5xFAD$^{-/-}$ and 5xFAD$^{+/-}$ vehicle injected mice ($F_{(1-4)}$ = 1.18, p=0.34 5xFAD$^{-/-}$ and 5xFAD$^{+/-}$, n=3). Compared to vehicle, AC-injection increased cadaverine fluorescence in the brain (HC: p=0.02; MC: p=0.04; VC: p=0.01; SSC: p=0.02, n=6 vs vehicle, Fig.6.3A) but no differences in cadaverine fluorescence were found between the genotypes following AC-injection ($F_{(1-4)}$ = 0.47, p=0.53 5xFAD$^{-/-}$ and 5xFAD$^{+/-}$, n=3).

AZ-injection alone had no effect on cadaverine expression in any brain region (HC: p=0.99; MC: p>0.99; VC: p=0.99; SSC: p=0.99, n=6 vs vehicle, Fig.6.3A).

There were also no genotype differences in cadaverine expression in the AZ-injected mice ($F_{(1-4)}$ = 0.007, p=0.94 5xFAD$^{-/-}$ and 5xFAD$^{+/-}$, n=3).

Finally, AZ-injection followed 1h later by AC-injection also had no influence on cadaverine expression compared to vehicle (HC: p=0.96; MC: p>0.99; VC: p=0.99; SSC: p=0.99, n=6 vs vehicle, Fig.6.3A). Further, no genotype differences were found ($F_{(1-4)}$ = 0.33, p=0.6 5xFAD$^{-/-}$ and 5xFAD$^{+/-}$, n=3).

6.3.1 AC-injection increases lectin expression in some brain regions.

To investigate blood vessels in the brain, vascular marker lectin (5 mg kg $^{-1}$) (Bravo-Ferrer *et al.*, 2025) was administered intravenously to label endothelial cells lining blood vessels to visualise vascular structures. Lectins, including isolectins such as Ricin Toxin B subunit (RTB), bind to glycoproteins on the endothelial surface and are widely used to map cerebrovascular architecture (Hanafy *et al.*, 2023). Lectin was given 5 min prior to brain fixation and removal. Mesolens imaging of lectin (Fig.6.2E-H) revealed no genotypic differences in lectin expression in vehicle injected mice ($F_{(1-4)}$ = 1.44, p=0.3 5xFAD$^{-/-}$ and 5xFAD$^{+/-}$, n=3). Unlike cadaverine, AC-injection did not alter lectin expression compared to vehicle-injection (HC: p=0.22; MC: p=0.38; VC: p=0.19; SSC: p=0.22, n=6 vs vehicle, Fig.6.3B). However, AC-injection did increase lectin expression in some brain regions when compared to AZ- followed by AC-injection (VC: p=0.036; SSC: p=0.051, n=6 vs AZ+AC, Fig.6.3B). Furthermore, lectin expression was unaffected by genotype following AC-injection ($F_{(1-4)}$ = 0.32, p=0.6 5xFAD$^{-/-}$ and 5xFAD$^{+/-}$, n=3).

AZ-injection alone had no effect on lectin expression (HC: p=0.99; MC: p=0.99; VC: p=0.99; SSC: p>0.99, n=6 vs vehicle, Fig.6.3B), and no genotypic differences were found ($F_{(1-4)}$ = 0.11, p=0.76 5xFAD$^{-/-}$ and 5xFAD$^{+/-}$, n=3).

Lastly, AZ-injection followed 1h later by AC-injection also did not alter lectin expression compared to vehicle in any brain region (HC: p=0.97; MC: p=0.83; VC: p=0.88; SSC: p=0.9, n=6 vs vehicle, Fig.6.3B). We also confirmed no differences in lectin expression between the genotypes ($F_{(1-4)}$ = 0.03, p=0.88 5xFAD$^{-/-}$ and 5xFAD$^{+/-}$, n=3).

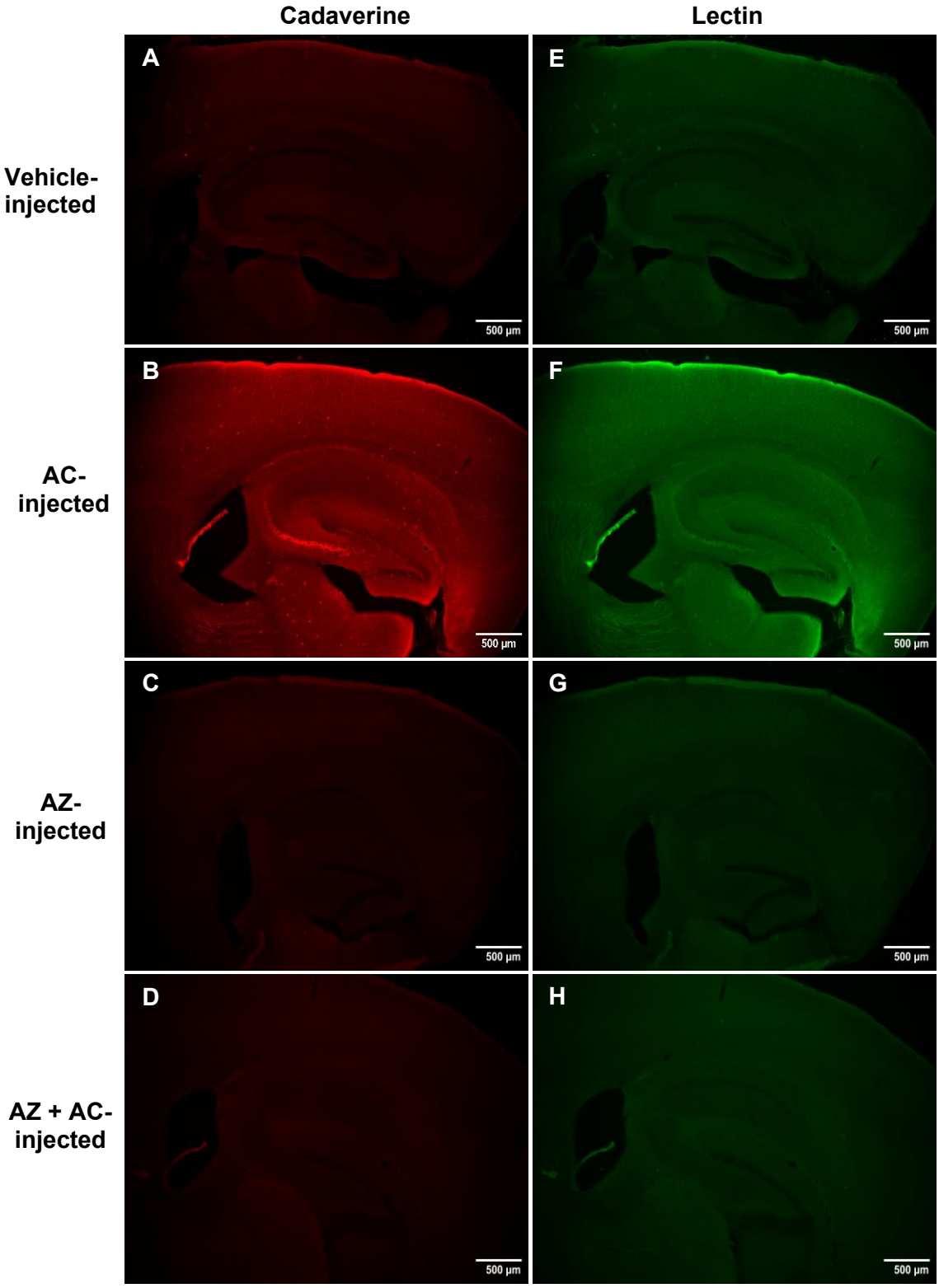

Figure 6.2: Representative Mesolens images of cadaverine and lectin expression in the hippocampus, VC and SSC. (A-D) Cadaverine expression was significantly increased following AC-injection but not AZ-injection or AZ + AC-injection. (E-H) Lectin expression was increased in the VC and SSC following AC-injection but not AZ-injection or AZ + AC-injection. Scale bar: 500 µm.

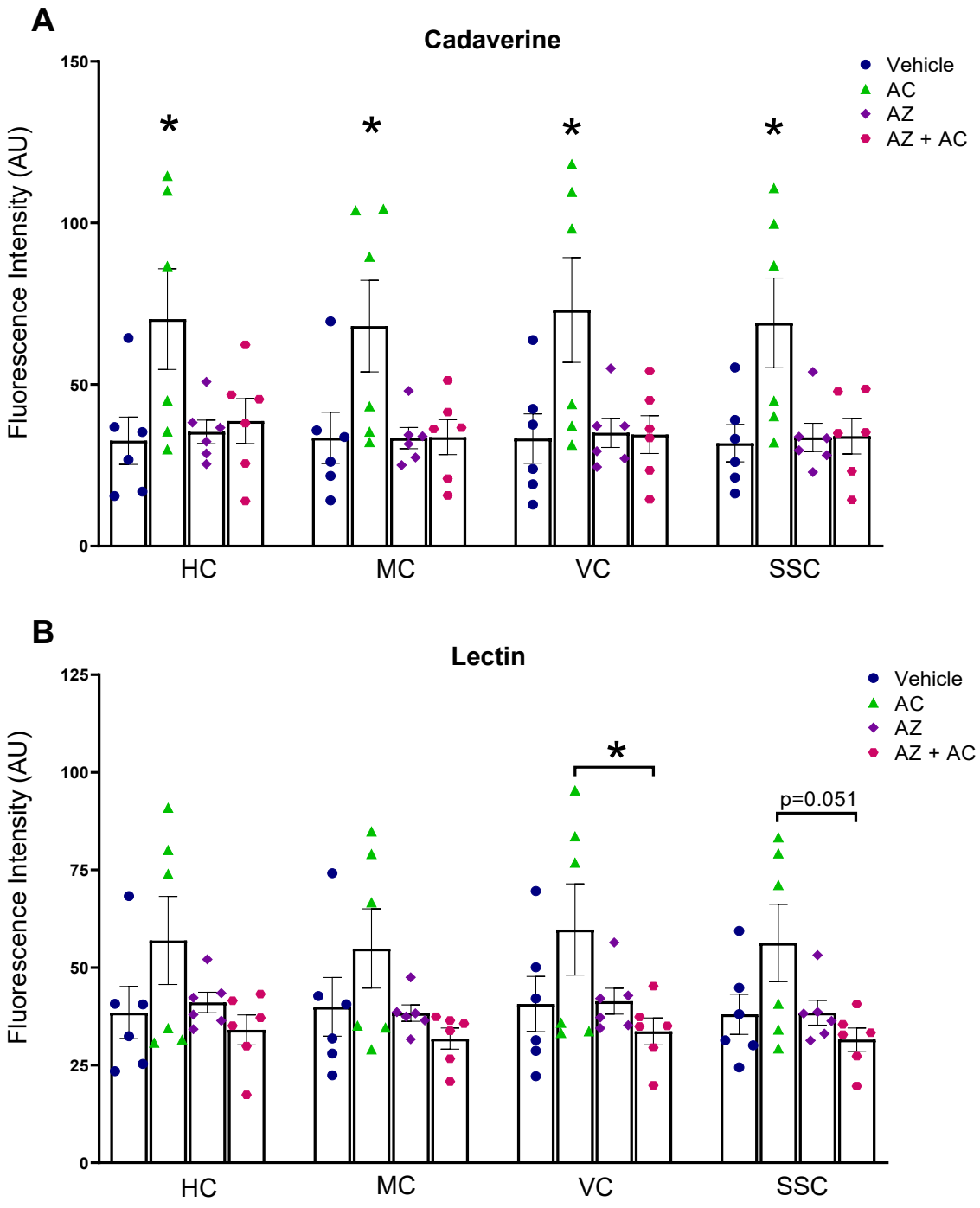

Figure 6.3: AC-injection increases cadaverine and lectin expression across brain regions. (A) Mesolens analysis demonstrated an increase in cadaverine fluorescence following AC-injection (*p<0.05 vs vehicle) in all examined brain regions. AZ-injection, and AZ + AC-injection had no effect on cadaverine fluorescence. (B) AC-injection significantly increased lectin expression in the VC and SSC (*p<0.05 vs AZ + AC) when compared to AZ + AC-injection. AZ alone, and AZ + AC–injection had no effect on lectin expression. Two-way repeated-measures ANOVA with Tukey's post hoc test (n= 6).

6.4. Confocal imaging reveals no increase in parenchymal cadaverine or vascular lectin in the CA1 following AC-injection.

6.4.1. AC-injection has no significant effect on cadaverine expression in the parenchyma.

Confocal imaging was also used to assess cadaverine extravasation into the parenchyma and lectin expression in the blood vessels. When parenchymal cadaverine fluorescence was examined (Fig.6.4A-D), no significant change was observed following AC-injection compared to vehicle (p=0.23 vs vehicle, n=5, Fig.6.5A).

Consistent with mesoscale imaging, AZ-injection alone had no effect on cadaverine fluorescence in the parenchyma compared to vehicle injection (p=0.71 vs vehicle, n=6, Fig.6.5A). Similarly, AZ-injection followed 1h later by AC-injection also did not alter parenchymal cadaverine fluorescence compared to vehicle (p=0.98 vs vehicle, n=6, Fig.6.5A).

No genotype differences were observed in cadaverine fluorescence in the parenchyma across any treatment groups ($F_{(1\text{-}15)}$ = 0.83, p=0.38 5xFAD$^{-/-}$, n=3 veh, AZ, AZ+AC, 2 AC and 5xFAD$^{+/-}$, n=3).

6.4.2. AC-injection has no significant effect on lectin expression in the blood vessels.

When lectin expression was examined in the vasculature in the CA1 (Fig.6.4E-H), AC-injection had no significant influence on lectin expression compared to vehicle (p=0.6 vs vehicle, n=5, Fig.6.5B).

In line with the mesoscale imaging, AZ-injection alone had no effect on lectin expression in the blood vessels (p=0.99 vs vehicle, n=6, Fig.6.5B). Similarly, AZ-injection followed 1h later by AC-injection also did not alter lectin expression compared to vehicle injection (p=0.68 vs vehicle, n=6, Fig.6.5B).

There was also no genotype differences found in vascular lectin expression across any treatment groups ($F_{(1-15)}$ = 1.82, p=0.2 5xFAD$^{-/-}$, n=3 veh, AZ, AZ+AC, 2 AC and 5xFAD$^{+/-}$, n=3).

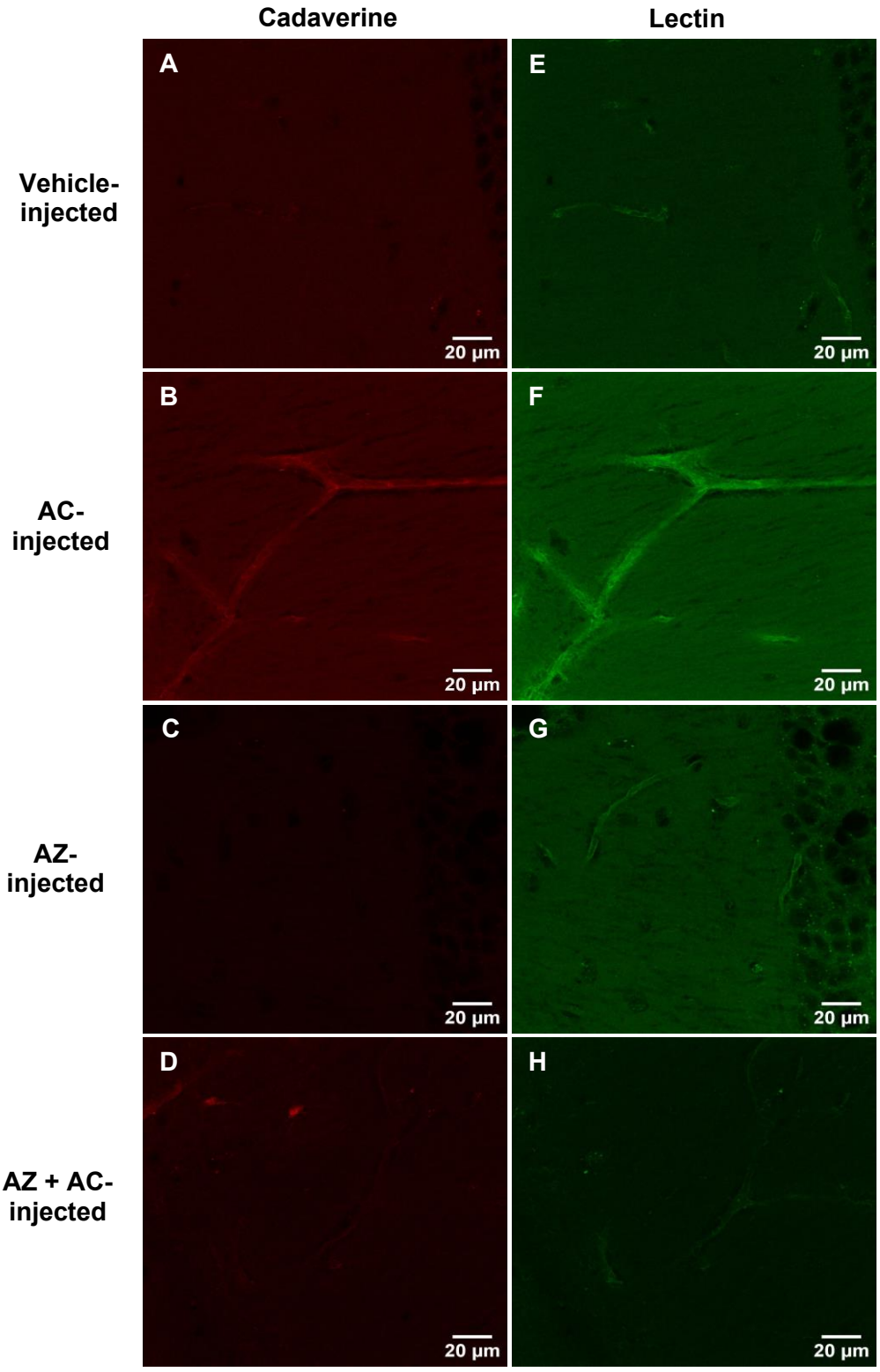

Figure 6.4: Representative confocal images of cadaverine and lectin expression in the hippocampal CA1 region. (A-D) Cadaverine expression in the parenchyma following vehicle, AC-injection, AZ-injection, and AZ + AC-injection. (E-H) Lectin expression in blood vessels following vehicle, AC-injection, AZ-injection, and AZ + AC-injection. Scale bar: 20 µm.

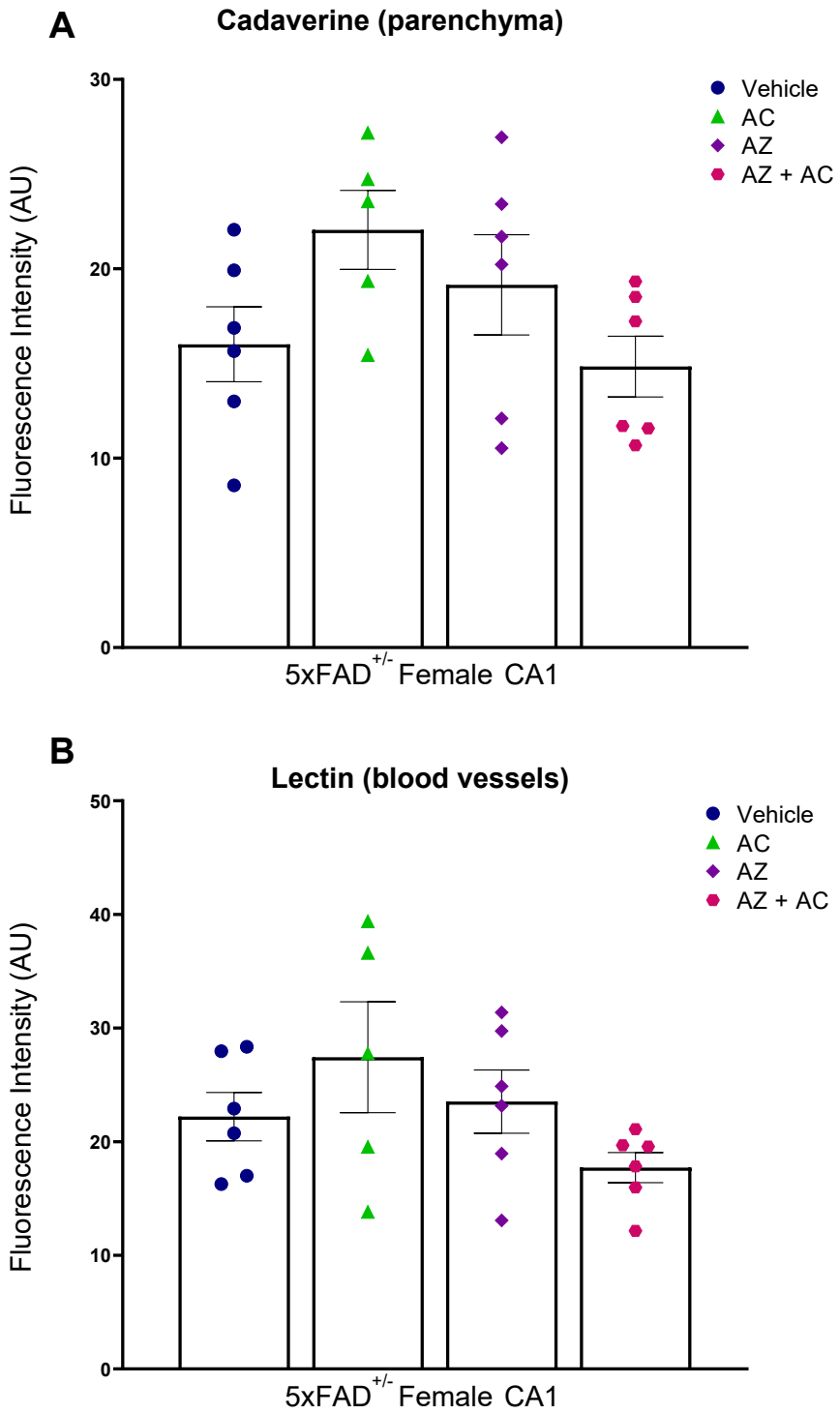

Figure 6.5: AC-injection did not significantly influence the expression of cadaverine in the parenchyma or lectin in the blood vessels in the CA1. (A) Confocal analysis of the CA1 found no significant effect of AC-injection on parenchymal cadaverine expression. AZ and AZ + AC also had no effect (B) AC-injection had no effect on lectin expression in CA1 blood vessels. AZ and AZ + AC did also not influence blood vessel lectin expression. One-way repeated-measures ANOVA with Tukey's post hoc test (n= 6 Vehicle, 5 AC, 6 AZ, 6 AZ + AC).

6.5. Discussion.

6.5.1. AZ8838 pre-treatment exacerbates AC264613-induced reductions in locomotor activity.

AZ is proposed to be a selective, competitive and potent PAR2 inhibitor, binding to the orthosteric site on the receptor to block PAR2 activation and inhibiting PAR2 downstream signalling pathways (Kennedy *et al.*, 2018). Hence, we expected AZ to inhibit PAR2 activation and competitively block AC binding, preventing or attenuating the AC-induced reductions in locomotor activity. Unpublished pharmacokinetics data within the research group, demonstrated AZ peaks at 1h post-injection, therefore, AZ was injected 1h prior to AC to ensure maximal inhibition of the receptor.

Interestingly, while AZ alone or AZ followed by vehicle injection had no effect on locomotor behaviour, AZ pre-treatment exacerbated AC-induced reduced locomotor activity, in contrary to our hypothesis that AZ would reduce AC's effects. We hypothesised that AZ may alter BBB permeability, thus allowing more AC to enter the brain, leading to enhanced reductions in locomotor activity. However, when BBB permeability was assessed using cadaverine and lectin, we found that AZ pre-treatment inhibited AC induced BBB leakage. These results suggest potential issues in functional selectivity of AZ or possible off-target interactions that alter neural activity and locomotor behaviour independently of BBB integrity.

Several PAR2 antagonists have reported complex signalling pathways. GB88, initially described as a selective antagonist that inhibits PAR2 $G_{q/11}/Ca^{2+}$/PKC signalling, was later found to exhibit partial agonist properties by activating

PAR2 cAMP, ERK and Rho thereby promoting PAR2 downstream signalling (Suen *et al.*, 2014; Lyu *et al.*, 2025). AZ may exhibit similar properties and while effectively inhibiting certain PAR2-mediated pathways, it may also act as a partial agonist in the presence of AC, thereby further enhancing PAR2 activation-induced effects on behaviour as observed in our study.

Another possibility is that AZ interacts with off-target receptors or pathways unrelated to PAR2. Like many GPCRs, PAR2 can activate multiple downstream signalling pathways, and while AZ is proposed to be selective, studies of other PAR2 antagonists have shown that pathway-specific inhibition or high concentrations can influence unrelated receptors or signalling pathways (Avet *et al.*, 2020; McIntosh *et al.*, 2020). Therefore, a combination of partial agonism, biased signalling or off-target activity may explain the unexpected enhancement of AC-induced behaviour effects following AZ pre-treatment.

6.5.2. PAR2 activation increases BBB permeability, whereas PAR2 inhibition preserves barrier integrity.

When we examined BBB integrity, we revealed, in contrast to our hypothesis, that PAR2 activation via AC-injection increased barrier permeability, whereas PAR2 inhibition with AZ alone, or AZ pre-treatment followed by AC, preserved barrier integrity. These findings suggest that PAR2 activation promotes barrier disruption, potentially through increased astrocytic reactivity and inflammatory responses, while PAR2 inhibition maintains endothelial stability.

The BBB is vital for maintaining homeostasis by tightly regulating the movement of ions, molecules and immune cells to the CNS (Profaci *et al.*, 2020). BBB dysfunction is a feature of many neurodegenerative diseases, including AD, where increased permeability allows peripheral inflammatory mediators and immune cells to enter the brain, thereby amplifying inflammatory responses and damage, contributing to disease progression (Nehra *et al.*, 2022). Astrocytes are crucial for BBB maintenance, providing trophic and structural support to endothelial cells, and increased astrocyte reactivity has been shown to increase BBB dysfunction and permeability (Argaw *et al.*, 2012; Kim *et al.*, 2022).

While we found AC-injection significantly reduced astrocytic GFAP and C3 expression in female 5xFAD$^{+/-}$ mice, these brains were examined 3 weeks post-mortem, by which time any initial neuroinflammatory or increased glial responses may have resolved or led to immunomodulatory responses. In contrast, the brains used in the BBB permeability experiments were fixed 2h post-injection, capturing potential acute effects of AC. PAR2 activation is known to trigger inflammatory signalling cascades in both glial and endothelial cells, including activation of NF-κB, MAPK, and calcium-dependent pathways within hours of activation, resulting in cytokine release and increased endothelial permeability (Zeng *et al.*, 2013; Bang *et al.*, 2021; Ushakumari *et al.*, 2022). Therefore, AC-induced PAR2 activation may have caused transient astrocyte activation and cytokine release, leading to disruption of the BBB, hence we observed an increase in cadaverine and lectin expression.

In contrast, AZ-injection appeared to inhibit PAR2 activation and downstream pro-inflammatory signalling, preventing BBB leakage. PAR2 inhibition has been shown to induce anti-inflammatory pathways, including reduced cytokine release and improved BBB integrity (Suen *et al.*, 2014; Ocak *et al.*, 2020). Interestingly, mice that received both AZ and AC did not exhibit BBB leakage, despite showing enhanced AC-induced reductions in locomotor activity. This dissociation, with preserved BBB integrity despite amplified behavioural effects, contrasts with our previous hypothesis that AZ induced BBB disruption leads to increased AC entering the brain thus inducing enhanced effects. Instead, the findings suggest that AZ may exert complex off-target effects or pathway-biased effects that alter neural activity and locomotor behaviour without directly affecting astrocytes and astrocytic mediated BBB regulation.

When confocal imaging was used to examine the brain sections, no significant increases in parenchymal cadaverine or vascular lectin expression were detected following AC-injection. However, this analysis was limited to the CA1 region of the hippocampus, whereas Mesolens imaging revealed widespread BBB alterations. It would therefore be of interest to assess BBB integrity using confocal microscopy in additional regions to better characterise the spatial profile of AC-induced permeability changes.

Across all treatment groups, we observed no differences between 5xFAD$^{-/-}$ and 5xFAD$^{+/-}$ mice in cadaverine or lectin expression. This suggests that, at the age of the mice used (12-18 weeks old), the neuroinflammation or amyloid pathology of the 5xFAD$^{+/-}$ model had not yet significantly impacted baseline BBB integrity. Disrupted BBB integrity has been reported in 5xFAD mice at 4–

6 months of age, with further deterioration observed with aging (Liu *et al.*, 2020; Bae *et al.*, 2024). Therefore, it is likely our mice were too young at the time of dosing to detect significant genotype differences.

It is important to note methodological considerations regarding the tracers used to assess BBB permeability and vasculature. Cadaverine, a small polar tracer is commonly used to detect BBB leakage, typically showing patchy or focal parenchymal distribution in cases of localised injury such as stroke or trauma (Boyé *et al.*, 2022; Munoz-Ballester *et al.*, 2022). However, in our study, cadaverine appeared relatively uniform across the brain following AC injection. Due to its small size, cadaverine can diffuse through the extracellular space where tight junctions are transiently compromised, and may reflect BBB disruption following AC injection, rather than focal leakage.

Similarly, lectin, used to label endothelial cells and visualise vasculature, did not clearly recapitulate the cerebrovascular architecture. Lectins bind glycoproteins on the endothelial surface, but staining intensity and pattern can be affected by perfusion efficiency, lectin binding issues, tissue sectioning, and imaging resolution (Battistella *et al.*, 2021). In our study, lectin primarily highlighted general vascular structures rather than detailed vessel networks, which may have limited interpretation of fine vascular changes following AC or AZ treatment.

Taken together, these observations highlight a limitation of using cadaverine and lectin to investigate BBB permeability. While both tracers provide useful insight into overall barrier changes, the tracers may not fully capture subtle or

region-specific leakage. Similar to the IHC data, cadaverine and lectin were quantified by fluorescence intensity which may not reflect absolute differences. Future studies would benefit from additional approaches, such as endogenous plasma protein extravasation with IgG or fibrinogen, radiolabelled tracers, or higher-resolution imaging methods, to provide more quantitative assessments of BBB and vascular integrity (Ryu *et al.*, 2009; Chung *et al.*, 2025).

6.5.3. Conclusion

From the work in this chapter, we conclude that the PAR2 inhibitor AZ alone does not influence behavioural changes in locomotor activity. However, when AC is administered in the presence of AZ, the AC-induced reduction in locomotor behaviour is further exacerbated. We also found that AC increases BBB permeability, whereas AZ maintains BBB integrity and effectively prevents AC-induced barrier leakage. Furthermore, we observed no differences in BBB integrity between 5xFAD$^{+/-}$ and 5xFAD$^{-/-}$ mice, suggesting that the mice used were too young to exhibit genotype-related BBB dysfunction. Our findings suggest that while AZ inhibits PAR2-mediated BBB disruption, its interaction with AC may produce unexpected or pathway-specific effects that enhance behavioural changes rather than attenuate them in the 5xFAD mouse model.

Chapter 7: General discussion

7.1. Summary of aims and results.

In this thesis, we aimed to assess the effects of PAR2 activation and LPS on behavioural, pathological, and molecular outcomes in a mouse model of amyloid pathology. We also investigated sex- and genotype-specific differences in both behaviour and pathology to further understand PAR2 and LPS immunomodulation in the 5xFAD mouse model. Additionally, we explored the effects of PAR2 inhibition on locomotor behaviour and blood brain barrier permeability to expand our understanding of PAR2 activators and antagonists *in vivo.*

The research in this thesis aimed to answer the following questions:

1. Does PAR2 activation and LPS induce depression-like behaviour in 5xFAD$^{-/-}$ and C57BL6/J wild-type controls?
2. Do 5xFAD$^{+/-}$ mice exhibit depression-like behaviour, and/or are 5xFAD$^{+/-}$ mice more susceptible to pharmacologically-induced depression-like behaviour compared to 5xFAD$^{-/-}$ littermate controls?
3. Does double-dose intervention or multi-dose intervention of pharmacologically induced depression-like behaviour exacerbate behavioural, inflammatory, and molecular pathology in 5xFAD$^{+/-}$ mice?
4. Does PAR2 inhibition affect the blood brain barrier integrity and influence behaviour and pathological changes following pharmacologically-induced depression-like behaviour in 5xFAD mice.

Overall, our results revealed that PAR2 activation via AC264613 and LPS induced behavioural changes associated with depression-like behaviour in

5xFAD$^{-/-}$ and C57BL6/J mice, with no significant sex or genotypic differences. At 3 months of age, 5xFAD$^{+/-}$ mice did not inherently exhibit depression-like behaviour but appear more susceptible to pharmacologically-induced depression-like behaviour, independent of sex. We also revealed that behavioural changes associated with depression-like behaviour can be exacerbated by stress-inducing environments. Additionally, AC264613 and LPS, administered either as two or four-injections, do not cause any lasting alterations to locomotor behaviour or general health in the 5xFAD model.

AC264613 and LPS induced transient immunomodulatory effects, reducing astrocyte reactivity and Aβ pathology at 3 weeks post-injection in 5xFAD$^{+/-}$ mice in a sex-specific manner. However, these effects appeared to be sensitive to environmental stress. Multiple dosing with AC264613 or LPS may have caused receptor desensitisation or signalling saturation, limiting their pharmacological effects on pathology. Both, AC264613 and LPS can induce pro- and anti-inflammatory peripheral cytokine changes, some of which correlate with MDD. However, AC264613 had minimal effects on cytokine levels in 5xFAD$^{+/-}$ mice suggesting peripheral cytokines do not contribute to the observed behavioural changes.

Finally, PAR2 inhibition via AZ8838 alone did not affect locomotor behaviour. However, in the presence of AZ8838, AC264613-induced reductions in locomotor activity were further exacerbated. Additionally, AC264613 increases blood brain barrier permeability, whereas AZ8838 preserves barrier integrity and prevents AC264613-induced disruption, independent of genotype.

7.2. Clinical relevance

Alzheimer's disease represents a major global health burden, with prevalence continuing to rise and current treatment options offering only limited efficacy (Zhang, Zhang, *et al.*, 2024). The development of novel therapeutic strategies and identification of new molecular targets remain critical for achieving effective disease-modifying interventions. Although most approaches have focused on targeting Aβ pathology (Cummings *et al.*, 2025), growing evidence highlights the important role of neuroinflammation in AD and other neurodegenerative diseases, offering it as a promising new avenue for therapeutic strategies (Lee and Chang, 2025).

PAR2 has been implicated in multiple inflammatory conditions (Reches *et al.*, 2024). In the present study we have built upon previous work in that PAR2 activation induces depression-like behavioural changes (Abulkassim *et al.*, 2016; Moudio *et al.*, 2022) but may also offer neuroprotective immunomodulatory properties *in vivo* that could be utilised in neurodegenerative research. We also observed that PAR2 activation influences BBB integrity, an effect that could be critical for understanding how inflammatory signalling impacts brain homeostasis and how therapeutics can be effectively delivered to the CNS. Further investigation into how the PAR2 activator AC264613 modulates glial cell activity, inflammatory pathways and BBB function would provide valuable mechanistic insight and may inform the development of targeted interventions for neurodegenerative diseases.

Lastly, major depressive disorder is the leading cause of disability worldwide, with treatment resistant depression affecting up to half of all cases (McIntyre

et al., 2023). As a recognised risk factor for AD, as well as other conditions (Berk *et al.*, 2023), identifying new molecular pathways could offer significant translational value. Our findings that PAR2 activation induces depression-like behavioural changes contribute to a deeper understanding of PAR2 function in neuropsychiatric disorders. Consequently, PAR2 inhibition could represent a potential therapeutic approach for alleviating depression-like behaviours and reducing associated neurodegenerative risk.

7.3. Limitations

The limitations of this study have been discussed throughout each results chapter, with the most significant being the major construction that took place in the animal facility during the study period. Although the effects of this stress-inducing environment were not initially apparent, subsequent analysis of behavioural and pathological data from the 10-week and multiple-injection cohorts revealed that environment had likely influenced previous results thereby limiting the interpretability and impact of these results. We believe that the excessive noise, vibrations from equipment and frequent room changes, contributed to elevated stress levels in the mice tested under these conditions, resulting in increased locomotor activity as well as altered sucrose preference and grooming behaviour. We also believe that environmental stress exacerbated amyloid plaque deposition and increased neuroinflammatory responses. In contrast, when mice were tested under calmer and quieter conditions, behavioural and pathological changes in response to PAR2 activation and LPS were markedly reduced or absent. Future studies should be conducted under tightly controlled environmental conditions, ideally

replicating key findings in stable housing facilities to ensure that behavioural and neuropathological outcomes reflect true pharmacological effects rather than environmental confounds.

Another limitation of this study was the poor quality of the brain tissue used to analyse phagocytosis in the 5xFAD$^{-/-}$ vs 5xFAD$^{+/-}$ 3-week post-injection mice. Due to inappropriate and prolonged storage, the tissue integrity was compromised, therefore potential mechanistic experiments were limited. Although these issues were rectified for the 10-week and multi-injection cohorts, they limit the reliability of the phagocytosis results from the 3-week cohort, particularly where AC and LPS appeared to influence pathology. Future studies should ensure that tissue processing and IHC are planned carefully to maintain high sample quality and reproducibility of histological data. In addition, IHC analyses relied primarily on fluorescence intensity as a quantitative measure, which can be influenced by technical factors and may not always reflect absolute differences. The absence of negative controls further limited interpretation of IHC interpretation between staining batches. Future studies should therefore include appropriate controls and potential complementary quantitative approaches such as cell burden and density. Furthermore, this study only investigated a single method of phagocytosis, limiting exploration of alternative mechanisms of Aβ plaque clearance. Future research should investigate additional pathways and assays to better understand the mechanisms underlying reduced astrocyte reactivity and Aβ burden.

Based on the results from the 3-week post-injection cohort, where drug-induced effects were observed exclusively in females, only female 5xFAD$^{+/-}$ mice were included in the 10 week-post injection cohort. However, disease pathology is known to progress more rapidly in female 5xFAD$^{+/-}$ mice than in males, meaning females are typically at a more advanced disease stage at the same age and may respond earlier to immunomodulatory interventions. Including male 5xFAD$^{+/-}$ mice could have provided valuable insight into whether drug-induced effects appear later in disease progression, as males generally develop pathology more slowly and may require a longer timeframe to exhibit comparable responses. Future studies should therefore include both sexes to provide more comprehensive and robust data.

The study utilised cadaverine and lectin tracers to examine BBB permeability and vascular structure. However, cadaverine distribution appeared relatively uniform rather than region-specific, and lectin staining did not clearly recapitulate cerebrovascular architecture, likely due to technical factors. While these tracers provide insight into overall barrier changes, they may not capture subtle or region-specific leakage. Future studies should consider alternative techniques such as endogenous plasma protein extravasation including IgG or fibrinogen, radiolabelled tracers, or higher-resolution imaging to better explore BBB integrity following PAR2 activation an inhibition.

Finally, while the experimental design and sample sizes allowed detection of main effects, the statistical analyses were limited by the use of two-way repeated-measures ANOVA. This approach assumes normality, homogeneity of variance, and sphericity, which may be less robust in complex designs

involving multiple variables such as treatment, genotype, and sex. Additionally, multiple comparisons were conducted across behaviours, sexes, genotypes, and treatment groups, which increases the risk of false-positive results. Consequently, some effects may be over- or under-represented. Future studies could employ linear mixed-effects models to better account for repeated measures and interactions between variables, improving the robustness and interpretability of statistical outcomes.

7.4. Future directions

This study builds upon previous investigations into the potential neuroprotective properties of PAR2 activation (Greenwood *et al.*, 2010) and advances our understanding of its role in amyloid pathology and neuroinflammation *in vivo*. Although we demonstrated clear behavioural and pathological outcomes following PAR2 activation, these findings would benefit from mechanistic studies to determine how AC264613 alters glial activation, as well as downstream inflammatory pathways, and the broader neuroimmune environment.

While the present work focused on early pathological and behavioural changes, future studies should investigate whether PAR2 activation also influences cognitive outcomes, as reducing or slowing cognitive decline remains a fundamental goal in AD therapeutics. Although amyloid pathology is often considered the initiating event in AD, tau pathology is more directly associated with cognitive decline (Zhang *et al.*, 2023). Therefore, it would also be valuable to determine whether PAR2 activation affects tau phosphorylation,

aggregation, or propagation, thereby providing deeper insight into how PAR2 signalling might influence cognitive function and disease progression.

Future studies should also aim to replicate key findings under tightly controlled environmental conditions to eliminate confounding effects of external stressors on behaviour and pathology. Furthermore, it would be informative to assess whether earlier intervention with PAR2 modulation provides greater neuroprotective benefit, particularly when applied prior to substantial amyloid deposition. Similarly, using a less aggressive or more slowly progressing model of AD could allow for a clearer assessment of long-term effects and potential therapeutic windows for PAR2 targeted interventions.

Finally, exploring the relationship between the PAR2 agonist AC264613 and the antagonist AZ8838 may clarify how receptor activation and inhibition differentially modulate neuroinflammation, BBB integrity, and behavioural outcomes. Given that PAR2 activation induced depression-like behavioural changes in this study, evaluating whether PAR2 inhibition could prevent or reverse existing depression-like behaviours represents an interesting area of investigation with potential relevance to both neuropsychiatric and neurodegenerative disorders.

References

Abulkassim, R. *et al.* (2016) “Proteinase-activated receptor 2 is involved in the behavioural changes associated with sickness behaviour,” *Journal of Neuroimmunology*, 295–296, pp. 139–147. Available at: https://doi.org/10.1016/j.jneuroim.2016.04.016.

Afkhami-Goli, A. *et al.* (2007) “Proteinase-activated receptor-2 exerts protective and pathogenic cell type-specific effects in Alzheimer’s disease.,” *Journal of immunology (Baltimore, Md. : 1950)*, 179(8), pp. 5493–5503. Available at: https://doi.org/10.4049/jimmunol.179.8.5493.

Ahangari, N. *et al.* (2023) “Cognitive resilience and severe Alzheimer’s disease neuropathology.,” *Aging brain*, 3, p. 100065. Available at: https://doi.org/10.1016/j.nbas.2023.100065.

Aizenstein, H.J. *et al.* (2008) “Frequent amyloid deposition without significant cognitive impairment among the elderly.,” *Archives of neurology*, 65(11), pp. 1509–1517. Available at: https://doi.org/10.1001/archneur.65.11.1509.

Alberelli, M.A. and De Candia, E. (2014) “Functional role of protease activated receptors in vascular biology,” *Vascular Pharmacology*, 62(2), pp. 72–81. Available at: https://doi.org/10.1016/j.vph.2014.06.001.

AlDawsari, A. *et al.* (2022) “Use of sedative-hypnotic medications and risk of dementia: A systematic review and meta-analysis,” *British Journal of Clinical Pharmacology*, 88(4), pp. 1567–1589. Available at: https://doi.org/10.1111/bcp.15113.

Allen Institution of Brain Sciences (2004) *Allen Institute for Brain Science: Allen Mouse Brain Atlas*. Available at: https://atlas.brain-map.org/atlas?atlas=2#atlas=2&plate=100884070&structure=502&x=6336.80029296875&y=3916.799997329712&zoom=-4&resolution=16.75&z=5.

Alonso, A.D. *et al.* (2018) “Hyperphosphorylation of Tau Associates With Changes in Its Function Beyond Microtubule Stability.,” *Frontiers in cellular neuroscience*, 12, p. 338. Available at: https://doi.org/10.3389/fncel.2018.00338.

Alzheimer’s Society (2024) *Facts for the media about dementia Alzheimer’s Society*. Available at: https://www.alzheimers.org.uk/about-us/news-and-media/facts-media.

Alzheimer, A. (1906) “Uber einen eigenartigen schweren Er Krankungsprozeb der Hirnrinde.,” *Neurologisches Centralblatt*, 23, pp. 1129–1136.

Alzheimer, A. *et al.* (1995) “An English translation of Alzheimer’s 1907 paper, ‘Uber eine eigenartige Erkankung der Hirnrinde’.,” *Clinical anatomy (New York, N.Y.)*, 8(6), pp. 429–31. Available at: https://doi.org/10.1002/ca.980080612.

Amare, A.T. *et al.* (2020) “Bivariate genome-wide association analyses of the broad depression phenotype combined with major depressive disorder, bipolar disorder or schizophrenia reveal eight novel genetic loci for depression,” *Molecular Psychiatry*, 25(7), pp. 1420–1429. Available at: https://doi.org/10.1038/s41380-018-0336-6.

Amidfar, M. *et al.* (2019) “The role of NMDA receptor in neurobiology and treatment of major depressive disorder: Evidence from translational research,” *Progress in Neuro-Psychopharmacology and Biological Psychiatry*, 94, p. 109668. Available at: https://doi.org/10.1016/j.pnpbp.2019.109668.

Argaw, A.T. *et al.* (2012) “Astrocyte-derived VEGF-A drives blood-brain barrier disruption in CNS inflammatory disease.,” *The Journal of clinical investigation*, 122(7), pp. 2454–2468. Available at: https://doi.org/10.1172/JCI60842.

Atrooz, F., Alkadhi, K.A. and Salim, S. (2021) “Understanding stress: Insights from rodent

models.," *Current research in neurobiology*, 2, p. 100013. Available at: https://doi.org/10.1016/j.crneur.2021.100013.

Avet, C. *et al.* (2020) "The PAR2 inhibitor I-287 selectively targets Gαq and Gα12/13 signaling and has anti-inflammatory effects," *Communications Biology*, 3(1), p. 719. Available at: https://doi.org/10.1038/s42003-020-01453-8.

Bae, J. *et al.* (2024) "Feasibility of measuring blood-brain barrier permeability using ultra-short echo time radial magnetic resonance imaging.," *Journal of neuroimaging : official journal of the American Society of Neuroimaging*, 34(3), pp. 320–328. Available at: https://doi.org/10.1111/jon.13199.

Bains, N. and Abdijadid, S. (2023) *Major Depressive Disorder*, *StatPearls*. Available at: http://www.ncbi.nlm.nih.gov/pubmed/30396512.

Baldwin, K.T., Murai, K.K. and Khakh, B.S. (2024) "Astrocyte morphology.," *Trends in cell biology*, 34(7), pp. 547–565. Available at: https://doi.org/10.1016/j.tcb.2023.09.006.

Balogun, W.G. *et al.* (2023) "Plasma biomarkers for neurodegenerative disorders: ready for prime time?," *Current opinion in psychiatry*, 36(2), pp. 112–118. Available at: https://doi.org/10.1097/YCO.0000000000000851.

Bang, E., Kim, D.H. and Chung, H.Y. (2021) "Protease-activated receptor 2 induces ROS-mediated inflammation through Akt-mediated NF-κB and FoxO6 modulation during skin photoaging.," *Redox biology*, 44, p. 102022. Available at: https://doi.org/10.1016/j.redox.2021.102022.

Bangasser, D.A. and Cuarenta, A. (2021) "Sex differences in anxiety and depression: circuits and mechanisms," *Nature Reviews Neuroscience*, 22(11), pp. 674–684. Available at: https://doi.org/10.1038/s41583-021-00513-0.

Barnes, C.A. (1979) "Memory deficits associated with senescence: A neurophysiological and behavioral study in the rat.," *Journal of Comparative and Physiological Psychology*, 93(1), pp. 74–104. Available at: https://doi.org/10.1037/h0077579.

Bartels, C. *et al.* (2018) "Impact of SSRI Therapy on Risk of Conversion From Mild Cognitive Impairment to Alzheimer's Dementia in Individuals With Previous Depression.," *The American journal of psychiatry*, 175(3), pp. 232–241. Available at: https://doi.org/10.1176/appi.ajp.2017.17040404.

Bateman, R.J. *et al.* (2012) "Clinical and biomarker changes in dominantly inherited Alzheimer's disease.," *The New England journal of medicine*, 367(9), pp. 795–804. Available at: https://doi.org/10.1056/NEJMoa1202753.

Batista, C.R. *et al.* (2019) "Lipopolysaccharide-Induced Neuroinflammation as a Bridge to Understand Neurodegeneration," *International Journal of Molecular Sciences*, p. 2293. Available at: https://doi.org/10.3390/ijms20092293.

Batiuk, M.Y. *et al.* (2020) "Identification of region-specific astrocyte subtypes at single cell resolution," *Nature Communications*, 11(1), p. 1220. Available at: https://doi.org/10.1038/s41467-019-14198-8.

Battistella, R. *et al.* (2021) "Not All Lectins Are Equally Suitable for Labeling Rodent Vasculature," *International Journal of Molecular Sciences*, p. 11554. Available at: https://doi.org/10.3390/ijms222111554.

Bay-Richter, C. and Wegener, G. (2022) "Antidepressant Effects of NSAIDs in Rodent Models of Depression—A Systematic Review," *Frontiers in Pharmacology*, 13. Available at: https://doi.org/10.3389/fphar.2022.909981.

Becker, M., Pinhasov, A. and Ornoy, A. (2021) "Animal Models of Depression: What Can They Teach Us about the Human Disease?," *Diagnostics*, 11(1), p. 123. Available at:

https://doi.org/10.3390/diagnostics11010123.

Bekhbat, M. and Neigh, G.N. (2018) “Sex differences in the neuro-immune consequences of stress: Focus on depression and anxiety.,” *Brain, behavior, and immunity*, 67, pp. 1–12. Available at: https://doi.org/10.1016/j.bbi.2017.02.006.

Belessiotis-Richards, C. *et al.* (2025) “Systemic medications and dementia risk: a systematic umbrella review,” *Molecular Psychiatry*, 30(11), pp. 5578–5599. Available at: https://doi.org/10.1038/s41380-025-03129-3.

Belzung, C. and Lemoine, M. (2011) “Criteria of validity for animal models of psychiatric disorders: focus on anxiety disorders and depression.,” *Biology of mood & anxiety disorders*, 1(1), p. 9. Available at: https://doi.org/10.1186/2045-5380-1-9.

Berk, M. *et al.* (2013) “So depression is an inflammatory disease, but where does the inflammation come from?,” *BMC Medicine*, 11(1), p. 200. Available at: https://doi.org/10.1186/1741-7015-11-200.

Berk, M. *et al.* (2023) “Comorbidity between major depressive disorder and physical diseases: a comprehensive review of epidemiology, mechanisms and management.,” *World psychiatry : official journal of the World Psychiatric Association (WPA)*, 22(3), pp. 366–387. Available at: https://doi.org/10.1002/wps.21110.

Berrio, J.P., Hestehave, S. and Kalliokoski, O. (2024) “Reliability of sucrose preference testing following short or no food and water deprivation—a Systematic Review and Meta-Analysis of rat models of chronic unpredictable stress,” *Translational Psychiatry*, 14(1), p. 39. Available at: https://doi.org/10.1038/s41398-024-02742-0.

Berrio, J.P. and Kalliokoski, O. (2023) “Rethinking data treatment: The sucrose preference threshold for anhedonia in stress-induced rat models of depression,” *Journal of Neuroscience Methods*, 395, p. 109910. Available at: https://doi.org/https://doi.org/10.1016/j.jneumeth.2023.109910.

Beshir, S.A. *et al.* (2022) “Aducanumab Therapy to Treat Alzheimer’s Disease: A Narrative Review,” *International Journal of Alzheimer’s Disease*. Edited by giulia abate, 2022, pp. 1–10. Available at: https://doi.org/10.1155/2022/9343514.

Beurel, E., Toups, M. and Nemeroff, C.B. (2020) “The Bidirectional Relationship of Depression and Inflammation: Double Trouble,” *Neuron*, 107(2), pp. 234–256. Available at: https://doi.org/https://doi.org/10.1016/j.neuron.2020.06.002.

Bhol, N.K. *et al.* (2024) “The interplay between cytokines, inflammation, and antioxidants: mechanistic insights and therapeutic potentials of various antioxidants and anti-cytokine compounds,” *Biomedicine & Pharmacotherapy*, 178, p. 117177. Available at: https://doi.org/https://doi.org/10.1016/j.biopha.2024.117177.

Biesmans, S. *et al.* (2013) “Systemic immune activation leads to neuroinflammation and sickness behavior in mice.,” *Mediators of inflammation*, 2013, p. 271359. Available at: https://doi.org/10.1155/2013/271359.

Biesmans, S. *et al.* (2015) “Effect of stress and peripheral immune activation on astrocyte activation in transgenic bioluminescent Gfap-luc mice.,” *Glia*, 63(7), pp. 1126–1137. Available at: https://doi.org/10.1002/glia.22804.

Biesmans, S. *et al.* (2016) “Systematic Analysis of the Cytokine and Anhedonia Response to Peripheral Lipopolysaccharide Administration in Rats.,” *BioMed research international*, 2016, p. 9085273. Available at: https://doi.org/10.1155/2016/9085273.

Birrell, J.M. and Brown, V.J. (2000) “Medial Frontal Cortex Mediates Perceptual Attentional Set Shifting in the Rat,” *The Journal of Neuroscience*, 20(11), pp. 4320–4324. Available at: https://doi.org/10.1523/JNEUROSCI.20-11-04320.2000.

Bortolanza, M. *et al.* (2025) “Sex-Specific Properties of Astrocytes: From Development to Evolutionary Insights.,” *Neurochemical research*, 50(4), p. 267. Available at: https://doi.org/10.1007/s11064-025-04512-w.

Bouguiyoud, N. *et al.* (2022) “Anxiety and Depression Assessments in a Mouse Model of Congenital Blindness,” *Frontiers in Neuroscience*, Volume 15. Available at: https://doi.org/10.3389/fnins.2021.807434.

Boulle, F. *et al.* (2014) “Hippocampal and behavioral dysfunctions in a mouse model of environmental stress: normalization by agomelatine,” *Translational Psychiatry*, 4(11), pp. e485–e485. Available at: https://doi.org/10.1038/tp.2014.125.

Bowman, R., Frankfurt, M. and Luine, V. (2025) “Sex differences in anxiety and depression: insights from adult rodent models of chronic stress and neural plasticity.,” *Frontiers in behavioral neuroscience*, 19, p. 1591973. Available at: https://doi.org/10.3389/fnbeh.2025.1591973.

Boyce-Rustay, J.M. and Holmes, A. (2006) “Genetic Inactivation of the NMDA Receptor NR2A Subunit has Anxiolytic- and Antidepressant-Like Effects in Mice,” *Neuropsychopharmacology*, 31(11), pp. 2405–2414. Available at: https://doi.org/10.1038/sj.npp.1301039.

Boyé, K. *et al.* (2022) “Endothelial Unc5B controls blood-brain barrier integrity.,” *Nature communications*, 13(1), p. 1169. Available at: https://doi.org/10.1038/s41467-022-28785-9.

Braak, H. and Braak, E. (1991) “Neuropathological stageing of Alzheimer-related changes.,” *Acta neuropathologica*, 82(4), pp. 239–59. Available at: https://doi.org/10.1007/BF00308809.

Braak, H. and Braak, E. (1995) “Staging of alzheimer’s disease-related neurofibrillary changes,” *Neurobiology of Aging*, 16(3), pp. 271–278. Available at: https://doi.org/https://doi.org/10.1016/0197-4580(95)00021-6.

Braak, H. and Del Tredici, K. (2011) “The pathological process underlying Alzheimer’s disease in individuals under thirty.,” *Acta neuropathologica*, 121(2), pp. 171–81. Available at: https://doi.org/10.1007/s00401-010-0789-4.

Bravo-Ferrer, I. *et al.* (2025) “Multiregional blood-brain barrier phenotyping identifies the prefrontal cortex as the most vulnerable region to ageing in mice,” *Brain Communications*, 7(5), p. fcaf332. Available at: https://doi.org/10.1093/braincomms/fcaf332.

Brendel, M. *et al.* (2015) “Depressive symptoms accelerate cognitive decline in amyloid-positive MCI patients,” *European Journal of Nuclear Medicine and Molecular Imaging*, 42(5), pp. 716–724. Available at: https://doi.org/10.1007/s00259-014-2975-4.

Bühm, S.K. *et al.* (1996) “Mechanisms of Desensitization and Resensitization of Proteinase-activated Receptor-2*,” *Journal of Biological Chemistry*, 271(36), pp. 22003–22016. Available at: https://doi.org/https://doi.org/10.1074/jbc.271.36.22003.

Burton, A.L. and Abbott, M.J. (2019) “Processes and pathways to binge eating: development of an integrated cognitive and behavioural model of binge eating,” *Journal of Eating Disorders*, 7(1), p. 18. Available at: https://doi.org/10.1186/s40337-019-0248-0.

Bushell, T. (2007) “The emergence of proteinase-activated receptor-2 as a novel target for the treatment of inflammation-related CNS disorders,” *The Journal of Physiology*, 581(1), pp. 7–16. Available at: https://doi.org/10.1113/jphysiol.2007.129577.

Bushell, T.J. *et al.* (2006) “Characterization of proteinase-activated receptor 2 signalling and expression in rat hippocampal neurons and astrocytes,” *Neuropharmacology*, 50(6), pp. 714–725. Available at: https://doi.org/10.1016/j.neuropharm.2005.11.024.

Cabezas, R. *et al.* (2014) “Astrocytic modulation of blood brain barrier: perspectives on Parkinson’s disease.,” *Frontiers in cellular neuroscience*, 8, p. 211. Available at:

https://doi.org/10.3389/fncel.2014.00211.

Campbell, S.N. *et al.* (2015) “Increased tau phosphorylation and aggregation in the hippocampus of mice overexpressing corticotropin-releasing factor.,” *Journal of Alzheimer’s disease : JAD*, 43(3), pp. 967–76. Available at: https://doi.org/10.3233/JAD-141281.

Canet, G. *et al.* (2019) “Is AD a Stress-Related Disorder? Focus on the HPA Axis and Its Promising Therapeutic Targets.,” *Frontiers in aging neuroscience*, 11, p. 269. Available at: https://doi.org/10.3389/fnagi.2019.00269.

Carli, M. *et al.* (1983) “Effects of lesions to ascending noradrenergic neurones on performance of a 5-choice serial reaction task in rats; implications for theories of dorsal noradrenergic bundle function based on selective attention and arousal,” *Behavioural Brain Research*, 9(3), pp. 361–380. Available at: https://doi.org/10.1016/0166-4328(83)90138-9.

Carregosa, D. *et al.* (2024) “Locomotor and gait changes in the LPS model of neuroinflammation are correlated with inflammatory cytokines in blood and brain.,” *Journal of inflammation (London, England)*, 21(1), p. 39. Available at: https://doi.org/10.1186/s12950-024-00412-y.

Cartwright, C. *et al.* (2016) “Long-term antidepressant use: patient perspectives of benefits and adverse effects.,” *Patient preference and adherence*, 10, pp. 1401–1407. Available at: https://doi.org/10.2147/PPA.S110632.

Cassano, T. *et al.* (2019) “Pharmacological Treatment of Depression in Alzheimer’s Disease: A Challenging Task,” *Frontiers in Pharmacology*, 10. Available at: https://doi.org/10.3389/fphar.2019.01067.

Cathomas, F. *et al.* (2015) “The translational study of apathy—an ecological approach,” *Frontiers in Behavioral Neuroscience*, 9. Available at: https://doi.org/10.3389/fnbeh.2015.00241.

Ceyzériat, K. *et al.* (2018) “Modulation of astrocyte reactivity improves functional deficits in mouse models of Alzheimer’s disease.,” *Acta neuropathologica communications*, 6(1), p. 104. Available at: https://doi.org/10.1186/s40478-018-0606-1.

Chai, H.-H. *et al.* (2019) “The chemokine CXCL1 and its receptor CXCR2 contribute to chronic stress-induced depression in mice,” *The FASEB Journal*, 33(8), pp. 8853–8864. Available at: https://doi.org/https://doi.org/10.1096/fj.201802359RR.

Chakrabarti, M. *et al.* (2014) “Estrogen receptor agonists for attenuation of neuroinflammation and neurodegeneration,” *Brain Research Bulletin*, 109, pp. 22–31. Available at: https://doi.org/https://doi.org/10.1016/j.brainresbull.2014.09.004.

Chartier-Harlin, M.-C. *et al.* (1991) “Early-onset Alzheimer’s disease caused by mutations at codon 717 of the β-amyloid precursor protein gene,” *Nature*, 353(6347), pp. 844–846. Available at: https://doi.org/10.1038/353844a0.

Chatterjee, P. *et al.* (2023) “Plasma Aβ42/40 ratio, p-tau181, GFAP, and NfL across the Alzheimer’s disease continuum: A cross-sectional and longitudinal study in the AIBL cohort,” *Alzheimer’s & Dementia*, 19(4), pp. 1117–1134. Available at: https://doi.org/10.1002/alz.12724.

Chen, C. *et al.* (2012) “Transient early neurotrophin release and delayed inflammatory cytokine release by microglia in response to PAR-2 stimulation,” *Journal of Neuroinflammation*, 9(1), p. 142. Available at: https://doi.org/10.1186/1742-2094-9-142.

Chen, G.F. *et al.* (2017) “Amyloid beta: Structure, biology and structure-based therapeutic development,” *Acta Pharmacologica Sinica*, 38(9), pp. 1205–1235. Available at: https://doi.org/10.1038/aps.2017.28.

Chen, J. *et al.* (2025) “Refining the interactions between microglia and astrocytes in

Alzheimer's disease pathology," *Neuroscience*, 573, pp. 183–197. Available at: https://doi.org/https://doi.org/10.1016/j.neuroscience.2025.03.033.

Chen, Y. *et al.* (2023) "Blood-brain barrier dysfunction and Alzheimer's disease: associations, pathogenic mechanisms, and therapeutic potential," *Frontiers in Aging Neuroscience*, Volume 15. Available at: https://doi.org/10.3389/fnagi.2023.1258640.

Chen, Z. *et al.* (2024) "Roles of Cytokines in Alzheimer's Disease.," *International journal of molecular sciences*, 25(11). Available at: https://doi.org/10.3390/ijms25115803.

Cheng, R.K.Y. *et al.* (2017) "Structural insight into allosteric modulation of protease-activated receptor 2," *Nature*, 545(7652), pp. 112–115. Available at: https://doi.org/10.1038/nature22309.

Chistyakov, D. V *et al.* (2019) "Cellular Model of Endotoxin Tolerance in Astrocytes: Role of Interleukin 10 and Oxylipins.," *Cells*, 8(12). Available at: https://doi.org/10.3390/cells8121553.

Chung, K.J. *et al.* (2025) "Quantitative PET imaging and modeling of molecular blood-brain barrier permeability," *Nature Communications*, 16(1), p. 3076. Available at: https://doi.org/10.1038/s41467-025-58356-7.

Cisternas, P. *et al.* (2022) "The reduction of astrocytic tau prevents amyloid-β-induced synaptotoxicity," *Brain Communications*, 4(5), p. fcac235. Available at: https://doi.org/10.1093/braincomms/fcac235.

Colla, M. *et al.* (2007) "Hippocampal volume reduction and HPA-system activity in major depression," *Journal of Psychiatric Research*, 41(7), pp. 553–560. Available at: https://doi.org/10.1016/j.jpsychires.2006.06.011.

Colom-Cadena, M. *et al.* (2020) "The clinical promise of biomarkers of synapse damage or loss in Alzheimer's disease," *Alzheimer's Research & Therapy*, 12(1), p. 21. Available at: https://doi.org/10.1186/s13195-020-00588-4.

Colonna, M. and Butovsky, O. (2017) "Microglia Function in the Central Nervous System During Health and Neurodegeneration.," *Annual review of immunology*, 35, pp. 441–468. Available at: https://doi.org/10.1146/annurev-immunol-051116-052358.

Corder, E.H. *et al.* (1993) "Gene dose of apolipoprotein E type 4 allele and the risk of Alzheimer's disease in late onset families.," *Science (New York, N.Y.)*, 261(5123), pp. 921–923. Available at: https://doi.org/10.1126/science.8346443.

Cornell, J. *et al.* (2022) "Microglia regulation of synaptic plasticity and learning and memory.," *Neural regeneration research*, 17(4), pp. 705–716. Available at: https://doi.org/10.4103/1673-5374.322423.

Costello, H., Roiser, J.P. and Howard, R. (2023) "Antidepressant medications in dementia: evidence and potential mechanisms of treatment-resistance.," *Psychological medicine*, 53(3), pp. 654–667. Available at: https://doi.org/10.1017/S003329172200397X.

Couch, Y. *et al.* (2016) "Low-dose lipopolysaccharide (LPS) inhibits aggressive and augments depressive behaviours in a chronic mild stress model in mice," *Journal of Neuroinflammation*, 13(1), p. 108. Available at: https://doi.org/10.1186/s12974-016-0572-0.

Crary, J.F. *et al.* (2014) "Primary age-related tauopathy (PART): a common pathology associated with human aging.," *Acta neuropathologica*, 128(6), pp. 755–766. Available at: https://doi.org/10.1007/s00401-014-1349-0.

Crespo-Castrillo, A. and Arevalo, M.-A. (2020) "Microglial and Astrocytic Function in Physiological and Pathological Conditions: Estrogenic Modulation.," *International journal of molecular sciences*, 21(9). Available at: https://doi.org/10.3390/ijms21093219.

Crilly, A. *et al.* (2012) "Immunomodulatory role of proteinase-activated receptor-2," *Annals of*

the Rheumatic Diseases, 71(9), pp. 1559–1566. Available at: https://doi.org/https://doi.org/10.1136/annrheumdis-2011-200869.

Cui, L. *et al.* (2024) "Major depressive disorder: hypothesis, mechanism, prevention and treatment," *Signal Transduction and Targeted Therapy*, 9(1), p. 30. Available at: https://doi.org/10.1038/s41392-024-01738-y.

Cuijpers, P. *et al.* (2023) "Cognitive behavior therapy vs. control conditions, other psychotherapies, pharmacotherapies and combined treatment for depression: a comprehensive meta-analysis including 409 trials with 52,702 patients," *World Psychiatry*, 22(1), pp. 105–115. Available at: https://doi.org/10.1002/wps.21069.

Cummings, J. (2021) "New approaches to symptomatic treatments for Alzheimer's disease," *Molecular Neurodegeneration*, 16(1), p. 2. Available at: https://doi.org/10.1186/s13024-021-00424-9.

Cummings, J. *et al.* (2024) "Anti-Amyloid Monoclonal Antibodies for the Treatment of Alzheimer's Disease.," *BioDrugs : clinical immunotherapeutics, biopharmaceuticals and gene therapy*, 38(1), pp. 5–22. Available at: https://doi.org/10.1007/s40259-023-00633-2.

Cummings, J. *et al.* (2025) "Alzheimer's disease drug development pipeline: 2025," *Alzheimer's & Dementia: Translational Research & Clinical Interventions*, 11. Available at: https://doi.org/10.1002/trc2.70098.

Dadkhah, M. *et al.* (2023) "Major depressive disorder: Biomarkers and biosensors," *Clinica Chimica Acta*, 547, p. 117437. Available at: https://doi.org/https://doi.org/10.1016/j.cca.2023.117437.

Dafsari, F.S. and Jessen, F. (2020) "Depression—an underrecognized target for prevention of dementia in Alzheimer's disease," *Translational Psychiatry*. Springer Nature. Available at: https://doi.org/10.1038/s41398-020-0839-1.

Dang, R. *et al.* (2019) "Predictable chronic mild stress promotes recovery from LPS-induced depression," *Molecular Brain*, 12(1), p. 42. Available at: https://doi.org/10.1186/s13041-019-0463-2.

Dantzer, R. (2006) "Cytokine, sickness behavior, and depression.," *Neurologic clinics*, 24(3), pp. 441–60. Available at: https://doi.org/10.1016/j.ncl.2006.03.003.

Dantzer, R. *et al.* (2008) "From inflammation to sickness and depression: when the immune system subjugates the brain.," *Nature reviews. Neuroscience*, 9(1), pp. 46–56. Available at: https://doi.org/10.1038/nrn2297.

Daria, S. *et al.* (2020) "Serum interferon-gamma level is associated with drug-naïve major depressive disorder.," *SAGE open medicine*, 8, p. 2050312120974169. Available at: https://doi.org/10.1177/2050312120974169.

Das, R. *et al.* (2021) "Higher levels of serum IL-1β and TNF-α are associated with an increased probability of major depressive disorder," *Psychiatry Research*, 295, p. 113568. Available at: https://doi.org/https://doi.org/10.1016/j.psychres.2020.113568.

Dayton, A. *et al.* (2016) "Breaking the Cycle: Estrous Variation Does Not Require Increased Sample Size in the Study of Female Rats.," *Hypertension (Dallas, Tex. : 1979)*, 68(5), pp. 1139–1144. Available at: https://doi.org/10.1161/HYPERTENSIONAHA.116.08207.

De-Paula, V.J. *et al.* (2012) "Alzheimer's Disease," in *Protein Aggregation and Fibrillogenesis in Cerebral and Systemic Amyloid Disease*. Springer Netherlands, pp. 329–352. Available at: https://doi.org/10.1007/978-94-007-5416-4_14.

Deacon, R.M.J. (2006) "Assessing nest building in mice," *Nature Protocols*, 1(3), pp. 1117–1119. Available at: https://doi.org/10.1038/nprot.2006.170.

Deal, A. *et al.* (2021) "Early life stress induces hyperactivity but not increased anxiety-like

behavior or ethanol drinking in outbred heterogeneous stock rats.," *Alcohol (Fayetteville, N.Y.)*, 91, pp. 41–51. Available at: https://doi.org/10.1016/j.alcohol.2020.11.007.

DeKosky, S.T. and Scheff, S.W. (1990) "Synapse loss in frontal cortex biopsies in Alzheimer's disease: Correlation with cognitive severity," *Annals of Neurology*, 27(5), pp. 457–464. Available at: https://doi.org/https://doi.org/10.1002/ana.410270502.

Deng, I. *et al.* (2020) "Lipopolysaccharide animal models of Parkinson's disease: Recent progress and relevance to clinical disease.," *Brain, behavior, & immunity - health*, 4, p. 100060. Available at: https://doi.org/10.1016/j.bbih.2020.100060.

Deutsch, J.A. (1971) "The Cholinergic Synapse and the Site of Memory," *Science*, 174(4011), pp. 788–794. Available at: https://doi.org/10.1126/science.174.4011.788.

Dhiman, K. *et al.* (2020) "Cerebrospinal fluid neurofilament light concentration predicts brain atrophy and cognition in Alzheimer's disease.," *Alzheimer's & dementia (Amsterdam, Netherlands)*, 12(1), p. e12005. Available at: https://doi.org/10.1002/dad2.12005.

Ding, H. *et al.* (2018) "Depression-like behaviors induced by chronic corticosterone exposure via drinking water: Time-course analysis," *Neuroscience Letters*, 687, pp. 202–206. Available at: https://doi.org/10.1016/j.neulet.2018.09.059.

Ding, Z.-B. *et al.* (2021) "Astrocytes: a double-edged sword in neurodegenerative diseases.," *Neural regeneration research*, 16(9), pp. 1702–1710. Available at: https://doi.org/10.4103/1673-5374.306064.

Dionisio-Santos, D.A., Olschowka, J.A. and O'Banion, M.K. (2019) "Exploiting microglial and peripheral immune cell crosstalk to treat Alzheimer's disease," *Journal of Neuroinflammation*, 16(1), p. 74. Available at: https://doi.org/10.1186/s12974-019-1453-0.

Domingues, C., da Cruz E Silva, O.A.B. and Henriques, A.G. (2017) "Impact of Cytokines and Chemokines on Alzheimer's Disease Neuropathological Hallmarks.," *Current Alzheimer research*, 14(8), pp. 870–882. Available at: https://doi.org/10.2174/1567205014666170317113606.

Dong, H. *et al.* (2014) "Effects of corticotrophin-releasing factor receptor 1 antagonists on amyloid-β and behavior in Tg2576 mice," *Psychopharmacology*, 231(24), pp. 4711–4722. Available at: https://doi.org/10.1007/s00213-014-3629-8.

Dong, H. *et al.* (2018) "Corticotrophin releasing factor receptor 1 antagonists prevent chronic stress-induced behavioral changes and synapse loss in aged rats," *Psychoneuroendocrinology*, 90, pp. 92–101. Available at: https://doi.org/10.1016/j.psyneuen.2018.02.013.

Dong, H. and Csernansky, J.G. (2009) "Effects of stress and stress hormones on amyloid-beta protein and plaque deposition.," *Journal of Alzheimer's disease : JAD*, 18(2), pp. 459–469. Available at: https://doi.org/10.3233/JAD-2009-1152.

Dong, Y. *et al.* (2016) "Dental noise exposed mice display depressive-like phenotypes.," *Molecular brain*, 9(1), p. 50. Available at: https://doi.org/10.1186/s13041-016-0229-z.

Dou, K.-X. *et al.* (2018) "Comparative safety and effectiveness of cholinesterase inhibitors and memantine for Alzheimer's disease: a network meta-analysis of 41 randomized controlled trials.," *Alzheimer's research & therapy*, 10(1), p. 126. Available at: https://doi.org/10.1186/s13195-018-0457-9.

Dowlati, Y. *et al.* (2010) "A meta-analysis of cytokines in major depression.," *Biological psychiatry*, 67(5), pp. 446–57. Available at: https://doi.org/10.1016/j.biopsych.2009.09.033.

Drummond, E. and Wisniewski, T. (2017) "Alzheimer's disease: experimental models and reality.," *Acta neuropathologica*, 133(2), pp. 155–175. Available at: https://doi.org/10.1007/s00401-016-1662-x.

van Dyck, C.H. *et al.* (2023) “Lecanemab in Early Alzheimer’s Disease,” *New England Journal of Medicine*, 388(1), pp. 9–21. Available at: https://doi.org/10.1056/NEJMoa2212948.

Edinoff, A.N. *et al.* (2021) “Brexpiprazole for the Treatment of Schizophrenia and Major Depressive Disorder: A Comprehensive Review of Pharmacological Considerations in Clinical Practice.,” *Psychopharmacology bulletin*, 51(2), pp. 69–95. Available at: https://doi.org/10.64719/pb.4399.

Eftekhari, R. *et al.* (2024) “Blockade of Proteinase-Activated Receptor 2 (PAR2) Attenuates Neuroinflammation in Experimental Autoimmune Encephalomyelitis.,” *The Journal of pharmacology and experimental therapeutics*, 388(1), pp. 12–22. Available at: https://doi.org/10.1124/jpet.123.001685.

Eid, R.S., Gobinath, A.R. and Galea, L.A.M. (2019) “Sex differences in depression: Insights from clinical and preclinical studies,” *Progress in Neurobiology*, 176, pp. 86–102. Available at: https://doi.org/https://doi.org/10.1016/j.pneurobio.2019.01.006.

Ennaceur, A. and Delacour, J. (1988) “A new one-trial test for neurobiological studies of memory in rats. 1: Behavioral data,” *Behavioural Brain Research*, 31(1), pp. 47–59. Available at: https://doi.org/10.1016/0166-4328(88)90157-X.

Escartin, C. *et al.* (2021) “Reactive astrocyte nomenclature, definitions, and future directions,” *Nature Neuroscience*, 24(3), pp. 312–325. Available at: https://doi.org/10.1038/s41593-020-00783-4.

Estanislau, C. *et al.* (2013) “Context-dependent differences in grooming behavior among the NIH heterogeneous stock and the Roman high- and low-avoidance rats,” *Neuroscience Research*, 77(4), pp. 187–201. Available at: https://doi.org/10.1016/j.neures.2013.09.012.

Eyre, H.A. *et al.* (2016) “A meta-analysis of chemokines in major depression,” *Progress in Neuro-Psychopharmacology and Biological Psychiatry*, 68, pp. 1–8. Available at: https://doi.org/https://doi.org/10.1016/j.pnpbp.2016.02.006.

Fagan, A.M. *et al.* (2006) “Inverse relation between in vivo amyloid imaging load and cerebrospinal fluid Abeta42 in humans.,” *Annals of neurology*, 59(3), pp. 512–9. Available at: https://doi.org/10.1002/ana.20730.

Fan, Y.-Y. and Huo, J. (2021) “A1/A2 astrocytes in central nervous system injuries and diseases: Angels or devils?,” *Neurochemistry International*, 148, p. 105080. Available at: https://doi.org/https://doi.org/10.1016/j.neuint.2021.105080.

Fanelli, G. *et al.* (2019) “Reduced CXCL1/GRO chemokine plasma levels are a possible biomarker of elderly depression.,” *Journal of affective disorders*, 249, pp. 410–417. Available at: https://doi.org/10.1016/j.jad.2019.02.042.

Fang, Y. *et al.* (2022) “Fluoxetine inhibited the activation of A1 reactive astrocyte in a mouse model of major depressive disorder through astrocytic 5-HT2BR/β-arrestin2 pathway,” *Journal of Neuroinflammation*, 19(1), p. 23. Available at: https://doi.org/10.1186/s12974-022-02389-y.

Fekadu, N., Shibeshi, W. and Engidawork, E. (2017) “Major Depressive Disorder: Pathophysiology and Clinical Management.,” *Journal of Depression and Anxiety*, 06(01). Available at: https://doi.org/10.4172/2167-1044.1000255.

Ferencz, B. and Gerritsen, L. (2015) “Genetics and Underlying Pathology of Dementia,” *Neuropsychology Review*, pp. 113–124. Available at: https://doi.org/10.1007/s11065-014-9276-3.

Ferrari, C. and Sorbi, S. (2021) “The complexity of Alzheimer’s disease: an evolving puzzle,” *Physiological Reviews*, 101(3), pp. 1047–1081. Available at: https://doi.org/10.1152/physrev.00015.2020.

Ferrell, W.R. *et al.* (2010) “Protease-activated receptor 2: a novel pathogenic pathway in a murine model of osteoarthritis,” *Annals of the Rheumatic Diseases*, 69(11), pp. 2051–2054. Available at: https://doi.org/10.1136/ard.2010.130336.

First, M.B. *et al.* (2021) “An organization- and category-level comparison of diagnostic requirements for mental disorders in ICD-11 and DSM-5.,” *World psychiatry : official journal of the World Psychiatric Association (WPA)*, 20(1), pp. 34–51. Available at: https://doi.org/10.1002/wps.20825.

Forner, S. *et al.* (2021) “Systematic phenotyping and characterization of the 5xFAD mouse model of Alzheimer’s disease,” *Scientific Data*, 8(1), p. 270. Available at: https://doi.org/10.1038/s41597-021-01054-y.

Frick, E.A. *et al.* (2024) “Serum proteomics reveal APOE-ε4-dependent and APOE-ε4-independent protein signatures in Alzheimer’s disease,” *Nature Aging*, 4(10), pp. 1446–1464. Available at: https://doi.org/10.1038/s43587-024-00693-1.

Fu, H. *et al.* (2012) “Complement component C3 and complement receptor type 3 contribute to the phagocytosis and clearance of fibrillar Aβ by microglia.,” *Glia*, 60(6), pp. 993–1003. Available at: https://doi.org/10.1002/glia.22331.

Fujita, Y. *et al.* (2020) “Engulfment of Toxic Amyloid β-protein in Neurons and Astrocytes Mediated by MEGF10,” *Neuroscience*, 443, pp. 1–7. Available at: https://doi.org/https://doi.org/10.1016/j.neuroscience.2020.07.016.

Gallagher, D. *et al.* (2018) “Depression and Risk of Alzheimer Dementia: A Longitudinal Analysis to Determine Predictors of Increased Risk among Older Adults with Depression,” *The American Journal of Geriatric Psychiatry*, 26(8), pp. 819–827. Available at: https://doi.org/10.1016/j.jagp.2018.05.002.

Gan, J. *et al.* (2011) “Indirect modulation of neuronal excitability and synaptic transmission in the hippocampus by activation of proteinase-activated receptor-2.,” *British journal of pharmacology*, 163(5), pp. 984–94. Available at: https://doi.org/10.1111/j.1476-5381.2011.01293.x.

Gao, C. *et al.* (2023) “Microglia in neurodegenerative diseases: mechanism and potential therapeutic targets,” *Signal Transduction and Targeted Therapy*, 8(1), p. 359. Available at: https://doi.org/10.1038/s41392-023-01588-0.

Gao, P. *et al.* (2022) “Daphnetin ameliorates Aβ pathogenesis via STAT3/GFAP signaling in an APP/PS1 double-transgenic mouse model of Alzheimer’s disease,” *Pharmacological Research*, 180, p. 106227. Available at: https://doi.org/https://doi.org/10.1016/j.phrs.2022.106227.

Gao, S. *et al.* (2023) “A terrified-sound stress causes cognitive impairment in female mice by impairing neuronal plasticity,” *Brain Research*, 1812, p. 148419. Available at: https://doi.org/https://doi.org/10.1016/j.brainres.2023.148419.

Gardell, L.R. *et al.* (2008) “Identification and Characterization of Novel Small-Molecule Protease-Activated Receptor 2 Agonists,” *The Journal of Pharmacology and Experimental Therapeutics*, 327(3), pp. 799–808. Available at: https://doi.org/10.1124/jpet.108.142570.

Gatchel, J.R. *et al.* (2017) “Depressive Symptoms and Tau Accumulation in the Inferior Temporal Lobe and Entorhinal Cortex in Cognitively Normal Older Adults: A Pilot Study,” *Journal of Alzheimer’s Disease*. Edited by K. Lanctôt, 59(3), pp. 975–985. Available at: https://doi.org/10.3233/JAD-170001.

Gatchel, J.R. *et al.* (2019) “Longitudinal Association of Depression Symptoms With Cognition and Cortical Amyloid Among Community-Dwelling Older Adults,” *JAMA Network Open*, 2(8), p. e198964. Available at: https://doi.org/10.1001/jamanetworkopen.2019.8964.

Gautam, M. *et al.* (2020) “Cognitive Behavioral Therapy for Depression.,” *Indian journal of*

psychiatry, 62(Suppl 2), pp. S223–S229. Available at: https://doi.org/10.4103/psychiatry.IndianJPsychiatry_772_19.

Gencturk, S. and Unal, G. (2024) "Rodent tests of depression and anxiety: Construct validity and translational relevance," *Cognitive, Affective, & Behavioral Neuroscience*, 24(2), pp. 191–224. Available at: https://doi.org/10.3758/s13415-024-01171-2.

Ghosh, S. *et al.* (2013) "Sustained interleukin-1β overexpression exacerbates tau pathology despite reduced amyloid burden in an Alzheimer's mouse model.," *The Journal of neuroscience : the official journal of the Society for Neuroscience*, 33(11), pp. 5053–64. Available at: https://doi.org/10.1523/JNEUROSCI.4361-12.2013.

Glenner, G.G. and Wong, C.W. (1984) "Alzheimer's disease: Initial report of the purification and characterization of a novel cerebrovascular amyloid protein," *Biochemical and Biophysical Research Communications*, 120(3), pp. 885–890. Available at: https://doi.org/10.1016/S0006-291X(84)80190-4.

Go, M. *et al.* (2016) "Microglial response to LPS increases in wild-type mice during aging but diminishes in an Alzheimer's mouse model: Implication of TLR4 signaling in disease progression," *Biochemical and Biophysical Research Communications*, 479(2), pp. 331–337. Available at: https://doi.org/10.1016/j.bbrc.2016.09.073.

Goedert, M. *et al.* (1989) "Multiple isoforms of human microtubule-associated protein tau: sequences and localization in neurofibrillary tangles of Alzheimer's disease.," *Neuron*, 3(4), pp. 519–526. Available at: https://doi.org/10.1016/0896-6273(89)90210-9.

Gold, S.M. *et al.* (2020) "Comorbid depression in medical diseases," *Nature Reviews Disease Primers*, 6(1), p. 69. Available at: https://doi.org/10.1038/s41572-020-0200-2.

Gomes, C. *et al.* (2024) "Induction of astrocyte reactivity promotes neurodegeneration in human pluripotent stem cell models," *Stem Cell Reports*, 19(8), pp. 1122–1136. Available at: https://doi.org/https://doi.org/10.1016/j.stemcr.2024.07.002.

González-Arias, C. and Perea, G. (2025) "When the Stars Misfire: Astrocytic Dysfunctions in Major Depressive Disorder.," *Neurochemical research*, 50(4), p. 231. Available at: https://doi.org/10.1007/s11064-025-04483-y.

González-Reyes, R.E. *et al.* (2017) "Involvement of Astrocytes in Alzheimer's Disease from a Neuroinflammatory and Oxidative Stress Perspective," *Frontiers in Molecular Neuroscience*, 10. Available at: https://doi.org/10.3389/fnmol.2017.00427.

Goodwin, N.L. *et al.* (2024) "Simple Behavioral Analysis (SimBA) as a platform for explainable machine learning in behavioral neuroscience," *Nature Neuroscience*, 27(7), pp. 1411–1424. Available at: https://doi.org/10.1038/s41593-024-01649-9.

Gourley, S.L. *et al.* (2008) "Acute hippocampal brain-derived neurotrophic factor restores motivational and forced swim performance after corticosterone.," *Biological psychiatry*, 64(10), pp. 884–90. Available at: https://doi.org/10.1016/j.biopsych.2008.06.016.

Gozlan, E., Lewit-Cohen, Y. and Frenkel, D. (2024) "Sex Differences in Astrocyte Activity," *Cells*. Available at: https://doi.org/10.3390/cells13201724.

Grande, G. *et al.* (2025) "Blood-based biomarkers of Alzheimer's disease and incident dementia in the community," *Nature Medicine* [Preprint]. Available at: https://doi.org/10.1038/s41591-025-03605-x.

Green, K.N. *et al.* (2006) "Glucocorticoids increase amyloid-beta and tau pathology in a mouse model of Alzheimer's disease.," *The Journal of neuroscience : the official journal of the Society for Neuroscience*, 26(35), pp. 9047–56. Available at: https://doi.org/10.1523/JNEUROSCI.2797-06.2006.

Green, R.C. *et al.* (2003) "Depression as a risk factor for Alzheimer disease: the MIRAGE

Study.," *Archives of neurology*, 60(5), pp. 753–9. Available at: https://doi.org/10.1001/archneur.60.5.753.

Green, T., Flash, S. and Reiss, A.L. (2019) "Sex differences in psychiatric disorders: what we can learn from sex chromosome aneuploidies," *Neuropsychopharmacology*, 44(1), pp. 9–21. Available at: https://doi.org/10.1038/s41386-018-0153-2.

Greenwood, E.K. and Brown, D.R. (2021) "Senescent Microglia: The Key to the Ageing Brain?," *International journal of molecular sciences*, 22(9). Available at: https://doi.org/10.3390/ijms22094402.

Greenwood, S.M. and Bushell, T.J. (2010) "Astrocytic activation and an inhibition of MAP kinases are required for proteinase-activated receptor-2-mediated protection from neurotoxicity," *Journal of Neurochemistry*, p. no-no. Available at: https://doi.org/10.1111/j.1471-4159.2010.06737.x.

Griciuc, A. and Tanzi, R.E. (2021) "The role of innate immune genes in Alzheimer's disease," *Current Opinion in Neurology*, 34(2), pp. 228–236. Available at: https://doi.org/10.1097/WCO.0000000000000911.

Grundke-Iqbal, I. *et al.* (1986) "Microtubule-associated protein tau. A component of Alzheimer paired helical filaments.," *Journal of Biological Chemistry*, 261(13), pp. 6084–6089. Available at: https://doi.org/https://doi.org/10.1016/S0021-9258(17)38495-8.

Guerreiro, R.J., Gustafson, D.R. and Hardy, J. (2012) "The genetic architecture of Alzheimer's disease: beyond APP, PSENs and APOE," *Neurobiology of Aging*, 33(3), pp. 437–456. Available at: https://doi.org/10.1016/j.neurobiolaging.2010.03.025.

Guo, J. *et al.* (2020) "Memantine, Donepezil, or Combination Therapy—What is the best therapy for Alzheimer's Disease? A Network Meta-Analysis," *Brain and Behavior*, 10(11). Available at: https://doi.org/10.1002/brb3.1831.

Guo, S., Wang, H. and Yin, Y. (2022) "Microglia Polarization From M1 to M2 in Neurodegenerative Diseases," *Frontiers in Aging Neuroscience*, 14. Available at: https://doi.org/10.3389/fnagi.2022.815347.

Guo, Z. *et al.* (2022) "Maternal Deprivation Increased Vulnerability to Depression in Adult Rats Through DRD2 Promoter Methylation in the Ventral Tegmental Area," *Frontiers in Psychiatry*, 13. Available at: https://doi.org/10.3389/fpsyt.2022.827667.

H., van D.C. *et al.* (2023) "Lecanemab in Early Alzheimer's Disease," *New England Journal of Medicine*, 388(1), pp. 9–21. Available at: https://doi.org/10.1056/NEJMoa2212948.

Haass, C. and Selkoe, D.J. (1993) "Cellular processing of beta-amyloid precursor protein and the genesis of amyloid beta-peptide.," *Cell*, 75(6), pp. 1039–1042. Available at: https://doi.org/10.1016/0092-8674(93)90312-e.

Habib, N. *et al.* (2020) "Disease-associated astrocytes in Alzheimer's disease and aging," *Nature Neuroscience*, 23(6), pp. 701–706. Available at: https://doi.org/10.1038/s41593-020-0624-8.

Habibi, A., Ruf, W. and Schurgers, L. (2025) "Protease-activated receptors in vascular smooth muscle cells: a bridge between thrombo-inflammation and vascular remodelling," *Cell Communication and Signaling*, 23(1), p. 57. Available at: https://doi.org/10.1186/s12964-025-02066-6.

Hacimusalar, Y. and Eşel, E. (2018) "Suggested Biomarkers for Major Depressive Disorder.," *Noro psikiyatri arsivi*, 55(3), pp. 280–290. Available at: https://doi.org/10.5152/npa.2017.19482.

Han, H. *et al.* (2025) "Implications of neurogenesis in depression through BDNF: rodent models, regulatory pathways, gut microbiota, and potential therapy," *Molecular Psychiatry*,

30(9), pp. 4409–4421. Available at: https://doi.org/10.1038/s41380-025-03044-7.

Han, J. *et al.* (2021) “Uncovering sex differences of rodent microglia,” *Journal of Neuroinflammation*, 18(1), p. 74. Available at: https://doi.org/10.1186/s12974-021-02124-z.

Han, K.-S. *et al.* (2011) “Activation of protease activated receptor 1 increases the excitability of the dentate granule neurons of hippocampus,” *Molecular Brain*, 4(1), p. 32. Available at: https://doi.org/10.1186/1756-6606-4-32.

Han, X. *et al.* (2021) “Protease-Activated Receptors (PARs),” in *Encyclopedia of Molecular Pharmacology*. Cham: Springer International Publishing, pp. 1–13. Available at: https://doi.org/10.1007/978-3-030-21573-6_10078-1.

Hanafy, A.S. *et al.* (2023) “Subcellular analysis of blood-brain barrier function by micro-impalement of vessels in acute brain slices,” *Nature Communications*, 14(1), p. 481. Available at: https://doi.org/10.1038/s41467-023-36070-6.

Hansen, D. V, Hanson, J.E. and Sheng, M. (2018) “Microglia in Alzheimer’s disease.,” *The Journal of cell biology*, 217(2), pp. 459–472. Available at: https://doi.org/10.1083/jcb.201709069.

Hara, T., Sata, M. and Fukuda, D. (2023) “Emerging roles of protease-activated receptors in cardiometabolic disorders,” *Journal of Cardiology*, 81(4), pp. 337–346. Available at: https://doi.org/https://doi.org/10.1016/j.jjcc.2022.09.013.

Hardy, J.A. and Higgins, G.A. (1992) “Alzheimer’s disease: The amyloid cascade hypothesis,” *Science*, pp. 184–185. Available at: https://doi.org/10.1126/science.1566067.

Hassler, S.N. *et al.* (2020) “The cellular basis of protease-activated receptor 2–evoked mechanical and affective pain,” *JCI Insight*, 5(11). Available at: https://doi.org/10.1172/jci.insight.137393.

Hauss-Wegrzyniak, B., Vannucchi, M.G. and Wenk, G.L. (2000) “Behavioral and ultrastructural changes induced by chronic neuroinflammation in young rats.,” *Brain research*, 859(1), pp. 157–66. Available at: https://doi.org/10.1016/s0006-8993(00)01999-5.

He, J.-G. *et al.* (2023) “Dysfunction of Glutamatergic Synaptic Transmission in Depression: Focus on AMPA Receptor Trafficking,” *Biological Psychiatry Global Open Science*, 3(2), pp. 187–196. Available at: https://doi.org/10.1016/j.bpsgos.2022.02.007.

Heneka, M.T. *et al.* (2015) “Neuroinflammation in Alzheimer’s disease,” *The Lancet Neurology*, 14(4), pp. 388–405. Available at: https://doi.org/10.1016/S1474-4422(15)70016-5.

Heneka, M.T. *et al.* (2024) “Neuroinflammation in Alzheimer disease,” *Nature Reviews Immunology* [Preprint]. Available at: https://doi.org/10.1038/s41577-024-01104-7.

Herber, D.L. *et al.* (2004) “Time-dependent reduction in Aβ levels after intracranial LPS administration in APP transgenic mice,” *Experimental Neurology*, 190(1), pp. 245–253. Available at: https://doi.org/10.1016/j.expneurol.2004.07.007.

Hernández, F. and Avila, J. (2007) “Tauopathies,” *Cellular and Molecular Life Sciences*, 64(17), pp. 2219–2233. Available at: https://doi.org/10.1007/s00018-007-7220-x.

Herring, W.J. *et al.* (2020) “Polysomnographic assessment of suvorexant in patients with probable Alzheimer’s disease dementia and insomnia: a randomized trial.,” *Alzheimer’s & dementia : the journal of the Alzheimer’s Association*, 16(3), pp. 541–551. Available at: https://doi.org/10.1002/alz.12035.

Heuberger, D.M. and Schuepbach, R.A. (2019) “Protease-activated receptors (PARs): mechanisms of action and potential therapeutic modulators in PAR-driven inflammatory diseases,” *Thrombosis Journal*, 17(1), p. 4. Available at: https://doi.org/10.1186/s12959-019-0194-8.

Hoeijmakers, L. *et al.* (2016) “Microglial Priming and Alzheimer’s Disease: A Possible Role for (Early) Immune Challenges and Epigenetics?,” *Frontiers in Human Neuroscience*, 10. Available at: https://doi.org/10.3389/fnhum.2016.00398.

Vom Hofe, I. *et al.* (2025) “Long-Term Exposure to Non-Steroidal Anti-Inflammatory Medication in Relation to Dementia Risk.,” *Journal of the American Geriatrics Society*, 73(5), pp. 1484–1490. Available at: https://doi.org/10.1111/jgs.19411.

Howard, D.M. *et al.* (2019) “Genome-wide meta-analysis of depression identifies 102 independent variants and highlights the importance of the prefrontal brain regions.,” *Nature neuroscience*, 22(3), pp. 343–352. Available at: https://doi.org/10.1038/s41593-018-0326-7.

Howlett, J. *et al.* (2021) “Disease Modelling of Cognitive Outcomes and Biomarkers in the European Prevention of Alzheimer’s Dementia Longitudinal Cohort,” *Frontiers in Big Data*, 4. Available at: https://doi.org/10.3389/fdata.2021.676168.

Hsiao, K. *et al.* (1996) “Correlative Memory Deficits, Aβ Elevation, and Amyloid Plaques in Transgenic Mice,” *Science*, 274(5284), pp. 99–103. Available at: https://doi.org/10.1126/science.274.5284.99.

Hsu, A.I. and Yttri, E.A. (2021) “B-SOiD, an open-source unsupervised algorithm for identification and fast prediction of behaviors.,” *Nature communications*, 12(1), p. 5188. Available at: https://doi.org/10.1038/s41467-021-25420-x.

Hu, C. *et al.* (2017) “Re-evaluation of the interrelationships among the behavioral tests in rats exposed to chronic unpredictable mild stress.,” *PloS one*, 12(9), p. e0185129. Available at: https://doi.org/10.1371/journal.pone.0185129.

Hu, X. *et al.* (2018) “BACE1 deletion in the adult mouse reverses preformed amyloid deposition and improves cognitive functions,” *Journal of Experimental Medicine*, 215(3), pp. 927–940. Available at: https://doi.org/10.1084/jem.20171831.

Huang, M. *et al.* (2025) “Astrocyte in Neurological Disease: Pathogenesis and Therapy.,” *MedComm*, 6(8), p. e70299. Available at: https://doi.org/10.1002/mco2.70299.

Huang, Q. *et al.* (2022) “Acetylcholine bidirectionally regulates learning and memory,” *Journal of Neurorestoratology*, 10(2), p. 100002. Available at: https://doi.org/https://doi.org/10.1016/j.jnrt.2022.100002.

Huang, Y.-Y. *et al.* (2024) “Depression in Alzheimer’s Disease: Epidemiology, Mechanisms, and Treatment,” *Biological Psychiatry*, 95(11), pp. 992–1005. Available at: https://doi.org/10.1016/j.biopsych.2023.10.008.

Hulshof, L.A. *et al.* (2022) “The Role of Astrocytes in Synapse Loss in Alzheimer’s Disease: A Systematic Review.,” *Frontiers in cellular neuroscience*, 16, p. 899251. Available at: https://doi.org/10.3389/fncel.2022.899251.

Husain, M.A., Laurent, B. and Plourde, M. (2021) “APOE and Alzheimer’s Disease: From Lipid Transport to Physiopathology and Therapeutics,” *Frontiers in Neuroscience*, 15. Available at: https://doi.org/10.3389/fnins.2021.630502.

Hutton, M. *et al.* (1998) “Association of missense and 5’-splice-site mutations in tau with the inherited dementia FTDP-17.,” *Nature*, 393(6686), pp. 702–705. Available at: https://doi.org/10.1038/31508.

Ishihara, H. *et al.* (1997) “Protease-activated receptor 3 is a second thrombin receptor in humans,” *Nature*, 386(6624), pp. 502–506. Available at: https://doi.org/10.1038/386502a0.

Isingrini, E. *et al.* (2010) “Association between repeated unpredictable chronic mild stress (UCMS) procedures with a high fat diet: a model of fluoxetine resistance in mice.,” *PloS one*, 5(4), p. e10404. Available at: https://doi.org/10.1371/journal.pone.0010404.

Jack, C.R. *et al.* (2013) “Tracking pathophysiological processes in Alzheimer’s disease: an

updated hypothetical model of dynamic biomarkers," *The Lancet Neurology*, 12(2), pp. 207–216. Available at: https://doi.org/10.1016/S1474-4422(12)70291-0.

Jäkel, L. *et al.* (2022) "Prevalence of cerebral amyloid angiopathy: A systematic review and meta-analysis," *Alzheimer's & Dementia*, 18(1), pp. 10–28. Available at: https://doi.org/10.1002/alz.12366.

Jang, H.Y. *et al.* (2020) "Antidepressant Use and the Risk of Major Adverse Cardiovascular Events in Patients Without Known Cardiovascular Disease: A Retrospective Cohort Study," *Frontiers in Pharmacology*, Volume 11. Available at: https://doi.org/10.3389/fphar.2020.594474.

Jankowsky, J.L. *et al.* (2004) "Mutant presenilins specifically elevate the levels of the 42 residue β-amyloid peptide in vivo: evidence for augmentation of a 42-specific γ secretase," *Human Molecular Genetics*, 13(2), pp. 159–170. Available at: https://doi.org/10.1093/hmg/ddh019.

Jawhar, S. *et al.* (2012) "Motor deficits, neuron loss, and reduced anxiety coinciding with axonal degeneration and intraneuronal Aβ aggregation in the 5XFAD mouse model of Alzheimer's disease," *Neurobiology of Aging*, 33(1), pp. 196.e29-196.e40. Available at: https://doi.org/10.1016/j.neurobiolaging.2010.05.027.

Jellinger, K.A. (1998) "The neuropathological diagnosis of Alzheimer disease," *Journal of Neural Transmission, Supplement*, 5(53), pp. 97–118. Available at: https://doi.org/10.1007/978-3-7091-6467-9_9.

Jendresen, C. *et al.* (2019) "Systemic LPS-induced Aβ-solubilization and clearance in AβPP-transgenic mice is diminished by heparanase overexpression," *Scientific Reports*, 9(1), p. 4600. Available at: https://doi.org/10.1038/s41598-019-40999-4.

Jha, M.K. *et al.* (2019) "Microglia-Astrocyte Crosstalk: An Intimate Molecular Conversation," *The Neuroscientist*, 25(3), pp. 227–240. Available at: https://doi.org/10.1177/1073858418783959.

Jiang, X. *et al.* (2009) "Impaired hypothalamic-pituitary-adrenal axis and its feedback regulation in serotonin transporter knockout mice.," *Psychoneuroendocrinology*, 34(3), pp. 317–31. Available at: https://doi.org/10.1016/j.psyneuen.2008.09.011.

Jin, G. *et al.* (2005) "Deficiency of PAR-2 gene increases acute focal ischemic brain injury.," *Journal of cerebral blood flow and metabolism : official journal of the International Society of Cerebral Blood Flow and Metabolism*, 25(3), pp. 302–313. Available at: https://doi.org/10.1038/sj.jcbfm.9600021.

Jong Huat, T. *et al.* (2024) "The impact of astrocytic NF-κB on healthy and Alzheimer's disease brains," *Scientific Reports*, 14(1), p. 14305. Available at: https://doi.org/10.1038/s41598-024-65248-1.

Jung, H. *et al.* (2023) "LPS induces microglial activation and GABAergic synaptic deficits in the hippocampus accompanied by prolonged cognitive impairment," *Scientific Reports*, 13(1), p. 6547. Available at: https://doi.org/10.1038/s41598-023-32798-9.

Kabra, M. *et al.* (2013) "JAABA: interactive machine learning for automatic annotation of animal behavior," *Nature Methods*, 10(1), pp. 64–67. Available at: https://doi.org/10.1038/nmeth.2281.

Kahn, M.S. *et al.* (2012) "Prolonged elevation in hippocampal Aβ and cognitive deficits following repeated endotoxin exposure in the mouse," *Behavioural Brain Research*, 229(1), pp. 176–184. Available at: https://doi.org/10.1016/j.bbr.2012.01.010.

Kalueff, A. V. *et al.* (2016) "Neurobiology of rodent self-grooming and its value for translational neuroscience," *Nature Reviews Neuroscience*, 17(1), pp. 45–59. Available at: https://doi.org/10.1038/nrn.2015.8.

Kalueff, A. V. and Tuohimaa, P. (2004a) “Contrasting grooming phenotypes in C57Bl/6 and 129S1/SvImJ mice,” *Brain Research*, 1028(1), pp. 75–82. Available at: https://doi.org/10.1016/j.brainres.2004.09.001.

Kalueff, A. V *et al.* (2007) “Analyzing grooming microstructure in neurobehavioral experiments,” *Nature Protocols*, 2(10), pp. 2538–2544. Available at: https://doi.org/10.1038/nprot.2007.367.

Kalueff, A. V and Tuohimaa, P. (2004b) “Grooming analysis algorithm for neurobehavioural stress research,” *Brain Research Protocols*, 13(3), pp. 151–158. Available at: https://doi.org/https://doi.org/10.1016/j.brainresprot.2004.04.002.

Kamran, M. *et al.* (2022) “Major Depressive Disorder: Existing Hypotheses about Pathophysiological Mechanisms and New Genetic Findings,” *Genes*, 13(4), p. 646. Available at: https://doi.org/10.3390/genes13040646.

Kang, J. *et al.* (1987) “The precursor of Alzheimer’s disease amyloid A4 protein resembles a cell-surface receptor,” *Nature*, 325(6106), pp. 733–736. Available at: https://doi.org/10.1038/325733a0.

van der Kant, R., Goldstein, L.S.B. and Ossenkoppele, R. (2020) “Amyloid-β-independent regulators of tau pathology in Alzheimer disease,” *Nature Reviews Neuroscience*, 21(1), pp. 21–35. Available at: https://doi.org/10.1038/s41583-019-0240-3.

Karch, C.M. and Goate, A.M. (2015) “Alzheimer’s Disease Risk Genes and Mechanisms of Disease Pathogenesis,” *Biological Psychiatry*, 77(1), pp. 43–51. Available at: https://doi.org/10.1016/j.biopsych.2014.05.006.

Katsouri, L. *et al.* (2020) “Ablation of reactive astrocytes exacerbates disease pathology in a model of Alzheimer’s disease.,” *Glia*, 68(5), pp. 1017–1030. Available at: https://doi.org/10.1002/glia.23759.

Keller, J. *et al.* (2017) “HPA axis in major depression: cortisol, clinical symptomatology and genetic variation predict cognition.,” *Molecular psychiatry*, 22(4), pp. 527–536. Available at: https://doi.org/10.1038/mp.2016.120.

Kempuraj, D. *et al.* (2016) “Neuroinflammation Induces Neurodegeneration.,” *Journal of neurology, neurosurgery and spine*, 1(1).

Kennedy, A.J. *et al.* (2018) “Structural Characterization of Agonist Binding to Protease-Activated Receptor 2 through Mutagenesis and Computational Modeling.,” *ACS pharmacology & translational science*, 1(2), pp. 119–133. Available at: https://doi.org/10.1021/acsptsci.8b00019.

Kennedy, A.J. *et al.* (2020) “Protease-activated receptor-2 ligands reveal orthosteric and allosteric mechanisms of receptor inhibition,” *Communications Biology*, 3(1), p. 782. Available at: https://doi.org/10.1038/s42003-020-01504-0.

Keren-Shaul, H. *et al.* (2017) “A Unique Microglia Type Associated with Restricting Development of Alzheimer’s Disease,” *Cell*, 169(7), pp. 1276-1290.e17. Available at: https://doi.org/10.1016/j.cell.2017.05.018.

Kessing, L.V. *et al.* (2009) “Antidepressants and dementia.,” *Journal of affective disorders*, 117(1–2), pp. 24–9. Available at: https://doi.org/10.1016/j.jad.2008.11.020.

Keszycki, R. *et al.* (2023) “Characterization of apathy-like behaviors in the 5xFAD mouse model of Alzheimer’s disease,” *Neurobiology of Aging*, 126, pp. 113–122. Available at: https://doi.org/10.1016/j.neurobiolaging.2023.02.012.

Khoon, L. and Piran, R. (2025) “A New Strategy in Modulating the Protease-Activated Receptor 2 (Par2) in Autoimmune Diseases.,” *International journal of molecular sciences*, 26(1). Available at: https://doi.org/10.3390/ijms26010410.

Kim, D. *et al.* (2021) “Depression and Increased Risk of Alzheimer’s Dementia: Longitudinal Analyses of Modifiable Risk and Sex-Related Factors.,” *The American journal of geriatric psychiatry : official journal of the American Association for Geriatric Psychiatry*, 29(9), pp. 917–926. Available at: https://doi.org/10.1016/j.jagp.2020.12.031.

Kim, H. *et al.* (2022) “Reactive astrocytes transduce inflammation in a blood-brain barrier model through a TNF-STAT3 signaling axis and secretion of alpha 1-antichymotrypsin,” *Nature Communications*, 13(1), p. 6581. Available at: https://doi.org/10.1038/s41467-022-34412-4.

Kim, J. *et al.* (2024) “Repeated LPS induces training and tolerance of microglial responses across brain regions,” *Journal of Neuroinflammation*, 21(1), p. 233. Available at: https://doi.org/10.1186/s12974-024-03198-1.

Klyucherev, T.O. *et al.* (2022) “Advances in the development of new biomarkers for Alzheimer’s disease,” *Translational Neurodegeneration*, 11(1), p. 25. Available at: https://doi.org/10.1186/s40035-022-00296-z.

Knopman, D.S. *et al.* (2021) “Alzheimer disease,” *Nature Reviews Disease Primers*, 7(1), p. 33. Available at: https://doi.org/10.1038/s41572-021-00269-y.

Kohler, O. *et al.* (2016) “Inflammation in Depression and the Potential for Anti-Inflammatory Treatment.,” *Current neuropharmacology*, 14(7), pp. 732–42. Available at: https://doi.org/10.2174/1570159x14666151208113700.

Konishi, H., Koizumi, S. and Kiyama, H. (2022) “Phagocytic astrocytes: Emerging from the shadows of microglia.,” *Glia*, 70(6), pp. 1009–1026. Available at: https://doi.org/10.1002/glia.24145.

Köpke, E. *et al.* (1993) “Microtubule-associated protein tau. Abnormal phosphorylation of a non-paired helical filament pool in Alzheimer disease.,” *The Journal of biological chemistry*, 268(32), pp. 24374–24384.

Kosel, F. *et al.* (2021) “Reduced social investigation and increased injurious behavior in transgenic 5xFAD mice,” *Journal of Neuroscience Research*, 99(1), pp. 209–222. Available at: https://doi.org/10.1002/jnr.24578.

Kosel, F., Pelley, J.M.S. and Franklin, T.B. (2020) “Behavioural and psychological symptoms of dementia in mouse models of Alzheimer’s disease-related pathology,” *Neuroscience & Biobehavioral Reviews*, 112, pp. 634–647. Available at: https://doi.org/10.1016/j.neubiorev.2020.02.012.

Kouba, B.R. *et al.* (2024) “Role of Inflammatory Mechanisms in Major Depressive Disorder: From Etiology to Potential Pharmacological Targets.,” *Cells*, 13(5). Available at: https://doi.org/10.3390/cells13050423.

Krabbe, G. *et al.* (2013) “Functional Impairment of Microglia Coincides with Beta-Amyloid Deposition in Mice with Alzheimer-Like Pathology,” *PLoS ONE*. Edited by J. Priller, 8(4), p. e60921. Available at: https://doi.org/10.1371/journal.pone.0060921.

Kraeuter, A.-K., Guest, P.C. and Sarnyai, Z. (2019) “The Nest Building Test in Mice for Assessment of General Well-Being,” in, pp. 87–91. Available at: https://doi.org/10.1007/978-1-4939-8994-2_7.

Kraft, A.W. *et al.* (2013) “Attenuating astrocyte activation accelerates plaque pathogenesis in APP/PS1 mice.,” *FASEB journal : official publication of the Federation of American Societies for Experimental Biology*, 27(1), pp. 187–198. Available at: https://doi.org/10.1096/fj.12-208660.

Krishnan, V. and Nestler, E.J. (2011) “Animal Models of Depression: Molecular Perspectives,” in, pp. 121–147. Available at: https://doi.org/10.1007/7854_2010_108.

Kruyer, A., Kalivas, P.W. and Scofield, M.D. (2023) “Astrocyte regulation of synaptic signaling in psychiatric disorders,” *Neuropsychopharmacology*, 48(1), pp. 21–36. Available at: https://doi.org/10.1038/s41386-022-01338-w.

Kwatra, M. *et al.* (2021) “Lipopolysaccharide exacerbates chronic restraint stress-induced neurobehavioral deficits: Mechanisms by redox imbalance, ASK1-related apoptosis, autophagic dysregulation,” *Journal of Psychiatric Research*, 144, pp. 462–482. Available at: https://doi.org/https://doi.org/10.1016/j.jpsychires.2021.10.021.

Kwon, H.S. and Koh, S.-H. (2020) “Neuroinflammation in neurodegenerative disorders: the roles of microglia and astrocytes,” *Translational Neurodegeneration*, 9(1), p. 42. Available at: https://doi.org/10.1186/s40035-020-00221-2.

La-Vu, M. *et al.* (2020) “To Approach or Avoid: An Introductory Overview of the Study of Anxiety Using Rodent Assays,” *Frontiers in Behavioral Neuroscience*, Volume 14. Available at: https://doi.org/10.3389/fnbeh.2020.00145.

Landeiro, F. *et al.* (2024) “The economic burden of cancer, coronary heart disease, dementia, and stroke in England in 2018, with projection to 2050: an evaluation of two cohort studies,” *The Lancet Healthy Longevity*, 5(8), pp. e514–e523. Available at: https://doi.org/10.1016/S2666-7568(24)00108-9.

Lasselin, J. *et al.* (2020) “Comparison of bacterial lipopolysaccharide-induced sickness behavior in rodents and humans: Relevance for symptoms of anxiety and depression,” *Neuroscience & Biobehavioral Reviews*, 115, pp. 15–24. Available at: https://doi.org/https://doi.org/10.1016/j.neubiorev.2020.05.001.

Lawrence, J.M. *et al.* (2023) “Roles of neuropathology-associated reactive astrocytes: a systematic review,” *Acta Neuropathologica Communications*, 11(1), p. 42. Available at: https://doi.org/10.1186/s40478-023-01526-9.

Lee, D. *et al.* (2024) “Brexpiprazole for Agitation Associated With Dementia Due to Alzheimer’s Disease,” *Journal of the American Medical Directors Association*, 25(10), p. 105173. Available at: https://doi.org/https://doi.org/10.1016/j.jamda.2024.105173.

Lee, E. and Chang, Y. (2025) “Modulating Neuroinflammation as a Prospective Therapeutic Target in Alzheimer’s Disease,” *Cells*. Available at: https://doi.org/10.3390/cells14030168.

Lee, H.-G. *et al.* (2024) “Disease-associated astrocyte epigenetic memory promotes CNS pathology,” *Nature*, 627(8005), pp. 865–872. Available at: https://doi.org/10.1038/s41586-024-07187-5.

Lee, J.R. *et al.* (2019) “Anhedonia and Dysphoria Are Differentially Associated with the Risk of Dementia in the Cognitively Normal Elderly Individuals: A Prospective Cohort Study,” *Psychiatry Investig*, 16(8), pp. 575–580. Available at: https://doi.org/10.30773/pi.2019.06.07.

Lee, J.W. *et al.* (2008) “Neuro-inflammation induced by lipopolysaccharide causes cognitive impairment through enhancement of beta-amyloid generation,” *Journal of Neuroinflammation*, 5(1), p. 37. Available at: https://doi.org/10.1186/1742-2094-5-37.

Lee, S.-I. *et al.* (2025) “Astrocyte priming enhances microglial Aβ clearance and is compromised by APOE4,” *Nature Communications*, 16(1), p. 7551. Available at: https://doi.org/10.1038/s41467-025-62995-1.

Lee, S.Y. and Chung, W.-S. (2021) “The roles of astrocytic phagocytosis in maintaining homeostasis of brains,” *Journal of Pharmacological Sciences*, 145(3), pp. 223–227. Available at: https://doi.org/https://doi.org/10.1016/j.jphs.2020.12.007.

Leng, F. and Edison, P. (2021) “Neuroinflammation and microglial activation in Alzheimer disease: where do we go from here?,” *Nature Reviews Neurology*, 17(3), pp. 157–172. Available at: https://doi.org/10.1038/s41582-020-00435-y.

van Lengerich, B. *et al.* (2023) “A TREM2-activating antibody with a blood–brain barrier transport vehicle enhances microglial metabolism in Alzheimer’s disease models,” *Nature Neuroscience*, 26(3), pp. 416–429. Available at: https://doi.org/10.1038/s41593-022-01240-0.

Lenouvel, E. *et al.* (2024) “Antidepressants for treating depression among older adults with dementia: A systematic review and meta-analysis,” *Psychiatry Research*, 340, p. 116114. Available at: https://doi.org/https://doi.org/10.1016/j.psychres.2024.116114.

Levey, D.F. *et al.* (2021) “Bi-ancestral depression GWAS in the Million Veteran Program and meta-analysis in >1.2 million individuals highlight new therapeutic directions,” *Nature Neuroscience*, 24(7), pp. 954–963. Available at: https://doi.org/10.1038/s41593-021-00860-2.

Levine, S. (2005) “Developmental determinants of sensitivity and resistance to stress.,” *Psychoneuroendocrinology*, 30(10), pp. 939–46. Available at: https://doi.org/10.1016/j.psyneuen.2005.03.013.

Levy-Lahad, E. *et al.* (1995) “Candidate gene for the chromosome 1 familial Alzheimer’s disease locus.,” *Science (New York, N.Y.)*, 269(5226), pp. 973–977. Available at: https://doi.org/10.1126/science.7638622.

Li, K. *et al.* (2019) “Reactive Astrocytes in Neurodegenerative Diseases.,” *Aging and disease*, 10(3), pp. 664–675. Available at: https://doi.org/10.14336/AD.2018.0720.

Li, L. *et al.* (2024) “Astrocytes Excessively Engulf Synapses in a Mouse Model of Alzheimer’s Disease.,” *International journal of molecular sciences*, 25(2). Available at: https://doi.org/10.3390/ijms25021160.

Li, R. *et al.* (2015) “The effects of apigenin on lipopolysaccharide-induced depressive-like behavior in mice,” *Neuroscience Letters*, 594, pp. 17–22. Available at: https://doi.org/https://doi.org/10.1016/j.neulet.2015.03.040.

Li, X. *et al.* (2022) “Seeding, maturation and propagation of amyloid β-peptide aggregates in Alzheimer’s disease.,” *Brain : a journal of neurology*, 145(10), pp. 3558–3570. Available at: https://doi.org/10.1093/brain/awac202.

Li, Y. *et al.* (2023) “TREM2: Potential therapeutic targeting of microglia for Alzheimer’s disease,” *Biomedicine & Pharmacotherapy*, 165, p. 115218. Available at: https://doi.org/https://doi.org/10.1016/j.biopha.2023.115218.

Li, Z. *et al.* (2020) “APOE2: protective mechanism and therapeutic implications for Alzheimer’s disease,” *Molecular Neurodegeneration*, 15(1), p. 63. Available at: https://doi.org/10.1186/s13024-020-00413-4.

Lian, H. *et al.* (2016) “Astrocyte-Microglia Cross Talk through Complement Activation Modulates Amyloid Pathology in Mouse Models of Alzheimer’s Disease.,” *The Journal of neuroscience : the official journal of the Society for Neuroscience*, 36(2), pp. 577–89. Available at: https://doi.org/10.1523/JNEUROSCI.2117-15.2016.

Liddelow, S.A. *et al.* (2017) “Neurotoxic reactive astrocytes are induced by activated microglia,” *Nature*, 541(7638), pp. 481–487. Available at: https://doi.org/10.1038/nature21029.

Liddelow, S.A., Marsh, S.E. and Stevens, B. (2020) “Microglia and Astrocytes in Disease: Dynamic Duo or Partners in Crime?,” *Trends in Immunology*, 41(9), pp. 820–835. Available at: https://doi.org/10.1016/j.it.2020.07.006.

Litvinchuk, A. *et al.* (2018) “Complement C3aR Inactivation Attenuates Tau Pathology and Reverses an Immune Network Deregulated in Tauopathy Models and Alzheimer’s Disease.,” *Neuron*, 100(6), pp. 1337-1353.e5. Available at: https://doi.org/10.1016/j.neuron.2018.10.031.

Liu, C.-C. *et al.* (2013) “Apolipoprotein E and Alzheimer disease: risk, mechanisms and therapy.,” *Nature reviews. Neurology*, 9(2), pp. 106–18. Available at: https://doi.org/10.1038/nrneurol.2012.263.

Liu, D. *et al.* (2011) “Anti-inflammatory effects of fluoxetine in lipopolysaccharide(LPS)-stimulated microglial cells,” *Neuropharmacology*, 61(4), pp. 592–599. Available at: https://doi.org/10.1016/j.neuropharm.2011.04.033.

Liu, H. *et al.* (2021) “Dissection of the relationship between anxiety and stereotyped self-grooming using the Shank3B mutant autistic model, acute stress model and chronic pain model,” *Neurobiology of Stress*, 15, p. 100417. Available at: https://doi.org/10.1016/j.ynstr.2021.100417.

Liu, J. *et al.* (2019) “The Role of NMDA Receptors in Alzheimer’s Disease,” *Frontiers in Neuroscience*, 13. Available at: https://doi.org/10.3389/fnins.2019.00043.

Liu, M.-Y. *et al.* (2018) “Sucrose preference test for measurement of stress-induced anhedonia in mice,” *Nature Protocols*, 13(7), pp. 1686–1698. Available at: https://doi.org/10.1038/s41596-018-0011-z.

Liu, Y. *et al.* (2022) “PET imaging of reactive astrocytes in neurological disorders.,” *European journal of nuclear medicine and molecular imaging*, 49(4), pp. 1275–1287. Available at: https://doi.org/10.1007/s00259-021-05640-5.

Liu, Y., Huber, C.C. and Wang, H. (2020) “Disrupted blood-brain barrier in 5×FAD mouse model of Alzheimer’s disease can be mimicked and repaired in vitro with neural stem cell-derived exosomes,” *Biochemical and Biophysical Research Communications*, 525(1), pp. 192–196. Available at: https://doi.org/https://doi.org/10.1016/j.bbrc.2020.02.074.

Livingston, G. *et al.* (2024) “Dementia prevention, intervention, and care: 2024 report of the Lancet standing Commission,” *The Lancet*, 404(10452), pp. 572–628. Available at: https://doi.org/10.1016/S0140-6736(24)01296-0.

Locci, A. *et al.* (2021) “Comparison of memory, affective behavior, and neuropathology in APPNLGF knock-in mice to 5xFAD and APP/PS1 mice,” *Behavioural Brain Research*, 404, p. 113192. Available at: https://doi.org/10.1016/j.bbr.2021.113192.

Long, S., Benoist, C. and Weidner, W. (2023) “International AS. World Alzheimer Report 2023: Reducing dementia risk: never too early, never too late.” Available at: https://www.alzint.org/u/World-Alzheimer-Report-2023.pdf.

Lopez-Lee, C. *et al.* (2024) “Mechanisms of sex differences in Alzheimer’s disease,” *Neuron*, 112(8), pp. 1208–1221. Available at: https://doi.org/https://doi.org/10.1016/j.neuron.2024.01.024.

Lovick, T.A. and Zangrossi, H.J. (2021) “Effect of Estrous Cycle on Behavior of Females in Rodent Tests of Anxiety.,” *Frontiers in psychiatry*, 12, p. 711065. Available at: https://doi.org/10.3389/fpsyt.2021.711065.

Lyketsos, C.G. *et al.* (2011) “Neuropsychiatric symptoms in Alzheimer’s disease.,” *Alzheimer’s & dementia : the journal of the Alzheimer’s Association*, 7(5), pp. 532–9. Available at: https://doi.org/10.1016/j.jalz.2011.05.2410.

Lynch, M.A. (2022) “Exploring Sex-Related Differences in Microglia May Be a Game-Changer in Precision Medicine.,” *Frontiers in aging neuroscience*, 14, p. 868448. Available at: https://doi.org/10.3389/fnagi.2022.868448.

Lyu, Z. *et al.* (2025) “Structural basis for the activation of proteinase-activated receptors PAR1 and PAR2,” *Nature Communications*, 16(1), p. 3931. Available at: https://doi.org/10.1038/s41467-025-59138-x.

Mahase, E. (2024) “NICE rejects Alzheimer{\textquoteright}s drug donanemab owing to cost

and {\textquotedblleft}significant health risks{\textquotedblright},” *BMJ*, 387. Available at: https://doi.org/10.1136/bmj.q2342.

Maier, S.F. and Seligman, M.E.P. (2016) “Learned helplessness at fifty: Insights from neuroscience.,” *Psychological review*, 123(4), pp. 349–67. Available at: https://doi.org/10.1037/rev0000033.

Mallach, A. *et al.* (2024) “Microglia-astrocyte crosstalk in the amyloid plaque niche of an Alzheimer’s disease mouse model, as revealed by spatial transcriptomics,” *Cell Reports*, 43(6), p. 114216. Available at: https://doi.org/https://doi.org/10.1016/j.celrep.2024.114216.

Markov, D.D. (2022) “Sucrose Preference Test as a Measure of Anhedonic Behavior in a Chronic Unpredictable Mild Stress Model of Depression: Outstanding Issues,” *Brain Sciences*, 12(10), p. 1287. Available at: https://doi.org/10.3390/brainsci12101287.

Martín-Sánchez, A. *et al.* (2021) “Comorbidity between Alzheimer’s disease and major depression: a behavioural and transcriptomic characterization study in mice,” *Alzheimer’s Research & Therapy*, 13(1), p. 73. Available at: https://doi.org/10.1186/s13195-021-00810-x.

Maschio, C. and Ni, R. (2022) “Amyloid and Tau Positron Emission Tomography Imaging in Alzheimer’s Disease and Other Tauopathies,” *Frontiers in Aging Neuroscience*, 14. Available at: https://doi.org/10.3389/fnagi.2022.838034.

Mason, B.N. *et al.* (2023) “PAR2 activation in the dura causes acute behavioral responses and priming to glyceryl trinitrate in a mouse migraine model,” *The Journal of Headache and Pain*, 24(1), p. 42. Available at: https://doi.org/10.1186/s10194-023-01574-5.

Matejuk, A. and Ransohoff, R.M. (2020) “Crosstalk Between Astrocytes and Microglia: An Overview,” *Frontiers in Immunology*, 11. Available at: https://doi.org/10.3389/fimmu.2020.01416.

Mathis, A. *et al.* (2018) “DeepLabCut: markerless pose estimation of user-defined body parts with deep learning,” *Nature Neuroscience*, 21(9), pp. 1281–1289. Available at: https://doi.org/10.1038/s41593-018-0209-y.

McAlpine, C.S. *et al.* (2021) “Astrocytic interleukin-3 programs microglia and limits Alzheimer’s disease.,” *Nature*, 595(7869), pp. 701–706. Available at: https://doi.org/10.1038/s41586-021-03734-6.

McConnell, G. *et al.* (2016) “A novel optical microscope for imaging large embryos and tissue volumes with sub-cellular resolution throughout,” *eLife*, 5. Available at: https://doi.org/10.7554/eLife.18659.

McCulloch, K. *et al.* (2018) “Rheumatic Disease: Protease-Activated Receptor-2 in Synovial Joint Pathobiology.,” *Frontiers in endocrinology*, 9, p. 257. Available at: https://doi.org/10.3389/fendo.2018.00257.

McDade, E. *et al.* (2022) “Lecanemab in patients with early Alzheimer’s disease: detailed results on biomarker, cognitive, and clinical effects from the randomized and open-label extension of the phase 2 proof-of-concept study,” *Alzheimer’s Research & Therapy*, 14(1), p. 191. Available at: https://doi.org/10.1186/s13195-022-01124-2.

McIntosh, K.A. *et al.* (2020) “The development of proteinase-activated receptor-2 modulators and the challenges involved,” *Biochemical Society Transactions*, 48(6), pp. 2525–2537. Available at: https://doi.org/10.1042/BST20200191.

McIntyre, R.S. *et al.* (2023) “Treatment-resistant depression: definition, prevalence, detection, management, and investigational interventions.,” *World psychiatry : official journal of the World Psychiatric Association (WPA)*, 22(3), pp. 394–412. Available at: https://doi.org/10.1002/wps.21120.

McShane, R. *et al.* (2019) “Memantine for dementia,” *Cochrane Database of Systematic*

Reviews [Preprint]. Available at: https://doi.org/10.1002/14651858.CD003154.pub6.

Medeiros, R., Baglietto-Vargas, D. and LaFerla, F.M. (2011) “The role of tau in Alzheimer’s disease and related disorders.,” *CNS neuroscience & therapeutics*, 17(5), pp. 514–24. Available at: https://doi.org/10.1111/j.1755-5949.2010.00177.x.

Medina-Vera, D. *et al.* (2023) “Transcending the amyloid-beta dominance paradigm in Alzheimer’s disease: An exploration of behavioural, metabolic, and gut microbiota phenotypes in 5xFAD mice,” *Neurobiology of Disease*, 187, p. 106295. Available at: https://doi.org/10.1016/j.nbd.2023.106295.

Michaud, J.-P. *et al.* (2013) “Toll-like receptor 4 stimulation with the detoxified ligand monophosphoryl lipid A improves Alzheimer’s disease-related pathology.,” *Proceedings of the National Academy of Sciences of the United States of America*, 110(5), pp. 1941–6. Available at: https://doi.org/10.1073/pnas.1215165110.

Miguel-Hidalgo, J.J. (2022) “Astroglia in the Vulnerability to and Maintenance of Stress-Mediated Neuropathology and Depression,” *Frontiers in Cellular Neuroscience*, Volume 16. Available at: https://doi.org/10.3389/fncel.2022.869779.

Mikulska, J. *et al.* (2021) “HPA Axis in the Pathomechanism of Depression and Schizophrenia: New Therapeutic Strategies Based on Its Participation,” *Brain Sciences*, 11(10), p. 1298. Available at: https://doi.org/10.3390/brainsci11101298.

Miller, A.H. and Raison, C.L. (2016) “The role of inflammation in depression: from evolutionary imperative to modern treatment target,” *Nature Reviews Immunology*, 16(1), pp. 22–34. Available at: https://doi.org/10.1038/nri.2015.5.

Miller, O.H. *et al.* (2014) “GluN2B-containing NMDA receptors regulate depression-like behavior and are critical for the rapid antidepressant actions of ketamine,” *eLife*, 3. Available at: https://doi.org/10.7554/eLife.03581.

Min, X. *et al.* (2023) “Association between inflammatory cytokines and symptoms of major depressive disorder in adults.,” *Frontiers in immunology*, 14, p. 1110775. Available at: https://doi.org/10.3389/fimmu.2023.1110775.

Misra, A., Chakrabarti, S.S. and Gambhir, I.S. (2018) “New genetic players in late-onset Alzheimer’s disease: Findings of genome-wide association studies.,” *The Indian journal of medical research*, 148(2), pp. 135–144. Available at: https://doi.org/10.4103/ijmr.IJMR_473_17.

Mlyniec, K. (2015) “Zinc in the Glutamatergic Theory of Depression.,” *Current neuropharmacology*, 13(4), pp. 505–13. Available at: https://doi.org/10.2174/1570159x13666150115220617.

Mo, M. *et al.* (2025) “Antidepressant use and cognitive decline in patients with dementia: a national cohort study,” *BMC Medicine*, 23(1), p. 82. Available at: https://doi.org/10.1186/s12916-025-03851-3.

Monterey, M.D. *et al.* (2021) “The Many Faces of Astrocytes in Alzheimer’s Disease,” *Frontiers in Neurology*, 12. Available at: https://doi.org/10.3389/fneur.2021.619626.

Morales, I. *et al.* (2014) “Neuroinflammation in the pathogenesis of Alzheimerâ€™s disease. A rational framework for the search of novel therapeutic approaches,” *Frontiers in Cellular Neuroscience*, 8. Available at: https://doi.org/10.3389/fncel.2014.00112.

Morris, R.G.M. *et al.* (1982) “Place navigation impaired in rats with hippocampal lesions,” *Nature*, 297(5868), pp. 681–683. Available at: https://doi.org/10.1038/297681a0.

Moudio, S. *et al.* (2022) “Protease-activated receptor 2 activation induces behavioural changes associated with depression-like behaviour through microglial-independent modulation of inflammatory cytokines,” *Psychopharmacology*, 239(1), pp. 229–242. Available

at: https://doi.org/10.1007/s00213-021-06040-1.

Moudio, S., Nuthall, H.N. and Bushell, T.J. (2025) “Neuroprotection induced by protease-activated receptor 2 activation is independent of Gq signalling.,” *Brain and neuroscience advances*, 9, p. 23982128251345670. Available at: https://doi.org/10.1177/23982128251345673.

Munhoz, C.D. *et al.* (2006) “Chronic unpredictable stress exacerbates lipopolysaccharide-induced activation of nuclear factor-kappaB in the frontal cortex and hippocampus via glucocorticoid secretion.,” *The Journal of neuroscience : the official journal of the Society for Neuroscience*, 26(14), pp. 3813–3820. Available at: https://doi.org/10.1523/JNEUROSCI.4398-05.2006.

Munoz-Ballester, C. *et al.* (2022) “Mild Traumatic Brain Injury-Induced Disruption of the Blood-Brain Barrier Triggers an Atypical Neuronal Response.,” *Frontiers in cellular neuroscience*, 16, p. 821885. Available at: https://doi.org/10.3389/fncel.2022.821885.

Munoz-Ballester, C. *et al.* (2024) “Assessment of Blood-Brain Barrier Integrity Using Dyes and Tracers,” *Preprints* [Preprint]. Preprints. Available at: https://doi.org/10.20944/preprints202409.0341.v1.

Murta, V., Seiffe, A. and Depino, A.M. (2023) “Sex Differences in Mouse Models of Autism Spectrum Disorders: Their Potential to Uncover the Impact of Brain Sexual Differentiation on Gender Bias,” *Sexes*, pp. 358–391. Available at: https://doi.org/10.3390/sexes4030024.

National Institute for Health and Care Excellence (2018) “Dementia: assessment, management and support for people living with dementia and their carers,” *NICE Guidelines*, (June 2018), pp. 2–43. Available at: www.nice.org.uk/guidance/ng97.

National Institute for Health and Care Excellence (2022) “Depression in adults : treatment and management,” *NICE Guidelines* [Preprint], (June 2022).

Nazem, A. *et al.* (2015) “Rodent models of neuroinflammation for Alzheimer’s disease,” *Journal of Neuroinflammation*, 12(1), p. 74. Available at: https://doi.org/10.1186/s12974-015-0291-y.

Nehra, G., Bauer, B. and Hartz, A.M.S. (2022) “Blood-brain barrier leakage in Alzheimer’s disease: From discovery to clinical relevance,” *Pharmacology & Therapeutics*, 234, p. 108119. Available at: https://doi.org/https://doi.org/10.1016/j.pharmthera.2022.108119.

Nelson, P.T. *et al.* (2012) “Correlation of Alzheimer disease neuropathologic changes with cognitive status: a review of the literature.,” *Journal of neuropathology and experimental neurology*, 71(5), pp. 362–381. Available at: https://doi.org/10.1097/NEN.0b013e31825018f7.

Nestler, E.J. and Hyman, S.E. (2010) “Animal models of neuropsychiatric disorders.,” *Nature neuroscience*, 13(10), pp. 1161–9. Available at: https://doi.org/10.1038/nn.2647.

Neuner, S.M. *et al.* (2022) “Translational approaches to understanding resilience to Alzheimer’s disease,” *Trends in Neurosciences*, 45(5), pp. 369–383. Available at: https://doi.org/10.1016/j.tins.2022.02.005.

Nichols, H.L. *et al.* (2012) “β-Arrestin-2 mediates the proinflammatory effects of proteinase-activated receptor-2 in the airway,” *Proceedings of the National Academy of Sciences*, 109(41), pp. 16660–16665. Available at: https://doi.org/10.1073/pnas.1208881109.

Nollet, M. (2021) “Models of Depression: Unpredictable Chronic Mild Stress in Mice,” *Current Protocols*, 1(8), p. e208. Available at: https://doi.org/https://doi.org/10.1002/cpz1.208.

Noorbakhsh, F. *et al.* (2003) “Proteinase-activated receptors in the nervous system,” *Nature Reviews Neuroscience*, 4(12), pp. 981–990. Available at: https://doi.org/10.1038/nrn1255.

Noorbakhsh, F. *et al.* (2006) “Proteinase-activated receptor 2 modulates neuroinflammation

in experimental autoimmune encephalomyelitis and multiple sclerosis," *Journal of Experimental Medicine*, 203(2), pp. 425–435. Available at: https://doi.org/10.1084/jem.20052148.

Norden, D.M. and Godbout, J.P. (2013) "Review: microglia of the aged brain: primed to be activated and resistant to regulation.," *Neuropathology and applied neurobiology*, 39(1), pp. 19–34. Available at: https://doi.org/10.1111/j.1365-2990.2012.01306.x.

Nordgreen, J. *et al.* (2018) "The effect of lipopolysaccharide (LPS) on inflammatory markers in blood and brain and on behavior in individually-housed pigs," *Physiology & Behavior*, 195, pp. 98–111. Available at: https://doi.org/https://doi.org/10.1016/j.physbeh.2018.07.013.

Novikova, G. *et al.* (2021) "Integration of Alzheimer's disease genetics and myeloid genomics identifies disease risk regulatory elements and genes," *Nature Communications*, 12(1), p. 1610. Available at: https://doi.org/10.1038/s41467-021-21823-y.

Nystedt, S. *et al.* (1994) "Molecular cloning of a potential proteinase activated receptor.," *Proceedings of the National Academy of Sciences of the United States of America*, 91(20), pp. 9208–12. Available at: https://doi.org/10.1073/pnas.91.20.9208.

O'Leary, T.P. and Brown, R.E. (2024) "Age-related changes in species-typical behaviours in the 5xFAD mouse model of Alzheimer's disease from 4 to 16 months of age," *Behavioural Brain Research*, 465, p. 114970. Available at: https://doi.org/https://doi.org/10.1016/j.bbr.2024.114970.

Oakley, H. *et al.* (2006) "Intraneuronal β-Amyloid Aggregates, Neurodegeneration, and Neuron Loss in Transgenic Mice with Five Familial Alzheimer's Disease Mutations: Potential Factors in Amyloid Plaque Formation," *The Journal of Neuroscience*, 26(40), pp. 10129–10140. Available at: https://doi.org/10.1523/JNEUROSCI.1202-06.2006.

Oblak, A.L. *et al.* (2021) "Comprehensive Evaluation of the 5XFAD Mouse Model for Preclinical Testing Applications: A MODEL-AD Study," *Frontiers in Aging Neuroscience*, 13. Available at: https://doi.org/10.3389/fnagi.2021.713726.

Ocak, U. *et al.* (2020) "Inhibition of PAR-2 Attenuates Neuroinflammation and Improves Short-Term Neurocognitive Functions Via ERK1/2 Signaling Following Asphyxia-Induced Cardiac Arrest in Rats.," *Shock (Augusta, Ga.)*, 54(4), pp. 539–547. Available at: https://doi.org/10.1097/SHK.0000000000001516.

Oddo, S. *et al.* (2003) "Triple-Transgenic Model of Alzheimer's Disease with Plaques and Tangles," *Neuron*, 39(3), pp. 409–421. Available at: https://doi.org/10.1016/S0896-6273(03)00434-3.

Office for National Statistics (ONS) (2024) "Deaths registered in England and Wales: 2023." Available at: https://www.ons.gov.uk/peoplepopulationandcommunity/birthsdeathsandmarriages/deaths/bulletins/deathsregistrationsummarytables/2023.

Olton, D.S. and Samuelson, R.J. (1976) "Remembrance of places passed: Spatial memory in rats.," *Journal of Experimental Psychology: Animal Behavior Processes*, 2(2), pp. 97–116. Available at: https://doi.org/10.1037/0097-7403.2.2.97.

Ownby, R.L. *et al.* (2006) "Depression and risk for Alzheimer disease: systematic review, meta-analysis, and metaregression analysis.," *Archives of general psychiatry*, 63(5), pp. 530–8. Available at: https://doi.org/10.1001/archpsyc.63.5.530.

Pádua, M.S., Guil-Guerrero, J.L. and Lopes, P.A. (2024) "Behaviour Hallmarks in Alzheimer's Disease 5xFAD Mouse Model.," *International journal of molecular sciences*, 25(12). Available at: https://doi.org/10.3390/ijms25126766.

Pákáski, M. and Kálmán, J. (2008) "Interactions between the amyloid and cholinergic mechanisms in Alzheimer's disease," *Neurochemistry International*, 53(5), pp. 103–111.

Available at: https://doi.org/https://doi.org/10.1016/j.neuint.2008.06.005.

Park, G. *et al.* (2024) “Clearing Amyloid-Beta by Astrocytes: The Role of Rho GTPases Signaling Pathways as Potential Therapeutic Targets,” *Brain Sciences*. Available at: https://doi.org/10.3390/brainsci14121239.

Park, G.H. *et al.* (2010) “Activation of microglial cells via protease-activated receptor 2 mediates neuronal cell death in cultured rat primary neuron,” *Nitric Oxide*, 22(1), pp. 18–29. Available at: https://doi.org/https://doi.org/10.1016/j.niox.2009.10.008.

Peach, C.J. *et al.* (2023) “Protease-activated receptors in health and disease.,” *Physiological reviews*, 103(1), pp. 717–785. Available at: https://doi.org/10.1152/physrev.00044.2021.

Peng, X. *et al.* (2021) “Blood-Brain Barrier Disruption by Lipopolysaccharide and Sepsis-Associated Encephalopathy,” *Frontiers in Cellular and Infection Microbiology*, Volume 11. Available at: https://doi.org/10.3389/fcimb.2021.768108.

Perez-Caballero, L. *et al.* (2019) “Monoaminergic system and depression,” *Cell and Tissue Research*, 377(1), pp. 107–113. Available at: https://doi.org/10.1007/s00441-018-2978-8.

Petersen, R.C. (2004) “Mild cognitive impairment as a diagnostic entity,” *Journal of Internal Medicine*, 256(3), pp. 183–194. Available at: https://doi.org/https://doi.org/10.1111/j.1365-2796.2004.01388.x.

Petković, A. and Chaudhury, D. (2022) “Encore: Behavioural animal models of stress, depression and mood disorders,” *Frontiers in Behavioral Neuroscience*, Volume 16. Available at: https://doi.org/10.3389/fnbeh.2022.931964.

Pitzer, C., Kurpiers, B. and Eltokhi, A. (2022) “Sex Differences in Depression-Like Behaviors in Adult Mice Depend on Endophenotype and Strain,” *Frontiers in Behavioral Neuroscience*, 16. Available at: https://doi.org/10.3389/fnbeh.2022.838122.

Planchez, B., Surget, A. and Belzung, C. (2019) “Animal models of major depression: drawbacks and challenges.,” *Journal of neural transmission (Vienna, Austria : 1996)*, 126(11), pp. 1383–1408. Available at: https://doi.org/10.1007/s00702-019-02084-y.

Poon, C.H. *et al.* (2023) “Sex Differences between Neuronal Loss and the Early Onset of Amyloid Deposits and Behavioral Consequences in 5xFAD Transgenic Mouse as a Model for Alzheimer’s Disease.,” *Cells*, 12(5). Available at: https://doi.org/10.3390/cells12050780.

Porsolt, R.D., Le Pichon, M. and Jalfre, M. (1977) “Depression: a new animal model sensitive to antidepressant treatments,” *Nature*, 266(5604), pp. 730–732. Available at: https://doi.org/10.1038/266730a0.

Price, B.R. *et al.* (2025) “Sex differences and the role of estrogens in the immunological underpinnings of Alzheimer’s disease,” *Alzheimer’s & Dementia: Translational Research & Clinical Interventions*, 11(3), p. e70139. Available at: https://doi.org/https://doi.org/10.1002/trc2.70139.

Price, R., Mercuri, N.B. and Ledonne, A. (2021) “Emerging Roles of Protease-Activated Receptors (PARs) in the Modulation of Synaptic Transmission and Plasticity,” *International Journal of Molecular Sciences*, 22(2), p. 869. Available at: https://doi.org/10.3390/ijms22020869.

Primo, M.J. *et al.* (2023) “Sucrose preference test: A systematic review of protocols for the assessment of anhedonia in rodents,” *European Neuropsychopharmacology*, 77, pp. 80–92. Available at: https://doi.org/https://doi.org/10.1016/j.euroneuro.2023.08.496.

Profaci, C.P. *et al.* (2020) “The blood-brain barrier in health and disease: Important unanswered questions.,” *The Journal of experimental medicine*, 217(4). Available at: https://doi.org/10.1084/jem.20190062.

Prut, L. and Belzung, C. (2003) “The open field as a paradigm to measure the effects of

drugs on anxiety-like behaviors: a review," *European Journal of Pharmacology*, 463(1), pp. 3–33. Available at: https://doi.org/https://doi.org/10.1016/S0014-2999(03)01272-X.

Puentes-Orozco, M., Albarracin, S.L. and Velásquez, M.M. (2024) "Neuroinflammation and major depressive disorder: astrocytes at the crossroads.," *Frontiers in cellular neuroscience*, 18, p. 1504555. Available at: https://doi.org/10.3389/fncel.2024.1504555.

Qian, X. *et al.* (2023) "Repeated reserpine treatment induces depressive-like behaviors accompanied with hippocampal impairment and synapse deficit in mice," *Brain Research*, 1819, p. 148541. Available at: https://doi.org/https://doi.org/10.1016/j.brainres.2023.148541.

Quarta, S. *et al.* (2024) "Inhibition of Protease-Activated Receptor-2 Activation in Parkinson's Disease Using 1-Piperidin Propionic Acid," *Biomedicines*. Available at: https://doi.org/10.3390/biomedicines12071623.

Ragsdale, S.M. *et al.* (2025) "Dual orexin receptor antagonists as promising therapeutics for Alzheimer's disease," *npj Biological Timing and Sleep*, 2(1), p. 11. Available at: https://doi.org/10.1038/s44323-025-00025-5.

Rambaran, R.N. and Serpell, L.C. (2008) "Amyloid fibrils: abnormal protein assembly.," *Prion*, 2(3), pp. 112–117. Available at: https://doi.org/10.4161/pri.2.3.7488.

Ramos-Cejudo, J. *et al.* (2024) "Antidepressant exposure and long-term dementia risk in a nationwide retrospective study on US veterans with midlife major depressive disorder.," *Alzheimer's & dementia : the journal of the Alzheimer's Association*, 20(6), pp. 4106–4114. Available at: https://doi.org/10.1002/alz.13853.

Reches, G. and Piran, R. (2024) "Par2-mediated responses in inflammation and regeneration: choosing between repair and damage," *Inflammation and Regeneration*, 44(1), p. 26. Available at: https://doi.org/10.1186/s41232-024-00338-1.

Reichenbach, N. *et al.* (2019) "Inhibition of Stat3-mediated astrogliosis ameliorates pathology in an Alzheimer's disease model.," *EMBO molecular medicine*, 11(2). Available at: https://doi.org/10.15252/emmm.201809665.

Reinert, K.R.S. *et al.* (2014) "Short-term effects of an endotoxin on substantia nigra dopamine neurons.," *Brain research*, 1557, pp. 164–170. Available at: https://doi.org/10.1016/j.brainres.2014.02.005.

Ren, Z. *et al.* (2016) "Bidirectional Homeostatic Regulation of a Depression-Related Brain State by Gamma-Aminobutyric Acidergic Deficits and Ketamine Treatment," *Biological Psychiatry*, 80(6), pp. 457–468. Available at: https://doi.org/10.1016/j.biopsych.2016.02.009.

Richardson-Jones, J.W. *et al.* (2011) "Serotonin-1A autoreceptors are necessary and sufficient for the normal formation of circuits underlying innate anxiety.," *The Journal of neuroscience : the official journal of the Society for Neuroscience*, 31(16), pp. 6008–18. Available at: https://doi.org/10.1523/JNEUROSCI.5836-10.2011.

Richardson, B., MacPherson, A. and Bambico, F. (2022) "Neuroinflammation and neuroprogression in depression: Effects of alternative drug treatments.," *Brain, behavior, & immunity - health*, 26, p. 100554. Available at: https://doi.org/10.1016/j.bbih.2022.100554.

Ricks, T.K. and Trejo, J. (2009) "Phosphorylation of protease-activated receptor-2 differentially regulates desensitization and internalization.," *The Journal of biological chemistry*, 284(49), pp. 34444–34457. Available at: https://doi.org/10.1074/jbc.M109.048942.

Ridder, S. *et al.* (2005) "Mice with genetically altered glucocorticoid receptor expression show altered sensitivity for stress-induced depressive reactions.," *The Journal of neuroscience : the official journal of the Society for Neuroscience*, 25(26), pp. 6243–50. Available at: https://doi.org/10.1523/JNEUROSCI.0736-05.2005.

Ries, M. and Sastre, M. (2016) "Mechanisms of Aβ Clearance and Degradation by Glial

Cells," *Frontiers in Aging Neuroscience*, 8. Available at: https://doi.org/10.3389/fnagi.2016.00160.

Roberson, E.D. *et al.* (2007) "Reducing endogenous tau ameliorates amyloid beta-induced deficits in an Alzheimer's disease mouse model.," *Science (New York, N.Y.)*, 316(5825), pp. 750–4. Available at: https://doi.org/10.1126/science.1141736.

Roccati, E. *et al.* (2024) "Modifiable dementia risk factors and AT(N) biomarkers: findings from the EPAD cohort," *Frontiers in Aging Neuroscience*, 16. Available at: https://doi.org/10.3389/fnagi.2024.1346214.

Rodda, J., Morgan, S. and Walker, Z. (2009) "Are cholinesterase inhibitors effective in the management of the behavioral and psychological symptoms of dementia in Alzheimer's disease? A systematic review of randomized, placebo-controlled trials of donepezil, rivastigmine and galantamine," *International Psychogeriatrics*, 21(5), pp. 813–824. Available at: https://doi.org/10.1017/S1041610209990354.

Rodríguez-Giraldo, M. *et al.* (2022) "Astrocytes as a Therapeutic Target in Alzheimer's Disease–Comprehensive Review and Recent Developments," *International Journal of Molecular Sciences*, 23(21), p. 13630. Available at: https://doi.org/10.3390/ijms232113630.

Roohi, E., Jaafari, N. and Hashemian, F. (2021) "On inflammatory hypothesis of depression: what is the role of IL-6 in the middle of the chaos?," *Journal of Neuroinflammation*, 18(1), p. 45. Available at: https://doi.org/10.1186/s12974-021-02100-7.

Rostami, J. *et al.* (2021) "Crosstalk between astrocytes and microglia results in increased degradation of α-synuclein and amyloid-β aggregates," *Journal of Neuroinflammation*, 18(1), p. 124. Available at: https://doi.org/10.1186/s12974-021-02158-3.

Rozkalne, A. *et al.* (2009) "A single dose of passive immunotherapy has extended benefits on synapses and neurites in an Alzheimer's disease mouse model.," *Brain research*, 1280, pp. 178–85. Available at: https://doi.org/10.1016/j.brainres.2009.05.045.

Rush, A.J. *et al.* (2006) "Acute and longer-term outcomes in depressed outpatients requiring one or several treatment steps: a STAR*D report.," *The American journal of psychiatry*, 163(11), pp. 1905–17. Available at: https://doi.org/10.1176/ajp.2006.163.11.1905.

Russell, F.A. and McDougall, J.J. (2009) "Proteinase activated receptor (PAR) involvement in mediating arthritis pain and inflammation.," *Inflammation research : official journal of the European Histamine Research Society ... [et al.]*, 58(3), pp. 119–126. Available at: https://doi.org/10.1007/s00011-009-8087-0.

Rygula, R. *et al.* (2008) "Pharmacological validation of a chronic social stress model of depression in rats: effects of reboxetine, haloperidol and diazepam," *Behavioural Pharmacology*, 19(3), pp. 183–196. Available at: https://doi.org/10.1097/FBP.0b013e3282fe8871.

Ryu, J.K. and McLarnon, J.G. (2009) "A leaky blood-brain barrier, fibrinogen infiltration and microglial reactivity in inflamed Alzheimer's disease brain.," *Journal of cellular and molecular medicine*, 13(9A), pp. 2911–2925. Available at: https://doi.org/10.1111/j.1582-4934.2008.00434.x.

Sabedra Sousa, F.S. *et al.* (2019) "Lipopolysaccharide-induced depressive-like, anxiogenic-like and hyperalgesic behavior is attenuated by acute administration of α-(phenylselanyl) acetophenone in mice," *Neuropharmacology*, 146, pp. 128–137. Available at: https://doi.org/https://doi.org/10.1016/j.neuropharm.2018.11.028.

Sabic, D., Sabic, A. and Bacic-Becirovic, A. (2021) "Major Depressive Disorder and Difference between Genders.," *Materia socio-medica*, 33(2), pp. 105–108. Available at: https://doi.org/10.5455/msm.2021.33.105-108.

Sachan, V. *et al.* (2019) "HIV-induced neuroinflammation: impact of PAR1 and PAR2

processing by Furin.," *Cell death and differentiation*, 26(10), pp. 1942–1954. Available at: https://doi.org/10.1038/s41418-018-0264-7.

Sadleir, K.R. *et al.* (2015) "Aβ reduction in BACE1 heterozygous null 5XFAD mice is associated with transgenic APP level.," *Molecular neurodegeneration*, 10, p. 1. Available at: https://doi.org/10.1186/1750-1326-10-1.

Saito, T. *et al.* (2014) "Single App knock-in mouse models of Alzheimer's disease," *Nature Neuroscience*, 17(5), pp. 661–663. Available at: https://doi.org/10.1038/nn.3697.

Sáiz-Vázquez, O. *et al.* (2021) "Depression as a Risk Factor for Alzheimer's Disease: A Systematic Review of Longitudinal Meta-Analyses.," *Journal of clinical medicine*, 10(9). Available at: https://doi.org/10.3390/jcm10091809.

Sakata, S. (2023) "SaLSa: A Combinatory Approach of Semi-Automatic Labeling and Long Short-Term Memory to Classify Behavioral Syllables," *eNeuro*, 10(12). Available at: https://doi.org/10.1523/ENEURO.0201-23.2023.

Salazar, A. *et al.* (2012) "Indoleamine 2,3-dioxygenase mediates anhedonia and anxiety-like behaviors caused by peripheral lipopolysaccharide immune challenge.," *Hormones and behavior*, 62(3), pp. 202–209. Available at: https://doi.org/10.1016/j.yhbeh.2012.03.010.

Santiago, J.A. and Potashkin, J.A. (2021) "The Impact of Disease Comorbidities in Alzheimer's Disease," *Frontiers in Aging Neuroscience*, 13. Available at: https://doi.org/10.3389/fnagi.2021.631770.

Sarkar, S., Guha, S. and Biswas, S.C. (2022) "Role of Reactive Astrocytes in Alzheimer's Disease," in *The Biology of Glial Cells: Recent Advances*. Singapore: Springer Singapore, pp. 199–242. Available at: https://doi.org/10.1007/978-981-16-8313-8_9.

Sarmin, N. *et al.* (2024) "Evaluation of serum interleukin-12 and interleukin-4 as potential biomarkers for the diagnosis of major depressive disorder," *Scientific Reports*, 14(1), p. 1652. Available at: https://doi.org/10.1038/s41598-024-51932-9.

Sasmita, A.O. *et al.* (2025) "Parental origin of transgene modulates amyloid-β plaque burden in the 5xFAD mouse model of Alzheimer's disease," *Neuron*, 113(6), pp. 838-846.e4. Available at: https://doi.org/https://doi.org/10.1016/j.neuron.2024.12.025.

Scheggi, S., De Montis, M.G. and Gambarana, C. (2018) "Making Sense of Rodent Models of Anhedonia.," *The international journal of neuropsychopharmacology*, 21(11), pp. 1049–1065. Available at: https://doi.org/10.1093/ijnp/pyy083.

Schöll, M. *et al.* (2016) "PET Imaging of Tau Deposition in the Aging Human Brain," *Neuron*, 89(5), pp. 971–982. Available at: https://doi.org/https://doi.org/10.1016/j.neuron.2016.01.028.

Seibenhener, M.L. and Wooten, M.C. (2015) "Use of the Open Field Maze to measure locomotor and anxiety-like behavior in mice.," *Journal of visualized experiments : JoVE*, (96), p. e52434. Available at: https://doi.org/10.3791/52434.

Selkoe, D.J. and Hardy, J. (2016) "The amyloid hypothesis of Alzheimer's disease at 25 years.," *EMBO molecular medicine*, 8(6), pp. 595–608. Available at: https://doi.org/10.15252/emmm.201606210.

Sens, J. *et al.* (2017) "Lipopolysaccharide administration induces sex-dependent behavioural and serotonergic neurochemical signatures in mice," *Pharmacology Biochemistry and Behavior*, 153, pp. 168–181. Available at: https://doi.org/https://doi.org/10.1016/j.pbb.2016.12.016.

Serrano-Pozo, A. *et al.* (2011) "Neuropathological alterations in Alzheimer disease.," *Cold Spring Harbor perspectives in medicine*, 1(1), p. a006189. Available at: https://doi.org/10.1101/cshperspect.a006189.

Setiawan, E. *et al.* (2018) "Association of translocator protein total distribution volume with

duration of untreated major depressive disorder: a cross-sectional study.," *The lancet. Psychiatry*, 5(4), pp. 339–347. Available at: https://doi.org/10.1016/S2215-0366(18)30048-8.

Sevigny, J. *et al.* (2016) "The antibody aducanumab reduces Aβ plaques in Alzheimer's disease," *Nature*, 537(7618), pp. 50–56. Available at: https://doi.org/10.1038/nature19323.

Sevil-Pérez, A. *et al.* (2024) "The Association Between Major Depression and Alzheimer's Disease Risk: Evidence from a 12-Year Longitudinal Study.," *Journal of clinical medicine*, 13(23). Available at: https://doi.org/10.3390/jcm13237039.

Shaftel, S.S. *et al.* (2007) "Sustained hippocampal IL-1 beta overexpression mediates chronic neuroinflammation and ameliorates Alzheimer plaque pathology.," *The Journal of clinical investigation*, 117(6), pp. 1595–604. Available at: https://doi.org/10.1172/JCI31450.

Shakya, R. *et al.* (2020) "Immune contexture analysis in immuno-oncology: applications and challenges of multiplex fluorescent immunohistochemistry.," *Clinical & translational immunology*, 9(10), p. e1183. Available at: https://doi.org/10.1002/cti2.1183.

Shavit-Stein, E. *et al.* (2017) "Protease Activated Receptor 2 (PAR2) Induces Long-Term Depression in the Hippocampus through Transient Receptor Potential Vanilloid 4 (TRPV4)," *Frontiers in Molecular Neuroscience*, Volume 10. Available at: https://doi.org/10.3389/fnmol.2017.00042.

Sheline, Y.I. *et al.* (2014) "An Antidepressant Decreases CSF Aβ Production in Healthy Individuals and in Transgenic AD Mice," *Science Translational Medicine*, 6(236). Available at: https://doi.org/10.1126/scitranslmed.3008169.

Shen, L. and Jia, J. (2016) "An Overview of Genome-Wide Association Studies in Alzheimer's Disease.," *Neuroscience bulletin*, 32(2), pp. 183–90. Available at: https://doi.org/10.1007/s12264-016-0011-3.

Sheng, J.G. *et al.* (2003) "Lipopolysaccharide-induced-neuroinflammation increases intracellular accumulation of amyloid precursor protein and amyloid β peptide in APPswe transgenic mice," *Neurobiology of Disease*, 14(1), pp. 133–145. Available at: https://doi.org/https://doi.org/10.1016/S0969-9961(03)00069-X.

Sherrington, R. *et al.* (1995) "Cloning of a gene bearing missense mutations in early-onset familial Alzheimer's disease.," *Nature*, 375(6534), pp. 754–760. Available at: https://doi.org/10.1038/375754a0.

Shi, Q. *et al.* (2017) "Complement C3 deficiency protects against neurodegeneration in aged plaque-rich APP/PS1 mice.," *Science translational medicine*, 9(392). Available at: https://doi.org/10.1126/scitranslmed.aaf6295.

Shin, H.S. *et al.* (2024) "Prolonged stress response induced by chronic stress and corticosterone exposure causes adult neurogenesis inhibition and astrocyte loss in mouse hippocampus," *Brain Research Bulletin*, 208, p. 110903. Available at: https://doi.org/https://doi.org/10.1016/j.brainresbull.2024.110903.

Shiota, N. *et al.* (2016) "Water spray-induced grooming is negatively correlated with depressive behavior in the forced swimming test in rats," *The Journal of Physiological Sciences*, 66(3), pp. 265–273. Available at: https://doi.org/https://doi.org/10.1007/s12576-015-0424-1.

Shlomi-Loubaton, S. *et al.* (2025) "Chronic stress leads to earlier cognitive decline in an Alzheimer's mouse model: The role of neuroinflammation and TrkB," *Brain, Behavior, and Immunity*, 127, pp. 303–314. Available at: https://doi.org/https://doi.org/10.1016/j.bbi.2025.03.021.

Si, X. *et al.* (2004) "Age-dependent reductions in the level of glial fibrillary acidic protein in the prefrontal cortex in major depression.," *Neuropsychopharmacology : official publication of the American College of Neuropsychopharmacology*, 29(11), pp. 2088–96. Available at:

https://doi.org/10.1038/sj.npp.1300525.

Sil, A. *et al.* (2022) “Sex Differences in Behavior and Molecular Pathology in the 5XFAD Model,” *Journal of Alzheimer’s Disease*. Edited by O. Wirths, 85(2), pp. 755–778. Available at: https://doi.org/10.3233/JAD-210523.

Sims, J.R. *et al.* (2023) “Donanemab in Early Symptomatic Alzheimer Disease: The TRAILBLAZER-ALZ 2 Randomized Clinical Trial.,” *JAMA*, 330(6), pp. 512–527. Available at: https://doi.org/10.1001/jama.2023.13239.

Singh, D. (2022) “Astrocytic and microglial cells as the modulators of neuroinflammation in Alzheimer’s disease,” *Journal of Neuroinflammation*, 19(1), p. 206. Available at: https://doi.org/10.1186/s12974-022-02565-0.

Singh, T.D. *et al.* (2010) “MEGF10 functions as a receptor for the uptake of amyloid-β,” *FEBS Letters*, 584(18), pp. 3936–3942. Available at: https://doi.org/https://doi.org/10.1016/j.febslet.2010.08.050.

Sly, L.. *et al.* (2001) “Endogenous brain cytokine mRNA and inflammatory responses to lipopolysaccharide are elevated in the Tg2576 transgenic mouse model of Alzheimer’s disease,” *Brain Research Bulletin*, 56(6), pp. 581–588. Available at: https://doi.org/10.1016/S0361-9230(01)00730-4.

Smith-Swintosky, V.L. *et al.* (1997) “Protease-activated receptor-2 (PAR-2) is present in the rat hippocampus and is associated with neurodegeneration.,” *Journal of neurochemistry*, 69(5), pp. 1890–6. Available at: https://doi.org/10.1046/j.1471-4159.1997.69051890.x.

Sofroniew, M. V (2020) “Astrocyte Reactivity: Subtypes, States, and Functions in CNS Innate Immunity.,” *Trends in immunology*, 41(9), pp. 758–770. Available at: https://doi.org/10.1016/j.it.2020.07.004.

Soraci, L. *et al.* (2023) “Toll-like receptors and NLRP3 inflammasome-dependent pathways in Parkinson’s disease: mechanisms and therapeutic implications.,” *Journal of neurology*, 270(3), pp. 1346–1360. Available at: https://doi.org/10.1007/s00415-022-11491-3.

Spires-Jones, T.L. *et al.* (2009) “Passive immunotherapy rapidly increases structural plasticity in a mouse model of Alzheimer disease.,” *Neurobiology of disease*, 33(2), pp. 213–20. Available at: https://doi.org/10.1016/j.nbd.2008.10.011.

Sri, S. *et al.* (2019) “Emergence of synaptic and cognitive impairment in a mature-onset APP mouse model of Alzheimer’s disease,” *Acta Neuropathologica Communications*, 7(1), p. 25. Available at: https://doi.org/10.1186/s40478-019-0670-1.

Srivastava, S., Ahmad, R. and Khare, S.K. (2021) “Alzheimer’s disease and its treatment by different approaches: A review,” *European Journal of Medicinal Chemistry*, 216, p. 113320. Available at: https://doi.org/10.1016/j.ejmech.2021.113320.

Stedenfeld, K.A. *et al.* (2011) “Novelty-seeking behavior predicts vulnerability in a rodent model of depression.,” *Physiology & behavior*, 103(2), pp. 210–216. Available at: https://doi.org/10.1016/j.physbeh.2011.02.001.

Steiner, J. *et al.* (2011) “Severe depression is associated with increased microglial quinolinic acid in subregions of the anterior cingulate gyrus: Evidence for an immune-modulated glutamatergic neurotransmission?,” *Journal of Neuroinflammation*, 8(1), p. 94. Available at: https://doi.org/10.1186/1742-2094-8-94.

Steru, L. *et al.* (1985) “The tail suspension test: A new method for screening antidepressants in mice,” *Psychopharmacology*, 85(3), pp. 367–370. Available at: https://doi.org/10.1007/BF00428203.

Striggow, F. *et al.* (2001) “Four different types of protease-activated receptors are widely expressed in the brain and are up-regulated in hippocampus by severe ischemia.,” *The*

European journal of neuroscience, 14(4), pp. 595–608. Available at: https://doi.org/10.1046/j.0953-816x.2001.01676.x.

Suen, J.Y. *et al.* (2014) “Pathway-selective antagonism of proteinase activated receptor 2.,” *British journal of pharmacology*, 171(17), pp. 4112–4124. Available at: https://doi.org/10.1111/bph.12757.

Sulakhiya, K. *et al.* (2016) “Lipopolysaccharide induced anxiety- and depressive-like behaviour in mice are prevented by chronic pre-treatment of esculetin,” *Neuroscience Letters*, 611, pp. 106–111. Available at: https://doi.org/https://doi.org/10.1016/j.neulet.2015.11.031.

Tachibana, M. *et al.* (2019) “APOE4-mediated amyloid-β pathology depends on its neuronal receptor LRP1.,” *The Journal of clinical investigation*, 129(3), pp. 1272–1277. Available at: https://doi.org/10.1172/JCI124853.

Takatori, S., Kondo, M. and Tomita, T. (2025) “Unraveling the complex role of microglia in Alzheimer’s disease: amyloid β metabolism and plaque formation,” *Inflammation and Regeneration*, 45(1), p. 16. Available at: https://doi.org/10.1186/s41232-025-00383-4.

Tejera, D. *et al.* (2019) “Systemic inflammation impairs microglial Aβ clearance through <scp>NLRP</scp> 3 inflammasome,” *The EMBO Journal*, 38(17). Available at: https://doi.org/10.15252/embj.2018101064.

The World Health Organisation (2012) *Dementia as a Public Health Priority*. Available at: https://www.who.int/publications/i/item/dementia-a-public-health-priority.

Thygesen, C. *et al.* (2018) “Diverse Protein Profiles in CNS Myeloid Cells and CNS Tissue From Lipopolysaccharide- and Vehicle-Injected APPSWE/PS1ΔE9 Transgenic Mice Implicate Cathepsin Z in Alzheimer’s Disease,” *Frontiers in Cellular Neuroscience*, 12. Available at: https://doi.org/10.3389/fncel.2018.00397.

Tolboom, N. *et al.* (2009) “Relationship of cerebrospinal fluid markers to 11C-PiB and 18F-FDDNP binding.,” *Journal of nuclear medicine : official publication, Society of Nuclear Medicine*, 50(9), pp. 1464–70. Available at: https://doi.org/10.2967/jnumed.109.064360.

Tran, T. *et al.* (2021) “Male-Female Differences in the Effects of Age on Performance Measures Recorded for 23 Hours in Mice.,” *The journals of gerontology. Series A, Biological sciences and medical sciences*, 76(12), pp. 2141–2146. Available at: https://doi.org/10.1093/gerona/glab182.

Troubat, R. *et al.* (2021) “Neuroinflammation and depression: A review,” *European Journal of Neuroscience*, 53(1), pp. 151–171. Available at: https://doi.org/10.1111/ejn.14720.

Turner, V. and Husain, M. (2022) “Anhedonia in Neurodegenerative Diseases BT - Anhedonia: Preclinical, Translational, and Clinical Integration,” in D.A. Pizzagalli (ed.). Cham: Springer International Publishing, pp. 255–277. Available at: https://doi.org/10.1007/7854_2022_352.

Tzioras, M. *et al.* (2023) “Synaptic degeneration in Alzheimer disease,” *Nature Reviews Neurology*, 19(1), pp. 19–38. Available at: https://doi.org/10.1038/s41582-022-00749-z.

Ushakumari, C.J. *et al.* (2022) “Neutrophil Elastase Increases Vascular Permeability and Leukocyte Transmigration in Cultured Endothelial Cells and Obese Mice,” *Cells*. Available at: https://doi.org/10.3390/cells11152288.

Valiukas, Z. *et al.* (2025) “Microglial activation states and their implications for Alzheimer’s Disease.,” *The journal of prevention of Alzheimer’s disease*, 12(1), p. 100013. Available at: https://doi.org/10.1016/j.tjpad.2024.100013.

Vaquero-Puyuelo, D. *et al.* (2021) “Anhedonia as a Potential Risk Factor of Alzheimer’s Disease in a Community-Dwelling Elderly Sample: Results from the ZARADEMP Project.,”

International journal of environmental research and public health, 18(4). Available at: https://doi.org/10.3390/ijerph18041370.

Verharen, J.P.H. *et al.* (2023) "A computational analysis of mouse behavior in the sucrose preference test," *Nature Communications*, 14(1), p. 2419. Available at: https://doi.org/10.1038/s41467-023-38028-0.

Verkhratsky, A. *et al.* (2023) "Astrocytes in human central nervous system diseases: a frontier for new therapies," *Signal Transduction and Targeted Therapy*, 8(1), p. 396. Available at: https://doi.org/10.1038/s41392-023-01628-9.

Viejo, L. *et al.* (2022) "Systematic review of human post-mortem immunohistochemical studies and bioinformatics analyses unveil the complexity of astrocyte reaction in Alzheimer's disease.," *Neuropathology and applied neurobiology*, 48(1), p. e12753. Available at: https://doi.org/10.1111/nan.12753.

Villa, A. *et al.* (2018) "Sex-Specific Features of Microglia from Adult Mice," *Cell Reports*, 23(12), pp. 3501–3511. Available at: https://doi.org/10.1016/j.celrep.2018.05.048.

Villano, G. and Pontisso, P. (2024) "Protease activated receptor 2 as a novel druggable target for the treatment of metabolic dysfunction-associated fatty liver disease and cancer," *Frontiers in Immunology*, Volume 15. Available at: https://doi.org/10.3389/fimmu.2024.1397441.

Vogel, J.W. *et al.* (2021) "Author Correction: Spread of pathological tau proteins through communicating neurons in human Alzheimer's disease," *Nature Communications*, 12(1), p. 4862. Available at: https://doi.org/10.1038/s41467-021-25193-3.

Vu, T.-K.H. *et al.* (1991) "Molecular cloning of a functional thrombin receptor reveals a novel proteolytic mechanism of receptor activation," *Cell*, 64(6), pp. 1057–1068. Available at: https://doi.org/https://doi.org/10.1016/0092-8674(91)90261-V.

Walker, L.C., Schelle, J. and Jucker, M. (2016) "The Prion-Like Properties of Amyloid-β Assemblies: Implications for Alzheimer's Disease.," *Cold Spring Harbor perspectives in medicine*, 6(7). Available at: https://doi.org/10.1101/cshperspect.a024398.

Wallensten, J. *et al.* (2023) "Stress, depression, and risk of dementia - a cohort study in the total population between 18 and 65 years old in Region Stockholm.," *Alzheimer's research & therapy*, 15(1), p. 161. Available at: https://doi.org/10.1186/s13195-023-01308-4.

Walsh, S. *et al.* (2021) "Aducanumab for Alzheimer's disease?," *BMJ*, p. n1682. Available at: https://doi.org/10.1136/bmj.n1682.

Wang, F. *et al.* (2020) "Lipopolysaccharide exposure during late embryogenesis triggers and drives Alzheimer-like behavioral and neuropathological changes in CD-1 mice.," *Brain and behavior*, 10(3), p. e01546. Available at: https://doi.org/10.1002/brb3.1546.

Wang, H.-Q., Wang, Z.-Z. and Chen, N.-H. (2021) "The receptor hypothesis and the pathogenesis of depression: Genetic bases and biological correlates," *Pharmacological Research*, 167, p. 105542. Available at: https://doi.org/10.1016/j.phrs.2021.105542.

Wang, H. *et al.* (2012) "Consequences of Inhibiting Amyloid Precursor Protein Processing Enzymes on Synaptic Function and Plasticity," *Neural Plasticity*, 2012, pp. 1–24. Available at: https://doi.org/10.1155/2012/272374.

Wang, H. *et al.* (2022) "Microglia in depression: an overview of microglia in the pathogenesis and treatment of depression.," *Journal of neuroinflammation*, 19(1), p. 132. Available at: https://doi.org/10.1186/s12974-022-02492-0.

Wang, H. *et al.* (2024) "Chronic Corticosterone Administration-Induced Mood Disorders in Laboratory Rodents: Features, Mechanisms, and Research Perspectives.," *International journal of molecular sciences*, 25(20). Available at: https://doi.org/10.3390/ijms252011245.

Wang, J. *et al.* (2014) “Fluoxetine Improves Behavioral Performance by Suppressing the Production of Soluble β-Amyloid in APP/PS1 Mice,” *Current Alzheimer Research*, 11(7), pp. 672–680. Available at: https://doi.org/10.2174/1567205011666140812114715.

Wang, L.-M. *et al.* (2018) “Lipopolysaccharide endotoxemia induces amyloid-β and p-tau formation in the rat brain.,” *American journal of nuclear medicine and molecular imaging*, 8(2), pp. 86–99. Available at: http://www.ncbi.nlm.nih.gov/pubmed/29755842.

Wang, Q. *et al.* (2017) “The recent progress in animal models of depression.,” *Progress in neuro-psychopharmacology & biological psychiatry*, 77, pp. 99–109. Available at: https://doi.org/10.1016/j.pnpbp.2017.04.008.

Wang, Y.-C. *et al.* (2018) “Increased Risk of Dementia in Patients with Antidepressants: A Meta-Analysis of Observational Studies.,” *Behavioural neurology*, 2018, p. 5315098. Available at: https://doi.org/10.1155/2018/5315098.

Wang, Y., Luo, W. and Reiser, G. (2007) “Activation of protease-activated receptors in astrocytes evokes a novel neuroprotective pathway through release of chemokines of the growth-regulated oncogene/cytokine-induced neutrophil chemoattractant family.,” *The European journal of neuroscience*, 26(11), pp. 3159–3168. Available at: https://doi.org/10.1111/j.1460-9568.2007.05938.x.

Watanabe, T. *et al.* (2025) “Ameliorative Effect of Ninjinyoeito on Reductions in Self-grooming in Lipopolysaccharide-Injected Mice: Involvement of Alpha7 Nicotinic Acetylcholine Receptor,” *Biological and Pharmaceutical Bulletin*, 48(5), pp. 728–732. Available at: https://doi.org/10.1248/bpb.b24-00510.

Waters, J.C. (2009) “Accuracy and precision in quantitative fluorescence microscopy,” *Journal of Cell Biology*, 185(7), pp. 1135–1148. Available at: https://doi.org/10.1083/jcb.200903097.

Webster, S.J. *et al.* (2014) “Using mice to model Alzheimer’s dementia: an overview of the clinical disease and the preclinical behavioral changes in 10 mouse models.,” *Frontiers in genetics*, 5, p. 88. Available at: https://doi.org/10.3389/fgene.2014.00088.

Wendeln, A.-C. *et al.* (2018) “Innate immune memory in the brain shapes neurological disease hallmarks,” *Nature*, 556(7701), pp. 332–338. Available at: https://doi.org/10.1038/s41586-018-0023-4.

Wightman, D.P. *et al.* (2021) “A genome-wide association study with 1,126,563 individuals identifies new risk loci for Alzheimer’s disease,” *Nature Genetics*, 53(9), pp. 1276–1282. Available at: https://doi.org/10.1038/s41588-021-00921-z.

Willner, P. (1984) “The validity of animal models of depression,” *Psychopharmacology*, 83(1), pp. 1–16. Available at: https://doi.org/10.1007/BF00427414.

Willner, P. *et al.* (1987) “Reduction of sucrose preference by chronic unpredictable mild stress, and its restoration by a tricyclic antidepressant,” *Psychopharmacology*, 93(3), pp. 358–364. Available at: https://doi.org/10.1007/BF00187257.

Willner, P. (1997) “Validity, reliability and utility of the chronic mild stress model of depression: a 10-year review and evaluation.,” *Psychopharmacology*, 134(4), pp. 319–29. Available at: https://doi.org/10.1007/s002130050456.

Willner, P. (2017) “The chronic mild stress (CMS) model of depression: History, evaluation and usage.,” *Neurobiology of stress*, 6, pp. 78–93. Available at: https://doi.org/10.1016/j.ynstr.2016.08.002.

Willner, P. and Belzung, C. (2015) “Treatment-resistant depression: are animal models of depression fit for purpose?,” *Psychopharmacology*, 232(19), pp. 3473–3495. Available at: https://doi.org/10.1007/s00213-015-4034-7.

Wippold, F.J. *et al.* (2008) “Neuropathology for the Neuroradiologist: Plaques and Tangles,” *American Journal of Neuroradiology*, 29(1), pp. 18–22. Available at: https://doi.org/10.3174/ajnr.A0781.

World Health Organisation [WHO] (2023) “Dementia fact sheet,” *WHO.int* [Preprint]. Available at: https://www.who.int/news-room/fact-sheets/detail/dementia.

Wu, T. *et al.* (2019) “Complement C3 Is Activated in Human AD Brain and Is Required for Neurodegeneration in Mouse Models of Amyloidosis and Tauopathy,” *Cell Reports*, 28(8), pp. 2111-2123.e6. Available at: https://doi.org/https://doi.org/10.1016/j.celrep.2019.07.060.

Wu, Y. and Eisel, U.L.M. (2023) “Microglia-Astrocyte Communication in Alzheimer’s Disease.,” *Journal of Alzheimer’s disease : JAD*, 95(3), pp. 785–803. Available at: https://doi.org/10.3233/JAD-230199.

Xiao, X. *et al.* (2021) “APP, PSEN1, and PSEN2 Variants in Alzheimer’s Disease: Systematic Re-evaluation According to ACMG Guidelines,” *Frontiers in Aging Neuroscience*, 13. Available at: https://doi.org/10.3389/fnagi.2021.695808.

Xie, J. *et al.* (2021) “Low-grade peripheral inflammation affects brain pathology in the App(NL-G-F)mouse model of Alzheimer’s disease.,” *Acta neuropathologica communications*, 9(1), p. 163. Available at: https://doi.org/10.1186/s40478-021-01253-z.

Xie, J., Van Hoecke, L. and Vandenbroucke, R.E. (2022) “The Impact of Systemic Inflammation on Alzheimer’s Disease Pathology,” *Frontiers in Immunology*. Frontiers Media S.A. Available at: https://doi.org/10.3389/fimmu.2021.796867.

Xu, B. *et al.* (2022) “Meningitic Escherichia coli-Induced Interleukin-17A Facilitates Blood–Brain Barrier Disruption via Inhibiting Proteinase 3/Protease-Activated Receptor 2 Axis,” *Frontiers in Cellular Neuroscience*, Volume 16. Available at: https://doi.org/10.3389/fncel.2022.814867.

Xu, W. *et al.* (1998) “Cloning and characterization of human protease-activated receptor 4,” *Proceedings of the National Academy of Sciences*, 95(12), pp. 6642–6646. Available at: https://doi.org/10.1073/pnas.95.12.6642.

Yang, Y. *et al.* (2022) “Sustained Inflammation Induced by LPS Leads to Tolerable Anorexia and Fat Loss via Tlr4 in Mice.,” *Journal of inflammation research*, 15, pp. 5635–5648. Available at: https://doi.org/10.2147/JIR.S358518.

Yang, Y. *et al.* (2023) “LPS priming before plaque deposition impedes microglial activation and restrains Aβ pathology in the 5xFAD mouse model of Alzheimer’s disease,” *Brain, Behavior, and Immunity*, 113, pp. 228–247. Available at: https://doi.org/10.1016/j.bbi.2023.07.006.

Yao, Y. *et al.* (2023) “Complement C3a receptor antagonist alleviates tau pathology and ameliorates cognitive deficits in P301S mice,” *Brain Research Bulletin*, 200, p. 110685. Available at: https://doi.org/https://doi.org/10.1016/j.brainresbull.2023.110685.

Yin, R. *et al.* (2023) “Lipopolysaccharide-induced depression-like model in mice: meta-analysis and systematic evaluation,” *Frontiers in Immunology*, 14. Available at: https://doi.org/10.3389/fimmu.2023.1181973.

Yohn, C.N., Gergues, M.M. and Samuels, B.A. (2017) “The role of 5-HT receptors in depression,” *Molecular Brain*, 10(1), p. 28. Available at: https://doi.org/10.1186/s13041-017-0306-y.

Yokoyama, M. *et al.* (2022) “Mouse Models of Alzheimer’s Disease,” *Frontiers in Molecular Neuroscience*, 15. Available at: https://doi.org/10.3389/fnmol.2022.912995.

Yu, X. *et al.* (2022) “Comparison of LPS and MS-induced depressive mouse model: behavior, inflammation and biochemical changes,” *BMC Psychiatry*, 22(1), p. 590. Available

at: https://doi.org/10.1186/s12888-022-04233-2.

Yue, Q. and Hoi, M.P.M. (2023) “Emerging roles of astrocytes in blood-brain barrier disruption upon amyloid-beta insults in Alzheimer’s disease.,” *Neural regeneration research*, 18(9), pp. 1890–1902. Available at: https://doi.org/10.4103/1673-5374.367832.

Van Zeller, M. *et al.* (2021) “NLRP3 Inflammasome: A Starring Role in Amyloid-β- and Tau-Driven Pathological Events in Alzheimer’s Disease.,” *Journal of Alzheimer’s disease : JAD*, 83(3), pp. 939–961. Available at: https://doi.org/10.3233/JAD-210268.

Zeng, X. *et al.* (2013) “Activation of protease-activated receptor 2-mediated signaling by mast cell tryptase modulates cytokine production in primary cultured astrocytes.,” *Mediators of inflammation*, 2013, p. 140812. Available at: https://doi.org/10.1155/2013/140812.

Zeng, X. *et al.* (2023) “Astrocyte-specific knockout of YKL-40/Chi3l1 reduces Aβ burden and restores memory functions in 5xFAD mice.,” *Journal of neuroinflammation*, 20(1), p. 290. Available at: https://doi.org/10.1186/s12974-023-02970-z.

Zetterberg, H. and Bendlin, B.B. (2021) “Biomarkers for Alzheimer’s disease—preparing for a new era of disease-modifying therapies,” *Molecular Psychiatry*, 26(1), pp. 296–308. Available at: https://doi.org/10.1038/s41380-020-0721-9.

Zhang, A.Y., Elias, E. and Manners, M.T. (2024) “Sex-dependent astrocyte reactivity: Unveiling chronic stress-induced morphological changes across multiple brain regions,” *Neurobiology of Disease*, 200, p. 106610. Available at: https://doi.org/https://doi.org/10.1016/j.nbd.2024.106610.

Zhang, C. *et al.* (2016) “Corticotropin-releasing factor receptor-1 antagonism mitigates beta amyloid pathology and cognitive and synaptic deficits in a mouse model of Alzheimer’s disease,” *Alzheimer’s & Dementia*, 12(5), pp. 527–537. Available at: https://doi.org/10.1016/j.jalz.2015.09.007.

Zhang, C. *et al.* (2018) “NSAID Exposure and Risk of Alzheimer’s Disease: An Updated Meta-Analysis From Cohort Studies ,” *Frontiers in Aging Neuroscience* . Available at: https://www.frontiersin.org/articles/10.3389/fnagi.2018.00083.

Zhang, F. *et al.* (2012) “Fluoxetine protects neurons against microglial activation-mediated neurotoxicity.,” *Parkinsonism & related disorders*, 18 Suppl 1(0 1), pp. S213-7. Available at: https://doi.org/10.1016/S1353-8020(11)70066-9.

Zhang, J. *et al.* (2011) “Deficiency of antinociception and excessive grooming induced by acute immobilization stress in Per1 mutant mice.,” *PloS one*, 6(1), p. e16212. Available at: https://doi.org/10.1371/journal.pone.0016212.

Zhang, J. *et al.* (2022) “Fluoxetine shows neuroprotective effects against LPS-induced neuroinflammation via the Notch signaling pathway,” *International Immunopharmacology*, 113, p. 109417. Available at: https://doi.org/10.1016/j.intimp.2022.109417.

Zhang, J. *et al.* (2024) “Recent advances in Alzheimer’s disease: mechanisms, clinical trials and new drug development strategies,” *Signal Transduction and Targeted Therapy*, 9(1), p. 211. Available at: https://doi.org/10.1038/s41392-024-01911-3.

Zhang, M. *et al.* (2022) “Resilience and resistance to the accumulation of amyloid plaques and neurofibrillary tangles in centenarians: An age-continuous perspective,” *Alzheimer’s & Dementia* [Preprint]. Available at: https://doi.org/10.1002/alz.12899.

Zhang, X. *et al.* (2021) “Role of Astrocytes in Major Neuropsychiatric Disorders,” *Neurochemical Research*, 46(10), pp. 2715–2730. Available at: https://doi.org/10.1007/s11064-020-03212-x.

Zhang, X. and Song, W. (2013) “The role of APP and BACE1 trafficking in APP processing and amyloid-β generation,” *Alzheimer’s Research & Therapy*, 5(5), p. 46. Available at:

https://doi.org/10.1186/alzrt211.

Zhang, Y. *et al.* (2023) “Amyloid β-based therapy for Alzheimer’s disease: challenges, successes and future,” *Signal Transduction and Targeted Therapy*, 8(1), p. 248. Available at: https://doi.org/10.1038/s41392-023-01484-7.

Zhao, J. *et al.* (2019) “Neuroinflammation induced by lipopolysaccharide causes cognitive impairment in mice,” *Scientific Reports*, 9(1), p. 5790. Available at: https://doi.org/10.1038/s41598-019-42286-8.

Zhao, J., O’Connor, T. and Vassar, R. (2011) “The contribution of activated astrocytes to Aβ production: Implications for Alzheimer’s disease pathogenesis,” *Journal of Neuroinflammation*, 8(1), p. 150. Available at: https://doi.org/10.1186/1742-2094-8-150.

Zhao, Y. *et al.* (2024) “Astrocyte-Mediated Neuroinflammation in Neurological Conditions,” *Biomolecules*. Available at: https://doi.org/10.3390/biom14101204.

Zheng, C., Zhou, X.-W. and Wang, J.-Z. (2016) “The dual roles of cytokines in Alzheimer’s disease: update on interleukins, TNF-α, TGF-β and IFN-γ,” *Translational Neurodegeneration*, 5(1), p. 7. Available at: https://doi.org/10.1186/s40035-016-0054-4.

Zhong, M.Z. *et al.* (2024) “Updates on mouse models of Alzheimer’s disease,” *Molecular Neurodegeneration*, 19(1), p. 23. Available at: https://doi.org/10.1186/s13024-024-00712-0.

Zhou, J. *et al.* (2023) “BACE1 regulates expression of Clusterin in astrocytes for enhancing clearance of β-amyloid peptides,” *Molecular Neurodegeneration*, 18(1), p. 31. Available at: https://doi.org/10.1186/s13024-023-00611-w.

Zhou, R. *et al.* (2021) “PET Imaging of Neuroinflammation in Alzheimer’s Disease.,” *Frontiers in immunology*, 12, p. 739130. Available at: https://doi.org/10.3389/fimmu.2021.739130.

Zhou, Y. and Danbolt, N.C. (2014) “Glutamate as a neurotransmitter in the healthy brain,” *Journal of Neural Transmission*, 121(8), pp. 799–817. Available at: https://doi.org/10.1007/s00702-014-1180-8.

Zhuo, X. *et al.* (2022) “The Yin-Yang roles of protease-activated receptors in inflammatory signalling and diseases,” *The FEBS Journal*, 289(14), pp. 4000–4020. Available at: https://doi.org/10.1111/febs.16406.

Ziar, R., Tesar, P.J. and Clayton, B.L.L. (2025) “Astrocyte and oligodendrocyte pathology in Alzheimer’s disease,” *Neurotherapeutics*, 22(3), p. e00540. Available at: https://doi.org/https://doi.org/10.1016/j.neurot.2025.e00540.